RWTH edition





RWTH AACHEN UNIVERSITY

Fritz Klocke

Manufacturing Processes 4

Forming

Springer

RWTHedition

For further volumes:
http://www.springer.com/series/7858

Fritz Klocke

Manufacturing Processes 4

Forming

Springer

Fritz Klocke
Lehrstuhl für Technologie der Fertigungsverfahren
RWTH Aachen
Aachen
Germany

ISSN 1865-0899 ISSN 1865-0902 (electronic)
ISBN 978-3-642-36771-7 ISBN 978-3-642-36772-4 (eBook)
DOI 10.1007/978-3-642-36772-4
Springer Heidelberg New York Dordrecht London

Library of Congress Control Number: 2013933111

Translation from the German edition "Fertigungsverfahren 4: Umformen", 2006, ISBN 978-3-540-23650-4 published by Springer.

© Springer-Verlag Berlin Heidelberg 2013
This work is subject to copyright. All rights are reserved by the Publisher, whether the whole or part of the material is concerned, specifically the rights of translation, reprinting, reuse of illustrations, recitation, broadcasting, reproduction on microfilms or in any other physical way, and transmission or information storage and retrieval, electronic adaptation, computer software, or by similar or dissimilar methodology now known or hereafter developed. Exempted from this legal reservation are brief excerpts in connection with reviews or scholarly analysis or material supplied specifically for the purpose of being entered and executed on a computer system, for exclusive use by the purchaser of the work. Duplication of this publication or parts thereof is permitted only under the provisions of the Copyright Law of the Publisher's location, in its current version, and permission for use must always be obtained from Springer. Permissions for use may be obtained through RightsLink at the Copyright Clearance Center. Violations are liable to prosecution under the respective Copyright Law.
The use of general descriptive names, registered names, trademarks, service marks, etc. in this publication does not imply, even in the absence of a specific statement, that such names are exempt from the relevant protective laws and regulations and therefore free for general use.
While the advice and information in this book are believed to be true and accurate at the date of publication, neither the authors nor the editors nor the publisher can accept any legal responsibility for any errors or omissions that may be made. The publisher makes no warranty, express or implied, with respect to the material contained herein.

Printed on acid-free paper

Springer is part of Springer Science+Business Media (www.springer.com)

Foreword to the Compendium "Manufacturing Processes"

Key factors in the quality and economic efficiency of industrial production are the choice of manufacturing processes and their design. Manufacturing technology is an elementary part of the basic knowledge of mechanical engineers. Also design engineers must gain knowledge of this field since they are highly responsible for the manufacturing costs. However, students as well as practising experts willing to enhance their knowledge experience difficulty in obtaining information. To the present day, there is no extensive yet clear description of manufacturing processes focusing on the technology itself.

In order to counter this necessity, the present compendium is meant to present an overall picture of the most common machining and non-machining manufacturing processes. In addition to the description of techniques, these volumes seek to deliver an insight into the underlying principles whenever it is necessary for the understanding of the processes.

The design of machine components, drives and controls is dealt with elaborately in the book "Machine Tools" from M. Weck/C. Brecher. W. Eversheim and G. Schuh go into detail about questions concerning cost-effectiveness as well as an optimized integration of machines in the production process in "Organisation in Production Techniques".

Techniques with similar active principles have been grouped together into the following volumes:

Volume 1: Turning, Milling, Drilling
Volume 2: Grinding, Honing, Lapping
Volume 3: Electrical Erosion and Hybrid Processes
Volume 4: Forming
Volume 5: Casting, Sintering, Rapid Prototyping

At the beginning of the first volume is appended a section spanning all branches on the subject of tolerances and the workpiece measuring techniques used in manufacturing.

Within the individual volumes, we have tried to avoid an encyclopaedic listing of the methods. The book series is primarily intended for junior scientists in the fields of manufacturing technology and construction. In addition, the practitioner will be able to refurbish or extend his knowledge. The variety of manufacturing

problems is as large as the multiplicity of products, and manufacturing problems cannot be solved with textbooks alone. We hope that this book offers starting points and approaches to its readers, points upon which they can come up with their own successful solutions using an engineer’s way of thinking.

Aachen, September 2008 Fritz Klocke

Foreword to Volume 4, "Forming"

The present volume of the compendium "Manufacturing Processes" deals with manufacturing methods of bulk and sheet forming. This book is based on the lecture series "Manufacturing Technology II" and the associated theoretical and practical exercises which I hold at the RWTH Aachen. In the process of revising the entire book series, the volumes "Massive Forming" and "Sheet forming" were combined to make the single volume "Forming". The contents were also expanded, updated and restructured.

The chapters on massive and sheet forming are preceded by a chapter on "Basic Principles". Therein, forming basics are addressed as well as methods of calculating problems in forming technology. The finite element method (FEM) is introduced as an important tool for analyzing complex forming processes using examples of its application. Methods of analyzing materials and components are introduced, as well as ways of determining material properties—especially flow curves. We present all tool and workpiece materials frequently used in all forming processes including the basic tribological aspects of forming engineering.

The chapter "Massive Forming" is dedicated to the most common processes of cold, warm and hot forming. It includes, among others, the processes of upsetting, impact extrusion and forging as well as superplastic forming and thixoforging. This chapter also addresses rolling as a finishing process. The chapter "Sheet Forming" contains the fundamentals required to analyze sheet forming processes. Among others, it includes the processes of deep drawing, stretch drawing, metal spinning and bending as well as several special sheet forming techniques.

The cutting processes of blanking and fine blanking are given a detailed presentation in the chapter "Sheet Metal Cutting". Finally, the chapter "Joining by Forming" deals with punch rivetting, crimping and seaming.

For their assistance in the production of this volume, I would like to thank my assistants and employees, Dr.-Ing. V. Bäcker, Dr.-Ing. B. Feldhaus, Dipl.-Ing. P. Mattfeld, Dipl.-Ing. F. Schongen, Mrs. M. Schröder, Dipl.-Ing. Dipl.-Wirt.Ing. M.Sc. M. Terhorst, Dr.-Ing. A. Timmer, Dipl.-Ing. Dipl.-Wirt.Ing. D. Trauth and Dipl.-Ing. M. Zimmermann, who substantially contributed to the appearance of the English translation of this book. I would also like to extend my thanks to my former assistants who contributed to the previous editions of the volumes upon

which this book is based, “Massive Forming” and “Sheet Forming”, and who now have leading positions in industry. Furthermore, I want to thank Springer for the thorough inspection of the manuscript.

Aachen, December 2012 Fritz Klocke

Contents

1 Introduction 1

2 Basic Principles 3
2.1 Introduction 3
2.2 Metallurgical Foundations for Determining the Condition of the Material 3
2.2.1 Crystal Structure 3
2.2.2 Elastic and Plastic Deformation of Crystals 5
2.2.3 Recrystallization 10
2.2.4 Difference Between Cold and Hot Forming 13
2.3 Plastomechanical Foundations 15
2.3.1 Comparison of Crystal Physics and Continuum Mechanics 15
2.3.2 State of Stress 15
2.3.3 Yield Criterion 17
2.3.4 Kinematics of the Continuum 21
2.3.5 Volume Constancy 24
2.3.6 Flow Rule 25
2.3.7 Limits of Plastic Formation 28
2.4 Possible Solutions to Forming Problems from the Field of Plasticity Theory 33
2.4.1 Solution Methods of Elementary Plasticity Theory 34
2.4.2 Energy Method 35
2.4.3 Calculation Method with the Strip, Disc and Pipe Model 36
2.4.4 Strict Solution 38
2.4.5 Slip Line Method 38
2.4.6 Visioplasticity and the Measuring Grid Method 39
2.4.7 Upper Bound Method 41
2.4.8 Error Compensation Method 42

2.5 Finite Element Method . . . 42
2.5.1 Basic Concepts of the Finite Element Method . . . 43
2.5.2 Lagrangian and Eulerian Representations of the Continuum . . . 45
2.5.3 Explicit and Implicit Solution Methods . . . 46
2.5.4 Thermal Coupling . . . 46
2.5.5 Element Types . . . 47
2.5.6 Non-Linearities . . . 48
2.5.7 Constitutive Laws . . . 48
2.5.8 Software . . . 49
2.5.9 Hardware . . . 50
2.5.10 Phases of a Finite Element Analysis . . . 50
2.5.11 The Use of FEM in Forming Engineering . . . 52
2.6 Metallography and Analysis . . . 62
2.6.1 Introduction . . . 62
2.6.2 Optical Microscopy . . . 63
2.6.3 Microhardness Testing . . . 63
2.6.4 Electron Microscopy . . . 65
2.6.5 Preparation Methods . . . 70
2.7 Materials in Forming Technology . . . 73
2.7.1 Workpiece Materials . . . 73
2.7.2 Tool Materials . . . 93
2.7.3 Determining the Flow Curve and Materials Testing . . . 101
2.8 Tribology in Forming Technology . . . 117
2.8.1 The Tribological System . . . 117
2.8.2 Friction . . . 119
2.8.3 Wear . . . 127
2.8.4 Lubrication in Forming Technology . . . 134
2.8.5 Tool Influences . . . 145
2.8.6 Effects of Topography . . . 153
2.8.7 Tribological Test Methods in Forming Technology . . . 157

3 Massive Forming . . . 169
3.1 Cold Forming . . . 169
3.1.1 Upsetting . . . 169
3.1.2 Extrusion . . . 172
3.1.3 Force and Energy Requirements . . . 188
3.1.4 Lubrication and Lubricants . . . 194
3.1.5 Manufacturing Accuracy and Surface Quality . . . 195
3.1.6 Economic Feasibility . . . 197
3.2 Warm Forming . . . 201
3.3 Hot Forming . . . 204
3.3.1 Definitions and Process Overview . . . 204
3.3.2 Open-Die Forging . . . 206

3.3.3 Closed-Die Forging 217
3.3.4 Swaging 229
3.3.5 Heating 232
3.3.6 Open-Die Forging Tools 236
3.3.7 Closed-Die Forging Tools 236
3.3.8 Lubrication in Closed-Die Forging 241
3.3.9 Design and Properties of Forgings 243
3.4 Special Massive Forming Processes 248
3.4.1 Special Closed-Die Forging Processes 248
3.4.2 Cold, Warm and Hot Working Combinations 253
3.4.3 Superplastic Forming 254
3.4.4 Thixoforging 258
3.5 Rolling as Remachining and Finish Machining Process 264
3.5.1 Profile Rolling of Prefabricated Components 264
3.5.2 Surface Fine Rolling 281
3.5.3 Materials Used in Rolling Processes 289
3.5.4 Tool Materials Used for Rolling Processes 290
3.5.5 Friction and Lubrication 290

4 Sheet Metal Forming 293
4.1 Deep Drawing 293
4.1.1 Principles of Deep Drawing 293
4.1.2 Process Variants and Examples of Use 304
4.1.3 Tools 314
4.1.4 Workpiece Materials 317
4.1.5 Manufacturing Accuracy 320
4.2 Flange Forming 323
4.2.1 Principles of Flange Forming 323
4.2.2 Process Variants and Manufacturing Examples 327
4.2.3 Tools 330
4.2.4 Materials 330
4.2.5 Manufacturing Accuracy 331
4.3 Stretch Drawing 332
4.3.1 Process Principle 332
4.3.2 Process Variants 333
4.3.3 Strains, Workpiece Materials and Forces 340
4.3.4 Tools 341
4.4 Metal Spinning 342
4.4.1 Process Principle 342
4.4.2 Admissible Strains 346
4.4.3 Forces 348
4.4.4 Manufacturing Examples 350
4.4.5 Tools 353
4.4.6 Materials 355

4.4.7 Manufacturing Quality 356
4.4.8 Metal Spinning: Advantages and Disadvantages, Criteria for Use 357
4.5 Bending 358
4.5.1 Principles of Bending 359
4.5.2 Process Variants 364
4.5.3 Tools and Workpiece Shapes 373
4.6 Special Processes of Sheet Metal Forming 382
4.6.1 Internal High-Pressure Forming 382
4.6.2 Superplastic Sheet Metal Forming 392
4.6.3 Forming with Laser Radiation 394
4.6.4 High Rate Forming 399

5 Sheet Metal Separation 407
5.1 Cutting 407
5.1.1 Cutting Principles 407
5.1.2 Process Characteristics and Variants 417
5.1.3 Manufacturing Accuracy 426
5.2 Fine Blanking 429
5.2.1 Principles of Fine Blanking 430
5.2.2 Tools 443
5.2.3 Materials 446
5.2.4 Process Variants and Manufacturing Examples 450
5.2.5 Manufacturing Accuracy and Component Properties . . . 453

6 Joining by Forming 457
6.1 Punch Riveting and Clinching 457
6.1.1 Punch Riveting 457
6.1.2 Clinching 459
6.1.3 Static and Dynamic Strength 463
6.2 Flanging and Seaming 464
6.2.1 Flanging 465
6.2.2 Seaming 465
6.3 Examples of Use 467

References 471

Index 509

Symbols and Abbreviations

Upper Case

A	Working zone; resurgence; crossover point
A	Failure strain (%)
A	Cross-section area (mm^2)
A_0	Initial surface area; initial cross-section area; face surfaces of the undeformed specimen (mm^2)
A_0/A_1	Degree of stretch
A_1	Final cross-section (mm^2)
A_{10}	Failure strain $l_0/d_0 = 10$ (%)
A_5	Failure strain $l_0/d_0 = 5$ (%)
A_g	Uniform elongation (%)
A_{max}	Face surfaces, deformed specimen (mm^2)
A_{min}	Cross-sectional area of the specimen, smallest (mm^2)
A_N	Surface area, loaded by the blank holder (mm^2)
A_q	Surface area cutting proportion (mm^2)
A_S	Cutting area (mm^2)
A_v	Impact energy
A_z	Surface area finished part (mm^2)
B	Back gauge width (mm)
C	Size, material specific
D	Diameter (mm)
D_{krit}	Damage value, critical
D_{makro}	Failure criterion, macro-mechanical
D_{mikro}	Failure criterion, micro-mechanical
E	Young's modulus (MPa)
E	Crack within the reference standard; entry point; load relieving zone
E_1	Heat-affected zone
F	Neutral surface
F	Force (N)
$F_1; F_b$	Punch force, lateral (N)
F_a	Axial force (N)
F_G	Counteracting force (N)

F_{Gf}	Counteracting force, fixed roll (N)
F_{GH}	Counterholding force (N)
F_{Gl}	Counteracting force, loose roll (N)
F_i	Surface force (N)
F_N	Normal force; blank holder force (N)
F_q	Shear force (N)
F_r	Radial force (N)
F_R	Friction force (N)
F_S	Cutting force (N)
F'_S	Reaction force (N)
F_{SB}	Strip bending force (N)
F_{SG}	Strip counteracting force (N)
F_{SP}	Clamping force (N)
F_{SR}	Strip friction force (N)
F_{St}	Punch force (N)
F_t	Tangential force (N)
F_U	Forming force (N)
F_Z	Drawing force (N)
F_{Zf}	Strip drawing force (N)
$F_{Z,id}$	Drawing force, ideal (N)
$F_{Z,max}$	Drawing force, maximal (N)
G	Shear modulus (MPa)
K	Penalty constant
L	Wavelength; rolling width (mm)
L	Grain size (μm)
L_c	Load, critical (N)
M	Momentum (Nm)
N	Load cycle
N_b	Bending cycle
P_i	Internal pressure (MPa)
P_N	Blank holder pressure (MPa)
P_Z	Drawing force (N)
Ra	Surface roughness/mean roughness index (μm)
R_m	Tensile strength (MPa)
Rp	Grading depth (μm)
R_p	Yield point (MPa)
$R_\mathrm{p}/R_\mathrm{m}$	Yield ratio
$R_{p0,2}$	Yield point at 0.2 % plastic strain (MPa)
Rt	Surface roughness (μm)
$R(T0)$	Preparation surface roughness (μm)
Rz	Surface roughness, averaged (μm)
S	Fineness
S_F	Surface (mm^2)
T	Time, duration (s)
T	Temperature (°C)

T_F	Melting point, pure metal (°C)
T_G	Die temperature (°C)
T_L	Liquidus temperature (°C)
T_S	Solidus temperature (°C)
T_U	Ambient temperature (°C)
T_W	Workpiece temperature (°C)
U	Deformed zone
U	Flange circumference (mm)
V	Geometric volume; material volume (mm^3)
$V(x, y, z)$	Velocity field
V_s	Wear coefficient, volumetric (m^3/Nm)
W_B	Bending energy (J)
W_{eff}	Deformation energy, effective (J)
W_{id}	Deformation energy, ideal (J)
W_S	Cutting energy (J)
W_{Sch}	Displacement work (J)
W_{ST}	Deformation force, stationary process (N)
Z	Reduction in area (%)

Lower Case

a	Minimal distance (mm)
a	Material constant
a	Ironing angle (°)
a_z	Distance ironing rings (mm)
b	Drawing ratio; part
b	Center hole distance; width; width of gearing (mm)
b	helix angle (°)
b_0	Initial width (mm)
b_1	Width, after deformation (mm)
b_E	Roll-over width (mm)
b_G	Burr width (mm)
c	Minimal curve factor; correction factor
c_1	Shear strength factor
d	Grain diameter (μm)
d	Reference diameter (mm)
d_0	Initial diameter (mm)
$d_{0,max}$	Initial diameter, maximal (mm)
d_1	Action circle diameter (mm)
d_a	Tip diameter (mm)
d_b	Base diameter (mm)
d_f	Root diameter (mm)
d_f	Void increase
$d_{f,Neubildung}$	Void increase due to regeneration of voids
$d_{f,Wachstum}$	Void increase due to void growth

d_i	Drilling diameter (mm)
d_M	Inner cup diameter (mm)
d_m	Die diameter (mm)
d_{St}	Wall diameter, mean (mm)
d_W	Punch diameter (mm)
f	Spinning roll diameter (mm)
f	Deflection
f_a	Void volume; friction factor
f_l	Feed, axial
Δh	Liquid phase proportion (mm)
h	Height variation (mm)
h_0	Height, punch stroke (mm)
h_1	Initial height (mm)
h_E	Roll-over depth (mm)
h_g	Burr height (mm)
h_R	Total height knife-edged ring; fracture depth (mm)
h_S	Sheared edge (mm)
i	Number of cuts
k	Shear yield stress (MPa)
k_f	Yield stress (MPa)
k_{f0}	Initial yield stress (MPa)
k_{fm}	Yield stress, mean (MPa)
k_S	Shear resistance
l	Length (mm)
l_0	Gearing length; initial length (mm)
l_1	Length after deformation (mm)
l_G	Cutting lengths, sum
l_R	Total length of knife-edged ring (mm)
l_S	Length of cutting line (mm)
m	Velocity exponent; module; friction factor
m	Length after deformation (mm)
m_h	Mass of the enveloping body (kg)
m_s	Mass of the die forging (kg)
n	Strain hardening coefficient
n_R	Rolling head drive (min^{-1})
p	Pressure (MPa)
p_i	Inner pressure (MPa)
p_m	Pressure, hydrostatic (MPa)
p_{max}	Surface pressure, maximal (MPa)
$\bar{p}_{St}$	Punch load, specific (MPa)
q_g	Counteracting force, specific (N)
Δr	Anisotropy, plane
r	Anisotropy value
r	Radius, limiting radius (mm)
$\bar{r}$	Anisotropy, mean

$r_{0°}$	Anisotropy, 0° to the direction of rolling
$r_{45°}$	Anisotropy, 45° to the direction of rolling
$r_{90°}$	Anisotropy, 90° to the direction of rolling
r_A	Radius resurgence (mm)
r_E	Radius entry point (mm)
$r_F; r_s$	Radius neutral surface (mm)
r_i	Inner radius (mm)
$r_{i,min}$	Bending radius, minimal (mm)
r_k	Radius, formable (mm)
r_{max}	Radius of the largest cross-section after upsetting (mm)
r_R	Drawing die radius; rounding radius (mm)
r_{St}	Punch rounding (mm)
Δs	Pressure touch time (s)
s	Burr height; distance (mm)
s	Aperture angle (°)
s_0	Axial feed (mm/s)
s_1	Sheet thickness; wall thickness after forming (mm)
s_2	Thickness after deformation (mm)
s_{ax}	Feed rate (mm/s)
s_B	Test distance (mm)
s_k	Penetration depth (mm)
s_v	Punch stroke (mm)
s_w	Length, metal spinned (mm)
Δt	Time difference (s)
t	Time (s)
t_R	Fracture depth (mm)
ü	Number of re-rolls
u_i	Surface velocity field
u_s	Clearance (mm)
u_z	Punch offset; drawing clearance (mm)
v	Velocity; sliding speed (mm/s)
v_0	Velocity of the forming tool (mm/s)
v_R	Relative velocity (mm/s)
v_{rel}	Relative velocity (mm/s)
v_{wz}	Material velocity in the undeformed shank of the workpiece (mm/s)
v_x, v_y, v_z	Components of the velocity field; surface velocity field
w	Angular deviation (°)
w_{id}	Deformation energy, volume-specific ideal (J/mm^3)
w_m	Deformation energy, volume-varying specific (J/mm^3)
w_{pl}	Deformation energy, plastic volume-specific (J/mm^3)
x	Cutting distance (mm)
x_g	Total cutting distance (mm)
x, y, z	Coordinates of the Cartesian coordinate system
z	Number of teeth

Greek Letters

α	Angle of inclination; angle of taper; Drawing clearance aperture angle (°)
α	Ratio between true and apparent contact area; viscosity factor
α_K	Impact value; stress concentration factor
α_s	Pivoting angle (°)
α_{Walz}	Angle of elevation tool (°)
α_{Wst}	Angle of elevation workpiece (°)
β	Draw ratio; spinning ratio
β	Fracture angle; shaft angle (°)
β_{100}	Sheet thickness ratio for $d_0/s_0 = 100$
β_{max}	Maximum drawing ratio
γ	Shearing angle (°)
$\dot{\gamma}$	Shear rate (s^{-1})
δ	Elongation at fracture
ε	Specific elongation
$\varepsilon_1, \varepsilon_2, \varepsilon_3$	Principal elongations
$\dot{\varepsilon}_1, \dot{\varepsilon}_2, \dot{\varepsilon}_3$	Principal elongation rates (s^{-1})
ε_A	Change in section, specific
ε_{aB}	Maximum allowable elongation in the outer fibre
ε_h	Height decrease; distortion; upsetting, specific
$\varepsilon_{h\ddot{o}}$	Distortion, local
$\dot{\varepsilon}_{ii}$	Distortion, volumetric (s^{-1})
ε_{pl}	Elongation, plastic
ε_s	Specific thickness change
$\dot{\varepsilon}_v$	Strain rate field (s^{-1})
η	Dynamic viscosity (Pa s)
η_F	Deformation efficiency
η_{Sch}	Apparent viscosity (Pa s)
η_∞	Equilibrium viscosity (Pa s)
λ	Relaxation time (s)
$\dot{\lambda}$	Proportionality factor
λ_R	Degree of stretch
$\lambda_{R,ges}$	Degree of stretch, total
μ	Friction coefficient, friction factor
μ_{Grenz}	Limiting frictional coefficient
μ_{SZ}	Strip friction value
ν	Kinematic viscosity (mm^2/s)
$\delta\pi$	Power variation with velocity field variation (W)
π	Deformation and friction power (W)
π_f	Deformation efficiency
ρ	Density (g/cm^3)

ρ	Curvature radius of the necking zone (mm)
ρ	Adhesion factor
ρ_a	Curvature radius of the bulged specimen (mm)
ρ_w	Curvature radius of the spinning roll (mm)
ρ_{wf}	Rolling force, areic (N/mm^2)
σ	Normal stress (MPa)
$\sigma_1, \sigma_2, \sigma_3$	Principal stress (MPa)
$\sigma'_1, \sigma'_2, \sigma'_3$	Main values of the stress deviators (MPa)
σ_{bw}	Bending fatigue strength (MPa)
σ_E	Limit of elasticity (MPa)
σ_{ES}	Residual stress (MPa)
σ_m	Principal stress, mean (MPa)
σ_{max}	Normal stress, maximal (MPa)
σ_N	Contact normal stress (MPa)
σ_r	Radial stress (MPa)
σ_r	Tangential stress (MPa)
σ_v	Effective stress field(MPa)
$\sigma_x, \sigma_y, \sigma_z$	Normal stresses (MPa)
σ_z	Axial stress (MPa)
τ	Shear stress (MPa)
τ	Partition
τ_B	Shear strength (MPa)
τ_{max}	Shear stress, maximal (MPa)
τ_R	Friction shear stress (MPa)
$\tau_{R,max}$	Friction shear stress, maximal (MPa)
τ_S	Cutting stress (MPa)
$\tau_{xy}, \tau_{yz}, \tau_{zx}$	Shear stresses (MPa)
φ	True strain
$\dot{\varphi}$	Strain rate (s^{-1})
$\varphi_1, \varphi_2, \varphi_3$	Principal strains
φ_b	True strain in latitudinal direction
φ_{BR}	True strain at fracture
φ_g	True strain of the uniform elongation
φ_{ges}	Total true strain
φ_s	True strain in thickness direction
φ_v	Effective strain
$\dot{\varphi}_v$	Effective strain rate (s^{-1})
φ_{v0}	Effective strain prior to the process
φ_{v1}	Effective strain after the process
φ_{vB}	True strain at fracture
φ_{vG}	Limiting strain
$\varphi_{v,max}$	Limiting effective strain
$\varphi_x, \varphi_y, \varphi_z, \varphi_{xy}, \varphi_{yz}, \varphi_{zx}$	Components of the strain tensor
$\dot{\varphi}_x, \dot{\varphi}_y, \dot{\varphi}_z, \dot{\varphi}_{xy}, \dot{\varphi}_{yz}, \dot{\varphi}_{zx}$	Components of the strain rate tensor (s^{-1})

Abbreviations

AFP	Age hardenable ferritic-pearlitic steel
bcc	Body-centered cubic
BH	Bake hardening steel
cBN	Cubic boron nitride
CP	Complex phase steel
DP	Dual-phase steel
fcc	Face-centered cubic
FEM	Finite element method
GKZ	Heat treated to globular cementite
HB	Brinell hardness
HRC	Rockwell hardness
HV	Vickers hardness
hdp; hex	Hexagonal crystal structure
IF	Interstitial free steel
ODS	Oxide dispersion hardening
TRIP	Transformation induced plasticity steel

Chapter 1
Introduction

It cannot escape the attention of the cost and quality-conscious manufacturing engineer that the number of forming processes in the manufacture of serial parts is increasing. Besides the classic advantages—e.g. the extraordinary properties of forged parts—it is the thinking in manufacturing sequences and substitution possibilities above all that reveals the chances within forming engineering of accelerating or improving the efficiency of the finishing process and of using forming for property improvement.

Forming processes are summarized in DIN 8582 and grouped in accordance with their "strain", i.e. the predominant stresses. Independently of this, the present volume preserves the subdivision customary in practice between massive and sheet forming.

Increasing accuracy of cold massive forming and forging technology enables the production of ready-to-install parts. Such a process substitution has often not only cost advantages, but also leads to product advantages. The favourable structure alignment and resultantly higher fatigue strength of the workpieces permit smaller dimensioning without reducing the load capacity. In automotive engineering, this development has found use in the lightweight construction of axes, gear shafts and hubs. Massive forming offers manifold possibilities of component formation for a variety of applications. The processes used in massive forming are presented in this book using several examples.

The rolling of thin iron sheets in the 18th Century formed the basis for a broad application of sheet forming. Hollow parts, which were already being manufactured in the Middle Ages by "thimbles" and "bell makers", were increasingly produced by means of drawing with the help of devices from which the 19th Century drawing presses originated. This created, together with the development of ingot steel, the foundation for the major industrial use of the processes of sheet forming, especially that of deep drawing, which in the 1920s obtained a decisive impulse by the rising demands of the automobile industry.

Intensive work in the area of material engineering and process development have led sheet forming to a level that makes it possible to manufacture sheet metal components that previously could be only made by casting, forging or using a cutting process.

F. Klocke, *Manufacturing Processes 4*, RWTHedition,
DOI: 10.1007/978-3-642-36772-4_1, © Springer-Verlag Berlin Heidelberg 2013

With the further development of tools, materials and machines, it has been possible to raise the flexibility of individual processes to such an extent that even average-sized and small numbers of units can be manufactured economically. Moreover, further areas of applications have become accessible which were previously unattainable for either economical or technical reasons. Sheet forming is thus in a state of constant competition with other technologies and materials, especially with the processes of plastics technology and its products.

The finite element method (FEM) places in the hands of the user a tool for component/process design that can save considerable costs already in the product development phase.

A familiarity with the forming properties and the processed materials is of fundamental importance for the further development of forming processes and the discovery of new areas of application. Besides the known material parameters, testing methods and characteristic values have been compiled in practice which, along with the common foundations of sheet and massive forming, comprise the starting point of this book.

Chapter 2
Basic Principles

2.1 Introduction

In this chapter the process group of forming will be described in detail. First, a series of basic problems in forming engineering will be discussed in order to understand, classify and evaluate the relevant technological idiosyncrasies involved. Thereby, the material to be formed along with its plastic behaviour under mechanical stress and under the effects of temperature will be in focus. This chapter serves to help understanding the material properties under various stresses which arise within the sphere of forming engineering. Thereby, the basic insights of metallurgy and plasticity theory will be explicated as well as the tribological relations between the tool and the workpiece. Furthermore, different ways to determine the material data of the workpiece materials will be described and various computational solution possibilities for problems in theory of plasticity will be shown.

2.2 Metallurgical Foundations for Determining the Condition of the Material

2.2.1 Crystal Structure

Metals make up the largest group among the workpiece materials. They consist of atoms that are metallically bonded. The common property of all ferrous and non-ferrous metals is their crystalline structure, i.e. their regular, definite arrangement of atoms. Metal physics has developed models of crystal structure as shown in Fig. 2.1 in atomic and macroscopic views using the unit cell of α-iron as an example.

Most metals have either a cubic or hexagonal crystal system. In the case of cubic crystal systems, we distinguish between a body-centred and a face-centred lattice structure.

F. Klocke, *Manufacturing Processes 4*, RWTHedition,
DOI: 10.1007/978-3-642-36772-4_2, © Springer-Verlag Berlin Heidelberg 2013

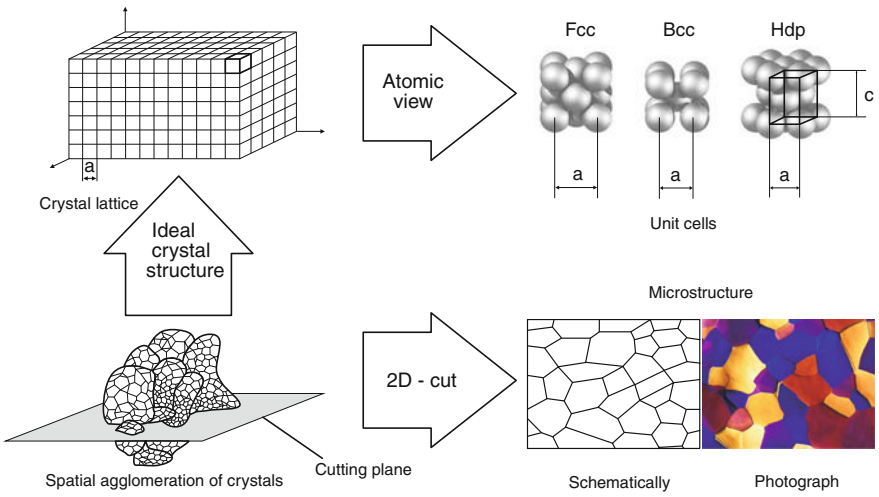


Fig. 2.1 Atomic and macroscopic views of metal structure; *bottom right*: grain structure, schematic and real

Examples for body-centred cubic (bcc) lattices are ferritic steel, chrome (Cr), tungsten (W), molybdenum (Mo), vanadium (V), niobium (Nb) and tantalum (Ta). Austenitic steel, aluminium (Al), copper (Cu), nickel (Ni), silver (Ag), platinum (Pt), gold (Au) and lead (Pb) are examples of face-centred cubic (fcc) crystal structures. Magnesium (Mg), zinc (Zn) and beryllium (Be) are hexagonally (hdP) structured. Many metals can exhibit different lattice structures. For example, titanium (Ti) is hexagonally oriented below 1,155 K, while above this temperature it transforms into a body-centred cubic structure. Iron (Fe) has a similar behaviour. At room temperature, iron has a bcc lattice structure, and at 1,184 K (911 °C) it changes to a fcc lattice structure. Iron reverts back to a body-centred cubic crystal structure above 1,665 K (1,392 °C).

The unit cell is the smallest geometrically cohesive unit of a crystal lattice. The lattice constants are in the range of 0.2–0.5 nm for a large number of metals. If theoretically unit cells are put together in all three spatial coordinates, a crystal lattice is formed (see Fig. 2.1, top left). Basically, the unit cell already contains the most important regularities and properties of the entire crystal. By geometrically stringing together unit cells, ideal crystals are created, i.e. faultless crystals which do not occur in practice. The real space lattice of the metals exhibit a variety of deviations (lattice defects). Fundamentally, we distinguish between three types of lattice fault:

- Zero-dimensional lattice faults (point-shaped lattice faults): if the atoms are embedded at interstitial sites, we speak of interstitial atoms. If the atom sites are occupied by foreign atoms, we refer to them as exchange or substitute atoms. If foreign atoms are located at interstitial sites, they are called interstitial impurity atoms. Sites, that are not occupied by atoms are called vacancies. Lattice

vacancies, or vacancy density, are especially important for thermally activated processes such as diffusion.

- One-dimensional lattice faults: one-dimensional lattice faults are linear structural faults (dislocations), see Fig. 2.3. The most important dislocations are edge dislocations and screw dislocations. Figure 2.3 provides a schematic view of an edge dislocation. Dislocations make plastic forming possible and are therefore of especial importance.
- Two-dimensional lattice faults: two-dimensional lattice faults result from surface effects. The most important two-dimensional lattice faults are grain boundaries and phase interfaces. Crystallization from the fluid state generally initiates at many different locations. Proceeding from seeds, the crystals grow towards each other. If a crystal encounters a second crystal during the growth phase (either from the fluid phase or during recrystallization), the lattice planes generally form a larger angle to each other. Large angle grain boundaries are formed, or in general usage: grain boundaries.

Due to lattice faults, real crystals differ from ideal ones considerably. For example, the tensile strength of iron is more than two orders of magnitude below that of the theoretically possible strength of the ideal crystal. An explanation for this phenomenon was only made possible when the effects of lattice defects were fundamentally understood so that corresponding model representations could be made, which will be considered more closely in the following chapter.

In the unit cells, the distances of the atoms to each other varies in different directions (Fig. 2.1 top right). Therefore, the fact can be already derived that certain properties of metals depend on the direction. This direction dependence is called anisotropy. Iron monocrystals have a modulus of elasticity between 130 and 290 GPa depending on the crystal orientation. In multicrystalline materials, the crystallites are frequently distributed in a statistically random fashion. From the outside, the material then generally appears isotropic (quasi-isotropic).

When technical melts solidify, impurities are for the most part pushed in front of the solidification front and collect at the grain boundaries. Figure 2.1 (bottom right) shows schematic representation of a grain structure and a real grain structure as seen in a metallographic specimen through a light microscope. We can recognize the shape, size and arrangement of the crystals, but not their internal structure.

2.2.2 Elastic and Plastic Deformation of Crystals

Deformation of a body occurs due to external forces affecting the body. Such deformation is subdivided in elastic and plastic strain.

If the deformed body returns completely to the initial shape and dimensions after the external strain is removed, it is referred to as an elastic strain. This results from a shifting of the atoms from their stable position of equilibrium where they

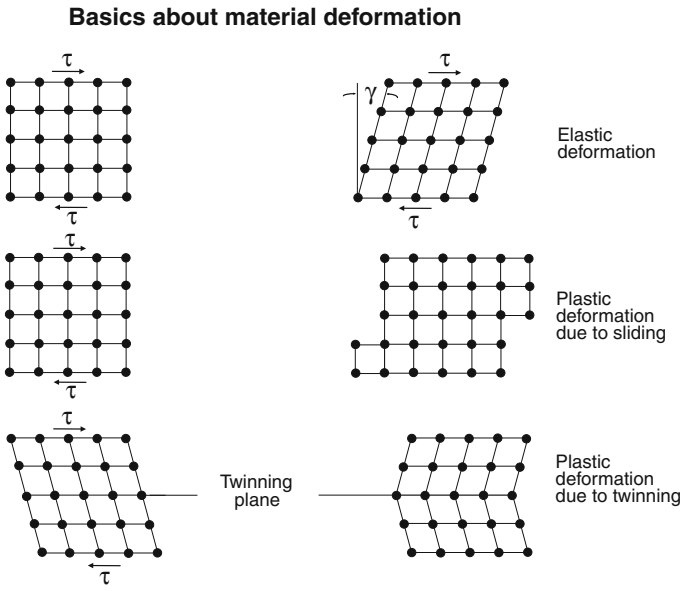


Fig. 2.2 Atomic representation of elastic and plastic deformation of the crystal lattice

exhibit a minimum of potential energy (Fig. 2.2). The respective amount of shifting is smaller than one interatomic distance. From materials mechanics, Hooke's law for tensile and compressive stress is well-known for the functional description of this process.

$$\sigma = E \cdot \varepsilon \tag{2.1}$$

Given a shear stress of τ, the following linear relation results for the resulting displacement γ:

$$\tau = G \cdot \gamma \tag{2.2}$$

In forming technology, elastic deformation is generally very small compared to plastic deformation. For this reason, elastic deformation can often be neglected. One undesirable property of elastic behaviour during forming processes is known as spring-back. This phenomenon occurs especially when deep drawing large-scale components and will be considered in more detail in Sect. 4.1.

In the case of plastic deformation, there is a dislocation of atoms into a new position of stable equilibrium. The amount of dislocation can be much larger than one atomic distance and the deformation remains after the external forces have been removed. Metallurgy recognizes essentially two mechanisms of plastic deformation: sliding (translation) and twinning (Fig. 2.2). In considering these processes, one first proceeds from a monocrystal so that varying orientations and grain boundaries can be neglected. Mechanical twinning involves a shifting of atoms that lie on planes parallel to the twin plane.

The amount of dislocation is proportional to the distance of these planes from the twin plane. The lattice area deformed by twinning appears as a reflection of the non-deformed area on the twin plane. In comparison to sliding, it requires relatively large external stresses to trigger the twinning process. It is therefore more rarely seen. Hexagonal and body-centred cubic metals and metals under abrupt stress are exceptions in this regard.

On the other hand, the mechanism of sliding is of higher importance in forming engineering. According to the atomic interpretation of this process, entire lattice areas are shifted relative to one another along a sliding plane. The amount of dislocation can be much larger than the atomic distance, sometimes by a large whole number multiple. To this end, a shear stress must be applied that is sufficient to overcome the elastic reset forces.

Interatomic bonding forces are lowest in the lattice areas that are the most densely occupied. Given an external force, sliding will therefore begin first where the resulting shear stress is largest (e.g. in the uniaxial tensile test below 45° to the direction of tension) while at the same time there are favourably oriented, densely occupied slide planes. The number and orientation of the potential slide planes vary in different crystal systems. For example, a hexagonal lattice has only one slide plane, a face-centred cubic lattice structure has four non-parallel slide planes. Slide planes and sliding directions together comprise the slide system (fcc: 12; bcc: 12; hcp: 3). This can explain, for example, how iron, copper and aluminium (i.e. metals with a cubic crystal structure) are more easily deformable than zinc and magnesium, which have hexagonal lattice structures.

Dislocation migration is assumed to be a basic mechanism of sliding in metal physics. Figure 2.3 left provides as an example a cross-section of an edge dislocation, which is characterized by the fact that atom row "2" is additionally inserted into the otherwise regular cubic lattice structure. Now already a small shear stress is sufficient to dislocate atom "A" with the underlying atoms into row "2". The discontinuity is thus pushed to the left. This process repeats itself several times until the discontinuity has left the lattice area under consideration and all atoms of the slide plane have shifted places.

Since in this case all individual atomic rows and not an entire plane migrates, the critical shear stress required to initiate sliding is small, the theoretically calculated value of which agrees well with experimental results.

For the purposes of forming engineering, a clearer conception is often useful, in which the material volume is understood as a card deck made of lattice layers and inter-adjacent slide planes. Figure 2.4 shows material behaviour under tension, pressure and shear strain for this model conception.

In the process of cold forming, metals have been observed to undergo a change in their strength values (Fig. 2.5). Tensile strength (R_m), elastic limit (R_p) and hardness (HB) are increased, while reduction in area (Z) and uniform elongation (A_{10}) are reduced.

This behaviour is called strain hardening. The dislocations migrating through the lattice mutually impede each other or accumulate at the grain boundaries and

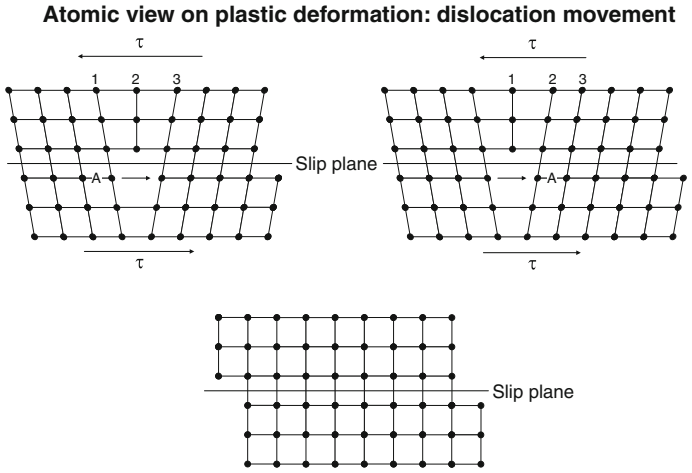


Fig. 2.3 Atomic representation of plastic deformation as dislocation migration

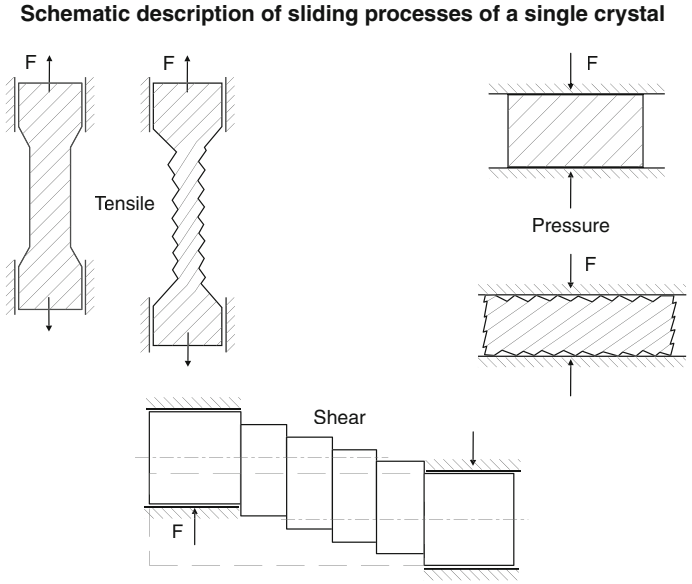


Fig. 2.4 Simplified representation of sliding processes in the monocrystal

phase interfaces. Moreover, the dislocation density is increased with progressive forming. In order to maintain plastic flow nonetheless, less favourable slide systems must also be activated. The force requirement is increased and the slide possibilities (ductility) are reduced. When the failure limit of the workpiece material is reached, cracks appear or fracture occurs. The metal is embrittled. The dependence of the stress required for flow k_f on the true strain described by the

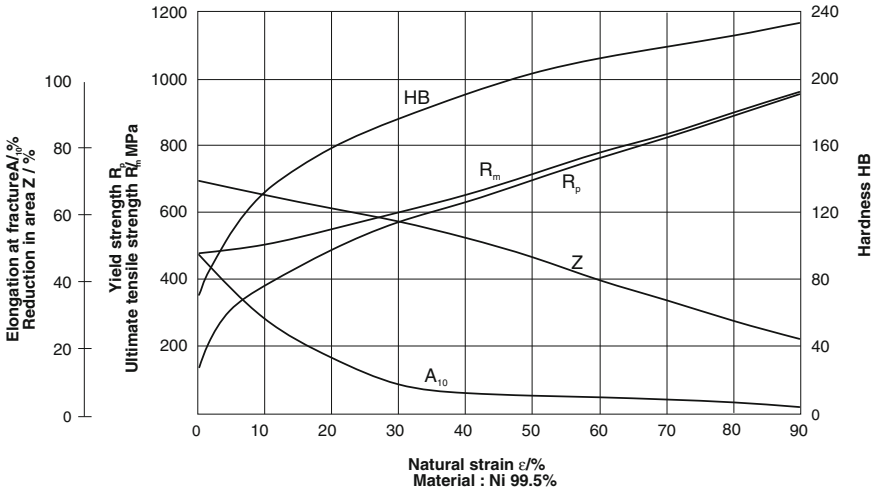


Fig. 2.5 Effect of true strain on strength and deformation parameters

flow curve. The flow stress is the stress that has to be applied for initiating plastic flow and for overcoming hardening (Fig. 2.6). Besides true strain the flow stress also depends on the crystal lattice type and orientation (Fig. 2.7) as well as on the strain rate and the forming temperature. The dependence on strain rate and forming temperature will be described in detail in later chapters. The gradient of the flow curve is a measure for hardening. It depends on the lattice type and is considerably affected by the alloying elements. In the case of certain materials, change in the crystal lattice can also be initiated by the forming process, changes which intensify strain hardening. This occurs for example when forming martensite is created by the occurring sliding processes.

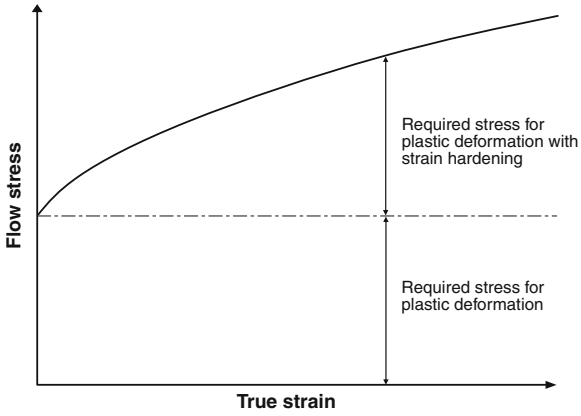


Fig. 2.6 Schematic sequence of the flow curve of a monocrystal

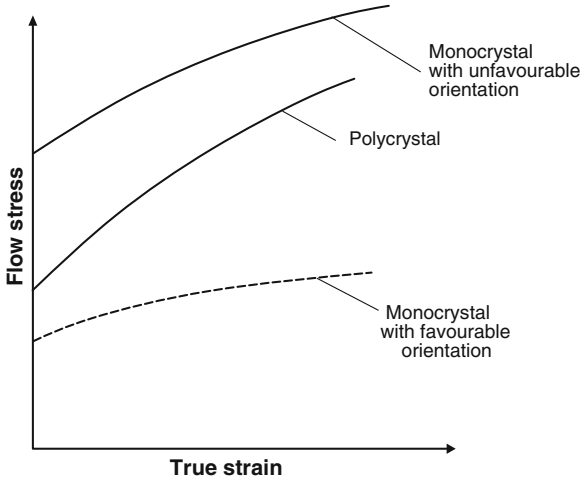


Fig. 2.7 Influence of the type and orientation of the crystals on flow behaviour

2.2.3 Recrystallization

From the technical point of view, a forming process is described by the flow capability, the deformability of the material and the therefor required energy. For a correct evaluation of the technological parameters involved in forming, the most important material processes on the atomic level must be also understood. An especially important role play thermally activated processes and changes in the metal lattice at high temperatures. A material system no longer changes in equilibrium. Plastic forming raises the energy content of the material considerably. Elastic distortions of the lattice are primarily brought about by dislocations. With progressive forming, i.e. as the dislocation density is increased, an increasing state of disequilibrium is produced. When heated up, the atoms strive again towards the state of equilibrium—the higher the temperature, the more quickly this process takes place. Fundamentally, two processes should be distinguished: crystal regeneration and recrystallization (Fig. 2.8). Both processes involve a thermally activated change of location in the lattice. In order to initiate these processes, a certain energy threshold must be exceeded, which is called activation energy.

The energy applied in plastic forming is converted for the most part into heat. The rest remains stored in the lattice as internal energy, as potential energy of elastic deformation. Of interest for forming are twins and dislocations as well as lattice vacancies and interstitial atoms. The largest amount of elastic deformation energy can be attributed to dislocations, the number of which is significantly increased in the case of cold forming. When the activation energy is exceeded, the lattice defects are recovered and rearranged.

Lattice defects also react with each other, for example opposing dislocations in one slide plane cancel each other. Aligned dislocations migrate into lower-energy

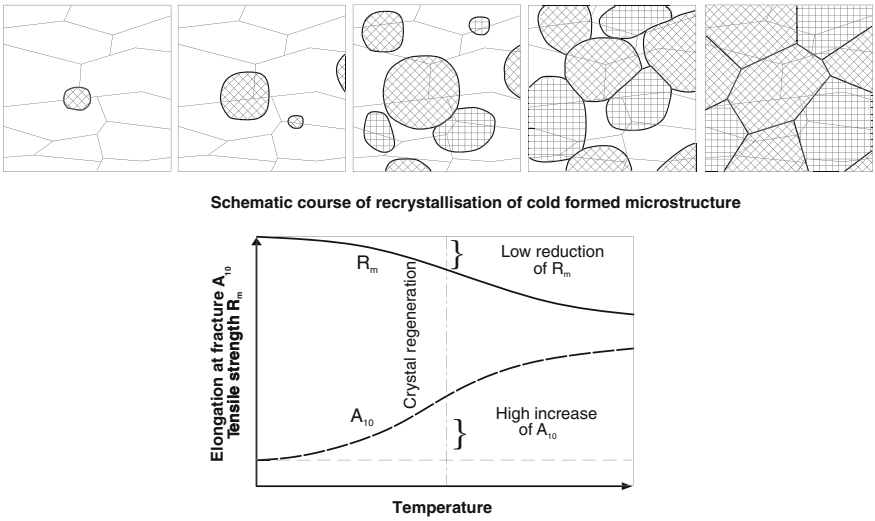


Fig. 2.8 Effect of crystal regeneration and recrystallization on tensile strength and strain of a cold-formed material

positions and form sub-grain boundaries. The randomly distributed dislocations become ordered in rows, and in this way small-angle grain boundaries are created within the grains. This process is also known as polygonization. Important for technical applications is the fact that while these processes take place on the atomic level, they nonetheless already cause changes in important macroscopic properties of the material (Fig. 2.8). Internal stresses are reduced and the elongation at fracture and tensile strength are slightly reduced. However, the deformation structure basically remains the same during crystal regeneration. The characteristics of crystal regeneration is essentially determined by the existence of impurity atoms, true strain, dislocation density (strain hardening) and temperature. When the temperature is increased, the regeneration processes proceed further because dislocations now become capable of climbing due to the onset of diffusion. While mechanical properties are only relatively slightly changed during crystal regeneration, other material properties such as electric conductivity and resistance practically reach their initial values already in the regeneration phase. Moreover, residual stresses are significantly reduced by crystal regeneration.

If temperature is further increased, these areas serve as the seeds of a complete reorganization of the microstructure. Now, new grain areas become visible, the old grains and the forming structure are completely consumed (Fig. 2.8). A completely new, unstressed and undeformed initial structure is formed. The crystallization fronts growing towards each other from different locations form new grain boundaries, grain sizes and grain forms. The most important process in this respect is the movement of the grain boundaries. The grain size is a function of true strain and the recrystallization temperature (Fig. 2.9). From this diagram we can derive the following basic facts regarding forming and recrystallization:

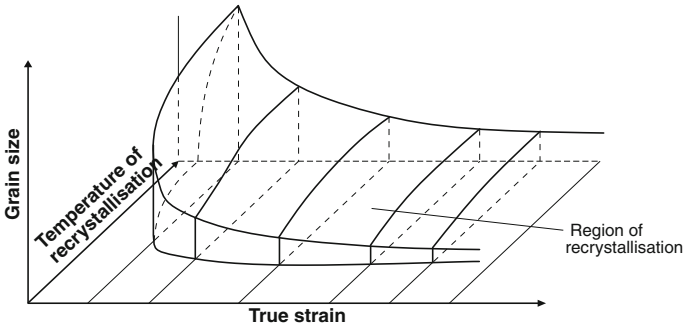


Fig. 2.9 The effect of the deformation level and temperature on the grain size during recrystallization [EISE66]

- The deformation level must exceed a certain minimum.
- Under otherwise identical conditions, low deformation levels lead to coarser grain sizes; high deformation levels lead to fine-grained structures.
- The temperature of recrystallization must exceed a certain minimum.
- In the case of higher deformation levels, recrystallization takes place at lower temperatures.

This summary makes it clear that the recrystallization temperature T_R is not a fixed characteristic value of the material. Nevertheless, we can proceed from the following relation as a reference value [GOTT98]:

$$T_R \approx 0.4 \cdot T_S, \tag{2.3}$$

into which the melting point T_s of the metal is to be inserted in Kelvin.

Often, previous deformation textures are dismantled after recrystallization. Under certain conditions of deformation and with certain materials however, it is also possible that the deformation texture remains intact even after recrystallization. These are called recrystallization textures. In general, textures are undesirable because they result in anisotropic properties. However, they are of great importance in a practical application from engine technology. In FeSi magnetic sheets, textures are created by annealing which later result in lower re-magnetization losses.

In forming technology, recrystallization is of central importance. In many cases, forming cannot advance up to the level predetermined by the manufacturing task because either the pressing force available is insufficient for sustaining plastic flow in the case of progressing strain hardening or because the forming capacity of the material is depleted and the first cracks appear.

It is then possible to recreate the original undeformed structure via recrystallization and to continue the forming process on the ductile material with low pressing force in a second stage. For the flow curve, this entails a shift on the abscissa (Fig. 2.10). In principle, alternation between strain hardening and recrystallization can be repeated to an arbitrary extent.

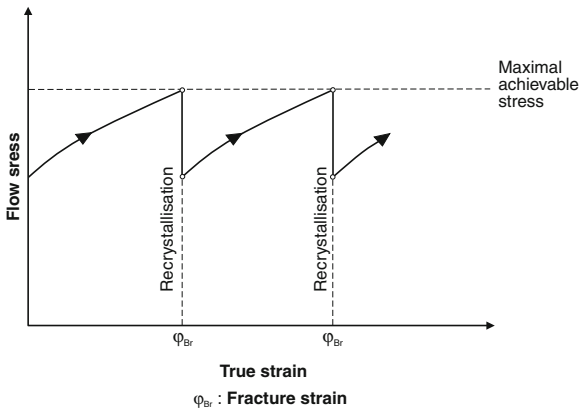


Fig. 2.10 Stress requirement in strain hardening with intermediary recrystallization annealing

Important in the heat treatment process however is precise control of the conditions. As one can see in the schematic representation in Fig. 2.9, the recrystallized microstructure is very coarse-grained in the case of "critical" combinations of temperature and deformation level, which has a negative effect on later component properties. The tendency to form coarse grains is also influenced by the carbon content and other alloying elements. With increasing amounts of C, the maximum grain size flattens quickly however, so that extreme coarse grain is no longer formed above a C-content of 0.3 % [EISE66].

2.2.4 Difference Between Cold and Hot Forming

One definition of cold and hot forming that is often used in practice is as follows:

In hot forming, the forming temperature is above the recrystallization temperature; in cold forming the forming temperature is lower than the recrystallization temperature. Since metals have very different recrystallization temperatures, this definition frequently leads to misunderstandings. For pure iron for example, Eq. 2.3 results in a recrystallization temperature of ca. 450 °C ($T_R \approx (1,536\ \text{K} + 273\ \text{K}) \cdot 0.4 = 723\ \text{K}$). Lead has a melting point of $T_S = 327\ ^\circ\text{C}$, so the recrystallization temperature of lead is about 3 °C. That means that forming lead at room temperature is already hot forming.

A more exact definition of hot forming takes the recrystallization rate and the forming rate into consideration. It states that in the case of hot forming the recrystallization rate is higher than the forming rate. Hereby, the structure is constantly reformed and no strain hardening occurs. In the case of low forming rates, the yield stress would then be independent of the true strain (Fig. 2.11 bottom). However, when very high forming rates above the recrystallization temperature occur, the time required for recrystallization can sometimes be

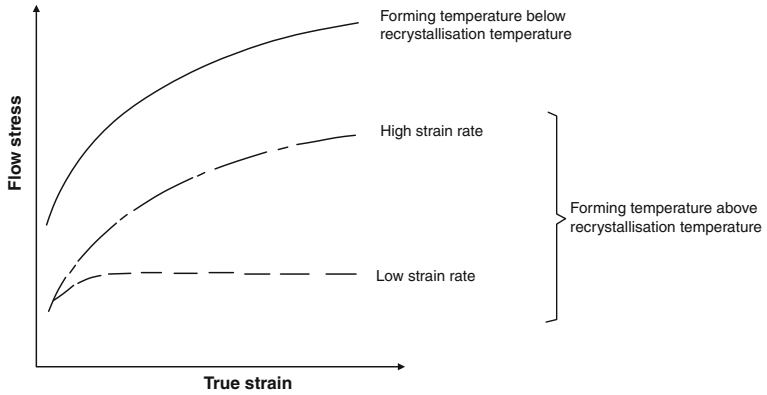


Fig. 2.11 The influence of forming temperature and rate on the flow curve

insufficient to reverse the strain hardening processes caused by forming. In this case, the yield stress exceeds the true strain, although forming takes place above T_R (Fig. 2.11 centre). This behaviour can become important if the working temperature is near T_R at high forming rates (accelerations) which can occur in certain forging processes in warm forming (also see Sect. 3.2).

Another important material property which can be exploited technically is when forming above the recrystallization temperature but with a very low forming rate. Due to the high thermal mobility, not only the atoms inside the crystal participate in restructuring processes, but the much weaker bonded atoms on the grain boundaries also participate in the reduction of lattice distortions. Grain boundary sliding can arise, which in the case of many metallic materials leads to a very high level of formability. This behaviour is called superplasticity. The prerequisites for this are a fine-grained microstructure, suitable temperature control and low forming rates (also see Sects. 3.4.3 and 4.6.2).

In the case of superplastic materials, true strain can be several times higher at low formation rates. One essential prerequisite is that the initial grain size of the material can be very small and also does not become coarse during forming. For this reason, a second phase must be present in the material in order to maintain superplasticity. Eutectic or eutectoid alloys are favourable in this context.

In practice, cold forming is preferred over hot forming in many cases. Advantages include:

- no energy cost for heating,
- low tool material costs,
- little influence on forming speed,
- no material losses and finishing treatment due to scale formation,
- no dimensional faults due to shrinkage,
- superior surface quality and
- increased component strength.

The disadvantages, such as the

- higher force and work requirement and
- limited formability

make clear, why usually hot forming is only applied when excessive forces in cold forming threaten tool fracture or machine overload, or when the strength of the material does not permit the required deformation. In this context, it has to be also examined, whether a gradual cold forming with respective recrystallization annealing is more economical.

2.3 Plastomechanical Foundations

2.3.1 Comparison of Crystal Physics and Continuum Mechanics

Large forces or pressures are usually required for the plastic forming of metallic workpiece materials. For this reason, it should be always proved by means of suitable calculation methods whether the target process is realisable with the given machines and tools and whether the workpiece material permits the planned deformation. Moreover, it has to be known in many cases how the mechanical properties of the material are altered by the forming process. One possibility would be to model the physical crystal processes on the atomic level to make them the basis of calculation models. This is the approach of molecular dynamic calculation approaches [RAPA04]. While the latter are not sufficiently developed for engineering practice in manufacturing, they are used in research. For practical application, the workpiece material is assumed to be a homogeneous continuum such that the physical values are described by space and time coordinates and their functions are constant and differentiable. The errors arising from these marginal conditions are by and large tolerable. Without going more deeply into the mathematical minutiae of plastomechanical solution methods, in the following we will show the physical relations that are required to understand forming engineering processes.

2.3.2 State of Stress

The force exerted by the forming tool on the workpiece creates a state of stress in the interior of the workpiece. As opposed to the vectorial force (first-order tensor), this is a two-directional quantity, i.e. a second-order tensor. For a general description of the stress tensor, six of its component must be known, the normal stresses

$$\sigma_x,\ \sigma_y,\ \sigma_z$$

and the shear stresses

$$\tau_{xy} = \tau_{yx},\ \tau_{xz} = \tau_{zx},\ \tau_{yz} = \tau_{zy}$$

While the components of the stress tensor change when the coordinate system is rotated, the sum of the normal stresses remains constant:

$$\sigma_x + \sigma_y + \sigma_z = \text{const.} \tag{2.4}$$

The sum of the normal stresses is an invariant and corresponds to three times the average principal normal stress σ_m, resulting in:

$$3\sigma_m = \sigma_x + \sigma_y + \sigma_z. \tag{2.5}$$

Often, σ_m is also described by the hydrostatic pressure p_m

$$\sigma_m = -p_m \tag{2.6}$$

Therefore, considering Eq. 2.5, the hydrostatic pressure is also invariant if the coordinate system is rotated. It exerts an equal stress in all directions of the continuum.

In every body subjected to external forces, three perpendicular planes resting upon each other can be defined, in which the shear stress components of the stress tensor become zero and in which only the normal stresses σ_1, σ_2, and σ_3 have an effect. These stresses are called principal normal stresses, while the planes are called principal stress planes. According to this definition, the principal normal stresses are described as follows:

$$\sigma_1 \geq \sigma_2 \geq \sigma_3.$$

In many cases, the position of the principal stress planes can be estimated from the type of external stress on the body.

In the top of Fig. 2.12, we can assume for the sake of simplification in the absence of friction that, in all planes of the square bar that lie parallel to the pressure pads, the principal stress σ_3 caused by force F_3 is in effect. The stress state is uniaxial. If the square bar is also stressed laterally by a second punch pair with pressure F_2, the state of stress is biaxial, for besides σ_3 there is now a second principal normal stress σ_2 being exerted in all planes lying perpendicular to F_2. Finally, a triaxial state of stress is created if a third punch pair exerts a force F_1 on the still free sides of the square bar, and principal normal stress σ_1 is generated. The planes in which σ_1 exerts an effect, stand both perpendicularly on the active planes of $\sigma_2\psi$ as well as on those of σ_3.

The right side of Fig. 2.12 contains the Mohr's circle belonging to the states of stress. With them, the components of the stress tensor can be determined for any arbitrary Cartesian coordinate system.

The hydrostatic state of stress is a special case of the general state of stress. In this case, the three principal normal stresses are equally large so that the Mohr's circles overlap at one point.

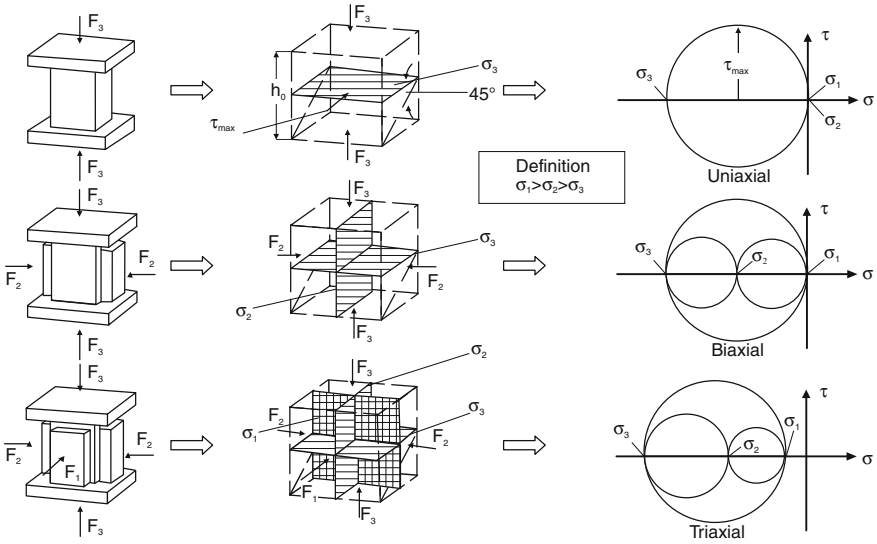


Fig. 2.12 States of stress with respective Mohr's stress circles

Every state of stress can be broken down into a deviatoric and a hydrostatic portion.

	Deviatoric portion		Hydrostatic portion
$\sigma_1 =$	σ_1	+	σ_m
$\sigma_2 =$	σ_2	+	σ_m
$\sigma_3 =$	σ_3	+	σ_m

The deviatoric part is relevant for forming. The maximum shear stresses and the position of the shear stresses can be derived directly from the Mohr's stress circles. The hydrostatic part determines the position of the Mohr's circles on the normal stress axis. In the case of the conditions selected in Fig. 2.12, only the states of pressure stress are taken into consideration. If there are tensile stresses, the circles are shifted to the right.

2.3.3 Yield Criterion

The yield criterion answers the question of how a state of stress must be constituted such that plastic flow occurs. The yield criterion establishes a functional relation between the yield stress k_f and the state of stress. In the following, an idealized thought experiment will be carried out on this subject.

Figure 2.13 again shows a square bar, which can be pressure-loaded on all sides by three punch pairs. The principal stresses inside the test bar should build up

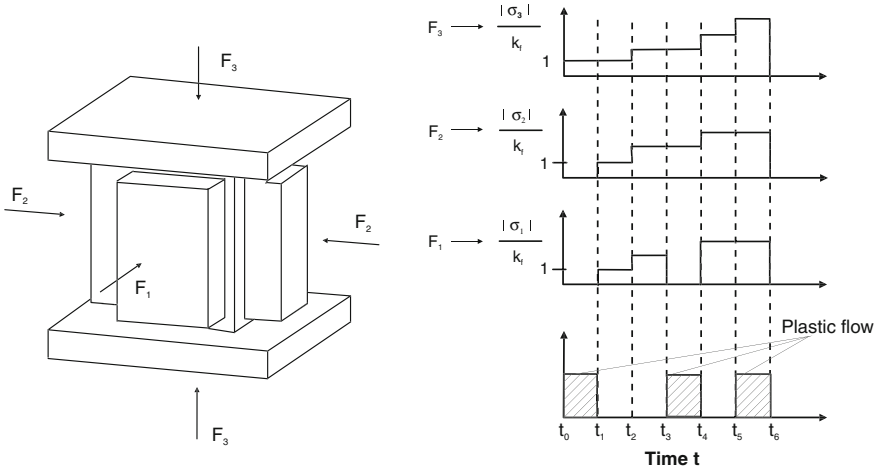


Fig. 2.13 Start of flow

independently of each other, so that F_3 produces σ_3, F_2 σ_2 and F_1 σ_1. The start of flow is indicated by a lasting deformation of the workpiece.

First, F_3 is applied and increased until plastic flow is initiated $(t_0 \text{ to } t_1)$. The state of stress is uniaxial and the only principal normal stress σ_3 corresponds to the yield stress

$$\sigma_3 = -k_f \tag{2.7}$$

Now, the lateral punch forces F_2 and F_1 produce stresses $\sigma_2 = -k_f$ and $\sigma_1 = -k_f$, and one observes that the flow is interrupted $(t_1 \text{ to } t_2)$. Even if all punch forces are simultaneously doubled during time t_2 to t_3, flow is not reintroduced. On the other hand, if we remove one punch force between t_3 and t_4, say F_2, flow begins again provided the remaining punch forces remain constant between t_3 and t_4. Renewed flow would also not result if all forces were to be simultaneously increased between t_4 and t_5. Only if one of the forces were alone increased between t_5 and t_6 would flow start again. The experiment would proceed quite similarly with respect to the start of flow if the punches were to pull on the sides of the square bar, thus creating tensile stresses. In summary, the experiment described here suggests the following conclusions (Fig. 2.13):

- The start of flow is a function of a principal normal stresses σ_1, σ_2 and σ_3;
- It is *no* function of the average principal normal stress σ_m,

$$\sigma_m = \frac{1}{3}(\sigma_1 + \sigma_2 + \sigma_3)$$

and therefore

- it must be a function of the deviatoric portion of the stress tensor and thus a function of the absolute amounts of the differences of the principal normal stress:

$$g(|\sigma_1 - \sigma_2|, |\sigma_1 - \sigma_3|, |\sigma_2 - \sigma_3|) = 0 \tag{2.8}$$

The formulaic relations for g generally used were provided with a different physical and mathematical background by Tresca (1864) [TRES64] and later by von Mises (1913) [MISE13].

According to the shear stress theory of Tresca, plastic flow is only dependent on the shear stresses and begins when the largest shear stress reaches a value of $\tau_{max} = k$ (Fig. 2.14).

The largest shear stress can be taken from the Mohr's circle. It corresponds to the radius of the largest stress circle or half the largest principal stress difference. One can therefore also formulate Tresca's yield criterion in this way:

$$\max\{|\sigma_i - \sigma_j|\} = k_f = 2k \tag{2.9}$$

(i and j extend from 1 to 3, $i \neq j$)

The following is valid for the case shown in Fig. 2.14:

$$k_f = |\sigma_1 - \sigma_3| = 2\tau_{max}.$$

Von Mises's yield criterion is based on energy. Before plastic flow is initiated in a volume element of the workpiece, mechanical energy w must be applied to it. The energy w is divided into w_m, which only changes the volume, and w_{pl}, which deforms the shape of the body at constant volume. Since metallic materials, barring lattice transformations and precipitations, do not change their volume lastingly, i.e. plastically, w_m can only be elastically stored and cannot contribute to

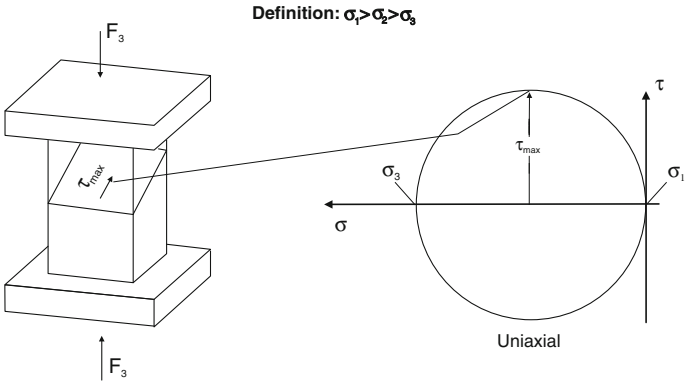


Fig. 2.14 Tresca's yield condition

plastic flow. If we separate w_m from w, only w_{pl} remains, which strives to deform the volume element and to cause plastic flow (Fig. 2.15).

With the help of Hooke's law, we can formulate w_{pl} as a function of the principal stresses σ_1, σ_2 and σ_3 as well as the shear modulus G:

$$w_{pl} = \frac{1}{12G}\left\{(\sigma_1 - \sigma_2)^2 + (\sigma_2 - \sigma_3)^2 + (\sigma_3 - \sigma_1)^2\right\} \tag{2.10}$$

The yield criterion can now be stated in the following way: plastic flow is initiated in one volume element of the workpiece if w_{pl} has reached a critical value. Since this critical value is independent of the type of state of stress, it can, for example, be determined in the tension test ($\sigma_1 = k_f$, $\sigma_2 = \sigma_3 = 0$) or in the compression test ($\sigma_3 = -k_f$, $\sigma_2 = \sigma_1 = 0$).

If we assume

$$(w_{pl})_{tension/compression\,test} = (w_{pl})_{general}$$

then Eq. 2.10 results in

$$\frac{1}{12G} \cdot 2 \cdot k_f^2 = \frac{1}{12G}\left\{(\sigma_1 - \sigma_2)^2 + (\sigma_2 - \sigma_3)^2 + (\sigma_3 - \sigma_1)^2\right\} \tag{2.11}$$

the yield criterion according to von Mises:

$$(\sigma_1 - \sigma_2)^2 + (\sigma_2 - \sigma_3)^2 + (\sigma_3 - \sigma_1)^2 = 2k_f^2 \tag{2.12}$$

or

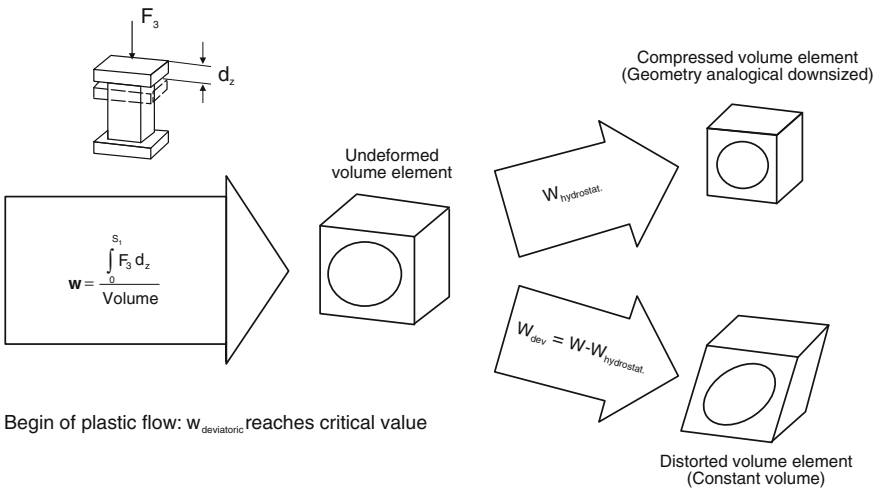


Fig. 2.15 Von Mises's yield criterion

$$(\sigma_1 - \sigma_m)^2 + (\sigma_2 - \sigma_m)^2 + (\sigma_3 - \sigma_m)^2 = \frac{2}{3} k_f^2. \tag{2.13}$$

The yield criteria of Tresca and von Mises only deviate from each other to a small extent depending on the state of stress. In the case of a pure tensile or compressive state of stress, they provide the same results; in the case of pure torsion, the maximum difference is 15 %. Trials have shown that the flow behaviour of technical workpiece materials are better described by the yield criterion of von Mises than that of Tresca [LANG90a].

In the calculations of forming engineering, usually arithmetic reasons decide which yield criterion will be used. For example, Tresca's yield criterion can be advantageous because it contains the principal stresses only as linear terms; however, it must be determined prior to the calculation which principal stress difference is maximal. This disadvantage is not encountered in the case of von Mises's yield criterion—it is a constantly differentiable function of all principal stresses. The quadratic principal stress terms can be detrimental.

2.3.4 Kinematics of the Continuum

If the state of stress fulfils the yield criterion and therefore plastic flow occurs inside the workpiece, the question arises how the geometry of the workpiece is changed during plastic flow. In classic flow curves, in which important strength and ductility characteristic values are recorded in the uniaxial tension test, the elongations and stresses are generally referred to the output variables (see also p. 119). Stress σ is equal to the ratio F/A_0 and elongation ε corresponds to the ratio $\Delta l/l_0$. The reference variables are the cross-sectional area A_0 and the output length l_0. These characteristic values are generally sufficient for strength calculations during design because the components are designed with respect to strength in the elastic range. In this case, both elongation and change in cross-section are minimal. The behaviour of materials above the yield point are interesting in the case insofar as information can be derived from it about whether the material tends to be brittle or ductile outside of the elastic range.

On the other hand, the plasticity of materials is in the foreground in forming technology. For this reason, true stress and true elongation characteristic values are used. In the case of true stress, the forming force is related to the actual (true) surface. The true stress is usually designated as strain strength or yield stress k_f. Elongations are also related to the actual reference value changing with deformation (the true value). In the German literature, true elongation is designated with the letter φ. For the reference elongation, usually the letter ε is used. In the English literature, this distinction is not made. ε designates both the reference elongation (nominal elongation) and for true elongation (true strain). Which variable is meant can often only be determined by context.

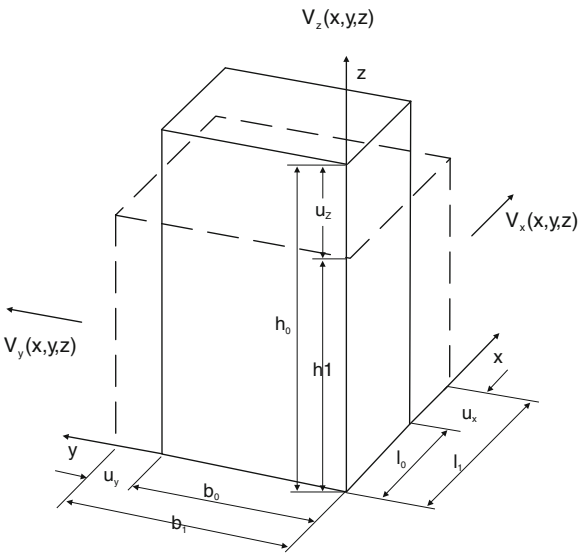


Fig. 2.16 Kinematics of an idealized upsetting process

The following example shows why nominal elongations are not suitable for describing plastic deformations. Let us first assume that the punch displacement u_z in Fig. 2.16 is small compared to the height h_0 of the square bar. Then the following is valid for the principal elongation ε_3:

$$\varepsilon_3 = \frac{h_1 - h_0}{h_0} = -\frac{u_z}{h_0}. \tag{2.14}$$

If a 50 % height reduction was to be achieved by means of upsetting, then

$$\varepsilon_3 = \frac{0.5h_0 - h_0}{h_0} = -0.5.$$

In case of a further 50 % height reduction, the workpiece material is elongated again by $\varepsilon_3 = -0.5$. But if the elongation is calculated with the output height h_0, the result is

$$\varepsilon_3 = \frac{0.25h_0 - 0.5h_0}{h_0} = -0.25.$$

This consideration makes clear that, in the case of large elongations such as are found in forming engineering, a fixed reference variable cannot be used to calculate elongation.

On the other hand, true elongation is a suitable variable, for which the Greek letter φ has been introduced. Its reference variable is the actual geometrical configuration of the continuum. For a small punch displacement du_z in Fig. 2.16, the increase in elongation amounts to

$$d\varphi_3 = \frac{du_z}{h}. \tag{2.15}$$

If the square bar is compressed from height h_0 to height h_1, then:

$$\varphi_3 = \int_{h_0}^{h_1} \frac{du_z}{h} = \int_{h_0}^{h_1} \frac{dh}{h} = \ln \frac{h_1}{h_0}. \tag{2.16}$$

This parameter is called true strain, logarithmic elongation or true elongation. The true strain is positive if a section is elongated and negative if a section is compressed. As in the z direction, two further true strains can be introduced for the x and y directions:

$$\varphi_1 = \int_{l_0}^{l_1} \frac{dl}{l} = \ln \frac{l_1}{l_0}$$

and

$$\varphi_2 = \int_{b_0}^{b_1} \frac{db}{b} = \ln \frac{b_1}{b_0}. \tag{2.17}$$

Referring to the example in Fig. 2.16, the first height reduction from h_0 to h_1 using the true strain to describe the illustrated upsetting process amounts to:

$$\varphi_3 = \ln \frac{h_1}{h_0} = \ln \frac{0.5h_0}{h_0} = \ln 0.5 \approx -0.69.$$

The second height reduction from h_1 to h_2 follows as:

$$\varphi_3 = \ln \frac{h_2}{h_1} = \ln \frac{0.25h_0}{0.5h_0} = \ln 0.5 \approx -0.69.$$

In contrast to the nominal elongations, the true strains are the same for both height reductions.

In many forming problems, the situation is not as simple as in the idealized upsetting process described in Fig. 2.16, in which a homogeneous (i.e. equally distributed in all points of the continuum) forming process is assumed. Depending on the problem, determining the true strain can be very difficult, and it can be advantageous to calculate with forming rates. Forming rates are obtained via differentiation of the velocity field $v_x(x, y, z)$, $v_y(x, y, z)$, $v_z(x, y, z)$:

$$\begin{aligned}\dot{\varphi}_1 &= \frac{\partial v_x}{\partial x},\\ \dot{\varphi}_2 &= \frac{\partial v_y}{\partial y} \text{ and}\\ \dot{\varphi}_3 &= \frac{\partial v_z}{\partial z}.\end{aligned} \tag{2.18}$$

Elongation and elongation rates are 2nd-order tensors. While for the special case in Fig. 2.16 the true strains defined via Eqs. 2.16 and 2.17 correspond to the principal elongations, the forming rates defined in Eq. 2.18 are the principal elongation rates.

In the case of a general position of the coordinate system, the coordinates of the elongation tensor are

$$\begin{gathered}\varphi_x,\ \varphi_y,\ \varphi_z\\ \varphi_{xy} = \varphi_{yx},\ \varphi_{yz} = \varphi_{zy},\ \varphi_{zx} = \varphi_{xz}\end{gathered} \tag{2.19}$$

and those of the tensor of the elongation rates are

$$\begin{aligned}&\dot{\varphi}_1 = \frac{\partial v_x}{\partial x}, \dot{\varphi}_2 = \frac{\partial v_y}{\partial y}, \dot{\varphi}_3 = \frac{\partial v_z}{\partial z},\\ &\dot{\varphi}_{xy} = \dot{\varphi}_{yx} = \frac{1}{2}\left\{\frac{\partial v_x}{\partial y} + \frac{\partial v_y}{\partial x}\right\},\\ &\dot{\varphi}_{yz} = \dot{\varphi}_{zy} = \frac{1}{2}\left\{\frac{\partial v_y}{\partial z} + \frac{\partial v_z}{\partial y}\right\} \text{ and}\\ &\dot{\varphi}_{xz} = \dot{\varphi}_{zx} = \frac{1}{2}\left\{\frac{\partial v_x}{\partial z} + \frac{\partial v_z}{\partial x}\right\}.\end{aligned} \tag{2.20}$$

The result of Eqs. 2.19 and 2.20 is that the elongation tensor and the tensor of elongation rates are similar to the stress tensor. Above all, both can be broken up into deviatoric and hydrostatic parts. The deviatoric part is a measure of the deformation (elongation tensor) or the deformation rate of the continuum (elongation rate tensor). The hydrostatic part corresponds to the volume change or volume change rate of the continuum.

2.3.5 Volume Constancy

In plastic flow processes, the volume of the continuum remains as good as unchanged. For this reason, the elongations and elongation rates described by the hydrostatic stress become equal to zero. As proof, Fig. 2.17 shows the square bar again with the edge lengths h_0, b_0, l_0 before upsetting and h_1, b_1, l_1 after upsetting. Volume constancy then requires that

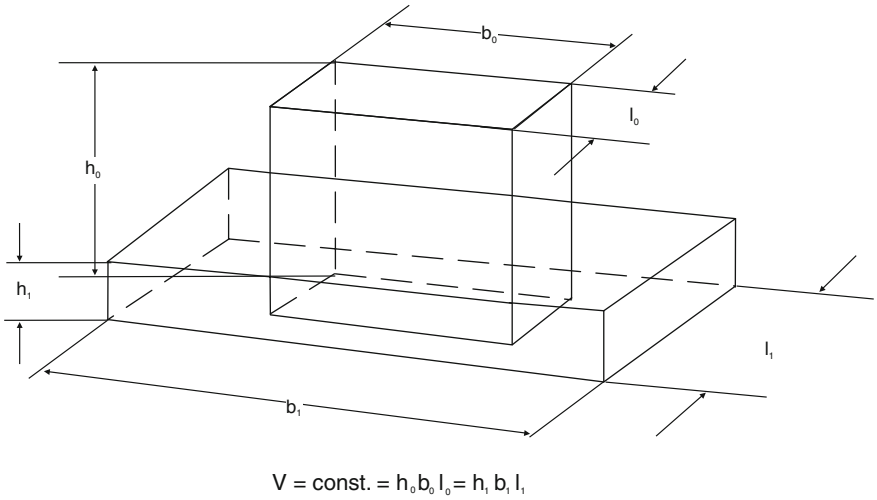


Fig. 2.17 Volume constancy in forming processes [LANG90a]

$$h_1 \cdot b_1 \cdot l_1 = h_0 \cdot b_0 \cdot l_0.$$

If we divide the left side of the equation just given by the right side and logarithmize, we obtain

$$\ln\left(\frac{h_1}{h_0} \cdot \frac{b_1}{b_0} \cdot \frac{l_1}{l_0}\right) = \ln 1 = 0$$

and thus

$$\ln\frac{h_1}{h_0} + \ln\frac{b_1}{b_0} + \ln\frac{l_1}{l_0} = \varphi_1 + \varphi_2 + \varphi_3 = 0. \tag{2.21}$$

Since similar considerations are also applicable for the forming rates, the following is also true

$$\dot{\varphi}_1 + \dot{\varphi}_2 + \dot{\varphi}_3 = 0. \tag{2.22}$$

2.3.6 Flow Rule

While stresses and deformations were previously treated separately, it is necessary for plastomechanical calculations to obtain a mathematical description of the relation between stresses and elongations.

To this end, we will again consider the example of upsetting a square bar. As the compressive force is applied, first elastic elongations arise, which are proportional to the stresses in accordance with Hooke's law. After the yield point is

reached, the stress $\sigma_3 = -k_f$ remains approximately constant, while with further upsetting the amounts of the elongations φ_1, φ_2, φ_3 increase monotonously. Therefore, a similarly simple relation such as Hooke's law cannot be given in the plastic range. Moreover, it has to be also assumed for real forming processes that the principal axes of the stress tensor change their directions, so that both the stress and elongation tensors no longer have the same principal directions.

To overcome this difficulty, the forming process is subdivided into small steps considering the tensor of elongation increase. It has the principal values

$$d\varphi_1,\ d\varphi_2,\ d\varphi_3.$$

Since the principal axes of this tensor now coincide with the principal axes of the stress tensor at every forming interval, proportionality can be applied between both tensors. However, it must be considered that the trace of the tensor of elongation increase must disappear due to Eq. 2.21 so that only the deviatoric part of the stress tensor comes into consideration for the proportionality:

$$\begin{aligned} d\varphi_1 &= d\lambda(\sigma_1 - \sigma_m), \\ d\varphi_2 &= d\lambda(\sigma_2 - \sigma_m) \text{ and} \\ d\varphi_1 &= d\lambda(\sigma_1 - \sigma_m). \end{aligned} \tag{2.23}$$

By division with dt, Eq. 2.23 can also be put into the form

$$\begin{aligned} \dot{\varphi}_1 &= \dot{\lambda}(\sigma_1 - \sigma_m), \\ \dot{\varphi}_2 &= \dot{\lambda}(\sigma_2 - \sigma_m) \text{ and} \\ \dot{\varphi}_3 &= \dot{\lambda}(\sigma_3 - \sigma_m). \end{aligned} \tag{2.24}$$

With a general position of the coordinate system, Eq. 2.24 becomes

$$\begin{aligned} \dot{\varphi}_x &= \frac{dv_x}{\partial x} = \dot{\lambda}\{\sigma_x - \sigma_m\}, \\ \dot{\varphi}_y &= \frac{dv_y}{\partial y} = \dot{\lambda}\{\sigma_y - \sigma_m\}, \\ \dot{\varphi}_z &= \frac{dv_z}{\partial z} = \dot{\lambda}\{\sigma_z - \sigma_m\}, \\ \dot{\varphi}_{xy} &= \frac{1}{2}\left\{\frac{\partial v_x}{\partial y} + \frac{\partial v_y}{\partial x}\right\} = \dot{\lambda}\tau_{xy}, \\ \dot{\varphi}_{yz} &= \frac{1}{2}\left\{\frac{\partial v_y}{\partial z} + \frac{\partial v_z}{\partial y}\right\} = \dot{\lambda}\tau_{yz} \text{ and} \\ \dot{\varphi}_{zx} &= \frac{1}{2}\left\{\frac{\partial v_z}{\partial x} + \frac{\partial v_x}{\partial z}\right\} = \dot{\lambda}\tau_{zx}. \end{aligned} \tag{2.25}$$

Equations 2.23–2.25 are called the flow law or flow rule. The flow rule, together with the yield criterion, describes the behaviour of the workpiece material in the state of plastic flow. $d\lambda$ and $\dot{\lambda}$ are scalar parameters, but no constants. Otherwise, doubling the elongation rate, for example, would also lead to a doubling of stress.

To derive a functional relation for $\dot{\lambda}$, Eq. 2.24 is squared line for line and then added up:

$$\dot{\varphi}_1^2 + \dot{\varphi}_2^2 + \dot{\varphi}_3^2 = \dot{\lambda}^2 \left\{ (\sigma_1 - \sigma_m)^2 + (\sigma_2 - \sigma_m)^2 + (\sigma_3 - \sigma_m)^2 \right\}. \tag{2.26}$$

The state of stress must constantly fulfil the yield criterion during plastic flow as well. Thus, the right side of Eq. 2.26 can be substituted with von Mises's yield criterion with Eq. 2.13,

$$\dot{\varphi}_1^2 + \dot{\varphi}_2^2 + \dot{\varphi}_3^2 = \dot{\lambda}^2 \frac{2}{3} k_f^2 \tag{2.27}$$

so that for $\dot{\lambda}$

$$\dot{\lambda} = \frac{\sqrt{\frac{3}{2}\left(\dot{\varphi}_1^2 + \dot{\varphi}_2^2 + \dot{\varphi}_3^2\right)}}{k_f} \tag{2.28}$$

or with elongations increments for $d\lambda$:

$$d\lambda = \frac{\sqrt{\frac{3}{2}\left(d\varphi_1^2 + d\varphi_2^2 + d\varphi_3^2\right)}}{k_f}. \tag{2.29}$$

If the yield stress k_f is constant in Eqs. 2.28 and 2.29, then it is a case of ideally plastic material behaviour. The flow curve in Fig. 2.18 then has a horizontal gradient. In order to take real workpiece material behaviour into consideration, k_f is determined is as function of natural strain, forming speed and also temperature. For this, flow curves are experimentally determined. This is done using uniaxial tests (see p. 118). We must therefore make a connection between the general state of strain of the given forming process and the particular uniaxial forming process with which the flow curve was determined.

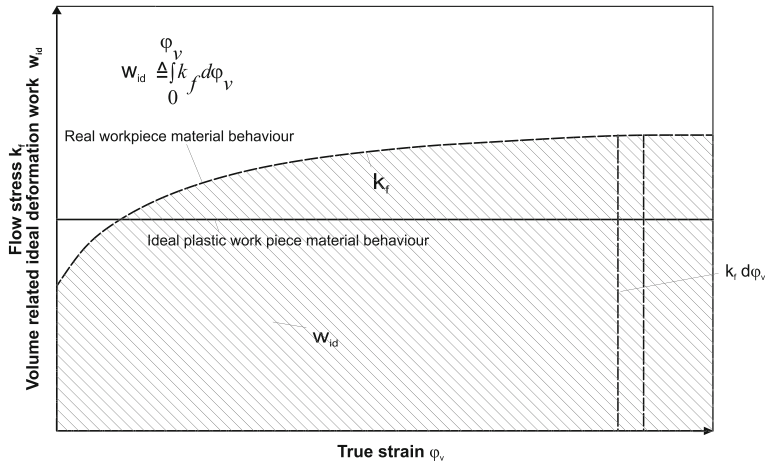


Fig. 2.18 Schematic representation of a flow curve

To this end, it is assumed that the flow curve of a workpiece material has been subjected to the idealized compression test described above.

The only principal stress that is not zero during the upsetting process is $\sigma_3 = -k_f$. With Eqs. 2.23 and 2.29, we can write for the increase in elongation $d\varphi_3$ in the direction of compression:

$$\begin{aligned} d\varphi_3 &= -\frac{\sqrt{\frac{3}{2}\left(d\varphi_1^2 + d\varphi_2^2 + d\varphi_3^2\right)}}{k_f}\left(k_f - \frac{1}{3}k_f\right) \\ d\varphi_3 &= -\sqrt{\frac{2}{3}\left(d\varphi_1^2 + d\varphi_2^2 + d\varphi_3^2\right)}. \end{aligned} \tag{2.30}$$

Following conclusions can be derived from Eq. 2.30: If a volume element is formed in time dt by a general forming process by $d\varphi_1$, $d\varphi_2$, $d\varphi_3$, this elongation, given the same workpiece material behaviour, corresponds to the increase in elongation $d\varphi_3$ in the tensile or compressive direction of a uniaxial tension or compression test.

Using integration the parameter is obtained

$$\varphi_v = \sqrt{\frac{2}{3}\left(\varphi_1^2 + \varphi_2^2 + \varphi_3^2\right)}, \tag{2.31}$$

which is called effective elongation or effective strain.

Quite similarly, the effective elongation rate/effective forming speed can be introduced with Eqs. 2.24 and 2.28:

$$\dot{\varphi}_v = \sqrt{\frac{2}{3}\left(\dot{\varphi}_1^2 + \dot{\varphi}_2^2 + \dot{\varphi}_3^2\right)}. \tag{2.32}$$

With Eqs. 2.31 and 2.32, the information in a flow curve can be applied to general forming processes. Both equations thus form an important foundation for calculating forming engineering problems.

2.3.7 Limits of Plastic Formation

In the literature, formability and the forming limit are utilized to describe the limits of plastic forming. Formability is a parameter specific to the material that restricts the forming process while the forming limit is a process-specific parameter. Both of these characteristic values will be described in more detail in the following.

2.3.7.1 Formability

Formability is a general expression for the property of a metallic material to sustain lasting deformations without damage (crack formation or fracture) [VDI76]. The fracture strain φ_{vB} is often used as a measure for the formability of a material. However, the fracture strain depends not only on the material but much more decisively on the temperature of the workpiece and the state of stress arising during the forming process [KOPP99]. Workpiece failure, described by formability, depends on the following parameters:

- workpiece material,
- workpiece temperature,
- forming rate and
- the type of stress in the workpiece.

Workpiece Material. The condition of the material is a result of the chemical composition (e.g. alloying elements), the material's microstructure (e.g. grain size), heat treatment (e.g. spheroidizing, sub-critical annealing, tempering, hardening and tempering) and the process steps in the course of component manufacture (e.g. casting, forging, rolling) [GRÄF93]. The condition of the material thus has a large influence on the formability of the material. For further details, the reader is referred to Sect. 2.7.1.2.

Workpiece Temperature. As a rule, the formability of a material increases with the workpiece temperature. This is due to the recovery and recrystallization processes that take place during forming (see Sects. 2.2.3 and 2.2.4). In the case of carbon steels, the blue brittleness range between 200 and 400 °C shows an exception to this behaviour (see Sect. 3.2, p. 222). The effect of temperature on a material can be represented with the help of a Charpy test in the impact work-temperature curve $(A_V - T - diagram)$. The steel's properties are all the more favourable the higher the impact work is at low temperatures.

Forming Rate. The forming rate also has a considerable influence on the limit of a material's formability. For example, formability generally decreases with higher forming rates [LANG90a]. In many cases, this is accompanied by an increased tendency to brittle fracture. However, it must be taken into consideration that increasing rates of load lead to more intense heating of the workpiece since the forming heat cannot be removed quickly enough. This effect is superimposed over the embrittlement of the material, leading to a higher level of material formability at significantly higher forming rates since the forming heat generated has a stronger effect on material behaviour [ELMA01].

Type of Stress in the Workpiece. Formability is strongly dependant on the state of elongation and stress in the workpiece. The latter can be broken down into a deviatoric and a hydrostatic part. While deviator stresses are decisive for plastic flow, the hydrostatic part has little effect on flow itself. It does however have a major effect on the formability of the material. Hydrostatic stress σ_m, with reference to the yield stress k_f, can be utilized as a measure for the effect of the state of

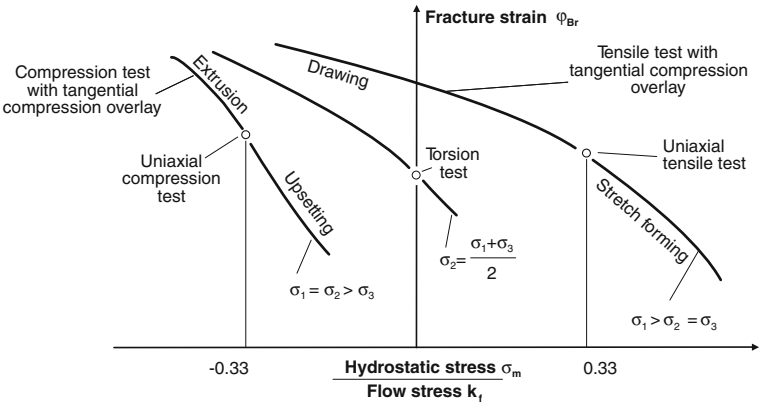


Fig. 2.19 The effect of the state of stress on formability according to Stenger [STEN65]

stress (see Fig. 2.19). For example, a value of 0.33 is obtained in a uniaxial tension test for σ_m/k_f, of 0 in a torsion test and of -0.33 in a uniaxial compression test. The smaller this value is, the larger the fracture strain φ_B, assuming that the second principal normal stress σ_2 is constant. If σ_2 shifts to the smallest principal normal stress σ_3, the formability of the material is increased assuming that the reference stress average σ_m/k_f is constant. In summary, we must bear in mind that both σ_m and σ_2 are functions of position and time depending on the forming process.

It has also been pointed out that formability depends on the stress history as well [PUGH70]. In a first test, Pugh upset a sample without external surrounding pressure until fracture. In a second test, he pre-upset a sample with surrounding external pressure and then upset the same sample without surrounding pressure until fracture. This experiment led him to the conclusion that formability was several times higher in the second test than in the first. This can be explained physically in the following way: During the forming process, microscopically small cracks in the workpiece material attempt to open and propagate through the entire workpiece. Compressive stresses on all sides strive to close these microcracks and to hinder their propagation. It immediately follows from this interpretation that only average compressive stresses, i.e. negative values of σ_m, can increase the maximum obtainable true strain. Average tensile stresses on the other hand are extremely unfavourable since they promote the opening and propagation of cracks.

Many technical forming processes are designed so that a hydrostatic pressure builds up in the workpiece. For example, in fine blanking (Sect. 5.2), hydromechanical deep drawing (Sect. 4.1.2) and roll bending with an additional press cylinder [MEIE01], a state of compressive stress is brought about in the forming zone by means of additional tool elements. This additional stress significantly increases the formability of the material. In this way, even high-strength and brittle materials can be plastically deformed.

2.3.7.2 Damage Criteria

As already described, the deformability of a material depends on different factors and is difficult to describe by means of a single material characteristic value. Thus, different fracture criteria have been developed that describe ductile material failure on the basis of the state of stress and deformation introduced and formulate this in the form of a characteristic value. If these characteristic values reach a level specific for that process, the appearance of a crack in the material is indicated. These fracture criteria can be subdivided into macromechanical and micromechanical fracture hypotheses. In the case of macromechanical criteria, these are further subdivided into elongation-independent and elongation-dependent hypotheses.

Time-independent Macromechanical Fracture Criteria. In the case of macromechanical, time-independent fracture criteria, the individual parameters of the stress and deformation state are determined as limit values. The forming history including crack development is not taken into consideration. In the simplest case for example, the critical effective stress of von Mises σ_V can be used as a limit value. More complex criteria calculate a limit value using a more comprehensive stress relation [GOSH76]. Among these criteria, the fracture true strain φ_B has a special position. The fracture true strain is an elongation-dependent variable, but it is assigned to this class as well because it is subject to the same restrictions as apply to the other macromechanical criteria. This class of fracture criteria is very important in sheet metal forming and is used as forming limit diagrams (see Sect. 2.7.3.5). In massive forming, these criteria have not been implemented since the dominated multiaxial states of stress lead to the extremely varied workpiece failure configurations, and these combinations can only be accounted for insufficiently with these criteria.

Time-dependent Macromechanical Fracture Criteria. As opposed to time-independent fracture criteria, macromechanical time-dependent fracture criteria are also called integral fracture criteria. They are based on the work introduced during forming, which is stored as plastic energy in the material on the one hand and converted as forming energy into elastic springback and heat on the other. This class of fracture criteria has the following structure:

$$D_{\text{makro}} = \int_0^{\varphi} f(\varphi, \sigma, a) d\varphi. \tag{2.33}$$

Here, elongations are taken into account with φ, stresses with σ and different material constants with a. The calculation thus sums up the incremental stress and deformation increases of a material element caused by forming. If the forming energy added to the workpiece reaches a critical damage value D_{crit}, then the deformability of the material has been exhausted in this area. The integral fracture criteria differ in the configuration of the energy terms. The best-known criteria are integrated in most FEM codes [FREU50, STEN65, COCK66, BROZ72, AYAD84].

Micromechanical Fracture Criteria. Micromechanical fracture criteria have also been developed parallel to the integral criteria [MCCL68, RICE69, GURS77,

OYAN80]. These attempt to calculate directly the material behaviour and thus the damage by proceeding from a pore volume f and adding up a pore increase df caused by new pore formation and pore growth.

$$D_{micro} = f + df_{newformation} + df_{growth} \tag{2.34}$$

The reduced strength of the damaged material area compared to the undamaged area is mostly considered in the form of a special flow function that represents the pore volume f. If the calculated pore volume f in combination with pore increase df reaches a critical amount, then the deformability of the material is exhausted and the workpiece experiences macroscopic material separation and cracking.

Summary. A number of micromechanical and macromechanical damage criteria are integrated in most FEM programs and are utilized to assess the deformability of a material. The forming areas heavily loaded during the forming process can be determined very effectively by these means. Difficulties arise in the determination of the maximum damage value for the individual damage criteria, materials and forming processes. For example, it is decisive in the determination of the material's formability for a particular forming process that a test method is selected, which exhibits a forming behaviour very close to the forming method so that its forming history at the location of the first crack formation agrees with or closely approximates the forming history at the critical location of the component.

Taking into account different forming histories to determine workpiece failure compensates for the disadvantage of macromechanical and micromechanical fracture criteria that a critical damage value can vary with the forming process. Zitz [ZITZ95] has shown that a subdivision can be made between a crack-free and crack-affected area by determining the largest reference principal normal stress as a function of the effective strain for different test piece geometries. To this end, deformability was determined in a compression test run with rotation-symmetrical test pieces of the most varied geometries. By means of an FE simulation, the forming history of the crack-endangered areas could be determined. The stress and deformation space was then subdivided into a crack-free area and a crack-affected area by means of a line connecting the end points. By representing the forming history of a crack-endangered area, a limiting strain for this process can be determined using the point of intersection of the limit curve and the profile of the forming history. The focus of further investigations is to consider not only one part of the stress and deformation state at the time of crack formation but to incorporate both the complete stress and deformation state as well as the variation of this state as a function of the forming process into the fracture prediction [KLOC03a, KLOC04a].

2.3.7.3 Forming Limit

In the case of the forming limit, it is not material failure that leads to process breakdown, but process-specific parameters such as:

- tool fracture,
- insufficient machine power,
- impermissible form and dimension deviations,
- impermissible surface quality.

According to VDI guideline 3,137 [VDI76], the maximum effective true strain reached in the component is designated as limiting strain φ_{vG} upon reaching the above process limits. It is thus an index for the forming limit. In general, the forming limit can be at most equal to the deformability of the material, but in most cases it is smaller. This is especially apparent in massive forming with high tool strains (e.g. cold extrusion, hot drop forging), whereby $\varphi_{vG} \leq \varphi_{vB}$, while in sheet forming failure mostly stems from the workpiece, and so $\varphi_{vG} = \varphi_{vB}$.

2.4 Possible Solutions to Forming Problems from the Field of Plasticity Theory

Building upon the foundations from Sect. 2.3, this chapter introduces different possibilities for analyzing problems in forming technology.

If the three components v_x, v_y and v_z of the velocity field, the proportionality factor $\dot{\lambda}$ and the six components of the stress tensor are understood as unknowns of a plastomechanical boundary value problem, then these seven quantities result, with the constitutive law, i.e. the yield criterion (Eq. 2.12) and the flow rule (Eq. 2.25), in seven equations. The three equations still lacking provide the equilibrium conditions

$$\begin{aligned} \frac{\partial \sigma_x}{\partial x} + \frac{\partial \tau_{xy}}{\partial y} + \frac{\partial \tau_{xz}}{\partial z} &= 0, \\ \frac{\partial \tau_{yx}}{\partial x} + \frac{\partial \sigma_y}{\partial y} + \frac{\partial \tau_{yz}}{\partial z} &= 0 \text{ and} \\ \frac{\partial \tau_{zx}}{\partial x} + \frac{\partial \tau_{zy}}{\partial y} + \frac{\partial \sigma_z}{\partial z} &= 0, \end{aligned} \tag{2.35}$$

because depending on whether elastic deformation or plastic flow is taking place, the state of stress must be constituted such that all areas of the workpiece are in a state of static equilibrium. Dynamic effects are generally negligible [PAWE76]. Although this basically proves the solvability of the plastomechanical boundary value problem, the number of partial differential equations suggests that a closed solution is only possible in rare cases.

For this reason, a variety of solution methods have been developed. A classification of these methods can be made in accordance with their approaches and procedures (see Fig. 2.20).

The solution methods of elementary plasticity theory assume geometrical, kinematic and material simplifications and convert the general equation system

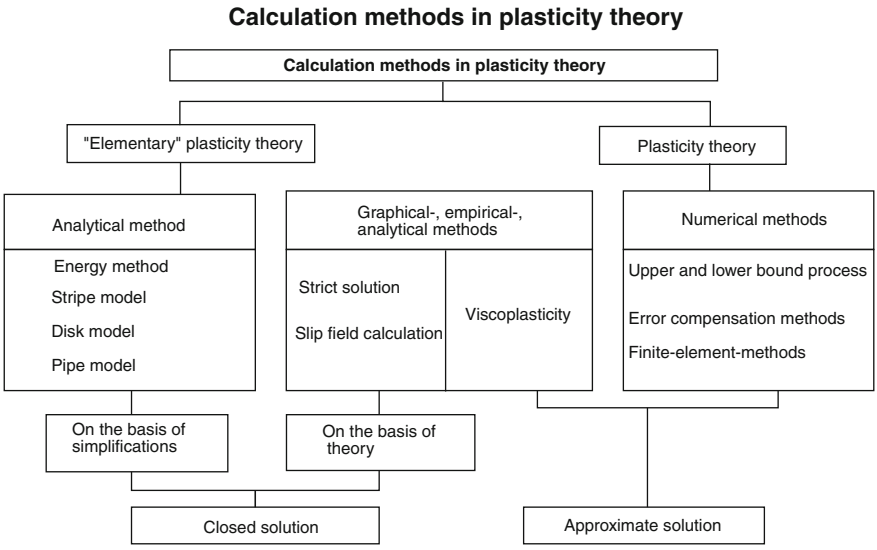


Fig. 2.20 Solution methods in forming engineering from plasticity theory (acc. to Roll)

into a system of analytically solvable equations. Today, high-performance computers enable the calculation of complex problems. The basics for such calculations are numerical calculation methods, which are used to solve the analytical approaches.

2.4.1 Solution Methods of Elementary Plasticity Theory

The basic assumption of elementary plasticity theory is that originally level sections do not experience any warping during the forming process. If the velocity in the normal direction is known for one section, then the speed at another location can be calculated by means of the condition of volume constancy, and thus information can be obtained about the forming rate at that location.

As a result of these assumptions concerning the kinematics of the forming process, simple equations are obtained for forming force and stresses. Moreover, the level state of motion implies a homogeneous deformation state in the entire section.

The following assumptions characterize the possibilities and limits of the elementary theory:

- the material behaves homogeneously and isotropically,
- a rigid/ideal-plastic material model is assumed,
- level deformation kinematics are assumed and

- material behaviour in the plastic state is described by the yield criterion and volume constancy.

These conditions reduce the problem of plastic deformation to a statically defined system.

2.4.2 Energy Method

The energy method requires the least amount of calculation. Using this method forming forces and performance can be approximated. It is applicable when the kinematics of plastic flow of a manufacturing process can be estimated. One disadvantage of the energy method is that the stress history can only be determined roughly.

We will consider upsetting a square bar as an example for this method [FINK74]. Let us assume the yield stress k_f as a function of the effective strain φ_v, i.e. the flow curve of the workpiece material. If the sample has a square cross-section, then the true strains φ_1 and φ_2 are the same during the upsetting process for reasons of symmetry. It then follows from Eqs. 2.21 and 2.31

$$\varphi_v = |\varphi_3|$$

During one forming step $|d\varphi_3| = d\varphi_v$, the compression paths perform the work

$$dW_{id} = F_{St}|dh| = A \cdot k_f|dh|. \tag{2.36}$$

After division with the volume of the compression sample, it is obtained

$$dw_{id} = \frac{A \cdot k_f|dh|}{Ah} = k_f \frac{|dh|}{h} = k_f|d\varphi_3| = k_f d\varphi_v. \tag{2.37}$$

By integrating Eq. 2.37, the ideal forming work relative to the volume w_{id} follows as:

$$w_{id} = \int_0^{\varphi_v} k_f(\varphi_v)d\varphi_v. \tag{2.38}$$

It has the dimension of a stress and corresponds to the surface beneath the flow curve (Fig. 2.18). Frequently, a diagram contains not only the yield point $k_f(\varphi_v)$ but also the curve progression $w_{id}(\varphi_v)$.

The reference forming work of a general forming process can be calculated by means of the effective strain, so the following steps are taken when determining forming work, forming force and workpiece strength:

1. Assumptions are made concerning material flow from tool movement during the forming process, the geometrical properties of the problem, the continuity equation and also from tests and the true strains φ_1, φ_2 and φ_3 are estimated.

2. With Eq. 2.31 the effective strain φ_v is determined and with the help of the flow curve the yield stress $k_f(\varphi_v)$ and ideal forming work relative to volume $w_{id}(\varphi_v)$ are determined.

3. From

$$W_{id} = \int_V w_{id} dV \tag{2.39}$$

the ideal forming work to be applied to the forming process is obtained.

4. The forming force is calculated from tool displacement and forming work.

It is known from practice that an effective forming work W_{eff} is necessary for most forming processes, which is larger than the ideal forming work W_{id}.

$$\frac{W_{id}}{W_{eff}} = \eta_F$$

is designated as the efficiency of deformation.

The cause of the difference between ideal and effective forming work is essentially the previously ignored friction between the tool and the workpiece. Friction in forming processes is dealt with in Sect. 2.8.2, p. 138.

2.4.3 Calculation Method with the Strip, Disc and Pipe Model

Characteristic of this method are the strip, disc and pipe-shaped volume elements the calculation is based on (Fig. 2.21). The tool shape and forming process determine which model is used. The application of equilibrium conditions leads in all three models to a linear, inhomogeneous differential equation of the first order. It is analytically solvable at least in some sections. By joining the solutions of several sections, an overall solution is obtained.

Drawing wire or bars will be considered as an example [PAWE76]. In accordance with Fig. 2.22, the equilibrium condition in the drawing direction leads to

$$\sigma_z + A\frac{d\sigma_z}{dA} + p(1 + \mu \cot \alpha) = 0. \tag{2.40}$$

The yield criterion after Tresca reads

$$p + \sigma_z = k_f. \tag{2.41}$$

In this way, both p as compressive stress and σ_z as tensile stress are defined positively. The cross-sectional surface A is selected as an independent variable.

Eliminating p, a common 1st order differential equation is obtained:

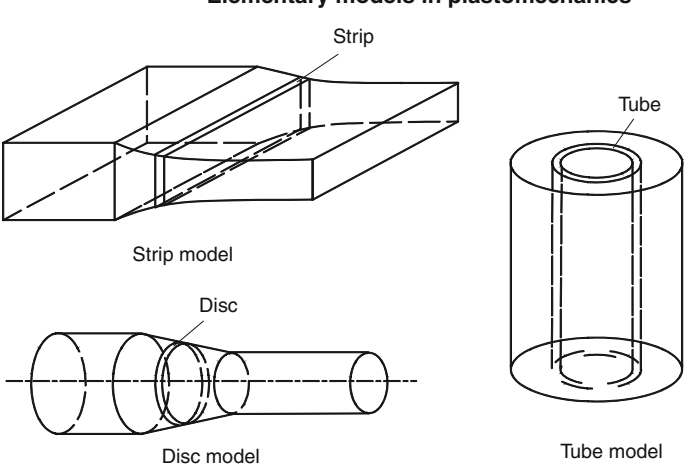


Fig. 2.21 Volume elements in elementary plastomechanics for different models (acc. to Pawelski)

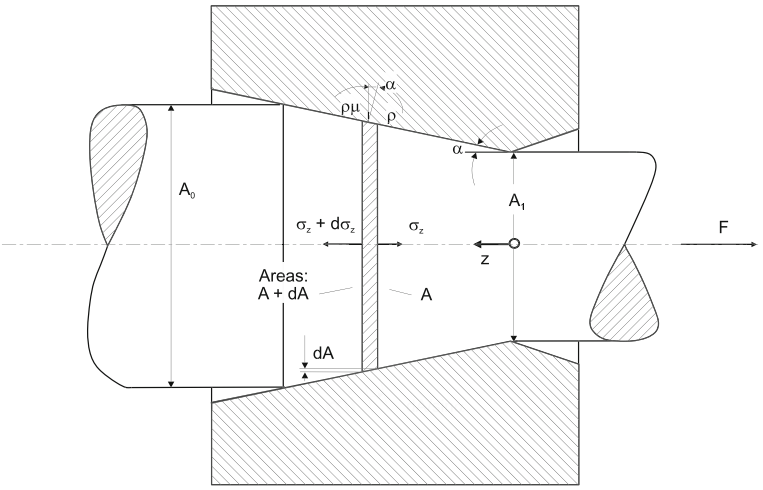


Fig. 2.22 Stresses on a disc-shaped volume element when drawing a wire or bar acc. to Pawelski [PAWE76]

$$\frac{d\sigma_z}{dA} - \frac{\mu \cot \alpha}{A}\sigma_z + \frac{k_f(1+\cot \alpha)}{A} = 0. \tag{2.42}$$

It corresponds to the type of differential equation

$$\sigma_z' + f(x)\sigma_z + g(x) = 0, \tag{2.43}$$

as is always encountered in the foundation of elementary plasticity theory. The functions $f(x)$ describe the forming geometry and the influence of friction. Such differential equations can be solved sometimes analytically, but always numerically (e.g. using the Runge-Kutta method). For constant values of k_f and μ, the solution leads to the drawing force formula acc. to [SACH27]:

$$P_z = \sigma_z(A_1)A_1 = k_f\left(1 + \frac{1}{\mu \cot \alpha}\right)\left[1 - \left(\frac{A_1}{A_0}\right)^{\mu \cot \alpha}\right] \tag{2.44}$$

2.4.4 Strict Solution

"Strict solutions" can only be applied in the case of very simple, straightforward problems. A strict solution means that there are functions for stress distribution and the state of motion in the entire plastic area that fulfil the continuity equation, equilibrium conditions, the yield criterion as well as von Mises's constitutive law. They must also comply with the marginal conditions. Usually we are dealing with tasks in which the geometry of the tools has partially determined the stress and deformation state. Examples of processes that can be solved in a strict way are provided in [PRAG54].

2.4.5 Slip Line Method

Slip lines are lines that have the direction of maximum shear stress at each of its points. The theory of the slip line method is based on the plane consideration of the forming process. The three unknown stresses σ_x, σ_z and τ_{zx} are subject to the equilibrium conditions in the x and z directions and the yield criterion. The task is thus statically determined. From these three static basic equations we obtain a system of partial differential equations of the first order. The latter represent two orthogonal curve sets corresponding to the slip lines. They are subdivided into α- and β- slip lines.

One disadvantage is that this theory is only valid for a planar formation and for an ideal-plastic material. Wall friction on the tool is also difficult to take into consideration.

If the slip line method is applied to axial symmetrical problems, formulations result that previously could only by solved with numerical iteration methods. We then refer to them as principal line methods. A detailed description of this method can be found in [HILL50, PRAG54, DIET86].

2.4.6 Visioplasticity and the Measuring Grid Method

Using the visioplasticity method, better approximations can be made of actual forming processes using plasticity theory than is possible with pure theory. The test piece to be formed is subdivided in a symmetry plane, and a line mesh is applied to the joint. In this way, the velocity field can be approximated by means of the mesh distortion arising during the forming process. With these input parameters, the stresses and forces can be calculated using the theory of plasticity. This will be explained in accordance with [LANG90a] in an abbreviated form using an axially symmetrical extrusion process (Fig. 2.23).

It will be assumed that the punch velocity and thus the velocity of the material in the undeformed shaft of the workpiece has the value v_{wz}. Then a line I-I in the shaft (Fig. 2.23) switches to line II-II in time

$$\Delta t = \frac{\Delta s_0}{\Delta v_{wz}} \tag{2.45}$$

In the same time, the intersection point A of the mesh migrates in the forming zone to A'. If the projection of the path AA' on the r-axis is designated with Δs_r and that on the z-axis with Δs_z, then with

$$\bar{v}_r = \frac{\Delta s_r}{\Delta t} \text{ and} \tag{2.46}$$

$$\bar{v}_z = \frac{\Delta s_z}{\Delta t}. \tag{2.47}$$

We obtain approximate values for the velocity components of point A. These are the more accurate the more tight the mesh selected.

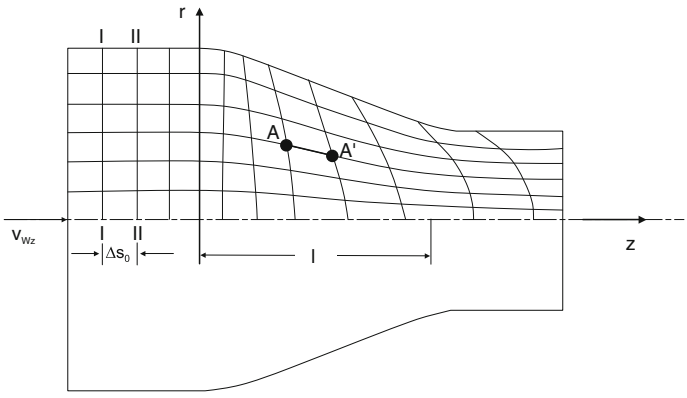


Fig. 2.23 Determining the velocity field from a distorted mesh for a stationary process, acc. to [LANG90a]

In the case of unstable processes, we obtain the velocities in a similar way if we determine the change in lattice distortion for two steps of the forming process that are in close sequence.

From the velocities v_i we can now determine the deformation rates graphically by plotting the calculated velocity components $\bar{v}_r$ and $\bar{v}_z$ over r and z and connecting them with a series of curves.

$$\dot{\bar{\varepsilon}}_r = \frac{\partial \bar{v}_r}{\partial r} \quad \dot{\bar{\varepsilon}}_r = \frac{\partial \bar{v}_r}{\partial r} \tag{2.48}$$

$$\dot{\bar{\varepsilon}}_z = \frac{\partial \bar{v}_z}{\partial z} \quad \dot{\bar{\varepsilon}}_{rz} = \frac{1}{2}\left(\frac{\partial \bar{v}_r}{\partial z} + \frac{\partial \bar{v}_z}{\partial r}\right) \tag{2.49}$$

The selected mesh must be fine enough to make an interpolation of $\bar{v}_r$ and $\bar{v}_z$ on lines $r = \text{const.}$ and $z = \text{const.}$ possible with sufficient precision. Now, the deformations can also be approximated from the deformation rates by integrating the deformation rates that a particle experiences on its way along a flow line. If the effective strain is also calculated, the yield stress can be obtained from the flow curve and thereby calculate the approximate values for the deviator components of the state of stress as functions of the spatial coordinates using the von Mises flow rule. In this method, a line mesh of a particular geometry, the "measuring grid", is applied to the sheet surface to be formed and evaluated after forming. The grid nets commonly used in practice are almost exclusively composed of circles, but these can also be combined with square grids. Evaluation is significantly simpler in the case of circular grids, as the forming process distorts them into ellipses, the principal axes of which indicate both the size and direction of the principal deformations. On the other hand, square grids are usually distorted into undefined rhombi that are very difficult to evaluate [KÜBE80]. Circular grids have a diameter of about 3–10 mm depending on the size of the drawn part. Small dimensions make measurement more difficult, but they allow for a more differentiated evaluation of smaller areas. Great demands are made on methods for plotting measuring grids. In order to determine deformations accurately, the grid must survive the deformation of the sheet without damage. This requires good adhesive power, while at the same time the deformation behaviour of the sheet must be influenced as little as possible. Furthermore, the accuracy of the dimensions must be guaranteed to such an extent that measurement prior to deformation is superfluous [MÜSC69].

Mechanical application of measuring grids with the help of scribers or scribing compasses, formerly widely utilized, is the most inexpensive method with respect to device-related costs, but it is also very time-consuming and low in precision. Moreover, the notch effect brought about by the scribing process and the resulting influence on the material surface cannot be neglected, especially in the case of fine sheets.

The most precise and, with respect to grid quality, best results can be obtained by means of electrochemical and photochemical processes. However, the device-related costs are considerably higher. In the case of electrochemical application, the sheet is covered with a template and etched. In the photochemical method, the

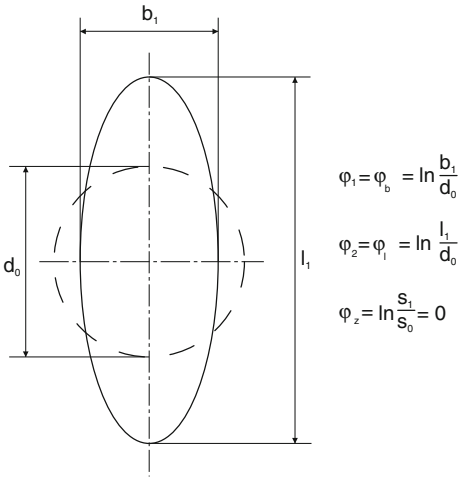


Fig. 2.24 Determining the true strain from a deformed measuring grid

grid is first applied to the sheet with a photosensitive lacquer by means of a grid negative. Then the surface not protected by lacquer is etched.

Other simple and economical ways to apply a line mesh include imprinting with rubber roll stamps, the screen printing method or the offset method. Due to the low abrasion resistance, these methods generally cannot be employed for deep drawing, but they can be for stretch drawing or tension test.

When evaluating a deformed circular grid, the length of both axes of the ellipse generated is measured and applied to the output diameter d_0 of the circle to determine the true strain in the longitudinal direction (φ_1) and the direction of width (φ_2). With the help of volume constancy, deformation in the direction of thickness (φ_3) or the local sheet thickness can be calculated from both true strains (Fig. 2.24).

In the case of curved surface areas, it has to be considered that deformations on the top and bottom sides of the sheet are approximately identical.

2.4.7 Upper Bound Method

In case the exact solution for forming performance cannot be determined for a forming process, often the upper and lower bound, between which lies the exact solution, are sufficient. Of primary interest in performing measurements on forming machines is the upper bound.

In the case of an exact solution, both the calculated stress field as well as the calculated velocity field fulfils the equilibrium conditions, the constitutive law, the condition of volume constancy and all marginal and starting conditions of the

problem. As a rule, there are several stress and velocity fields that fulfil part of these conditions independently of each other.

When calculating the lower bound for forming performance, only a statically permissible stress field is required; kinematics are not taken into consideration. Such a field needs only to satisfy the equilibrium conditions, the yield criterion and the marginal stress conditions. When calculating the upper bound, we start from a kinematically permissible velocity field which must fulfil the condition of volume constancy and the marginal velocity conditions [LANG90a].

2.4.8 Error Compensation Method

ECM originated in the direct treatment of variational calculus problems. It is basically restricted to planar and axially symmetrical forming processes.

In one section of a continuum, a function is sought (velocity field, stress field) that is determined by a differential equation and a marginal condition. For the unknown solution, a method of approximation is set up, e.g. in the form of a power series. If this approximate solution is inserted into the differential equation, it will not be satisfied exactly. The error depends on the form of the method and the choice of parameters. These parameters must be set so that the error distribution satisfies the target requirements. This can be done, for example, by using the method of least squares. In the first approach, usually viscous constitutive equations are applied. Then the plastic attributes of the material are taken into consideration. In the practical calculation, we alternately calculate a stress field from the constantly held velocity field and vice versa. This is repeated until the errors no longer exhibit diminutions or the velocity and stress fields no longer change.

With the error compensation method, we can calculate the local velocity distributions, deformation rate distributions, deformations/distortions, stress distributions as well as the yield stress, friction coefficient, forming force/performance and temperature fields. Areas that remain rigid during the forming process cannot be measured well using ECM. Errors arise with respect to satisfying the yield criterion that are also propagated in the plastic section. The consequence is an inexact calculation of the stress distribution. The use of this method is often limited by geometrical eventualities.

[LANG90a] includes an extensive description of the use of ECM in the upsetting of a cylindrical body. Further examples can inter alia be found in [ROLL81].

2.5 Finite Element Method

In the last 20 years, simulation has been established both in sheet and massive forming as an indispensable tool in research and industrial practice. The most frequently utilized method for simulating forming processes is the finite element

method (FEM). This is a numerical method for finding approximate solutions to continuous field problems. These are problems in which the behaviour of the continuum can be described by partial, time-dependant and location-dependent differential equations. Each state variable (e.g. stress, temperature) of a continuum possesses infinitely many values, since it is a function of every point of the continuum. The problem thus has an infinite number of unknowns. The basic principle of FEM consists in breaking down the continuum into a finite number of parts called finite elements. Thus, an initially complex, continuous problem is subdivided into a finite number of simple, mutually dependent problems. Applied to forming processes, FEM enables to make assertions about the size and distribution of various state variables in the material and tools during and after forming. It is thus a valuable aid in the interpretation and analysis of forming processes. FEM enables the investigation of such processes in forming engineering that, due to their complexity, can be handled with analytical methods only with great difficulty if at all.

Since the development of the basic concepts of FEM took place at the same time and with the same motivations in the spheres of mathematics, physics and engineering sciences, the exact time point of FEM's origination cannot be determined exactly. The designation "finite element method" was first used however in the year 1960 by Clough [CLOU60]. [HUEB82, KNOT92], among others, provide a history of FEM with reference to the three abovementioned areas of specialization.

In the following, the basic concepts of FEM will be introduced in addition to some application examples from forming technology. The goal is not to provide an introduction to the foundations of FEM, but rather to communicate the basic concepts as well as some of the technical terms. A good introduction into the foundations of FEM for engineers can be found, for example, in [KNOT92, BETT03, HUEB82]. In [ROLL93, KOBA89], the method is explained with particular reference to forming technology. More advanced standard works on the topic include [BATH96, ZIEN00, REDD93].

2.5.1 Basic Concepts of the Finite Element Method

Even in the case of the use of forming-specific program packages, it is helpful to be acquainted with the basic concepts of FEM in order to avoid errors and to evaluate correctly the results of the calculation. The user should be conscious of the assumptions made by the software and their potential effects on the results. The process analysis by means of FEM is also called finite element analysis (FEA). The following steps are taken in every FEA [HUEB82, ZIEN00, REDD93, ROLL93]:

1. discretizing the continuum,
2. selecting interpolation functions,

3. determining the element properties,
4. assembling the element equations and
5. solving the system equations.

During continuum discretization, the solution domains (e.g. the workpiece) is subdivided into a finite number of subdomains, the finite elements. In the process, the type, number, size and distribution of the elements is set.

The selection of interpolation functions, which are often designated as shape or basis functions, takes place in practice at the same time that the element type is selected. The interpolation functions serve to approximate the progress of the state variables within an element. The element nodes function as support points for interpolation. In the case of "linear elements", these are the vertices of an element. Higher-order elements have available a set number of additional nodes on the element edges or within the elements and, because of the larger number of nodes, supply a more exact solution. Due to their differentiability or integrability, polynomials are frequently used as interpolation functions. The order of the polynomials depends here on the number of element nodes, the number of unknowns of each node as well as on the continuity conditions at the nodes. Since the interpolation functions represent the behaviour of the state variables in the inside of the element, the values of the state variables at the nodes represent the unknowns of the discretized problem.

After selecting the element types and the associated interpolation functions, the element equations (element matrices) are determined. These equations describe the relations between the primary unknowns (e.g. velocity, dislocation, temperature) and the secondary unknown (e.g. stresses). To determine the element equations, several approaches are possible. The basic variation formulation for plastic problems is [ROLL93, KOBA89]:

$$\delta\pi = \int_V \sigma_V \delta\dot{\varepsilon}_V dV + K \int_V \dot{\varepsilon}_{ii} \delta\dot{\varepsilon}_{ii} dV - \int_{S_F} F_i \delta u_i dS = 0 \tag{2.50}$$

with:

π	power generated by forming and friction
$\delta\pi$	variation of power with the variation of the velocity field
σ_V	effective stress field
$\dot{\varepsilon}_V$	field of forming velocity
V	volume
K	penalty constant to limit volume change
$\dot{\varepsilon}_{ii}$	volumetric shape change
S_F	surface
F_i	surface forces
u_i	surface velocity field

With the help of numerical methods, the velocity field is sought that satisfies Eq. 2.50. This velocity field minimizes power consumption and thus the energy

cost. The "penalty term" ensures that volumetric deformation is kept low, and so the condition of volume constancy is nearly fulfilled. In addition, the velocity field sought must satisfy the marginal conditions.

One of the fundamental differences between FEM and other numerical approximation methods is that the solution is first formulated for every single element. In order to approximate the properties of the overall system built of these elements, the element matrices are assembled into the global matrix of the problem. Also, the marginal conditions (clampings, external forces, etc.) are introduced. Assembly of the element equations yields the system equations, which are then solved with the help of suitable methods. The numerical integration methods employed to integrate the element matrices require the evaluation of the integrals at certain points within an element, so-called integration points. In the process, the number of required integration points can be reduced without affecting accuracy by carefully selecting their positions. The Gaussian quadrature is a very common method used for numerical integration in FEM. The positions of the integration points within an element are exactly determined and represent the positions at which stresses and elongations are calculated [KOBA89, ROLL93, ZIEN00]. Even if the basic procedure of all FEM-based calculations is the same, the programs used differ in a few fundamental aspects.

2.5.2 *Lagrangian and Eulerian Representations of the Continuum*

The continuum can be discretized using different approaches. The most common approaches in FEM are the Lagrangian and Eulerian [BATH96].

The Lagrangian method is the most dominant in forming engineering. In this case, the nodes of an element move along with the material. An observer travelling on a node would observe change in the state variables of a particular particle throughout the entire forming process. One disadvantage of the Lagrangian approach is the mesh distortion entailed by large-scale plastic deformations, which can sometimes require remeshing. The interpolations of the state variables from the distorted to the new mesh lead to an undesirable, more or less distinct smoothing of the state variables depending on the number of remeshing cycles.

The Eulerian approach proceeds from the movement of a continuum through a fixed mesh. An observer on a node of such a mesh would observe the changes of all particles that pass his fixed point of observation. The method is especially appropriate for investigating stationary processes and is frequently employed in flow simulation. The "arbitrary Lagrangian-Eulerian" (ALE) method is being increasingly used. This is a combination of the above methods permitting the mesh a motion independent of the material as long as the shape of the domains under considerations remains intact [KOBA89, WU03].

2.5.3 Explicit and Implicit Solution Methods

Most programs employed in massive forming make use of so-called implicit methods, whereas in sheet forming and for highly dynamic applications (e.g. crash simulations) explicit time integration is widely used. Explicit methods consider the process under investigation as a dynamic problem subdivided into time increments. The target variables at time $t + \Delta t$ are determined only from the values available at time t. This is done usually by means of difference schemes. Yet this method is only stable if time increment Δt is smaller than the time required for an elastic wave to cover a distance corresponding to the shortest element edge. In this way, the possible size of the time increment is contingent on the sonic velocity c present in the material. The following is valid for solid bodies:

$$c = \sqrt{\frac{E}{\rho}}.$$

The maximum possible time increment thus depends on the density ρ and modulus of elasticity E of the material. Since the time increment can be in the range of microseconds, a very large amount of calculation steps is sometimes required. "Mass scaling", the artificial increase of material density or artificial shortening of process time, represents an attempt to increase the possible size of the time increments. The mass effects caused by such interventions have to be compensated by suitable measures [ROLL93, CHUN98].

This limitation does not exist when using implicit methods. Implicit solvers seek the solution for every time $t + \Delta t$ under consideration of the values of the target variables both at time t and at time $t + \Delta t$ [HUEB82]. Due to the non-linearities involved, this requires the solution of a non-linear equation system by means of an iteration process (e.g. Newton-Raphson) [ROLL93, ZIEN00]. To the advantage of the up to 1,000 times larger possible time increments compared to the explicit method is thus joined the disadvantage of the calculation time required for the iterative equation solution.

2.5.4 Thermal Coupling

When considering thermal processes, the mechanical and thermal calculations must be coupled. In the case of simultaneous coupling, this is achieved by setting up a completely coupled equation system. Non-simultaneous coupling proceeds from a purely mechanical formulation, in which the temperature serves only to determine temperature-dependent material characteristic values (e.g. the flow curve). The mechanical calculation calculates frictional heat, heat from plastic deformation and heat exchange with other objects or the environment. These data are then the input variables for the thermal calculation. This coupling can take

place at every iteration (iterative coupling) or at every time increment (incremental coupling) [KOPP99].

2.5.5 Element Types

Basically, three different categories of elements are used in forming engineering [ROLL93]:

- volume elements (continuum elements),
- membrane elements and
- shell elements.

In massive forming, mainly continuum elements are used. In this case, we distinguish between planar, axially symmetrical and three-dimensional elements, depending on the state of deformation. Continuum elements make it possible to capture all normal and shear stresses. The complete definition of an element type includes the element shape, number of nodes, type of node variables and the interpolation functions. In massive forming, so-called isoparametric elements without centre nodes have become established [ROLL93]. An element is isoparametric if it has the same interpolation function both for the state variables within the element and for the coordinate transformation from the global into the local coordinate system (element coordinate system) [ZIEN00, ROLL93]. Figure 2.25 shows

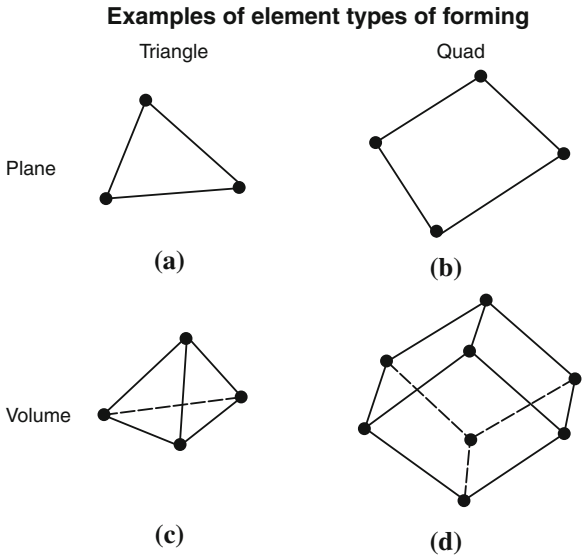


Fig. 2.25 Examples of element shapes used in forming engineering triangle (**a**), square (**b**), tetrahedron (**c**), and hexahedron (**d**)

some examples of element types that are used in forming engineering. Typical element shapes are triangular and quadratic elements with three or four nodes as well as tetrahedral and hexahedral elements with four or eight nodes [HUEB82]. In sheet forming, mainly membrane and shell elements are employed, in rare cases continuum elements as well. Membrane elements cannot convey bending moments, are not suitable for capturing wrinkle formation and are thus hardly used anymore. Shell elements on the other hand are capable of capturing bending moments and of taking wrinkle formation in shell forming into consideration. "Thin" shell elements (acc. to Kirchhoff) have a finite bending and shear stiffness [ROLL93]. Since triangular shell and membrane elements only differ in the freedom of their nodes, the representation in Fig. 2.25a is valid for both element types.

2.5.6 Non-Linearities

A linear analysis is the analysis of a problem that exhibits a linear relation between the loads applied and the answer of the system. Linear analysis represents a simplification, since every real physical system is non-linear. These non-linearities can however be neglected in many cases. If we speak of non-linearities in FEM, this indicates that these non-linearities must be taken into consideration.

Basically, we differentiate between three different kinds of non-linearities:

- material non-linearities,
- geometric non-linearities and
- non-linearities in the boundary conditions.

Material non-linearities result, for example, from a non-linear relation between stress and displacement which occurs in metallic materials after leaving Hooke's range. Further causes for material non-linearities include material behaviour that is dependent on the forming rate and/or temperature as well as material failure.

Geometric non-linearities are caused by an alteration of geometry during the calculation. As soon as the displacements arising are large, thus influencing the behaviour of the system, it is considered a non-linearity.

Non-linearities in the marginal conditions are caused, for example, by a change in the external loads or by new contact or loss of contact between two objects (e.g. tool—workpiece). As a rule, we encounter all three types of non-linearity in a typical forming process simulation.

2.5.7 Constitutive Laws

The constitutive laws implemented in the simulation of forming processes for the representation of metallic materials can be subdivided into two main groups: those

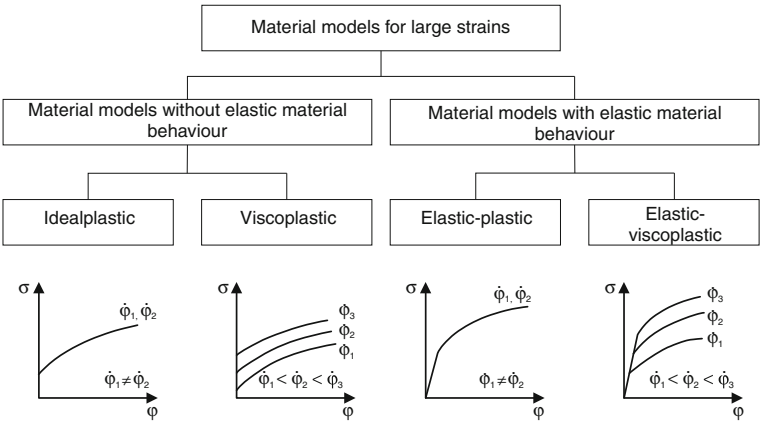


Fig. 2.26 Classification of material models for large plastic deformations [ROLL93]

that take elastic material properties into consideration by regarding the material first elastically and upon further deformation plastically, and those that consider the material as rigid until the plastic limit is reached (Fig. 2.26). The use of a rigid-plastic constitutive law accelerates the calculation and provides satisfactory simulation results for many applications in massive forming, since the amount of plastic deformation compared to elastic deformation is significantly larger [ROLL93]. Elastic-plastic material models are important when elastic effects (such as spring-back and residual stresses remaining in the component) are no longer negligible. The velocity-dependence of the material's properties, such as the "viscous" constitutive laws take into account, plays a role for steel materials mainly in hot and warm forming. Most programs permit the inclusion of temperature-dependence of material behaviour. The consideration of textures and the associated geometrical anisotropic material behaviour is especially significant in sheet forming, but it is growing in importance in massive forming as well with the increasing demands on component quality. Observation of anisotropism in the stress space (Bauschinger effect) is becoming increasingly important as well, especially in massive forming.

2.5.8 Software

Both commercially available FEM packages as well as packages specially tailored for forming processes have become established for process simulation in forming engineering. An overview of such packages can be found in [ADLO04]. These programs offer user interfaces that are adjusted to the needs of forming engineering and make the design and execution of simulations easier for the user. The simplified operability of such specialized program systems usually entails a restriction

on the possibilities of the model's control. So-called "general purpose" systems on the other hand are indeed flexible and can be used for diverse applications outside the field of forming technology, but the modelling process often requires a large amount of experience and a larger expenditure of time. Depending on the application spectrum, the use of different FEM programs by one company is quite common.

Among programs specialized for forming engineering, a distinction is drawn between programs for sheet forming and programs for massive forming. This distinction is the result of various demands that manufacturing processes make on the simulation as well as the possible ways to describe material behaviour.

The decision of whether a problem should be investigated in two dimensions or spatially depends on the problem definition and the dominant state of deformation. Many problems exhibit axis or rotation symmetry, i.e. we can assume a level state of elongation or stress [ROLL93]. By exploiting existing symmetries, the calculation time required can be significantly reduced in comparison to the three-dimensional of an entire component.

2.5.9 Hardware

With the rapid development of the computer industry, processors are becoming continuously more powerful. While a few years ago cost-intensive computer systems were required to carry out calculations with FEM, these days many personal computers (PCs) used as workstations are equipped with the necessary requirements with respect to working memory and processing power for calculating simple calculations. Personal computers for calculating larger problems are already available at moderate prices. To handle very demanding problems with a large number of elements, such hardware can also be used for operation in "clusters". In this case, several computers are networked in such a way that a substantial problem can be calculated on several computers simultaneously. The precondition for this is the support of this functionality with FE software. The computation time for a problem does not become reduced in a linear way with the number of nodes (here: computers) in the cluster. The effective increase in speed depends rather on the hardware and software employed. The behaviour of a specific software as a function of the available processing power is called scalability. A software scales well is the calculation time required for a task is approximately halved when the available processing power is doubled.

2.5.10 Phases of a Finite Element Analysis

From the user's point of view, a typical finite element analysis (FEA) takes place in three phases:

- data preparation with a pre-processor,
- calculation and
- evaluation of the results with the postprocessor.

With the help of the preprocessor, the user provides the software with all information necessary for the modelling of the problem. The problem must be rendered abstract enough for it to be represented with the help of the software. The simplifications made and the quality of the data the user provides to the system have a decisive effect on the quality of the simulation results. As a rule, preprocessing contains the following steps:

- geometry definition,
- networking,
- material data input and
- defining the marginal conditions.

Modern programs are equipped with import filters for common CAD formats. The geometries of the objects involved in the simulation can thus often be taken from the 2D or 3D CAD data sets present in the design in electronic form.

Meshing of the objects (discretization) takes place after the object geometries are defined. For mesh creation, most software manufacturers provide tools that permit a rapid meshing of geometries. If these tools reach their limits, separately available commercial meshers can be used. If several element types are available, then the user can select one. Specialized software packages frequently provide a specific element type. The size and distribution of the elements are determined by the user. The element type and element density of a mesh have a significant effect on the quality of the simulation result. Basically, using a larger amount of elements leads to more precise results. To save calculation time, often adaptive meshes with a locally varying density are used in order better to resolve local gradients in the state variables. Some programs offer the possibility of automatic adaptive remeshing, in which the element density is automatically adjusted to existing gradients.

After discretization, the mechanical and thermophysical material data are inputted. This step requires that the corresponding data is available under the conditions of the simulation. Then the boundary conditions are indicated such as external loads, contact conditions, friction between different objects and velocities.

After calculation, the results are evaluated in the postprocessor. Depending on the software, a number of possibilities are available for representing the results graphically and for further processing. Evaluation of the results also includes the critical judgement of the user. A comparison of the results with experience, roughly estimated calculations or experimental results is essential.

Possible sources of error of FE analysis include:

- discretization errors from the interpolation of the geometry during meshing and interpolation of the state variables,
- faulty input data (e.g. material data, process data, friction conditions),
- numerical errors (e.g. from numerical integration) and

- rounding errors due to the limited accuracy of the floating-point representation in the computer.

2.5.11 The Use of FEM in Forming Engineering

Due to the varying process kinematics and differing focal points in the consideration of the process, many FEM programs are tailored to special processes of massive and sheet forming. Only a few programs are suited to both areas. Due to the geometry of the components and the arising states of deformation, in most cases volume elements are used in massive forming and shell elements are applied in sheet forming. The focus of the evaluation of the results is also significantly different. While in massive forming the material flow and with it the mould filling behaviour, deformability and tool load are investigated, the foci of investigation in sheet forming engineering are deformability (thinning and crack probability), wrinkle formation and spring-back of the component.

2.5.11.1 Massive Forming

In the 1990s, finer and more detailed models have led—hand in hand with increasing processing power—to drastic improvements in massive forming simulation. Commercial FEM systems allow for the calculation of the 3D material flow of a forming level with high precision in a few hours. In the simulation of massive forming processes, the focus on the workpiece side is generally on material flow, mould filling, subsequent grain flow, material hardening, grain structure formation and the deformability of the material. With respect to the tool, the mechanical, thermal and tribological tool stresses and tool flexibility are determined. Several applicable programs for massive forming have thus been established for industrial use in recent years [ADLO04]. The uses of FE simulation and its savings potential can, according to [FELD01], no longer be ignored.

Tool Design

Mechanical Tool Stresses. To calculate tool stresses, the elastic properties of the material must be known. Figure 2.27 shows the die stresses that arise as a result of a lateral extrusion operation for manufacturing a helical gearing. Observation of the stresses induced in the die shows that the maximum principal normal stresses σ_1 can be significantly reduced by prestressing the die. Thus, the maximum tensile stresses are encountered in the non-prestressed die in the area of the tooth base. The tooth base acts as a chamfer on the die and can, in combination with the high tensile stresses, lead to crack formation in this area of the die. After a short period of use, a non-prestressed die exhibits hair cracks in almost every tooth base that

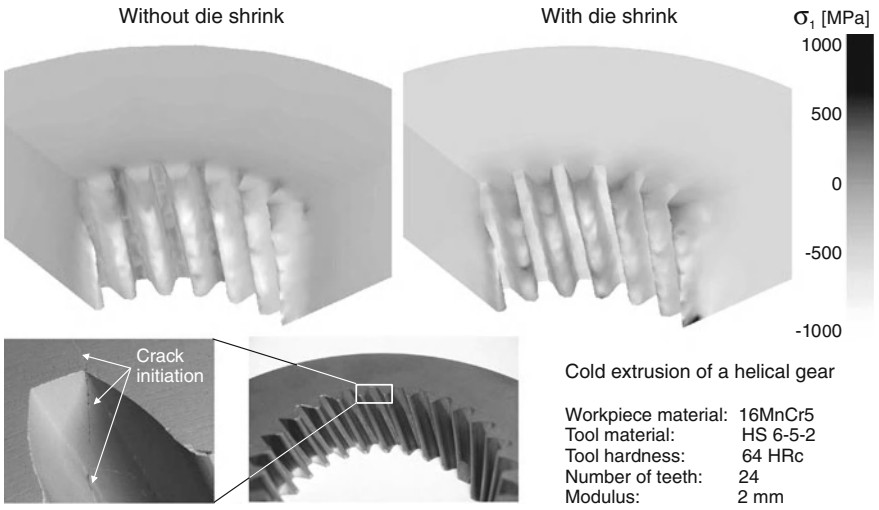


Fig. 2.27 3D simulation of the stresses of a tool die for lateral extrusion of a helical gearing

grow radially and outwardly. Crack formation can be prevented with the help of die prestressing. In that case, the first principal normal stresses in the tooth base of the die may not lie in the positive range (the tensile stress range) when under maximum load by the forming process.

Tribological and Thermal Tool Stresses. The following will show, using the example of fine blanking, how FE simulation can be used to determine tribological conditions like contact stress distribution, the relative velocities of the contact partners and temperature distribution. Analytical considerations can only deliver rough reference values about the order of magnitude of the contact normal stresses to be expected. Thermal processes are very transient, so elementary considerations are not accurate enough to be consulted for correlation with wear processes. Furthermore, the temperatures encountered in fine blanking can only be captured metrologically with great effort, whereby the measurement results are generally unsatisfactory on the whole. The area of interest, in which the danger of adhesion formation is the greatest, is the area directly over the punch edge. It is almost impossible to reach this area with thermoelements. Also, the area affected by high temperature is very small, so there is a large drop in temperature already after tool opening, making a pyrometrical (optical) measurement meaningless at that point. For these reasons, FE simulation makes sense for this process as well. For the example shown in Fig. 2.28, the temperature field has been calculated once with and once without friction. A free friction law was utilized for the friction model, which characterizes dry contact between the friction partners and will be described in more detail in Sect. 2.8.2.3. For the parameters given in Fig. 2.28, the calculated maximum temperatures are equally high for both cases. At the start of the partial cutting process, the contact zone temperatures are not significantly different. At the end, much higher temperatures were calculated for the case with friction. From

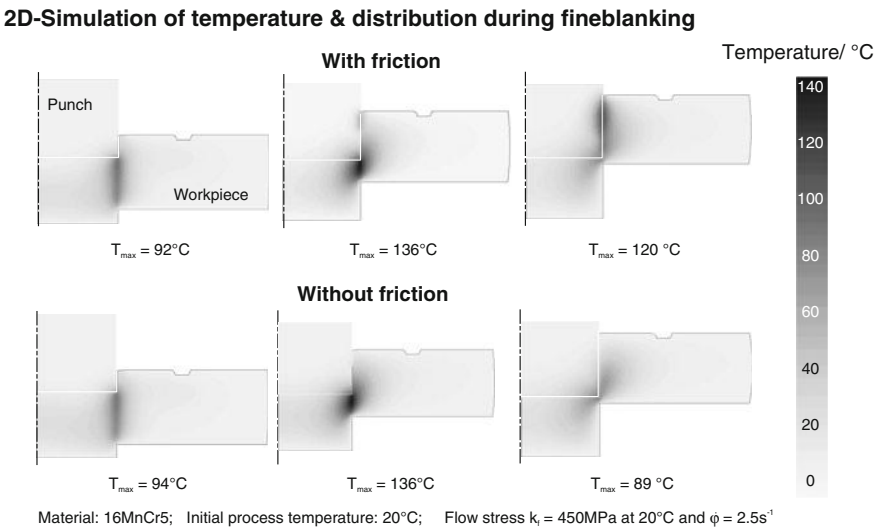


Fig. 2.28 2D simulation of the temperature field during the fine blanking process [RAED02]

these results, we can also derive for the case at hand that the amount of heat created by the forming process is much larger than that caused by friction. This is however not generally the case, but is valid only for the conditions shown in Fig. 2.28.

Workpiece Design

Determining Workpiece Geometries. Fine blanking is a sheet cutting manufacturing process. However, the forming processes taking place in the shape forming zone correspond to those of massive forming. For this reason, fine blanking processes are generally evaluated with the methods of massive forming. Up to the point of final separation of the material, fine blanking is a pure material forming process that is characterized by strong shearing. The heavily localized shearing and surface regeneration result in special marginal conditions of the simulation: The elements on the surfaces and in the peripheral zone near the surface in particular can become considerably distorted very quickly. In order to nonetheless proceed stably with the simulation, meshes must be regenerated frequently, whereby the calculated new information must be transferred to the new mesh. This is generally done automatically.

A special problem is encountered in case of fine blanking of fine contours (e.g. gearings). Here, the material is especially strongly drawn in the cutting direction at the edges at the beginning of the fine blanking process. This phenomenon is called edge draw-in. Edge draw-in is not desirable because it reduces the useful functional surface. It is thus of particular importance in designing the active elements

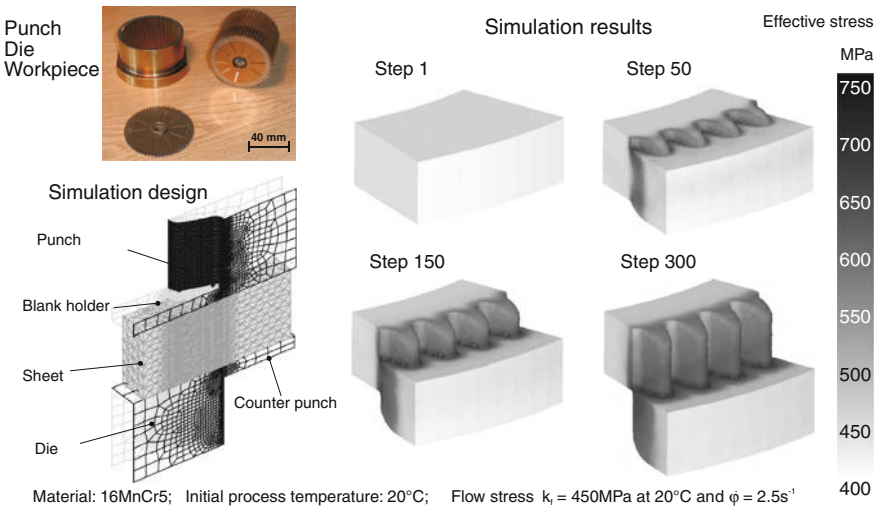


Fig. 2.29 3D simulation of a fine blanking process with respect to the formation of draw-in on the sheet surface [KLOC02a]

of a fine blanking tool [i.e. the punch and pressure pad as well as the die and knife-edged ring (holding-down device)] that the expected edge draw-in be determined beforehand in order to introduce countermeasures via tool design and process design, if required. Figure 2.29 shows the structure of a 3D simulation for the gear fine blanking and the formation of draw-in on the sheet surface. By exploiting the level symmetry of the gear, it is sufficient to model only half of a gear width. The four tool elements concerned have been represented as rigid, while elastic/plastic material properties (constitutive law) were assumed for the workpiece. The numerical results show that the edge draw-in is very distinct on the tip, since the stresses are not sufficient for plastic flow as the cutting process is introduced on the sheet surface. The material is curved near the gear tip due to the relative motion between the punch and the die so that plastic deformation of the gear tip takes place in the direction of the tooth width. In summary, it can be concluded that the simulation of fine blanking is comparable to the simulation of a cold forming process.

Let us consider orbital forging of a wheel hub made of C55E as an example of hot forming. Figure 2.30 shows the simulation of the orbital forging process with the help of FEM. This is an incrementally working forming process in which the contact surface between the upper die and the workpiece is small in comparison to the overall surface and rotates around the workpiece axis with progressive forming. Incremental forming can significantly reduce the forming force in contrast to massive forming. Figure 2.30 shows the stationary lower die and an upper die which carries out a linear feed motion superimposed with a gyrating feed motion. Due to the complex process kinematics, the calculation must be 3-dimensional even is the component being manufactured is rotation-symmetrical.

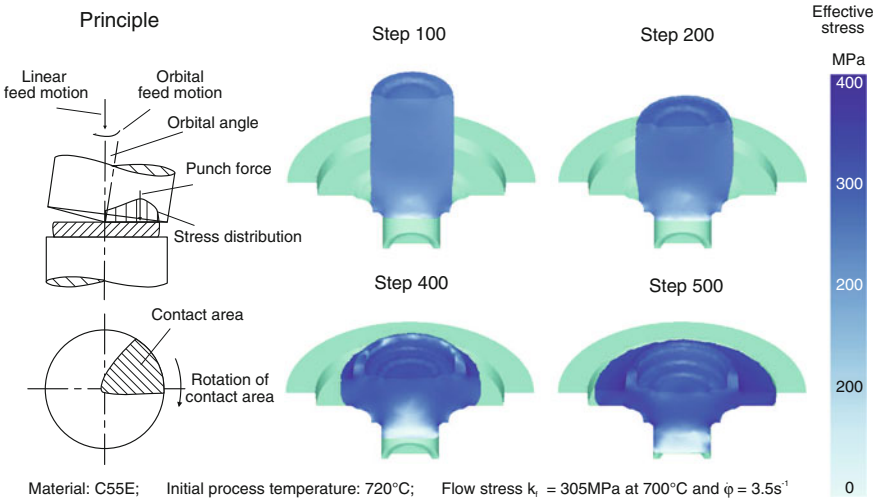


Fig. 2.30 3D simulation of orbital forging

The cut through the main component shows that the effective stresses in the area of the lower pin hardly exceeds the yield stress k_f of the material. This is not the case near the flange, which is well-moulded. Because of such complete mould filling, material flow ceases in the flange area. Despite increased punch forces, the yield criterion cannot be maintained in the area of the pin. Complete mould filling of the pin is not possible with the indicated parameters.

Determining the Sequence of Stages. With the stage sequence the most important working steps in the forming process chain are determined until the final shape is obtained. As an example the forging of an eccentric shaft for a fully variable valve control will be considered here. Figure 2.31 shows the material flow simulation of this complex forging part. Figure 3.55 shows the actual component and the individual intermediate stages. The cylindrical output blank (section) is heated to the process starting temperature of 1,250 °C by means of induction. Since the tooth segment in the centre of the eccentric shaft required a highly inhomogeneous material distribution across the length of the forging part, in the first forming stage a material agglomeration is applied to this area by pre-upsetting. A preforming stage follows and then the finishing stage. In the finishing stage, the final contour of the eccentric shaft is obtained with the forging measurements to a large extent. Since almost complete mould filling is already realized in the pre-stage, the finishing stage serves primarily again to reduce the tolerance width and to compensate for any dimensional deviations resulting from tool wear in the pre-stage. Comparison of the simulation results with the real component in Fig. 3.55 shows that the simulation represents the process well, which also manifests itself in the reduced flash formation. In this way, simulation can help realize a sequence of stages with an optimal use of material.

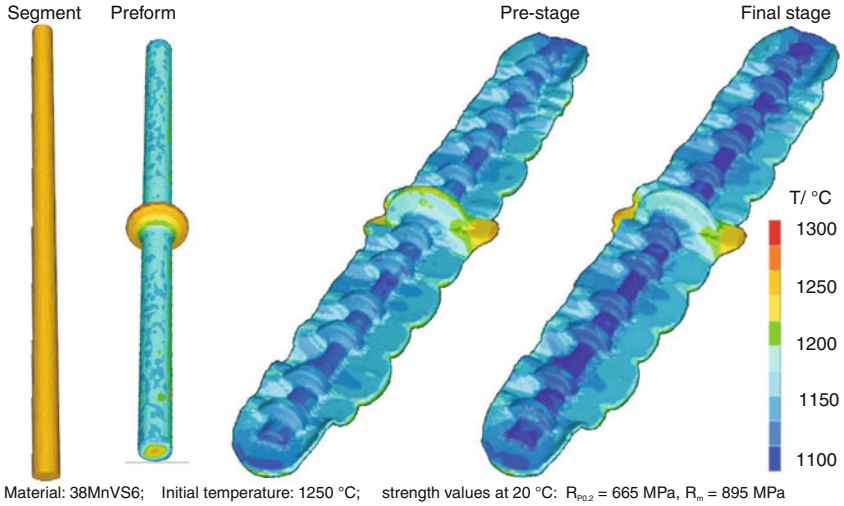


Fig. 2.31 3D FEM material flow simulation for the forging of an eccentric shaft in three stages (*Source* Hirschvogel Umformtechnik GmbH)

FE simulation can also be used to help calculate the obtainable component quality of a laterally extruded spur-toothed gear, in which case both procedural principles of radial lateral extrusion and "divided flow" are employed. The top row of images in Fig. 2.32 shows the first forming stage, in which a ring-shaped punch introduces divided flow in both axial and radial directions.

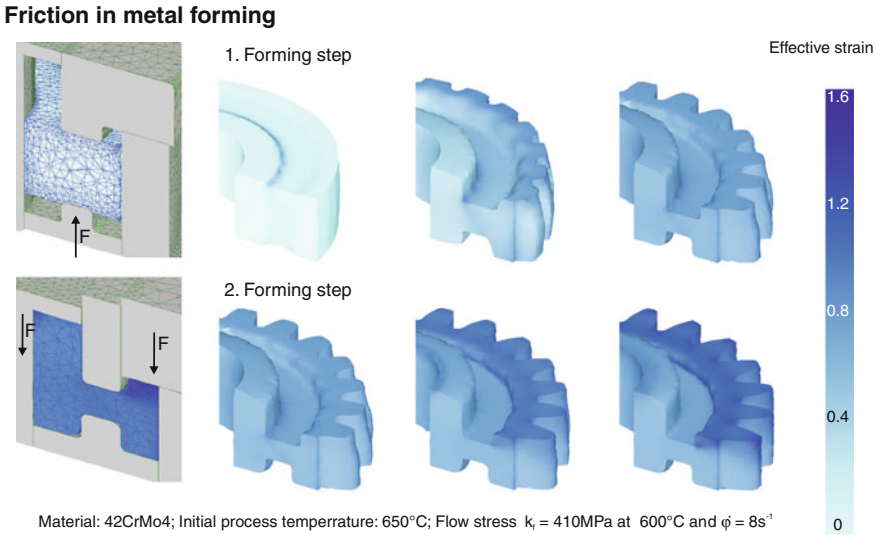


Fig. 2.32 3D simulation of the lateral extrusion of helical spur gears in two stages with the procedural principle of "divided flow"

In the internal component area, there is a flow of material in the axial direction, and in the external component area, the flow is in the outward direction. In the first forming stage, radial material flow is not sufficient enough to provide a complete material filling of the teeth. Thus, in the second forming stage the material is pressed radially outwards in the axial direction into the tooth mould and radially inwards by upsetting the external gear area. In this way, the tooth shape is formed along the entire width of the tooth.

Both examples show that FE simulation is an important aid in designing individual forming stages in massive forming. If the designer recognizes problems in the simulation calculation, many ways to intervene are opened up. On the one hand, the final result can be affected positively by varying the feeding positing into the cavity. On the other hand, it may be necessary to change the tool geometry of the corresponding forming stage. Changing the previous forming stage would be much more difficult and is not at all desirable. Attempts are thus being made to determine the individual stages of forming proceeding from the geometry of the finished part via reverse simulation. A definite prediction of material flow is absolutely necessary here, since it would be otherwise impossible to determine the individual forming stages [BEHR04a].

Modelling Heat Treatment Processes. During heat treatment, many mutually influential thermal, transformation-related and mechanical processes take place simultaneously. This affects the input data required for the simulation of heat treatment. Besides temperature-dependent elastic and plastic material behaviour, one must also possess information on structural transformation (e.g. TTT and TTS diagrams), diffusion coefficients, carbon distribution as well as carburizing and diffusion times. Many of these variables are difficult to determine or are highly imprecise. This is especially true when the mutual dependence of the processes on each other has to be taken into consideration. For this reason, the determination of these material data is usually very difficult and costly, and such calculations are usually undertaken only for especially sophisticated components. Figure 2.33 left shows martensite formation on the tooth flanks of a bevel gear made of carbon-manganese steel, which forms when cooling from an austenitizing temperature of 850 °C to room temperature. Oil is used as a cooling medium.

The right side of Fig. 2.33 shows a grain size distribution adjusted to the recrystallization behaviour of the material when hammer forging a low-pressure compressor disc made of Inconel 718. Grainsize plays an important role in components subjected to high thermal and mechanical loads, whereby an opposing tendency can be recognized. With a diminishing grain size, the strength of the material increases, but the creep strength is reduced [GOTT98]. In turbine components, the attempt is made to use different grain sizes for different component areas. This can be done by means of a focused thermomechanical design of the forming process that is inhomogeneous along the cross-section of the component.

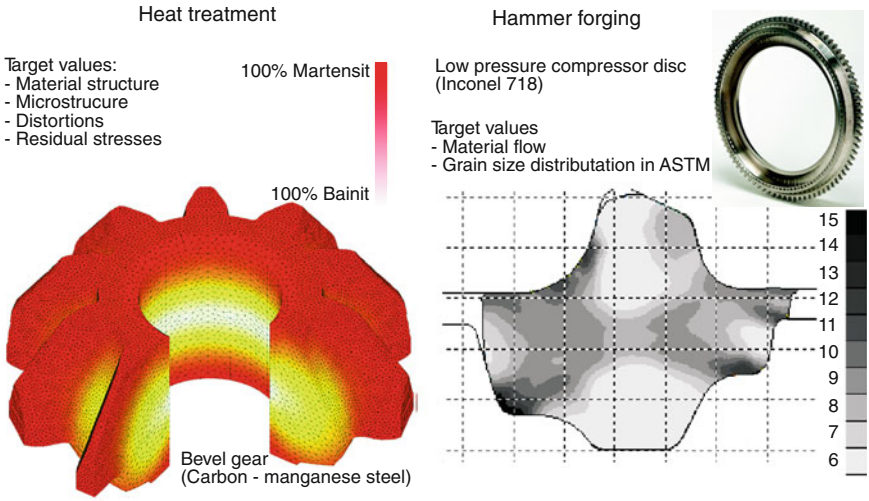


Fig. 2.33 Modelling heat treatment processes—*left* calculation of martensite formation on a bevel gear caused by heat treatment (*Source* SFTC); *right* calculation of the grain size distribution for the hammer forging of a low-pressure compressor disc (*Source* MTU Aero Engines und Thyssen Umformtechnik GmbH)

2.5.11.2 Sheet Forming

The focus of FEM development in the area of sheet formation has been in feasibility studies of particular forming operations. In addition, the crash behaviour of automobiles has been the subject of analysis since the end of the 1980s. In the latter case, the centre of attention is on the deformation of body parts, which are almost exclusively sheet forming parts. Figure 2.34 shows an example of such a FEM crash simulation.

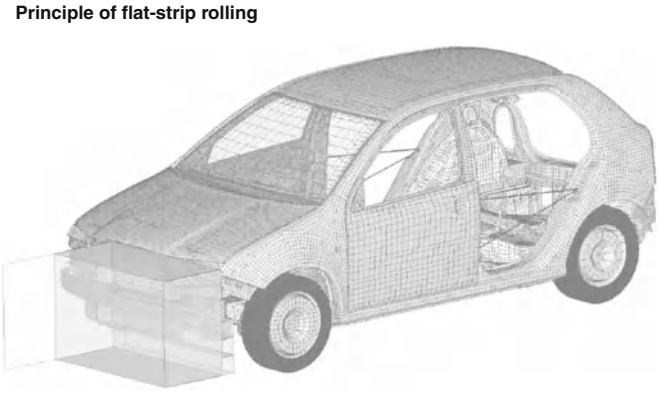


Fig. 2.34 Structure of a crash simulation with the program Pam-Crash by ESI GmbH

Due to the development of the automobile industry, the largest user of FEM simulation in the area of sheet forming, specifications have also been adjusted to modern simulation technology. With the help of FEM, concepts can be tested for their feasibility in the production process already at an early development stage. This leads to shorter product cycles with correspondingly short development times overall.

At the same time, growing environmental consciousness has led the automobile industry to develop fuel-efficient vehicles based on lightweight designs. Motor vehicles should be both light and safe. With an eye to this goal, new materials have been developed not only for components and body parts but for interior equipment as well. The industry is now using aluminium alloys and new steel types such as DP, CP and TRIP steel, the capability of which lies far above the range of earlier steel types (see Sect. 2.7.1.1). Components made of these materials can only be implemented in forming simulation with a high degree of precision.

The uses of present-day FEM simulation in the area of sheet forming are concentrated on deformation prediction. With the help of common software tools, usually feasibility analyses of different sheet metal geometries are undertaken. Of particular importance is recognizing and predicting material thinning. Such effects during the deep drawing process lead to weak points in the component, increasing the danger of failure. Besides thinning, material agglomeration along the component geometry also occurs frequently. With the right process design, the areas in which thinning occurs can subsequently be supplied with sufficient material, while the material can be used more effectively in those areas in which agglomeration takes place [FRIE02]. Figure 2.35 shows an example of the simulation of sheet thickness alteration in the mudguard of a passenger car.

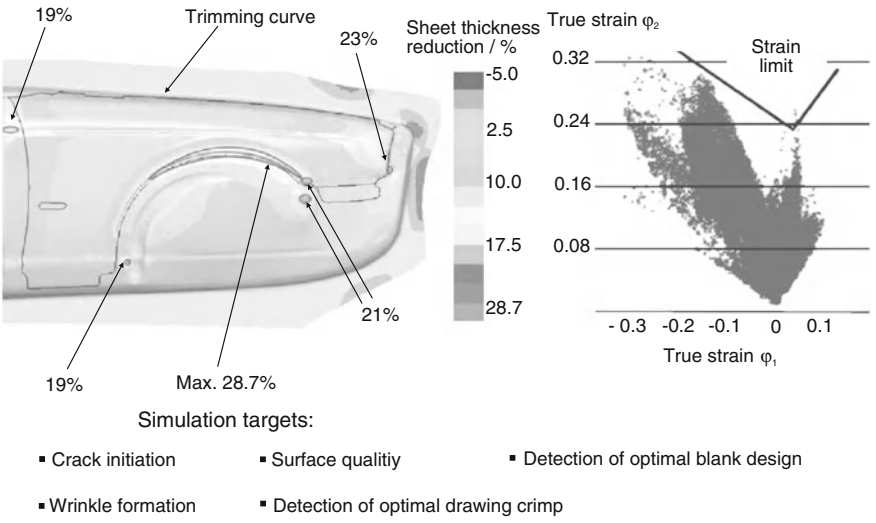


Fig. 2.35 Simulation of a mudguard with calculation of sheet thickness change and local true strain with respect to cracking (*Source* Thyssen Nothelfer GmbH)

Material flow is predominantly controlled in sheet forming with the help of drawbeads (Sect. 4.1.2.1). These can be designed and constructively adjusted for the load case at hand with the help of FEM. In this way, the sheet forming process can be optimized already, without taking geometrical component changes into consideration.

Wrinkle formation during the process is an important influencing parameter in sheet forming operations. It is especially important in the outer skin of body parts that no wrinkling occurs, as it remains visible even after finishing. Moreover, wrinkling can also produce weak areas in the component leading to failure under strain. For these reasons, wrinkles must be avoided—see Sect. 2.7.1.1 for more on this subject.

In most cases, shell elements are used in sheet forming simulations. Variation in material thickness during the process is calculated using shell elements by means of special algorithms. If volume elements are used, the actual change in sheet thickness can be calculated more accurately. However, a volume element has more degrees of freedom than a shell element, leading to an increase in calculation time. In the last several years, further development in the computer industry has made it possible to increase the element numbers or element information used without slowing down the simulation. For this reason, the use of volume elements is on the rise [WU00]. In sheet forming, the use of shell elements is sufficient in most cases however, since sheet thickness change is desired in only a few processes [KUBL95].

One of the greatest problems is calculating the springback that occurs after a forming process. It is essentially caused by free bending and is difficult to calculate beforehand. This problem is currently still under investigation.

Besides complete calculation approaches, partial approaches are also used in sheet forming in order to answer specific questions:

1. Cross-Section Simulation

In cross-section simulation, the complete component is not considered, but only the cross-section presumed to be in danger. The durations of the simulation is drastically reduced by considering only a part of the entire workpiece.

A further advantage of investigating only a single cross-section is that it enables the reduction the required input data. Only the data required in the cross-section being considered and not the exact definition of the entire component are necessary to obtain an executable simulation.

The disadvantage is that the cross-section to be investigated must be selected such that it also illustrates the effects that are to be analyzed. The correct selection of the cross-section is not trivial, and there is also the danger that the effects to be analyzed do not arise in the selected cross-section. Also, investigating only a small cross-section of the entire forming problem involves a large amount of simplification. This simplification allows mostly for qualitative and only rarely quantitative predictions using the obtained results.

2. One-Step Simulation

One-step simulation is used for inspecting geometry. With the help of this simulation, feasibility analyses can be carried out quickly and efficiently without

the necessity of long calculation times. The only crucial factor for the calculation is the change in geometry from the blank to the component. With the reverse method, the sheet cut required for the forming operation can be determined. In the forwards direction, the amount of true strain can be estimated from the change in geometry. Stress on the workpiece beyond its deformability limit can thereby be determined and prevented at an early development stage.

By calculating the phenomenon to be investigated in only one simulation step, calculation time is significantly reduced. In this case too, the specifications of the input data are normally not as high as in full simulations. In this way, it is possible to obtain valuable results quickly. Example of the use of this procedure include the initial feasibility estimations in product creation. A detailed consideration of the overall process is not possible with this method however.

2.6 Metallography and Analysis

2.6.1 Introduction

Metallography is the investigation of grain structure for the sake of qualitative and quantitative description. Structural investigation permits inferences regarding physical, chemical and mechanical properties of a material. The required microscopic analytical methods are applied to forming tools and unformed components during development and current quality control in the manufacture of forming parts as well as in the clarification of damage cases.

Grain structure is characterized by size, shape, distribution and volumetric content of the phases. Qualitative or quantitative evaluation of structure provides information regarding phase boundaries, precipitations, segregations, grain size distribution, lattice defects, deformation structures and their regeneration and recrystallization. Information regarding cracks, pores and other irregularities can also be obtained.

The most important methods and devices in metallography will be briefly described in this chapter from the standpoint of the manufacturing engineer. Using practical examples, the possibilities of metallography in manufacturing technology will be shown both in general and in the field of forming engineering specifically. The relevant literature will be referred to at corresponding locations for more in-depth study. An extensive treatment of the topic with ample reference to praxis can be found in [SCHU04b].

2.6.2 Optical Microscopy

For metallographic investigations, visible light with a wavelength between 350 and 780 nm is the most relevant. Here, the wavelength represents the limiting factor for the maximum resolution in light microscopes. The obtainable depth of sharpness is less than one in the case of a magnification of 1,000 depending on the aperture of the lens system [DOMK86, SCHU04a].

Only reflected-light microscopes are used for metallurgical optical microscopy. As opposed to the transmission electron microscope (medicine), only the reflected light beams enters the tube and can be captured by the human eye or by cameras or optic sensors (digital cameras). Figure 2.36 shows examples of micrographs taken with a reflected-light microscope at relatively low magnifications.

The contrast between different metallographic constituents arises from the varying reflecting power of individual constituents (light absorption, index of refraction, roughness/reflexion angle [DOMK86, SCHU04a]). Since the refraction/reflexion power of metals is very similar, in most cases different measures must be applied to increase the contrast such as etching, multiple reflection through vapour deposit coatings etc. [DOMK86, PETZ94, SCHU04a]. The individual methods are treated in Sect. 2.6.5 in more detail.

Methods of quantitative structural analysis are used for a more exact characterization of metallic materials [EXNE86, SCHU04b]. These yield structural characteristic values that describe things like the volumetric percentage, size, distance and orientation of individual phases and metallographic constituents. To this end, diverse arithmetic and metrological processes can be used, including comparative methods with rating charts.

2.6.3 Microhardness Testing

Besides the traditional hardness testing methods of Rockwell, Brinell, Knoop and Vickers, which are carried out using relatively large test loads, testing methods with extremely small test loads are practical for conducting tests on metallographic specimens. The Vickers test according to DIN EN ISO 6507-1 thus distinguishes between the Vickers hardness test, Vickers small load hardness test and the Vickers microhardness test [ISO04a]. The latter is suitable for use in metallography [SCHU04b]. The test loads in this case are between 0.09807 and 1.961 N (0.001–0.2 kp). The designation of the determined value depends on the test load (e.g. HV 0.2 corresponds to a test load of 1.961 N). Should the application require an especially low indenter penetration depth, often a Knoop pyramid is used instead of the Vickers pyramid [SCHU04b].

With the help of microhardness measurements, high-resolution hardness profiles can be obtained along the cross-section of metallic samples in addition to measurements of finely structured surfaces or thin layers. Depending on the grain

size of the metallic sample to be investigated, hardness differences between individual grains can also be determined. In the case of coatings, this is also the only method with which hardness and the modulus of elasticity can be established (see Sect. 2.8.5.3).

In many applications, microhardness testing is used to investigate the hardness gradients in the peripheral zone of components. Figure 2.36 shows two typical examples. On the left is the etched cross-section through the area near the surface of a forged and induction-hardened component made of 100Cr6. After exposure of the etched specimen, on which the effective hardening depth can be clearly recognized (change in colour), the sample was repolished and numerous microhardness impressions with a test load of 1,000 mN were made (corresponding to HV 0.1). In this way, the hardness of the peripheral layer can be quantified for quality control purposes (see Fig. 2.36 left).

The second example shows the loss of hardness in the peripheral zone of a sample from the intersection between the impression and die land of an overheated and plastically deformed die (see the SEM image, Fig. 2.36 top right). Here, the hardness measurement was utilized for damage analysis. The die is a forging die made of plasma-nitrided hot-working steel X 38 CrMoV 5-1. The hardness of the nitrided layer, which is completely worn out after damaging, can be seen clearly in the diagram in Fig. 2.36 right (in the microgram in Fig. 2.36 no longer recognizible).

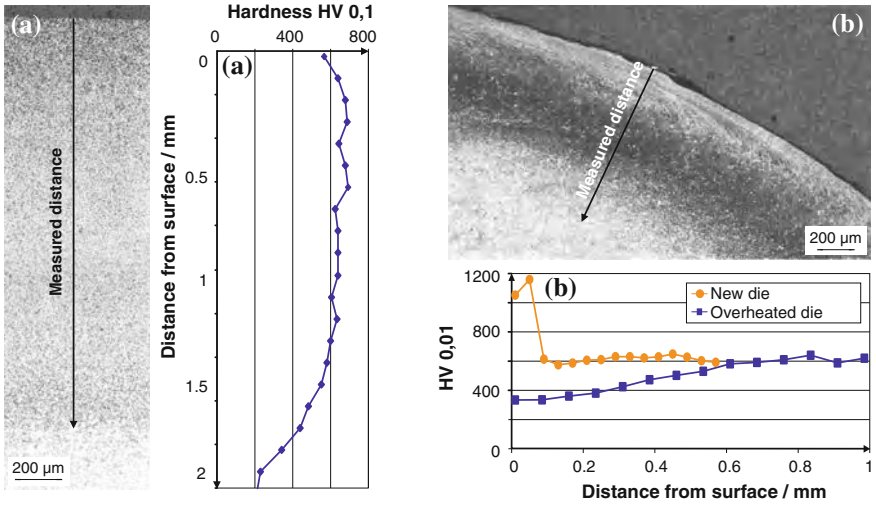


Fig. 2.36 Examples of optical micrographs of etched metallographic specimens and associated depth profiles of microhardness acc. to Vickers. **a** Sample taken from the surface of a forged induction-hardened and ground component made of 100Cr6, magnified 100x. **b** Sample from the intersection between the impression and die land of a significantly overheated, plastically deformed forging die made of plasma-nitrided hot-working steel X 38 CrMoV 5-1, magnified 50x

2.6.4 Electron Microscopy

As opposed to optical microscopy, which works with visible light, in electron microscopy electrons are sent in high vacuum ($<10^{-3}$ mbar) through/on the preparation, where they are diverted in different directions. Detectors capture the electrons generated through various interactions and convert them into electric voltage. Amplified and modulated, a visible light spot is created on a screen. In this way, the electron beam gradually scans the surface area to be displayed.

The object under investigation must be subjected to a suitable preparation technology and be completely free of water. Depending on whether the electrons scan the surface of a preparation or penetrate it, it is distinguished between scanning electron microscopy (SEM) and transmission electron microscopy (TEM) (Fig. 2.37).

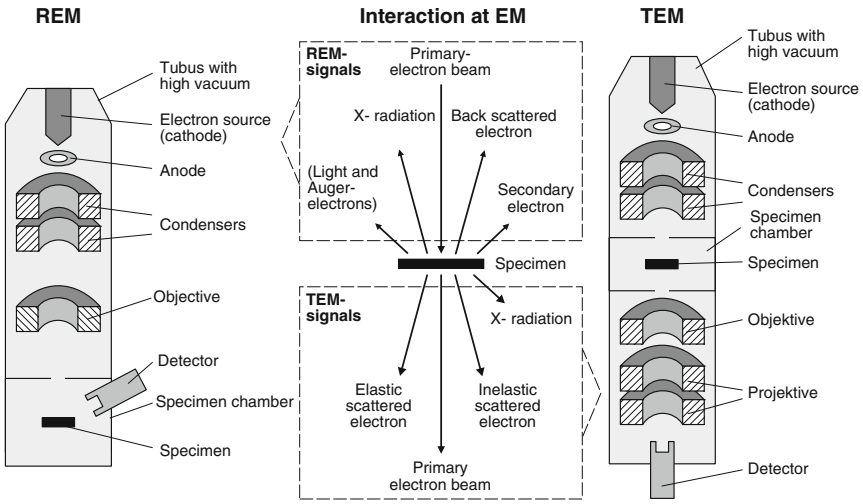


Fig. 2.37 Simplified diagram of SEM and TEM as well as the interactions between the electron beam and the sample

To create the image, signals are used that arise in the interaction between the electron beam and the preparation. Figure 2.37 right shows these signals, whereby the illustration above the sample represents signals significant for SEM. Under the sample are those signals that are used for TEM.

2.6.4.1 Scanning Electron Microscopy

Introduction. With the scanning electron microscope, it is possible to scan a surface by means of a highly focused beam of electrons. As opposed to the magnification of an optical microscope (maximum ca. 1,000 times), a very large

range of magnification is possible with the scanning electron microscope, between 10 and 150,000. The resolution amounts to a few nm, which corresponds to the size of large molecules. Since lenses are superfluous, associated deficiencies (highly limited depth of sharpness range, distortion) are avoided. One can thus obtain very plastic images of the geometrical surface configuration of the sample, which permits both the representation of coarse, gorge-like structures and the recording of very fine details in a nanometer range. Figure 2.38 shows an example of an image of a cemented carbide structure in the cross section through the surface of a forming tool. Here, we can observe a washing out of the cobalt binder phase, which can subsequently lead to chipping.

SEM is suitable for depicting surface configurations from the millimeter to the nanometer range, for looking for structural anomalies and damage to component surfaces and cross sections, such as corrosion islands, wear etc. Furthermore, it serves as an ideal search monitor for EDX analyses (see Sect. 2.6.4.3 and Fig. 2.38 right).

Structure. The scanning electron microscope has the following structure (Fig. 2.37 left) [SCHM94]:

- Electron generation system, consisting of a tungsten thermionic cathode from which electrons are emitted, a control cylinder (Wehnelt cylinder) and an anode. The electrons are accelerated by the electrical voltage between the cathode and the anode.
- XY deflexion system for producing a line raster.
- Electromagnetic lens system, consisting of two condenser lenses and a final lens (objective lens), which sharply focuses the primary electron beam, as well as several spray blinds.

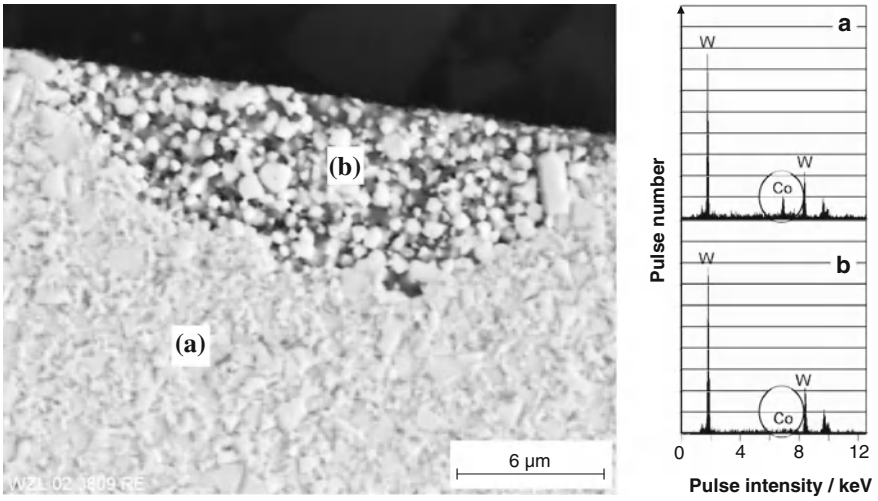


Fig. 2.38 Scanning electron microscopic image and EDX analysis of a metallographic specimen perpendicular to the surface of a damaged cemented carbide forming tool **a** undamaged matrix, and **b** structure of the damaged spot (cobalt washout)

- Secondary electron detector, which registers the secondary electrons accelerated away from the sample upon impact of the electron beam. There are also other detectors: RE detectors register backscatter electrons, EDX detectors register X-rays (Sect. 2.6.4.3). Different detectors are used depending on the method of application.
- One or more monitor screen to display the observation area.
- Electronic signal processing, which controls the brightness of the corresponding light point on the monitor.
- Raster generator, which synchronizes the XY deflexion system of the SEM tube and the monitor.
- Sample chamber, into which the preparation can be housed.
- Vacuum pumps, which create a high vacuum ($<10^{-3}$–10^{-8} mbar) in the EM tube.

The electron microscope tube and the monitor work analogously and in correspondence, but they are two separate units.

Functionality. As a rule, the entire process of microscoping takes place in high vacuum, in order to prevent interactions with atoms and molecules in the air. The electrons are generated with a tungsten hot cathode in the Wehnelt cylinder and are concentrated to a saturated electron cloud.

By applying high voltage (1–30 kV) between the cathode and the anode, the electrons are formed out of the electron cloud into a beam. The electron beam thus generated is then deflected and focused with the help of magnetic coils. These magnetic coils serve as lenses (two condenser lenses, 1 objective lens), i.e. they focus the electron beam. The final lens of the multi-stage condenser lens system, consisting of a stigmator and a multi-stage deflexion coil system, is frequently referred to as an "objective". In addition to beam focusing, XY deflexion also occurs here with the help of deflexion coils, with the help of which the object is scanned. Deflexion is controlled by a raster generator and takes place synchronously both in the EM tube and on the monitor.

If the electron beam strikes the sample surface, the electrons are then decelerated. They release kinetic energy to the sample. In this way, secondary electrons are detached from the sample surface (Fig. 2.37). By analyzing this, especially the topography of the surface becomes visible (topography contrast). Furthermore, backscatter electrons can be analyzed, which are diverted by attraction to the positive atomic nuclei and accelerated back. This gives them an energy that is characteristic of the material of the atomic nucleus, which is why the corresponding image presents different materials at varying brightness levels (material contrast). While light materials appear dark, heavy materials are bright. Further signals include x-rays, light impulses and "Auger electrons" (Sect. 2.6.4.3).

2.6.4.2 Transmission Electron Microscopy

In contrast to the much more frequently used SEM, which structurally resembles a reflected-light microscope, transmission electron microscopes (TEM) can radiate electrons through solid bodies [SCHU04b]. This method is especially practical for showing crystal defects and the finest structures in the nanometer range. It is used in particular to investigate precipitation and recrystallization processes in steel. Magnification can extend to up to 800,000 times the normal size. Details of a few tenths of a nanometer can be resolved. Figure 2.39 shows examples of images from TEM.

The structure of TEM is very similar to SEM, whereby additional projective lenses and an objective lens below the sample are required in addition (Fig. 2.37). Furthermore, TEM is generally equipped with a much stronger radiation source than SEM. This is why the acceleration energy of the generated electron beams amounts to several hundred keV.

Even when most of the electrons pass unaffected through the sample, numerous interactions between the primary beam electrons and the sample atoms occur, which contribute to the generation of the TEM image (Fig. 2.37 right). Elastically scattered electrons are electrons that interact with the atomic nuclei of the sample. These electrons are scattered at a large angle and do not lose any energy. Inelastically scattered electrons interact with the electrons of the sample atoms and so exhibit energy loss, but they are scattered at small angles.

TEM generates a transmitted light electron image of a very thin sample. Ultrathin cross-sections with thicknesses of <100 nm are required. For this, a very costly, high-precision technology is necessary (Sect. 2.6.5.1). In the case of a standard bright field image, as many electrons of the electron beam as possible have to be able to penetrate the sample. The quality of the image depends not only on the microscopy process used and the quality of the beam, but also on the quality on the sample preparation in particular. Image capture is currently almost exclusively digital.

In every transmission electron microscope, one can produce—in addition to structural images—so-called diffraction images. These contain information about the lattice structure and lattice constants of the sample material. If electrons strike a crystal, Bragg diffraction occurs [SCHU04b]. From the diffraction images, we can draw conclusions about the crystal structures at hand. If it is a polycrystalline substance, the electron beam that makes contact with the preparation is diffracted into different directions according to the structure and orientation of the individual crystals. “Debye-Scherrer rings” are formed. If we limit the diameter of the primary beam with a blind on a small section of the sample, then the electrons are only diffracted on a few monocrystals. As a result, the points of the diffraction rings are reduced in correspondence to the different crystal orientations (Fig. 2.39 bottom left). In the case of a monocrystal, we can then only recognize single, sharply differentiated points, as is shown in Fig. 2.39 (bottom right) using the example of a clearly monocrystal carbide [RAED02].

In summary, TEM is particularly suited to the following problems:

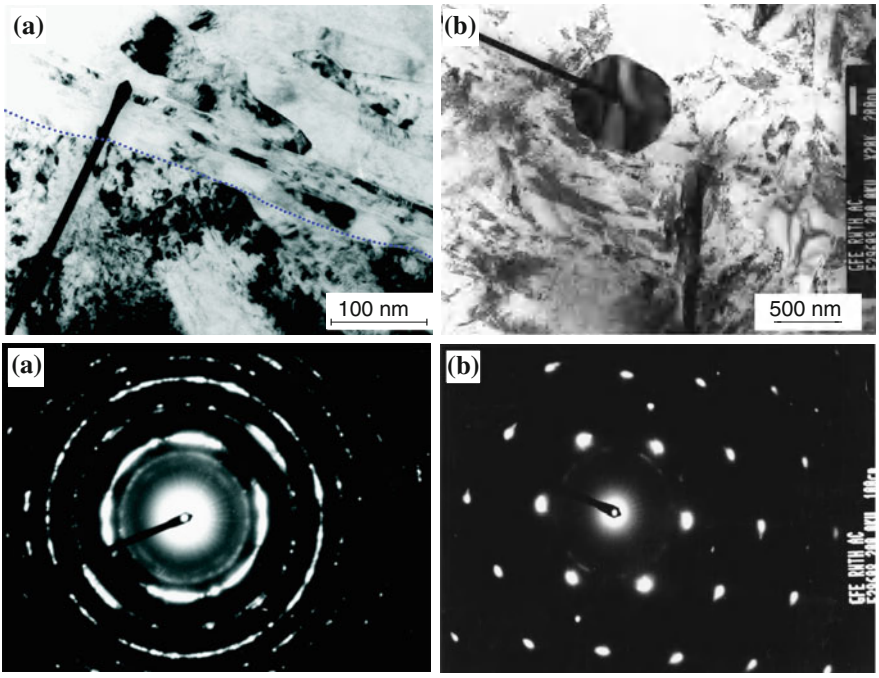


Fig. 2.39 Examples of transmission electron microscopic (TEM) images and associated TEM diffraction images **a** smeared workpiece material 16MnCr5 on a forming tool made of powder-metallurgical HS-PM 6-5-3, and **b** visibly monocrystalline carbide in the matrix of HS-PM 6-5-3 [RAED02]

- detection, illustration and analysis of precipitations (>5 nm), Fig. 2.39 top right,
- illustration and analysis of crystal faults such as displacements, stacking faults and boundary laters in general, Fig. 2.39 top left,
- chemical composition of precipitations and phases (>5 nm) with the help of EDX analysis (Sect. 2.6.4.3) and/or electron area diffraction, Fig. 2.39 bottom.

2.6.4.3 X-Ray Microanalysis

In the case of chemical analysis with x-ray microanalysis, the sample is fired with a very finely focused beam of high-energy electrons such are used to create images in SEM or TEM devices [HANT94]. These electrons sometimes penetrate deep into the sample and can interact with the shell electrons of the sample's atoms, which can initiate many different processes.

Among other things, the electrons release x-rays (Fig. 2.37). A distinction is drawn here between x-ray braking radiation and characteristic x-rays. In the latter case, the energy of the ray is characteristic of the atom from which the x-ray quantum was emitted. The characteristic ray can be detected with a semiconductor

detector in both SEM and TEM. The term used is "energy dispersive x-ray spectroscopy" or EDX [HANT94, SCHU04b]. Less common is the use of crystal lattice spectrometers that use a different kind of evaluation called wavelength dispersive x-ray spectroscopy (WDX).

In the case of EDX, the x-rays are subdivided with an energy spectrometer (multichannel analyzer) according to energies. The respective radiant energy thus becomes an index for the atom type, while the number of evaluated impulses per chemical element represents a measure for its concentration (Fig. 2.38). In the case of SEM analysis, one must bear in mind that the location of the measurement reaches from the surface into the inside of the sample and covers an area of 1–10 μm depending on the material. Moreover, it needs to be taken into consideration that the energetic resolution is relatively low in comparison to other methods. Thus, the signals of single elements intersect, which can lead to mistakes. Detection of light elements (carbon, oxygen) is difficult and quantitatively uncertain. In summary, from an EDX or WDX analysis we obtain:

- Qualitatively: type of elements and laterally resolved distribution in the sample. Depending on intent, point, line and area scans are possible. Clear-cut identification of elements is sometimes difficult.
- Quantitatively: concentration of elements (with a corresponding statistical evaluation of the energy impulses detected).

2.6.5 Preparation Methods

2.6.5.1 Sampling and Embedding

The removal and preparation of metallographic samples should be adjusted as much as possible to the purpose of the investigation [SCHU04b] (lateral/longitudinal cross-section etc.) and should also avoid any structural changes resulting from excessive heat or deformation [PETZ94, SCHU04b]. To separate a sample from a metallic component, in principle all separation methods are conceivable [PETZ94]. As a rule however, the sample is removed by means of special cutting devices that work according to the principle of plunge grinding. Here, the component is affixed and cut with a quickly rotating disc. The disc material depends on the material to be cut. Also, spark-erosive cutting, also called electrical discharge machining (EDM), is ideal for more precise cuts—see Volume 3 of this series, "Electrical Erosion and Hybrid Processes".

To improve handling of the removed sample, they are either cramped or embedded hot or cold in plastic, depending on the size of the sample and the application case [PETZ94]. For cold embedding, two substances, an uncrosslinked polymer and a catalyst, are mixed to a liquid or paste and poured over the sample, which is lying in an embedding mould, where the embedding medium polymerizes and hardens. The advantage of cold embedding includes faster applicability and

low costs. In the case of hot pressing into special embedding presses, the sample is completely surrounded by plastic granules that fused under the influence of increased heat and high pressure. The advantage in this case is the improved bond between the sample and the embedding medium. In both cases, the result is a cylindrical, easily manageable sample that can be further prepared in the following step on the front face.

Sample removal for TEM studies represents a special case. Since the samples for TEM have to be extremely thin (<100 nm), special techniques are required that permit major thinning of the material. Recently, the FIB method (focused ion beam) has become established, in which the sample is cut with a heavily focused ion beam, resulting in thin lamellae [ENGE02, GIAN99].

2.6.5.2 Grinding and Polishing

To render the grain structure visible, an extremely smooth, generally polished surface is required. First, the depth of the faulty surface layer (e.g. thermally influenced or plastically deformed during sample removal) is reduced by gradual grinding until the actual structure is recognizable [DOMK86, PETZ94, SCHU04b].

The sample is ground with an aluminium oxide abrasive paper (Al_2O_3) on rotating discs. The sequence of abrasive papers is customarily 180, 240, 320, 400, 600, 800, 1,000. The size of the number stands for the finesse of the grain, not the grain size. It is defined by the number of meshes per square inch screening surface when screening the abrasive material.

After every grinding process, the sample is cleaned, rotated 90° and ground further in the same direction. In this way, grinding grooves from the previously used paper are removed. In modern, metallographic grinding devices, the samples are not manually pressed against the paper, but are clamped in special devices that also take over the function of rotating the sample. Sometimes even fully or semi-automatic grinding machines are used that can take over all grinding, polishing and cleaning steps autonomously.

Polishing removes the grinding grooves remaining from the grinding process. Diamond paste or diamond suspension (with a grain size of 15, 6, 3, 1 μm) applied on velvet or wool cloths serve as the polishing agents [DOMK86, PETZ94]. Formerly, de-mudded aluminium oxide (Al_2O_3), green rouge (chromium oxide) (Cr_2O_3) and other abrasive substances were utilized.

2.6.5.3 Contrasting

In the polished state, pores, cracks, cavities and other such things can be recognized under the microscope. One can also easily recognize many non-metallic inclusions since these generally have a different reflectivity than metals—e.g. graphite in cast iron or precipitations in Al-Si alloys [SCHU04b]. However, in order to render differences in the microstructure visible, contrasting methods are

still required that are adjusted to the application case. Therefore, a variety of preparation and etching formulae are available for metallic and ceramic materials as well as for plastics [PETZ94].

A distinction is drawn between contrasting without changing the polished surface (optical contrasting methods) and contrasting with a change of the polished surface (chemical and physical contrasting methods) [PETZ94, SCHU04b]. Optical methods make use of the interaction of the incident light and the ground metallic surface. This requires a specially equipped reflected-light microscope. In the case of electrochemical and physical methods, the polished surface is treated further. The term etching is also used in this context. What both methods have in common is that they amplify the difference in reflectivity of various structural components. This is done either by creating a variously strong oxide formation and/or by setting back individual structural components (relief formation) so that they become visible under the microscope.

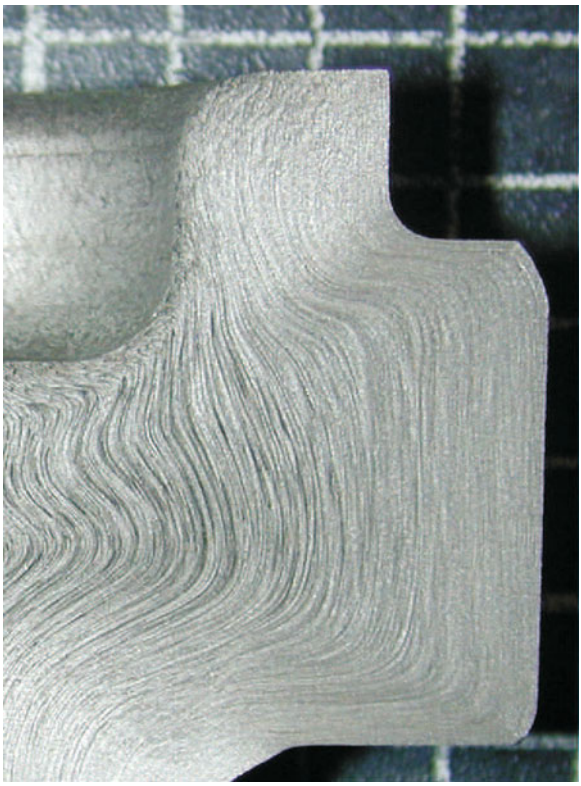


Fig. 2.40 Cross-section through part of a cold-formed gear shaft made of case hardening steel 16MnCr5, etching agent: lukewarm to boiling hydrochloric acid (*Source* Hirschvogel Umformtechnik GmbH)

The "classic" etching process is dip etching. It makes use of etching agents that act purely chemically and act upon different structural components with various levels of intensity.

We distinguish between macroetching and microetching. Macroetching is meant to provide a complete overview of segregations and primary structure (Fig. 2.40). The magnifications involved in such evaluations are in the area of 1:1–30:1. In the investigation of microetched surfaces, magnifications of 50:1–1,000:1 are used. The purpose of microetching is the development of the microstructure. In the following, several details concerning macroetching will be described since these are typically used in forming technology. The best-known macroetching process is "Oberhofer etching", in which the sample is held at room temperature in an etching agent composed of distilled water, ethanol (96 %), hydrochloric acid (32 %), copper(II) chloride, iron(III) chloride and tin(II) chloride [PETZ94].

In this etching method, segregation-free areas appear dark, while segregation areas are unaffected. In this way, the "fibre structure" of a component becomes quite visible, which makes it interesting to forming engineers. Formed components (such as crankshafts, screws, etc.) exhibit a continuous fibre flow and are thus more prone to stress than components that were manufactured by machining (interrupted fibre structure). Figure 2.40 shows an example of a microetched cross-section through part of a cold-formed gear shaft made of case-hardening steel 16MnCr 5. The fibre structure of the sample is rendered visible in this case by cleaning it with lukewarm to boiling hydrochloric acid.

2.6.5.4 Coating

Since scanning electron microscopy can only be used on conductive surfaces, non-conductive samples (e.g. ceramics, sometimes also ceramic coatings) must be specially prepared [GÖCK94]. By vapour-depositing a metal film (e.g. gold), the surfaces of the objects can be rendered conductive. One must bear in mind that the coating is not deposited too thickly, or else the fine structures of the object would be covered. Since scanning with the electron beam takes place in a vacuum, the objects must also be prepared prior to vapour-depositing so that they are absolutely anhydrous.

2.7 Materials in Forming Technology

2.7.1 Workpiece Materials

2.7.1.1 Sheet Metal

Modern sheet metal materials as used in sheet metal processing are following the demand for increasingly lightweight design. Based originally on classic soft deep

drawing grades, a development in the last several years in direction of higher and higher strength steels can be observed.

As before, there is still no exact definition of soft steel as opposed to a high-strength material. In accordance with the current state of materials development, the following classification is suitable:

- soft steel: tensile strength <300 Mpa
- higher-strength steel: tensile strength >300 MPa
- high-strength steel: tensile strength >500 MPa
- highest-strength steel: tensile strength >950 Mpa.

Which nomenclature is finally used is not really decisive. Comparative forms such as "ultra high-strength" or even "mega high-strength" are already in use. In general, the obtainable tensile strength should be used for a clear distinction of sheet metal qualities. Figure 2.41 shows the development of sheet materials with varying quality and strength properties. In the following, we will pursue individual steel materials and their active mechanisms in more detail.

The development of steel materials had already been advanced to high-strength sheet materials in the 1970s. First, microalloyed and phosphorus-alloyed steels were developed. In the case of microalloyed steels (alloy contents up to about 0.1 %), finely distributed carbides and carbon nitrides are formed in the grain structure which both refine the grain and have a hardening effect. The cause of the grain refining effect is that finely precipitated particles hinder grain growth during hot forming are available as germs in the transformation of austenite into ferrite.

Typical representatives of microalloys steels are the IF steels (interstitial free). An IF steel is a steel without interstitially incorporated alloying elements, i.e. no iron atoms are substituted by carbon or nitrogen atoms in the metal lattice. In this steel type, the C and N atoms are bound by titanium or niobium, which must be present in hyperstoichiometric amounts. In this way, IF steels obtain a ferritic microstructure without perlite or cementite. That guarantees favourable cold-formability and good deep drawing properties in particular. Because they lack interstitial atoms, these steel types are free of aging symptoms.

In the case of phosphorus-alloyed steels, the element phosphorus is added. This element helps to solidify the mixed crystal phase.

"Dual phase" steels (DP) were developed in the 1980s. As with the microalloyed steels, solidification is brought about by the second phase. In the case of DP steels, we make use of the fact that the martensitic components become hardened by the unavoidable solution of carbon in its crystal structures. How high the obtainable increase in strength is, depends on the amount, hardness and distribution of the martensite and bainite islands in the softer ferritic matrix. The microstructural development can be controlled by the conditions of the manufacturing process.

What makes "bake-hardening" steels special is that they have both good cold formability and attain a large increase in strength during subsequent heat treatment

(e.g. baking the body paint). This is achieved by diffusion of interstitial carbon and nitrogen to displacements within the crystal structure.

IF steels can be further developed and their strength increased to a higher-strength steel quality by alloying with elements that solidify mixed crystals. The latter are normally not as strong as carbon or nitrogen, but they occupy different positions in the crystal structure. Thus, these foreign atoms, in analogy to microalloyed steels, represent obstacles to dislocations without introducing irregularity to the stress/elongation values.

Without attempting to achieve a significant increase in strength, isotropic steel sheets were developed in the 1990s. Since anisotropy has a decisive influence on the required size of the sheet section and on the quality of the target component, engineers attempted to create anisotropic steel by adding suitable alloying elements. It was discovered that isotropy could be affected by alloying with titanium and its precipitations. We can now avoid anisotropy-caused earing and flow lines to a much larger extent.

Since the turn of the century, sheet metals have been further developed with the aim of increasing strength values. The focus has largely been on further developing DP steels. Other multiphase steels such as complex phase steels (CP) and TRIP steels ("transformation induced plasticity") also belong to this development. In the case of TRIP steels, which fall into the category of residual austenite steels (RA), there is an elongation-induced transformation of the metastable residual austenite into martensite, substantially increasing strength. In future, lightweight design will also be advanced further, and with it the development towards higher-strength materials. L-IP steels ("lightweight steels with induced plasticity") are a further development of TRIP steels. In this case, by adding further alloying elements, density is reduced while the strength remains the same in comparison to TRIP steels.

In Fig. 2.41, the stainless steel family is not explicitly indicated. This group of materials lies above the materials developments shown. What is special about this group is its high resistance against corrosion. This is a result of the high amounts

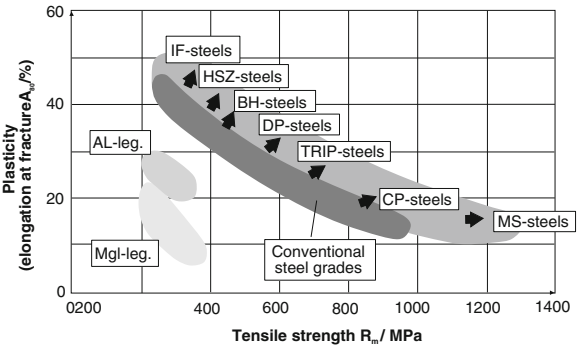


Fig. 2.41 The development of sheet materials of varying quality and strength [NN01a]

of the alloying constituents chrome (>12 %) and nickel, for which reason they are also known as chrome-nickel steels. This advantage is always exploited whenever components without additional protection (e.g. lacquering, zinc and eloxal) against corrosion are to be used. Stainless steels have a relatively high amount of residual austenite. For this reason, they are highly adhesive in production. In addition, deformation martensite can be formed when austenite is transformed to martensite during deformation.

The Anisotropy Coefficient r. In many sheet forming processes, it must be taken into consideration that a material does not have the same properties in all directions, but is anisotropic. The anisotropy of a multicrystalline material is characterized by the fact that the atomic lattices of the grains are not oriented in a statistically random way, but tend to prefer certain levels and directions. Such a preferential orientation, also called texture, can arise both during manufacture (e.g. casting) as well as during subsequent processing (rolling, forming, heat treatment). Consequently, the plastic deformations required for sheet manufacture lead to orientation changes as a result of sliding in the grains and thus to the formation of typical rolling textures [MACH81]. Due to this, tensile strength and plastic properties are to some extent direction-dependent, among other things.

To measure the anisotropy of the plastic properties of sheets, the perpendicular anisotropy is determined in the tension test—the so-called r coefficient. This is defined as the ratio of true strain in the width and thickness directions of a tensile specimen (Fig. 2.42).

$$r = \frac{\varphi_2}{\varphi_3} = \frac{\varphi_b}{\varphi_s}. \tag{2.51}$$

If $r = 1$, the material behaves isotropically and the same deformations take place in the width and thickness directions. In case of values of $r > 1$, the sheet is more resistant to changes in thickness under tensile stress and is deformed more in width. If $r < 1$, deformation occurs more in the thickness direction.

The r coefficient is generally not constant in the sheet plane, but rather has varying values depending on the position of the sample relative to the rolling

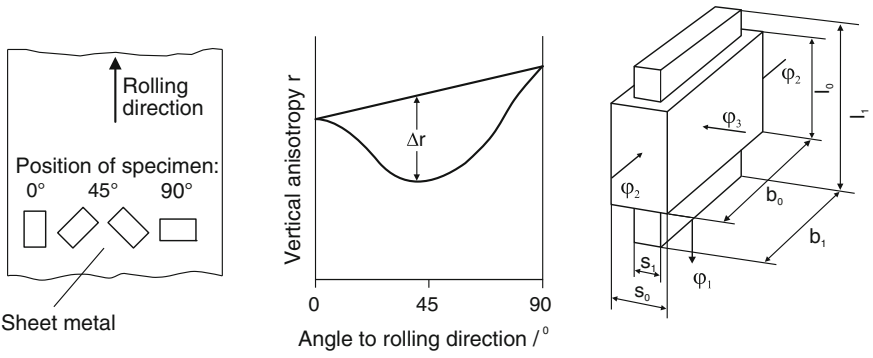


Fig. 2.42 Definition of the anisotropy coefficient

direction. We thus define the average for this reason, which is measured at certain angles (0°, 45°, 90°) to the rolling direction:

$$\bar{r} = \frac{r_{0^\circ} + 2 \cdot r_{45^\circ} + r_{90^\circ}}{4}. \tag{2.52}$$

The variation of the r coefficient with direction is called plane anisotropy and is defined:

$$\Delta r = \frac{r_{0^\circ} + r_{90^\circ}}{2} - r_{45^\circ}. \tag{2.53}$$

The experimental determination of anisotropy coefficients is standardized in DIN EN 10130 [EN04]. Accordingly, perpendicular anisotropy is determined after executing a tension test up to a deformation of 20 % from the change in length and width of the sample. It is recommended that one record length variation (L, L_0) instead of thickness variation. Then perpendicular anisotropy can be determined with the law of volume constancy using the following formula:

$$r = \frac{\ln \frac{b_0}{b}}{\ln \frac{L \cdot b}{L_0 \cdot b_0}}. \tag{2.54}$$

The Effect of Anisotropy in Deep Drawing. A cup produced by deep drawing often exhibits a wall of varying height and thickness despite symmetrical stress. This phenomenon is called "earing" and is due to the distinct plane anisotropy of the sheet material (Fig. 2.43).

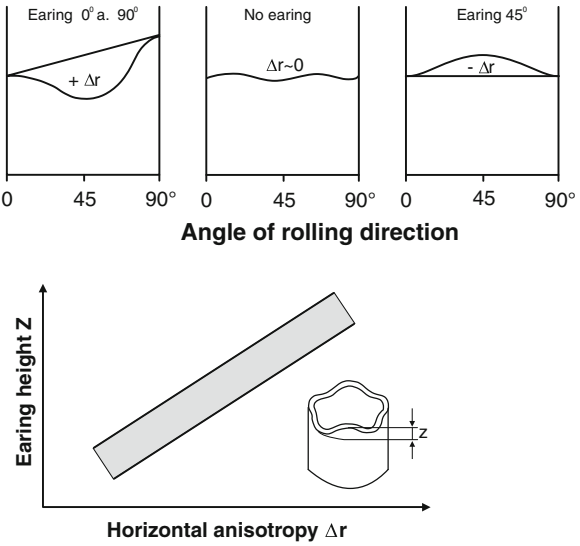


Fig. 2.43 Dependence of earing on plane anisotropy

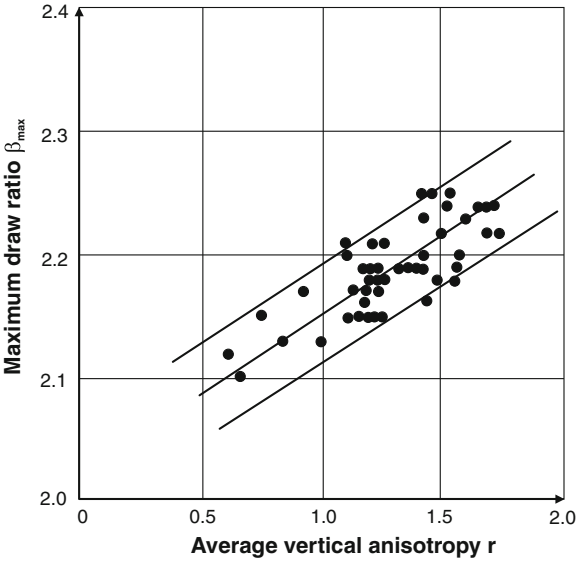


Fig. 2.44 Limiting draw ratio as a function of the average perpendicular anisotropy (acc. to Whiteley)

Given higher coefficients of perpendicular anisotropy, the sheet material tends to be constricted in width/the circumferential direction. The sheet is highly resistant to thickness changes. The material flows from neighbouring areas. As a result, both earing as well as larger wall thicknesses (relative to the circumference) arise here. At locations of minimal *r* coefficients on the other hand, valleys appear. The height of the tip is all the higher the higher the coefficient of plane anisotropy Δr is. In the case of a positive coefficient, the tips are under 0° and 90°—in the case of a negative coefficient, under 45° to the rolling direction. Since usually a smooth edge is usually required for technical and optical reasons, the cups require post-processing, which is associated with additional costs and a reduction of the useful cup height.

Large coefficients of perpendicular anisotropy can sometimes have a positive effect. For example, the limiting draw ratio rises with increasing r coefficients (Fig. 2.44). This can be explained with the help of Hill's yield locus curves for various *r* coefficients [HILL50] (Fig. 2.45). Yield locus curves describe the geometrical location for the start of flow in the stress area. These curves are applicable under the assumption of a level state of stress for materials that exhibit only a perpendicular anisotropy but no plane anisotropy [PÖHL84].

The yield locus curve is closed [Fig. 2.45 only shows the range between ideal stretch forming (tension-tension) and ideal deep drawing (tension-compression)], convex and generally cannot be described by an analytical function. In order to determine the represented yield locus curves experimentally, it is necessary to determine the start of flow for two-axis states of stress [PÖHL84].

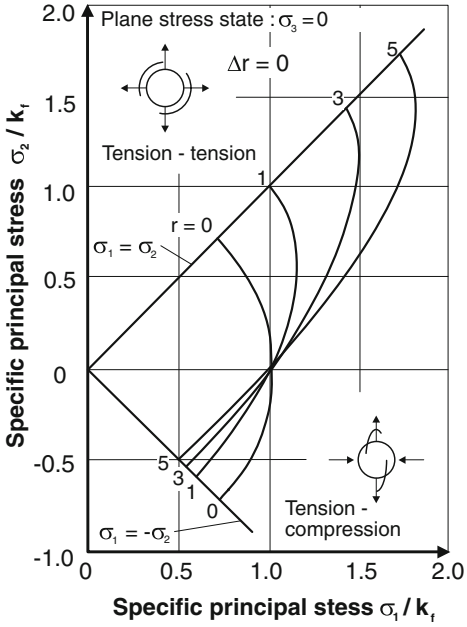


Fig. 2.45 Yield locus curves of sheet materials as a function of the *r* coefficient (acc. to Hill/ Pankin)

We can determine the yield locus curve experimentally, for example, with the help of tension or crush tests. In this case, the individual samples must have a different orientation to the rolling direction. The tests are carried out in analogy to the test procedure used for isotropic material. From the measurements, information about the yield locus curve is derived [PÖHL84].

We can see that in the case of two-axis tensile stress, which is predominant in the wall of a cup during deep drawing, the state of stress required for plastic flow rises with increasing *r* coefficients. On the other hand, in the case of a tension-compression state of stress, which is found in the flange, there is a reduction of the stresses required for flow. Applied to the conditions of cup-drawing, the conclusion is that the forming force drops in the flange area with increasing coefficients of perpendicular anisotropy, while the force transferable in the wall rises. Thus, larger limiting draw ratios can be obtained.

2.7.1.2 Cold Massive Forming

The following criteria are desirable for all workpiece materials that come into consideration for the manufacture of extrusion parts:

- minimal flow stress k_f,
- low tendency to strain-hardening,

- homogeneous grain structure along the entire initial cross-section and
- high formability.

To initiate flow, a quite distinct stress is required for each material. This can be used as a feature for classifying extrusion materials. With increasing flow stress, we obtain the following ranking:

- lead and lead alloys,
- tin and tin alloys,
- aluminium and aluminium alloys,
- zinc and zinc alloys,
- copper and copper alloys,
- unalloyed and alloyed steels up to about 0.45 % C in an annealed state,
- corrosion-resistant ferritic and martensitic Cr steels,
- austenitic CrNi steels,
- nickel and nickel alloys in a solution-annealed state and
- titanium and titanium alloys.

Of the non-ferrous metals indicated, lead and tin alloys are of relatively little importance although they are the easiest to form. These alloys are used especially for thin-walled parts such as cups, sheaths and tubes.

Aluminium and Aluminium Alloys. Aluminium materials are much more important. They can be roughly subdivided into

- ultra-pure and pure aluminium,
- non-age hardenable alloys and
- age-hardenable alloys.

Ultra-pure aluminium contains more than 99.98 % aluminium. The aluminium content of pure aluminium is between 99 and 99.9 %. The main alloying element is magnesium, of which up to 0.5 % is permissible. Ultra-pure and pure aluminium types have low strength (Table 2.1). They can be cold-formed already at low pressures. In this case, from large to very large deformations are possible. This is universally applicable however only for the soft state. In a semi-hard or hard state, strength is higher and the required pressure as well. Formability is accordingly reduced. Ultra-pure or pure aluminium is always in a semi-hard or hard state after cold-forming. This can be removed again by means of recrystallization annealing.

Alloyed aluminium materials contain mainly copper, magnesium, manganese, zinc and silicon as alloying elements. They are subdivided into non-age hardenable and age-hardenable alloys.

Among the non-age hardenable alloys are mainly the groups AlMg, AlMn and some variations of these. They obtain their higher strength compared to ultra-pure and pure aluminium from the effect of the alloying elements and from cold-forming. For this reason, they are often referred to as wrought alloys. Their strain-hardening tendency limits the formability of these materials.

Table 2.1 Non-ferrous metals for cold-forming

Material denomination/ number	Elastic limit R_p MPa	Tensile strength R_m MPa	Elongation at fracture A %	Hardness *HB*	Notes
Al9,5 EN AW1050A	20	70	23	20	Electrical parts, ferrules, pipes
AlMg5 EN AW5019	110	240	17	55	Self-hardening, container and vehicle construction
AlCuMg1 EN AW2017A	260	400	10–15	100	Age hardening, vehicle and engineering parts
Zn99,95 2.2035	–	120–140	52–62	32–34	
ZnAl4 2.2140	200–230	250–300	3–6	70–90	Pressed parts, profiles, armatures
ZnAl4Cu1 2.2141	220–250	280–350	2–5	85–105	
E Cu57 Cu-ETP	120	200–290	38	45–70	Semifinished goods for electrical engineering
CuSn2 –	150	260–280	35–50	60	Pipes, springs, screws
CuZn37 CW508L	180–250	300–380	45–50	70–75	Main alloy for cold forming, universally applicable
CuZn33 CW506L	150–180	270–370	46–50	65–70	Well cold formable, screws, rivets, formed parts
CuZn28 CW504L	(150)	280	44	70	Very well cold formable, versatile applications
Ti99,7 3.7035	250–350	400–550	22	150	Aircraft industry, jet engine parts, chemical apparatus and reactor construction
Ti6Al4V 3.7165	820–940	880–1,130	8	260–310	Aircraft and jet engine industry

Examples of age-hardenable alloys include those of the groups AlMgSi, Al-ZnMg, AICuMg and AlZnMgCu. In this case, phases that increase strength are eliminated by natural or artificial aging. Cold forming increases this strength again. Forming age-hardened alloys is more difficult than other alloy types. Table 2.2 [BILL73] provides a qualitative overview of the cold-formability of aluminium materials.

Zinc and Zinc Alloys. Zinc and zinc alloys are used only to a very limited extent for cold forming parts. The main reason for this is that zinc already starts to creep under low amounts of stress. This disadvantage can indeed be compensated to some extent by adding aluminium and copper, but the consequence is a very distinct reduction of elongation at fracture (Table 2.1).

The variety of workpieces composed of zinc materials comprises rivets and bolt-shaped parts, moulds, fittings and pressed parts.

Table 2.2 Classification of some aluminium materials in accordance with their cold formability [BILL73]

Good formability	Medium formability	Low formability
Ultra-pure aluminium	AlMgSi soft	AlMgSi warm age-hardened
Pure aluminium soft	AlMg3 soft	AlMgMn semi hard
AlMn soft	AlCuMg soft	AlMg5 semi hard
	AlMgSi cold age-hardened	
Pure aluminium semi hard	AlMg5 soft	AlCuMg age-hardened
AlMn semi hard	AlMgMn soft	AlMg7 semi hard
		AlCuMg age-hardened
	Pure aluminium hard	AlMn hard
	AlMg3 semi hard	AlMgMn hard
	AlMg7 soft	AlZnMg1
	AlCuMg soft	AlZnMgCu1.5

Copper and Copper Alloys. Copper and copper alloys have become very important as materials for cold-forming parts. This is due to the diverse potential applications of this material group and, with a corresponding alloy composition, their high deformability in the cold state.

The highest deformability can be obtained with pure copper types. Here, the copper content is between 99.50 and 99.90 %. They have trace amounts of residue from deoxidation agents (e.g. phosphorus or arsenic). Certain types (electrolytic copper) contain up to 0.04 % oxygen. Figure 2.46 illustrates the change in the mechanical properties R_m, R_p and A of electrolytric copper during cold forming.

The cold forming of pure copper materials is primarily applied to the manufacture of semi-finished products like solid and hollow profiles of the most varied cross-sections. These are made further use of predominantly in the electronics

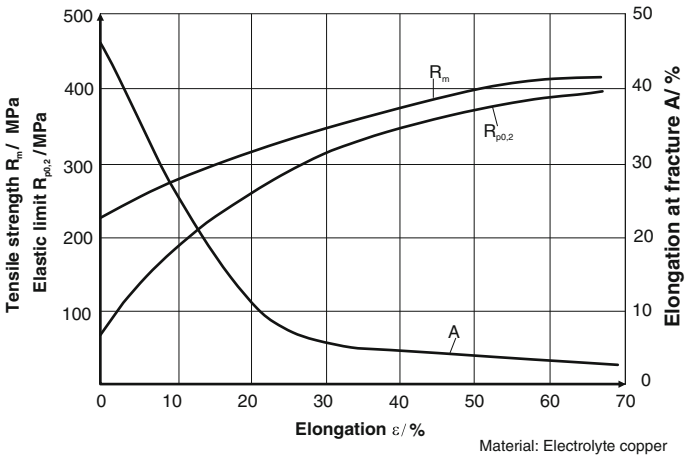


Fig. 2.46 Effect of cold forming on the mechanical properties of electrolytic copper [NN86, NN01b]

industry. Pure copper in the form of sheets and tubes functions as a workpiece material when there are high requirements concerning thermal or electrical conductivity [NN01b, NN86].

Most important of the alloyed copper materials are the copper-zinc alloys—commonly known as brass—with a production share of about 70 % of all copper alloys [NN03]. Their properties, including their formability in the cold state, depend on their zinc content. If the latter is under 37.5 %, then the alloy consists in solid state completely of α -mixed crystals (α -brass). Among others, these include the alloys CuZn20, CuZn28 and CuZn37. Alloys that contain only α -mixed crystals are very easy to form (Fig. 2.47). They exhibit high elongation at fracture, making forming operations with high degrees of deformation possible.

In the case of zinc contents of over 37.5 %, a second phase is formed in addition to the α -mixed crystal, the β -mixed crystal. Both crystal types are encountered side by side when the zinc content is up to 46 %. $(\alpha + \beta)$ alloys are especially interesting because the phase boundaries shift according to temperature. Thus, the properties of these materials can be influenced by heat treatment. The $(\alpha + \beta)$ alloys group includes CuZn40 and CuZn40Pb2 among others. In the case of CuZn40Pb2, the amount of β is in the area of 30–50 % [NN88]. The appearance of the second phase is of considerable influence on cold formability, which is poorer in materials then in pure α-alloys. Increasing zinc contents lead to a larger amount of β in the grain structure and thus in ever poorer formability in the cold state. On the other hand, these alloys are very well suited to hot forming.

If copper-zinc alloys contain still other elements, then they are called special brass. These materials consist of 56–79 % copper. What remains is composed of zinc and one or more other elements. As a whole, the content of such additional elements is usually 4 % at most [NN88]. These are aluminium, iron, magnesium,

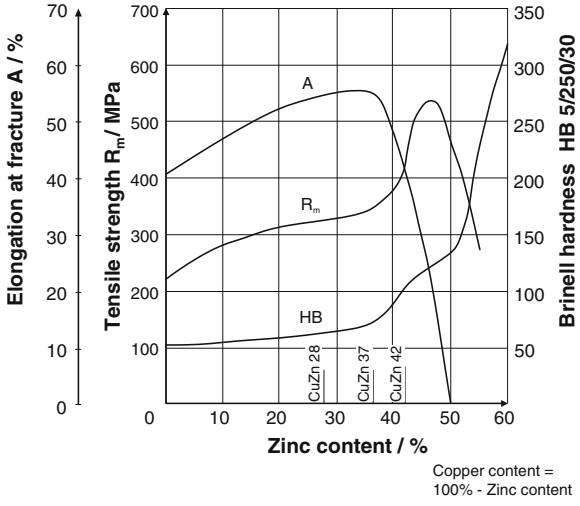


Fig. 2.47 Mechanical properties of copper-zinc alloys as a function of their zinc content [NN88]

Table 2.3 Relative cold formability of copper-zinc wrought alloys [NN88]

Good formability	Medium formability	Low formability
CuZn20	CuZn20Al2	–
CuZn28	CuZn28Sn1	–
CuZn31Si1	–	–
CuZn35	CuZn35Ni2	–
–	CuZn39Pb0,5	CuZn39Pb2
–	CuZn40Mn2	CuZn40Mn1Pb

manganese, nickel, silicon or tin. Their effect on the alloy's mechanical properties varies. With respect to the properties of special brass types in cold forming, they can be considered from the standpoint of the shifting of phase boundaries. For example, nickel like copper causes an increase of the amount of α. The other additional elements function like zinc, i.e. the amount of β in the microstructure is increased. As a result, formability in the cold state generally becomes more difficult. Table 2.3 shows some frequently used special brass types along with a classification with reference to cold formability.

Other binary and multinary alloys based on copper are of minor importance as materials for cold-forming parts in comparison to copper-zinc alloys. All wrought alloys can indeed be formed into construction parts as well, but their main area of application is in the manufacture of semi-finished products like sheets, belts, rods, pipes and moulds of all kinds.

A further area of alloyed copper materials includes copper-tin alloys, commonly called bronze. In Germany, they have a production share of about 14 % of all copper alloys [NN03]. Copper-tin alloys are easily formable using processes such as rolling, drawing, bending, cornering and deep drawing. The high strain hardening of these materials is the reason for their wide-spread use as a material for resilient contact elements in the electronics industry [NN04].

High Temperature Non-Ferrous Metals. High temperature and chemically resilient non-ferrous metals such as nickel and titanium as well as certain alloys are also processed into construction elements using cold forming, if only in special cases.

Of nickel materials, the technical pure nickel types are the easiest to cold form. They contain 99.5 % or more nickel as well as some carbon, manganese, iron, silicon and copper. High degrees of deformation are obtainable with these materials (Fig. 2.5), so intermediate annealing is required to restore formability only in case of extreme deformations. Cold forming increases strength and hardness. Elongation at fracture on the other hand is reduced already with small amounts of true strain. Pure nickels have attributes similar to steel within a range of comparable degrees of deformation with 0.2–0.25 % carbon [NN75] (Fig. 2.48).

Nickel wrought alloys have much higher mechanical characteristic values as pure nickel types depending on their composition. With respect to deformability in the cold state, they have similar properties concerning potential true strain and the tendency to strain hardening. Their higher strength in the undeformed state is

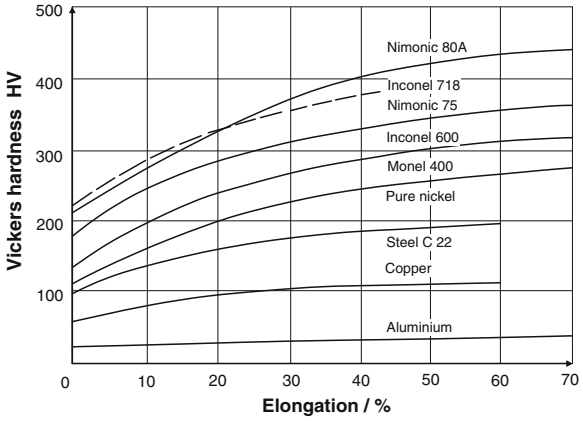


Fig. 2.48 Increase in hardness via cold forming [NN75]

further increased with higher degrees of deformation (Fig. 2.48). This also increases the demands made on machines and tools.

For reasons of material savings, the cold forming of nickel alloys is of great economical interest. They are also interesting because they can be machined only with difficulty [BILL73, LANG90a].

Titanium and Titanium Alloys. Metallic titanium and titanium alloys are, due to their favourable relation of density $(\rho \approx 4.5\ \mathrm{g/cm^3})$ to strength, of interest as construction materials when a combination of minimal component weight and high strength are essential. Since these materials also have good resistance to many chemicals, they are often used in the construction of chemical apparatus and plants. Titanium is a very expensive metal that is difficult to machine. For these reasons, the possibility of cold forming is highly interesting. The high strength of titanium is, however, an obstacle. Large forming forces then become necessary. The true strain obtainable with pure titanium are roughly comparable to ultrahard steels. Technical pure titanium types have tensile strengths in the range of R_m = 300–700 MPa elastic limits of $R_{p0.2}$ = 200–600 MPa and elongations at fracture of $A_5 = 20\,\mathrm{to}\,35\%$. These variables change considerably with the degree of cold forming, as the example of cold rolling pure titanium makes clear (Fig. 2.49).

Titanium alloys become increasingly difficult to cold form with increasing amount of alloying elements. The cause is not the content of additional elements alone however, but rather their effects with respect to the phases that they form. Technical titanium materials are subdivided into α-, β- and $(\alpha + \beta)$ alloys. The α-phase has a hexagonal lattice, the β-phase has a body-centred cubic crystal structure. β-alloys stand behind pure titanium with respect to their deformability in the cold state, but before the α- and $(\alpha + \beta)$ alloys. They contain vanadium, chrome, molybdenum, niobium, tantalum or manganese as their main alloying elements. Among others, this group includes the technical alloys TiV13Cr11Al3, TiV8Fe5Al1 and TiV16Al2,5.

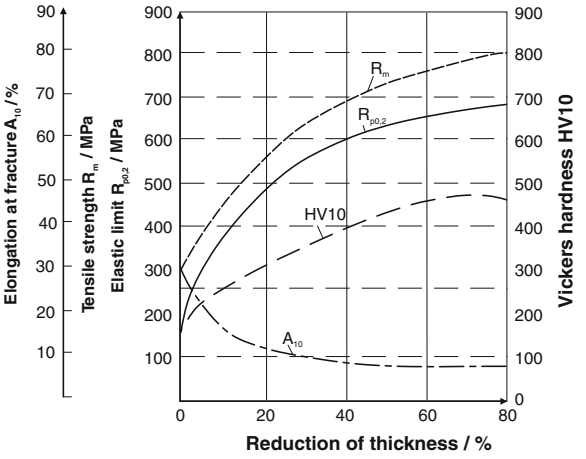


Fig. 2.49 Effect of height reduction in the rolling of titanium [ZWIC74]

The main alloying elements of α- alloys are aluminium, tin or zircon. The materials of this group are much more difficult to cold form than the β-alloys. Mentionable examples of technical α- alloys are TiAl5, TiAl5Sn2,5 and TiAl8-Mo1V1. One of the most well-known titanium materials is the $(\alpha + \beta)$ alloy TiAl6V4, which is considered poorly formable (Table 2.1).

Should titanium alloys be cold-processed into moulded parts, this generally is done for special cases in chemical apparatus manufacture, in reactor construction as well as in the aerospace industry.

Steel and Steel Alloys. Presently, steel is the most commonly utilized material for cold forming parts. Due to its high strength compared to most non-ferrous metals, steel must fulfil special requirements with respect to homogeneity, microstructure and mechanical properties in order for cold forming to be economical. This is especially true for ultra-high strength alloyed steels, the field of application of which is being continually expanded.

The formability of ferrous materials essentially depends on the type and content of the alloying elements. The formability of unalloyed carbon steels improves as the carbon content decreases, i.e. with increasing proportion of proeutectoid ferrite within the microstructure. Ferrite (α-iron) is a low-carbon iron mixed crystal that is highly cold-formable. With increasing carbon content, another microstructural component is formed, perlite. This is a lamellar-structured mixture of ferrite and iron carbide (Fe_3C, cementite). Carbides are exceedingly hard (>1,000 HV), brittle and almost undeformable. An increase in carbon content leads to a larger perlite proportion in the microstructure and thus to a higher strength and a diminished formability, which in return requires an even higher expenditure of energy. These characteristics of carbon steels can within limits be influenced by a suitable heat treatment. The goal of this is to transform the carbides in the perlite from a lamellar to a globular structure. In this form, the carbides hinder yielding

during forming to a lesser degree. Material behaviour becomes more homogeneous as a whole and the ductility is increased. Globular shaping of the carbides is achieved by annealing to spherical cementite (GKZ). Soft-annealing often suffices as well. But since the long annealing times are frequently not realizable for economic reasons, blanks to be formed often have mixed microstructures still containing some amounts of perlite with lamellar carbides.

As for the homogeneity and the yielding the effect of hard and brittle nonmetallic inclusions can be evaluated in the same way as that of cementite. However, the essential difference is that the shape of such inclusions cannot be influenced by heat treatment. Consequentially, especially high demands must be placed on the purity level of extrusion steels.

Unalloyed steels specially produced for extrusion contain the capital letter "C" in their designation as an attachment to the carbon content. C15C and C45C are examples of steels from this group. In such materials, the accompanying elements phosphorus and sulphur are undesirable because they cause inhomogeneities in the microstructure already during steel production, therefore reducing the deformability of the steels. In special cases however, steels containing higher amounts of sulphur are also cold-processed. These cases comprise simple forming processes with small strains where no special demands are made in terms of the final strength of the workpieces and where difficult finish-machining operations are to be performed on the workpieces.

Especially due to cost reasons, extrusion is also noteworthy as a manufacturing process for higher-loaded construction and machine parts. This is why alloyed case hardening steels and quenched and tempered steels are being increasingly processed. They are still relatively easy to cold form in the soft-annealed state. The strengthening associated with cold forming is frequently utilized purposefully (Table 2.4) and is already taken into consideration along with the dimensioning of workpieces.

Stainless steels are being increasingly subjected to cold forming as well. Because of the higher prices of these steels, the cost savings due to lower usage of materials is more significant than in the case of construction steels. Moreover, machining these materials is often difficult to execute because of increased tool wear and unfavourable chip shapes.

Stainless steels are generally classified as follows:

- austenitic CrNi and CrNiMo steels
- ferritic Cr steels
- martensitic Cr steels.

Depending on the respective content of alloying elements and the crystalline structure the characteristics of steels from different groups differ widely when being cold formed. Figure 2.50 illustrates this aspect with a juxtaposition of the yielding behaviour of three steels (including a stainless austenitic steel).

Table 2.4 Steels for cold forming [LANG90c]

Material denotation	Before/after forming	Elastic limit R_p MPa	Tensile strength R_m MPa	Elongation at fracture A %	Examples of use
C15	Before	280	400–450	20	Screws, nuts,
	after	500	600–700	8	trusses, levers,
C15C	Before	280	400–450	20	Pressure pads,
	after	500	600–700	8	shafts,
C35E	Before	320	420–500	18	Small machine
	after	600	700–800	6	parts
C45C	Before	340	500–600	16	
	after	650	750–850	6	
16MnCr5	Before	340	420–500	18	Gear wheels
	after	500	650–750	8	
41Cr4	Before	400	600–750	18	Gear wheels,
	after	650	750–850	8	screws
42CrMo4	Before	500	650–750	14	Steering arm
	after	750	900–1,000	8	
100Cr6	Before	450	600–750	12	Wear part
	after	650	800–900	6	
X10Cr13	Before	450	600	18	Corrosion-
	after	600	750	10	resistant parts
X5CrNi18-9	Before	220	550–700	50	Acid-resistant
	after	600	800–900	6	parts

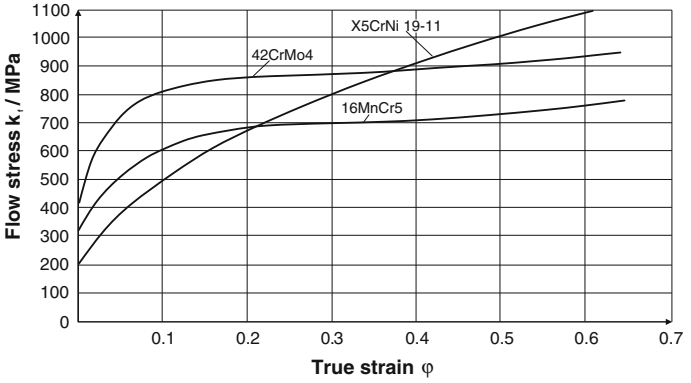


Fig. 2.50 Profile of yield stress for various steels

The difference in the strain hardening exponent n is very clear in the case of ferritic and austenitic steels. The major tendency of austenitic stainless steels to strain hardening makes it necessary to carefully adjust the blanks with respect to the deformations arising in the course of the forming process.

2.7.1.3 Hot Massive Forming

Hot forming is always utilized when the yield stresses are to be reduced and the formability of the material has to be increased. In general, all formable metals are suitable for this. Above all, unalloyed and alloyed steels are of technical importance today, moreover magnesium, aluminium, titanium, copper, nickel and their alloys as well. Also used, though to a much more limited extent, are highly heat resisting materials like niobium, tantalum, molybdenum, tungsten and their alloys.

The most important material for hot forming is steel, which can be adjusted within broad limits by means of alloy additives and heat treatment to different specifications concerning hardness, yield strength, tensile strength, failure strain, toughness, fatigue strength, high temperature strength, machinability and corrosion resistance.

Tables 2.5, 2.6 and 2.7 provide an overview of the types of steel used in forging.

Precipitation-hardening ferritic-perlitic steels were developed specially for hot forming and documented in DIN EN 10267. They are generally referred to as AFP steels. They obtain a ferritic-perlitic matrix by means of targeted cooling from the forming temperature. Due to simultaneously transpiring precipitation processes, dispersion hardening occurs in the ferrite, resulting in high strength. The obtainable strength parameters are comparable with those of heat-treated steels. The cost advantages of these steels are caused by their low price as well as by the omission of hardening, annealing and flattening costs.

The forming behaviour of metallic materials depends on the temperature, the forming speed and the formability [BARG83]. In hot forming the upper temperature limit is determined by the solidus temperature, phase transformations or chemical reactions (oxidation processes) and grain growth. Since areas with eutectic composition can arise in heavily segregated alloys, the highest temperature must be lower than the eutectic temperature in such cases. The lower temperature limit is theoretically the temperature limit of recrystallization, below which—due to the advent of strain hardening—the deformability is reduced respectively the resistance to forming is increased.

The strain rate as well should be regarded along with the recrystallization. At the respective temperature, the strain rate must not exceed the recrystallization rate in order to avoid strain hardening.

In addition to the minimum temperature set by recrystallization, a forming temperature must be selected for which homogeneous mixed crystals are to be expected corresponding to the phase diagram. Varying deformation properties among several structural constituents can thereby be avoided, and, in particular, secondary phases at the grain boundaries can be re-dissolved. If phases of differing lattice types exist, the more formable lattice type at hand is preferred for plastic deformation (e.g. face-centred cubic).

Since the deformability of the material must be maintained during the forming process, yet cooling is unavoidable due to the temperature difference between the

Table 2.5 Steels for hot forming I

Denomination (DIN/steel–iron-mat.data sheet)	Application characteristics	Examples of use	Tensile strength[a] (MPa)	Forming temperature[a] (°C)
General construction steels (DIN EN 10025)	Application in forged state	Flanges, bosses, levers, bushes, bodies, rings	300–800	850–1,150
Quenched and tempered steels (DIN EN 10083)	Through heat treatment (quenching and tempering) broadest influencing of mechanical characteristics: high toughness along with defined strength	Drive and gear parts: waved parts for force and torque transmission (e.g. crank shafts); gear wheel; wheel bosses, stub axles, piston rods etc.	500–1,500	850–1,100
Case-hardened steels (DIN EN 10084)	High hardness of case-hardened surface layer along with high core toughness → wear parts	Cam shafts, control shafts, gear wheels, measuring devices, bosses, levers, gear and steering shafts	500–1,500	850–1,150
Nitriding steels (DIN EN 10085)	High surface hardness, good wear resistance, good fatigue resistance, rust inertance	Wear parts of high surface hardness: heavy machine parts of large dimensions	800–1,600	850–1,100
Steels for flame and induction hardening (DIN 17212)	Hardenability of the surface layer without influencing the core characteristics	Drive shafts, gear wheels, bevels, crank shafts, cam shafts, gudgeon pins	500–1,300	850–1,100
Heat-resisting steels (DIN EN 10269) (DIN EN 10273)	Load temperature up to 540 °C	Forgings for turbine engineering, steam boiler engineering, former apparatus construction: flanges, screws, nuts, high pressure pipes	450–1,000	850–1,100
AFP-steels (DIN EN 10267)	Hardening through targeted cooling from forming heat	Dynamically highly loaded parts such as piston rods, stub axles, suspension arms	700–900	900–1,100

[a] according to: Stahlschlüssel

workpiece and the tool, the forming process is initiated with the highest permissible temperature.

In case of larger cross-sections and in case of materials with lower heat conductivity along with elevated high temperature strength an even temperature

Table 2.6 Steels for hot forming II

Denomination (DIN/steel–iron-mat.data sheet)	Application characteristics	Examples of use	Tensile strength[a] (MPa)	Forming temperature[a] (°C)
Highly heat resisting steels (W 670-69)	Load temperature up to 800 °C; additional demand of toughness, fatigue strength and corrosion resistance	Parts for container and apparatus construction for thermal power plants and reactors: armatures, valves, pipes, pressure containers, turbine blades etc.	500–1,250	850–1,250
Corrosion and acid-resistant steels	High corrosion resistance	Construction and apparatus engineering parts for chemical industry, food industry (armatures, shafts, srews, bolts, bushes)	450–900	750–1,150
Bearing steels (W 350-53)	High surface hardness, high strength martensitic-carbidic microstructure (→high tension-compression cyclic stress and wear)	Rolling bearing rings through partial forging (preform)	(only hardness data) 60–66 HRC	800–1,100
Tool steels				
Non-Alloyed tool steels (W 150-63)	Surface hardening (low hardening depth)	Hand tools, simple shearing tools	58–65 HRC	800–1,100
Cold work steel[a] (W 200-69)	Up to 200 °C surface temperature	Shearing and cold forming tools	55–67 HRC	800–1,100
Hot work steel[a] (W 250-63)	Permanent temperature above 200 °C; high heat resistance, high hot wear resistance	Forming tools (hot forming) plastics molding tools	900–2,000	800–1,150
High speed steel[a] (W 320-69)	High tempering resistance and hot hardness up to app. 600 °C, hot wear resistance	Big tools of chipless forming	64–67 HRC	900–1,150

[a] according to: Stahlschlüssel

Table 2.7 Non-ferrous metals and hard alloys for hot forming

Denomination	Application characteristics	Examples of use	Tensile strength (MPa)	Forming temperature (°C)
Pure aluminium and AL-alloys	Low part weight along with high continuous load; high corrosion resistance	Forgings for aircraft industry, vehicle manufacturing and shipbuilding; pressure vessels, electrical engineering	Up to 400	350–550
Magnesium alloys	Lowest density of metallic materials along with medium strength properties; good machinability; high hot resistance (Mg-Zr-alloys) problem: high chemical reactivity	Die forgings: mechanical parts of medium to high mechanical and thermal load (Zr-alloys); housing in turbine manufacturing	Up to 260	370–400
Titanium alloys	High strength along with low density and excellent corrosion resistance	Aircraft and jet engine manufacturing (compressors, turbine blades), armatures, chemical apparatus	300–750	700–1,000
Copper alloys	High electric and heat conductivity, good strength properties; corrosion resistant	Electrical engineering, vehicle manufacturing, fine mechanics. Apparatus construction (armatures)	Up to 600	700–900
Hard alloys with nickel, cobalt and tungsten basis	Very high heat resistance	Turbo jet engine parts: turbine blades and disks		1,050–1,250

distribution across the workpiece cross-section can only be realized through a long warm-up phase. As for large open-die forging pieces, uniform heating down to the core can last several days. Uneven heating with temperature gradients from the surface to the core can lead to thermal stresses and thus to damage.

The criterion for judging the level of forging difficulty is the so called "forgeability" of a material, a qualitative indicator of the formability respectively deformability.

According to Lange [LANG90b], the following qualitative ordering of material groups can be made with respect to hot forming:

1. aluminium alloys
2. magnesium alloys

3. copper alloys
4. carbon steels, alloyed steels
5. martensite-hardening steels
6. austenitic stainless steels
7. nickel alloys
8. titanium alloys
9. iron-based superalloys
10. cobalt-based superalloys
11. molybdenum alloys
12. nickel-based superalloys
13. tungsten alloys
14. beryllium.

2.7.2 Tool Materials

2.7.2.1 Casting Materials

Cast Iron. Cast irons are iron alloys with a high carbon content of about 2.7–3.8 % and a silicon content of 0.8–3 % as well as further components like manganese, chrome or nickel. The carbon in cast iron is mostly in the form of graphite and immediately leads to cracking during forming processes. For this reason, the material is poured into moulds and subsequently processed into tools using machining or dissociative material removal. Along with the disadvantages of low deformability and toughness in comparison to steel, it has significant cost advantages, high machinability as well as favourable sliding properties resulting from the graphite content. For the construction of forming tools, cast iron with lamellar graphite and spheroidal graphite are of primary interest.

Cast Iron with Lamellar Graphite. In this type of cast iron, the carbon in graphite form is predominantly lamellar. As a result of its low mechanical strength, the graphite flakes do not take part in load transmission but rather act as hollow spaces that reduce the load-bearing section and produce concentrations of stress at its edges as a result of the notch effect. The deformability and impact strength of this cast iron type is thus especially low. The mechanical properties are essentially determined by the microstructure and the graphite form. Thus, the Young's modulus of ferritic cast iron is in the area of 90,000 MPa and increases with perlitic cast iron content to about 150,000 MPa [BEIT01]. Beyond that, this material has the peculiarity that the Young's modulus decreases as the stress increases. Thus, there is no linear relation between stress and strain, which must be taken into consideration in the context of tool design. The tools should be subjected to as little tensile stress as possible, since the tensile strength of the material is only a fourth of the compressive strength [MERK03]. Because the high internal notch effect, caused by the graphite flakes, dominates tool failure, an notch-reduced surface construction is

Table 2.8 Cast iron materials with lamellar graphite [MERK03, OEHL01]

Cast type	Tensile strength/ MPa	Hardness/ HB	Application purpose
EN-GJL-150	150–250	100–175	Lowly loaded drawing punches, bonnets, base plates for column mounts for light cutting and shearing tasks
EN-GJL-200	200–300	120–195	Drawing tools for large and flat parts, car body pressing, furthermore for cylindrical Bowden cables at high load and simple geometry
EN-GJL-250	250–350	140–215	
EN-GJL-300	300–400	165–235	Drawing and forming tools for high wear resistance, base plates and bonnets for high strength load
EN-GJL-350	350–450	185–255	

not required for reasons of strength. Furthermore, the strength of cast iron with lamellar graphite depends on the fineness of the graphite distribution, which is increased with rising cooling rates. Thus, higher strengths can be realized in thin-walled workpiece areas. This is exploited especially in the production of stiffening ribs [OEHL01].

Table 2.8 shows some frequently used cast iron materials with lamellar graphite as well as their mechanical characteristic values and examples of their applications.

Cast Iron with Spheroidal Graphite. It is possible to create a graphite shape that is not lamellar but spheroidal by providing a scarceness of sulphur in addition to certain carbon and silicon contents. This form has the advantage of reduced internal notch effects and therefore a considerably increased material strength. Furthermore, the Young's modulus is increased to about 175,000 MPa [BEIT01].

By means of appropriate heat treatments, the properties of this type of cast iron can be improved to a greater extent than those of cast iron with lamellar graphite. To obtain the highest level of impact strength for example, heat treatments are undertaken that result in a ferritic microstructure. The machinability is good. For these reasons, this material represents an economical alternative for large tools exposed to higher loads.

Table 2.9 lists some frequently used cast iron materials with spheroidal graphite, their mechanical characteristic values and examples of their applications.

Steel Casting. Steel casting constitutes iron materials with carbon contents of up to 2 % that are poured into moulds. Here, the melting and alloying processes used

Table 2.9 Cast iron materials with spheroidal graphite [MERK03, OEHL01]

Cast type	Tensile strength/ MPa	Hardness/ HRC	Application purpose
EN-GJS-500	500	54	Drawing tools and molds for high wear resistance, base plates and bonnets for high strength load
EN-GJS-600	600	56	
EN-GJS-700	700	56	

Table 2.10 Cast steel materials [MERK03, OEHL01]

Cast type	Tensile strength/MPa	Hardness/ HRC	Application purpose
Cold working steel casting			
G45CrNiMo4-2	1,000 – 1,030	50 ± 2	Molds and embossing tools
GX100CrMoV5-1	800 – 900	60 ± 2	Embossing, cutting, drawing tools
G45CrNiMo4-2	800 – 900	60 ± 2	Molds and jigs
Hot working steel casting			
GX38CrMoV5-1		–	Dies; unsusceptible to hot cracking
GX40CrMoV5-1		–	Die inserts, parts for compression dies; very good tempering resistance
G37CrMoW5-1		–	Punches, dies, die inserts; very good tempering and hot wear resistance

correspond to those of rolled and forged steel. However, its strength properties are largely independent of direction since no distinct texture is created by subsequent forming processes. Compared to cast iron, it is of higher strength and sometimes higher toughness. For this reason, it is particularly suitable for large-format tools exposed to high mechanical loads [BEIT01]. Depending on the use, a distinction is made between hot and cold working cast steel. Table 2.10 lists some examples among the large number of possible alloys.

Zinc Alloy Casting. Zinc alloy casting can be poured simply. With them, dies and cutting tools are cast in order to produce corresponding tool pairs in a simple fashion. The good reproduction of the tool geometry permits a reduction of further treatment, keeping production costs to a minimum. The tools can withstand small loads such as those arising in the forming of soft light-metal sheets and spacious steel sheet parts with large radii and can be re-cast into other tool geometries after their use without a problem. The most common alloy for tool manufacture is ZnAl4Cu3 with a tensile strength of 335 MPa [MERK03].

2.7.2.2 Aluminium Bronze Alloys

Alloys composed of aluminium bronze, used in the manufacture of deep drawing tools, consist of about 80 % copper, 14 % aluminium, iron and sometimes nickel. They have a hardness of 300–400 Brinell and are characterized by their very low friction coefficient [MERK03]. Because of these properties, this material is employed for mounting or armouring highly stressed tool edges for the manufacture of drawing parts made of stainless steel sheets that are hard to form. With it, the surfaces of the drawing material are spared extremely well, and the formation of wrinkles, grooves and scratches is largely avoided.

2.7.2.3 Tool Steels

Tool steels are classified as unalloyed and alloyed cold working steels, hot working steels and high-speed steels. Cold working steels are suited to applications in which the operational surface temperature is generally under 200 °C. Hot working steels and high-speed steels on the other hand can be used in temperatures of up to 600 °C. Cold working and high-speed steels are used above all to produce tools for machining and forming. Hot working steels are used mainly to manufacture forming tools such as dies, die-cast moulds or tools for forging and extruding.

Unalloyed Cold Working Steels. Unalloyed cold working steels, also called carbon steels, obtain their hardness with a corresponding heat treatment by the formation of a martensitic microstructure. Besides the carbon content of up to 1.25 % C required for this, they also contain up to 1.5 % Cr, 1.2 % W, 0.5 % Mo and 1.2 % V. Wear resistance is increased with hardness and increasing carbon content. However, toughness is reduced at the same time, and thus the material's sensitivity during heat treatment and tool use becomes larger. All unalloyed tool steels are shell hardeners, that is, they only harden on the workpiece surface and not across the entire section. Complete hardening is only possible up to a diameter of 10 mm.

During operation, the surface temperature of the workpiece should not exceed 180 °C. Otherwise tempering phenomena are inherent which are associated with a decline in hardness.

Table 2.11 lists some frequently used unalloyed cold working steels as well as their hardness and typical applications.

Alloyed Cold Working Steels. The carbon content of alloyed cold working steels is between 0.18 and 2.30 %, therefore higher than that of unalloyed steels. In addition, they contain the alloying elements Cr, Mo, W and Mn, which contribute to a reduction of the critical cooling rate and thus to the favourable through hardenability of the materials as well as to the formation of carbides and thus to the increase of wear resistance [PÖHL99]. Also, they increase the tempering resistance and the high temperature strength. These steels as well can only be exposed to surface temperatures of up to 200 °C during operation (Table 2.12).

Hot Working Steels. Hot working steels are used for the chipless forming of steel, non-ferrous metals and their alloys under temperature far above 300 °C, frequently in a rot hot state. Thus, high demands are placed in terms of heat resistance, high temperature wear resistance, heat conductivity, toughness and

Table 2.11 Unalloyed cold working steels [MERK03]

Steel type	Hardness/HRC	Application purpose
C70U	57	Deburring tools, axes, cutting goods
C80U	58	Hot dies, hot rolls, machine cutting tools
C105U	61	Embossing and drawing tools, dies
C120U	62	Files, milling tools, band and bow saws

Table 2.12 Alloyed cold working steels [MERK03]

Steel type	Hardness/HRC	Application purpose
60WCrV8	58	Embossing, extrusion and shearing tools
90MnCrV8	60	Cutting, bending, deep drawing and embossing tools
X100CrMoV5	62	Cold pilger mandrels and cutting tools
X153CrMoV12	61	Cutting, thread rolling and pressing tools
45NiCrMo16	52	Embossing and bending tools

tempering resistance. The type of load determines the simultaneous presence of several or all of these properties. Essential for hot working steels is also their insensitivity to fire cracks, which results from a combination of toughness and heat conductivity [NN96].

Since in most cases the contact with the hot metal to be processed is intermittent and repeated at certain intervals, the inherent temperature changes result in an additional load that gradually leads to the formation of net-like cracks, called fire cracks [SPUR84].

In order to meet all these requirements, a large number of alloying elements are required that cause additional interactions among themselves, resulting in complex steels. Steels with the alloying components Cr-Mo-V and Ni-Cr-Mo-V are especially suited to meeting these requirements.

One essential property of these steels is a high hot hardness caused by a secondary hardening in the temperature range around 500 °C. This is due to additional carbide precipitations, which hinder plastic deformation of the material in this temperature range [MERK03].

A further important property of these steels is their high toughness, which is significantly higher than other steels that are applied within this temperature range. This attribute is the reason why these materials can also be applied in tools that are subjected to high loads such as forging dies. While hot working tools made of Cr-Mo-V steels are ideal for water cooling because of their thermal shock resistance, Ni-Cr-Mo-V steels are—due to their toughness—used for tools with abrupt and high compressive loads. Table 2.13 shows some frequently used hot working steels as well as their hardness and some typical applications.

High-Speed Steels. High-speed steels offer a good combination of high-temperature hardness, wear resistance and toughness. Especially the latter two properties have brought about their use predominantly for cold forming tools. The special properties of this steel group are based on the strong carbide formers W, Mo, V and Cr [BEIT01].

Table 2.13 Hot working steels [MERK03]

Steel type	Hardness/HRC	Application purpose
55NiCrMoV7	42	Forging dies, hot shear blades
32CrMoV12-28	46	Rod extrusion tools, dies
X37CrMoV5-1	48	Water coolable ros extrusion tools and dies
X40CrMoV5-1	50	Hot shear blades, rod extrusion tools

Table 2.14 High-speed steels [MERK03]

Steel type	Application purpose
HS 6-5-2	Punches, dies, fine blanking tools
HS 6-5-3	Press bushes, die inserts
HS 10-4-3-10	Mandrel

A distinction is drawn between high-speed steels fabricated by metallurgical melting processes and the more cost-intensive powder-metallurgically produced high-speed steels, which differ due to their finer and more uniform carbide distribution and their lack of segregation. This results not only in higher compressive strength but also in enhanced toughness properties [MERK03].

Table 2.14 lists some often used high-speed steels along with their hardness and typical applications.

2.7.2.4 Cemented Carbides

Cemented carbides are composite materials. They consist of a soft metallic binder phase such as cobalt or nickel and of carbides of the transition metals W, Ti, Ta, Nb. Carbides border between metals and ceramics. They exhibit some properties similar to metals, e.g. electrical conductivity, but are—as metallic hard materials—assigned to non-oxide ceramics [MERK03].

The hard materials are responsible for hardness and wear resistance. The task of the binder phase is to bind the brittle carbides and nitrides to a relatively solid body.

The advantages of cemented carbides are their good microstructural uniformity due to the powder-metallurgical production, their high hardness, compressive strength and high temperature wear resistance. Cemented carbides have the same hardness at 1,000 °C. as high-speed steel at room temperature. Furthermore, it is possible to produce cemented carbides with different properties by making targeted changes in terms of the hard material and binder contents [BEIT01].

The cemented carbide types used for forming purposes usually consist of tungsten carbide (WC) as a phase in a cobalt matrix (Co). The cobalt content is between 6 and 30 %, whereby the mixture ratio largely determines the properties of the cemented carbide. With increasing amounts of WC, the hardness, compressive strength and wear resistance increase. On the other hand, toughness, bending strength and buckling strength are increased along with the Co content.

Typical areas of application for cemented carbides in forming technologies are cutting tools, stamps, press bearing bushes and dies for both cold and hot forming, which must have high wear resistance and high compressive strength. Cemented carbides are especially often used for narrow-tolerance components, which are then produced in smaller series as well.

2.7.2.5 Ceramics

The material category ceramics includes all non-metallic, inorganic, temperature-resistant materials that are at least 30 % crystalline [SALM82, TIET94]. This does not however exclude the possibility of metallic and/or polymer components being present within a ceramic material as additives.

Besides artistic ceramics (e.g. porcelain), which are not used in metalworking, modern ceramic materials are classified into the two large groups "functional ceramics" and "structural ceramics" [WILL88]. Structural ceramics are used when high mechanical loads are expected. This is the case, for example, for indexable inserts in machining or for the balls of hip joint prostheses. Commonly used structural ceramics are either oxides, carbides or nitrides. Functional ceramics are used because of their special functional properties. Among these are good electrical insulating properties or heat conduction. High-performance ceramics are materials that can satisfy especially high requirements, including very high wear resistance and heat resistance. From a technical point of view, structural and high-performance ceramics are used for metal processing. They are summarized by the generic term of "technical ceramics" [SALM83, WILL88].

Technical ceramics are subdivided into the groups silicate ceramics, oxide ceramics, non-oxide ceramics and titanates. Table 2.15 lists some typical representatives of these ceramic groups.

Oxide and non-oxide ceramics are especially important for metal processing (forming).

Ceramics are usually manufactured according to the following schema:

1. forming process: ceramic powder and binder are pressed into a green body
2. green machining: the still soft green body is processed by near-net-shape machining
3. sintering: heat treatment at 1,200–2,200 °C to generate the actual ceramic
4. finishing: hard machining (grinding, lapping) is used to create the near-net-shaped ceramic.

For forming technological applications, the ceramics aluminium oxide (Al_2O_3), zirconium oxide (ZrO_2), silicon oxide (SiC) and silicon nitride (Si_3N_4) are of primary interest.

Table 2.15 Classification and examples of technical ceramics

Ceramic group	Ceramic examples		
Silicate ceramic	Steatite ($Mg_3(OH)_2(Si_4O_{10})$)	Cordierite ($Mg_2Al_4Si_5O_{18}$)	Kaoline ($Al_2O_3 \times 2SiO_2$)
Oxide ceramic	Aluminium oxide (Al_2O_3)	Zirconium oxide (ZrO_2)	Magnesium oxide (MgO)
Non-oxide ceramic	Silicon carbide (SiC)	Silicon nitride (Si_3N_4)	Aluminium nitride (AlN)
Titanate	Calcium titanate ($CaTiO_3$)	Barium titanate ($BaTiO_3$)	Lead zirconate titanate (PZT)

Application Examples. Because of the many advantages associated with the use of ceramic tool materials in forming technologies, a number of areas of application have already been opened up. It is current state of the art, for example, in wire manufacturing that the rolls have a fully ceramic core. The benefit of ceramic tools is that the high wear resistance of ceramics is a necessary prerequisite for the effective application in this manufacturing process.

In wire forming, the tools employed are subjected to high mechanical loads and heavy wear depending on the composition, microstructure and surface properties of the wire. In the case of some wire materials, such as copper alloys, there are additional problems due to the propensity to adhesion between the tool and the wire [WAGE00]. In addition to their high hardness, the tribological properties of ceramics make them suitable for the use in industrial applications and in the sphere of forming tools in particular. Here, their non-metallic bond character and thus their small adhesive tendency in the case of friction pairings make them particularly effective. As a result the total friction losses as well as the tendency to cold welding in the case of mixed or dry friction are reduced. This advantage has been practically proven in the case of drawing rings made of silicon nitride [WAGE99].

Various research projects have and still do set out to investigate the applicability of ceramic tools in sheet forming. In one case, the use of silicon nitride in rotationally symmetric deep drawing made it possible to boost tool life by up to 300 % compared to conventional tool steel. Considering that such ceramics are still much more expensive, such an increase in tool life is also necessary to make their use economical [KLOC03b].

The properties of ceramic materials are advantageous not only in deep drawing, but are also useful in other sheet metal forming operations. One example is the form roller as it is encountered in the manufacture of tins when forming the container edge [WAGE99].

A similar application was executed for the manufacture of welded pipes. In this case, ceramic form or pressure rollers are applicable in the welding unit, since they are not only wear resistant but also have a high temperature resistance and cannot be heated by eddy currents in the case of induction welding [WAGE99].

Another important field for the use of ceramic tools is massive forming. Impact extrusion involves very high contact stresses and internal tool pressures, especially in the case of higher reductions of cross-section. This increases the formation of weldings between the workpiece and the tool. The advantages of ceramics with respect to wear resistance and their low propensity to adhesion can be fully utilized in this case as well. Experiences with ceramics have already been made even in the case of steel-forging, where the high temperature resistance of ceramics is utilized in addition to the aforementioned advantages [WAGE00].

2.7.2.6 Plastics

Plastics are also used as tool materials in forming technologies. Since compared to metals they can only take a small amount of mechanical and thermal loads, their

use is currently limited to the deep drawing of thin sheets in small to medium-sized series in which high compressive strengths are not necessary [FRAN99]. In this case, the advantage of a lower volume price and a more economical shaping process via milling or casting compared to steel can be exploited [DEIL03].

Both epoxy resins and polyurethane are used, the properties of which are modified partially by means of fillers.

2.7.3 Determining the Flow Curve and Materials Testing

Besides the determination of quality characteristic values and material data, materials testing also serves to test the suitability of materials for various forming processes. In the following, material data determination and suitability testing with the help of standardized test methods will be introduced in more detail. The most crucial material characteristic value in forming technology is the flow curve $k_f = k_f(\varphi, \dot{\varphi}, \vartheta)$ of the material to be formed. With it, stress distribution, the power and energy requirement of the forming process and the strength of the manufactured part can be derived. Further characteristic values include the Young's modulus E for describing elastic resilience, the strain hardening exponent n for representing strain hardening of the material (Sect. 2.7.3.1) and the anisotropy r, which describes the dependence of the material's properties on the direction of load (Sect. 2.7.1.1).

For a lasting shaping of the workpiece material, plastic flow must be initiated in the material and be maintained during the process [SIEB62]. Here, stress—required for bringing about plastic flow of the workpiece material in the case of a uniaxial state of stress—is called yield stress. If the active force is designated as F and the actual surface as A, the yield stress is:

$$k_f = \frac{F}{A}. \tag{2.55}$$

Yield stress is generally plotted over the true strain as a flow curve. The yield stress of uniaxial states of stress can be transformed to multiaxial ones using the yield criteria of *Tresca* and *von Mises* (Sect. 2.3). To this end, an equivalent stress σ_v is calculated, which is then compared with the yield stress k_f at an effective strain φ_v.

The flow curves of the unalloyed and alloyed steels and non-ferrous metals that are most important for cold forming are compiled in the flow curve atlas of metallic materials [DOEG86].

Flow curves are usually determined by means of simple material tests. In special cases, they can also be calculated from the chemical composition of the material [LEYK78]. In order to determine the flow curve, three basic tests are applied as a rule: the tensile test, the compression test and the torsion test. The method used to record flow curves should be selected as a rule such that stress and

strain conditions come as close as possible to those of the forming process to be designed. Since this requirement is very difficult to meet except for a few cases, often simple compression and tensile tests on round specimens are preferred for determining the flow curves of massive-formed materials. In sheet forming, the tensile test with flat test pieces as well as the flat crush test and the hydraulic cupping test are used.

2.7.3.1 Determining the Flow curve with the Tensile Test

A large number of standards exist for the tensile test (Fig. 2.51), and it is the most commonly used test to determine material data. One advantage of the tensile test is that is can be executed without friction. Furthermore, it is especially suitable for determining the Young's modulus E in the range of elastic elongation. In the case of stress beyond the elasticity limit σ_E, the material begins to yield and shows lasting deformation after the stress is removed from the specimen. Until the maximum tensile force is reached, the strain is equally distributed in the tensile specimen and is designated as uniform elongation A_g. Uniform elongation is generally expressed as relative strain respectively nominal strain $(\varepsilon = \Delta l/l_0)$. After the maximum tensile force is reached, the specimen is constricted in the case of further stress. In the case of most metallic materials, this constriction begins already at relatively small true strains $(\varphi_g = 0.2...0,3)$. Since the state of stress in the tensile specimen shifts from a uniaxial to a multiaxial one with the onset of constriction, the flow curve has to be extrapolated or determined using special calculation rules above this point. The tensile test is described for both massive and flat specimen types in the standards DIN 50125, DIN EN 10002-1, DIN EN 10002-5 and DIN EN 10045-1.

The tensile test on round specimens is primarily used to determine material data for massive forming. This is because the round specimen largely eliminates the effects of the manufacturing process.

Flat bar tension specimens are frequently used to determine material data for sheet metal materials. The advantage of this is that not only the flow curve but also the anisotropy characteristic values can be determined (Sect. 2.7.1.1). Moreover, the flat tensile test also measures elongation at break, which can be used as a measure for the formability of a sheet metal material.

The disadvantage is that the flat tensile test is restricted to lower true strains, as it only permits the recording of flow curves below uniform elongation. Evaluation in the constriction range is not possible with the usual methods, the more so as the constriction generally does not progress perpendicular to the specimen's axis [JAHN81].

Determining the Flow Curve using the Tensile Test with a Uniaxial State of Stress. When executing a tensile test, a round specimen, the dimensions of which are specified by DIN 50125 [DIN04a] is continuously loaded until fracture (Fig. 2.51). Since within uniform elongation there is a largely uniform load across

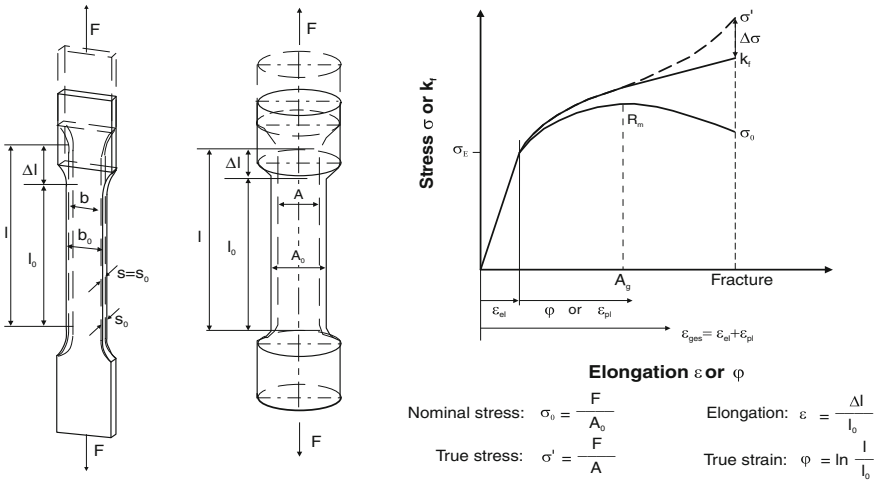


Fig. 2.51 Schematic stress-elongation profile from a tensile test on a metal without a pronounced yield point

the cross-section of the specimen, several relations are used to calculate yield stress in this range. The following is true for volume constancy:

$$l \cdot A = l_0 \cdot A_0, \tag{2.56}$$

which can also be represented as:

$$\frac{l}{l_0} \cdot \frac{A_0}{A} = 1 \text{ or } \ln \frac{l}{l_0} = \ln \frac{A_0}{A}. \tag{2.57}$$

The effective strain φ_v

$$\varphi_v = \ln \frac{A_0}{A}. \tag{2.58}$$

can also be represented as:

$$e^{\varphi_v} = \frac{A_0}{A}. \tag{2.59}$$

Thus the following is true for the yield stress k_f:

$$k_f = \frac{F}{A} = \frac{F}{A_0} \cdot e^{\varphi_v}. \tag{2.60}$$

For the forming velocity $\dot{\varphi}_v$, the following is valid:

$$\dot{\varphi}_v = \frac{d\varphi}{dt} = \frac{1}{l} \cdot \frac{dl}{dt}. \tag{2.61}$$

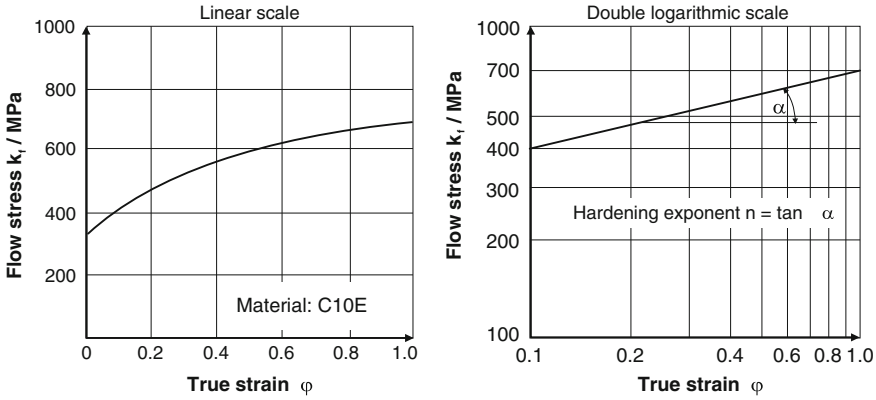


Fig. 2.52 Flow curve and solidification exponent n

Determining the Flow Curve using Tensile Strength and Uniform Elongation. The flow curves of most unalloyed and low-alloy steels as well as Al alloys at room temperature can be described for deformations $\varphi < 1.0$ in good approximation by the power function

$$k_f = C \cdot \varphi^n. \tag{2.62}$$

This "Ludwik equation" [LUDW09] does not take the elastic portion into consideration and is only valid assuming that the material is not pre-strain-hardened.

The strain hardening exponent n, which is a measure for the material strain hardening occurring during forming, and the value C are material-specific constants.

If the flow curve is plotted in a double logarithmic representation, it becomes a straight line, the slope of which corresponds to the strain hardening exponent (Fig. 2.52).

According to Reihle [REIH61], the following relations are true:

$$n = \varphi_g \tag{2.63}$$

and

$$C = R_m \cdot \left(\frac{e}{n}\right)^n. \tag{2.64}$$

Here, e is the basis of the natural logarithm. To determine the flow curve, only the uniform elongation strain φ_g and tensile strength R_m need be established.

The uniform elongation strain φ_g (true strain) can be determined from the uniform elongation A_g (relative strain) in the tensile test as follows:

$$A_g = \varepsilon_g = \frac{l_g - l_0}{l_0} = \frac{l_g}{l_0} - 1 \tag{2.65}$$

and

$$A_g + 1 = \frac{l_g}{l_0} \tag{2.66}$$

resulting for φ_g in:

$$\varphi_g = \ln \frac{l_g}{l_0} = \ln(1 + A_g). \tag{2.67}$$

Here, the accuracy with which uniform elongation Ag is determined has a direct effect on the accuracy of the flow curve.

The uniform elongation can also be determined approximately by the formula

$$A_g \approx 2 \cdot A_{10} - A_5 \tag{2.68}$$

[KOST51]. So it is often possible to make a first approximation of the flow curve when one knows the elongation at fracture A_{10} and A_5 as well as the tensile strength R_m. The accuracy of the flow curve thus depends heavily on the accuracy of the manufactured test pieces.

Determining the Flow Curve Using the Tensile Test with a Multiaxial State of Stress

Determining the Flow Curve using the Tensile Test with a Multiaxial State of Stress. Above uniform elongation, the state of stress is no longer uniaxial, as the specimen now begins to become constricted. Taking constriction into account, yield stresses with true strains of of up to $\varphi \approx 1$ can be calculated (Fig. 2.53). To this end, Siebel and Schwaigerer [SIEB48] developed for the constriction of a round specimen the following calculation rule, according to which the flow stress k_f is calculated as:

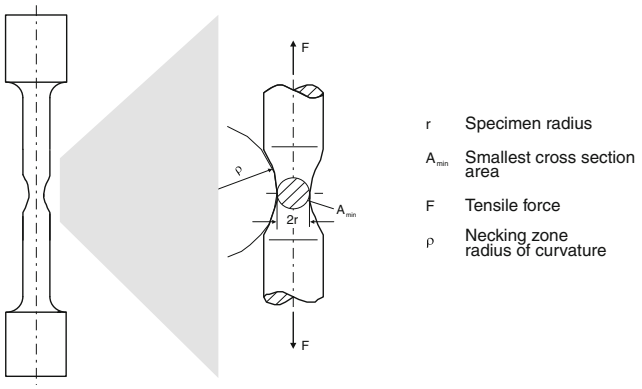


Fig. 2.53 Schematic representation of the constriction zone of a cylindrical tensile specimen

$$k_f = \frac{F}{A_{\min} \cdot \left(1 + \frac{r}{4\rho}\right)}. \tag{2.69}$$

Another possibility is to calculate the flow stress k_f in the case of the constriction of a round specimen with the following relation [BRID44]:

$$k_f = \frac{F}{A_{\min} \cdot \left(1 + \frac{2\rho}{r}\right) \cdot \ln\left(1 + \frac{r}{2\rho}\right)}. \tag{2.70}$$

The difference between both formulae is minor and in both cases the associated effective strain is calculated as follows:

$$\varphi_v = \ln \frac{A_0}{A_{\min}}. \tag{2.71}$$

However, this method requires that the constriction zone retains its circular cross-section. The largest possibilities of error in this method are the result of determining the radius of curvature ρ in the constriction zone and neglecting the effect of velocity, as there are higher strain rates in the constriction zone than in the other areas of the specimen. In determining the radius of curvature, the ratio r/ρ can be approximated as:

$$\frac{r}{\rho} \approx \sqrt{\ln\left(\frac{A_0}{A_{\min}}\right) - 0,1}. \tag{2.72}$$

2.7.3.2 Determining the Flow Curve with the Compression Test

Higher true strains are obtained in the crush test than in the tensile test, since the deformability of metals is generally higher in the case of a hydrostatic compressive stress than in that of a hydrostatic tensile stress. Thus, it is especially practical for determining flow curves in massive forming with high true strains. In the process, a cylindrical specimen is continuously compressed between two level parallel compression paths (Fig. 2.54).

Cylinder Crush Test with a Uniaxial State of Stress. A "uniaxial" cylinder crush test presumes a uniaxial state of stress and homogeneous deformation. This is the case when the specimen remains cylindrical during upsetting. Due to frontal friction, material flow is obstructed on the front faces however, so that the specimen bulges convexly. It is hardly possible in that case to capture the effective strain φ_v exactly. Homogeneous deformation can be maintained up to effective strains of $\varphi_v \approx 0.8$ by reducing frontal friction with the help of a suitable lubrication (Fig. 2.54). In the case of optimal lubrication, the specimen maintains its cylindrical shape during the forming process, while insufficient lubrication leads to convex bulging. In this case, the state of stress becomes multiaxial, and, in the case

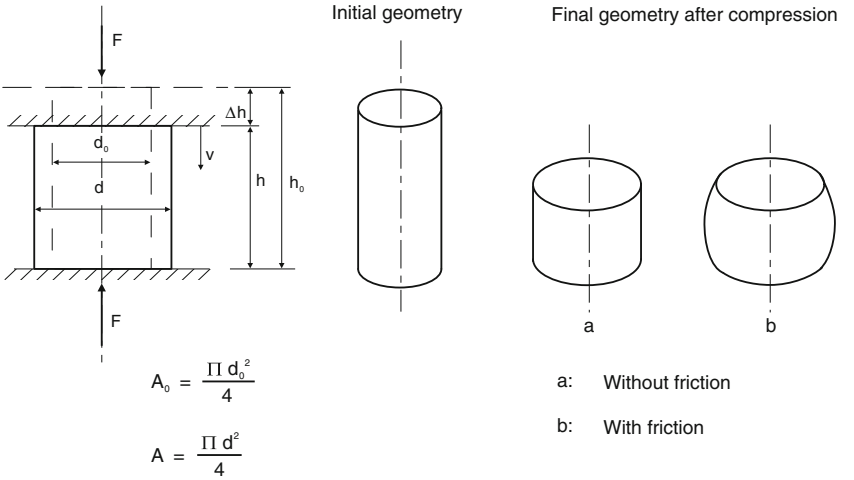


Fig. 2.54 Schematic representation of a cylinder compression test and the effect of friction on the test result

of a convex specimen shape, the yield stress k_f becomes larger than the resistance to forming, as the compressed surface is smaller than the average surface. Measures to reduce friction can include the use of plastic films or the turning of grooves into the front faces of the specimen, which then accommodate the lubricant. A deformation that is as homogeneous as possible can also be achieved by a discontinuous upsetting process, in which the specimen in the case of small amounts of bulging is brought back to its original shape by turning. The following laws are used to calculate the yield stress:

$$k_f = \frac{F}{A} = \frac{F}{A_0} \cdot e^{\varphi_v} \tag{2.73}$$

with

$$h \cdot A = h_0 \cdot A_0. \tag{2.74}$$

The following is true for the effective strain φ_v:

$$\varphi_v = \ln \frac{h}{h_0} = \ln \frac{A_0}{A} \tag{2.75}$$

and for the strain rate $\dot{\varphi}_v$

$$\dot{\varphi}_v = \frac{d\varphi}{dt} = \frac{1}{h} \cdot \frac{dh}{dt}. \tag{2.76}$$

Cylinder Crush Test with a Multiaxial State of Stress. Since homogeneous deformation of the compression specimen cannot be guaranteed in all cases, the yield stress can be determined by upsetting several specimens with the most varied

ratios of diameter d_0 to height h_0. The results are then extrapolated to $d_0/h_0 = 0$ [SACH24]. Such an extrapolation is undertaken because the effect of friction decreases as the ratio of diameter to height becomes smaller. Thus, a ratio of zero corresponds to a frictionless upsetting process.

Another way to calculate yield stress in the upsetting of cylindrical specimens taking multiaxiality into consideration requires the undeformed specimen have a slenderness ratio of $d/h < 1$ [REIC51]. Calculation of the yield stress k_f is based on [SIEB48]:

$$k_f = \frac{\frac{F}{A_{\max}}}{1 - \frac{r_{\max}}{4 \cdot \rho_a}}. \tag{2.77}$$

With a slenderness ratio of $d/h \geq 1$, the formula is as follows:

$$k_f = \frac{\frac{F}{A_{\max}}}{1 - \frac{r_{\max}}{4 \cdot \rho_a} + \frac{\mu \cdot (d-h)}{3 \cdot h}}. \tag{2.78}$$

The effective strain φ_v is calculated from the maximum specimen front sides with

$$\varphi_v = \ln \left| \frac{A_0}{A_{\max}} \right|. \tag{2.79}$$

However, the friction coefficient μ (Sect. 2.8.2), the undeformed front lateral surfaces of the specimen A_0 and the front lateral surfaces $A_{\max}$ of the deformed specimen must be known, as well as the radius rmax $r_{\max}$ of the largest cross-section after compression upsetting and the radius of curvature ρ_a of the bulged specimen. The latter can also be calculated approximately with the following formula:

$$\rho_a \approx \frac{h^2}{8 \cdot (r_{\max} - r)}. \tag{2.80}$$

Flat Crush Test. The flat crush test was developed in order to depict, also in one single test, the high true strains often reached in sheet metal forming processes and thereby to produce comparable flow curves. In this test, two opposing, flat punches are pressed into the specimen (Fig. 2.55). During the test, the compressive force is constantly measured at the corresponding height reduction. The loaded surface remains constant.

The width/height ratio of the flat specimen has to be $w/h > 6$ in order to assume a planar deformation. Under this assumption, the following is true for all ratios $h/a < 1$ with the yield criterion of Tresca [GREE51]:

$$k_f = \frac{F_{(\varphi_v)}}{a \cdot b} \tag{2.81}$$

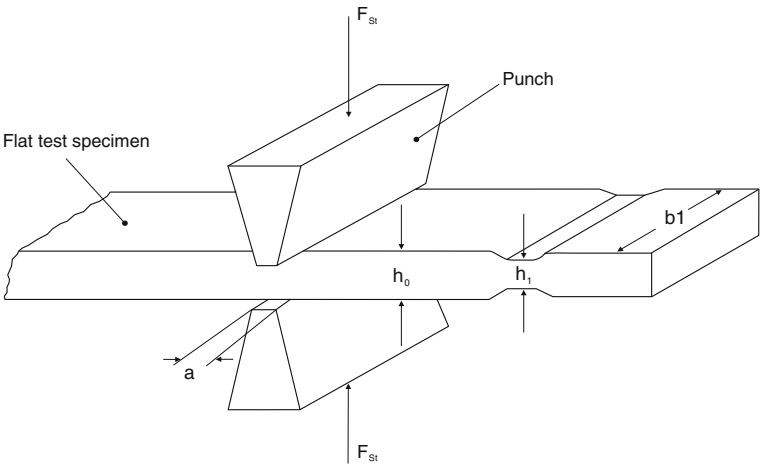


Fig. 2.55 Schematic representation of the flat compression test

with

$$\varphi_v = \ln \frac{h}{h_0}. \tag{2.82}$$

The yield stresses calculated with Eq. 2.81 are maximally 4 % too high, which has been verified experimentally. In general, higher true strains can be obtained in the flat crush test than in the tensile test. The selected thickness of the sheet metal cannot be too small, since otherwise the height reduction and thus true strain cannot be determined with sufficient accuracy. Moreover, the upsetting tools must be guided with high precision, since a lateral displacement decreases the contact surfaces and thus the upset volume. In comparison to the cylinder crush test, the results of the flat crush test are, with good lubrication, less affected by friction [KRAU62].

Taper Crush Test. Siebel and Pomp [SIEB27] have developed a crush test which avoids the effect of friction if the frontal surfaces of the specimen and the compression paths of the tools are conical. The cone angle must be chosen such that the radial shear stresses obtained are large enough to eliminate the frictional shear stresses. This requirement is met when the cone angle fulfils the following equation:

$$\alpha = \arctan(\mu). \tag{2.83}$$

The cone angle α is about 3°–7° when upsetting steel at room temperature, which corresponds to a friction coefficient of $\mu = 0.08...0.125$. Since a homogeneous deformation can thus be assumed in the forming process, the same laws apply for the calculation of yield stress as for a crush test with a uniaxial state of stress (Eqs. 2.73–2.76). Since the frontal surfaces of the specimens are conical,

average heights are used for the heights h and h_0. True strains of $\varphi_v \approx 0.5$ can thus be obtained without the specimen becoming bulged, making the deformation inhomogeneous. If larger true strains are to be reached, the specimen can be reduced in diameter until its original ratio of diameter to height is reached again. Re-upsetting can lead to true strains of $\varphi_v \approx 1.2$ with this method.

2.7.3.3 Other Tests for Determining Flow Curves

Hydraulic Cupping Test. In the hydraulic cupping test, which is especially suited to recording the flow curve of thin sheets, a sheet metal specimen of thickness s_0 whose circumference is firmly clamped is pressed into a usually circular die opening with a single-direction pressure (Fig. 2.56). The pressure, the depth of the outward bulge and the thickness of the sheet metal s_1 are measured on the pole of the cupped specimen. Fluids serve as the medium of load transmission. The sheet metal is formed in a pure stretch forming process, since the clamping precludes yielding. The bulging thus results in a reduction of the thickness of the sheet metal [PANK64].

With the help of the yield criterion of von Mises, the yield stress k_f can be calculated from the radius of curvature at the pole, the sheet metal thickness s_1 of the cupped specimen and the hydraulic pressure p [GOLO77]:

$$k_f = \frac{p \cdot \rho}{2 \cdot s_0} \cdot e^{\varphi} \cdot s \tag{2.84}$$

with

$$\varphi_v = -\varphi_s = \ln \frac{s_0}{s_1}. \tag{2.85}$$

With this process, the flow curve can be recorded up to a true strain of about 0.7, hence for a much higher range than in the tensile test. It is frequently observed that the flow curves obtained with the cupping test deviate from the data determined by the tensile test. The causes for this are the simplifications in the calculation (geometry, yield criterion) and the often high anisotropy of the sheet metal specimens, which cannot be specially taken into account in this method.

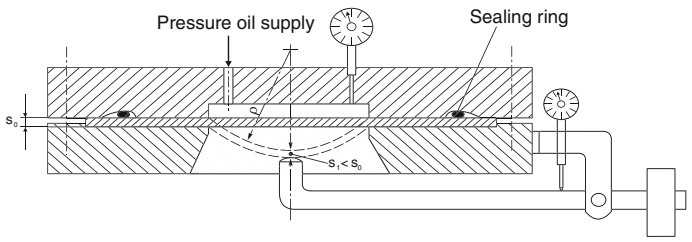


Fig. 2.56 Hydraulic cupping test

Often, the hydraulic cupping test is used to investigate the stretch drawing properties of thin sheet metals.

Torsion Test. In the torsion test, a cylindrical solid body is twisted by a torque around the longitudinal axis. With the measurement data of the torque and the torsion angle along with the specimen dimensions, the yield stress k_f and the effective strain φ_v can be calculated [DIET72]. Since the test is frictionless and can be executed at relatively low cost, it is good for determining flow curves in cold massive and hot massive forming up to high true strains.

Bending Test. In the bending test, a flat, rectangular specimen is bent. With the bending moment and the bending angle, the flow curve of the material can be determined. When calculating the flow curve, simplifications are applied that are only partially fulfilled. For example, instead of a uniaxial state of stress, there is actually a triaxial state of stress in the forming zone, which, among other things, leads to calculated yield stresses that are about 30 % below the values obtained in the tensile test. Thus, the bending test is in most cases not suitable for an exact flow curve determination [DIET72].

2.7.3.4 Comparison of the Methods Used to Determine the Flow Curve

The previous chapters have described the most important methods used to determine flow curves. Comparing the flow curves of a workpiece material recorded by different methods, considerable deviations can arise (Fig. 2.57). The cause of these deviations is primarily due to the individual processes, which have the following uncertainties:

- deviating testing approaches
- faulty measurements

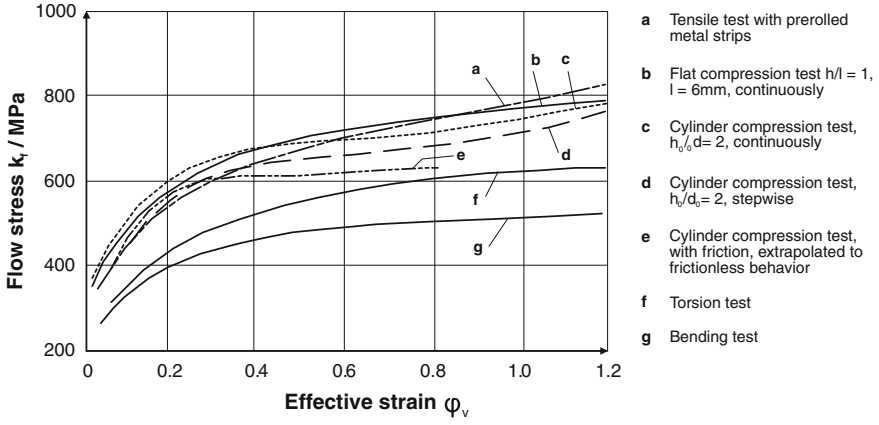


Fig. 2.57 Flow curves of the material C10 acc. to von Mises derived from different test methods [DIET72]

- requirements for test execution and test evaluation are not consistent
- inaccuracy of the method used to determine the reference value
- varying temperature and friction conditions in the different test methods
- varying changes of the test parameters during the test in the different test methods
- elastic resilience of the testing devices.

In addition, each test method involves varying test conditions with respect to

- anisotropy of the material
- microstructure of the material
- analytical errors concerning the material used
- temperature and frictional effects during the test.

These lead to deviations among the flow curves.

A comparison of the recorded flow curves shows that the cylinder crush test is affected by friction. Thus additional energy must be applied, which is reflected in the "higher" position of the flow curve. In addition, there is a clear increase in temperature in the entire specimen due to the forming process. This disadvantage does not arise in the case of the flat crush test, as in this case the heat generated can be diverted along the compression paths and the undeformed specimen areas. This advantage of frictionless test execution is accompanied by the disadvantage that deformation takes place inhomogeneously when the uniform elongation is exceeded. As a result, there is the possibility of errors in the calculation of the flow curves. The torsion test permits a simple variation of the strain rate and temperature in a frictionless test process, in which large true strains can be reached. However, complex test equipment is required. Furthermore, inhomogeneous deformation leads to lower yield stresses than those recorded, for example, in compression tests.

2.7.3.5 Sheet Metal Testing Methods

In order to predetermine the suitability of a sheet material for a certain forming operation, numerous model testing methods have been developed that, for example, simulate the load generated in principle in a stretch drawing, deep drawing or bending process. Since in practice many sheet forming processes represent a combination of deep drawing, stretch drawing and bending processes due to the variety of geometries, universally valid statements are not possible with the help of individual test procedures. For this reason, usually several testing methods are utilized in practice. The following will provide a short description of the most important ones.

Deep Drawing Test. To assess the suitability of sheet metals for deep drawing, cup deep drawing test methods are often used. In the case of the deep drawing test of Swift, cylindrical cups are drawn from sheet metal blanks with a gradually

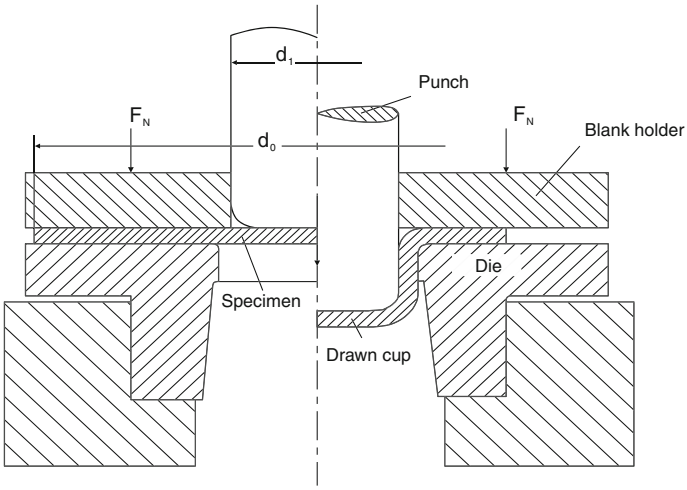


Fig. 2.58 Cup deep drawing (acc. to Swift)

increasing diameter at constant die diameter (Fig. 2.58). The characteristic value is the maximum drawing ratio β_{max}, at which the drawability limit of the sheet metal is reached due to an imminent cup base fracture [TÖLK70]:

$$\beta_{max} = \frac{d_{0max}}{d_1}. \tag{2.86}$$

Since the maximum drawing ratio can only be determined with sufficient accuracy on the basis of a series of tests, this test procedure is associated with relatively high costs. Moreover, the results from the deep drawing test cannot simply be applied to the deep drawing with large tools, since the maximum drawing ratio obtained from the test is generally larger than it is in the case of operational forming. This is because the effects of friction in the area of the blank holder become increasingly apparent in the case of large tools.

Stretch Drawing Test. The Erichsen cup test has become an essential tool for testing the suitability of a sheet material for stretch drawing [HESS91]. In this case, a firmly clamped sheet test piece is dented to the point of fracture (Fig. 2.59). The central characteristic value is the Erichsen cupping value, the depth to which the punch can deform the sheet without cracking. In this process, the cupping is determined in a biaxial state of stress. Thus, it is a measure for the formability of sheets via stretch drawing. There is no correlation between the limiting draw ratio and the cupping value, so this test method is of little value for deep drawing processes.

Bending Test. Bending counts among the most frequently employed forming processes, as, in addition to well-known bending procedures (e.g. die-bending, roll forming) many other processes, such as deep drawing, are combined with bending processes.

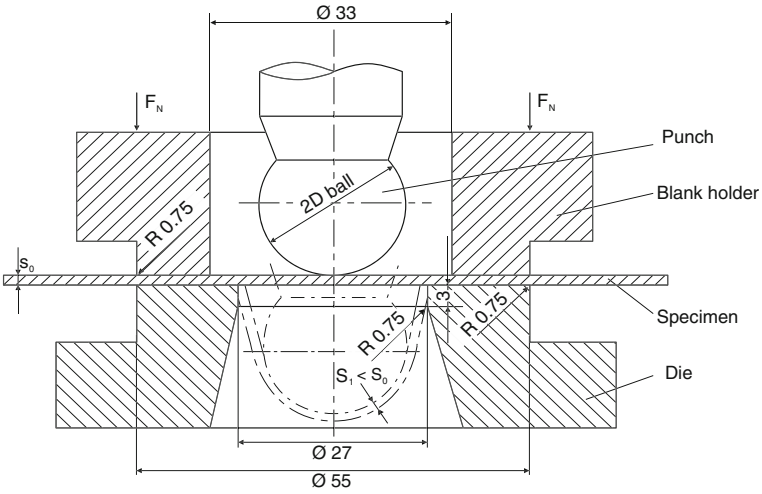


Fig. 2.59 Tool for the Erichsen cup test (acc. to DIN EN ISO 20482 [ISO03])

Among specific tests for the bending capability are the folding test (bending test) [KAEH92, ISO04b, EN01b] and, for nominal thicknesses of 0.3–3 mm, the to-and-fro bending test [PERE92a, ISO00].

As shown in Fig. 2.60, the bending test involves freely laying the test block on two rotatable rollers at a prescribed distance and bending it with a mandrel that is also exactly defined in its dimensions. The measure for the bendability of the sheet metal is the bending angle, the maximum of which can be reached without cracking on the tension side of the specimen. The elongation values obtained are larger in comparison to the tensile test, which can be derived from the supporting effect of the lower-lying "fibres".

In the case of the to-and-fro bending test, the specimen is clamped on one side between clamping jaws and bend alternately towards the left and the right into a horizontal position (Fig. 2.61). The number of bendings that the sheet metal can endure until cracking or fracture is defined as the bending number N_b and is used as the measure for bendability. Here, one bending is defined as bending the specimen into a horizontal position and bending it back into a vertical position.

Determining Forming Limit Diagrams. Deformations made during the drawing of irregular sheet metal parts can be highly different with respect to size and type in different areas of the same drawn part. For this reason, it is impossible to describe process limits with a universally valid characteristic value such as the limiting draw ratio for deep drawing symmetrical parts [DANN83].

One way to represent the process limits of a drawing process with a plane state of stress is the forming limit diagram (Fig. 2.62). The forming limit diagram serves as a tool for the assessment of the forming properties of sheet metals with the help of measuring grids. The theoretical basis of the measuring grid method has already been described in Sect. 2.4.6.

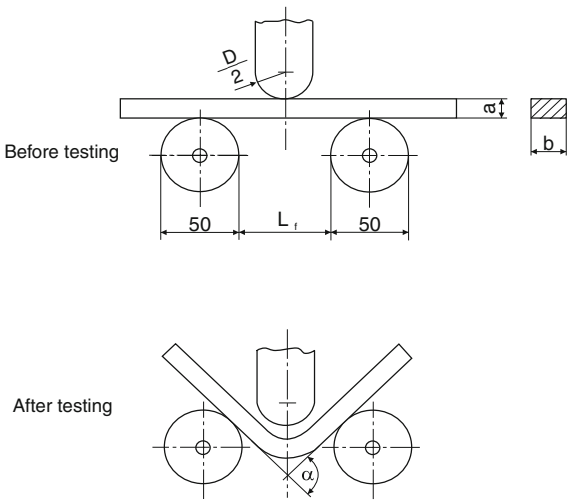


Fig. 2.60 Bending test (acc. to DIN EN ISO 7438 [ISO04b])

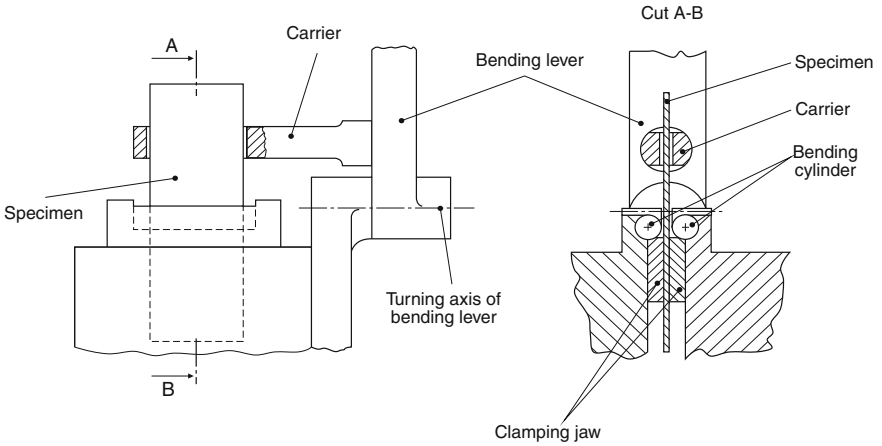


Fig. 2.61 To-and-fro bending apparatus for sheet metals, belts and strips (acc. to DIN EN ISO 7799 [ISO00])

The forming limit curve plotted in the diagram characterizes the combinations of both deformations φ_1 and φ_2, in which the sheet metal material tends towards failure due to necking or cracking. Above the forming limit curve, shown as a solid line, the material fails. In addition to the limit curve, the diagram also indicates the states of "pure deep drawing" $(\varphi_1 = -\varphi_2)$, "uniaxial tension" $(\varphi_1 = -2\varphi_2)$, and "pure stretch forming" $(\varphi_1 = \varphi_2)$. Since according to the definition, the second principal stress can never be larger than the first, pure stretch forming represents the natural limit of the diagram.

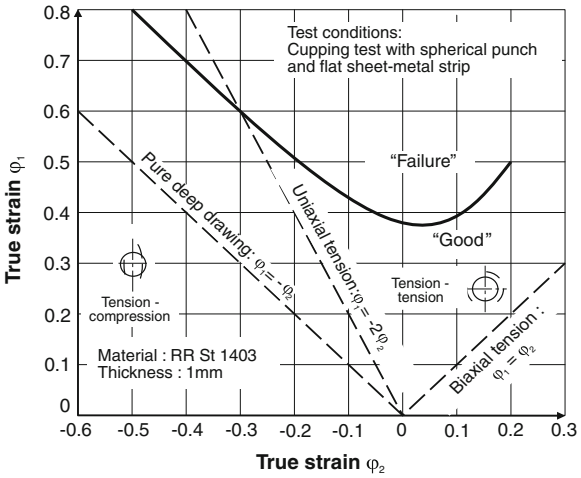


Fig. 2.62 Forming limit diagram [HASE77]

We can thus recognize critical areas by comparing the deformation distribution on a drawn part to be tested with the corresponding limit curve. With the help of this information, forming conditions such as the shape of the blank holder, blank holder force, lubrication, tool geometry (edge radii etc.) and the sheet blank size can be optimized so that a maximally uniform deformation distribution is obtained and load peaks are removed. With respect to cost effectiveness, it may then be possible to select sheet metals of lower quality but which can still safely sustain the deformations required.

Besides testing and designing new tools, deformation analysis is also often used in practice to monitor a running production. By determining the distance between the deformations of critical areas and the forming limit curve, which is a measure for production reliability, both differences in sheet metal quality and tool wear progress can be detected. This is important insofar as the geometry of a tool (die clearance etc.) sometimes alters considerably with progressive wear. The resulting new distribution of deformation is then frequently the cause for failure [SUY77].

If drawn parts are manufactured in several stages, one must bear in mind that the forming history (deformation path) also affects the position and shape of a forming limit curve [HASE80b].

Judging the forming suitability of different sheet metal materials is only possible to a limited extent with the help of forming limit diagrams. While materials with very different physical properties do also differ in their forming limit curves, the latter imperfectly reproduce the effects of the strain hardening exponent n and of perpendicular anisotropy r [LANG74]. It is thus possible that two sheet metal materials differing only in these two parameters have almost identical forming limit curves on the one hand but exhibit quite different deformation distributions after a drawing operation and as a result are not equally suitable for the forming process on the other hand.

In addition to the evaluation of cases of failed production parts, usually experimental test procedures are used in order to determine the forming limit curve. Among the most common processes are cupping tests with varying punch and blank shapes, the hydraulic cupping test as well as the tensile with notched specimens [HASE78]. They differ mainly by the shape of the specimen respectively blank as well as by the type of material load, whereby the resultant forming limit curves can deviate from each other considerably at times due to process-specific differences.

2.8 Tribology in Forming Technology

The term "tribology" was introduced in 1966 by an English commission and was derived from the words for "to rub" (tribein) and "theory" (logos) [JOST66]. Tribology is limited however not only to the study of friction, but also includes wear processes. It comprises the entire science and technology of surfaces acting upon each other under relative motion and thus aims for the scientific understanding of all types of friction, wear and lubrication as well as the technical application of tribological knowledge [GFT02].

2.8.1 The Tribological System

When observing tribological processes, it is important not only to take into consideration the individual bodies in contact but the entire tribological system and the collective load acting upon it (Fig. 2.63) [CZIC03].

The tribological system consists of bodies and counter-bodies (tool and workpiece in the case of manufacturing technology) as well as intermediate and surrounding media (lubricant and air as a rule). The sum of external load effects such as process forces, temperature or sliding speed makes up the tribological stress collective, which can be understood as the system input from a system's approach.

Within the system structure there are many influences at work, which effect the system's behaviour at exposure of the stress collective (Fig. 2.64). Besides the type of materials involved, the local load induced stress distributions, contingent on the microgeometry of the surfaces, has an important influence on the friction behaviour. In contrast to friction processes in bearing technology or gear drives, major plastic deformations of a friction partner (the workpiece) can arise during the forming process. These deformations are sometimes associated with considerable surface enlargements, so that the various influences on the system are subject to permanent change. This makes it difficult to capture the state of the system exactly.

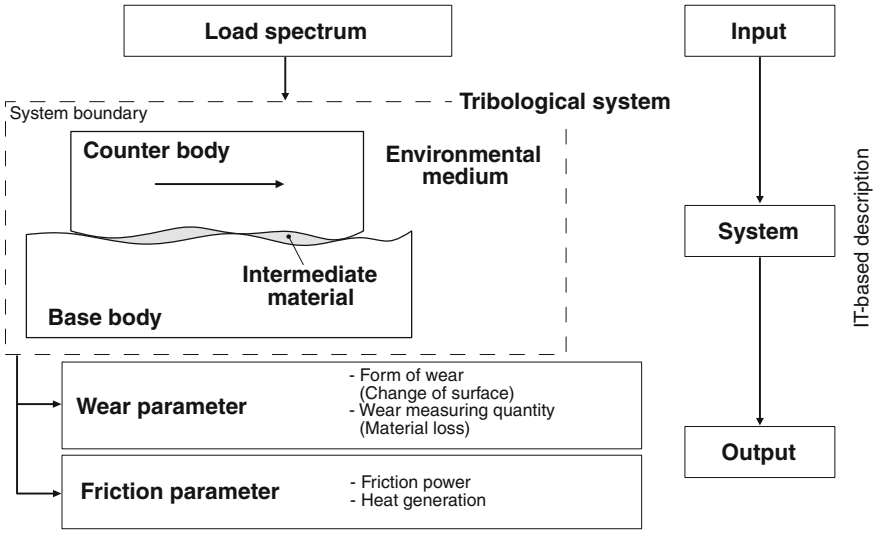


Fig. 2.63 The tribosystem and the system's approach

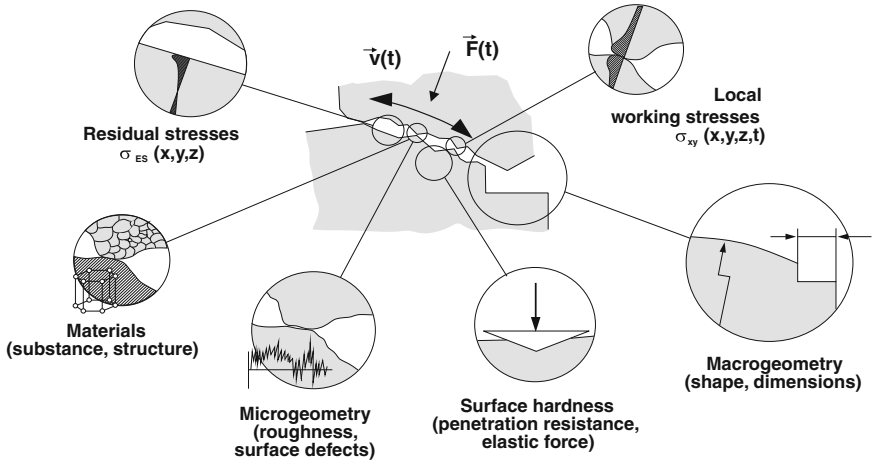


Fig. 2.64 Influences on the tribological system's behaviour within the system structure [FRIE97]

Both friction and wear are dependent on the structure of the tribological system and on the stress collective. They thus make up the system response or system output. Progressive wear and consequentially altered friction conditions retroactively affect both the system structure and the stress collective [CZIC03]:

- *friction, wear = f(system structure, stress collective)*
- *system structure, stress collective = f(friction, wear)*.

The tribological conditions within the system of a forming process have an effect on numerous characteristics of forming processes. Among these are:

- process limits
- cost-effectiveness
- workpiece quality
- impact on the environment and workplace
- resource conservation.

The aim of tribological process designs and optimizations is the improvement of one or more of the above factors. For example, changing the friction conditions can have a major effect on material flow. The latter determines the obtainable final geometry of the workpieces and thus the process limits as well. Furthermore, friction affects the process forces. A reduction of the process forces contributes to resource conservation due to a saving of energy. In addition, tool life is increased with lower loads, which has a positive effect on the cost-effectiveness of a forming process. One consequence of friction is tool wear, the type and characteristics of which affect the service life of the tools used (cost-effectiveness) and the surface quality of the forming parts produced. Many forming processes in manufacturing would not be economically viable at present without the tribological advances of the 20th century.

Given precise knowledge of the tribological conditions within a forming process, friction and wear can be influenced and minimized by carefully selecting the individual components of the tribological system. Essentially, this selection includes the tool materials being used, tool coatings and lubricants, which in turn codetermine the environmental friendliness of a process. In the following, the different types of friction and wear will be elucidated, as well as the potential ways to affect friction and wear by means of measures taken in terms of material and lubrication.

2.8.2 Friction

Friction occurs when there is relative motion between bodies in contact. We differentiate between two basic types of friction. External friction takes place between material areas of different bodies in contact. Internal friction involves contact between two substance areas within the same body. It arises within metallic bodies that are undergoing plastic deformation, leading to forming heat. What both types of friction have in common is that friction respectively the frictional force is directed against the relative motion [GFT02]. In the following, we will take a closer look at external friction.

2.8.2.1 Parameters Influencing Friction

A large number of parameters affect friction. Some of these parameters, such as the true contact surface or the state of lubrication, are difficult to capture formulaically. Figure 2.65 shows different influencing parameters [LI95] affecting friction conditions which arise within a dynamically changing contact surface in the microscopic order of magnitude. Friction is thus a complex process, the analytical calculation of which is very difficult in the sphere of forming technology.

The predominant stress collective has a decisive influence on the magnitude of the frictional force. Forming temperature, strain rate and surface pressure between the body and counter body are essential parameters in this context. In the realm of mixed and boundary friction, which is encountered in forming technology, it is especially surface pressure—also called contact normal stress—that is of paramount importance.

The condition of the tribological system is a further source of influence. This includes factors such as surface finish and the chemical composition of the tool and workpiece. One very important factor is the surface finish of the tool. The influence of machining is so considerable that the frictional force has different values depending on the sliding direction relative to the machining direction. Apart from sheet metal forming, the type of machining process used on the contact surface of the body to be formed is significant only in the initial stage of forming. With progressive deformation, the surface smoothens and becomes a replica of the tool surface.

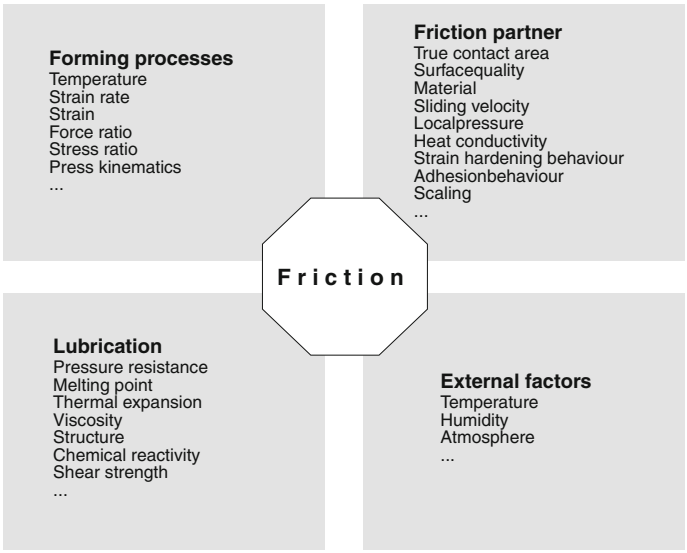


Fig. 2.65 Influencing parameters on friction [LI95]

The physical/chemical condition of the tool and workpiece surfaces has substantial influence on the force of friction. During the forming process, oxides and impurities are removed from the contact surfaces, causing an increase in friction and potentially an increase in the occurrence of wear phenomena. Thus, lubricants need to be employed. These ensure that the size of the frictional forces and the assault of wear on the tool remain within acceptable limits [LI95, RAED02].

2.8.2.2 Friction Laws for Movement Friction

Friction laws are mathematical/analytical approaches with which we can calculate the maximum transmissible frictional shear stress in a friction interface as a function of its main influencing parameters. In plasticity theory, two models have become established to describe the frictional shear stress τ_R—the Coulomb law and the shear friction law (Fig. 2.66). Newer approaches have adjusted the properties of these friction laws to the special requirements of forming technology and combine the advantages of both established models.

Generally speaking, greater accuracy in the calculation of forming processes is possible when the friction laws applied describe the reality more exactly and the characteristic values required for the calculation are all known. One must bear in mind that numerical values such as those that are valid for the friction of normal machine components should never be used to determine friction forces in the case of plastic deformation.

Coulomb Law. The first attempts to describe the underlying natural law stem from the work of Leonardo da Vinci in the 15th century [DAWN79]. Coulomb summarized these experiences in 1785 in a natural law named after himself [COUL85]. The Coulomb law describes the relation between the compressive

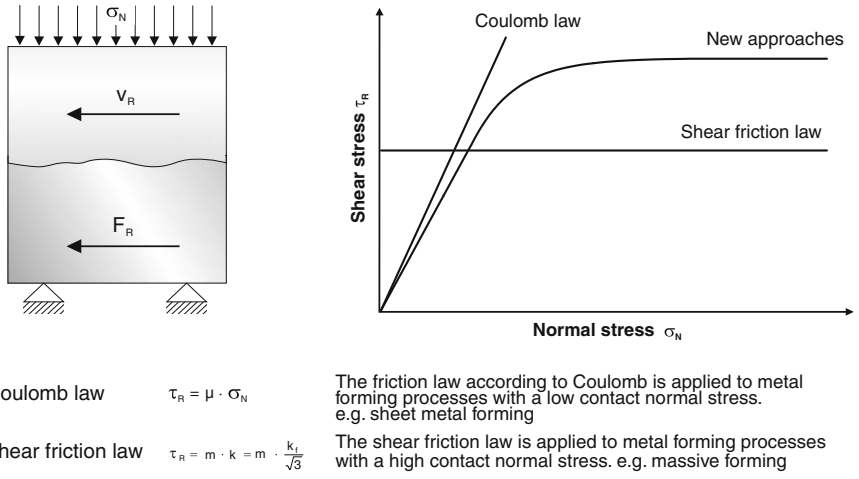


Fig. 2.66 Friction laws in forming technology

force F_N acting in the normal direction and the friction force F_R arising in the interstice in opposition to the direction of movement by the linear relation:

$$|F_R| = \mu \cdot |F_N|. \tag{2.87}$$

The proportionality factor is the friction coefficient μ, which is mostly viewed as constant throughout the duration of the friction process and along the friction surface. Thus, this friction law is based on the assumption that the force of friction is proportional to the load applied and independent of the contact surface and sliding speed. The normal force and friction force can be transferred to locally acting stresses by means of the following relation:

$$|\tau_R| = \mu \cdot |\sigma_N|. \tag{2.88}$$

Thus, the locally acting frictional shear stress τ_R is proportional to the contact normal stress σ_N.

If a relative motion arises in the contact surface of two bodies (workpiece/tool) under the condition that the contact normal stress σ_N is small compared to the flow stress k_f, then the frictional shear stress initially has a linear relation to the contact normal stress if the friction coefficient μ remains constant. Thereby the friction coefficient μ can arbitrarily be set to any positive constant value. A value of 0 describes a frictionless state. But if the frictional shear stress reaches the size of the shear flow stress k of the softer body, the softer body will react with shifting below the contact surface, and both bodies will adhere to each other in the contact zone. This condition is called static friction. The limiting friction coefficient at which adhesion initiates is calculated with $\mu_{limit} = k/|\sigma_N|$. With increasing normal stress, the frictional shear stress corresponds to $|\tau_{R\max}| = k$, whereby k represents a function of deformation in the case of solidifying materials. The Coulomb law is no longer valid in this case, since it does not take an upper limit for frictional shear stress $\tau_{R\max}$ into consideration.

Shear Friction Law. Another mathematical friction law used to describe friction is the shear friction law. This model assumes that the frictional shear stress τ_R must be linked with the shear flow stress k of the softer material with the relation

$$\tau_R = m \cdot k, \tag{2.89}$$

whereby the proportionality factor m is called the shear factor.

This law assumes that the frictional shear stress is constant and independent of the normal pressure. $m = 1$ results in the condition of adhesion, while $m = 0$ characterizes the frictionless state. With the shear factor $0 < m < 1$, the shear friction model is only a rough approximation, as there is no objective method for estimating the numerical value of m. By using the yield criterion of von Mises $k = k_f/\sqrt{3}$ with the flow stress k_f, we obtain the following relation for the shear friction model:

$$\tau_R = m \cdot \frac{k_f}{\sqrt{3}}. \tag{2.90}$$

Free Friction Laws. As opposed to two bodies that slide along each other, the surface of a counter body can tear open because of plastic deformation. In this way, the material from the inside of the plasticized material reaches the surface so that new particles are constantly participating in the friction process. Furthermore, the yield criterion shows that the frictional shear stress is only increased until plastic flow begins, so the friction coefficient is reduced in the case of high surface pressures and thus itself must be a function of surface pressure. This has been determined in numerous investigations, so the Coulomb law is only true for relatively small normal stresses, while the shear friction law is more suitable for high contact normal stresses [KLOC02b].

For this reason, Orowan [OROW43] suggested that the frictional shear stress τ_R should be calculated according to Coulomb's law in proportion to the contact normal stress σ_N in case of low contact normal stresses and that a constant frictional shear stress should be set equal to the shear flow stress k for high contact normal stresses. Figure 2.67 illustrates this law. One proven disadvantage of this approach is the discontinuous transition area, which insufficiently describes the actual conditions of friction.

Further studies have shown that the size of the friction coefficient is determined not only by the material combination but also by the geometry of the friction surface and by the physical and chemical influencing parameters active in the frictional interstice such as pressure, sliding speed and temperature. Dowden and Tabor [BOWD50] have shown that the Coulomb law is only valid as long as the true contact surface increases in proportion with the normal force. Shaw [SHAW63] pursued this problem and has formulated a friction law that describes a continuous transition (area 2) of frictional shear stress between low (area 1) and high contact normal stresses (area 3) (Fig. 2.67).

Building upon the work of Orowan and Shaw, Wanheim and Bay have developed a universal friction law as a combination of the Coulomb law and the shear friction law. This universal friction law describes on the one hand the continuous transition between both friction laws and on the other hand takes into consideration the true contact surface. In this way, the ratio between the true and the apparent contact surface becomes larger as the normal stress increases, and the

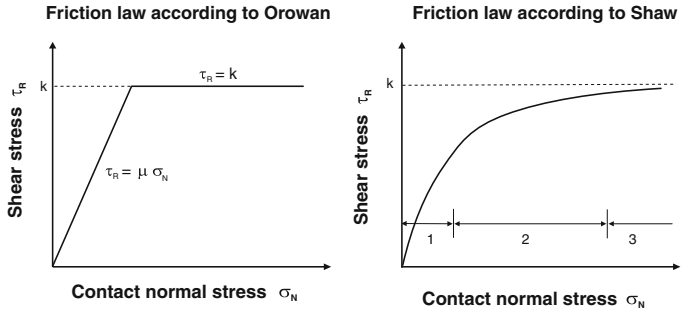


Fig. 2.67 Friction law acc. to Orowan and Shaw [OROW43, SHAW63]

ratio of friction shear stress to the shear flow stress proceeds asymptotically towards 1. This is described by the following relation:

$$\tau_R = f \cdot \alpha \cdot k \tag{2.91}$$

with

τ_R frictional shear stress,
f friction factor $0 \leq f \leq 1$,
α ratio between true and apparent contact surface and
k shear flow stress

Studies on the influence of the contact normal stress σ_N and shear flow stress k on the contact surface ratio α have shown that the course of α initially shows a linear increase and then approaches the value $\alpha = 1$ asymptotically [WANH87, WANH99]. The mathematical relation that describes this effect looks as follows:

$$\frac{\tau_R}{k} = \frac{\tau_R^*}{k} \cdot \frac{\frac{\sigma_N}{k_f}}{\frac{\sigma_N^*}{k_f}} \tag{2.92}$$

with

$$\frac{\sigma_N}{k_f} \leq \frac{\sigma_N^*}{k_f}$$

and

$$\frac{\tau_R}{k} = \frac{\tau_R^*}{k} + \left(f - \frac{\tau_R^*}{k}\right) \cdot \left[1 - \exp \frac{\left(\frac{\sigma_N^*}{k_f} - \frac{\sigma_N}{k_f}\right) \cdot \frac{\tau_R^*}{k}}{\left(f - \frac{\tau_R^*}{k}\right) \cdot \frac{\sigma_N^*}{k_f}}\right] \tag{2.93}$$

with

$$\frac{\sigma_N}{k_f} > \frac{\sigma_N^*}{k_f}$$

The friction stress τ_R and the normal stress σ_N are normalized with the shear flow stress k and the flow stress k_f respectively. The limits of proportionality for the frictional shear stress and the contact normal stress $\left(\tau_R^*, \sigma_N^*\right)$ are described by:

$$\frac{\tau_R^*}{k} = 1 - \sqrt{1 - f}, \tag{2.94}$$

$$\frac{\sigma_N^*}{k_f} = \frac{1 + \frac{\pi}{2} + \arccos(f) + \sqrt{1 - f^2}}{\sqrt{3} \cdot (1 + \sqrt{1 - f})}. \tag{2.95}$$

The friction model is based on contact tests between one smooth and one rough surface. Due to plastic deformation of the roughness peaks, the ratio α between the

true and the apparent contact surface is determined as a function of the normal stress σ_N and the friction factor f, which describes friction in the true contact surface $(0 \leq f \leq 1)$. In the case of low normal contact stress, the roughness peaks are deformed without being influenced by neighbouring peaks. If α is proportional to the normal stress, the Coulomb law is valid. In the case of higher contact normal stress, frictional shear stress is increased along with the normal stress (Eq. 2.92). The frictional shear stress here progresses towards a constant value, comparable to the shear friction model. Figure 2.68 left shows the normalized dimensionless frictional stress as a function of the normalized normal stress with the friction factor f in accordance with the Wanheim/Bay friction law.

In the calculation of forming processes, often either the Coulomb law or the shear friction model is used. The Coulomb law overestimates the frictional shear stress between the workpiece and the tool very frequently however, since the applied normal stress is often so large (e.g. in massive forming) that the frictional shear stress becomes larger than the shear flow stress. In the case of low normal stresses, the shear friction model overestimates the frictional stress, since the friction is not dependent on the current state of stress between the workpiece and the tool, but only on the properties of the workpiece material.

A comparison between a real and a FEM-calculated compression test of a conical specimen without lubrication shows that calculating with a Wanheim/Bay friction factor with $f = 1.0$ describes the deformation of the cone better than the calculated deformation with a friction factor of $m = 0.85$ obtained in the ring compression test (Fig. 2.68 right). The explanation for this is that the shear friction model overestimates the actual friction on the upper side of the workpiece/tool contact surface due to the low contact normal stress, and therefore the material on the top does not flow as much in the radial direction. On the contrary, the shear friction model underestimates friction on the bottom of the workpiece/tool contact surface, since here the contact normal stresses are significantly higher. Thus, the material in this area flows much more in the radial direction in the simulation (Fig. 2.68 right). This is especially clear in those areas in which the contact normal stress takes on small values, i.e. when the normalized normal stress is $\sigma_N / k_f < 1$. Guérin et al. [GUÉR99] have implemented this friction law into commercial FE software. The implementation included two-dimensional and three-dimensional applications.

2.8.2.3 The Effect of Friction on the Process

Many forming processes are heavily influenced by friction. Increased friction causes a larger power and energy requirement, increases surface temperature and affects material flow and with it the distribution of deformation and strength in the entire forming zone. As a result of the higher power requirement, tool load is also increased, leading to a shorter tool life. In sheet metal forming, the maximum drawing ratio is influenced. In the case of excessive frictional forces, cup base

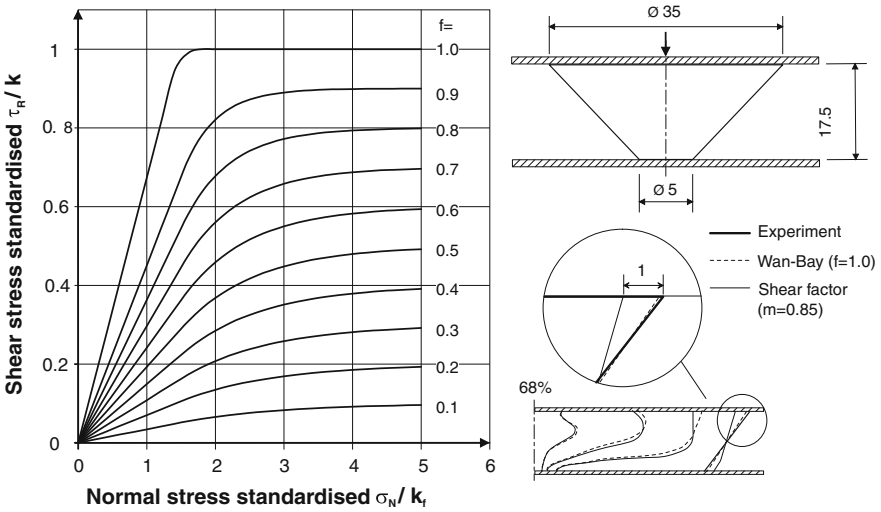


Fig. 2.68 Accuracy of the shear friction law and friction law according to Wanheim and Bay using the example of a conical test piece

fractures can occur. Moreover, the accuracy grade and surface quality of the workpiece can be significantly affected [KOPP99].

However, it is not justified automatically to consider friction merely from a negative light as something undesirable. In forming technology in particular, several processes absolutely require a certain amount of friction for the process to run stably, e.g. rolling (Sect. 3.5). Depending on the requirements of the application at hand, friction in forming technology thus represents a problem of either minimization or optimization.

The simplest example of how friction affects the forming output can be seen in the compression testing of a cylindrical specimen. Assuming frictionless compression, the specimen remains cylindrical during the entire process. The true strain tells a similar story as it remains constant within the cross-section of the specimen and increases with progressing deformation. If the compression process is subject to friction, the specimen bulges more and more with increasing deformation. The bulging is all the more apparent the higher the friction is between the workpiece and the tool. A cross-section through the compressed specimen shows the distribution of the true strain, which increases radially outwards along the contact surface between the workpiece and tool on the one hand and also increases in the axial direction on the other hand, so that the maximum true strains become arranged along the component diagonal.

In the case of reverse cup extrusion (Sect. 3.1.2.1), a variation of friction only leads to a small change in the component's geometry. Nonetheless, the process is heavily influenced by friction (Fig. 2.69). The evaluation of test series carried out with varying lubricants has shown that the punch force is strongly influenced by the lubricant. Dry contact surfaces lead to a high punch force. The friction laws

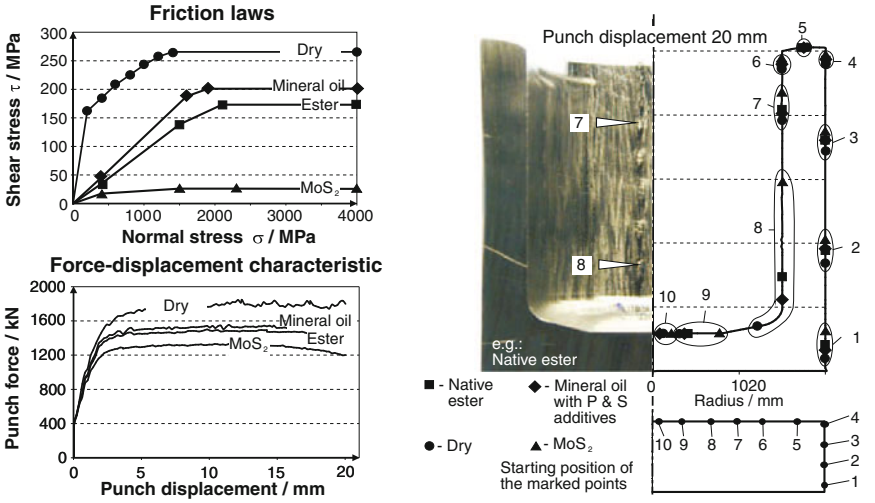


Fig. 2.69 Effects of different types of friction on the forming process using the example of reverse cup extrusion

shown in Fig. 2.69 were established by means of a combination of different test series with FEM simulations and approximately reproduce the actual course of frictional shear stress over contact normal stress. [KLOC04e] provides a detailed explanation of the procedure used to determine these laws.

When one considers surface enlargement during the forming process, one sees that high frictional shear stresses lead to minor displacements along the surface. To this end, in one experiment the surface of the initial test piece was equipped with markings (Fig. 2.69). After forming, the displacements of the points as a result of forming were evaluated. The result was that, in a forming process with dry contact surfaces, the displacement of the marking points relative to their initial coordinates is the smallest. This is especially clear in the case of marking point 8. While this point is shifted in a dry forming process maximally up to the beginning of the punch edge, in a forming process with a solid lubricant it is shifted up to half the height of the cup wall. These examples show that friction is a process-specific quantity which can have a decisive influence on the properties of the component and thus cannot be ignored.

2.8.3 Wear

In the case of constant load, the frictional stress of forming tools is accompanied by wear. According to worksheet 7 of the German Society for Tribology, wear refers to the progressive loss of material from the surface of a solid body from mechanical causes, i.e. contact and relative motion of a solid, liquid or gaseous

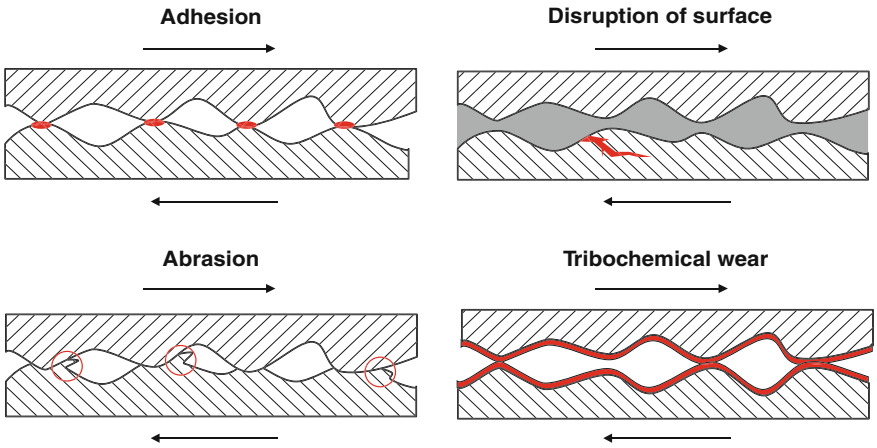


Fig. 2.70 Wear mechanisms in forming technology

counter body [GFT02]. In forming technology, wear is defined also as the transfer of workpiece material to the tool surface, which is commonly referred to as cold shut or wear due to scoring [LANG90a]. In addition to the possibility of cracks, tool fracture and plastic tool deformation, tool wear has a considerable influence on the life of forming tools. The tool life quantity is defined as the amount of produced workpieces till the end of tool life. This is reached when a required quality of workpiece, characterized by accuracy grade and surface quality, can not longer be maintained.

Wear is caused by the interaction of different mechanical and chemical processes. The basic processes involved in wear can be traced back to the following wear mechanisms [CZIC73]: abrasion, adhesion, disruption of surface and tribochemical reactions (Fig. 2.70).

Figure 2.71 shows some typical peculiarities of the wear natures produced by individual mechanisms with the help of selected scanning electron microscopic images. In most cases however, tool wear is the result of several mechanisms operating simultaneously. While the transfer of workpiece material can clearly be attributed to adhesion, material loss cannot always be clearly assigned to individual wear mechanisms.

It should be noted that a distinction must be made in the case of adhesive material transfer between two initiating mechanisms—adhesion due to interfacial bonding (adhesion in the classic sense) and mechanical clasping (Sect. 2.8.3.2). Figure 2.71 top left shows two examples that make the difference clear. The level areas with white points in the left image represent the surface of a polished, powder-metallurgical high-speed steel. The white points are the spherically formed carbides. The adhered workpiece material lies on this very smooth surface and adheres due to the formation of interfacial bondings on the surface. In the right image, a high-speed steel surface is also shown but in much lower magnification. In this case it is a turned surface and as such much rougher. The vertical grooves

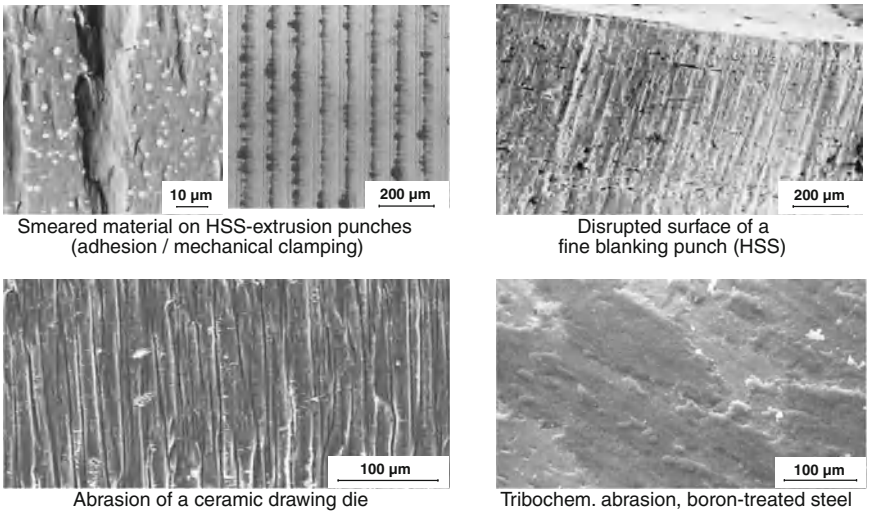


Fig. 2.71 Scanning electron microscopic images of typical forms of wear on forming tools caused by different wear mechanisms

can be easily seen. Workpiece material adheres to the raised transitions between the grooves. This material is sheared off by the elevations during the forming process and becomes mechanically anchored on the uneven patches.

2.8.3.1 Abrasion

Abrasion of the base body occurs in tribological contact classically when the base body is loaded by the roughness peaks of a harder counter body or by hard particles [BART00]. In forming technology, the tool is the base body, which due to the process is always harder than the workpiece to be formed, i.e. the counter body. Abrasive wear of forming tools is thus attributed to hard particles found in the frictional contact zones between the base and counter bodies. Among these are hard phases contained in the counter body material (workpiece material) such as the carbides of the alloying elements or intermetallic phases, as well as oxides (e.g. scale of forging blanks) or other compounds or impurities on the surface. The abrasive hard particles are pressed into the hard tool surface according to a kind of hydraulic principle. The position and shape of the abrasive particle is decisive [RAED02]: on the side of the workpiece, the particle is loaded with a relatively small pressure, which is maximally three time the value of the yield point of the softer material. If this particle has a small contact surface on the side of the tool, it exerts a corresponding amount of pressure there, since the equilibrium of forces must be maintained.

Even extremely hard tool materials such as cemented carbides or ceramics are subject to this wear mechanism, the results of which manifest themselves

microscopically in small furrows on the tool surface and material loss in the form of wear particles (Fig. 2.71 bottom left). The hardness of the abrasive particles in relation to the hardness of the tool material is decisive for the quantitative characteristics of abrasive wear. Beyond a certain hardness difference, there is a rapid increase in wear. The designation of low/high wear level is used for this [BERT00].

Depending on the material properties, different forms of abrasion can arise on the tool surface, individually or in combination [GAHR87]:

- **micro ploughing:** furrowing, plastic deformation of the base body with accumulations on the furrow edges, ideally without material removal
- **micro fatiguing:** separation of the material from the surface of the base body as a result of repeated micro ploughing
- **micro chipping:** formation of a "microchip" in front of the abrasively acting hard particle
- **micro fracture:** exceeding a critical load leads to cracking and thus to larger chippage, especially in the case of more brittle materials.

The wear particles originating from the mechanisms of micro chipping and micro fatiguing are harder than the base material of the tool, since they were subjected to plastic deformation before separation. These particles act abrasively in turn and can thus additionally enhance abrasive wear. It is therefore the task of lubrication to transport wear particles of any kind as quickly as possible from the contact zone between the tool and the workpiece.

2.8.3.2 Adhesion

Adhesive wear manifests itself in a transfer of material from the softer friction partner to the surface of the harder one. It originates under the effect of higher surface pressures between the base and counter bodies. Due to the extreme surface pressures and the friction combination of hard tool/soft workpiece, adhesive wear is of decisive importance in forming technology. In the case of adhesive wear, we differentiate between two initiating mechanisms—interfacial bonding and mechanical clasping (see also Fig. 2.71 top left and Sect. 2.8.3). Both mechanisms will be explained further in the following.

The wear mechanism of adhesion is, according to the classic definition, initiated by the formation of interfacial bonds when non-metallic surface layers like oxides tear open in tribological contact and are removed. This results in a purely metallic contact between the materials of the tool and the workpiece [RAED02].

On the workpiece side, enlargement of the surface with progressive plastic deformation is responsible for tearing open the oxide layers. On the tool side, local load peaks on roughness peaks lead to elastic material deformation, which also leads the brittle oxide layers to becoming torn open. Moreover, it is possible that the oxide layers are abrasively removed.

At the points of metallic contact, interfacial bonds can finally be formed under the high surface pressures. These interfacial bonds are also known as "cold welding" or "scorer". The mechanism involved is adhesion, to which all chemical bonds can contribute that can also bring about the inner cohesion of solid bodies. Among these are the strong primary valency bonds (ionic bonds, covalent bonds, metallic bonds) as well as the relatively weak secondary valency bonds (van der Waals bonds).

These interfacial bonds can be stronger than the cohesion inside the soft workpiece material, so that separation of the bond generally takes place inside the workpiece material via shearing. In this way, the workpiece material is permanently transferred to the tool surface (Fig. 2.71 top left, left image).

In numerous investigations, attempts have been undertaken to discover connections between the general tendency to adhesion and the basic material properties of different metals. The basic insights gained from this can be summarized in rules of thumb, which however are only valid for pure metals and only partially:

- The adhesive tendency of metals is reduced with increasing hardness [SIKO63].
- The adhesive tendency is reduced as a function of the lattice structure in the order fcc- bcc-hexagonal [BUCK68, HABI68]. The reason for this lies in the different number of glide planes, which effect the formation of true contact surfaces.
- The strength of adhesion is reduced in the order b-group metals—noble metals—transition metals [CZIC68]. This is founded in the differing electron configuration and the associated capability to form certain types of bonds.

Furthermore, adhesive wear is in many cases initiated by mechanical clasping. In this case, due to the high pressures arising during the forming process the soft material of the workpiece is pressed into surface defects (grinding grooves, burrs, coating defects etc.) of the tool and sheared off the workpiece by relative motion (Fig. 2.71 top left, right image). In this way, workpiece material also remains on the tool surface, bringing about in turn a metallic contact which in this case is between the workpiece material adhered to the tool surface and the workpiece itself.

Adhesive wear has different technological effects. Heavily roughened tool surfaces are the first result, resulting in turn in grooves on the workpieces. If the surface quality of the workpieces is exceeded to an impermissible extent, the end of the tool life has been reached. Mechanical reworking (e.g. grinding or polishing), or in some cases chemical treatment (e.g. in the case of aluminium buildup weldings), can remove these undesirable material transfers.

Furthermore, the buildups of workpiece material also causes local overloads of the tool surfaces in the case of repeated tribological load. These locally excessive and time limited stress peaks promote the mechanism of the disruption of the surface (Sect. 2.8.3.3). Thus, spontaneous cracking can occur that lead eventually to pitting-like disruptions from the tool surface.

Potential measures against adhesive wear are extremely numerous. In order to prevent the development of interfacial bonds effectively, one must separate the metallic surfaces of the tool and the workpiece (see Sects. 2.8.4 and 2.8.5). In order to prevent mechanical clasping, an optimal finishing processing of the tool surfaces is necessary. In many cases therefore, polished tools are employed since they lay themselves open for attack by mechanical material clasping to only a small extent.

2.8.3.3 Surface Disruption

Surface disruption is based on fatigue and crack initiation of the areas near the surface, brought about by tribological alternating loads in the surface layer zone of both contact partners, leading to material separation [CZIC03]. It is a wear mechanism brought about by the cyclical rollover and tangential and normal multiple loads on the same surface areas.

Surface disruption has certain similarities with fatigue and the fracture of massive components. Accordingly, fatigue is determined by the load amplitude and number of cycles. We differentiate in general between short-term and long-term fatigue. In the short-term fatigue range, load amplitudes are on the level of tensile strength. In these cases, cracking and fractures can develop after a very short amount of time. On the contrary, long-term fatigue is characterized by long tool life and low load amplitudes and represents the technologically most desirable variant of fatigue. The process of long-term fatigue on surfaces can, as opposed to short-term fatigue, be subdivided into the following phases [SUH73]:

- generation of dislocations below the tribologically loaded surface (tool surface),
- accumulation of dislocations,
- formation of crystallographic defects and submicroscopic "voids",
- merging of the voids into cracks parallel and perpendicular to the loaded surface and
- generation of wear particles when the cracks reach a certain critical length.

Surface cracks and platelet-shaped wear particles are the result (Fig. 2.71 top right). In order to obtain as many load cycles as possible without surface disruption (or high tool life quantities), the load amplitude must be kept as low as possible. In the case of surface fatigue, peak loads occur on the surface warping. Among these are, for example, roughness peaks or grinding grooves or burrs remaining from the tool manufacture. In analogy to the mechanism of adhesion via mechanical clasping, the result is the need for forming tools with surfaces of extremely low roughness. But even in the case of ideally smooth surfaces, buildup workpiece material transferred by the wear mechanism of adhesion to the tool surface can form imperfections that have a load-concentrating effect.

2.8.3.4 Tribochemical Wear

The tribological loading of both friction partners induces frictional energy into the surface areas of the contact partners. This generates chemical reactions between the base and counter bodies, intermediate material and the surrounding medium, in which surface layers of altered chemical composition form on the base and counter bodies, usually with significantly altered material properties (Fig. 2.71 bottom right). Brittle-hard reaction layers can only reduce tribologically induced stresses to a limited extent and are removed by brittle disruption when a critical thickness is reached, whereas softer reaction products are continuously regenerated and abrasively removed [FINK32, QUIN62]. Both kinds of removal of chemical reaction products from tool surfaces are designated as tribochemical wear. Loss of material from the tool surface is common to both of them.

Tribochemical reactions can generally be accelerated by different processes [HEID75, THIE67]:

- removal of reaction-inhibiting surface layers
- acceleration of the transport of the reaction participants
- enlargement of the reactive surface
- temperature increase as a result of frictional heat
- generation of surface atoms with free valancies as a result of lattice distortions resulting from plastic deformation processes.

In forming, all five of these processes take place simultaneously. In addition to the friction energy mentioned, dissipated forming energy and potentially process heat (such as is required for forging) also lead to further temperature increases on the tool surface. Chemical reactions between the tool and the surrounding or intermediate medium thus arise in all forming processes, even if they differ considerably with respect to their magnitude or technological effect. We will briefly list two examples to elucidate this:

- The surfaces of forging tools are exposed to high temperatures. As a result, increased oxidation (reaction of the base body and the surrounding medium) takes place compared to room temperature. As a result of thermal and mechanical activation, these occur especially on microcontact areas (roughness peaks). Disruptions of the resulting oxide islands result, resulting in turn in undesirable loss of material from the tool in the form of wear particles.
- In cold forming, lubricants are often provided with reaction layer-forming additives. The reaction layers are generated continuously and again removed and per definition contribute to tribochemical wear. This is intentional in this case however and is accepted in order to prevent adhesive wear via the surface-removing effect of reaction products (e.g. iron chloride in the case of chlorinated oils, Sect. 2.8.4.4), as adhesive wear has a much stronger effect.

2.8.4 Lubrication in Forming Technology

Lubrication is extremely important in forming technology. Very different materials are used to prevent tool wear and to work against the effects of friction. Due to the exceedingly high tribological loads, many forming processes are not even executable without special lubrication techniques.

In most applications, liquid lubricants based on minerals or synthetic oils or natural oils serve as the base lubricants. These base lubricants are also called base oils (Sect. 2.8.4.3). However, pasty, fatty and solid substances or foils are also employed, as these have an increased surface-separating effect or, in the case of solid lubricants, can withstand higher temperatures such as those that are found in forging (Sect. 2.8.4.5). In order to obtain a technologically effective lubricant, different additives must be mixed into the base oils, emulsions or greases (Sect. 2.8.4.4). In many cases, the lubricants can be applied to the workpieces directly. In the case of complicated processes, cold massive forming in particular, often it is necessary to apply a lubricant carrier layer, which then itself receives the lubricant (Sect. 2.8.4.2).

Work sheet 2 of the German Society for Tribology [GFT91] provides an overview of the lubricating media suitable for forming. This guideline also contains information regarding the type of application that is best suited for the respective lubricant.

The reason for the above mentioned diversity of lubricants used in forming technology has to do with the array of process-dependent tribological loads with respect to mechanical tool load and relative velocity between the tool and workpiece surfaces. From hydrodynamic states of lubrication, as sometimes found in the blank holder area of deep drawing tools, to extreme conditions of boundary friction in massive forming, the entire spectrum of lubrication states is thus covered by all individual forming process (Fig. 2.72).

2.8.4.1 Forming Lubricant Requirements

The most important tribological function of a lubricant consists in separating the surfaces of the tool and workpiece, thereby shifting the friction conditions from the boundary friction area in the direction of hydrodynamic friction (Fig. 2.72). Optimal friction conditions are the prerequisite for good workpiece surfaces as well as minimal forming forces and thus for a low mechanical load and low tool wear.

A further tribological function consists in the removal of heat from the lubrication gap. This function is of particular importance above all in forging processes. By spraying the forging die between every working stroke, it is guaranteed that the tool material does not overheat and prematurely fail due to softening and oxidative wear. But high temperatures are encountered in the case of “cold” forming as well. In the reverse cup extrusion of soft-annealed case-hardening steel 16MnCr5 for

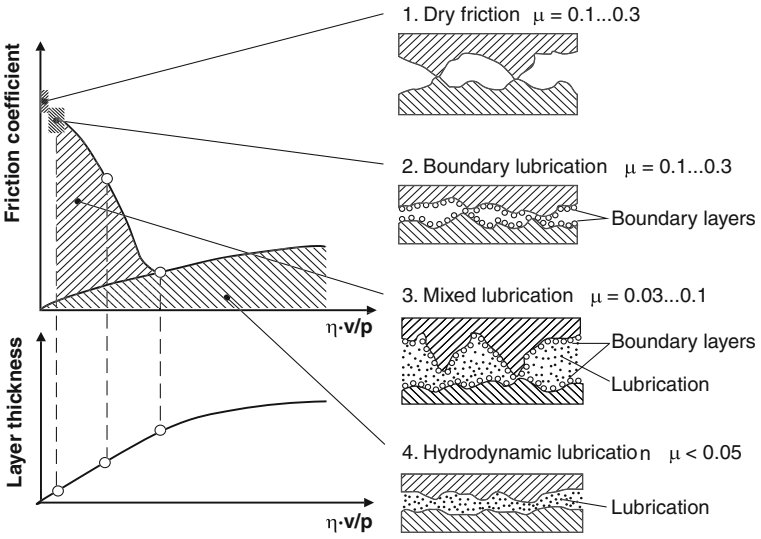


Fig. 2.72 Stribeck diagram for different states of lubrication, with η dynamic viscosity, v sliding speed, p pressure/surface pressure [CZIC03]

example, contact temperatures of more than 350 °C can arise, in the case of stainless steel even more than 500 °C [RAED02, STEE99]; similar temperatures are found in fine blanking.

Yet in addition to the tribological properties of lubricants (reduction of friction and wear as well as heat removal), lubricants must also perform many other tasks and meet a large number of requirements. Figure 2.73 gives an overview of the requirements of forming lubricants. Each requirement can be met in a different way, as will be shown in the following by means of describing individual lubricants and their functionality.

2.8.4.2 Release Agent and Lubricant Carrier Coatings

In cold forming operations, in which enhanced surface enlargement of the workpiece is to be expected, the material to be formed is equipped with a lubricant carrier layer (conversion coating) in chemical baths. Conversion coatings are crystalline, highly porous salt layers that originate via chemical conversion with the base material and are firmly fused to it. The task of these layers is to separate the metallic surfaces of the tool and workpiece even in the case of major surface enlargements and to serve as a tie coat or conversion partner for the lubricant to be applied.

Besides extrusion, conversion coatings are also utilized for wire, tube and profile drawing and sometimes in sheet metal processing, e.g. in the case of difficult wall ironing operations [MANG83]. While bulk solids are coated by

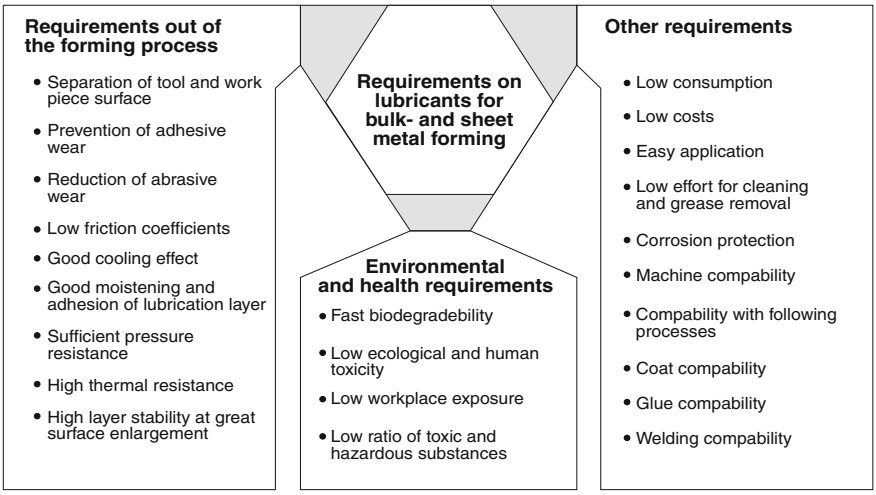


Fig. 2.73 Requirements for lubricants for massive and sheet metal forming

immersion in multi-chamber systems, tunnel machines tend to be used for wire and sheet metal.

Especially important are metal phosphate and metal oxalate coatings which are used for the extrusion of high-strength chrome and/or nickel steels [MANG83, LANG90a, NITT04a]. Zinc phosphating is the most common pretreatment method for steel extrusion parts. However, sometimes manganese phosphate or zinc manganese phosphates are also used. For the extrusion of high-strength aluminium materials, very often calcium aluminate coatings are also employed in addition to zinc phosphates [NITT04a]. Titanium alloys are equipped with titanium fluoride coatings.

Zinc phosphate coatings are stable to about 400 °C, while oxalate coatings already begin to disintegrate after 140 °C [MANG83]. For a short time however, both can withstand much higher thermal loads in forming processes.

As an example, let us briefly consider zinc phosphating. First of all, it is important that the blanks have a consistent, homogeneous surface quality, as present-day phosphating facilities are highly automated. In order to obtain this, the blanks often undergo a form of mechanical pretreatment such as peeling, sand-blasting or shot peening [BAY94].

To better fix the phosphate coating on the workpiece surface, first iron atoms are removed from the composite by means of a pickling process using sulphuric, phosphoric or hydrochloric acid. After rinsing, actual film-forming begins. The phosphating solution involved consists of a phosphoric acid solution of the primary zinc phosphate. First there is a pickling reaction of the workpiece surface with the free phosphoric acid. This alters the solution equilibrium at the workpiece/solution interface; the primary zinc phosphate in the solution breaks down into poorly soluble tertiary zinc phosphate and free phosphoric acid. The poorly

soluble tertiary zinc phosphate is deposited on the workpiece surface as a crystalline film, while the iron atoms released from the surface react with the solution to form Fe-III phosphate. The latter collects at the bottom of the phosphating bath and has to be disposed of as phosphate sludge.

General tips on phosphating metals, also regarding chipless shaping, can be found in DIN EN 12476 [EN01a]. More recent developments in conversion treatment have been focused on reducing the use of chemicals and lubricants, diminishing processing times and lowering process temperatures during the coating process in order to make the process more environmentally friendly and cost-efficient [KÖNI93a].

The form of the film structure depends on how long it spends in the phosphating bath. Figure 2.74 clarifies the effect of the phosphate film structure on the extrusion process.

While the characteristic of the phosphate film has indeed an influence on friction and thus press force, however it itself does not have any properties that reduce friction [MANG83]. Rather, it provides, depending on the porosity of its structure, an extremely large surface, which is an ideal tie coat for additional lubricants of various kinds. The better the layer fulfils its function as a lubricant carrier, the better the lubricants can perform.

Depending on the expected process temperature, suitable lubricants can include oils, different soaps and polymer dry films, or solid lubricants like molybdenum disulfide (MoS_2) or graphite [LANG90a, MANG83, NITT04b]. Extrusion oils with different high pressure additives are preferred for the manufacture of screws, bolts, nuts and small parts on automated multistage presses.

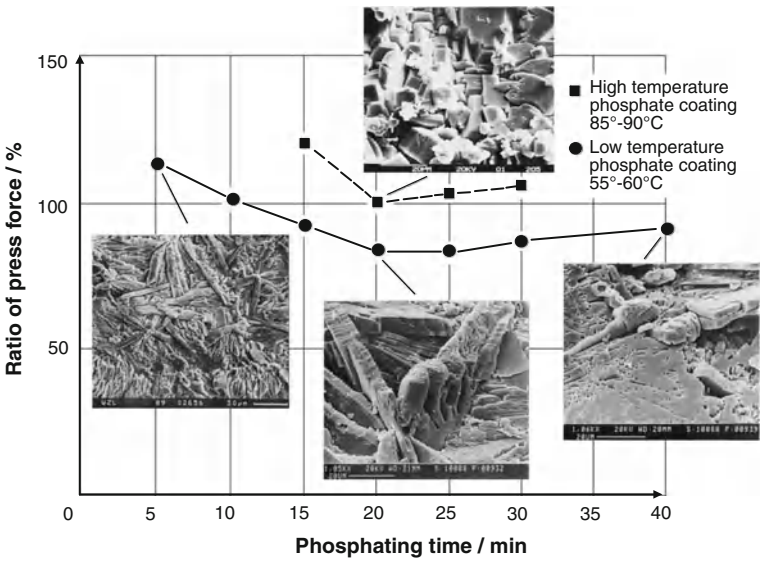


Fig. 2.74 Effect of the phosphate film structure on the press force in the extrusion of helical gears

Soap lubricants are of particular interest for most extrusion and drawing processes, as the fatty acid in the soap can react with the zinc phosphate film in hot, aqueous solution to form highly friction-reducing zinc soap (e.g. zinc stearate in the case of stearic acid). This reaction has two advantages:

- good bonding of the lubricant to the carrier layer and
- the resulting zinc soap has a higher melting point than alkali soaps (sodium soaps).

These soaps are functional until about 200 °C. An important disadvantage of these lubricants is that the soap film cannot endure greater surface enlargements of the workpiece and tears open. This results in the dreaded metallic contact between tool and workpiece, which the still existing phosphate layer can no longer prevent. In the case of more difficult forming processes and higher temperatures, solid lubricants such as molybdenum disulfide (MoS_2) and graphite thus tend to be utilized (Sect. 2.8.4.5).

In some cases, polymer dry films are used instead of MoS_2, as they allow a further increase in performance compared to MoS_2 [NITT04b]. This is of interest for near-net-shape applications, which require optimal mould filling. Certain components can be produced with the use of polymer films even without zinc phosphating and soap. Cold massive forming without a zinc phosphate film is also significantly aided by the use of CVD and PVD coatings [RUPP97].

2.8.4.3 Oils, Greases and Emulsions

Liquid and fatty lubricants are those based on oil and water. Alone they generally have no sufficient wear/friction-reducing effects for forming applications. Oil and water serve as base substances for lubricants in forming technology and thus as carriers for additives or solid lubricants. In order to obtain a lubricant that is technologically attractive and meets all requirements, additives and/or solid lubricants must be added in emulsified, dissolved or dispersed form (Sects. 2.8.4.4 and 2.8.4.5).

Greases. Oils in there pure state are often called base oils. By adding soaps (e.g. sodium soap), solid greases (e.g. wool grease), solids (e.g. chalk), gelling agents (e.g. silica gel) or polyureas, thickened products can be produced that are called greases or pasty substances [MANG01]. Greases are frequently employed because of their rheological properties or for the stable introduction of solid materials that cannot precipitate in grease. The consistency and tribological properties of greases depend heavily on the base oil used, the thickening system and the additives and/or solid lubricants mixed in.

Emulsions. Both oils and greases are often used in the form of emulsions. In the case of emulsions, one liquid is dispersed in another. That is, one liquid is in droplet form (disperse or internal phase) and is surrounded by another liquid (continuous or external phase) [MANG01]. Depending on the type of dispersion, a

distinction is drawn between oil-in-water (OW, oil/grease as the disperse phase) and water-in-oil emulsions (WO, water as the disperse phase). The advantage of emulsions is the enhanced cooling effect resulting from their heat conductivity being five times higher than that of oil and the three times higher heat capacity of water. In the case of hot forming processes, there is also the more rapid vaporization of water, which also has a cooling effect. Moreover, when emulsions are used, the need for oil—which is significantly more expensive than water—is much smaller. However, the higher cost of maintenance and upkeep is a disadvantage, since emulsions are susceptible to contamination from bacteria and fungus as well as to frost. Essential for the quality of an emulsion is that the water used be of consistent quality, as water can fluctuate greatly with respect to pH, ion content and the microorganisms it contains. It is also true for emulsions that their performance depends greatly on the base oil used as well as its additive content.

Viscosity. Probably the most important characteristic value of oils and emulsions is viscosity. As a rule, it is labelled as kinematic viscosity v at 40 °C in mm^2/s (SI-unit) or *cSt* (centistokes) and describes the fluidity of liquid substances [MANG01]. Forming technology covers a wide range of viscosity, from low-viscous, thin oils (e.g. residue-free vapourizing punching and drawing oils, $v \approx 3\,mm^2/s$) up to extremely viscous, hardly flowable oils (e.g. oils for mandrel lubrication in pipe manufacture, $v \approx 1,000\,mm^2/s$) [MANG83].

Viscosity changes as a function of temperature and applied pressure [MANG01]. Viscosity-temperature behaviour (VT behaviour) is described by the viscosity index (VI). The higher the VI given for a certain lubricant is, the less its viscosity drops with increasing temperature. Viscosity-pressure behaviour (VP behaviour) on the contrary is characterized by a viscosity-pressure coefficient α [GOLD01]. A high α value stands for a high increase in viscosity with increasing pressure.

Since viscosity is also a measure for the carrying capacity of a lubricant film, a reduction of viscosity under increased temperature has a negative effect in most forming processes, while the tendency to increase viscosity with increasing pressure is a positive one. Favourable lubricant behaviour is thus indicated by high values of VI and α.

Mineral Oils. Base oils are classified as mineral oils, synthetic oils and natural oils [HUBM94, MANG83, MANG01, SEID04]. Mineral oils are, as before, still the most important group with the greatest market strength.

Depending on the properties desired, different components of mineral oil are used, called raffinates. Paraffinic or naphthenic mineral oil raffinates are used, aromatic oils on the other hand to only a very limited extent. Aromatic mineral oils do have properties that are attractive for forming, as they have a very good VP behaviour and the high solubility for additives, but they frequently contain carcinogenic compounds. While paraffin oils, quantitatively the most important group, have the best VT behaviour and lowest dissolving power for additives, aromates are the exact opposite. Napthenes represent the compromise between VT behaviour and dissolving power. Table 2.16 provides an overview.

Table 2.16 Evaluation of the properties of different mineral oils with respect to forming processes [HUBM94, MANG83]

	VT behaviour	VP behaviour	Wettability	Dissolving of additives	Dispersing power	Evaporation
Paraffin	+	−	−	−	−	+
Naphthene	○	○	○	○	○	○
Aromates	−	+	+	+	+	−

Synthetic Oils. The most important synthetic oils are polyolefins, alkyl benzenes, polyglycols and carboxylic acid esters [HUBM94, MANG83, MANG01]:

- Polyolefins have properties similar to paraffinic mineral oils. Especially common are polyalphaolefins, which depolymerize at high pressures or temperatures. That means that their viscosity may sink with use, but they are ideally suited for forming parts that have not been degreased prior to thermal postprocessing.
- Alkyl benzenes as a whole are very similar to aromatic mineral oils and thus provide similarly good dissolving power for additives. Their absolute lack of sulphur makes the use of these materials especially attractive.
- Polyglycols are water soluble in most cases, often oil soluble simultaneously. Compared to emulsions, they thus make more stable oil-water mixtures available. These materials are of interest for solid lubricant dispersions for hot and warm forming because of the possibility of using aqueous oil-based dispersions. Compared to water-based dispersions, they thus provide an enhanced lubricative effect, and compared to oil-based dispersions, a greater cooling effect.
- Synthetic carboxylic acid esters are fabricated by esterifying natural fatty acids (obtained from natural fats, e.g. rapeseed oil) or synthetic carboxylic acids (oxidation of mineral oils). Their greatest advantage is their polar character, leading to a very adhesive lubricant film and a very good lubricative effect in the mixed friction range.

Natural Oils. In the last several years, natural oils have become increasingly important due to their improved biodegradability compared with mineral oils [AHLR04, GERB03, KLOC04c]. Although they have many favourable properties, they have not become dominant because of their high prices and variable quality. The saturated and unsaturated fatty acids (e.g. oleic acid) contained in natural oils and different ester compounds (e.g. triglyceride) exhibit polar groups that become deposited on surfaces via adsorption, thus greatly aiding lubricant film adhesion and stability. In their pure form, they thus lead to significantly lower friction coefficients than pure mineral oils (Fig. 2.75). They are also frequently superior to mineral oils containing additives [KLOC04e]. Native fatty acids and ester compounds are therefore often used as additives (polar additives) in lubricants based on mineral oils. Furthermore, they are distinguished by a better VT behaviour than mineral oils and a much lower degree of vaporization. Since most forming

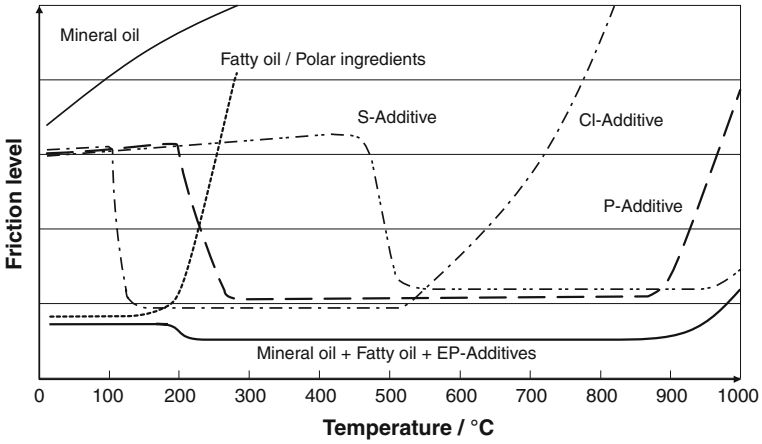


Fig. 2.75 Qualitative profile of the friction coefficients for different base oils and additives over temperature [HORL89, MANG83, SCHU04a]

processes work without circular lubrication but rather with loss lubrication, their low ageing stability is of a little importance in forming technology.

2.8.4.4 Additives

Forming lubricants, including oils, greases and emulsions, are generally provided with additives. A distinction is drawn between stabilizing additives such as oxidation, hydrolysis and foam inhibitors, emulsifiers and surface-active additives [BART94, MANG83, MANG01]. Among the latter are included anti-corrosion additives as well as friction and wear reducing materials. Surface-active friction/wear-reducing materials have the greatest effect on the respective forming process [ULLM04]. What they all have in common is that they reduce the friction coefficient to a greater or lesser degree and protect the surface from wear. The biggest difference is in their mechanisms of action (physisorption, chemisorption and chemical reaction), of which one or more are active simultaneously. Depending on the type of tribological conditions dominant in the lubrication gap, each additive varies in terms of how well it can be used or combined with lubricants. Figure 2.75 shows the friction-reducing potential of different liquid lubricants and additives over temperature.

It is difficult to subdivide additives into different classes, and this is undertaken in various ways in the literature. In the following, we will differentiate between polar agents and EP additives.

Polar Agents. The most important polar agents are natural fats (ester compounds like triglycerides), fatty acids, synthetic carboxylic acids and carboxylic acid esters, fatty alcohols, fatty acid amides and amines and metallic soaps [ULLM04]. They deposit themselves to a great extent on metallic surfaces via

physisorption, creating van-der-Waals bondings between the polar molecular end and the metal surface. In this way, they influence the wetting behaviour of the lubricants and, already at room temperature, form friction-reducing and slightly wear-protective forms of the thickness of one molecular length. At temperatures above 100 °C, the polar bonds begin to be released, eliminating the friction-reducing effect (Fig. 2.75). Moreover, fatty acids are capable of reacting with the surfaces of metallic materials. This results in metallic soaps that also have a friction-reducing effect and are stable to about 200 °C.

Extreme Pressure (*EP*) *Additives.* The EP additive group is needed for difficult forming processes when the use of additives with polar materials is no longer sufficient. The metallic surfaces newly created during forming react with the EP additives during the process to form shear-soft reaction layers that prevent undesirable metallic contact between the tool and workpiece. Under mechanical load, these films are easily sheared off and thus have a friction-reducing effect (Fig. 2.75). The reaction layers are thus constantly built up and rubbed off again, consuming the EP agents.

The class of EP additives is dominated by three especially common material classes [HORL89, KORF94, MANG83, MANG01, SCHU04a, ULLM04]:

- **Sulphur-containing additives:** The most effective and commonly used reaction layers are sulphidic. The reaction of metallic surfaces with sulphur contained in oil takes place at high temperatures (generally above 500 °C) and leads to very stable and temperature-resistant separating layers. The effectiveness of sulphur carriers is based on the fact that they become deposited on the metal surface through physical adsorption and separate sulphur via chemisorption, which then reacts with the metal to form a sulphide. Sulphurized oils are produced by the addition of pure sulphur powder (also called flower of sulphur, which also has the properties of solid lubricants), sulphurized fats (e.g. sulphurized fatty acid esters) or by sulphurized hydrocarbons (e.g. alkyl polysulfides) and contain between 10 and 50 % sulphur. The particular additives used differ with respect to polarity (physisorption capability), which increases from hydrocarbon to fat, sulphur activity (chemisorption capability) and sulphur content, which is reduced from hydrocarbon to fat. In order to cover a wide range of applications therefore, often different sulphur carriers are used in combination.
- **Phosphoric additives:** Phosphoric additives partially cause a phosphatizing of the surfaces of both tool and workpiece. By means of its synergy with sulphur carriers, they are being used nowadays increasingly in combination as a substitute for chlorinated paraffins [WÜNS02]. The most important phosphorous additives are phosphoric acid esters. In the phosphate part of the molecule, oxygen can be replaced by sulphur, resulting in thiophosphates, of which previously zinc dialkyldithiophosphates were preferrably used. They are utilized in almost all lubricant areas and are being increasingly substituted by zinc-free compounds. In the case of these materials, there is not only phosphatizing but also the release of reactive sulphur, so that sulphidic separating layers are also obtained. The stability of the phosphate films created is very limited in the high

pressure range, which is why phosphorous carriers are often not labelled as EP additives but rather merely as AW (anti-wear) additives. Besides their wear-protective effect, they often function as oxidation and corrosion inhibitors.

- **Chloric additives:** The most important group of chlorine-containing additives are the oily, usually highly viscous chlorinated paraffins with chlorine contents between 35 and 70 %. Their effect is based on a similar mechanism as is seen with the sulphur additives (physisorption—chemisorption—reaction). They have a friction-reducing and wear-protective effect from their mere presence alone, being very polar compounds. When the activation temperature (>100 °C) is reached, an iron chloride layer is formed consisting of iron(II) and iron(III) chloride, which is stable up to a maximum temperature of 670 °C (melting point of iron(II) chloride). Different information is provided in the litarature regarding their exact workings and thermal limits of use. A good description can be found in [SCHU04a]. Chlorinated paraffins bring about extremely low friction coefficients. The latter is of interest especially for processing high-alloyed Cr-Ni steels, since in this case polar additives can only bring about a small reduction of friction. Despite their excellent tribological effect and relatively low price, their use is rapidly declining at present. The reason for this is the ban on short-chained chlorinated paraffins (10–13 C atoms) in Europe since December 31st, 1999 because they were found to be toxic, carcinogenic and difficult to degrade [AHLR04, NN95]. Medium and long-chained chlorinated paraffins may indeed still be used, but are suspected to break down into short-chained chlorinated paraffins during use. Their disposal is expensive, since dioxin is formed when they are burned. Moreover, the hydrochloric acids freed during consumption often cause corrosion problems for the parts produced along with associated high cleaning requirements. Nonetheless, they are still used for some forming processes, e.g. in the case of difficult deep drawing operations of austenitic, stainless steels or in certain fine blanking processes [KLOC03c, KLOC04d]. Substitute products are often less effective, much more expensive or frequently entail a rearrangement of downstream cleaning stages.

Passive Extreme Pressure Additives (*PEP*). This class of additives is characterized by very good high-pressure properties without a chemical reaction with the metal surface taking place, such as is the case with sulphur-containing or chloric additives. They are called passive extreme pressure additives (PEP) for this reason. Typical representatives of this class are overbased sulphonates. These compounds contain, besides conventional petroleum sulphonate (calcium, sodium), the corresponding carbonate in very fine distribution, so that the entire mixture appears as an amorphous liquid. The carbonates function as a solid lubricant and bring about at least a partial physical separation of the tool and the workpiece. In this way, the pressure absorption of the oils is heavily increased. At the same time, overbased sulphonates provide good corrosion protection and act as acid scavengers.

2.8.4.5 Solid Lubricants

It is impossible to find a generally binding definition for dry or solid lubricants, terms which the literature often uses synonymously. Fundamentally, a classification can however be made into structurally effective, mechanically effective and chemically effective solid lubricants. Furthermore, it is possible to subdivide the solid lubricants used in the metalworking industry according to their chemical character into organic and inorganic solid lubricants. In the following, we will look at the solid lubricants that are common in forming technology along with their properties [HORT01, KORF94, LANG90a, MANG83, SEID04, ZIBU04]:

Solid Lubricant Powder. Among the most important of all solid lubricants are the structurally effective inorganic lubricants. The most significant representatives of this group are graphite, molybdenum disulfide (MoS_2) and hexagonal boron nitride (hBN, not to be confused with the cutting material cBN). These are used both in cold massive forming as substitutes for soap at higher temperatures as well as in forging in suspensions with water or oil. Moreover, they are also used in greases. Their structure consists of superimposed multilayered platelets that can withstand high pressures and large true strains. The layers in the platelets shift against each other, but this does not tear open the lubricant film. MoS_2 can be used up to about 400 °C, graphite up to about 700 °C and hBN up to about 1,000 °C. At higher temperatures, oxidation sets in.

In cold forming, the good lubrication properties of graphite and MoS_2 are bought at a high price, which is about 15 times more than that of soaps and thus places economic limits on a broader use. Solid lubricants can be applied on previously phosphated workpieces by tumbling, dipping in suspension and by a combination of phosphating/oxalating and coating.

Forging processes work primarily with graphite. The advantages of hBN come to play at temperatures above 600 °C, where hBN has a lower friction coefficient than graphite. The disadvantage of hBN is its high cost.

Titanium iodide (TiJ_2) and chrome chloride ($CrCl_3$) have properties similar to molybdenum disulfide.

Plastic Foils. Plastics are used in various forms as foils and strippable paints and as additives in liquid and pasty lubricants. Their use is limited predominantly to the manufacture of decorative sheet metal forming parts made of stainless noble steel, aluminium, copper and bronze materials, where they significantly improve the friction conditions and protect from undesirable grooves. Foils are applied or glued to the sheet metal, while strippable paints are applied in liquid form and then dried. PVC, PE and PP are examples of suitable materials. Thickness ranges between 10 and 50 μm. Both paints and foils are employed only in combination with other lubricants, since they generally tear during the forming process, though they can withstand an elongation of up to 300 %.

Dry Lubricants. "Dry lubricants" are also being increasingly used. A distinction is drawn between "dry lubes" and "hot melts". The former are quickly volatilizing suspensions that are applied at room temperature and leave behind a solid film after drying that often contains combinations of diverse polymers and

waxes as well as PTFE (Teflon). The waxy hot melts on the other hand are applied in a heated form (60–80 °C), often already just after cold rolling as a corrosion inhibitor. In many application examples, their properties are the same as or better than those of oils with high amounts of additives, making them a more environmentally friendly alternative in sheet metal forming or in the extrusion of aluminium.

Prepainted Sheets. In more recent developments in sheet metal forming, prepainted sheet metals are being used to an increasing extent because of the savings potential in painting as well as because of the enhanced corrosion protection. The paint layers often have a positive influence on friction conditions during forming and thus can be included among the dry lubricants.

Salts and Glasses. When forging, especially in the case of some bar extrusion processes and when forging special materials like nickel-titanium alloys, salts or glassy materials can lead to tribological improvements. Their effect is based on the formation of a highly viscous lubricant film above the melting temperature of these materials. They are often sprayed on as a suspension in organic carriers and water. Salts are provided in aqueous solution as well.

Soaps. Some authors also include soaps, such as the often-used, water-soluble and reactive sodium stearate, along with the solid lubricants, since they have a solid character at room temperature. However, sodium stearate is applied in most cases in aqueous solution, e.g. as a soaping on phosphated press blanks. In the extrusion of non-ferrous metals, especially pure aluminium and aluminium alloys, metallic soaps like zinc stearate or zinc behenate or cadmium stearate are used in powder form. They are applied on the blanks by "tumbling", i.e. the blanks are put in large revolving drums along with the soap powder, resulting in a solid lubricant film on the blanks. Metallic soaps are also required in order to thicken greases based on mineral oil or synthetic oils (colloidal dispersion of metallic soap and hydrocarbon oil) or serve as polar additives in liquid lubricants.

Soft Metals. Finally, the literature also includes soft metals such as Pb, Sn, In, Ag and Au among the solid lubricants. They are used as highly adhesive metallic coatings (e.g. tin for drawing steel bushes) when other kinds of lubrication are uneconomical. The resulting frictional shear stress depends directly on the shear strength of the soft metal and on the strain hardening of the soft metal to be expected in the process temperature.

2.8.5 Tool Influences

In addition to the lubricant used, the tool material also has a decisive influence on the forming tribological system. The tool material and especially the characteristics of its edge zone and surface determine the resistance of the tool to wear and affect the friction conditions in the lubrication gap.

2.8.5.1 Influence of the Tool Material

Section 2.7.2 described the tool materials that can be used in forming technology as well as their properties and areas of application. In order to keep the assault of wear at bay as much as possible, it is important that one also bears the tribological material properties in mind when selecting material. Depending on the primary mechanism of wear, corresponding material properties can be exploited for wear reduction [ESCH04, FINZ03, FÜLL04, GEIL04, SCHR04]:

- **Abrasion—**The hardness of a material is a measure of its resistance against abrasive wear (Sect. 2.8.3.1). From the standpoint of abrasive wear protection therefore, the active elements of forming tools subjected to friction should be as hard as possible. The hardness of tool materials increases in the following order: plastics—cast—quenched and tempered steel—cemented carbide—ceramics. Besides the selection of material, heat treatment is also important in this context, as it determines the ultimate hardness of the tool. In the case of forging dies, a high required red hardness is also important. For tool steels, hardness is determined primarily by the carbide-forming alloying elements (Cr, W, Mo, V) and the carbon content. Tungsten, molybdenum and especially cobalt result additionally in an increase in red hardness.
- **Adhesion—**The assault of adhesive wear and the formation of interfacial bonds is among other things affected by the electron configuration of the friction partner materials respectively their alloying elements (Sect. 2.8.3.2). We also refer in this context to the mutual solubility of the friction partners. In connection with the development of adhesion therefore, this indicates the potential of two materials to form common interfacial bonds. The more different the material character of the tool and workpiece materials is, the lower the probability of adhesive wear. For example, especially strong adhesive wear by austenitic, stainless noble steels cannot be prevented by using tool steels with high chrome or nickel contents. Cemented carbide and especially ceramic tools on the contrary reduce adhesion; yet they are only usable under special conditions because of their susceptibility to cracking [FÜLL04].
- **Surface disruption**—Prerequisites for high resistance to surface disruption are both good toughness properties and high mechanical and thermal (especially for forging dies) fatigue strength of the tool material. These properties can suppress cracking (Sect. 2.8.3.3). Toughness is enhanced by means of alloying elements such as cobalt or nickel. Furthermore, the danger of cracking can be diminished by minimizing inclusions and defects in the tool steel and by means of a surface that is as smooth and groove-free as possible. In addition, crack propagation can be hindered with a fine-grained microstructure. Powder-metallurgically manufactured steels are especially important in this context.
- **Tribochemical wear—**Tribochemical reactions arise due to the reaction of the tool material with the lubricant and/or the oxygen in the surrounding air. Wear originates when the reaction products are rubbed off of the tool surface (Sect. 2.8.3.4). Thus, the tool material must be as oxidation-resistant and as inert as

possible. Furthermore, high heat conductivity leads to a more rapid removal of heat, reducing surface temperatures. This generally decelerates chemical reactions. A certain amount of tribochemical wear is unavoidable however; indeed, it is even desirable if reactive EP additives are being used. Most wear-protective additives are designed for the surfaces of metals. When changing from uncoated to coated tool steels respectively to cemented carbide or ceramic tools, we must therefore check whether the additives are still effective. In the case of cemented carbides, one must also guarantee that the lubricant does not bring about any cobalt erosion. Even ceramic materials are subject to a certain amount of chemical attack. Si_3N_4 ceramics, for example, can react with water to form SiO_2 and NH_3, resulting in extremely thin friction-affecting films [KAJD98].

For coated tools, it is essential that the tool material (in this case also called substrate material) has a sufficient supporting effect, i.e. strength, and that it is not subject to plastic deformation. Therefore, a high compression yielding point is required [ESCH04, EVER04]. In principle, it is indispensable for a consistent, faultless layer structure that one ensures flawlessly machined substrate surfaces with a poreless surface structure. Roughness values of $Rz < 1$ µm are to be recommended, while visible grinding grooves and burrs are to be avoided.

In addition, one must ensure that tool manufacture affects the edge zones as little as possible. White layers from eroding or grinding processes are not permissible. This is especially true for surfaces to be coated. In hard machining, any reduction of hardness under the influence of heat is also impermissible.

2.8.5.2 Modification of the Tool Rim Zone

With the help of surface technology, we can affect the tribological properties of forming tools in a specific way by changing the composition of the tool rim zone or by coating the tool. Manipulation of the rim zone involves the targeted treatment of the upper edge layer of a workpiece in order to create certain properties. A distinction can be made in this context between pure heat treatment, thermochemical pretreatment or thermomechanical pretreatment. Careful heat treatment that is adapted to the respective tool steel is indispensible. Thermochemical pretreatment is an additional measure with which the wear resistance of forming tools can be increased and the effect of tool coatings can be influenced positively. This includes, among some other methods, case hardening, nitriding, borating, or chromizing [LANG90a, LUIG93]. What all variants of thermochemical surface treatment have in common is that the chemical composition of a material is intentionally altered by one or several elements diffusing into the material or out. Thermochemical surface treatment can be used to realize the following properties within the tool rim zone:

- increase in hardness,
- increase in high temperature strength,

- increase of the supportive effect against tool coatings,
- material modification to decrease adhesion.

The most common procedure, nitriding, involves a diffusion saturation of the edge layer of a workpiece with nitrogen in order to increase hardness, wear resistance, fatigue strength or corrosion resistance. The presence of elements that form special nitrides can, for example, bring about a higher edge hardness than can case hardening. However, the disadvantage is the steeper decrease in hardness towards the inner workpiece. After nitriding, the rim zone consists of an upper nitride layer (compound layer) and an underlying layer composed of nitrogen-enriched mixed crystals and precipitated nitrides (diffusion layer). Generally we distinguish between gas nitriding in an ammoniac gas flow at 500–550 °C, salt bath nitriding in cyan salt baths at about 520–580 °C and plasma nitriding at 450–550 °C. In the recent past, plasma nitriding, which is easy to combine with plasma-guided coating processes and requires shorter nitriding periods than gas nitriding, has become especially economical. This process is used in order to realize continuous distributions of hardness between the base material and the hard material coatings applied on it. Here, the nitride layer assumes the function of a supportive layer, while the hard material layer applied upon it takes over the actual function of wear protection. The disadvantage of gas nitriding is the long period of time required for nitriding, which can be shortened by glow discharging (plasma nitriding), which ionizes the nitrogen.

Other methods include carburetion, carbonitriding, borating and vanadizing. The advantages of these methods can partially be derived from the indications given in Sect. 2.8.5 concerning the influence of alloying elements. For example, in [BARN04], a reduction of material transfer via borating is observed in the case of non-lubricated hammer forging, while nitriding leads to more material transfer than with an untreated tool. In lubricated experiments, nitrided, carbonitrided and borated upsetting paths diminish wear (material loss) compared to untreated paths in a similar way. [HUSK02] proposes a duplex treatment (plasma nitriding followed by PVD coating) as an effective measure for increasing both wear resistance and the fatigue strength of cold extrusion tools.

2.8.5.3 Tool Coatings

Since tool wear largely depends on the properties of the tool surface, it is obvious that the properties of the surface should be intentionally influenced. Modern thin-film technology gives us the possibility of improving the surfaces of forming tools with CVD and PVD processes by applying supporting layers in a targeted way [ESCH04, EVER04, VDI92]. The high hardness of the hard material layers thereby obtainable provides increased resistance against abrasive wear, while their non-metallic material properties lead to a reduced tendency to adhesion.

However, the use of tool coatings also has a drastic effect on the forming process as a tribological system, since the, as a rule, metallic surface of the tool is

replaced by a non-metallic and much harder one. This means a huge change in the physical and chemical processes involved in tribological contact, i.e. during the forming process, affecting the mechanisms of friction and wear. While wear is heavily limited by coatings as a rule, only a few coating systems are capable of reducing friction.

Coating Methods. The most important methods of coating are CVD (chemical vapour deposition) and PVD (physical vapour deposition) as well as their variants. With them, extremely different wear-protective and sometimes friction-reducing hard material coatings of a few µm thickness can be created. Volume 1 of this series contains a detailed description of these methods [KÖNI02]. Besides them, there are still other methods such as galvanic or galvanochemical coating (e.g. hard chrome coatings) as well as plasma spraying. Large tools are often weld-clad or laser-treated (e.g. laser-beam cladding, surface alloying). These procedures are also used in the repair of large tools.

Layer Properties. The properties of a coating are characterized by defined values. An overview and exact indications on the execution of the most important test methods are provided in the various sections of DIN 1071 as well as in VDI guidelines 3198 and 3824 [DIN94, DIN03a, DIN03b, DIN04a, ISO04a, VDI92, VDI01] (Table 2.17).

Further characteristics include residual stresses, the exact chemical composition across the thickness of the layer, heat properties and surface energy. Beyond these, the tribological properties of coatings can be tested in many different experimental tests (Sect. 2.8.7). The importance of these coating properties for its function will be described in the following.

The coating thickness is generally between 1 and 5 µm. In the case of CrN, coating thicknesses of up to 10 µm are possible. Thicker coatings often have excessive residual stresses and tend to crack under elastic elongation, flaking off as a result. We refer to the so-called "egg-shell effect" or adhesive coating failure when the layer completely detaches from the substrate, and to cohesive coating failure when only some areas of the layer flake off without exposing the substrate. The inclusion of "relaxation layers" can decrease residual stresses, making it possible to generate larger coating thicknesses (up to about 15 µm).

In order to keep coating wear low, high hardness (protection from abrasive wear) and as possible a low Young's modulus (high ductility, protection from

Table 2.17 Important values for characterizing hard material coatings and associated test methods

Quantity unit	Coating thickness µm	Hardness HV 0.05	Young's modulus MPa	Adhesion adhesion class or critical load L_c in N
Range	1–5	1,700–4,200	2,000–5,000	1–4 respectively 10–90
Typical test methods	Light microscopic measurement at calotte cut	Microhardness or universal hardness	Universal hardness	Rockwell C test or scratch test

cracking) are required [RAED02, RENT97]. This contradictory ratio of Young's modulus and hardness can be obtained by means of multilayer technology (see below). The adhesion of a layer is determined qualitatively in indenter or scratch tests and is not directly transferable to forming process behaviour. Basically however, a high adhesion class is required, especially in the case of high local tool loads. Buildups can be influenced by the selection of the coating material (Sects. 2.8.3.2 and 2.8.5.1).

Furthermore, hard metal coatings possess other properties that affect their performance, but which usually cannot be determined by a standard characterization. Roughness is indeed sometimes indicated, but it depends primarily on the roughness of the substrate and thus does not characterize the coating but the coating-substrate composite. Nonetheless, it should be as low as possible in order to prevent local overloads at the roughness peaks. Tools to be coated should thus not exceed a surface roughness of 1 μm. Profile methods are used to determine roughness. Porosity, which should be kept as low as possible for reasons of high-load behaviour and protection against tool corrosion, is also rarely indicated.

Heat properties are important when high process temperatures are to be expected (e.g. forging, cold massive forming or fine blanking with a high number of strokes). As a rule, low temperatures are desirable in order to minimize thermal alternating load on the layer and thermal load on the lubricant. This can be obtained with high values of heat conductivity, thermal capacity and layer density [RAED02].

Often, good wettability of the tool surface by the respective lubricant is also required. Wettability can be evaluated in "contact angle measurements". In these, droplets of reference liquids are added to the coating in order to cite the angle between the droplet surface and the coating surface as a measure for wettability. With this method, the polar and disperse surface energies of solids and liquids can also be determined, which is indicated in mN/m [BOBZ00].

The properties of tool coatings are essentially a function of the following influences:

- coating method,
- layer material,
- layer construction and internal structure,
- substrate material and pretreatment.

Coating Materials and Internal Structure. Figure 2.76 lists the layer materials that can be used for PVD and CVD coatings. We distinguish between oxide, nitride, carbide and boride coatings. Detailed descriptions of different layer materials can be found in VDI guideline 3824-1 [VDI02]. Carbon layers have distinctive properties, differing fundamentally in their behaviour from the others. They are treated separately in VDI guideline 3840 [VDI04]. Most common are nitride and carbide layers as well as those based on C_xN_y. Inside monolayers, they form columnar crystallites, the structure of which depends on the parameters of the coating process and on the substrate and its pretreatment (Fig. 2.76 bottom left)

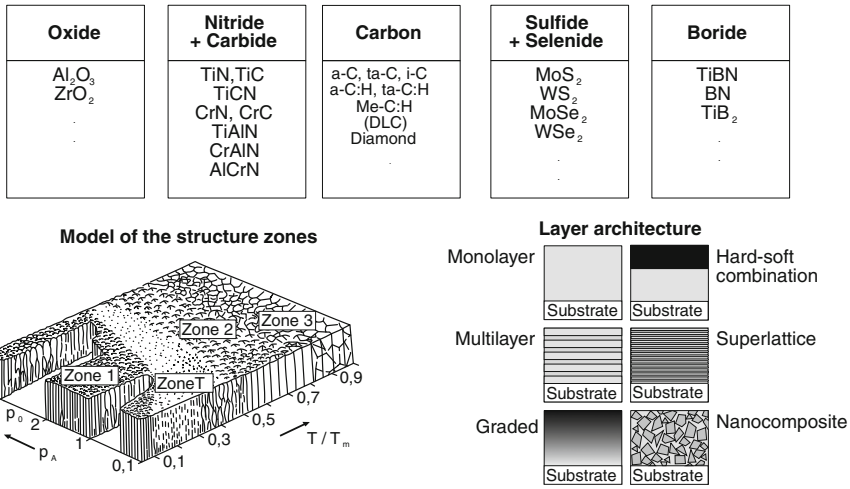


Fig. 2.76 Materials, structure and architecture of CVD and PVD coatings

[HAEF87]. The characteristics of the crystallites influence the mechanical properties of the layer, porosity, microtopography and wetting behaviour.

Nitride and carbide layers are often implemented as multilayer coatings or in recent times as nanolayer (or superlattice) coatings to increase ductility (Fig. 2.76 bottom right). In the latter case, the thickness of a single layer is only 5–20 nm, while the thickness of the entire coating is a few μm [BOBZ04]. So-called nanocomposite layers represent another variant with improved mechanical properties compared to monolayers. Their structure resembles those of cemented carbides, i.e. a hard phase is embedded in a somewhat softer matrix, also a hard phase. The hard-soft combinations and graduated layers consist on the surface of friction-reducing materials generally containing high amounts of carbon.

Carbon layers have a unique role within coating technology. Amorphous diamond-like carbons (DLC) are extremely wear-resistant and highly low-friction coatings deposited with CVD or PVD methods. The properties of these layers can be varied within broad limits depending on the manufacturing process, deposition conditions and composition. Depending on the amount of the predominant bond-type (sp^2- or sp^3- hybridization), the hydrogen content and the content of metallic and non-metallic doping elements, we obtain properties ranging between graphite-like and diamond. The exact designation of all variants along with an overview of their properties is specified in VDI guideline 2840 [VDI04].

Application Areas of Tool Coatings. Particular coatings are more or less appropriate for various forming processes. Figure 2.77 shows a rough classification. The extremely attractive low-friction, adhesion-reducing carbon coatings are especially suited for forming processes in which the tool surfaces are subject to only moderate mechanical loads. Hitherto they have mostly been employed in sheet metal forming processes (e.g. deep drawing or hydroforming) and in

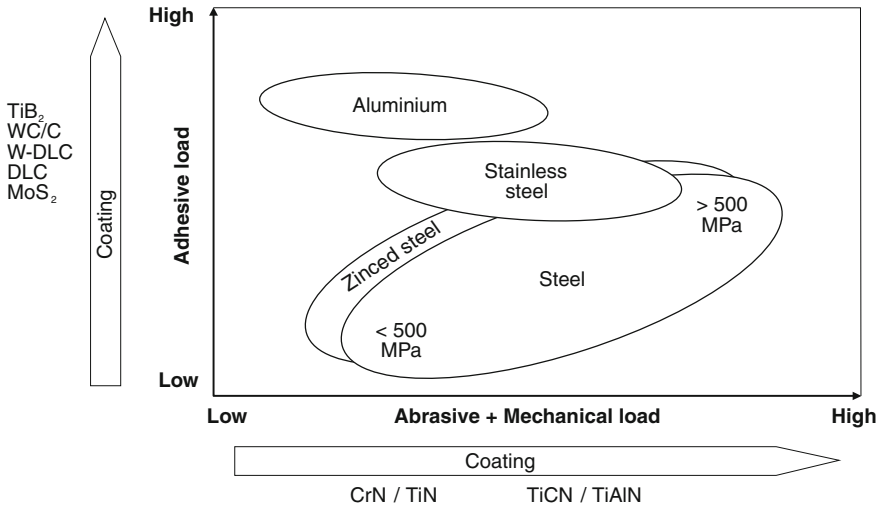


Fig. 2.77 Application areas for tool coatings in forming technology

aluminium processing [HORT01, KLOC04d, WEBE04]. For example, the use of amorphous carbon coatings led to significant tool life increases in the manufacture of caps for aluminium beverage cans. For the workpiece material aluminium in particular, boride layers (TiB and TiBN) are also of interest [HORT01]. If extremely low loads are to be expected and minimal friction coefficients are required, MoS_2 coatings as monolayers or as the top layer in multilayer coatings are an interesting alternative.

The adhesive strength of friction-reducing layers is often insufficient in the case of larger tool loads. In the areas of highest tool loads, multilayer coatings fit for heavy loads like TiCN, TiAlN, CrAlN and recently AlCrN (increased aluminium content compared to CrAlN) are used [EVER04, RAED02, RENT97]. These may not necessarily reduce friction, but they lead to significantly higher tool life quantities. The layers most suited to heavy loads are deposited nowadays using CVD methods on the basis of TiCN systems. The CVD coating here has the advantage of having greater adhesive strength.

In die forging tests, wear was reduced with a multilayer coating of type TiN-TiCN-TiC by a factor of three compared to plasma-nitrided dies and by a factor of two compared to TiN-coated dies [BARN04, DOEG01]. Similar CVD multilayer coatings are to be recommended for shearing electrical sheets and offer the possibility in cold massive forming of working without a zinc phosphate layer [RUPP97, TOUS00].

Yet in the case of moderate abrasive and adhesive loads, TiN is still a standard coating with high industrial acceptance. CrN is also used in the case of moderate loads when adhesive load is significantly more predominant or when increased temperature resistance is required [RUPP97]. TiAlN however—fit for heavy loads

and usually implemented as a multilayer or nanolayer coating—has the highest thermal stability (up to 800 °C).

For all coatings, one must bear in mind that the properties of coatings with the same name but made by different manufacturers can deviate considerably due to the variables mentioned above. Furthermore, when changing from uncoated to coated tools, one must check whether the lubricant used is suitable for the respective coating. As a rule, coating tools allows for a reduction of lubricant additives and/or lubricant amounts.

2.8.6 *Effects of Topography*

Even if the friction conditions in forming technology generally are in the range of mixed and boundary friction, in many cases of mixed friction local hydrostatic and/or hydrodynamic effects are nonetheless active that can sometimes have a positive influence on friction and wear (Fig. 2.72). Such effects arise when depressions are formed on the tool or workpiece surface in which lubricant is enclosed. These are called closed lubricant pockets, whereby a distinction is made between macroscopic pockets (e.g. in the case of sheet concavities in the flange area when deep drawing) and microscopic pockets (roughness/microtopography). Open pockets on the other hand can be so defined, that the lubricant contained in them can escape to neighbouring pockets or on the transition between the tool contact surface and free workpiece surface.

The lubricant enclosed in the pockets is compressed and exposed to high pressures due to the high contact normal stress in the lubrication gap, resulting in the formation of a hydrostatic cushion. This is especially the case when the affected pockets are on the surface of the workpiece [NEUD04]. During the forming process, workpiece surfaces are smoothened, reducing the volume of the pockets and heavily increasing the pressure in the lubricant. In the case of relative motion, hydrodynamic effects also become active on the flanks of the pockets. The most important influencing variables are as follows:

- size and geometry of the lubricant pockets and pockets flanks
- distribution of the lubricant pockets on the surface (stochastic or deterministic)
- ratio of closed to open lubricant pockets (especially in the case of miniature components in microforming [TIES02])
- viscosity and compressibility of the lubricant
- the stress collective, especially contact normal stress and relative velocity.

To calculate the effects of topography on friction, it is important that one uses meaningful three-dimensional surface parameters that permit a more extensive description of topography than simple roughness characteristics. Numerous new parameters and metrological methods have been developed for this in the last several years [PFES97, WAGN96].

The following will explain the most important examples for the intentional integration and exploitation of surface microtopographies.

2.8.6.1 Surface Microtopography of Sheet Metal Materials

In sheet metal forming procedures, especially deep drawing, mixed friction conditions are frequently predominant, in which case lubricant pockets can be formed on the sheet metal surface. Here, the rather long-wave microtopography of the initial sheet metal plays a decisive role, while the far more short-wave topography of zinc coatings has a much smaller effect [BÜLT96].

The microtopography of the base sheet metal material is determined in the manufacturing process. After cold rolling and annealing, the sheet is lightly post-formed with so-called skin pass rolls (degree of skin-pass 0.5–1 %), so that the surface of the skin pass roll can be transferred as a negative to the sheet metal surface [NEUD04, STAE98].

The various types of texturing differ therefore in the processing of the roll surface. The concept of texturing in this context should not be confused with the texture of the workpiece material. For some years now, a variety of different methods exist for the modification of roll surfaces. The most common fine sheet metal texturings that can thereby be created are listed below and have been tested for their tribological properties in many investigations (Fig. 2.78) [DINK97, STAE98, WAGN96]:

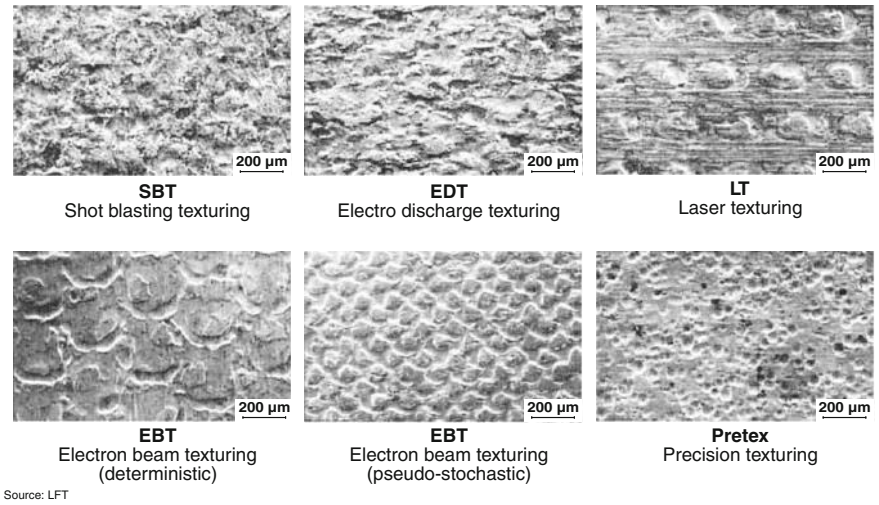


Fig. 2.78 SEM images of textured thin sheets [NEUD04]

- **MF—**mill finish (no texturing): ground skin pass rolls; hardly any lubricant pocket effects (depending on the drawing direction); improvements via cross-grinding possible; implementation declining [NEUD04]
- **SBT—**shot blasting texturing: roughening the roll surface by bombardment with a blasting agent accelerated by a shot blasting wheel [PANK90]
- **EDT—**electro-discharge texturing: roughening the roll surface in a spark-erosive process; less roughness and higher number of peaks as in SBT [HEBE87]
- **LT—**laser texturing (since 1982 [CRAH82]): pointwise fusing of the roll by means of a pulsed CO_2 laser; deterministic formation of small craters [CRAH82]
- **EBT—**electron beam texturing: similar to LT; fusing takes place by means of an electron beam; consistent, deterministic formation of ring-shaped craters; superimposition of craters leads to pseudo-stochastic distribution [DOLV91]
- **PRETEX—**precision texturing: application of an electrolytically generated, structured hard chrome layer; process control during coating leads to the formation of hard chrome droplets; stochastic distribution of calotte-shaped packets in the sheet metal [ZIMN98].

Texturing does not necessarily lead to friction coefficients that are lower than those of MF surfaces. However, they do shift the appearance of tool wear to higher surface pressures [STAE98].

2.8.6.2 Surface Topography of Materials for Massive Forming

Depending on the size of the workpiece, either wire or rod-shaped semifinished products are used as the starting material in massive forming. In cold forming, these are generally provided with a lubricant carrier layer, which is applied in the case of wire before and in the case of rods after the detachment of a blank (Sect. 2.8.4.2). Before applying these layers, the materials are often subjected to mechanical surface treatment, which influences the topography of the surface [BAY94].

It has been shown that blasting treatment (e.g. sand or shot blasting) leads to improved adhesion of the lubricant carrier layer compared to scalping, which due to the roughening of the surface in addition to the cleaning effect of the jet. But even without the use of carrier layers, the topographies created lead to improved friction conditions compared to fully untreated raw material. This can be attributed to the lubricant pocket effect.

2.8.6.3 Surface Topography of Forming Tools

In addition to the surface topography of workpieces, the formation of the tool surface also affects friction and wear. The essential difference is that the topography of tools is subject to significantly fewer changes. Those that nonetheless occur result less from plastic deformation, but are rather the result of tool wear.

Effect of Tool Finishing on Topography. Firstly, the tribological properties of a tool are influenced by the tool finishing process. In terms of wear, as a rule polished tools may be evaluated positively (Sects. 2.8.3.2 and 2.8.3.3).

It is also possible to create lubricant pockets by means of diverse blasting methods (e.g. shot blasting). These rarely used methods may indeed be used to strengthen the rim zone of tools and to induce compressive residual stresses, which can have positive effects on surface disruption. Since however blasting also involves a significant topographical alteration, the tool's tribological behaviour is also influenced.

Influence of Tool Coatings on Topography. While the roughness characteristic values of tool surfaces are only rarely significantly altered in most coating processes, layer microtopography does play a role in the interaction of surface and lubricant. For example, lubricants on the surface of columnar PVD layer crystals are much more adhesive than those on completely smooth layer surfaces. This can improve the effect of the lubricant (Fig. 2.76).

This effect can be exploited especially in the case of monolayers and multilayer coatings with relatively large single layer thicknesses, since the columnar layer structure can be created particularly prominently in this case. The lubricant penetrates into the hollow spaces between the crystallites and is thus borne into the action interstice between the tool and the workpiece. Depending on the selection of parameters in the coating process, the layer structure and its effects can vary. This was shown in [GERB02] using the example of CrN coatings.

Effect of Laser Processing on Topography. In some newer applications, laser-textured tools are being used in both massive and sheet metal forming [NEUD04, POPP04]. Similarly to the texturing of skin pass rolls for textured sheet metals, small pits are introduced into the tool surface by means of an excimer laser. These pits then serve as lubricant pockets in the forming process (Sect. 2.8.6.1). In principle, texturing can be carried out for all tool materials. In the case of coated tools, we differentiate between pockets introduced prior to and after coating [POPP04].

The pointwise laser remelting of tool surfaces is a special case. Here, hard material powder (e.g. TiC) is added to the surface of the tool and "implanted" into the surface using a laser beam [STEI99]. The implanted areas remain intact under tribological load, while the surrounding areas are reset by wear. The result is a self-sustaining surface structure.

Fundamentally, the same hydrostatic and hydrodynamic effects are found at the lubricant pockets as is the case with sheet metal materials, only that the shape of the lubricant pockets is not altered by plastic deformation during the forming process.

In exchange, workpiece material is squeezed into the pockets during the forming process, reducing the volume of the pockets and leading to an increase in pressure in the lubricant. This process can however also have a negative effect if the workpiece material is sheared off at the pocket flanks and remains in the pockets. On the other hand, it is advantageous that wear particles that can lead to abrasion during tool contact are collected in the pockets [POPP04]. While surface

quality is hardly affected in sheet metal forming, small elevations remain behind in the case of massive-formed components due to the imprinting of pocket geometries into the workpiece surface.

Overall, only in some cases an increase in tool life and a reduction of friction is possible by laser texturing forming tools.

2.8.7 Tribological Test Methods in Forming Technology

Tribological test methods are used in forming technology in order to test the tribological properties of materials and intermediates at little expense. Since it is often not possible for reasons of process reliability to test new tribologically effective products in everyday operation, simply designed experimental setups are used to help inspect those products. Tribological metrological and test engineering distinguishes between several task areas:

- experimental simulation of forming processes to discover friction and wear mechanisms
- determination of friction and wear parameters for the sake of process design and calculation
- comparison of materials and intermediates for process optimization
- quality surveillance and control of tribotechnical materials and lubricants.

In order to obtain meaningful test results that are applicable to real forming processes, it is important that the tribological conditions in the test process model those in the real process well. This requires material, kinematic and thermal similarity between the test and the forming process that is as close as possible. The test results are thus more or less relevant depending on the model test's degree of abstraction compared to the actual tribological system [GFT02]. Results from different experimental setups can deviate from each other considerably.

2.8.7.1 Equipment for Lubricant Testing

There are many simple standardized procedures for the general tribological testing of lubricants, whereby the highly abstracted tribological systems in the test devices used do not simulate a particular application. They serve rather to assist in the development of new lubricants in the selection of promising formulations and in quality assurance for existing products. A rough classification of lubricants with respect to additive content and wear protective effect is also possible with these processes. In some cases, a friction coefficient can also be determined, which cannot be used in the calculation of forming processes due to lacking applicability. Figure 2.79 provides an overview of the most important methods.

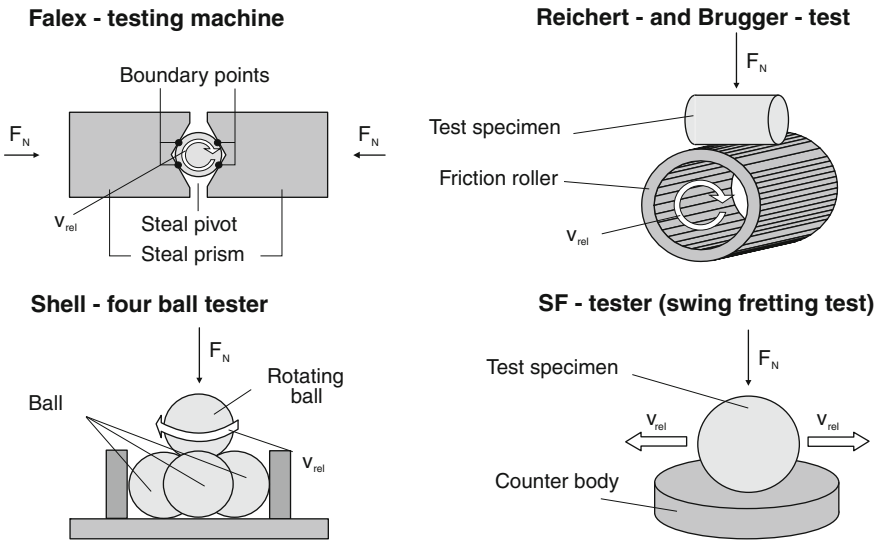


Fig. 2.79 Schematic representation of different lubricant test equipment [DIN77, DIN00, DIN04b]

These test methods differ not only with respect to geometric and tribological conditions but especially with respect to the response characteristics of particular additives (Fig. 2.80) [SCHU04a].

With respect to forming technology, the biggest disadvantage of these test methods is that the results obtained are not applicable to the tribological systems of forming processes. They are thus not suitable for selecting lubricants for particular applications. This is because both the tribological system components, which are usually manufactured from roller bearing steel 100Cr6, and the stress collective (surface pressure, relative velocity, temperature) are largely standardized and hardly correspond to those of forming processes. Only the SRV test provides the possibility of varying a large number of load parameters. But here too, it is impossible to take surface enlargement into consideration, which takes place in many forming processes. Nonetheless, the results of these standard tests are often the only tribological data provided by the lubricant supplier.

For a targeted choice of particular lubricants for particular forming processes therefore, further test methods must be used that approximate the tribological conditions in a better way (Sects. 2.8.7.3 and 2.8.7.4). In the following, the most common methods and devices used in lubricant testing will be briefly explained [SCHU04a]. It should be noted that in all of these processes, standard test objects (base and counter bodies) made of 100Cr6 are used. In this way, the results of the tests can be compared, yet they are generally not transferable to forming processes.

Falex Testing Machine. A soft steel pin rotates under load in an oil bath between two hardened steel prisms. The revolutions per minute (290 min^{-1}) is held constant; the load is increased in three stages. Contact of the test object takes

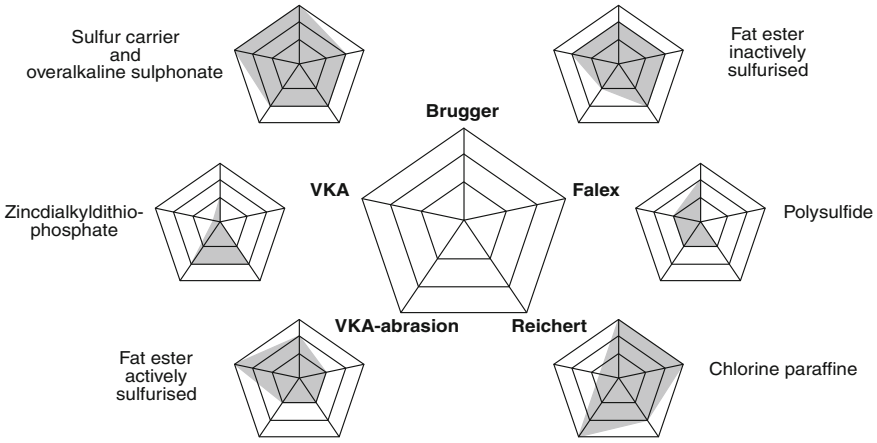


Fig. 2.80 Response characteristics of different wear-protective additives in various lubricant test equipment [SCHU04a]

place at four points in line contact. The test determines the scuffing load (fracture of the shaft at the predetermined breaking point) or, surviving all three load points, the wear on the steel pin.

Shell four ball tester. The lubricant is tested with a four ball system consisting of a rotating ball sliding on three balls identical to it [DIN77]. The test forces can either be increased gradually until the balls fuse, or, under constant test force, the calotte diameter of the three stationary balls is measured after a predetermined test time. Methods based on this standard function to determine characteristic values for lubricants with active substances that should allow for high surface pressures in the mixed friction range between surfaces in relative motion.

Reichert's Fretting Scale. In the case of this friction testing device, a firmly clamped test roller is pressed with a double lever assembly on a revolving slip ring, the lower third of which is submerged in the liquid to be tested. The revolutions per minute of the motor and of the slip ring revolving directly with it are set such that constantly enough liquid can enter the contact point (fretting location) between the test roller and the slip ring. Depending on the pressure absorption capacity of the liquid on the test roller, ground areas appear on the slip ring (elliptical wear marks), the size of which depends on the bearing capacity of the test liquid. The sharply delineated wear area allows for exact measurement, which is beneficial for an exact determination of the load bearing capacity of the test liquid. The pressure absorption capacity is the larger the smaller this wear mark is after a certain run time or distance (100 m of the circumferential path of the slip ring).

Brugger Lubricant Testing Device. To carry out a test run, a certain small amount of the lubricant to be tested is applied to the friction roller, and a cylindrical test piece is pressed against the still stationary roller with constant force. The test begins when the friction roller is set in rotational motion. The duration of the test is 30 s. According to Brugger, loading capacity, measured in N/mm^2, is the

quotient of the pressing force of the test piece on the friction roller and the size of the wear area on the test piece [DIN00].

SF (*Swing Fretting*) *Tester*. The metrological principle is that an upper test piece (ball—point contact, standing cylinder—surface contact, lying cylinder—line contact) is moved in an oscillating manner on a ground or lapped surface (bottom test piece—counter body) [DIN04b]. The substance under investigation is located between the test pieces. The friction coefficient is recorded throughout the entire test period. In addition, the lubricant and galling mark can either be optically evaluated, or the galling mark can be measured. The big difference of SF testing from other test methods in the mineral oil industry is that a large number of parameters can be altered. Not only the test force (surface pressure) but also the test temperature, frequency of oscillation, amplitude (path traversed by the upper test piece) and the test time can be adjusted. Also, it is possible to select within a wide spectrum both the material of the test pieces as well as their geometries. In this way, tool coatings can also be tested. This variety of variables makes it possible to adjust the test conditions so that the actual process for which the lubricant was developed can be simulated as well as possible.

2.8.7.2 Devices to Test Coatings

Since coating technology is much younger than lubricant technology, it has been subject to significantly less standardization. In practice however, besides investigations for layer characterization (Table 2.17), often simple friction tests are carried out in order to determine the Coulomb friction coefficient against steel or wear behaviour.

The friction coefficient is carried out in simple pin-disc or ball-disc tribometers. A cylindrical pin or a ball, as a rule consisting of 100Cr6, is pressed with a defined pressing force against a coated disc rotating with a defined rotation speed. The result is the average friction coefficient after a test period of several minutes or hours. Furthermore, conclusions can be drawn concerning the run-in behaviour of the layer with the help of the course of the friction coefficient. With most layers, the friction coefficient decreases with time and continues towards a constant minimum. Not until advanced layer wear occurs the friction coefficient goes up again. In the case of adhesive or cohesive layer failure, the test is prematurely aborted.

Moreover, by measuring the galling mark, information can be obtained regarding the worn volume, given as a wear coefficient. The volumetric wear coefficient V_s is defined as the magnitude of the wear volume of the loaded surface divided by the effective glide path and the effective normal force. This is specified with the unit m^3/Nm. Sometimes planimetric wear (cross-sectional area of the galling mark) or gravimetric wear (mass loss) are also evaluated.

In some cases, the calotte grinding method in accordance with DIN V ENV 1071-6 is applied [DIN02]. The resulting abrasive wear coefficient cannot be

compared with that resulting from the pin-disc or ball-disc test, since the frictional load is different in kind.

In addition the flexibly applicable SF test can be used for the examination of tribological properties of coatings (Fig. 2.79) [DIN04b].

2.8.7.3 Test Procedures for Massive Forming

In order to test tribotechnical materials and lubricants under the demanding conditions of massive forming processes, a number of model tests have been developed with which the most varied massive forming processes can be simulated. The transferability of the test results is especially important in the area of massive forming, since it is difficult to reproduce the tribological conditions with sufficient precision. In massive forming, one must take into consideration, in addition to the consideration of the characterizing tribological system magnitudes of surface pressure (contact normal stress), relative velocity and temperature, the enlargement of the workpiece surface, which also influences the mechanisms of friction and wear to a decisive degree.

Figure 2.81 provides a comparison of typical cold massive forming process with some common model tests [LANG81a]. A comparison of the characterizing tribological system magnitudes is helpful in selecting the right model test. Figure 2.81 shows this using the example of relative surface pressure $p_{\max}$ in relation to the initial yield stress k_{f0}.

It is clear that it is impossible to reproduce all cold massive forming processes equally well in model tests. Especially the extremely high requirements of reverse cup extrusion can not be met with these model tests. In this case however, it is possible to reproduce the process itself under laboratory conditions, in which case it is completely possible to make simplifications that reduce expense. For example, [RUPP97] suggests “free cup extrusion”. This is a reverse cup extrusion process without a die. One cup is not inserted into one single workpiece, but rather several cups side by side are inserted into a wire with a rectangular cross-section or in a semi-finished rod. With this model test, the major surface enlargement of the actual cup extrusion process, about 5 times that of the ring upsetting test, can be well approximated. In addition, [GRÄB83] proposes draw pressing (simultaneous reducing and drawing of a bar). This process is also characterized by relatively high surface pressures, relative speeds and surface enlargements, though not as high as in free cup extrusion.

Supplementing Fig. 2.81, Table 2.18 shows, next to the relative surface pressure, the values of maximum relative velocity v_R between the tool and workpiece in relation to the velocity v_0 of the forming tool as well as the surface enlargement A_1/A_0 of the workpiece [GRÄB83]. In contrast to the investigations in [LANG81a] (Fig. 2.81), here surface pressure $p_{\max}$ is not related to the initial yield stress k_{f0} but to the average yield stress, which takes into account the strain hardening of the workpiece material.

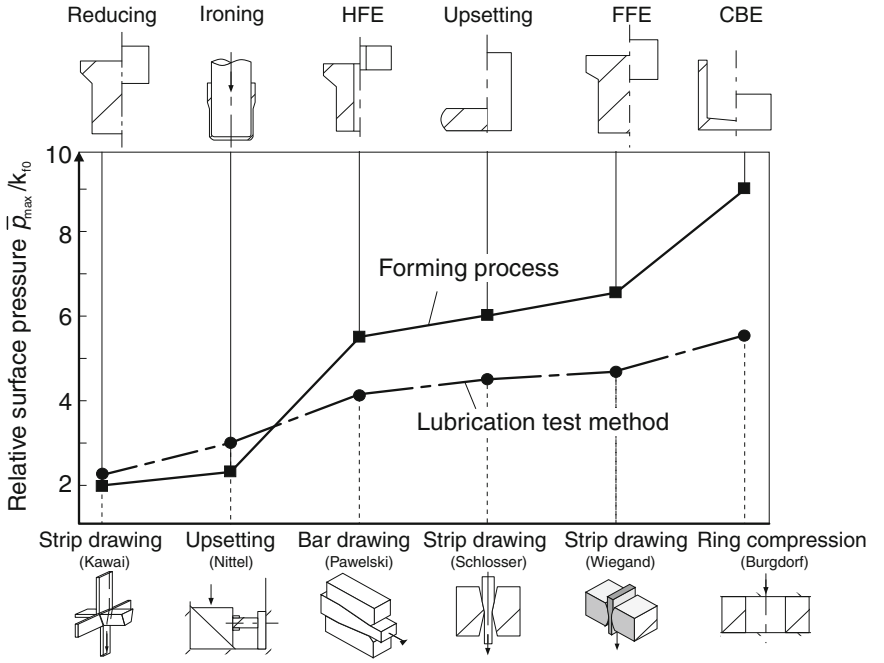


Fig. 2.81 Comparison of relative surface pressures in forming processes and model tests (acc. to Lange) [LANG81a]

Table 2.18 Comparison of characterizing tribological system magnitudes for different processes and model tests in massive forming [GRÄB83, RUPP97]

Process/model test	$\bar{p}_{max}/k_{fm}$	v_R/v_{WZ}	A_1/A_0
Reducing	1.4	1.5	1.2
Ironing	1.6	2.3	2.2
Upsetting	3.4	2.4	4.5
Hollow forward extrusion (HFE)	3.2	5	4
Solid forward extrusion (SFE)	3.8	5.7	2
Cup reverse extrusion (CRE)	5.2	6.3	11
Strip tension (Kawai)	1.6	1.5	1.5
Strip tension (Wiegand)	1.6	–	–
Strip tension (Schlosser)	1.8	2	2.0
Rod tension (Pawelski)	1.9	1.5	1.5
Beveled upsetting (Nittel)	1.9	2	2.4
Ring upsetting (Burgdorf)	1.7	2	1.8
Draw pressing (Gräbener)	2.8	2.6	2.5
Free cup extrusion (Rupp)	4.3	–	9

Although, in comparison to draw pressing or free cup extrusion, it has limitations with respect to tribological load, ring upsetting as a test procedure is a good compromise between applicability, reproducibility and expense. It is thus very common and is often cited in the literature for determining friction coefficients for different states of lubrication [HORL89, KLOC04e, LI95]. For this reason, ring upsetting will be explained in more detail in the following.

The ring upsetting test has been known since the 1960s and permits a reliable experimental determination of friction values (friction coefficient μ and friction factor m) at low cost [BURG67]. It is suitable for investigations of both cold and hot forming. The ring-shaped specimen consists of a cylindrical body with a hole in the center (Fig. 2.82 top left). This specimen is compressed axially between two level, parallel upsetting panels, whereupon the geometry is measured and compared with the starting geometry.

During upsetting, a neutral surface can be formed between the inner and outer diameter with which the limit radius r_s is designated. The limit radius divides the specimen into areas of opposed material flow (Fig. 2.82 bottom left) [BURG67]. If there is a lot of friction, the inner diameter becomes smaller and the outer diameter larger. In the case of little friction, the neutral surface radius r_s is shifted inwards and the inner diameter becomes larger. The friction shear stresses in the contact zone bring about an outward curvature of the free external lateral surface (bulging), while the internal lateral surface bulges inwards or outwards depending on the direction of material flow.

The size of the ring specimens must be adjusted to the available press. Limitation of the maximum pressing force simultaneously entails limitation of the starting cross-section of the specimen. To determine the permissible starting cross-

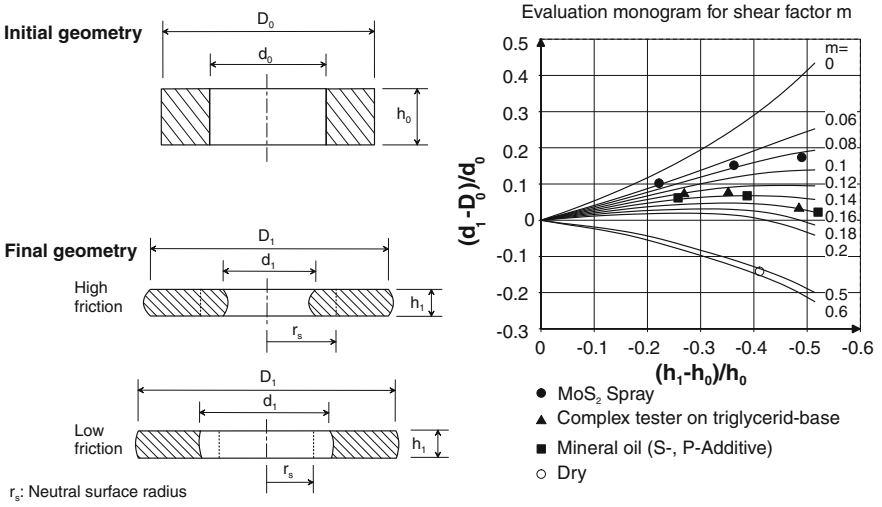


Fig. 2.82 Specimen geometry in ring upsetting and a monogram calculated via FEM simulation for the evaluation of ring upsetting tests; shear factor m for different lubricants [KLOC04e]

section, we assume that the largest height reduction occurring in the ring upsetting test is $\varepsilon_h = 0.5$ [BURG67]. Furthermore, a maximum allowable deformation resistance (yield stress) after a deformation of 2,000 MPa should not be exceeded. For a 200 t-press, the starting cross-section may not be larger than 500 mm^2. In order to prevent unsymmetrical deformations, the aim should be a wall thickness that is as large as possible or a large ratio of D_0/d_0. On the other hand, the inner diameter should not be too small, which can cause the hole to close. Height is limited upwards by buckling problems and downwards by an unnecessarily high deformation resistance.

Considering the marginal conditions mentioned, a ring geometry with an outer diameter of 20 mm, an inner diameter of 10 mm and a height of 7 mm has proved suitable [BURG67]. The upper and lower edges must in every case be plane-parallel to each other.

In order to determine friction values for executed experiments, so-called evaluation monograms are required, which can be obtained in different ways, e.g. with the upper bound process or with the help of FEM (Sects. 2.4 and 2.5) [LI95]. When calculating the ring upsetting process, the shear factor m in the action interstice is varied between zero and one. Alteration of the inner diameter, reacting sensitively to the friction, is calculated and represented as a function of the shear factor in an evaluation monogram (Fig. 2.82 right). For a ring upsetting test with an unknown friction coefficient or shear factor, these can be taken from the diagram once the inner diameter has been measured.

The monogram in Fig. 2.82 right shows results from ring upsetting tests with different states of lubrication, in which the above mentioned ring geometry was used [KLOC04e]. It should be taken into consideration that the determined friction coefficients are not absolute values but average values across the entire contact surface between the specimen and the tool that were also determined along the entire path traversed.

2.8.7.4 Test Procedures for Sheet Metal Forming

For the evaluation of friction conditions between the tool and sheet metal material, different model tests have been developed with which the effects of various lubricants and the surface condition of the sheet metal can be investigated.

Strip Drawing Test. The most important model test for determining and assessing friction conditions in sheet metal forming is the strip drawing test. Strip drawing tests are carried out either with or without baffle. In the case of the strip drawing test without baffle, the "flat path test", a metal strip is drawn through two friction pads that are pressed together with a defined normal force. The resultant frictional force on the metal strip is recorded with a metrological device, with which the Coulomb friction coefficient is determined. Instead of simple flat pads, it is also possible to integrate different shape elements into the friction pads for the flat path test. These days, both the simple blank holder area as well as draw beads are incorporated—the former with flat friction pads, the latter with corresponding

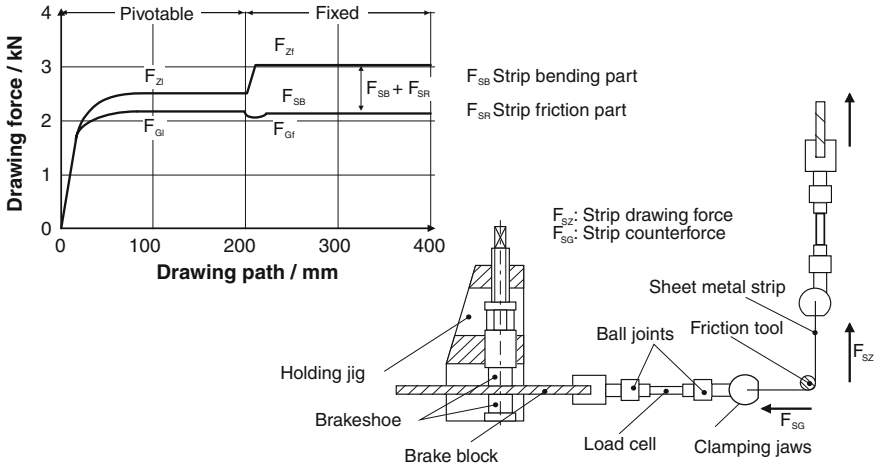


Fig. 2.83 Strip drawing test [WITT80]

shape elements in the friction pads. The strip drawing test with baffle shown in Fig. 2.83 serves to help investigate friction conditions on the die radius of deep drawing tools [WITT80]. In this short test procedure, a strip of the sheet metal material under investigation is drawn with a defined strip drawing force F_{SZ} over a cylindrical forming head, which represents the die radius. The required strip counterforce F_{SG} is applied with a holding device and measured with a force-measuring sensor.

The strip drawing force F_{SZ} consists of the sum of the counter-holding force F_{SG}, a force caused by friction F_R and a force required for bending the metal strip F_{SB} (Eq. 2.96):

$$F_{SZ} = F_{SG} + F_R + F_{SB}. \tag{2.96}$$

To determine the friction coefficient with the help of the Eytelwein equation (Eq. 2.98) however, the strip drawing force F_{SZ} must be reduced by the bending component F_{SB}. To determine its magnitude, a metal strip is pulled over a rotatably mounted forming head. In this way, the friction component disappears, and the bending component can be determined by measuring the drawing and counter-holding forces:

$$F_{SB} = F_{SZ} - F_{SG_1}. \tag{2.97}$$

With the forces F_{SG} and F_{SZ} measured with a stationary forming head, the strip friction coefficient is:

$$\mu_{SZ} = \frac{2}{\pi} \cdot \ln \frac{F_{SZ} - F_{SG_1}}{F_{SG}}. \tag{2.98}$$

The device developed by Pawelski is a variation on the classic strip drawing test [PAWE64]. In this case, friction measurements can be carried out under large specific surface pressures and large plastic deformations (Fig. 2.84).

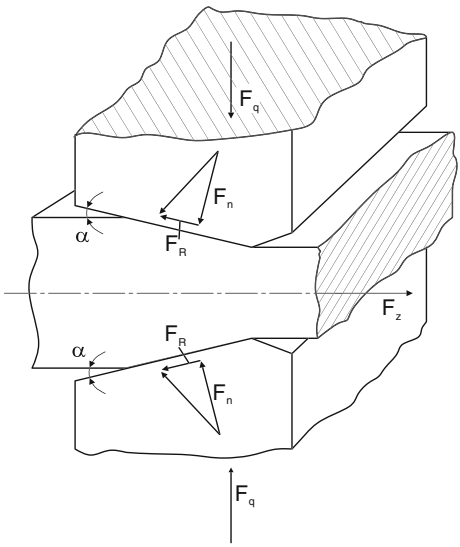


Fig. 2.84 Schematic representation of a test design for determining the friction coefficient in ironing [PAWE64]

The Coulomb friction coefficient μ is calculated from the drawing force F_z, lateral force F_q and the die clearance aperture angle α. It is an average value across the entire width of the test piece. For the friction coefficient we have:

$$\mu = \frac{\frac{F_z}{2F_q} - \tan\alpha}{1 + \frac{F_z}{2F_q} \cdot \tan\alpha}. \tag{2.99}$$

To determine the friction coefficient μ, only the condition of static equilibrium is used, while material equations for the elastic or plastic behaviour of both friction partners are not introduced into the calculation.

Ironing Test. With this test, it is possible to judge the quality of different lubricants used for ironing processes. To achieve this, the friction coefficient μ arising on the ironing ring is calculated from the particular forces active during ironing (Fig. 2.85). In order to obtain constant force conditions, an annealed cup that has already been ironed to a consistent wall thickness is used. While the punch force can be determined with a customary force-measuring device, the horizontal force is determined by means of the strain of the ironing ring with the help of an equation from elasticity theory. The test thus requires relatively high metrological

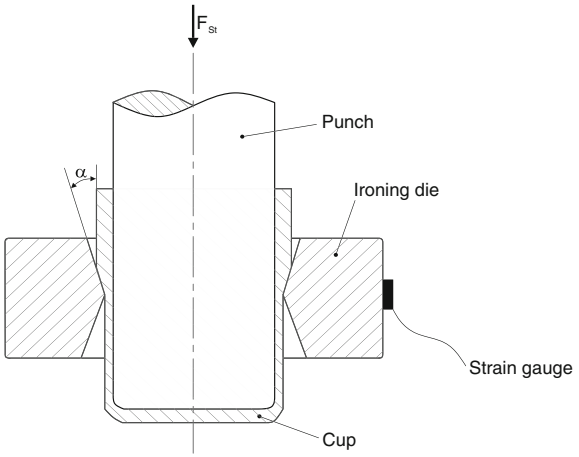


Fig. 2.85 Schematic representation of the test design used to determine the friction coefficient in ironing [SIEB54]

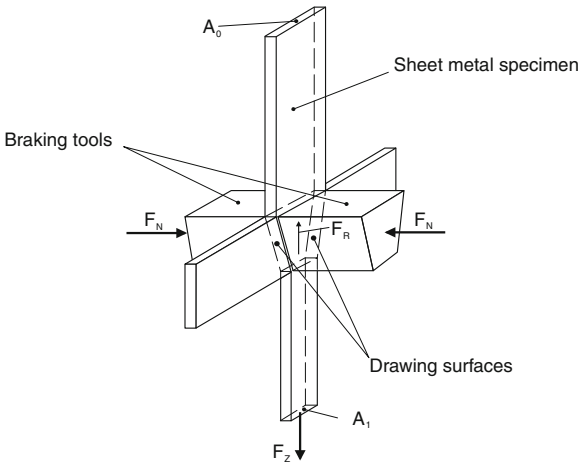


Fig. 2.86 Schematic representation of the test design used to determine the friction coefficient in the wedge draw test [REIH59]

expenditure (force and strain measurement). Making simplifying assumptions, the following determination equation is true for the friction coefficient at the ironing ring:

$$\mu = \frac{\frac{F_{St}}{2F_h} - \tan\alpha}{1 + \frac{F_{St}}{2F_h} \cdot \tan\alpha}. \tag{2.100}$$

Wedge Draw Test. In the wedge draw test according to Reihle [REIH59], a metal strip is pulled through two tapered drawing surfaces, whereby the starting cross-section A_0 is reduced to the final cross-section A_1 (Fig. 2.86). The frictional force F_R is measured in the drawing direction at both brake components, which are pressed on the test strip with a normal force F_N. These load conditions are similar to those encountered in the flange when deep-drawing a cylindrical hollow body. We obtain the frictional coefficient with:

$$\mu = \frac{F_R}{F_N}. \tag{2.101}$$

Chapter 3
Massive Forming

3.1 Cold Forming

Cold forming is characterized by the circumstances that the forming of the workpiece begins at room temperature and that no external heating takes place. In addition to this technical definition, there is also a metal-physical definition which states that a process can be referred to as cold forming as long as the forming temperature of the workpiece material is lower than its recrystallization temperature. The two most important cold massive forming processes are upsetting and extrusion.

3.1.1 Upsetting

3.1.1.1 Classification and Significance

Upsetting is classified in DIN 8582 [DIN03b], "Forming manufacturing processes" under Group 2.1, "Compressive forming". The category is further subclassified in DIN 8583-1 [DIN03c], which defines the manufacturing processes in greater detail. Open-dieing is referred to as upsetting if the workpiece dimensions between usually flat, parallel effective surfaces, i.e. so-called upsetting paths, are reduced. The upsetting path is constantly larger than the compressed workpiece surface [DIN03c]. A special process is partial upsetting (e.g. heading), in which a local mass concentration is created on the workpiece. In this process, parts of the workpiece are clamped in a clamping die, so as to prevent the complete deformation of the workpiece volume (Fig. 3.1). Upsetting is particularly important for model tests, serving among other things to determine yield stresses and friction coefficients.

F. Klocke, *Manufacturing Processes 4*, RWTHedition,
DOI: 10.1007/978-3-642-36772-4_3, © Springer-Verlag Berlin Heidelberg 2013

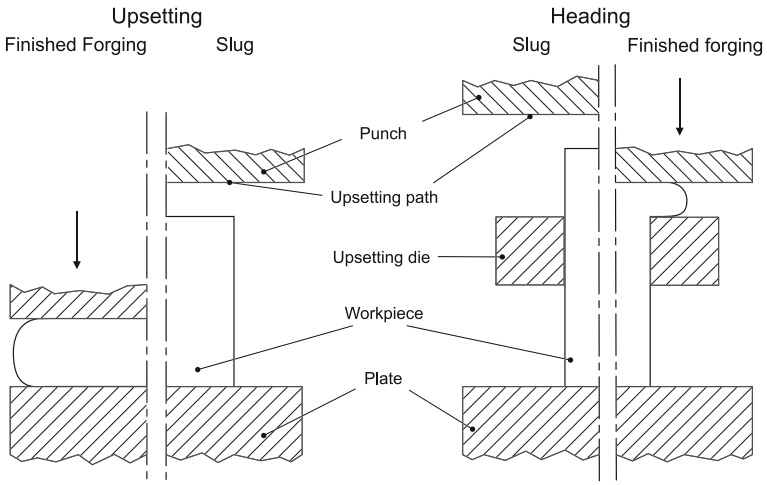


Fig. 3.1 Process steps in upsetting and partial upsetting (e.g. heading)

3.1.1.2 Upsetting: Manufacturing Examples

Upsetting is combined in most cases with other forming operations. In many cases, partial upsetting is employed to create plane-parallel surfaces on tube parts produced by sawing or shearing bars or wire sections. This is vital for the positioning of the blank in additional forming operations, such as forging or extrusion. Figure 3.2 shows different massive components produced by upsetting, among other processes. In these cases, upsetting is used to create local mass concentrations, to flatten the component or to produce parallel surfaces onto which other components can be fastened.

Typical production processes in which upsetting is applied includes the manufacturing of screws, nuts, bolts and cup-shaped parts. Figure 3.3 shows the way the process is integrated. Usually, a wire-shaped starting material is used. The wire first runs through a machine-integrated alignment station, in which it is usually pulled. The pulling movement guarantees a constantly identical diameter on the one hand, with the Bauschinger effect having a positive influence in subsequent upsetting operations, as the material already starts to flow at a lower stress because of the changing direction of loading. After aligning, a piece is sheared form the wire (Pos. 1) which is fed into the first die through automatic feed mechanisms (Pos. 2). In the first working stroke (Pos. 3), the screw end is partial upset and the later screw shank is reduced by extrusion. After this working stroke, the part used for the next work step is transported onwards (Pos. 4). There, the end of the screw is upset in a finish riveting die, thus receiving its final contour (Pos. 5). Finally, the finished part is ejected from the die with the aid of ejectors (Pos. 6). The number of forming steps depends on the shape of the part and the material used. When determining the forming steps, attention must be paid to the strain hardening of the material, as no heat treatment of the parts can be executed on such machines after the individual forming operations.

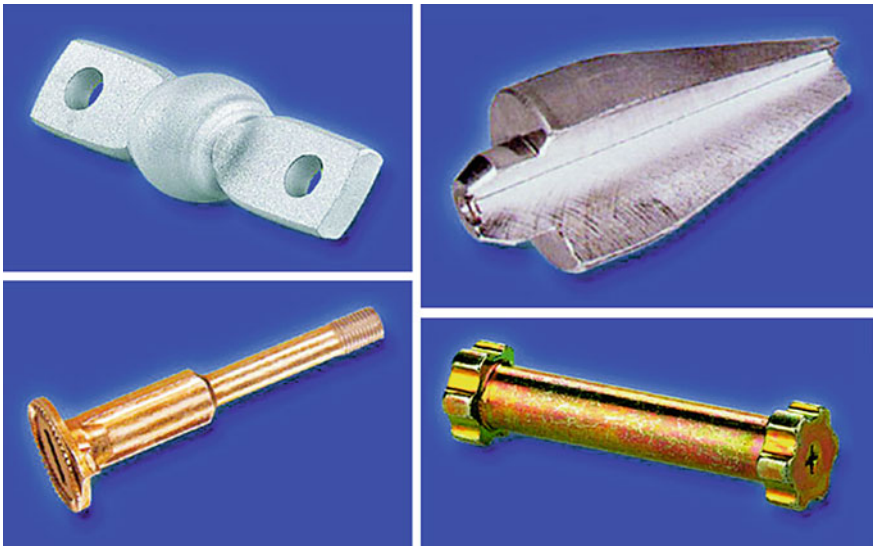


Fig. 3.2 Manufacturing examples of components whose manufacture includes an upsetting operation (*Source* A.&.E Keller GmbH)

Figure 3.4 shows another example in which upsetting is integrated as an intermediate operation into the operational sequence. Here, upsetting creates an optimal predistribution of the material, minimizing the tool loads in the subsequent forming stages.

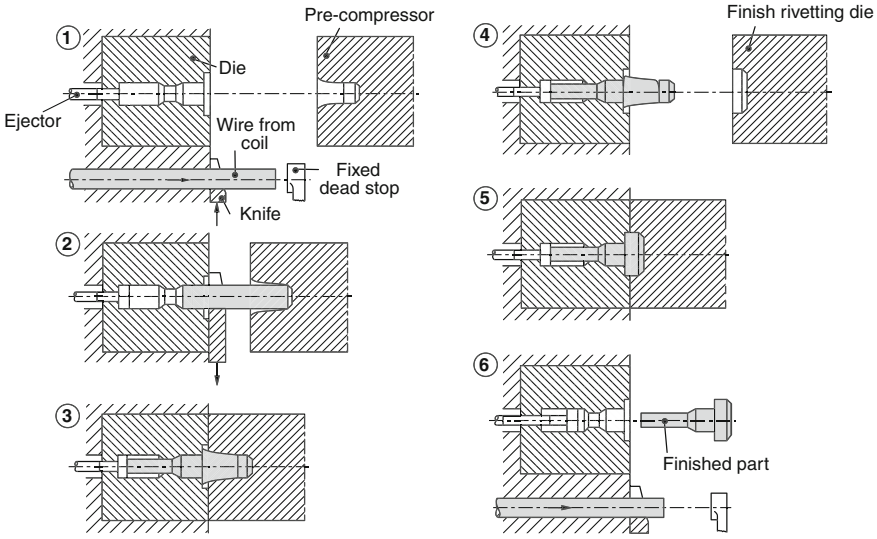


Fig. 3.3 Extrusion of screw blanks with the aid of upsetting processes

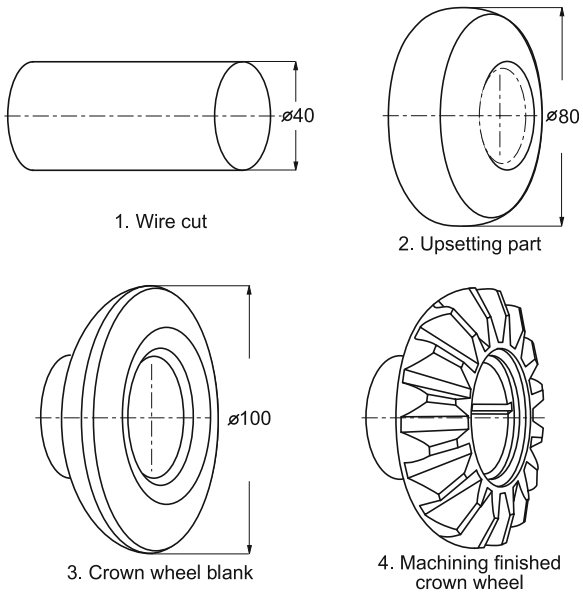


Fig. 3.4 Manufacture of a crown gear

3.1.2 Extrusion

Like upsetting, extrusion is also classified in DIN 8582 [DIN03b], "Forming manufacturing processes" under Group 2.1, "Compressive forming". DIN 8583-6 [DIN03g] defines extrusion as follows: "Extrusion is the pushing-through of a workpiece held between two tool parts, e.g. a bar section or sheet section, primarily in order to create individual workpieces. In comparison to reducing, greater deformations are possible with extrusion". Extrusion is subdivided according to the tool type used into (Fig. 3.5):

- extrusion with a rigid tools,
- extrusion with active media.

3.1.2.1 Classification and Special Features of Extrusion Processes

The principles of classification within the two different process groups distinguished according to tool type are:

- the direction of material flow relative to the effective machine direction,
- the shape of the workpieces produced.

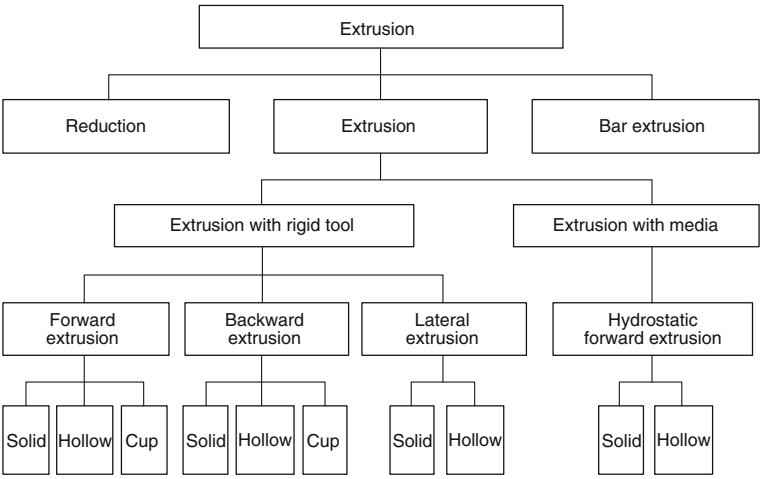


Fig. 3.5 Classification and designation of extrusion processes

A superordinate characteristic used to classify the processes is the direction of the material flow. This results in the subdivision of extrusion processes with rigid tools into.

- forward extrusion,
- backward extrusion,
- lateral extrusion.

The characteristic feature of these processes is that the workpieces is pressed with the aid of a punch through a die, in which it undergoes a plastic deformation. The term "die" refers to the container and the shaping tool aperture as a unit. Extrusion with active media (hydrostatic extrusion) differs from extrusion with rigid tools inasmuch as the workpiece is pressed through a die by means of a fluid. The fluid pressure in the tool required to do this is usually created with the aid of a forming press. The fluid can also be pressurized in other ways, e.g. by means of a pump. For process-related reasons, the use of active media allows only for forward extrusion.

The individual process variants are clearly determined by the direction of material flow and the basic shape of the workpieces. Figure 3.6 contains some examples. The highly simplified sketches show the starting shapes of the workpieces and the initial position of the punch on the left side. The right side shows the direction of flow of the material and the geometries the workpieces receive. The arrows represent the working motion of the punch.

Forward extrusion with rigid tools is subdivided according to the shape of the workpieces produced into the following process variants:

- solid forward extrusion
- hollow forward extrusion
- cup forward extrusion.

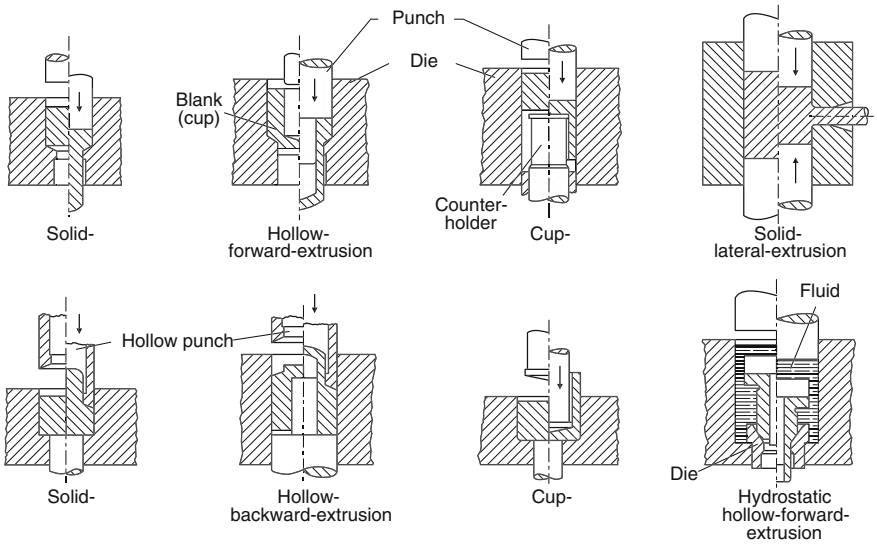


Fig. 3.6 Compressive forming manufacturing processes [DIN03b]

Table 3.1 Distinguishing features of forward extrusion [DIN03g]

Method	Blank	Final shape	Shaping tool opening
Solid forward extrusion	Solid body	Solid body with reduced cross-section	Die
Hollow forward extrusion	Cup or shell	Shell with reduced wall thickness	Gap between die and punch (shearing gap)
Cup forward extrusion	Solid body	Thin-walled hollow body	Gap between die and counterholder

The direction of the punch movement and the material flow are the same in all three variants. In terms of the remaining characteristics, they differ as indicated in Table 3.1. The blanks, referred to as "solid bodies" can either be bar sections, rod sections or sheet sections. With respect to tool construction and workpiece shape, cup forward extrusion and hollow forward extrusion are very similar. Differences lie in the shape of the starting material and the designated use of the parts after forming. In cup extrusion, a hollow body (cup, shell) is created from a solid body. In hollow extrusion, the blank is an already preformed cup or shell. The finished part is created by means of further forming steps. There are also three variants of backward extrusion with solid tools:

- solid backward extrusion
- hollow backward extrusion
- cup backward extrusion.

Table 3.2 Distinguishing features of backward extrusion [DIN03g]

Method	Blank	Final shape	Shaping tool opening
Solid backward extrusion	Solid body	Solid body with reduced cross-section	Inner contour of the punch
Hollow backward extrusion	Cup or shell	Shell with reduced wall thickness	Gap between inner contour of the punch and counterholder
Cup backward extrusion	Solid body	Thin-walled hollow body	Gap between die and counterholder

The material flow and the effective machine direction are opposed. With the exception of cup backward extrusion, hollow punches are used. Table 3.2 provides an overview of the remaining distinguishing features.

Lateral extrusion differs from forward and backward extrusion insofar as the work flow no longer runs with or opposite the effective machine direction, but rather transversely to it. It is subdivided into.

- solid lateral extrusion
- hollow lateral extrusion.

These processes are applied when, for example, solid or hollow profiles are to be attached to solid bodies. In solid lateral extrusion, the shaping tool opening for the attachment piece is the die, in hollow lateral extrusion the die and a dome for the inner contour of the attachment piece. In order to remove the workpiece from the tool after processing, the die must be divided in both cases. If the material flow in the radial direction is not routed through a die, the process is one of upsetting or partial upsetting.

A variant of forward extrusion is hydrostatic extrusion. In this process, the transfer of the forming force to the workpiece is not executed directly by the punch, but rather indirectly using a fluid. This fluid surrounds the workpiece on all sides, pressing it through the shaping die. Both solid and hollow bodies can be produced. However, the latter can only be produced if a mandrel is used. As a result of the application of hydrostatic pressure on all sides, this process has the advantage of increasing formability, as crack formation is deferred to higher true strains.

The production of extrusion parts (Sect. 3.1.2.3) usually takes place in multiple steps. Also, the extrusion processes discussed above can be applied simultaneously in various combinations or in sequence. Figure 3.7 contains some typical basic shapes of extrusion parts and the designations of the relevant process variants.

3.1.2.2 Extrusion Tools and Tool Design

Especially in extrusion, the cost-effective production of dimensionally accurate parts with good surfaces is influenced in a vital way by the design of the tools and the selection of suitable construction materials for the individual tool components.

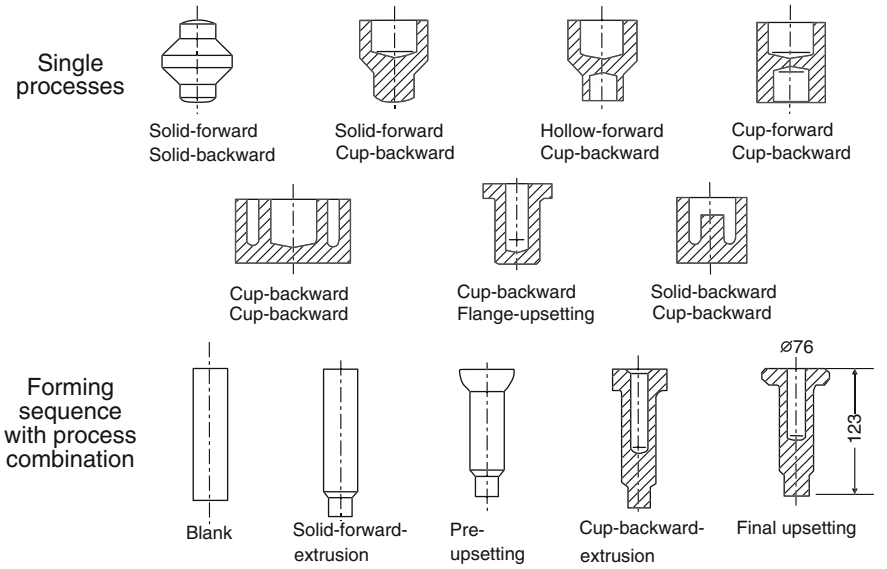


Fig. 3.7 Process combinations in the production of extrusion parts

These components fulfil different functions in the tool, thus placing divergent demands on the corresponding tool construction materials.

The shape of the workpiece to be produced determines the shapes of the punch, die and pressure pad (Figs. 3.8 and 3.9). During the extrusion process, these parts come into direct contact with the workpiece and are exposed to high stresses.

The forming force acts on the tool in a radial and axial direction. Axial compressive stresses are introduced into the press in the form of a force. The radial components act, however, as an internal pressure on the inner wall of the hollow tool. If pressures of more than 1,000 MPa develop on the inner surfaces of the dies, reinforcement rings are required (Figs. 3.8 and 3.9). These are designed in such a way that compressive stresses arise on the inner sides of the dies. A full or partial compensation of these compressive stresses occurs during the extrusion process through the opposing process stresses. It is recommendable for the tool design that a compressive residual stress remains intact to the greatest extent possible with every working stroke which exerts a positive influence on tool life. This applies in particular to tool made of hardened high-speed steels and hard metal, since these tool materials cannot absorb any larger tensile stresses.

Depending on the extrusion process, the punch presses the workpiece through a die (solid forward extrusion), or it shapes an inner contour (cup extrusion). The entire cross-section of the punch is exposed to high compressive stresses. Compressive load stresses in the marginal zone of the punch arise as a result of friction forces caused by contact with the workpiece. For this reason, the punch must have the highest possible fatigue strength. Loads bearable without plastic deformation of the tools lie at approximately $\sigma_{max} = 3.000$ MPa. The pressure pad is exposed

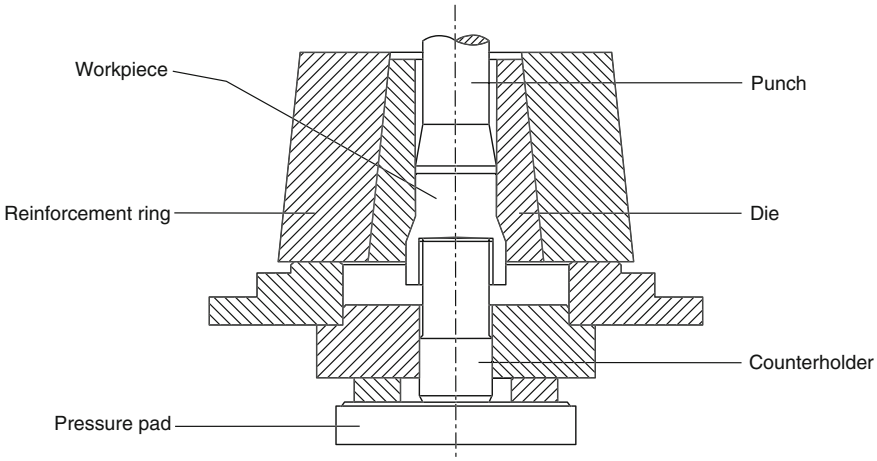


Fig. 3.8 Schematic tool construction for cup forward extrusion (acc. to Kunogi)

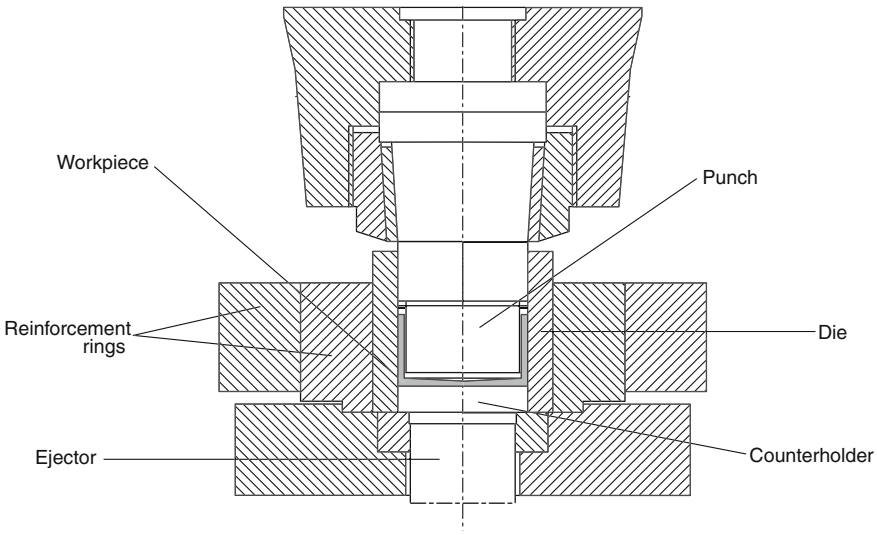


Fig. 3.9 Schematic tool construction for cup backward extrusion [VDI97]

to the same basic stresses as the punch. The ejectors needed for removing the workpieces or slugs (in piercing operations) are considerably less stressed. The stresses placed on extrusion tools may be composed of tension, compression, shear, bending, friction, oxidation and thermocycling. The wear developed when the tools are used generally causes an increase of any arising tool stresses. Different parts or areas of the tools may be especially affected by this. Critical locations in the tool tend to be those on which there are larger changes in workpiece cross-section (Fig. 3.10). The smaller the contact surface in the deformation

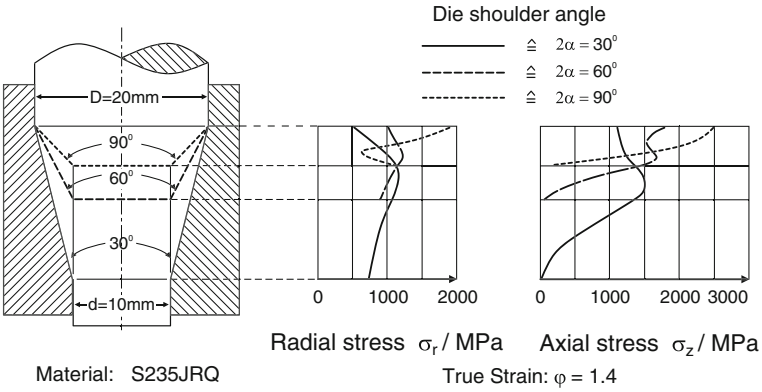


Fig. 3.10 Die load in solid forward extrusion (acc. to Geiger)

region is, the greater the tool loads. The production of components by means of cold extrusion requires manufacturing facilities for the following work steps:

- blank production (as circular sheets, rod sections, or similar items)
- heat treatment (annealing)
- surface treatment (phosphating, lubricating, etc.)
- forming (pressing)
- postprocessing and inspection.

When creating a phase plan specifying the overall processing sequence, a pressed part drawing is developed, into which the required dimensions and their tolerances, transitions with angles and radii, the material overrun and the admissible eccentricity is recorded. The individual pressing stages are determined in reverse, from the pressed part drawing to the blank. The following factors are taken into account during the process [SPUR84]:

- the forming limit for the respective forming process, given by
  - the loading capacity of the individual tool elements
    The attempt is made to distribute an equal amount of load to each forming stage in order to avoid increased wear in a single stage. [JAHN81, VDI99a] contain information on the forming limits achievable with the different extrusion processes.
  - the formability of the workpiece material (Sect. 2.3.7, p. 32).
- the limited ability of the individual forming processes with respect to
  - deformation (material flow)
    Only very few pressed parts can be produced in a single work step according to one of the basic extrusion processes. Usually, several forming steps are required (possibly with intermediate annealing), taking the process-specific material flow into account.

  - changing material properties
  - Additional demands, e.g. increased strength, can be placed on the pressed part.

- the limited ability of the individual forming processes to control the strain and the changes to material properties
  Pressed parts with very close shape and dimensional tolerances frequently require a processing sequence especially adapted to these tolerances, in part with additional calibration steps.
- unfavourable material flow
  If unfavourable conditions for the material flow are present, these can cause defects on the workpiece, such as chevrons and folds. Chevrons are V-shaped cracks which may form, for example, in the interior of a workpiece during solid forward extrusion. Defects of this kind can often be eliminated by changing the processing sequence.

Determining the phase sequence determines the shape and dimensions of the individual press steps of an extrusion part and thus also the shaping working surface of the active tool parts. The loading capacity of the extrusion tools limits not only the strains which can be achieved, but also the achievable die life. Proper constructive design, the selection of suitable tool materials and wear protection treatments and an optimized tool production are thus all essential to the achievement of economic tool lives. Varying demands are placed on tool construction materials. These depend on the tool part (punch, die, ejector, reinforcement rings), the workpiece material and the forming temperature. In order to keep tool costs to a minimum, it must not be neglected to guarantee the sufficient machinability of the tool construction materials, especially when producing complex tool geometries.

The following properties of tool construction materials for extrusion tools are particularly important:

- uniform, isotropic grain structure
- maximum possible dimensional stability during hardening and tempering
- good tempering resistance
- heat resistance and hot ductility
- insusceptibility to hot cracking
- thermal shock resistance
- resistance to oxidation and corrosion
- high wear resistance
- dimensional stability in use

Since tool construction materials only exhibit these properties in part, their selection should be based on the respective case of application. Sect. 2.7.2 provides an overview of the properties, advantages and disadvantages, as well as the fields of application of the different tool materials. Table 3.3 lists the steels largely used today for the production of extrusion tools. They are used exclusively in the quenched and tempered condition.

Table 3.3 Steels used for extrusion tools (acc. to Thyssen)

Material designation	Hardening/Quenching/ Tempering	Hardness HRC	Examples of application
100 V 1	Quenching in water, tempering shallow depth case hardening	60–64	Extrusion tools for low strain
115 CrV 3			
145 V 33			Ejectors
90 MnCrV 8	Quenching in oil, tempering shallow depth case hardening	58–62	Punch thrust pieces, guide rings
55 NiCr 10		52–58	Punches, counterholder, dies
X 45 NiCrMo 4		47–52	Reinforcement rings, pressure plates
X 155 CrVMo 12 1	Quenching in oil or air	54–62	Punches, counterholder, dies
X 210 Cr 12		56–62	Thrust pieces, guide plates
X 3 NiCoMo 18 8 5	Martensitic	50–54	Reinforcement rings
X 3 NiCoMoTi 18 9 5	Hardenable	54–56	Reinforcement rings, punches, pressure plates
HS 6-5-2 C	Quenching in oil or salt-bath	58–65	Punches, counterholder, dies
HS 2-10-1-8		62–67	Punches, punch heads
HS 10-4-3-10	Repeated tempering	62–67	Punches, punch heads

Surface treatments of especially highly stressed tool parts can be effective for increasing wear resistance and reducing the adhesion tendency between the workpiece and the tool. To this end, layers are applied to the surfaces which are characterized both by high hardness and by a corresponding brittleness. In order to avoid chipping under stress, they may not exceed a certain thickness. For nitriding, this thickness is ca. 25 μm, or 5–9 μm in the case of carbide, titanium and chrome-based hard material layers. Carbides exhibit high hardness and wear resistance. For extrusion dies, grades G 30–G 55 are primarily used (Table 3.4). These grades have preferred fields of application in accordance with their properties.

In extrusion tools, carbides may only be exposed to compressive stresses, since they only bear minimal tensile stresses. As a result, only minimal bending stresses are admissible. When designing the tools, therefore, great care is to be taken with respect to the reinforcement rings. Also, angles, radial transitions and die divisions

Table 3.4 Carbides used for extrusion tools

Type	Composition (%)			Hardness	Bending strength	Compressive strength	Examples of application
	WC	TiC+TaC	Co	HV30	(MPa)	(MPa)	
G 30	82	3	12	1,200	2,400	4,100	Piercing punches, forming pins, extrusion mandrels
G 40	77	3	20	1,050	2,600	3,800	Extrusion dies, extrusion punches (at low bending stresses)
G 55	75	–	25	850	2,800	3,000	Pre- und finish upsetting device, extrusion tools (standard type for extrusion)

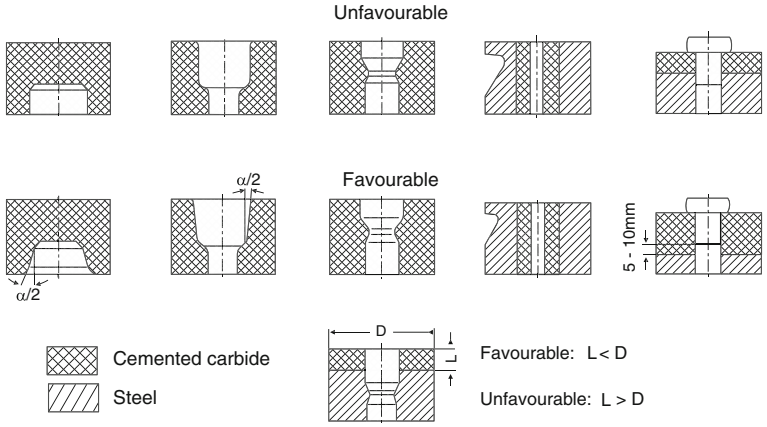


Fig. 3.11 Design of carbide inserts for extrusion (acc. to Kraft)

must be designed in such a way that tensile and bending stresses do not arise in the carbide. Figure 3.11 shows some typical design examples. Only tool constructions which are adapted to the special properties of carbides can fully exploit its superior wear and heat resistance. If wear stresses predominate, carbide-tipped dies can be used to achieve die lives ten to 40 times greater than when using tool steel.

In general, the following factors must be taken into account in designing extrusion tools:

- The extrusion dies must have single or multiple reinforcement rings, depending on the load.
- The extrusion mandrels should be as short as possible so as to reduce bending stresses.
- An exact guidance of the extrusion punch to the die must be ensured.
- Parts subject to wear should be as easily replaceable as possible.

Tables 3.5 and 3.6 summarize the limit stresses of extrusion tools.

Figure 3.12 shows the design of extrusion punches, mandrels and dies for the most frequently implemented extrusion processes. Figure 3.13 illustrates the basic construction of tools for cold massive forming on the example of a tool for solid forward extrusion of steel.

Table 3.5 Limit values for the internal pressure p_i of extrusion dies with different die shrink ring assemblies [LANG90b]

Die reinforcement	Limit value p_i / MPa
Non-reinforced dies	1,000
Single reinforced dies with steel core	1,600
Single reinforced dies with carbide core	1,500
Double reinforced dies with steel core	2,200
Double reinforced dies with carbide core	2,000

Table 3.6 Limit values for the relative punch load $\bar{p}_{St}$ for the extrusion punch and extrusion mandrel

Tool	Limit value $\bar{p}_{St}$/MPa
For punches and mandrels made of tool steel	1,800
For extrusion punches made of high-alloy high speed steel	2,500

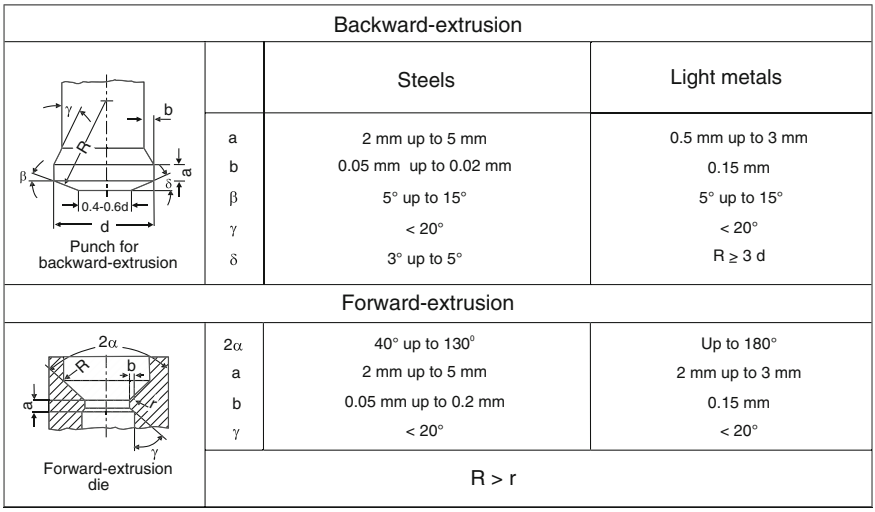


Fig. 3.12 Reference values for extrusion punches and dies

Among the two construction elements of an extrusion tool standing in direct contact with the workpiece during the forming process, the punch can generally be designed without great difficulty with respect to a more or less optimal load and low wear. Designing the die to withstand loads represents a considerably larger challenge. The determinant factors which affect the design of extrusion dies are the stresses arising during the forming process (Fig. 3.14). The dies are loaded during pressing above all by high internal pressures varying over the length of the bore. The maximum pressures are concentrated in the zone of the inner bore, in which the workpiece is found. Since the internal pressure acting on the die originates from the workpiece, both the internal pressure and the pressure chamber height change during the forming process. Under simplifying assumptions, such as static load, an even distribution of internal pressure and no residual stresses, stress calculations can be executed for the production of a thick-walled hollow cylinder. Disregarding axial stresses, tangential and radial stresses σ_t and σ_r result under the internal pressure p_i, as shown in Fig. 3.15 [SPUR84].

In the vicinity of the inner wall of the thick-walled hollow cylinder the magnitudes of the stresses σ_t and σ_r are approximately the same, taking on the value of the internal pressure. According to the Tresca yield criterion (shear stress hypothesis),

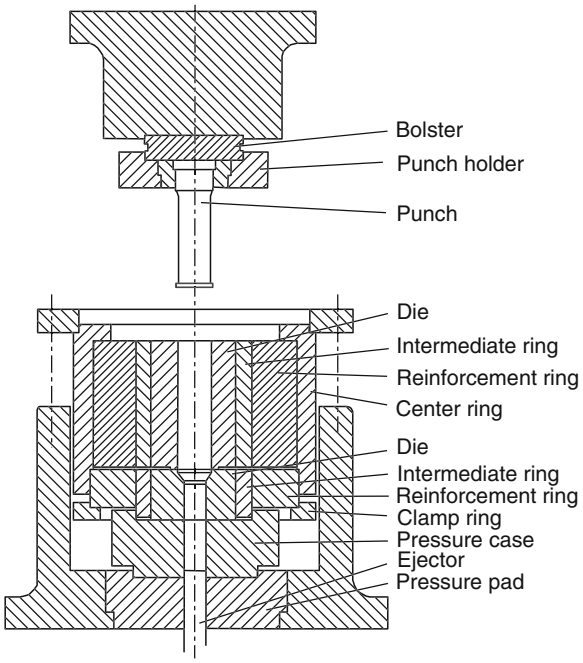


Fig. 3.13 Tool construction for solid forward extrusion

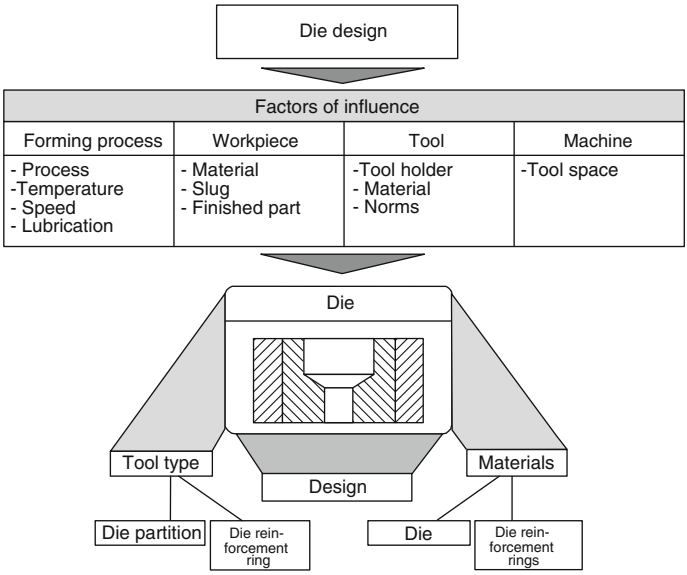


Fig. 3.14 Factors influencing the shape and design of dies

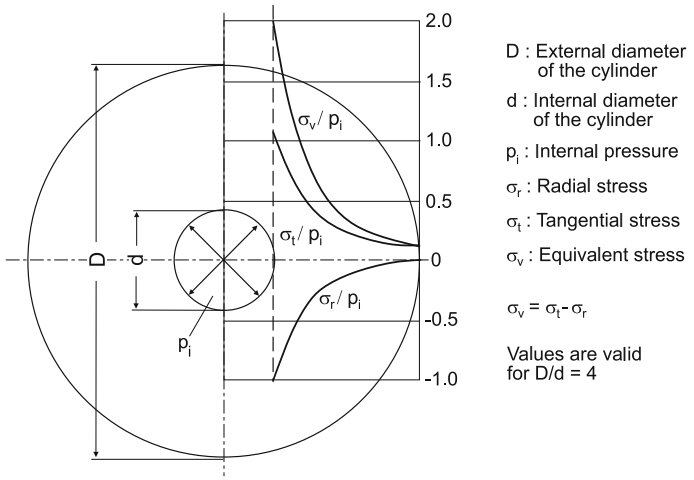


Fig. 3.15 Theoretical stress progression in a thick-walled hollow cylinder under internal pressure [SPUR84]

the internal pressure may not be greater than half of the elastic limit of the tool steel. However, in order to withstand higher pressures, a tangential compressive stress must be present on the inner wall when unpressurized, so that a lower resultant tangential stress results given internal pressure than without prestressing. Such prestressing is created by means of one or more reinforcement rings, whose hole is smaller than the outer diameter of the respective inner ring. As shown in Fig. 3.16,

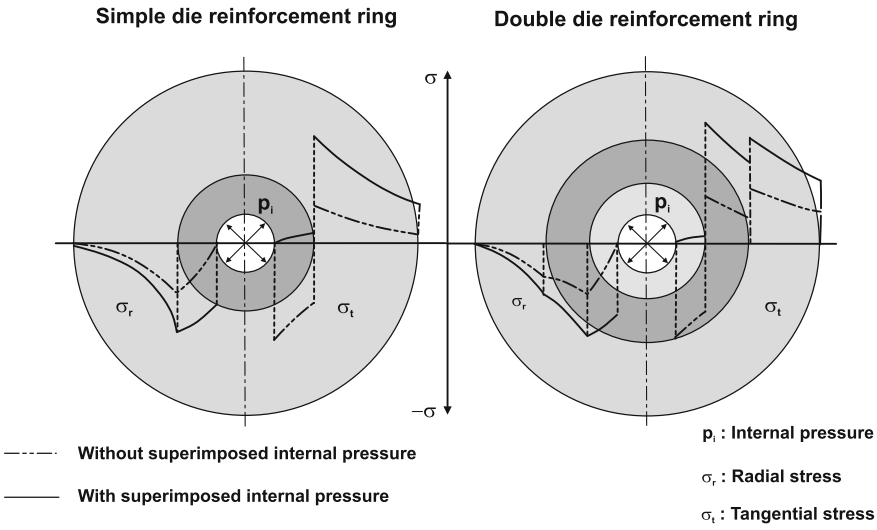


Fig. 3.16 Theoretical stress progressions with one (links) and two (right) reinforcement rings, with and without internal pressure [SPUR84]

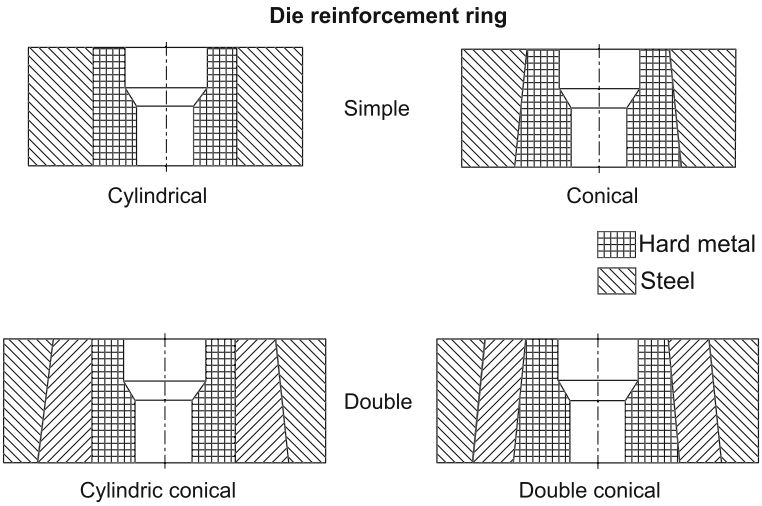


Fig. 3.17 Interference fit models

the resultant stress results from the sum of the prestressing and the stress caused by the internal pressure.

Figure 3.17 illustrates different interference fit models. The cylindrical joint has the advantage of simple production, although due to the maximum possible heating only relative interferences of $\rho < 0.4$ % are possible. With tapered designs, the stretch limit of the die shrink rings represents the limit for interference. As usual, the tapered seat offers the advantages of simplified joining and release.

The number of reinforcement rings depends on the internal pressure arising in the die during forming (Table 3.7), the tool materials employed and the available space.

The economic viability of massive forming processes is primarily determined by the service life of the tool elements. This in turn depends on many factors, the most important of which are the following:

Table 3.7 Increase of the admissible internal pressure through the installation of reinforcement rings [VDI86]

Parameter	Die		
	Not reinforced	Single reinforced	Double reinforced
$\rho_0 = d_i/D_a$	0.20	0.20	0.20
$\rho_1 = d_i/d_1$	0.20	0.44	0.56
$\rho_2 = d_1/d_2$	–	0.45	0.58
$\rho_3 = d_2/D_a$	–	–	0.61
$\sigma_{v1,zul}/MPa$	1,500	1,500	1,500
$\sigma_{v2,zul}/MPa$	–	1,400	1,400
$\sigma_{v3,zul}/MPa$	–	–	1,300
$p_{i,zul}/MPa$	690	1,160	1,395

- the process (forward, backward, solid, hollow, lateral extrusion)
- the workpiece material (strength, wear-causing inclusions, surface condition)
- the true strain
- friction conditions
- the tool shape (part-dependent)
- the constructive design of the tool
- the properties of the tool construction materials
- the required dimensional accuracy and surface quality of the workpiece.

For this reason, the following information can only be seen as guide values: The main causes of failure in the punch and the die differ according to the typical types of loading. The punch is primarily exposed to fluctuating compressive stresses. The tool life quantity of punches made of HSS used in solid forward extrusion of steel with up to 0.4 % carbon can amount to up to 100,000 workpieces. With hollow forward extrusion, this value lies between 50,000 and 100,000. The smallest value is for heat-treatable steels with up to 0.4 % carbon content (C35C, CrNiMo 8, 41Cr4) [SPUR84]. These tool life quantities are the same as the number of load cycles acting on the punch. In the extrusion of steel, the punch is exposed to high compressive loads of up to 3,000 MPa, causing signs of fatigue to appear which finally lead to fracturing. Lower punch loads occur when extruding light metals. If strongly abrasive inclusions are present, abrasive wear becomes the primary cause of failure. The dies are also subjected to a dynamic load. These reach tool life quantities between 30,000 and 100,000 workpieces when extruding soft steels. With unalloyed steels with more than 0.35 % carbon and alloyed steels, the tool life quantities are lower, amounting to only 5,000–20,000 pieces.

The dies usually fail as a result of transverse fractures. These form because of stress peaks or gradients caused by the forces transferred from the workpiece to the die. The maximum stresses can be reduced by means of a transverse division of the die [SU94]. If the load on the die is very high or if it is overloaded, longitudinal fractures develop. The risk of longitudinal fractures is increased if a high pressure load occurs in the region of the die end surface. This is almost always the case with head upsetting dies for screws or bolts. This risk can be reduced, albeit only to a limited extent, by a radial prestressing of the die in the region of the end surfaces.

3.1.2.3 Extrusion: Manufacturing Examples

Usually, multiple work steps are required to manufacture extrusion parts (Fig. 3.18). If the starting material is not continuously fed, as for example in the processing of wire into extrusion parts, then a blank, e.g. a rod section, must be produced through sawing or shearing. Shearing is more time- and cost-effective than sawing, although it causes an undesirable strain hardening on the shearing surfaces and can only be used for diameters of up to average size. Sawing is slow, with material going to waste in the process. An advantage, however, is that practically no surface strain hardening occurs. For economic reasons, shearing is

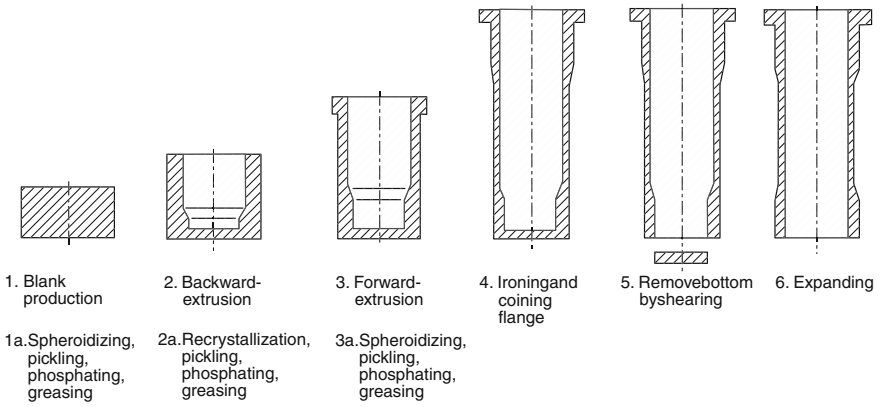


Fig. 3.18 Manufacture of a sliding sleeve

used for producing rod or wire sections whenever possible. The sections are then usually lightly upset so as to receive plane-parallel blanks.

In the case of difficult forming operations with high true strains, steel blanks are often soft-annealed beforehand in order to obtain a grain structure which is as uniform as possible. This can then be followed by the first forming operation, e.g. backward extrusion. Multiple heat and surface treatments may be necessary between the individual forming stages of the overall production process (Fig. 3.19). These serve to remove the strain hardening of the material through recrystallization, thus increasing the achievable total strain. Heat treatment prior to calibration is necessary to achieve close, uniform tolerances. This is especially

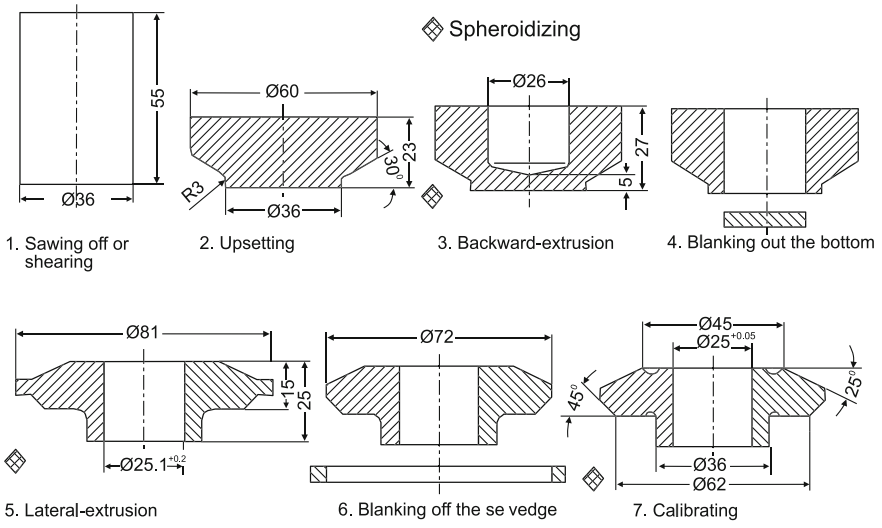


Fig. 3.19 Operational sequence for manufacturing a bevel gear (acc. to Komatsu Maypress)

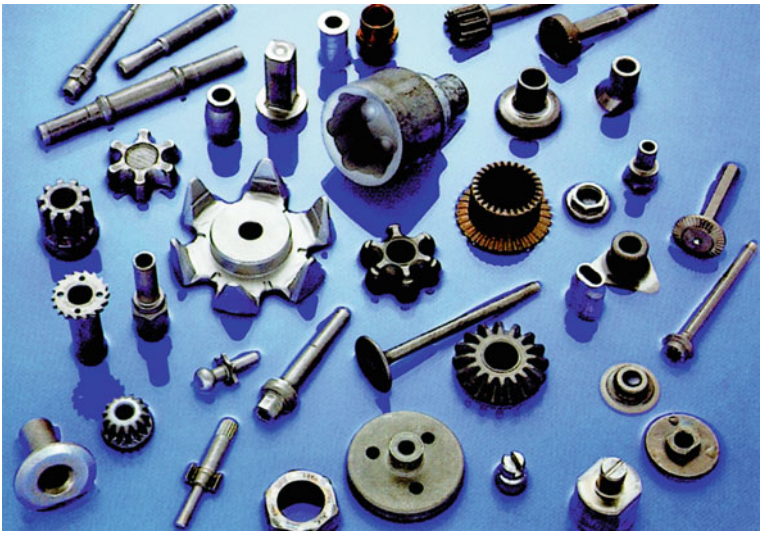


Fig. 3.20 Different cold extrusion parts (*Source* Sieber Forming Solutions)

important for the bore serving as an intake in gear cutting processes. In order to accommodate the tolerances of the blank and to ensure a good workpiece shape, a material overrun is pressed on and later removed.

Figure 3.20 illustrate some manufacturing examples of complex components. Extrusion is not only competitive with respect to the production of ready-to-install parts, but also as a process for producing blanks on which finishing operations are to be performed, e.g. to create sharp edges (Fig. 3.21).

Figure 3.22 provides an impression of the extreme material deformations which can be realized by means of extrusion. For example, a cup-shaped filter housing can be made from a circular aluminium sheet with a wall and bottom thickness of 1 mm. This component is produced in a single forming step by means of cup backward extrusion. The starting circular sheet has a diameter of 80 mm and a height of 25 mm. The circular sheet is lengthened during extrusion to 15 times its starting height.

3.1.3 Force and Energy Requirements

The forces and energy necessary for manufacturing cold forming parts depend on a number of factors. Among them are the forming process used, the strength properties of the material and their alteration over the course of forming, the shape of the workpieces, the friction relationships between the workpiece and the tool elements and the process control, i.e. above all the strain rate and the temperature.

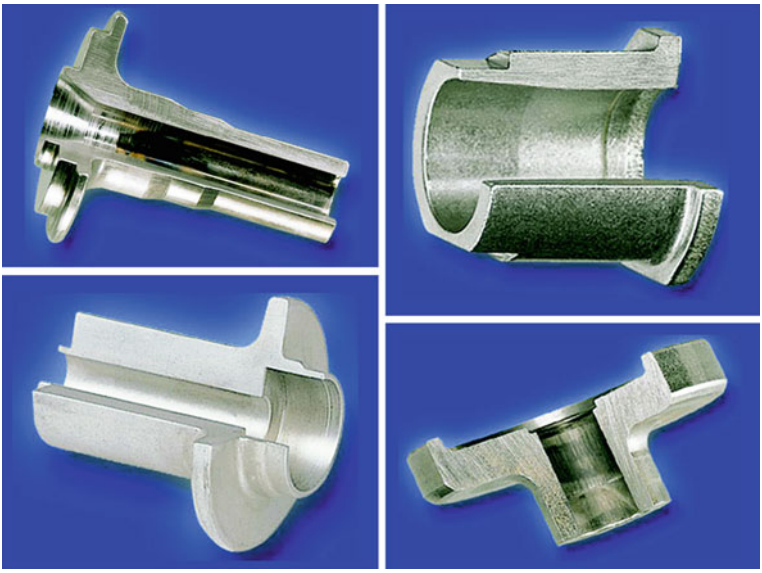


Fig. 3.21 Manufacturing examples of flanges (*Source* A.&.E Keller GmbH)

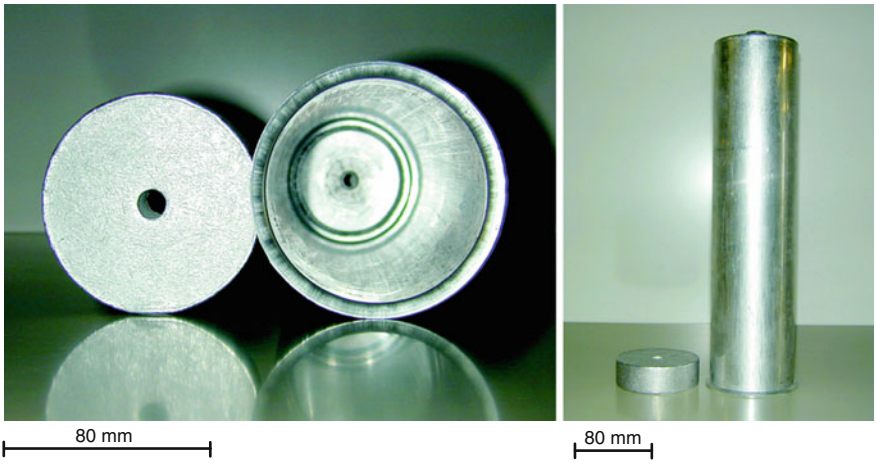


Fig. 3.22 Manufacturing examples of cup backward extrusion of aluminium (*Source* Schneider-Clauss GmbH)

An exact calculation of these influencing variables is not possible. Only the material behaviour and the admissible strain can be approximately determined as a function of the true strain. An analytic determination of punch forces can only be executed approximately for individual processes.

3.1.3.1 Admissible Strains

The material and the workpiece geometry to be obtained in the forming process are generally specified when manufacturing cold forming parts. The contour of the blank and, if forming is to occur in multiple steps, the division of the individual forming steps are to be coordinated as the individual case demands. For this, the following factors are important either alone or in combination with each other with respect to determining the admissible strain (Sect. 2.3.7):

- the material properties
- the forming process
- the loading capacity of the tool elements
- the available machine power.

The greatest importance is usually attributed to the material. Its properties determine the forces necessary to introduce and maintain flow during the forming process. They also determine the strain which can be achieved without setting off a local crack formation. The boundaries within which forming is performed are given by the transition from elastic to plastic deformation (lower boundary) and the appearance of the first material separations (upper boundary). The formability of materials as determined in model tests (Sect. 2.3.7) cannot always be fully exploited in the manufacture of extrusion parts. Constraints exist in the form, for example, of geometrically related flow hindrances, friction between the workpiece and the tool, limits to the loading capacity of the tools and accuracy requirements placed on the workpieces. Table 3.8 summarizes the strains typically achievable for some materials and forming processes, taking account of the constraints mentioned, including the process used. The table assumes a specific tool load of approximately 2,500 MPa.

It should be noted that, when forming in multiple steps, the individual true strains φ_1 to φ_n add up to a total true strain φ_{tot}.

Table 3.8 Reference values for the limiting strain in extrusion [JAHN81, VDI99a]

Material	Forward extrusion		Backward extrusion	
	φ_{vmax}	$\lvert\varepsilon_A\rvert/\%$	φ_{vmax}	$\lvert\varepsilon_A\rvert/\%$
Al 99.5, AlMg 1, AlMg 3, AlMg 5, AlMgSi 0.5, AlMgSi 1	3.0–5.0	95–99	2.5–4.5	90–98
AlCuMg 0.5, AlCuMg 1	2.5–3.0	90–95	1.4–1.8	70–85
E-Cu 99.9, R-Cu 99.5, CuZn 37, CuZn 28	1.4–2.0	70–85	1.4–1.6	70–80
C 2 E, C 4 C	2.2–3.0	85–95	1.4–1.8	70–85
C 10 C, C 10 E, C10	1.6–2.0	80–85	1.4–1.6	75–80
C 15 C, C 15 E, C15	1.4–1.6	70–80	1.1–1.3	65–70
C 22 C, C 22 E, C 25 E, C25, C 35 C, C 35 E, C35	0.8–1.0	55–65	0.7–0.8	50–60
15 Cr 3, 15 CrNi 6, 16 MnCr 5, 20 MnCr 5	0.7–1.1	50–67	0.5–0.8	40–65
34 CrMo 4, 41 Cr 4, C45, 42 CrMo 4, 25 CrMo 4	0.5–0.6	40–45	0.5–0.8	40–55

If this total true strain is greater at some location on the workpiece than the limiting strain of the material, material tears and folding will occur at this location, leading to the fracturing of the material. In order to avoid this, the formability of the material must be restored beforehand. This is achieved through a targeted heat treatment, i.e. either sub-critical or soft-annealing. If materials such as lead, tin or zinc are extruded, the recrystallization temperatures of which lie approximately at room temperature, then the abovementioned constraints with respect to the maximum possible true strain, above which a heat treatment becomes necessary, no longer applies, i.e. provided that the strain rate is lower than the recrystallization rate. For this reason, far higher strains are possible with such materials than those given in Table 3.8.

Greater strains than in a cold state are only possible for metals with higher recrystallization temperatures when the workpieces are preheated. In such a case, warm working is possible in principle (Sect 3.2). If the achievable strains are nevertheless insufficient, hot forming can also be performed (Sect. 3.3).

3.1.3.2 Stationary and Non-stationary Processes

The forming method used determines whether the forming process is stationary or non-stationary. Also, the flow and path lines of the individual workpiece points must be taken into consideration. Flow lines refer to the lines which have the velocity vectors as tangents. In contrast, path lines are defined as the paths actually described during the forming process. If the velocity vector is tangent to the path curve at all times, then the flow and path lines are identical for this point. If this applies to all workpiece points, then the process is one of stationary forming. A further characteristic is a constant velocity field. If the velocity field varies during forming, then the flow and path lines are not identical and the forming process is non-stationary [SPUR84] (Fig. 3.23).

Force Determination for Stationary Forming Processes

Extrusion is a stationary forming process. Thus the punch force is roughly constant during forming. Therefore, the punch or machine work can be approximately determined using the formula

$$W_{St} = \int_0^{s_w} F_{St}\, ds \approx F_{St} \cdot s_w. \tag{3.1}$$

In the formula, s_w refers to the punch path and F_{St} to the punch force.

The behaviour of the material can be roughly determined as a function of the true strain. It is advisable to determine the mean yield stress k_{fm} for all materials which strain-harden during forming. The mean yield stress is defined between the true strain at the start of forming φ_{v0} and after forming φ_{v1} as:

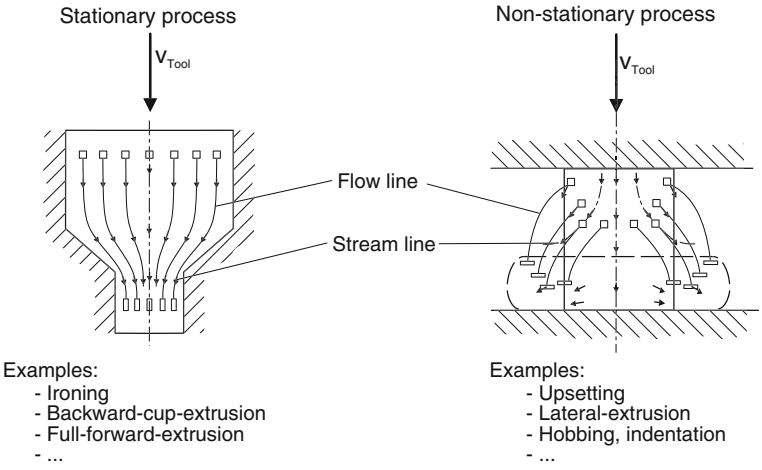


Fig. 3.23 Comparison of stationary and non-stationary forming processes

$$k_{fm} = \frac{1}{\varphi} \int_{\varphi_{v0}}^{\varphi_{v1}} k_f d\varphi. \tag{3.2}$$

In this equation, k_f is the yield stress specified in the flow curve (Sect. 2.3.7). With the aid of the mean yield stress k_{fm}, the material volume V affected by the forming process and the change to the reference true strain $\Delta\varphi_v$, one can calculate the ideal deformation energy W_{id}:

$$W_{id} = k_{fm} \cdot \varphi_v \cdot V. \tag{3.3}$$

The ideal deformation energy is part of the total energy which must be generated for a forming process. Further work components are

- friction work W_R,
- redundant work W_{Sch},
- bending work W_B.

The bending work is only applicable for asymmetric cross-sections. The determination of these work components is already very difficult for workpieces with simple geometrical shapes [JAHN81].

Since the forming force and deformation energy are linked over the punch path, the explanations of the deformation energy also apply to the force and its components. In practice, approximation formulas are often used to determine force and work. In these formulas, the friction, shear and bending components, which can only be determined with difficulty and in an imprecise way, are accounted for as a single coefficient, for example as the efficiency of deformation η_F [LANG90b].

The punch force can be roughly determined by equating the machine work with the total deformation energy:

$$W_{St} = \frac{1}{\eta_F} \cdot W_{id}. \tag{3.4}$$

The punch force is calculated for a stationary forming process as:

$$F_{St} = \frac{1}{\eta_F} \cdot k_{fm} \cdot \Delta\varphi_v \cdot \frac{V}{s_w} \quad \text{with} \quad \eta_F = 0.5 \ldots 0.8. \tag{3.5}$$

If the flow curve of the material to be processed is known, then it can be used to determine the ideal deformation energy w_{id} relative to the unit volume (Sect. 2.3.6). w_{id} corresponds to the surface beneath the flow curve between φ_{v0} and φ_{v1}:

$$w_{id} = \int_{\varphi_{v0}}^{\varphi_{v1}} k_f \cdot d\varphi \quad \text{with} \quad \varphi_{v0} < \varphi_{v1}. \tag{3.6}$$

Figure 3.24 shows the flow curves and the relative ideal deformation energies for two steels. If the material volumes participating in the forming process and the degrees of deformation are known, the necessary forces and work values can be derived from such diagrams.

Force Determination for Non-stationary Forming Processes

The determination of the punch force is more difficult for a non-stationary than for a stationary forming process. This is due to the fact that the punch force is not constant during forming. Instead, it rises as forming progresses due to the strain hardening of the material. For this reason, the punch or machine work can only be

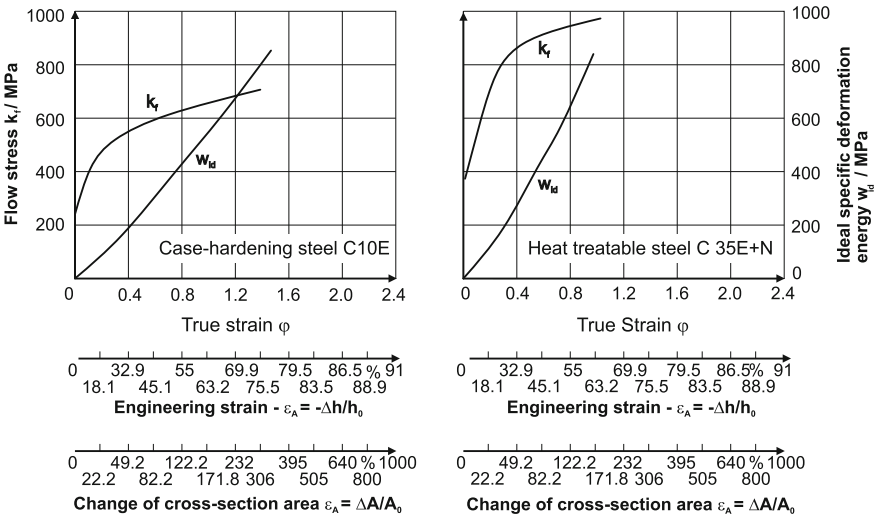


Fig. 3.24 Flow stress and ideal specific deformation energy of a C10E and a C35E + N

determined given an exact knowledge of the progression of the punch force. Since this is only known in the rarest of cases, the punch force must be redetermined for every point in time of the forming process.

The following will demonstrate a model punch force calculation on the example of a non-stationary upsetting process. It requires the knowledge of the progression of the normal contact stress on the punch surface. Siebel has developed a formula for the normal contact stress for axially symmetric upsetting on the basis of a tube model and with the aid of the Tresca yield criterion [SIEB32]:

$$\sigma_z = -k_f \cdot \left[1 + \frac{2 \cdot \mu}{l} \cdot \left(\frac{d}{2} - r\right)\right]. \tag{3.7}$$

Integrating the normal stress over the end face A of the sample yields the punch force

$$F_{St} = \int_A \sigma_z \, dA = A \cdot k_f \cdot \left[1 + \frac{\mu}{3} \cdot \frac{d}{l}\right] \tag{3.8}$$

with

A current contact surface
μ friction coefficient
k_f current flow stress of the material
d current workpiece diameter
l current workpiece height

Given the onset of strain hardening, k_f is replaced by the mean flow stress k_{fm}. The friction coefficient μ can be assumed as $\mu \approx 0.1$ for cold upsetting steel with lubrication. Since an analytic determination of the normal contact stress presents great difficulties and depends on a number of influence factors, numerous other equations are cited in the literature which account for the relevant process parameters in different ways [AMBA79]. What all these equations have in common is that the upsetting force can only be determined for a defined point in time. The only calculation generally made in practice is that of the maximum upsetting force reached due to the geometric ratio d/l at the end of forming.

3.1.4 Lubrication and Lubricants

When forming a blank with a tool, the two act together as a friction pairing. In the forming zone, large amounts of energy arise as a result of high mechanical forces, especially in cold extrusion. This energy output is required for forming and for overcoming friction forces. The resultant higher temperatures between the tool and the workpiece can amount to ca. 500 °C, with surface pressures rising up to ca. 3,500 MPa. With respect to cold extrusion, the function of lubrication is both to

dissipate heat and to create optimal friction relationships as a precondition for good workpiece surfaces and minimal forming forces, leading to low mechanical loads and low tool wear.

In simple forming operations, the lubricants can be applied directly to the workpieces. For complicated processes, it is frequently necessary to apply a lubricant carrier layer which then in turn accepts the lubricant. Different zinc phosphates and iron oxalates are used as carrier layers for corrosion-resistant steels. They are applied on the workpieces occurs through chemical bath deposition (layer thickness: 2–25 μm). They have a crystalline structure and a very high capacity for absorbing oil and soap, one which can amount to 13 times that of a metallic surface.

Section 2.8.4.2 describes lubricant carrier layers and their combination with different lubricants. New developments have been made to dispense with the costly phosphating process. Instead, wear protection is supposed to be ensured by a combined application of tool coatings and specially adapted lubricating oils [RUPP97]. However, this has only been feasible in individual cases. The selection of lubricants is already a crucial factor in planning the forming sequence. At this phase, one must already determine whether the selection of a more effective lubricant may allow for higher true strains and thus savings on heat treatments or entire intermediate stages.

3.1.5 Manufacturing Accuracy and Surface Quality

When shaping and manufacturing extrusion parts, the goal is to be able to implement the parts with as little subsequent machining as possible. This means that the geometrical dimensions must have close tolerances and that the surfaces must be of lasting quality.

Factors which affect the achievable dimensional and shape accuracy are the shape of the part, the material properties, the breakdown of the forming steps, the care taken in intermediate treatments such as annealing and lubricating, the condition of the tool and the machine and the process control.

With respect to the dimensional accuracy, extrusion can be classified between forging and machining (Fig. 3.25). Closer tolerances can be realized for cold extrusion than for warm or hot extrusion.

The absolutely achievable dimensions depend on the dimensions of the mould elements and the masses of the parts. Figure 3.26 provides a partial list of reference values which account for these factors on the basis of an exemplary component [VDI98].

Besides these dimensional tolerances, further deviations from the specified shape of the workpieces must be monitored. These above all include form and position errors on individual workpiece elements. Among form errors are shape deviations such as out-of-roundness, crowning and warpage. Position errors can arise in the form of offsets, eccentricities, hole offsets or angle errors.

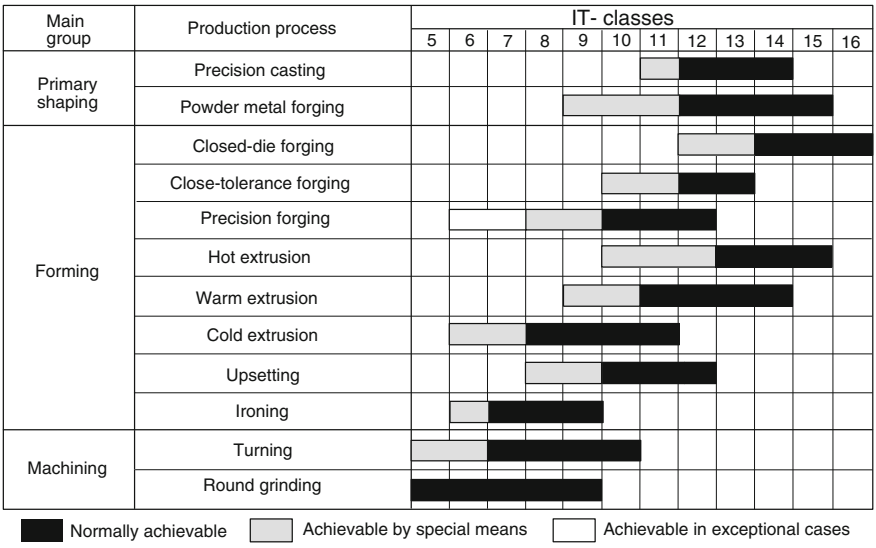
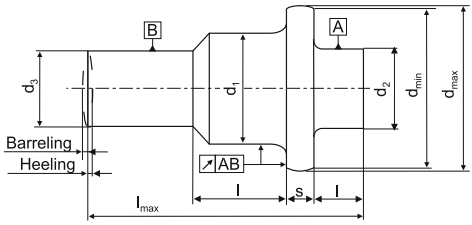


Fig. 3.25 Achievable accuracy for different manufacturing methods [VDI98]



Weight category	< 50 g	50 - 500 g	> 500 g
Basic size	Tolerances [mm]	Tolerances [mm]	Tolerances [mm]
Total length l_{max}	1 - 2	2 - 3	2 - 3
Crank lenght l	0.3 - 0.5	0.5 - 1	0.5 - 1.5
Flange Diameter, difference d_{max} - d_{min}	1 - 2	3 - 4	4 - 5
Diameter d_1 IT ...	0.05 - 0.2	0.1 - 0.3	0.3 - 0.5
Coastdown (conditional oversize) d_2 respectively d_3	0.1 - 0.3	0.3 - 0.5	0.5 - 1
Flange Thickness s	0.1 - 0.3	0.3 - 0.5	0.5 - 1
Concentricity AB	< 0.2	0.3	0.3 - 0.5
True running AB	< 0.2	0.3	0.3 - 0.5
Heeling or barreling (depending on forming type and true strain)	0.5 - 1	1 - 2	2 - 4

Fig. 3.26 Tolerances for the cold extrusion of steel [VDI98]

Another characteristic of workpiece quality besides dimensional accuracy is surface quality. The surface quality is especially important for extrusion parts, as they are generally intended to have functional surfaces ready for installation. Conditions which must be fulfilled in order to realize the lowest possible roughness include:

Table 3.9 Surface quality in the extrusion of steel

Process	Surface roughness R_t	
	Inner wall	Outer wall
Cup backward extrusion	1–3 µm	1–2 µm
(long measuring length)	–	8–20 µm
Steel forward extrusion	2–3 µm	3–4 µm
(long measuring length)	6–9 µm	8–15 µm

- the use of defect-free blanks or wire/rod sections
- a high surface quality of the shaping tool surfaces and their timely post-processing in the event of wear
- the use of suitable lubricants.

Table 3.9 lists the surface roughnesses which can be realized if the above conditions are fulfilled.

The numerical values in Table 3.9 apply for measurements in the pressing direction on a remaining phosphate layer. After the layer comes off, the values may rise by a factor of 2–3 if pores or surface scores were not previously filled in by the layer. This does not have to amount to disadvantages with respect to the performance characteristics of the workpieces. In the case of extruded bearing pins, bearing bushes or push rods, recesses in the surface contribute to lubrication in the form of lubrication pockets.

3.1.6 Economic Feasibility

Manufacturing methods which potentially compete with extrusion are machining, electric discharge machining, casting, forging and sintering. While casting and forging are generally excluded when it comes to the production of ready-to-install parts, this does not apply to the production of semi-finished products.

Criteria which are often consulted when comparing machining and forming include:

- savings on material
- reduction of manufacturing time
- more favourable workpiece strength properties in favour of forming.

Figure 3.27 uses a bevel gear blank as an example for the material savings achievable in extrusion in comparison to turning. In turning, the blank dimensions are determined by the largest outer diameter of the finished part. A material volume of up to 56 % is removed in the production of the outer contour and the bore. In contrast, extrusion can be used to form so closely to the final contour that the material removal volume only amounts to approximately 1 %. The extruded blank is also preferable with respect to its strength. Forming leads to an orientation

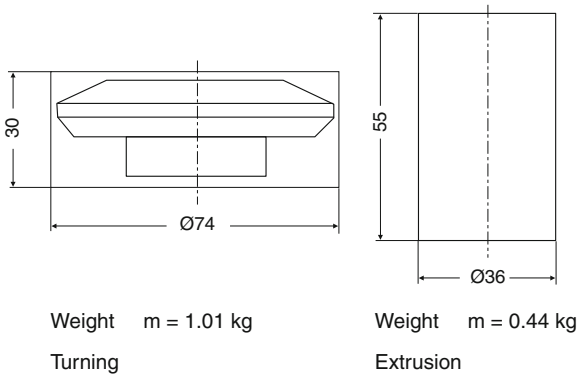


Fig. 3.27 Comparison of initial weights (masses) for a bevel gear

of the grain structure which is adjusted to the part. In machining, there is no orientation of the grain structure to the workpiece contour.

An even more significant savings on material costs can be achieved, for example, when manufacturing spark plug bodies by extrusion. Not only is the volume of removed material lower; also, cost-effective round material can be used instead of cost-intensive hexagon starting material. In addition, the material is strain hardened during forming, as a result of which an increase of torsional stiffness by about 20 % can be achieved.

Furthermore, extrusion generally allows for shorter processing times and thus a higher part output. This output can reach up to 60 parts per minute in the forming manufacture of spark plug bodies, for example, which is about 10 times higher than in machining on automatic lathes. The savings on material and the shorter manufacturing times have ultimately cut manufacturing costs in half.

The goal of cold massive forming is the manufacture of near-net-shape parts. The term "near-net-shape" is applied to workpieces which only barely differ from the ready-to-use final contour following their production by means of a primary forming or reforming process. The aim is to execute the cutting process in one clamping position or in a single step.

More and more, entire assembly functions can be integrated into a single formed part, as observable in the example of a gear shaft (Fig. 3.28). The centring bores as well as the running gears and splines are produced in a single forming operation. As a result, forming now often competes with manufacturing sequence, no longer to individual processes.

The increase in the accuracy of the formed parts with respect to shape, position and dimension and the improvement of the surface quality result in the fact that more and more functional elements and complete workpieces are ready for installation with no or little post-processing. The blank contour approximates the final contour more and more effectively. The example of a crosspiece (Fig. 3.29) clearly shows to what extent allowances and form errors can be reduced today. Such a high level of precision can translate directly into dispensing with



	Machining	Forming
Shaft	- Cut to length by sawing - Drilling of center hole -Turning of shaft profile - Cut into length - Cold rolling of toothed profile - Milling of fitting key slot - Cleaning - Grinding	- Cut to length by sawing - Phosphating of blanks - Cold forming of profiles - Dephosphating of shafts
Gear	- Parting-off of the blank -Turning of external diameter -Turning-off ends - Grinding of head area - Grinding out of middle hole - Hobbing of tooth system - Broaching of fitting key slot - Cleaning - Case-hardening - Grinding of the tooth profile - Join shaft with gear wheel	-Annealing - Phosphating workpiece - Extruding of gears and center holes - Dephosphating of the shaft -Turn-off extrusion ends - Case-hardening - Grinding of toothed profiles

Fig. 3.28 Comparison of manufacturing sequences for the production of gear shafts

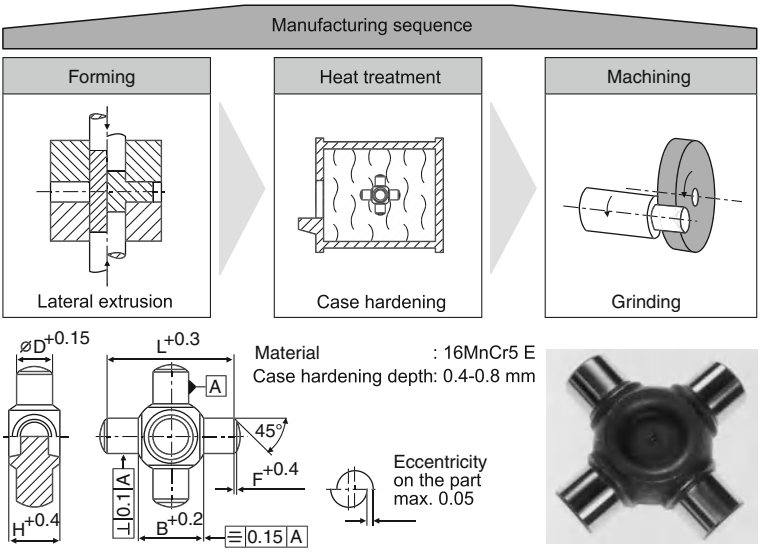


Fig. 3.29 Example of a near-net-shape manufacturing [NN87]

manufacturing steps. Once necessary, overwinding prior to case hardening is no longer executed. The parts are hardened directly after forming and then only have to be machined [NN87]. Reduced allowances on blanks increasingly allow finishing to be performed in one step. Even a machining allowance of 1–1.5 mm is currently often regarded as the upper limit.

Table 3.10 Reference values for minimal, economic lot sizes for the cold forming of steel [VDI99a]

Weight per part (mass in g)	Minimum size of lots (parts)	Weight per part (mass in kg)	Minimum size of lots (parts)
< 10	200,000	1–3	5,000
10–100	100,000	3–5	2,000
100–250	50,000	5–10	1,000
250–500	25,000	> 10	500
500–1000	10,000		

Different minimum quantities result for the economic manufacturing of extrusion parts depending on the material, the part mass and the type of manufacturing equipment. The numbers given in Table 3.10 apply for steel parts and complex parts made of non-ferrous metals. These are to be interpreted as guide values. For simple parts, the quantity is lower because the tools are more cost-effective. In addition, the tool wear is lower, so that higher tool life quantities can be reached than for geometrically complex parts.

In general, it can be stated that extrusion is economically viable in proportion to the extent of the possible strain and to how few working strokes are needed to manufacture the part. The elimination of joining operations is often a further cost-reducing factor in favour of extrusion parts.

In comparisons of economic efficiency, not only the forming work steps should subject to comparison, but also intermediate work steps, such as annealing and surface treatments. These work steps affect the overall costs to the disadvantage of extrusion. The relatively high exploitation of material speaks in favour of the process, however. Also, extrusion is distinguished by a good use of the material volume. Additional economic advantages can be derived from the strain hardening experienced by the material during cold forming. As a result, either the part can then have a lighter design or a less costly material can be used.

Table 3.11 provides a breakdown of the cost shares which together form the total cost of producing parts by forming. The reference methods used are warm extrusion and close-tolerance forging. The parts produced also lie between the two methods with respect to their accuracy.

Table 3.11 Cost shares for different forming methods expressed as ratios [LANG90b]

Cost shares	Cold extrusion	Warm extrusion, close-tolerance forging	Closed-die forging
Material costs	0.80	1.00	1.00
Tool costs (original production)	1.10	1.00	0.70
Tool costs (maintenance)	0.70	1.00	1.30
Costs for surface and heat treatment	2.00	1.00	1.00
Machine costs	1.20	1.00	0.90

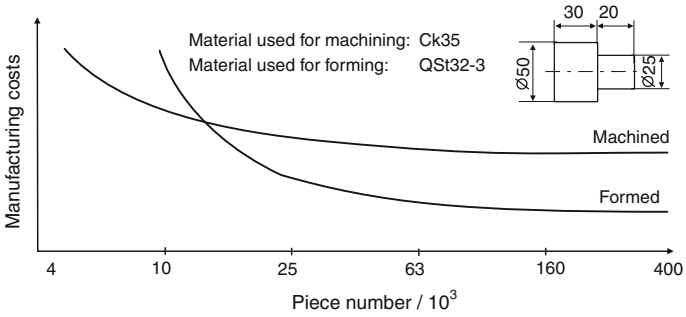


Fig. 3.30 Comparison of manufacturing costs, machining-forming [LANG90c]

In addition to the advantage in extrusion of a considerable savings on material, the long tool life of forming tools and short set-up times promote the economic viability of forming manufacturing processes, especially in high-volume production (Fig. 3.30).

3.2 Warm Forming

With respect to the process, warm working differs from cold and hot forming above all in terms of the starting temperature of the blanks, lying above that of cold forming and under that of hot forming. With respect to the workpiece, the goal is to reconcile some essential advantages of cold forming, such as strain hardening, close tolerances and high surface qualities with the higher achievable true strain offered by hot forming. In line with this marginal condition, the method is defined in the guideline VDI 3166 [VDI77] as a forming process prior to which the blank is heated only to the extent that permanent strain hardening effects are induced under the given forming conditions. With the forming of steel, this broad definition is limited to lower temperatures by the effect of blue brittleness, which results in a considerable reduction in toughness and an increased yield stress in unalloyed and low-carbon steels. The lower temperature range is limited by the effect of scale formation, i.e. the oxidation of iron with atmospheric oxygen, as the scale layer which forms thwarts the tight tolerance of the material volume and the creation of a high surface quality. Depending on the material, the temperature range lies between about 500 and 900 °C. If, for example, C15E steel is warm-worked within this temperature range its yield stresses can be cut in half and the possible true strain tripled in comparison to cold forming (Fig. 3.31).

In comparison to hot forming, however, the yield stresses are another three times higher and the achievable true strains considerably lower. Technically and economically sensible workpiece temperatures start for C15E at approximately 600 °C, as only then is the formability of the material high enough to justify the high technical effort required in comparison to cold forming. Different principles

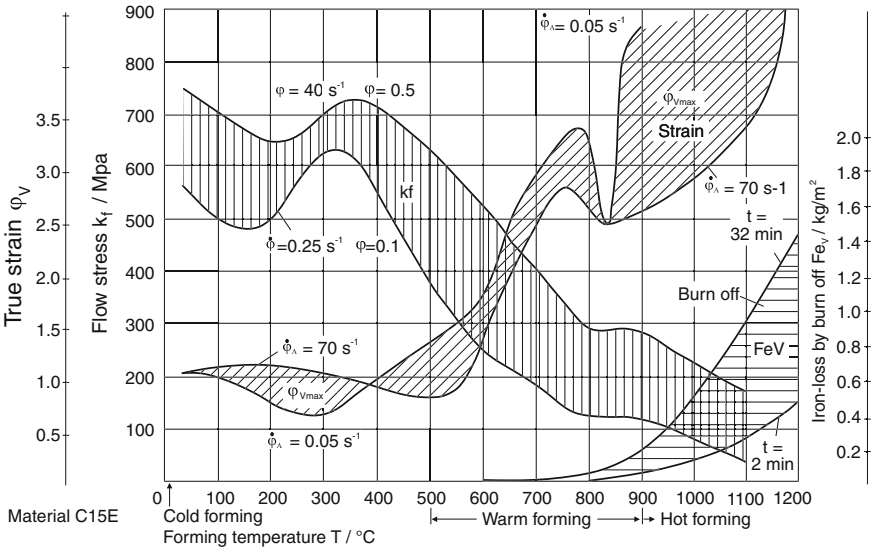


Fig. 3.31 Effect of the forming temperature on forming and workpiece properties; material: C15E [LIND65]

apply to austenitic steels. Since no blue brittleness occurs in these materials, a heating to 400 °C is already highly advantageous for forming. In the case of non-iron metals, however, warm extrusion has not yet proved useful.

If scale formation is avoided, surface qualities are possible ranging from $R_z = 20\mu$m to $R_z = 60\mu$m. Tolerances ranging from IT 11–12 can still generally be realized for tool-related dimensions (Fig. 3.25). Special measures can be used to achieve accuracies up to IT 9. These accuracies lie between the tolerances typical of cold and hot forming. By means of the tight achievable tolerances, but also by the direct creation of secondary shaped elements in the sense component production which approximates the final shape, both allowances and the material volume to be machined can be minimized for subsequent machining processes, increasing the economic viability of the entire process chain.

As a result of the repression of distinct recrystallization processes, the effects of strain hardening remains intact in the component, which leads to a considerable increase in the elastic limit and tensile strength of the material. This in turn has a positive effect on the static and dynamic loading capacity of the component. The spectrum of parts producible by warm extrusion basically corresponds to that of cold extrusion, which means that the parts are largely rotationally or axially symmetrical. However, secondary shape elements can also be created by means of more complex material flows, as in lateral extrusion. Warm working is primarily used to manufacture shafts, pegs, valves, stud-bolts or bevel gears. The blank masses generally range from about 0.1 to 5 kg and can even reach 30 kg in the manufacture of hollow bodies. Figure 3.32 shows a flanged cylinder used for diesel injection manufactured in a warm extrusion process.



Fig. 3.32 Warm extruded flanged cylinder for a diesel injection system (*Source* Hirschvogel Umformtechnik GmbH and Robert Bosch GmbH)

This component is subjected in its later application to internal, cyclical, hydraulic pressure increases and decreases, which exposes the wall of the workpiece to a fluctuating tensile stress. For the component to endure this, the transition from the flange to the shaft must exhibit particularly high fatigue strength. This has proved feasible for 100Cr6 steel in a process with a favourable process-related orientation of the grain structure. The cold extrusion of this workpiece is impossible due to the steel quality, but a hot forming by closed-die forging would yield a considerably higher machining allowance for this component, destined for large-series production. Warm working at 700 °C still allows for the use of a material annealed to globular cementite which is fully recrystallized after forming, thus practically regaining its initial state, which renders an annealing after forming unnecessary.

The high stresses arising during warm working entail similar tool designs to that of cold forming. The tools must be prestressed by means of die shrink rings and distributed on fillets and on locations in risk of fracture. As in cold forming, high-quality tool surfaces are necessary to achieve high workpiece surface qualities. As a rule, materials used for the tools are high-speed steels and carbides. They are cooled and lubricated by means of oil–water mixtures applied in spray form between every stroke. The workpieces can be coated with lubricant, as well. This is also executed via spraying or by immersing the pieces in fine graphite mixed with water. It is not necessary to phosphate the workpieces, as in cold forming.

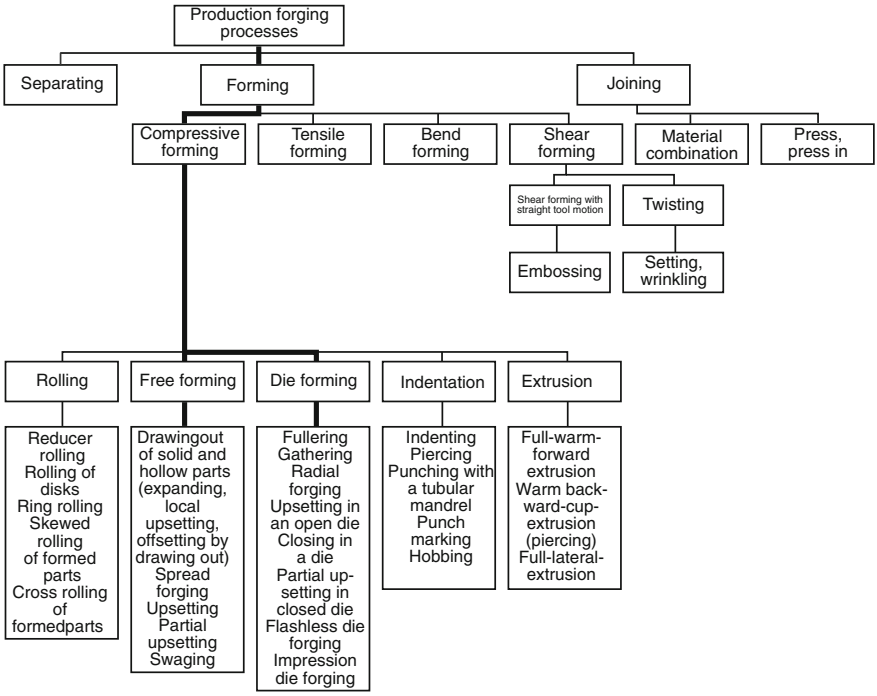


Fig. 3.33 Forging manufacturing processes [LANG90b]

3.3 Hot Forming

3.3.1 Definitions and Process Overview

According to Lange [LANG90b], the term "forging" comprises manufacturing methods from the different main groups (DIN 8580, [DIN03a]) used to produce forgings (Fig. 3.33).

Forging can accordingly be defined as "manufacturing by forming a workpiece using heating, separating and joining". Besides compressive forming processes, tensile forming, bend forming, shear forming processes, as well as rolling processes, the different combinations of which constitute different process variants or manufacturing sequences (Fig. 3.34).

This chapter is devoted to the basic forging processes and will explain the essential aspects of warming, workable materials and the tools used. However, the stress will be placed on using manufacturing examples to illustrate the broad range of application of forging technology and the application conditions with respect to component design, as well as using the achievable component geometries and accuracy to demonstrate process limitations of forging.

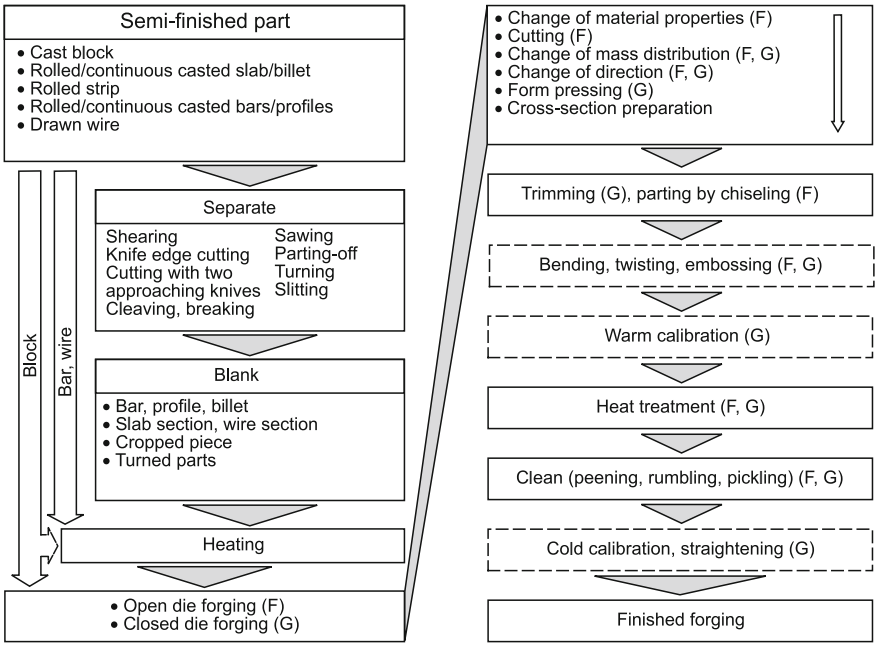


Fig. 3.34 Forging process flow [LANG90b]

Forging can be subdivided into the two basic processes of open-die forging and closed-die forging:

- In open-die forging, the forming process is "non-tool-based", which means the workpiece shape is created by means of targeted movements of the workpiece between individual tool strokes.
- In closed-die forging, the forming process is "tool-based", which means that the workpiece shape is created by means of the form (impression) of tool parts acting in opposition to each other.

Table 3.12 summarizes the distinguishing characteristics of the two basic processes.

Open-die forging is predominately applied in individual and small-series production of usually very large workpieces. The main objective is to influence the workpiece properties, i.e. especially to remove irregularities such as slag inclusions and blowholes, so as to create a grain structure which is as homogenous as possible. However, open-die forging is also effective as a forming process which is flexible due to being non-tool-based (partial forging), with which components close to the final shape can also be manufactured by means of targeted movements of the workpiece [KOPP87].

Table 3.12 Comparison of the process characteristics of open-die and closed-die forging

	Open-die forging	Closed-die forging
Process characteristics	Non-tool based, shaping by targeted movements of workpiece and partial or integral forming	Tool-based, shaping by form of tool parts (impression)
Application goals	- Improvement of mechanical properties (solidly forging) - Blank manufacturing (preform with distributed mass)	- Unfinished/semi-finished/finished part manufacturing - Near-net-shape and ready to install components
Target group	Individual and small-series production	Medium- and large-series production
Mass of workpieces	1 kg–500 t	50 g–1.5 t
Typical workpieces	Disks, rings, bushings, shafts, rods, billets, blocks, crankshaft parts	Crankshafts, front axles, wheel hubs, toroidal parts (rolling bearing rings), gears, baulk rings, turbine blades

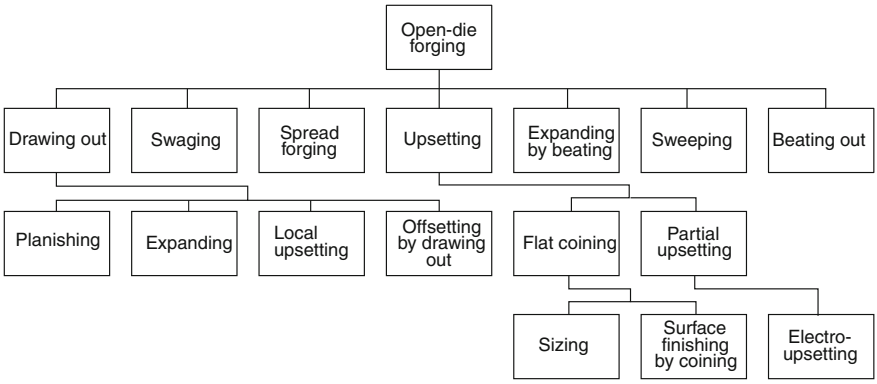


Fig. 3.35 Classification of open-die forging manufacturing processes according to DIN 8583-3 [DIN03e]

Closed-die forging is used to produce workpieces in medium- and large-scale manufacture. The forming tool is an essential determinant of the economic efficiency of the given process.

3.3.2 Open-Die Forging

Figure 3.35 provides an overview of the processes of open-die forging. Drawing out, spread forging and upsetting are the essential open-die forging processes performed on forging presses and special forging machines and used in industry.

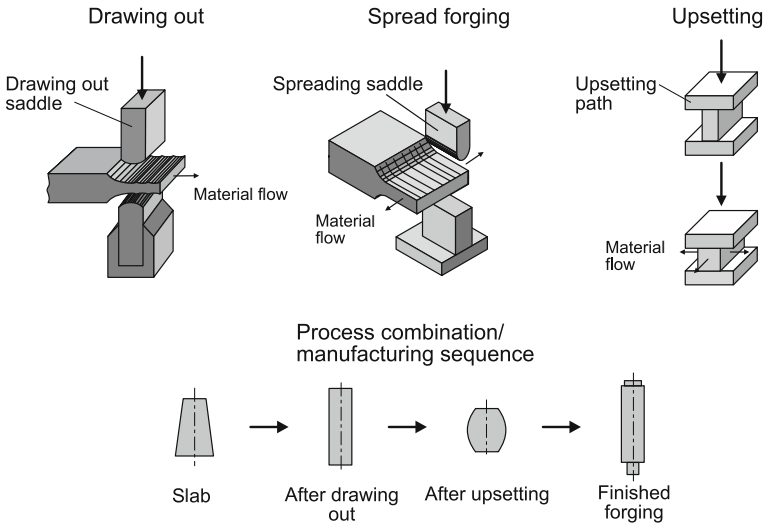


Fig. 3.36 Open-die forging processes

Figure 3.36 above shows the process principles of these processes for cross-sectional changes. The following chapters will explain the individual principles in detail. On the one hand, the processes are used to create preforms and semi-finished products. On the other, they are applied in the production of components close to the final forging. The individual process principles must be combined into a manufacturing sequence (Fig. 3.36).

Processes for changing direction (e.g. shear forming) and for creating hollow shapes (e.g. indentation) can also still be counted among open-die forging processes. These will also be explained in greater depth in Sect. 3.3.2.4.

Swaging will be treated separately in Sect. 3.3.4, as it is used both as an open-die and a closed-die forging method for reducing or shaping cross-sections executed on bar stock or tubes in a heated or unheated condition. The processes of expanding by beating, sweeping and beating out tend to find application in manual craftsmanship and will therefore not be treated here.

Section 3.3.2.6 will introduce the most important manufacturing sequences for open-die forging as well as provide some practical examples.

3.3.2.1 Drawing Out

Drawing out reduces the cross-section or the thickness of a workpiece gradually by means of a targeted combination of feed on the part of the manipulator and press strokes, with the material being predominately displaced in a longitudinal direction (Fig. 3.36 above left). In the case of hollow bodies, the workpiece is drawn out over a mandrel (Fig. 3.45). Put simply, drawing out can be seen as a sequence of

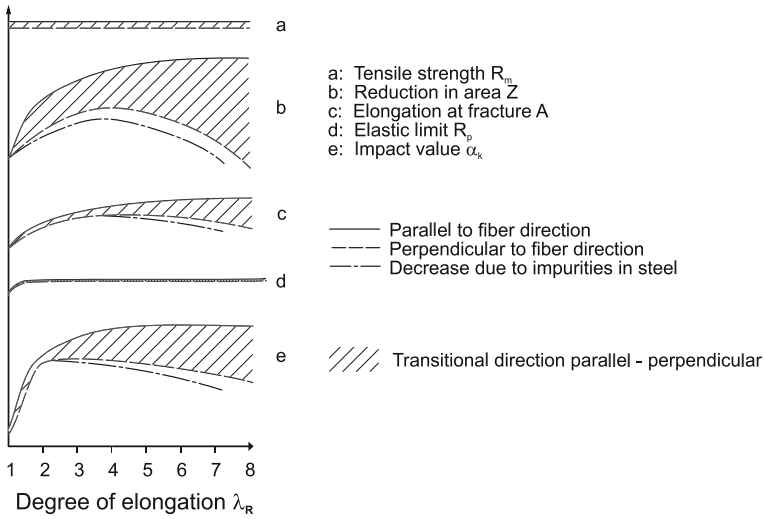


Fig. 3.37 Changes to mechanical properties with different rates of drawing-out [SPUR84]

incremental upsetting operations, as only one limited region of the workpiece is formed per press stroke. In the process, the cast microstructure is to be destroyed, i.e. segregations, inclusions and cavities removed, in order to realize a homogeneous grain structure and the required mechanical properties. Drawing out is favourable with respect to workpiece loading, as the fibre orientation remains intact and a fine-grained microstructure is created.

The most important parameter for describing the drawing-out process is the rate of drawing-out:

$$\lambda_R = \frac{A_0}{A_1}, \tag{3.9}$$

resulting from the ratio of the cross-sectional areas before and after drawing out or from the total rate of drawing out λ_{Rres}, resulting from the n individual rates of drawing out, which is calculated as follows [SPUR84]:

$$\lambda_{Rres} = \prod_{i=1}^{n} \lambda_{Ri} = \frac{A_0}{A_1} \cdot \frac{A_1}{A_2} \cdots \frac{A_{n-1}}{A_n}. \tag{3.10}$$

Another important parameter is the achievable bite ratio s_B/h ($s_B/d$for round cross-sections). s_B is the compressed length of the workpiece resulting from the feeding of the manipulator and h the workpiece height achieved per drawing-out operation (h_0 = starting height). Figure 3.37 left shows the effect of the rate of drawing-out on the mechanical properties of the workpiece material.

Figure 3.38 demonstrates the connection between the bite ratio s_B/h and the height of the forging h resp. the saddle width B.

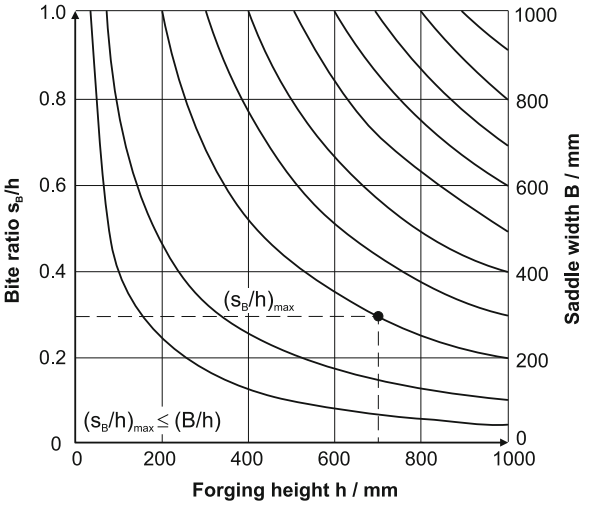


Fig. 3.38 Effect of height of forging h and saddle width B on the achievable bite ratio s_B [SPUR84]

Drawing out is used to create round, rectangular or flat cross sections as semi-finished products (bar and flat stock) which are further processed in an additional manufacturing sequence, e.g. rolling, closed-die forging, and other processes, into shaft-, disc-, ring- or cylinder-shaped products.

3.3.2.2 Upsetting

As opposed to drawing out, which is characterized by a partial forming, upsetting is predominately used to form the entire workpiece. However, no improvement of the properties of the forgings is achieved in the process. If the preform is upset in an axial direction, the material fibres are pushed apart. The homogeneity of the grain structure is achieved where required by combining upsetting with drawing out. Upsetting is thus often only a partial operation in a manufacturing sequence.

Considerably greater changes to height can be realized in upsetting in comparison to drawing out. These changes are described by the true upset strain

$$\lambda_s = \frac{A_1}{A_0} = \frac{h_0}{h_1}. \tag{3.11}$$

As a result of the friction arising between the workpiece and the tool, the workpiece tends to exhibit a varyingly severe barrel-shaped bulging depending on the height/diameter ratio h_0/d_0. Profiled upsetting plates can be used to reduce this effect. If the starting geometry is too slender, there is a risk of buckling. For this reason, the slenderness ratio $h_0/d_0 < 2 \ldots 2.5$ should not be exceeded.

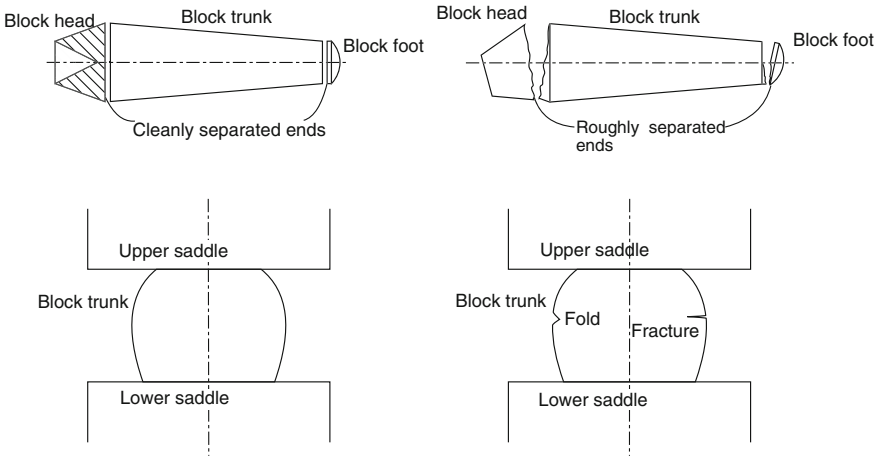


Fig. 3.39 Upsetting of a skimmed-off ingot [HALL71]

Upsetting can also be used to detect faults on ingots and semi-finished products. Irregularities form near the surface of the parts, including blowholes, scores, slag locations, edge fractures and stress cracking. Upsetting renders the faults visible, allowing them to be cut or burned off. The process is thus potentially effective for material testing.

Prior to upsetting the ingot, the head and foot must be separated in order to remove the impurities attached there (Fig. 3.39). If this operation, referred to as skimming-off, is not performed, the impurities from the head and the foot migrate during upsetting to the ingot body. Skimming-off is executed in the form of sawing or parting-off. If simple cutting is performed, slanted head and foot surfaces may form which lead in upsetting to folding and, in extreme cases, to fractures. Besides increasing the drawing-out rate and fault detection, upsetting is also used to form discs, rings and bushings.

3.3.2.3 Spread Forging

Spread forging reduces the cross-section or thickness of a workpiece gradually, i.e. through the targeted movement of the workpiece relative to the working stroke of the press or of the hammer. As opposed to drawing out, in spread forging the material is displaced predominately in a transverse direction, i.e. transverse to the longitudinal axis of the workpiece (Fig. 3.36).

Spread forging is used to produce so-called broad goods, such as scythes, heels and spades or for mass distribution prior to closed-die forging.

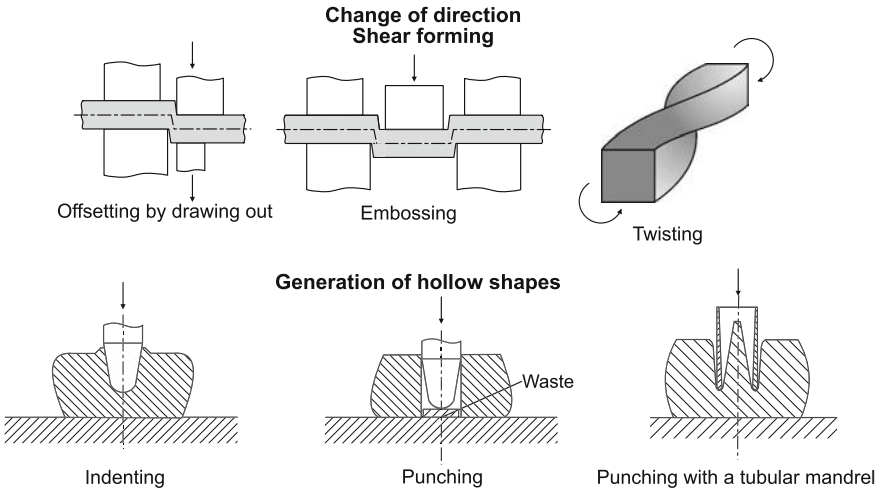


Fig. 3.40 Open-die processes for changing direction and creating a cavity [LANG90b, SPUR84]

3.3.2.4 Direction Changes and Cavity Creation

Figure 3.40 shows the principles underlying the processes of shear forming and indentation.

The shear forming processes embossing and offsetting are used to shift neighbouring cross-sectional areas of a workpiece parallel to each other in the direction of force. Shear forming is characterized by a pure shear stress state. Since the fibre orientation in the workpiece remains almost entirely unaltered, shear forming processes have a favourable effect on the mechanical properties. They are primarily used in the manufacture of crankshafts.

In the shear forming process referred to as twisting, neighbouring workpiece cross-sectional areas are shifted against each other by means of a rotating movement at a certain twisting angle. The twisting processes of warping or setting are applied, for example, in crankshaft manufacturing.

Indentation processes are used to create cavities by means of the displacement of material in a direction transverse (using a solid mandrel) or transverse and parallel (using a hollow mandrel) to the direction of force (Fig. 3.40). In contrast to solid mandrels, hollow mandrels are used exclusively for the creation of continuous cavities on one side and are predominately applied with larger forging.

3.3.2.5 Separation Processes

The cutting processes typically used in the open-die forging production sequence have been clarified in Fig. 3.41 using working principles and actual manufacturing examples.

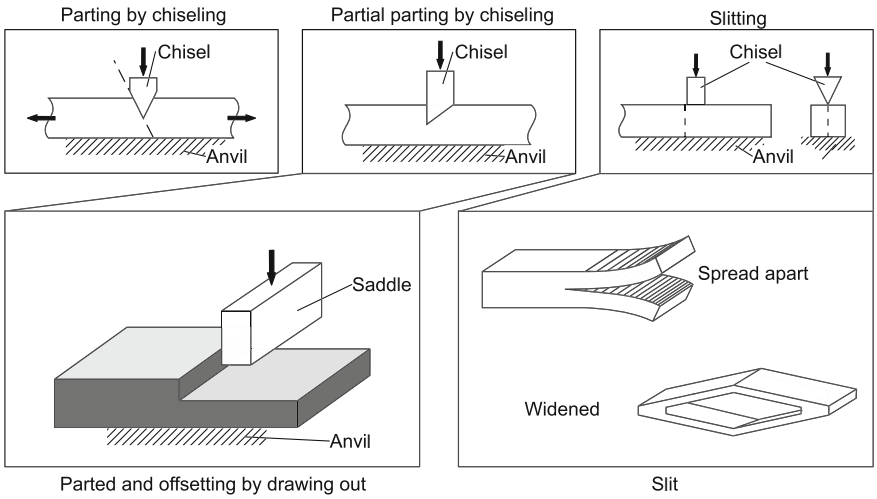


Fig. 3.41 Separation processes in open-die forging [LANG90b]

According to DIN 8588, these processes belong to the knife-edge cutting methods and are used to remove superfluous material parts, to create sharp-edged cross-sectional changes ("offsetting") in combination with drawing out or, in the form of a continuous slitting process, to prepare ring-shaped and spread parts [DIN03l].

3.3.2.6 Manufacturing Sequences and Application Examples

In open-die forging, the manufacturing sequence is divided principally into two partial sequences. Starting from the cast ingot, the individual steps for solid forging are executed in the first partial sequence. The grain structure is formed and any defects are sealed or welded. Generally, this partial sequence consists of a combination of the basic processes of drawing out and upsetting executed until the required drawing-out rate or true upset strain is reached. Depending on the number of individual steps and the workpiece mass, a repeated heating may be necessary. The second partial sequence consists of the forming steps, with different process variants integrated with varying tools, depending on the desired finished forging.

Besides billet and bar stock with round or polygon cross-section, preforms for large components produced by means of open-die forging for use in small-series or individual manufacture include discs, perforated discs, rings and hollow cylinders, as well as block-shaped or cubic blocks. The following will introduce some manufacturing examples typical for the open-die forging industry which should give an impression of the possible range of application of open-die forgings. The most important examples of large open-die forgings are heavy crankshafts and

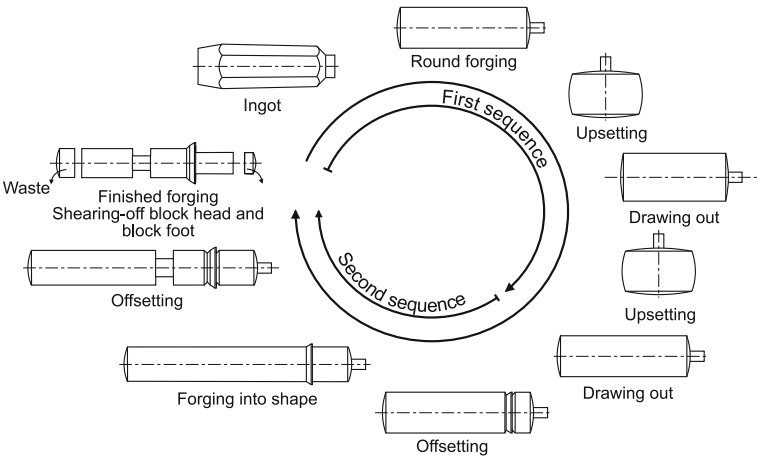


Fig. 3.42 Manufacturing sequence for forging a turbine rotor by upsetting/drawing-out [HALL71]

drive shafts for marine engines, turbine and compressor shafts for power plants, pressure vessel parts for nuclear power plants and large-scale tools for steel works and metal forming. This section will highlight and explain examples of manufacturing sequences for the following workpiece groups:

- wave-like components
- discs
- rings
- hollow bodies.

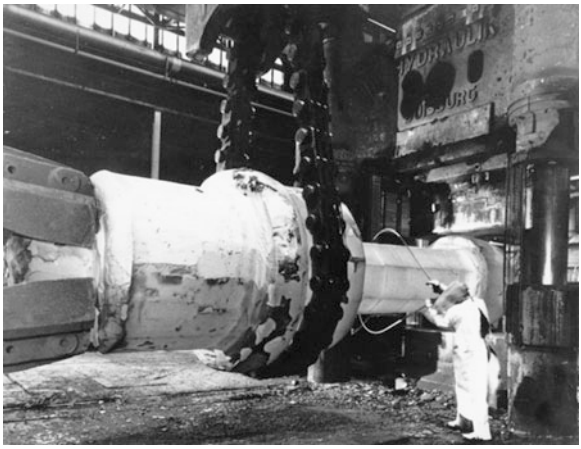


Fig. 3.43 Open-die forging of a hydro turbine shaft (*Source* Saarstahl AG Völklingen)

Wave-Like Components

The manufacturing sequence for wave-like workpieces is essentially determined either by the piece weight and the largest cross-section or from the required rate of drawing-out and the maximum rate of drawing-out achievable in individual steps. Wave-like workpieces include, for example [HALL71]:

- rotor shafts for turbines and generators (up to 100 t)
- flanged shafts (up to 65 t)
- crankshafts (10–250 t).

Figure 3.42 shows the first partial sequence of the manufacturing of a turbine rotor by means of combined upsetting and drawing out as well as the forge finishing process in the second partial sequence as an example for the manufacture of offset shafts.

Figure 3.43 illustrates the open-die forging process for producing a hydro turbine shaft. The rotor shaft shown has a piece weight of ca. 42 t, a maximum diameter of 2 m and a total length of ca. 6 m.

Large crankshafts, e.g. for marine propulsion, are constructed from forged or cast components. The following processes have been developed for the production of medium-sized crankshafts [SPUR84].

In some older process variants, only a rough adjustment of the contour is performed after heating the ingots to 1,000–1,300 °C. Pins are forged on by means of drawing out and the remaining shape elements, such as bearing seats and crank webs are created by machining. These material-intensive processes are only applied to smaller crankshafts suited to open-die forging.

Other process variants for producing larger crankshafts are characterized by their combination with the shear forming processes embossing and twisting crank strokes. However, twisting can be replaced by the use of partial dies. In this way, the strokes are forged in place, after which they are formed by notching and embossing.

In order to avoid damaging the fibre structure favourable for the properties of the component through unfavourable processing steps, such as machining, processes have been developed in which the fibre structure remains intact during forming and the target contour is largely achieved.

Characteristic of these processes is the simultaneous forging on of the crank webs by means of suitable machine and tool-side devices starting from a rolled or forged round bar and embossing of the crankpins. The respective additional devices are responsible for transforming certain portion of the pressure of the presses into a horizontal force component in order to partially upset the crank webs. This transformation occurs in the following:

- the RR method using slanted sliding surfaces (according to Röderer, France),
- the TR method using articulated lever arms or double toggles (according to T. Rut, Poland),

- the National Forge method using two interconnected presses arranged at a 90° offset angle (National Forge Company, USA)
- the MAN method using a suitable hydraulic system (MAN, Deutschland).

An example of the production of crankshafts with ca. 300–600 mm stroke and masses between 2 t and 10 t is stroke-to-stroke forging according to the Schloemann-Krupp method [LANG90b, SPUR84]. The method is characterized by three work steps with respective preheating and postheating and tool movements in two directions.

In the first step, the shaft bearings are pressed in and the swellings are embossed in an angular position. In the second step, the swellings are flattened in an angular position between the bearing points to the rough width of the web and crankpins. In this work step, the crank strokes are pressed out in an angular position and the crankpins are formed. Essential advantages of this process are the near-net-shape forming, which reduces the need for subsequent machining, as well as a fibre orientation favourable for operational stability.

Discs. A disc is a geometric shape whose thickness is several times smaller than its length and width. The outer shape is irrelevant, though usually a disc has the shape of a very flat cylinder.

Either integral or partial processes are applied, depending on the size of the disc. Since cracks can form in the core area due to tensile stresses, this area is further upset using a profiled tool following the pre-upsetting the disc. In order to minimize the risk of core tears, partial upsetting is used for medium-sized to large disc diameters (up to 4 m; disc height up to 1 m). First, the disc is integrally pre-upset and subsequently partially upset from the edge to the middle in an axial direction, so that the core area is formed last. The disc is turned between every press stroke. Further mentionable processes include upsetting a disc with pins using a profiled tool, partial upsetting outside of the press using a suitable power transmission and cube upsetting for manufacturing small and medium-sized discs.

Rings and Hollow Bodies. The term "ring" generally refers to a thin, closed, usually circular object. A ring differs from a disc both in wall thickness and in the defined circular outer contour.

Among the hollow bodies created by means of open-die forging are rings and hollow cylinders (Fig. 3.44). In order to distinguish these according to geometrical criteria, rings are characterized in that their height $h_0 \approx h_1$ during upsetting remains almost constant and their inner and outer diameters increase ($d_1 > d_0$; $D_1 > D_0$). With hollow cylinders, however, the inner diameter remains almost constant ($d_1 > d_0$), while their length and outer diameter change ($L_1 > L_0$; $D_1 > D_0$.)

Starting from the perforated disc as the interstage of the forging, there are different process variants for manufacturing rings and hollow cylinders. All variants share a characteristic radial expansion to the required inner diameter with the aid of an internal mandrel. In further steps of ring manufacturing, the ring heights are maintained and the diameters expanded to size.



Fig. 3.44 Rings and hollow cylinders manufactured by means of open-die forging (*Source* Schmidt + Clemens GmbH)

In the manufacture of hollow cylinders, the workpiece is drawn out after being expanded over a conical and water-cooled stretching mandrel in the longitudinal direction. The mandrel diameter corresponds to the inner diameter of the cylinder. Depending on the size, the worksteps of expanding (diameter) and drawing-out (length) must be repeated multiple times after previous reheating. Figure 3.45 illustrates the work sequence for open-die forging a hollow cylinder. Visible in the diagram are the round saddle, mandrel and manipulator gripper.

With respect to the main material flow direction, ring manufacturing is distinguished by a predominant material flow in the circumferential direction,

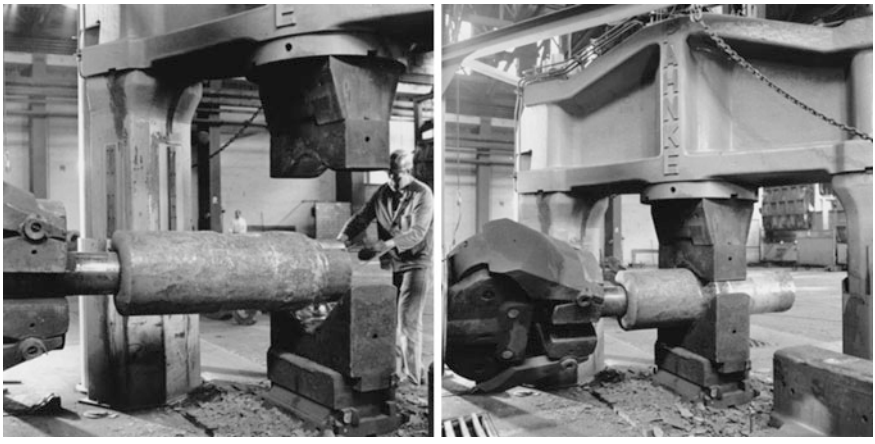


Fig. 3.45 Open-die forging of a hollow cylinder (*Source* Schmidt + Clemens GmbH)

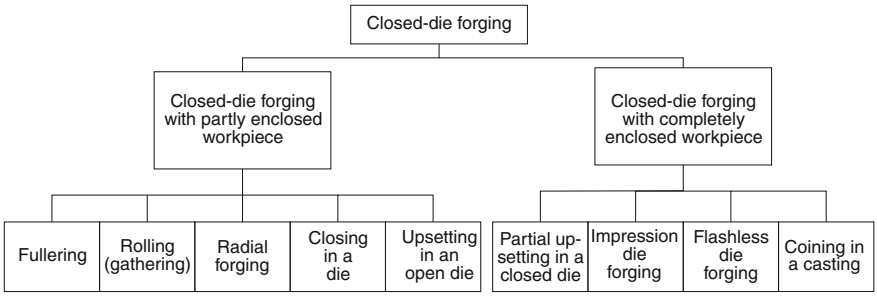


Fig. 3.46 Classification of closed-die forging manufacturing processes according to DIN 8583-4 [DIN03f]

as opposed to that of hollow cylinder manufacturing, whose predominant material flow is in the longitudinal direction.

Internally and externally stepped or profiled hollow bodies can be manufactured by using special form saddles or profiled mandrels. One-piece rings can be forged with an outer diameter up to 8 m and a height up to 4 m. Hollow-cylinder workpieces can be manufactured with lengths up to 30 m given a diameter of about 1.5 m as well as workpieces with diameters up to 4 m given a length of ca. 7 m.

The following will describe the radial forming method according to Lange [LANG83] as an example of a flexible, automated forging method. By means of a radial force transmission via four hydraulically activated rams mutually offset by 90°, workpieces are created with a strong longitudinal axis, e.g. offset shafts, double-T profiles, cross profiles with crosspieces and polygonal profiles. Circular cross-sections are approximated with polygons. By means of the regular and omnidirectional transmission of force and the even graduation of the individual steps allowed by the automated kinematics, a homogenous overall forming is achieved with respect to texture and strain distribution. This has a positive effect on the performance characteristics of the finished product.

3.3.3 Closed-Die Forging

Closed-die forging is defined according to DIN 8583-4 as a compressive forming process in which the workpiece geometry is created by the tool impression. The workpiece is either entirely or partially enclosed by the tool [DIN03f].

Due to the pressure acting on the workpiece, the tool forces a material flow in the same direction as the tool movement (upsetting), in the opposite direction of the tool movement (upward flow) or transverse to the tool movement (spread forging). Among these three basic processes of the "guided displacement" of the material, at least two occur simultaneously, although the transitions are fluid.

Figure 3.46 provides an overview of closed-die forging processes for changing cross-sections.

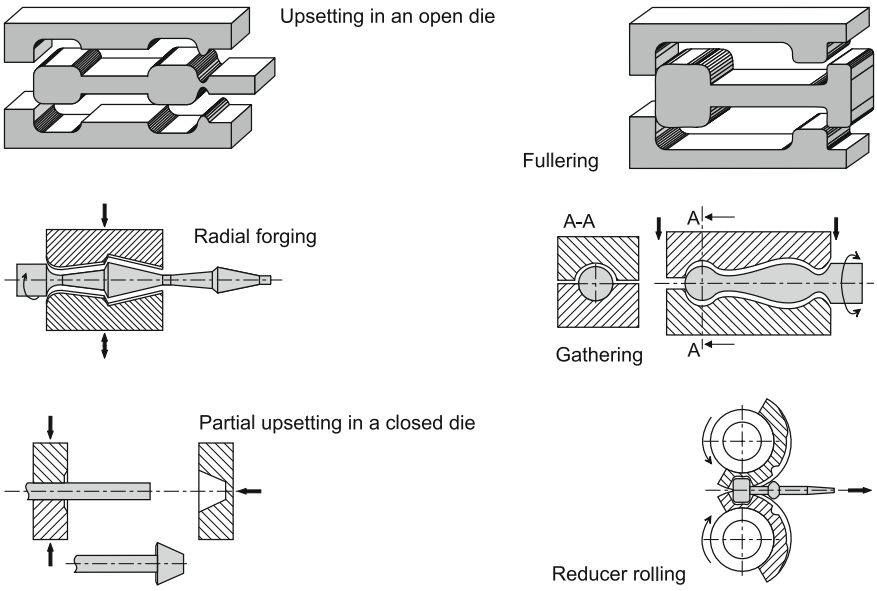


Fig. 3.47 Different processes for changing cross-sections and mass distribution [LANG90b, SPUR84, HALL71]

3.3.3.1 Closed-Die Forging Processes for Preforming

Starting from the blank, closed-die forging parts go through one or multiple interstages until reaching the finished forging, depending on the degree of difficulty. Three types of preforming are distinguished:

- Mass distribution—The blank is preformed in such a way that the main cross-sections match the finished forging as much as possible.
- Bending—Elongated workpieces are bent, offset or embossed in accordance with the final contour.
- Preshaping the cross-section—The cross-sections are profiled in such a way that forming is only required for dimensional accuracy in the finish impression.
- The finished forging can profit from preforming in the following ways:
- the avoidance of irregular or locally excessive flash formation,
- with elongated parts: the reduction of the material flow in the direction of the longitudinal workpiece axis,
- an improved filling of the finish impression with a lower expenditure of force,
- wear reduction of the finish impression,
- an improved fibre orientation in the workpiece,
- an increase in the quality of the finished forging.

The essential preforming processes are die forming processes with partially enclosed workpieces and partial upsetting in a die (Fig. 3.47). These processes are also used in isolated cases as end forming processes.

In the process of upsetting in an open die, the workpiece is formed between parallel, usually plane upsetting paths of two die halves. By means of partial upsetting in a die or on horizontal forging machines, the material is locally concentrated. In fullering, the workpiece is drawn out between two form saddles under constant rotation around the longitudinal workpiece axis. For more information on drawing out, cf. Sect. 3.3.2.1.

Radial forging is a die forming process with a rotating force application, with the workpiece being drawn out, upset or gathered in a continuous sequence. This method is also used to create the finished forging and is treated separately under the general term "swaging" in Sect. 3.3.4.

Rolling or gathering is also a process with a rotating force application, although forming by drawing out is predominant. The workpiece cross-section is sometimes reduced, sometimes increased. Gathering is used most often when die forming from a rod, predominately for preforming purposes.

Reducer rolling is a shape rolling method. The required form is imposed on the workpiece in the rolling direction by means of the profiled roll segments. It has proved valuable for mass distribution in closed-die forging. As it is characterized by a relatively high regularity in the created interstages, the process is also conducive to a reduction of flash losses. In order to achieve the desired mass distribution form, further rolling steps are usually integrated so as to avoid flash formation due to excessively high true strains.

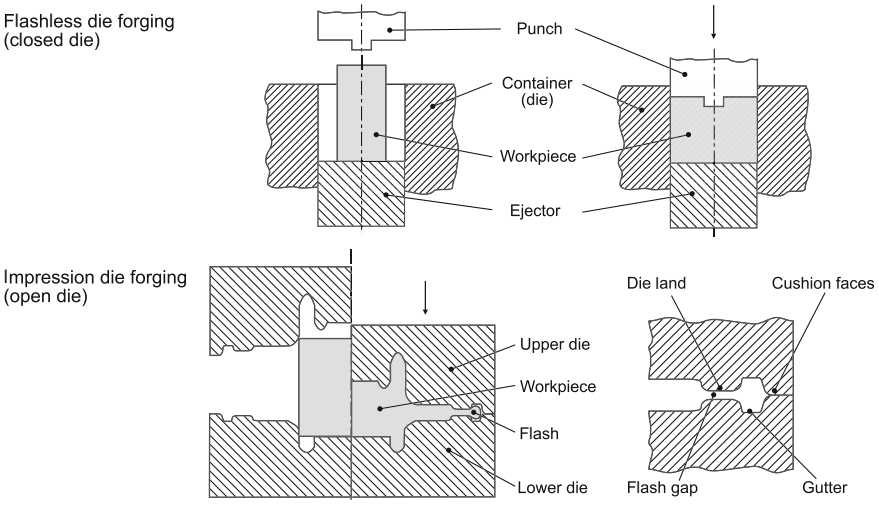


Fig. 3.48 Closed-die forging processes with a completely enclosed workpiece

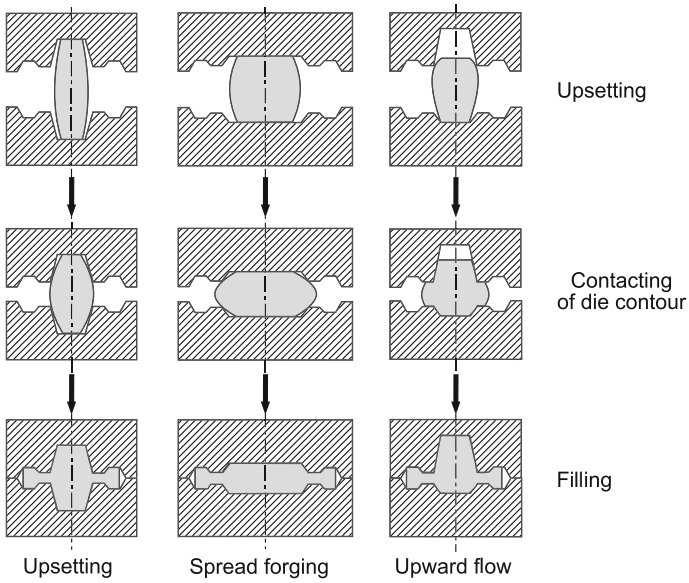


Fig. 3.49 Basic types of processes for filling forging dies [LANG90b]

The main process used for forming bolt and screw heads is partial upsetting in a die (Fig. 3.47). By using replaceable inserts, a large variety of workpieces can be manufactured on horizontal forging machines.

3.3.3.2 Impression Closed-Die Forging

The forging method used most frequently in industry is impression open-die forging (Fig. 3.48). Every impression closed-die forging process begins and ends with upsetting, with the superfluous material displaced through the flash gap after the complete filling of the impression. Figure 3.49 illustrates three basic possible types of "guided material displacement".

If the blank is upset, the starting height is reduced without an extensive spreading over small glide paths along the tool surfaces. The materials flows primarily parallel to the tool movement. With continued upsetting or with larger cross-sections, there is a lateral deviation of the material from the inside outwards. The material flow is characterized by long glide paths along the tool surfaces perpendicular to the tool movement under high normal pressures. This process is known as spreading.

If deep cavities in the impression must be filled, an upward flow of the material may be caused in the opposite direction of the tool movement, depending on the position of the die parting plane. Then there is a local increase of the starting height with partly long glide paths along the tool surfaces under high normal pressures.

A simultaneous upsetting is vital to this upward flow. However, it requires an accordingly high resistance to forming in the flash gap.

Due to the large amount of friction, wide and thin cross-sections are highly resistant to the material flow perpendicular to the tool movement, thus also opposing the filling of the impression in end forming. By means of a suitable interstage of the forging which allows for a reduced contact surface to the impression and thus reduced friction, the resistance arising during end forming is considerably reduced and the filling of the finished forging ensured, even in small edges.

Figure 3.48 illustrates the difference between filling the impression in flashless closed-die forging (upper half) and impression closed-die forging (lower half). It can clearly be seen that the superfluous material in impression closed-die forging flows off via the flash gap. However, the geometrical properties of the flash influence not only the amount of surplus material, but also in particular the stresses in the flash and thus in both the workpiece and the die. The forming of the finish impression is essentially influenced by the normal force in the flash outlet and by the resistance to forming of the workpiece material. The flash gap is geometrically defined, and is characterized by the die land width and the flash gap thickness or by the flash ratio of width to thickness.

The normal force at the flash outlet must be great enough that only a small amount of material deviates and the overpressure in the tool is great enough to fill the die impression completely. The shape and dimensions of the flash are in line with the form and size of the forging. If the upward flow of the material predominates because of the particular geometry of the impression, the flash gap must be designed in such a way that it is highly resistant to the material flowing out. In contrast, given a prevalent spreading of thin-walled workpieces without cross-sectional enlargements at the outer edge or a predominant upsetting, the resistance in the flash gap must be lower. The influence of temperature must also be taken into account. If the selected flash gap is too narrow (excessively low flash thickness) and the selected die land too wide (excessively high flash width), the cooling rate in the flash gap will be too high. The resistance to forming in the flash gap then increases and thus also the loading of the impression.

[HALL71] provides guidelines for designing the geometry of the flash gap, and [LANG90b] gives a detailed account of the effect of the flash geometry and the die land ratio on the forming force, the upward flow height and the surplus of material.

After closed-die forging, the flash is removed either warm (forging temperature) or cold (room temperature). The selection of a deflashing process depends on the geometry of the part and the workpiece strength. Smaller workpieces are disengaged from the stroke of the forging machine for cold deflashing, which results in a larger quantity output. The advantage of warm deflashing lies in the lower separating forces and the better, almost fracture-free sheared edges. It is therefore used predominately with larger forgings or difficult materials.

3.3.3.3 Flashless Closed-Die Forging

Flashless closed-die forging is executed in a closed tool (Fig. 3.48). Advantages of flashless closed-die forging include the following:

- a material savings of 10–40 % of the used mass
- no deflashing operation
- a reduction of subsequent machining work through smaller machining allowances and as a result of lower tolerances of the blank material
- lower forming forces.

However, flashless closed-die forging has the following disadvantages:

- Fluctuations in the volume of the blank can lead either to the overloading of the die when no compensatory spaces are provided, or to the impression not being entirely filled. This results in the requirement of a high volume accuracy (deviations <5 %) of the blank and thus in increased demands on blank production.
- An exact positioning of the blank in the impression is necessary to avoid eccentric loads and thus shape errors.
- The process requires a careful mass distribution, especially for elongated workpieces.

The cross-sections of the mass distribution form must be perpendicular to the main axis in all section planes and thus equal to those of the end cross-sections. Flashless closed-die forging is used above all in the production of forgings made of nonferrous metals and alloys. Combining processes with and without flash in a single manufacturing sequence allows for the use of less closely toleranced blank material. One process variant displaces the surplus volume in end forming as flash. Another possibility is displacing the surplus material during preforming with flash.

3.3.3.4 Manufacturing Sequences and Application Examples

The achievement potential of closed-die forging is informed on the one hand by overall developments in manufacturing technology, but on the other hand in particular by market developments and resultant demands on the components with respect to quality and costs. The trend which has led to this state of development [VOIG88] is still current and is characterized by the following demands on potential forgings:

- higher dimensional and shape accuracy,
- improved component properties with respect to higher loading capacity and thus further savings in weight,
- lower weight tolerances,
- higher functional integration (multifunctional components),

- the use of cost-effective materials and
- the reduction of the overall manufacturing costs through near-net-shape manufacture, especially of surfaces and shapes which are difficult to machine, thus the substitution or elimination of machining operations.

These demands cannot be met by the optimization of a single process or manufacturing step alone, but rather requires an integrated approach to the respective manufacturing task or manufacturing sequence.

The following will present typical forging manufacturing examples in order to illustrate the current status of closed-die forging technology in the context the respective overall manufacturing sequence.

Figure 3.34 already shows the principle work flow with all possible individual processes. Created either by separation from a rod, wire or strip section or by near-net-shape casting, the blank is frequently first subjected to a rough mass distribution. Also, different open-die forging processes are used, such as drawing out, upsetting or spreading. Otherwise, intermediate moulding operations such as reducer rolling can be used to create a precontour.

The finished forging is pressed to size in the final impression. In addition to separating the flash, straightening and calibration operations can also be added after end forming. Heat treatment and cleaning operations can also be integrated.

In principle, forging operations can be executed in a single, multiple impression or multi-stage die. Multiple impression dies shape one single mould element multiple times, whereas multi-stage dies unite several different forming operations in one die block. Forging in multiple impression dies allows for a higher quantity output and is advantageous for workpiece quality, as the material flow can be

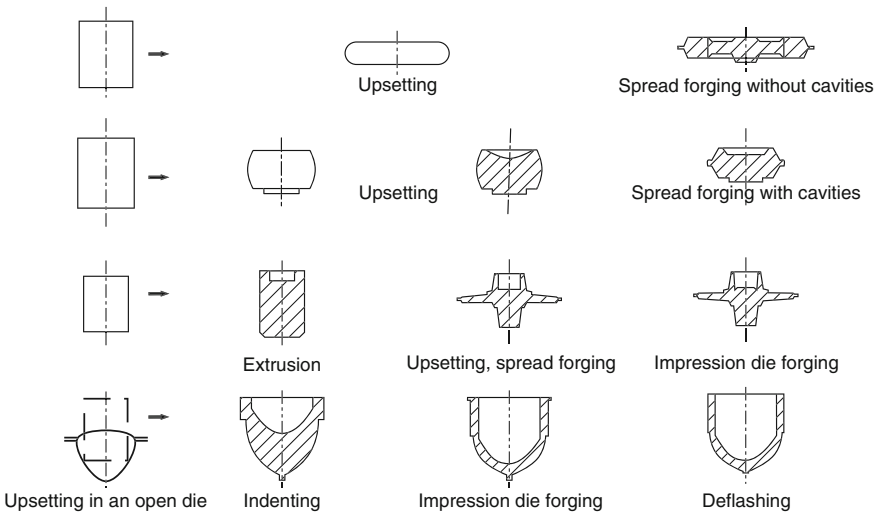


Fig. 3.50 Representation of four typical operating sequences in closed-die forging [LANG90b]

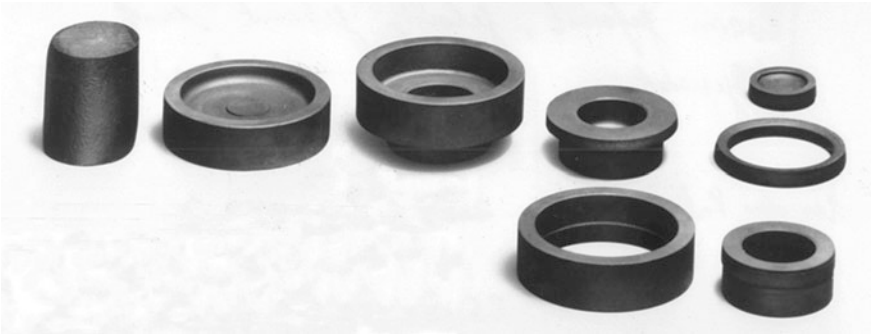


Fig. 3.51 Operating sequence for the rings of a ball bearing (*Source* Hatebur Umformmaschinen GmbH)

controlled in a more targeted way in some circumstances. In addition, the process allows for the symmetrical design of the impression, even for asymmetrical forgings, preventing die and punch tipping. Manufacturing sequences can be executed both on a single machine by using multi-stage dies and in individual work steps (individual tools) in a line or group of different forging machines.

The following will highlight and explain examples of manufacturing sequences for these workpiece groups:

- discs, rings and hollow cylinders,
- wave-like and elongated parts as well as
- complex forgings.

Discs, Rings, Hollow Cylinders. For preforming or mass distribution when forging round parts, various upsetting processes can be used (open die upsetting,

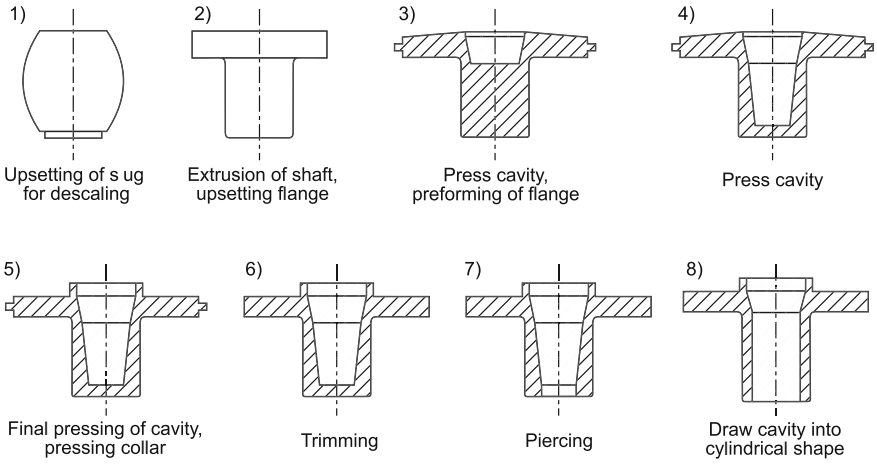


Fig. 3.52 Stages in the die casting of a hollow flange with a multiple impression die [HALL71]



Fig. 3.53 Operating sequence in the manufacture of an alloy wheel rim of AlMgSi1 (*Source* Otto Fuchs KG)

upsetting in a die) as well as hot extrusion operations. This is because other preforming processes result in asymmetric ratios. Figure 3.50 shows typical operating sequences. In order to manufacture axisymmetric moulding elements with large mass concentrations, upsetting processes are used, while axisymmetric hollow moulds are created via hot extrusion.

Rolling bearings are typical examples of rotation-symmetrical forging parts. They are among machine components subjected to the very highest amounts of stress (Fig. 3.51). They are forged in the average range of diameter (30–150 mm), starting with sections of rolled bar stock. Different ring dimensions (inner and outer ring) can be produced from one bar dimension. As opposed to customary through-hardened steels (e.g. 100Cr6), case-hardening steel also make it possible

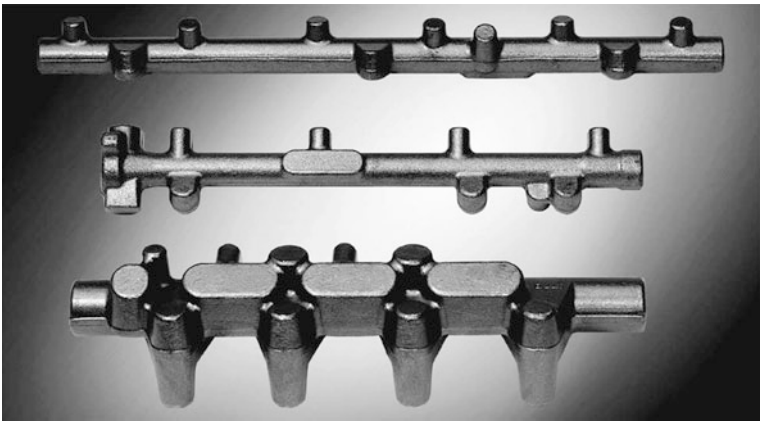


Fig. 3.54 Forged blanks of distributor tubes for the common rail diesel injection system, length 300–500 mm (*Source* Hirschvogel Umformtechnik GmbH)

via two cold extrusion steps to obtain, from a hot preform, a condition that no longer requires any roughing.

As an example of a hollow part, Fig. 3.52 shows the various operating sequences used in the forging of a hollow flange. The final shape is created with the help of a multiple impression die, whereby each interstage of the forging is formed further in the same impression.

By means of a combination with metal spinning techniques, forged alloy wheel rims are manufactured for use with automobiles (Fig. 3.53). Starting with a continuous casting blank, an interstage is produced via closed-die forging, in which case the gaps between the spokes are already punched (Fig. 3.53, second from the right). The actual rim geometry is then generated in a separate operating cycle by "spinning". The advantage compared with cast rims is the weight savings of about 15 % [BOET98].

Transmission parts, such as cylindrical and conical gears, clutch bodies and synchronizing rings, are another highly important area of application [WITT89]. However, for reasons of accuracy, they are manufactured predominantly with the techniques of warm working and precision forging (Sect. 3.2 and 3.4.1.1).

Shafts and Elongated Parts. A modern example of elongated closed-die forging parts are blanks made for the distributor tubes of common rail injection systems (Fig. 3.54). These components have to be able to withstand extreme pressures despite very small diameters and are, moreover, subject to alternating stress. Thus, such parts are produced advantageously by means of forging. They represent a typical use for forging in the automobile branch [NN01c].

With a share of almost 60 %, the automobile industry is the most important consumer of massive forming [NN01c]. Crankshafts and camshafts represent the classic types of forged parts.

The piece weights of crankshafts reach up to 15 kg for average-sized automobile engines and up to 180 kg for commercial vehicles [COEN88]. The most important component requirements are fatigue strength, narrow dimensional tolerances and sometimes high surface qualities. These properties are realized by means of a manufacturing chain consisting of forging, heat treatment and both chipless and machining finishing.

Economical processing of a forging blank requires minimal oversizes and at times installation-ready functional surfaces. For automobile crankshafts, a maximum of 3 mm forging oversize is permissible. With smaller oversizes and installation-ready surfaces, a narrow tolerance and thus small production-related variance can be expected.

By introducing "twisting"—i.e. twisting the crankshaft in the hot forging state into the final stroke position—five to six-stroke crankshafts can be manufactured in analogy to four-stoke shafts, without additional tool parts and with a small oversize. The use of microalloyed AFP-steels (precipitation-hardenable ferritic/perlitic steel) makes it possible to meet the required material properties without additional heat treatment after a controlled cooling from the forging heat level [EN98]. To increase fatigue strength, it is possible to append a targeted hardening of the outer layer via deep rolling (Sect. 3.5.2).

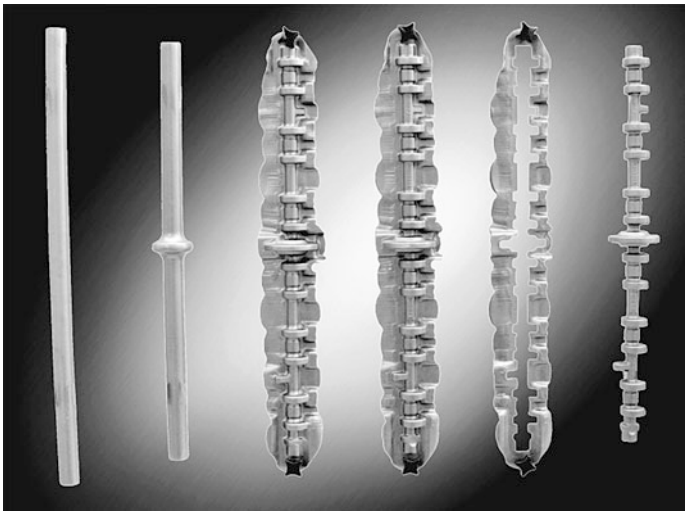


Fig. 3.55 Manufacturing sequence in the forging of eccentric shafts for Valvetronic systems; bar section–pre-upsetting blank–preliminary stage–finished stage–flash section–heat-calibrated finished forged piece, length 562 mm (*Source* Hirschvogel Umformtechnik GmbH)

The entire forging sequence starts with the billet section, which is pre-compressed or reducer rolled for the sake of a rough mass distribution. Subsequent pre- and final pressing are undertaken in two impressions. Trimming and alignment take place on their own special machines. In the case of twisted crankshafts, the twisting process takes place after trimming on a special machine.

The situation is similar in the case of forged camshafts. In the realm of automobile production however, "built" camshafts are being increasingly used (Fig. 4.106). In the case of such "built" camshafts, only the individual cams are die forged. They are mounted together with other components sequentially on a steel support pipe; the joining position is locally prepared by a rolling process.

The goal of larger functional integration is inevitably leading to increasingly complex yet simultaneously more precise components. Closed-die forging can be utilized to good advantage even for a component that is completely new in engine construction—an eccentric shaft for infinitely variable valve trains (Valvetronic, a development by BMW AG, Fig. 3.55). In addition to strength, the highest requirements are made upon the position and shape of the numerous moulded elements due to the high dynamic stresses, as these directly affect the precision of the valve lift to be set. This means for the component that it must be extremely straight as a whole and that the bearing and eccentric surfaces must have exact properties of concentricity and shape tolerances. In this case, this cannot be achieved by built shafts.



Fig. 3.56 Manufacturing examples of complex closed-die forging parts made of aluminium alloys for use in a chassis—*left* passenger car swivel bearing, length 250 mm (*Source* Hirschvogel Umformtechnik GmbH); centre and *right* passenger car triangle wishbone (ca. 2 kg) of AlMgSi1 and aircraft steering arm nose gear (ca. 180 kg) made of AlZnMgCu 1.5 (*Source* Otto Fuchs KG)

The first step consists of a material accumulation for the central tooth segment, achieved by means of drop-upsetting. This guarantees the formation of a consistent flash and an optimal utilization of material. Then there is a preform stage, in which we already nearly obtain the target geometry. In the finishing stage finally, we ensure high precision with respect to shape, position and mass tolerances. Only small forging oversizes distinguish this stage from the final geometry. The forming process concludes with a combined trimming and hot calibration process, which leads to an optimal initial inventory in the subsequent machining finishing process. The use of AFP-steel 38 MnVS 6 (precipitation-hardening ferritic/perlitic steel in accordance with DIN EN 10267) makes it possible to obtain the desired material properties safely by controlled cooling on the transport belt [EN98]. Additional heat treatment, as is required for Q & T steel, is thus rendered superfluous.

Complex Forged Parts. In the production of more complex forged parts such as chassis components for automobiles, often longer manufacturing sequences are necessary. As a rule, the first step is mass distribution via preform formation. To this end, both open-die forging and closed-die forging can be used. Viable preforming processes include drawing out, spread forging or upsetting (Figs. 3.36 and 3.47).

Figure 3.56 shows some examples of more complex components manufactured with closed-die forging. These are various chassis parts for motor vehicles and aircraft. Increasingly, light metals (aluminium alloys) are being used for such parts in the motor vehicle industry as well. Such light metals obtain significantly improved strength and tool life values via forging technology than is the case with foundry technology [LOWA01]. After mass distribution, which is usually indispensable with such complex structures, diverse multistage closed-die forging operations and sometimes piercing operations follow. In the case of certain geometries, bending is also necessary, taking place directly prior to closed-die forging or after trimming.

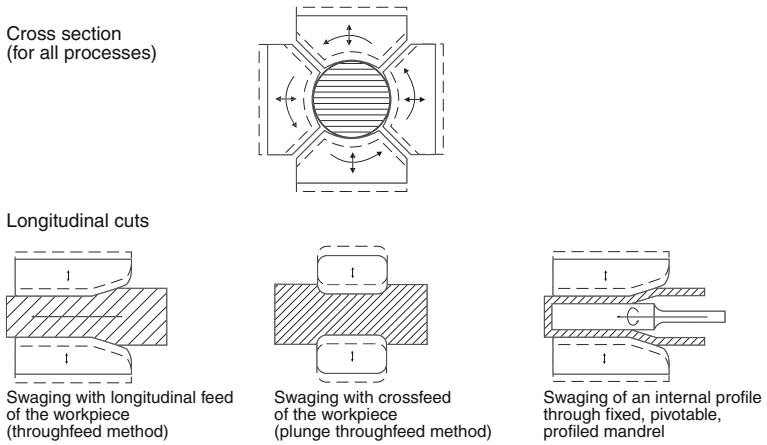


Fig. 3.57 Process principle and variants of swaging

3.3.4 Swaging

3.3.4.1 Process Principle

Swaging is a free or die moulding process for reducing or profiling the cross-sections of bars or pipes, either as a cold or hot working process (Fig. 3.57). Two or more tool segments acting upon each other exert radial pressure forces on a completely or partially enclosed workpiece in a rapid rotational sequence, executing limited path strokes perpendicularly to the workpiece axis.

A distinction is drawn between the feed or continuous flow process for the creation of long reduced cross-sections with comparatively flat transition elbows (Fig. 3.57, left), the plunge process for local reduction of cross-section (Fig. 3.57, centre) and the swaging of an internal profile with a fixed, rotatable profiling mandrel (Fig. 3.57).

In swaging, the radial strokes of the tool segments are carried out in high frequency. The incremental forming thus obtained permits very high degrees of deformation, even without intermediate or subsequent heat treatment for both not-heated and heated materials.

The tolerances obtainable on the external diameter, depending on the material, workpiece dimensions and forming task, are in the area of ±0.01 mm till ±0.1 mm (IT 8–9), thereby falling in the range of precision forging (Fig. 3.25). When processing the internal diameter with a mandrel, it is common to reach tolerances of even <0.03 mm. The processing range, depending on the machine size and type, includes diameters between 0.4 and 120 mm.

Swaging brings about a strain hardening that is nearly constant along the entirety of the material's cross-section. This can be taken into consideration in the component design. Swaged surfaces have a very low surface roughness and a high

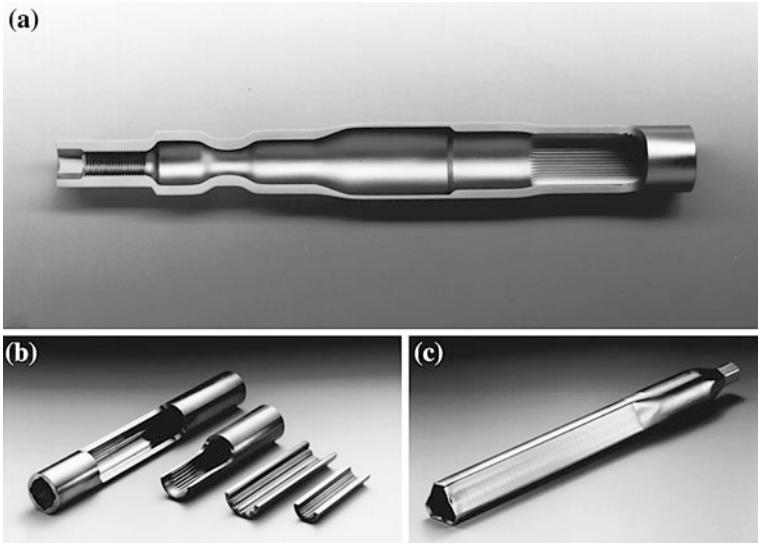


Fig. 3.58 Examples of swaged hollow shafts—**a** shaft (all geometries besides the internal toothing are swaged), **b** hollow profiles with serration and involute toothing as well as ball tracks (swaged with a profiled mandrel), **c** steering shaft with 3 and 4-edge on the workpiece ends (*Source* Gebr. Felss GmbH)

supporting proportion. In the case of plunging, mean roughness is usually $R_a < 0.1$ µm while it is $R_a < 1.0$ µm for feed swaging.

3.3.4.2 Application Examples

Swaging has a variety of possible applications in the forming of rods, pipes or wires with rotation-symmetric or axially symmetric cross-sections. Both internal and external profiles as positive locking elements (gears, wedge profiles, milled flats) and local constrictions such as the necking of a pipe can be produced via swaging (Fig. 3.58).

In the case of pipes, the wall thickness of an exit pipe can also be altered by using a mandrel during the swaging process. This can be done just as much to obtain a local strengthening of the component as purposely to thin out the end wall strength of the pipe for weight-optimized components (Fig. 3.59).

Pressure-tight sealing of a pipe can also be achieved by swaging in few operational steps (Fig. 3.60).

As we can see in the application example found in Fig. 3.61, in which a piston is form-fittingly joined with a pipe by swaging, the process has also opened up possibilities in the realm of joining.

Swaging's range of applications can be greatly expanded by combining forming operations such as beading, flanging, expanding, retracting and thread rolling with

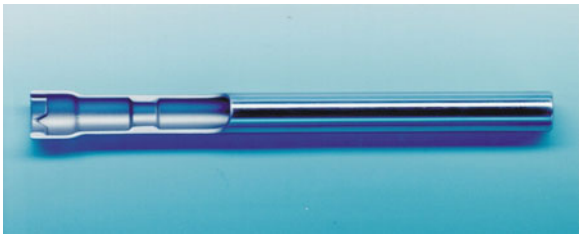


Fig. 3.59 Swaged piece for a jigsaw axis, wall-thickness variation by swaging with the use of a mandrel (*Source* Gebr. Felss GmbH)

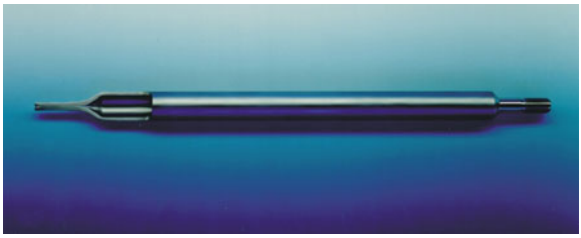


Fig. 3.60 Hollow shock absorber piston rod, sealed pressure-tight by swaging



Fig. 3.61 The attachment of a piston on a rack via swaging (*Source* Gebr. Felss GmbH)

cutting processes and joining operations. For example, a joining construction can be manufactured in which geared bolts are inserted into a pipe and form-fittingly and tightly joined with it by swaging. Furthermore, it is possible to manufacture on multistage processing machines with cutting stations of one cylindrical rod section. Manufacturing processes such as facing, chamfering and centring can be integrated into one single machine this way.

The most important problems surrounding this process include dynamic problems caused by the kinematics of "hammering"—manifesting themselves in the

form of fretting wear on both machine and tools—, high noise emission levels due to the "hammer blows", which however can be reduced by suitable encapsulation, and also problems concerning length tolerances in plunging and cranks.

3.3.5 Heating

The raw parts are heated to high temperatures for forging (about 1200 °C in the case of steel) in order to reduce yield stress resp. forming force and work as well as to improve formability.

3.3.5.1 Heating Means

The following methods are used for heating for the purpose of forging [LANG90b]:

- Heating in furnaces heated with gas, oil or electricity. Heat is transferred to the forging via radiation and convection.
- Heating by induction. Here, heat arises in the workpiece as the result of magnetic inductions via the formation of eddy currents.
- Resistance heating (conductive heating). Heat is also generated directly in the workpiece.

Different furnace types can be classified according to size, application area and mounting type (free-standing or continuous furnace) as follows (Table 3.13).

The problem with heating is the temperature difference between the workpiece edge and the core area, which can be minimized only by a suitable temperature/time sequence. An excessive temperature gradient results in a strong expansion in the fringe area and crack-promoting tensile stresses in the core. The speed of the

Table 3.13 Furnace types used to heat forgings

Furnace types	Free-standing furnace	Continuous furnace	Utilisation for
Large forging furnaces (cockle area ≥ 4 m^2)	Bogie hearth furnaces	Pusher-type furnaces	Large open-die forgings
	Chamber furnaces		Open-die and closed-die forgings
Small forging furnaces (cockle area <4 m^2)	Chamber furnaces	Rotating hearth furnaces, push-through furnaces	Closed-die forgings
	Chamber furnaces for heating bars and bolts		Closed-die forgings and upsetting parts

heating process is therefore dependent on the cross-section of the forging and on the crack-sensitivity of the material. Large open-die forgings made of steel, for example, can be heated with the following four-step cycle:

1. heat to 650 °C
2. balance (hold at 650 °C)
3. heat from 650 °C to the forging temperature
4. thorough heating (hold forging temperature for a long duration)

Heating speeds are between 2 K/h and 100 K/min depending on the hardness of the workpiece. The speed can be increased above 650 °C. The efficiency of heating in a furnace is especially contingent on the amount of useful heat generated by the furnace.

In the case of inductive heating units, the penetration depth of the induced flow depends on the frequency, as well as on the conductivity and permeability (i.e. for the induced flow) of the material. The higher the frequency, the smaller is the penetration depth of the induced flow. The core of the workpiece is heated by heat conduction from the fringe. Induction units work with frequencies between 50 Hz and 1 MHz. The selected frequency is smaller the larger the cross-section of the raw part.

In the case of conductive heating (resistance heating), the raw part is switched into the secondary circuit of a fine-tuneable transformator (current: ca. 10,000 A; voltages: 2 ... 6 V) as a resistor.

Since the necessarily good surface contact between the raw part and the electrode can only be realized with great difficulty, the use of electrical resistance heating is essentially limited to electrical headers and rivet heating devices.

Compared with furnace heating, heating with induction units has important advantages with respect to oxidation processes, which are damaging to the forging. As opposed to reactions with the furnace smoke, in the case of inductive and conductive heating essentially only reactions with atmospheric oxygen are taking place. Moreover, the last-mentioned process permits more rapid heating which is of great importance in the case of steel due to the significant increase in oxide formation above 730 °C.

3.3.5.2 Oxidation in the Heating and Forging of Steel

Oxidation processes at high temperatures generally cannot be completely avoided. Even when heating with protective gas, oxidation processes take place as a result of residual oxygen [MICH85]. A basic distinction is made between two reaction types, internal and external oxidation, as well as decarburization [SCHÜ73]:

Internal Oxidation (Peripheral Oxidation). Oxygen diffuses through the grain or along the grain boundaries in the workpiece fringe and reacts with alloying elements. These, as opposed to iron, have a strong affinity for oxygen. Such alloying elements include silicon, manganese and chrome. The impoverishment of

these alloying elements, usually added to improve hardenability, as a result of oxidation can lead to a non-martensitic fringe structure. This affects the state of residual stress in the fringe area and, because of the decrease in hardness, leads to increased wear and loss in strength, especially with case-hardened steels.

External Oxidation (Scaling). External oxidation, or scaling, is the product of reactions of oxygen with iron already on the surface. The formation of iron oxides can be attributed to a complex sequence of reactions characterized less by chemical reactions but rather by time/temperature-contingent diffusion processes and phase boundary reactions. Three oxide phases appear from the inside outwards between the pure iron and the atmospheric oxygen:

- FeO (wuestite)
- Fe_3O_4 (magnetite)
- Fe_2O_3 (iron oxide/hematite).

The scale that is formed as the workpiece is heated can consist of one or more of these oxide phases and is called primary scale. It must be removed because of its abrasive effect on the tool prior to forging. The amount of scale formation depends on the following factors:

- the time/temperature cycle during heating
- the atmosphere during heating
- the workpiece material.

The following measures can help reduce scale formation:

- a shorter heating duration, e.g. via inductive heating,
- heating with protective gas or inert gas,
- low forming temperature if possible (warm forging),
- the use of a protective coating.

The new oxide layer forming during the cooling phase of forging—the thin, firmly adherent secondary scale—also has a negative effect on tool life and, as a consequence, on dimensional and formal accuracy and the surface quality of the workpiece. This is especially problematic in the precision forging of installation-ready parts. Unlike primary scales however, it cannot be removed from the workpiece surface.

Decarburization. Decarburization occurs at high forging temperatures via reactions of carbon with the components of the surrounding atmosphere. Decarburization reactions then take place on the boundary surface steel/scale; reactions with the water vapour in the surrounding atmosphere are particularly important. Gaseous reaction products CO and H_2 result from pores and cracks in the scale layer. Important influential factors, as in scale formations, include furnace temperature, heating temperature and time and the alloy composition of the workpiece material [MICH85].

The depth of decarburization is contingent on the formation. Areas with material displacement have smaller and those with material accumulation larger decarburization depth.

Decarburization leads to a loss of hardness in the fringe and thus to losses in strength and to wear. This disadvantage can be compensated by means of blasting treatment. In the case of precision forging, heating and cooling must be undertaken under protective gas due to the high surface quality required.

3.3.5.3 Post-Forging Descaling Processes

Forming can be used to remove scales. Deformation of the surface puts bending stress on the brittle scale layer, which as a result tears open and flakes off. Depending on the position of the workpiece relative to the tool, a distinction is made between spherical roller upsetting, flat upsetting longitudinally and transversely relative to the workpiece axis, between level paths or between dual-diagonal paths as well as upsetting in prisms or rollers.

Hydraulic descaling with water jets striking the workpiece surface at high speed is another method [MICH85]. The descaling effect is here based on four different effects:

- Cooling effect—Due to the differentiated cooling of the base material and the scale layer, tangential shear forces arise on the metal/oxide boundary surface. These forces contribute to the separation of the layer from the base material. Exposure time and volume flow should be adjusted to the thickness and type of scale layer.
- Fragmentation effect of the jet—jet pressure causes the scale layer to break open and fall off. This effect depends on the pressure before the nozzle, nozzle shape

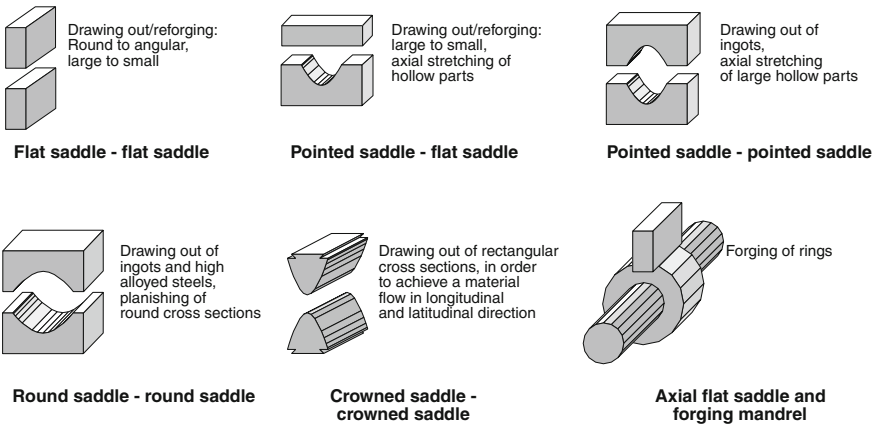


Fig. 3.62 Open-die forging tools [SPUR84]

and size, on the distance of the nozzle from the workpiece and on the impact angle.
- Vaporizing effect—water that penetrates into cracks in the scale layer can heat up in hollow spaces between the base material and the scale, explosively vaporizing and thereby dissolving the layer.
- Rinse effect—rinsing serves to remove the dissolved scale particles.

3.3.6 Open-Die Forging Tools

Tools used for open-die forging essentially are "forging saddles" of various geometries. Figure 3.62 can be consulted for an overview of these. The manufacture of bar material (also offset and non-cylindrical solid and hollow bodies) is done on long forging machines or forging mills, whereby six or eight forging saddles are arranged in a circle around the workpiece. Only three resp. four saddles move towards the workpiece, while the rest move away from it.

Forging saddles are subject to complex stresses as a result of pressure, friction, constant temperature change and, under higher temperatures, local plastic deformation [PHIL82]. While there is a relatively short dwell time under impact load when using forging hammers, in the case of forging with presses requires a relatively long dwell duration and thus strong heating, especially of the undersaddle. The tool surface then heats up to 500 °C or 700 °C, especially when processing steels with high deformation resistance such as hot working, cold working and high speed steels and heat and corrosion-resistant steels.

Forging with "red hot" saddles at 500–700 °C can however be advantageous in the case of especially sensitive steels. The very hot saddle surfaces permit more deformation in forging heat due to the low amount of heat removal [PHIL82]. The temperature range in which edge fractures occur on the workpiece is delayed to a later point in time by means of retarded cooling.

The high thermal load on the forging saddle considerably shortens tool life. Improvements therein can be obtained by using tool materials of high mechanical strength at high temperatures such as hot working steels or hardenable nickel alloys or by deposit welding or "hard surfacing" with wear-resistant, alloys that are strong at high temperatures (Sect. 2.8.5).

3.3.7 Closed-Die Forging Tools

Closed-die forging tools are bound to the workpiece shape to be created and can thus not be flexibly applied or altered. Die manufacture and maintenance is also very cost intensive. For these reasons, the cost-effectiveness of the forging process in relation to a particular application is essentially determined by the die costs.

With respect to the current trend in closed-die forging engineering (and thus in forming technology in general) regarding the economical production of complex, multifunctional components, in small batches as well, the design, processing and especially the functional security of the tool is very important.

3.3.7.1 Tool Design

Tools for closed-die forging can be differentiated or characterized according to different criteria. Dies with flashes (open die) are distinguished from those without (closed die) (Fig. 3.48). A further distinguishing feature is the number of tool separating surfaces. Workpieces with indentations can be manufactured with a multiply separated tool.

According to the number of identical impressions, simple or multiple dies are distinguished. The latter are used to boost quantitative performance. Instead of full dies, often die inserts are used. In this case, the die holder is made of a lower-quality material, while the replaceable die insert can be created with a high-quality material.

In contrast to single-stage tools, so called multistage tools allow a combination of several operating steps via intermediate forming.

Tool design must take into consideration not only workpiece dimensions and tolerances but also the following features:

- The impression geometry, especially impression depth, as well as the necessary impact surface determine the dimensions of the die block as well as minimal wall thickness and web thicknesses. Excessively high and slender webs and ribs have an adverse effect on material flow and increase forming resistance.
- In case of refinishing of the impression (re-setting), 10–25 mm allowance must be supplied respectively, relative to the die height.
- In order to minimize offset, various tool guides are provided depending on the precision requirements made on the forging to be manufactured.
- Position and progress of the choice of parting plane are important with respect to material flow, especially in the case of complex impressions, on the required material volume and on impression loading.
- The design of the die land and die groove is contingent on the impression and the shape's difficulty level. The dimensions of the die gap and die land influence the climbing height of the workpiece in the impression, the material surplus required to fill the impression and the arising compressive stresses and forming forces [SPUR84].
- Side shaping on internal and external surfaces in order to lift out the workpiece are measured as a function of the workpiece shape. They are omitted when hydraulically activated ejectors are utilized.
- Shrinkages must be taken into consideration when designing the final impression.

- Curves for fillets should not be measured to small when considering possible crack-promoting stress peaks.
- Forming small base thicknesses leads, with increasing ratio of base width and base thickness, to higher compressive stresses.
- The accuracies of the die dimensions should be 1–3 ISO quality levels more precise than the corresponding workpiece measurements.

3.3.7.2 Stress on Forging Dies

Closed-die forging tools are subjected to a complex stress collective, composed of the following basic stresses [LUIG90]:

- thermal,
- mechanical,
- tribological,
- chemical.

Among the thermal stress types are thermal fatigue stress caused by constant addition of energy and thermal alternating stress due to temporary temperature peaks that can exceed the annealing temperature of the tool material.

The temperature field determining thermal fatigue stress in the die is itself determined by the heat introduced into the tool by the respective forging process and removed by cooling. The basic tool temperature represents an equilibrium. It is generally between 200 °C and 300 °C.

Thermal alternating stress is concentrated on the tool area near the surface. Here, temporary peak temperatures of 500–700 °C are reached. The peak temperature arising during the contact phase is influenced by the die material mass and basic temperature, by the forging material mass and temperature, by the type of intermediate layer, the normal stress, the dwell time and the relative motion between workpiece and tool, which depends on material flow and is thus very large in certain areas. Figure 3.63 clarifies the progression of temperature on the impression surface in the course of one forging cycle.

Due to the deformation resistance of the workpiece material, locally and temporally varying mechanical stresses manifest themselves in the die. Towards the end of the forging process, these stresses increase sharply due to dynamic pressure. Contact normal stresses are of decisive importance for friction conditions and the transfer of heat.

The area of tension in the die is characterized by axial compression and radial and tangential expansion. There are high tensile stresses near fillets as a result of material diversion. Effective stresses assume their maximum values in these areas in comparison to the total impression surface.

The real state of stress in the tool is the result of the superimposition of thermal and mechanical loads. Thus, toward the end of the dwell time, there are high thermally based compressive stresses due to impeded heat expansion in addition to

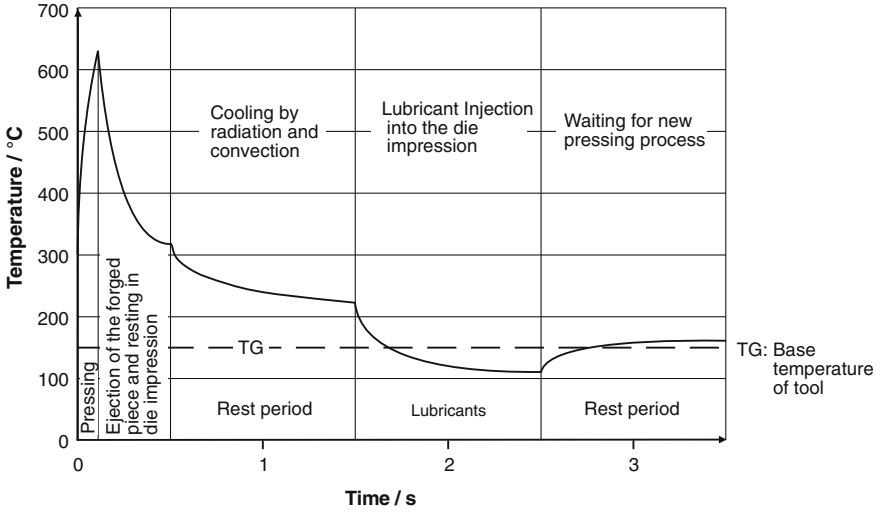


Fig. 3.63 Temperature profile on the impression surface of a forging die within one forging cycle [LUIG90]

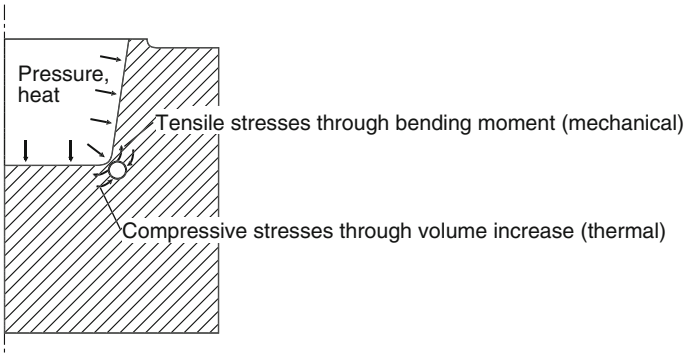


Fig. 3.64 Mechanical and thermal stress at the impression base of forging dies [LUIG90]

the maximum mechanical stresses. In the notch root of fillets, the risk of cracking can be reduced because thermally caused compressive stresses partially compensate tensile stresses of mechanical origin (Fig. 3.64).

In combination with temperatures in the region of 600–900 °C in the interaction area and under the effect of lubricant and reaction products (especially scales), the relative motions arising between the tool and workpiece result in a complex tribological system (Sect. 2.8). In the case of closed-die forging, boundary friction arises with sometimes highly differing states of friction [LUIG90]. Depending on the die form resp. material flow and state of stress, on lubrication and on the surface condition of the friction partner, all states of friction between solid body

and hydrostatic friction can appear. Chemical stresses are the result of oxidation processes on the tool surface and chemical reactions with the intermediate layer.

3.3.7.3 Types of Damage in Forging Dies

Figure 3.65 clarifies the different kinds of damage that can arise in forging dies.

Different types of damage usually appear in combination, whereby wear represents the cause for die failure up to 70 % of the time (position 1, Fig. 3.65). In the case of closed-die forging, adhesive and abrasive wear is predominant. Adhesive wear results from the high pressures and temperatures, which in turn lead to microweldings, which are sheared off again due to the relative motion of the friction partners (Sect. 2.8.3.2).

Abrasive wear in forging is primarily the result of hard scale particles found in the intermediate layer or are plastically embedded in the workpiece surface (Sect. 2.8.3.1). The worst wear appears where the relative movement with high contact normal stresses between tool and workpiece is the greatest, e.g. on the die land or on edge roundings.

In principle therefore, those tool areas are especially endangered by wear at which increased contact stresses and increased relative speeds between tool and workpiece are to be found. This is the case at the radii of the impression peaks (convex contours such as cone curves, die lands and mandrels). In combination with the increased temperatures compared to other surface areas, the result is a complex of stresses. Higher temperatures promote adhesion. Furthermore, the tool material can soften locally, leading to an increase in abrasive wear and the possibility of plastic deformation cannot be excluded (Fig. 3.65).

Plastic deformation occurs when the flow limit of the tool material is exceeded as a result of excessive local loads. Areas with high thermal and mechanical load are especially endangered, such as cone roundings and mandrels.

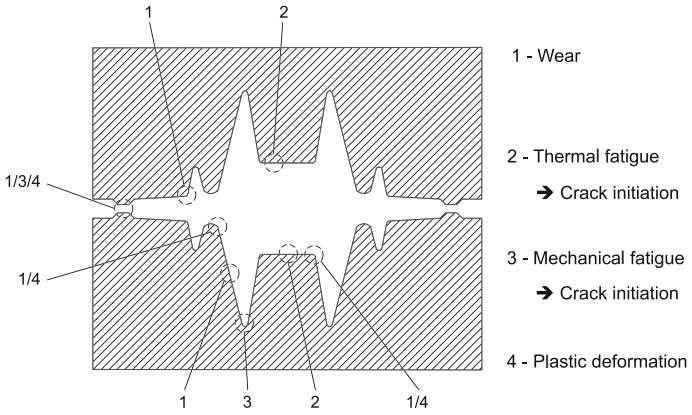


Fig. 3.65 Types of forging die damage [LANG90b]

The stationary temperature level in the die that comes about during operation is, in the case of conventional closed-die forging, between 200 °C and 300 °C. In the case of heavy thermal wear, the tool's basic temperature should be kept as low as possible by cooling. The best results are obtained with a combination of internal cooling and spraying the tools.

With respect to toughness and thermal alternating stress however, increased tool temperature is preferable. If required, tools are heated directly or prior to installation into the machine by means of suitable devices. The advantage of direct heating is a consistent distribution of temperature in the die. A maximally precise control of temperature is favourable for workpiece quality, since thermal expansions lead to deviations in impression size and thus to dimensional variance.

Cracking caused by mechanical fatigue is usually found at locations of high stress concentration (Fig. 3.65). Notch effects, especially in the case of bending fatigue stress, are characteristic of these areas. As a result, forced ruptures or fatigue fractures occur. Cracking and especially tool fracture may be most efficaciously reduced by die preheating and temperature control with a view to sufficient forging temperature.

Thermal cracking occurs on the impression surface as a result of fatigue phenomena, the latter arising from constant temperature change (Fig. 3.65). A large temperature gradient from the impression surface to the inside of the tool results from surface contact with the hot forging. Due to the impeded, thermally caused expansion, compressive stresses arise in the impression surface. Depending on the temperature, these can lead to plastic flow on the tool's surface layer. With subsequent cooling, residual tensile stresses are brought about. The periodic plastic deformations resulting from this load change lead to cracking when there are high residual tensile stresses.

On the other hand, hot cracking is purely mechanical in origin and arises when the thermal strength of the tool material is exceeded towards the end of the dwell time at which time the maximum mechanical stresses are found.

3.3.8 Lubrication in Closed-Die Forging

The functions of lubrication in closed-die forging are manifold and can be subdivided as follows [BARN04]:

- cooling of the dies via heat removal,
- wear protection by forming loadable separating layers in order to prevent metallic contact between tool and workpiece,
- reduction of friction in order to improve material flow and to decrease stress on the die,
- insulation in order to decrease heat transfer from the workpiece to the tool during dwell and

- creation of a propelling effect in order to make the separation of the workpieces from the impression easier.

Besides their actual tasks, lubricants must also satisfy the following requirements:

- They must be automatically sprayable.
- They must be environmentally friendly and may not be harmful to health.
- They may not have a corrosive effect on either the tool or the workpiece.
- If possible, they should leave no, or only easily removable residue in the die and on the forging.

Lubricants for forging purposes consist as a rule of a solid portion (graphite, molybdenum sulphide, boron nitride, alkali phosphates, glass, water glass + graphite), of a lubricant carrier (water, oils, fats) and of additives, e.g. for improved wettability.

Possible coolants for dies include air, air/water mixtures, water, or water with wetting agents (e.g. soap). They are applied separately. Wetting agents help to avoid the formation of a steam skin. See Sect. 2.8.4 on the functionality of and difference between particular materials.

Magnitudes of influence on lubrication coating formation include:

- type of lubricant (composition, solid content, additives),
- spray pressure, spray duration, angle of impact,
- tool temperature and tool material.

Mentionable factors influencing the effect of the lubrication during the forging process include:

- temperature in the lubrication gap (contingent on the workpiece and tool temperature),
- dwell time,
- degree of deformation and forming speed,
- workpiece material,
- lubricant type and lubricant film thickness.

The lubricant is sprayed on the dies between each forging cycle. If water is used as a carrier fluid, it vaporizes and the solid components remain on the surface as a separation layer. Oils and fats on the other hand form a continuous lubricant film, which only decomposes under high pressure in the forging process. Depending on the carrier fluid therefore, a variably high cooling effect is the result. Water not only has five times higher heat conductivity and twice the thermal capacity of oil, but it its evaporation also contributes to the cooling effect. On the other hand, oils lubricate better.

Propellants are employed when the forging is difficult to remove from the impression because the latter is deep or complex. Gas-forming substances are used for this (e.g. sawdust, hydrocarbons as lubricant additive or ingot mould varnish),

which slowly burn in the impression while gas pressure builds. This gas pressure then goes up towards the end of the forging process, thus aiding in the separation of the forging from the impression.

3.3.9 Design and Properties of Forgings

In this chapter, we will describe the properties of open-die and closed-die forgings. In closed-die forging engineering, careful component design is required to obtain these properties. The most important rules of design thus will need to be touched upon. The materials that come into question for forging have been treated in detail in Sect. 2.7.1.3.

3.3.9.1 Influencing Workpiece Properties with Open-Die Forging Methods

The primary goal of open-die forging is, given a cast input material, to obtain the required mechanical characteristics of the finished part by forming the cast structure, to close cavities and to produce a certain starting shape for further processing.

In order to meet this goal with a minimal defect risk, a theoretical and empirical forging plan is necessary, in which each operating step is provided under the following criteria [STEN82]:

- obtainable geometric relations (rate of drawing-out, true upset strain),
- required bite ratio,

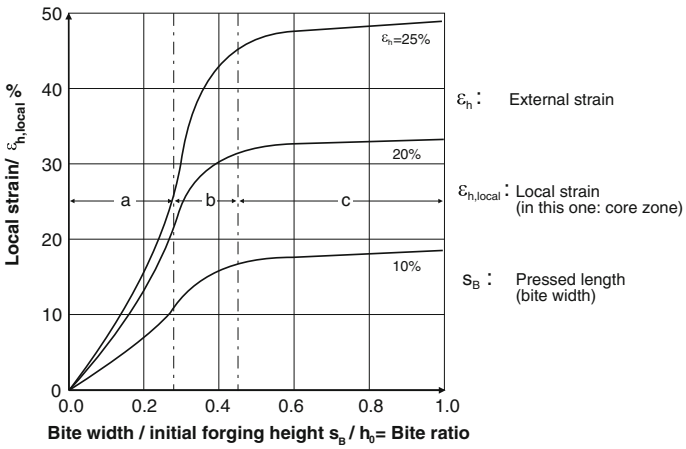


Fig. 3.66 Influence of the bite ratio on deformation $\varepsilon_{h,\text{local}}$ in the core zone [SPUR84]

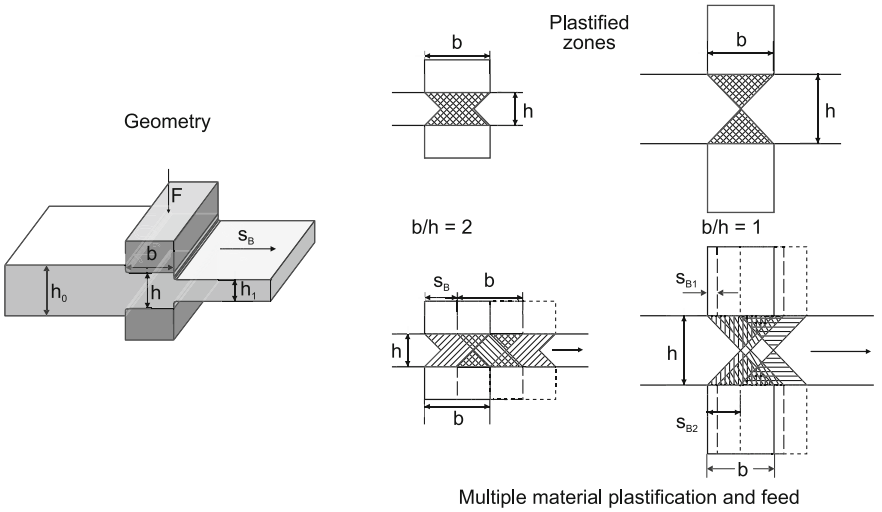


Fig. 3.67 Forging through in drawing out [LANG90b]

- theoretical process times (transport, manipulation, and forming times),
- obtainable core deformation degree,
- thermal conditions (number of heatings, time–temperature behaviour, temperature field in the workpiece).

The definitions of drawing-out rate and true upset strain and of the bite ratio were already introduced in Sect. 3.3.2.1 and 3.3.2.2. The consistent conversion of a coarse crystalline cast structure into a fine-grained wrought structure via drawing out and upsetting takes place in alternating order. There is a clear relation between changes in cross-section and mechanical properties which is clarified in Fig. 3.37 in Sect. 3.3.2.1. In accordance with this, especially the impact value α_k, the elongation at fracture A and the reduction in area Z are improved with an increasing drawing-out rate $\lambda_R = A_0/A_1$, as long as λ_R is smaller than 3.

The characteristic values of deformation ε and φ determined by external changes in geometry represent average values that are insufficient to describe the actual, inhomogeneous distribution of deformation. Deformation at the core, on the other hand, is valid as a measure for forging through. Through-core forging is contingent on the bite ratio and on workpiece feed. Figure 3.66 clarifies the affect of the bite ratio on the obtainable core deformation. In accordance with Fig. 3.67, workpiece feed must be adjusted as a function of the bite ratio s_B/h when drawing out.

3.3.9.2 Closed-Die Forging Design

Closed-die forgings need to be designed in a way that is consistent with stress, material flow, tools, dimensions and machining [NN94a].

Table 3.14 Basic die segmentation rules [LANG90b]

Construction perspectives	Explanation
Symmetric separation	Separation on centreline of workpiece, flash is not at workpiece-edge
Plane separation	Two-dimensional separation, thus easier die manufacturing
Flow feasible separation	Construe separation to ensure optimal material flow, possibly divide workpiece since smaller pieces are rather flow feasible
Processing feasible separation	Dependent on following processing steps, e.g. small surface with side-bevelling, sufficient surface to machine

A suitable choice of die segmentation may interfere with several aspects but should fulfil at least one

Since forged workpieces usually are subject to dynamic stress, component design and edge layer condition (edge hardness, state of residual stress, microgeometry) must be taken into consideration when designing the workpiece. By means of a suitable heat treatment, e.g. via controlled cooling from the forging heat or by abrasive blasting to strengthen the fringe, a higher level of fatigue strength is realizable.

Sharp edges, abrupt change in cross-section or high, narrow ribs (corresponding to deep, slender impression gaps) increase deformation resistance and thus can lead to faults in the forging. With a design that is true to material flow and the tool, extreme geometries can be avoided.

Limit deviations and tips regarding the design of closed-die forgings can be taken from the following standards:

steel	DIN EN 10243 [EN00]
aluminium and aluminium alloys	DIN EN 586 [EN02]
copper and copper alloys	DIN EN 12420 [EN99]
titanium and titanium alloys	DIN 17864 [DIN93]

The subdivision of the tool is very important for sake of forging designs that are true to flow and tool conditions. Table 3.14 shows the four most important basic rules for partitioning the die [LANG90b].

If force components come about as a result of a broken separation in the case of non-axial-symmetrical workpieces, these can lead to horizontal offset of the halves of the die. These transverse force components must be taken up by a "catch selvedge", or else one can create symmetrical force conditions by means of a pairwise multi-forging [LANG90b].

A dimensionally accurate design takes into account possible dimension deviations due to shrinkage (during workpiece cooling) and die size change (due to temperature changes, wear, uneven tool stress and the influence of the machine). In DIN EN 10243, tolerances have been set that take into consideration the effect of the workpiece mass, die separation, material and geometry [EN00] (Sect. 3.3.9.3).

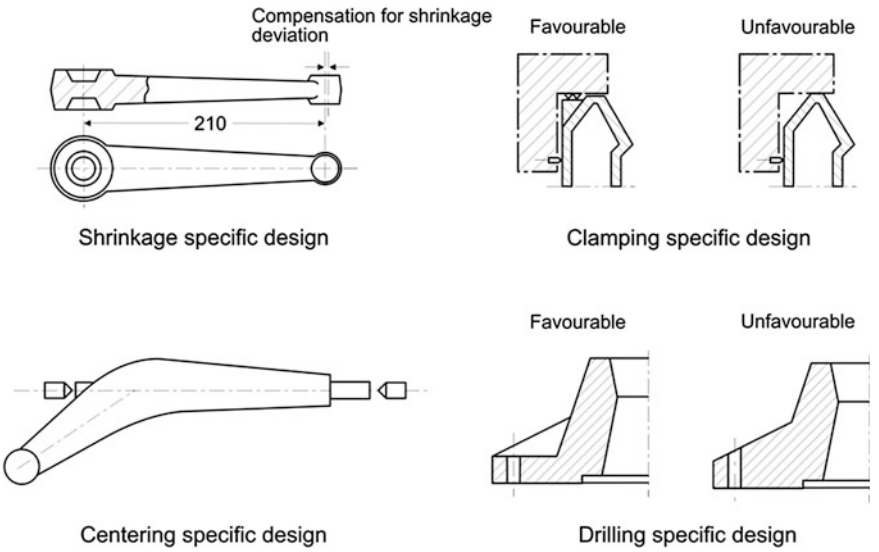


Fig. 3.68 Designs of various closed-die forgings that are machining-compatible

Subsequent improvement of dimensional and shape accuracy is possible by means of cold straightening or sizing.

A design that is compatible with machining reflects a consideration not only of machining allowances as a function of decarburization, scales or potential shrinkages, but also of clamping surfaces for subsequent machining (Fig. 3.68). Machining allowances for forgings made of steel are indicated in DIN 7523-2 [DIN86a]. Forgings—due to the mostly large dynamic stress associated with them—are often oversized using empirical methods without systematic optimization. The goal of design optimization is thus mass reduction whist maintaining the same fitting dimensions and the same material without reducing the tool life of the components [NN94a].

The characteristic variable for the service life of components is fatigue strength. Dynamic fatigue tests following investigations under different types of load, experimental stress analyses (e.g. by means of stress optics) and numerical stress and elongation analyses with the finite element method (FEM, Sect. 2.5) provide information regarding the distribution of stress in the component. A design that is truly accurate with regard to stress is now becoming possible by means of an iterative process.

3.3.9.3 Properties of Closed-Die Forgings

Workpiece properties include static and dynamic strength, dimensional and formal accuracy, surface quality and subsequent machinability.

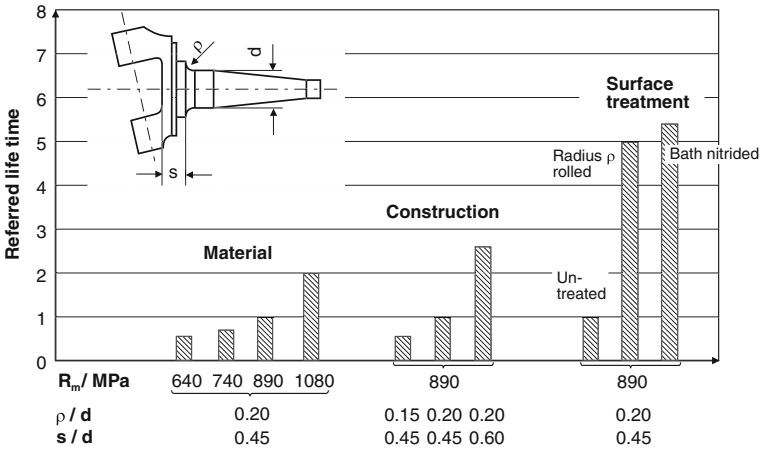


Fig. 3.69 Possible ways to increase the tool life of steering knuckles [LANG90b]

Table 3.15 The classifying feature material difficulty acc. to DIN EN 10243 [EN00]

Group	Alloy composition
M 1	C $\leq$ 0.65 mass % and aggregated alloy portions Mn, Cr, Ni, Mo, V, W $\leq$ 5 mass %
M 2	C $>$ 0.65 mass % or aggregated alloy portions Mn, Cr, Ni, Mo, V, W $>$ 5 mass %

The most important characteristic value for dynamic strength/fatigue strength is contingent on the following parameters:

- basic strength, determined by the material and heat treatment,
- edge layer condition (state of residual stress, hardness, microgeometry), dependent on final processing (machining, blasting, heat treatment),
- shape, characterized by the shape coefficient α_k at the critical location
- workpiece size,
- type and distribution of stress in the component,
- forging-specific characteristics such as flashes and fibre orientation.

Edge layer properties and component shape (shape coefficient) have the distinction of having the largest effect on the service life of the component (Fig. 3.69). Abrasive blasting strengths the edge layer, and residual compressive stresses arise that have a favourable effect on strength properties.

Table 3.16 The classifying feature constructional delicacy acc. to DIN EN 10243 [EN00]

Group	$S = m_s/m_H$
S1	$0.63 < S \leq 1.00$
S2	$0.32 < S \leq 0.63$
S3	$0.16 < S \leq 0.32$
S4	$0.00 < S \leq 0.16$

Accuracy in dimension and form of closed-die forgings are contingent on those of the tool. Tool accuracy must be two ISO tolerance level beneath those of the forgings so that the required forging accuracy is achieved. Dimensional accuracies of common closed-die forgings are set in DIN EN 10243 [EN00]. Indications about obtainable accuracy in the case of different forming processes can be seen in Fig. 3.25.

Surface quality is determined by the abrasive blasting process. The latter removes scales and provides for a relatively consistent structure. In relation with the indications regarding accuracy, DIN EN 10243 uses material difficulty and constructional delicacy as characteristics of classification [EN00]. The degree of material difficulty distinguishes two groups (M 1 and M 2) according to carbon content and the sum of alloying elements (Table 3.15).

Constructional delicacy acc. to DIN EN 10243 considers the fact that, in the case of thin-walled and branched parts, larger dimensional deviations arise than with simple, compact parts due to varying shrinkage, greater deformation resistance and, consequently, greater tool wear [EN00].

Constructional delicacy is described by the ratio of the mass of the closed-die forging to the body formed of the largest dimensions: $S = m_s/m_H$. The four groups of constructional delicacy are distinguished (Table 3.16).

Since the predominant share of closed-die forgings are subsequently subject to machining, their machinability, especially with regards to manufacturing cost, is an important feature.

Evaluation criteria for machinability include obtainable surface quality, machining forces, tool wear and chip shape (see Volume 1, “Turning, Milling, Drilling”, of this series).

3.4 Special Massive Forming Processes

3.4.1 Special Closed-Die Forging Processes

The following will introduce the process variants close-tolerance and precision forging, as well as isothermal forging.

3.4.1.1 Close-Tolerance and Precision Forging

By implementing special measures, close-tolerance forging is capable of an increase of dimensional and shape accuracy and of surface quality in comparison to conventional closed-die forging. Close-tolerance-forged components exhibit an accuracy which is two IT quality levels higher than possible with conventional forging. By taking proper measures, tolerance classes between IT 10 and 11 can be reached (Fig. 3.25). Some surfaces are often even ready for installation.

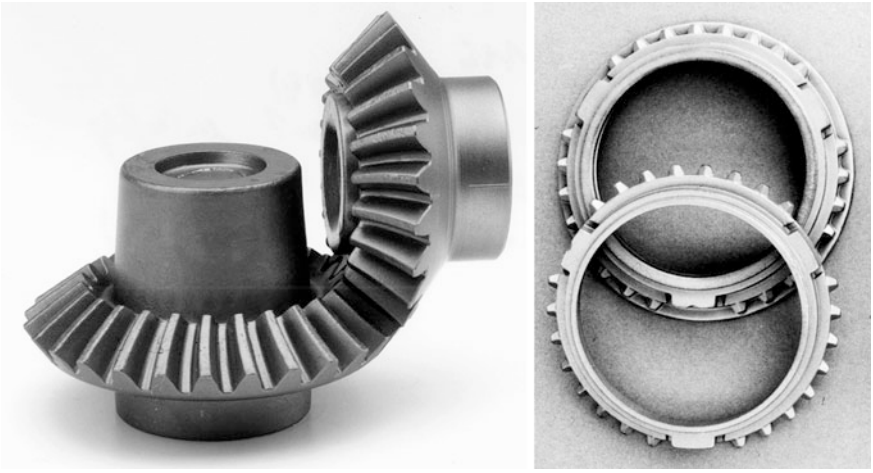


Fig. 3.70 Examples of precision-forged gear parts—*left* bevel gear pair (0.9/0.4 kg) with ready-to-install forged toothing; *right* precision-forged synchronizer rings, forged and additionally pre-turned design (*Source* ThyssenKrupp Präzisionsschmiede GmbH)

Precision forging can be used to further increase the quality up to IT 8–9 (Fig. 3.25). In special cases, such as when forging turbine blades, such refined forging methods can even be used to fulfil accuracy demands corresponding to IT 6. In addition, precision forgings are often installation-ready. This is due both to significantly improved surface quality and to increased shape and dimensional accuracy. The special measures which need to be taken are:

- extensive blank preparation,
- more precise tool manufacture,
- precise temperature control,
- uniform lubrication,
- improved adjustment of the intermediate shapes along with final calibration steps,
- the use of ejectors instead of the die taper.

A further alternative for reaching high accuracies is the combination of forging with downstream cold-forming processes. This topic will be treated in Sect 3.4.2.

The considerably greater effort involved in precision forging in comparison to conventional forging must be weighed against the total manufacturing sequence of a component. If time-consuming machining operations are omitted, precision forging remains economically feasible. It is thus an especially attractive option for the production of toothed gear parts whose machining production can be very costly (Fig. 3.70).

But there are also other reasons than economic feasibility which speak for the use of precision forging for toothings. Transmission manufacturers require their gearings to exhibit higher performance with simultaneously unaltered or even

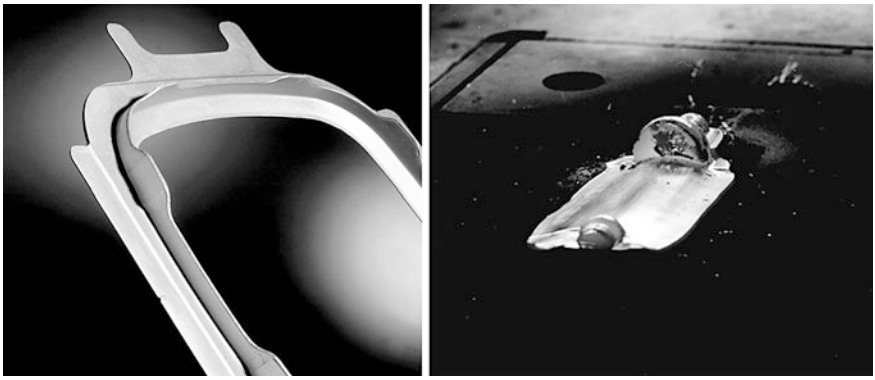


Fig. 3.71 Examples of precision-forged aircraft components—*left* window frame made of AlZn 5.5 MgCu(B), weight 1.2 kg (*Source* Otto Fuchs KG); *right* turbine blade made from a titanium alloy (*Source* ThyssenKrupp Präzisionsschmiede GmbH)

reduced size and lower noise emissions. In order to fulfil these demands, forging offers clear advantages over machining, especially thanks to a resulting fibre orientation which can withstand loading and which fits ideally to the tooth fillet [ADLO89]. This effect can lead to a 25–30 % increase in tooth root strength [NN01c].

The load distribution in the tooth engagement can be optimized by means of a precisely definable height and width crowning, by means of which a more uniform positioning of the contact pattern is achieved. The loading capacity of the tooth root of precision-forged toothings is ca. 25 % higher than those of machined toothings.

Adherence to close tolerances is especially difficult in the case of helical or spiral gears and pinions. Spiral-toothed gears can be manufactured in large series starting with a quality of IT 10 with a grinding allowance e.g. of 0.1 mm. A subsequent hard finishing, e.g. through CBN shape grinding, guarantees the required hardness penetration depth even after grinding. In the case of the bevel gear pair shown in Fig. 3.70, the toothing was precision-forged to be installation-ready with a profile tolerance of ±0.03 mm (IT 7).

Other examples of precision-forged gear parts are synchronizer rings and clutch bodies [ADLO89]. Precision-forged synchronizer rings for inner and outer synchronization are an example of the integration of multiple functions in a single component with higher transmitted torques and a resulting increase of geometrical complexity and loading capacity (Fig. 3.70, right).

A further application area of precision forging is aircraft construction. Many aircraft parts are precision-forged in order to minimize machining operations. For the window frame on the left of Fig. 3.71, only the bores for fixing the frame must be drilled. All functional surfaces are forged installation-ready. The right side of Fig. 3.71 illustrates the production of a turbine blade. In turbine blades, the highest IT qualities are reached, in some cases up to IT 6 (Fig. 3.25) [VOIG88]. As nickel-base

Table 3.17 Classification of different variants of closed-die forging according to the relative die temperature and the pressure dwell time [ADAM98, SCHR93b]

Method	Die temp. related to workpiece temp. T_D/T_W	Pressure dwell time [s]
Conventional forging (steel, Ni, Ti)	0.1–0.35	10^{-3}–1
Conventional forging of aluminium	0.55–0.8	10^{-3}–100
Hot die forging	0.6–0.9	5–500
Isothermal forging	ca. 1	100–1,000
Superplastic forming	ca. 1	Up to 5,000

and titanium alloys are frequently used whose microstructures are very sensitive to thermal treatments, another process besides precision forging particularly suited to the production of turbine blades is isothermal forging.

3.4.1.2 Isothermal and Hot-Closed-Die Forging

In special applications, it is especially important to guarantee a uniform temperature distribution in the workpiece which is constant over time over the entire duration of the forging process. This applies, for example, to the forming of materials whose microstructure is very sensitive to thermo-mechanical treatment. Constant die temperatures are also highly important when particular materials entail a slow forming process, as in superplastic forming.

Table 3.17 provides an overview of the die temperatures relative to the workpiece temperature and the pressure dwell time for conventional forging, aluminium forging, forging with hot dies, isothermal forging and superplastic forming [ADAM98, SCHR93b].

In order to maintain the temperature over in part long forming times, forging dies are required which can be heated to temperatures up to 1,200 °C. In part, this entails dies made of highly temperature-resistant molybdenum-base alloys, which due to their tendency to sublimate (for $T > 600$ °C) only allow for operation in a protective atmosphere [JANS99, SCHR84]. This requires special isothermal presses with an encapsulated press chamber. Other tool materials include nickel-base alloys used for the isothermal forging of titanium and hot-working steels used for isothermal forging of aluminium [SCHR84].

The insulation between the hot dies and the press table resp. press ram is achieved by a special ceramic which, at a thickness of only 50 mm, must ensure a temperature difference of 1,000 °C and simultaneously transmit the entire forming force [JANS99, SCHR84]. Lubricants used are glasses and mixtures of glasses with boron nitride (see Sect. 2.8.4.5) [SCHR84].

Typical applications of isothermal forging include the processing of titanium alloys or nickel-base alloys prepared by powder metallurgy with dispersed ceramic oxide (ODS super alloys) whose preferred use is in aerospace technology and in



Fig. 3.72 Isothermally forged hip joint prosthesis made of TiAl6V4, length ca. 20 cm (*Source* Otto Fuchs KG)

high-temperature turbines [ADAM98, SCHR84, SCHR93b, TERL01]. Decisive for forming titanium alloys is the transformation of the hexagonal α-phase to the body-centred cubic β-phase at temperatures between 910 °C and 1,050 °C (alloy-dependent) [ADAM98, PETE02, TERL01]. They only obtain their optimal strength upon the formation of a mixed α/β-structure with primary and secondary α content. As a result, they must be forged in the temperature region of the partial β-phase formation and of the partial formation of primary α-phase content. The central difficulty here, however, is preventing temperature gradients within the workpiece during forging. This is achievable by means of isothermal forging. Another problem is the high oxygen affinity above 580 °C. Isothermal forging is therefore performed in a protective atmosphere.

Without isothermal forging, titanium forgings require corresponding allowances and remachining and bear an irregular microstructure. On the other hand, isothermal forging entails considerably higher plant expenses, making it economical only starting with output quantities between 200 and 500 [SCHR93b]. The general rule is that the more highly alloyed the workpiece material is, the more cost-effective is the use of isothermal forging.

Figure 3.72 shows an isothermally forged hip joint prosthesis made of the titanium alloy TiAl6V4. This alloy can also be forged conventionally. In the case shown, however, isothermal forging was necessary both to achieve a regular grain structure over the thickness of the component (safety-relevant part) and to satisfy the high requirements placed on accuracy.

Another recent example is turbine blades made of γ-titanium aluminides [JANS99]. γ-titanium aluminides are intermetallic phases which are absolutely unformable using conventional forming methods and are therefore isothermally forged. Although no extraordinarily high true strains are achieved, this process can almost be classified under superplastic forming, as only extremely slow forming speeds lead to economically attractive true strains (see Sect. 3.4.3). For turbine blades made of γ-titanium aluminides, the process window within which crack free forming is possible lies in the temperature range of 1,100–1,200 °C and at a logarithmic forming speed $\dot{\varphi}$ of 10^{-3}–10^{-2} s^{-1}. At 1,150 °C, the yield stress varies between 70 and 150 MPa in the range of the above-named forming speed.

3.4.2 Cold, Warm and Hot Working Combinations

The massive forming methods explained in the chapters above exhibit different specific properties. By the sequential application of hot or warm working processes and cold forming operations, the advantages of different methods can be combined together. For example, the high forming capacity of hot and warm working can be exploited without dispensing with the high precision of cold forming. The achievable tolerance classes of combination methods thus correspond to those of cold forming (Fig. 3.25).

The primary forming shaping occurs at an increased temperature, which—at room temperature—can only be reached by repeated intermediate annealing in several stages. By means of subsequent calibration, sizing or extrusion in a cold state, final dimensions and surface qualities can be achieved for certain shape elements which satisfy the demand for installation-readiness.

The optimal method or combination of methods for a certain application must be decided on a case-by-case basis, taking the entire process chain into account. A combination is only worthwhile if pure cold forming would require at least one intermediate annealing. Nevertheless, it is possible that a combination of hot- or warm-working processes with a finish-machining process may represent the more cost-effective alternative. Thus while the finish machining is more time-consuming as a rule than cold calibration, machining is less expensive and more flexible for a smaller output, as the tool costs are ultimately lower. On the other hand, the service life of variably stressed components is negatively affected by machining operations, while cold working usually increases service life. Therefore, in order to find the optimal manufacturing strategy for a certain component, numerous factors must already be considered at an early developmental stage.

The following will present two examples in which a combined hot- and warm-working operation with subsequent cold forming has proved advantageous.

3.4.2.1 Combined Warm and Cold Massive Forming

The cardan shaft shown in Fig. 3.73 (left) represents a typical application for combined warm and cold forming. The part is made from Cf53 steel, which can only be cold-formed to a limited extent. Despite this, the demand exists for a near-net-shape forming in order to minimize the finishing of the running track on the inner side of the component, which is costly with respect to the high quantities required. As the corresponding demands placed on shape and dimensional accuracy cannot be fulfilled by conventional forging and the required true strains are clearly too high for a pure cold-forming process, these parts are initially warm-formed and then calibrated in a cold state.

The warm working is performed in multiple steps at a starting temperature of ca. 850 °C. By means of a downstream normalizing operation, the differences in the grain structure created as a result of the varying rates of cooling of the

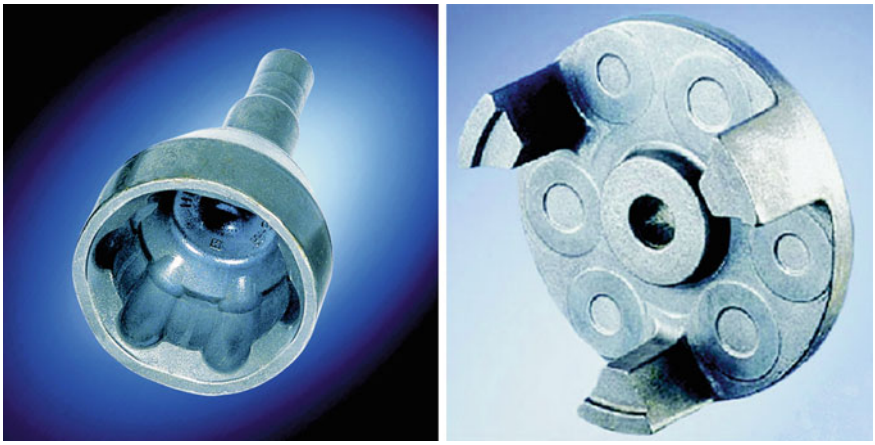


Fig. 3.73 Manufacturing examples of process combinations in massive forming; *left* fixed joint made of Cf53, combined warm- and cold-forming; *right* planetary gear carriers made of AFP steel, combined hot and cold forming (*Source* Hirschvogel Umformtechnik GmbH)

individual areas of the component are balanced out. The subsequently cold-pressed ball running tracks finally obtain a dimensional accuracy of ±0.1 mm. After hardening, the running tracks are finish-ground.

3.4.2.2 Combined Hot and Cold Massive Forming

The planetary gear carrier in Fig. 3.73 (right) is similar to the preceding example. Its function is to accommodate the planetary gears of a planetary gearbox. As there is only a very limited space for this part and it is also subject to high varying mechanical stresses, this component must be designed as a formed part. This is the only way the required strength can be guaranteed. Otherwise, the part must exhibit high accuracies to be implemented in gearboxes, which at first makes it a better candidate for a cold forming operation. However, here too the true strains involved are by far too large for pure cold forming. The basic geometry is thus created by means of a three-stage hot-forming process. The precise mounting dimensions are then calibrated in a cold forming step. Since the material is an AFP steel which receives its final strength through controlled cooling from the forging heat, heat treatment is omitted.

3.4.3 Superplastic Forming

In conventional forming processes, boundaries are set to the forming of components as a result above all of the limited formability of the material used and to the inadmissible loading of the forming tools. These restrictions can be removed to a

great extent by superplastic forming, so that even geometrically complex parts can be produced in a single forming step.

3.4.3.1 Process Principle and Preconditions

The state of a metallic material is referred to as superplastic if it exhibits an extremely low yield stress and a very high formability even at very low forming speeds. Within the region of superplasticity, the yield stress is almost independent from the preceding forming operation. It is thus not or hardly influenced by strain hardening, though it does depend directly on the forming speed. In this way, extremely high deformations are possible of up to 8,000 % at extremely low forming speeds. In order to achieve superplasticity, three preconditions must be fulfilled [SCHE76]:

1. a uniform grain structure (as a rule, two-phase) with a small grain size to below 1 μm, which must also be maintained during the forming process
2. low forming speeds in the region of $10^{-5}\,s^{-1} < \dot{\varphi} < 10^{-1}\,s^{-1}$
3. a forming temperature greater than half the melting temperature (in °C).

In order to hold the temperature constant over the entire workpiece cross-section during the sometimes very long forming times, tools are needed which can be heated to the required workpiece temperature. In such cases, the technology of isothermal forging is applied (see Sect. 3.4.1).

An effective way to explain what takes place in superplastic forming processes is to look at uniaxial tensile tests. A tensile specimen made of superplastic material does not have the usual necking at the end of uniform elongation which very rapidly further reduces the minimum cross-section. Instead, the necking retains its cross-section and spreads out lengthwise.

This behaviour can be explained as follows: In a tensile test with conventional material, a necked-down area is formed upon reaching the uniform elongation. The cross-section recedes in the necked-down area, which causes the normal stresses in this area to rise. As a result, only the necked-down area is formed, while the rest of the specimen remains at the uniform elongation. Due to the fact that a considerably shorter area of the material is being formed, the forming speed in the necked-down area also increases. With superplastic materials, the increased forming speed leads at this point to a very high strain hardening. The forming zone therefore moves out beyond the necking area, as a result of which the entire specimen is gradually uniformly elongated [PERE92a, PERE92b].

More recent studies have proved using transmission electron microscopy (see Sect. 2.6.4.2) that superplastic forming is realized not only through dislocation movement, but also through the parallel action of multiple elementary processes [ISLA03]. These mechanisms include:

- grain boundary sliding,
- grain rotation,

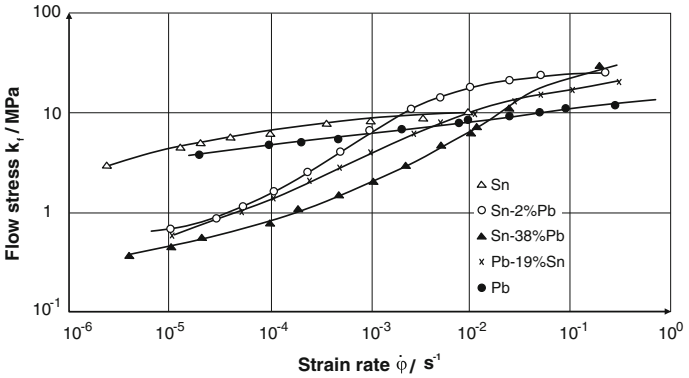


Fig. 3.74 Flow stress as a function of forming speed [CLIN67]

- grain boundary diffusion,
- dislocation movement.

3.4.3.2 Description of Superplastic Material Behaviour

Figure 3.74 illustrates the dependence of yield stress on the forming speed in the form of a diagram for different Sn–Pb alloys [CLIN67]. The curves are derived from tensile tests performed at 20 °C.

Several studies have been executed to describe the flow stress k_f for the behaviour of superplastic materials [LEE67, VULC04]. In the region of superplasticity, the influence of strain hardening, i.e. of the already achieved true strain,

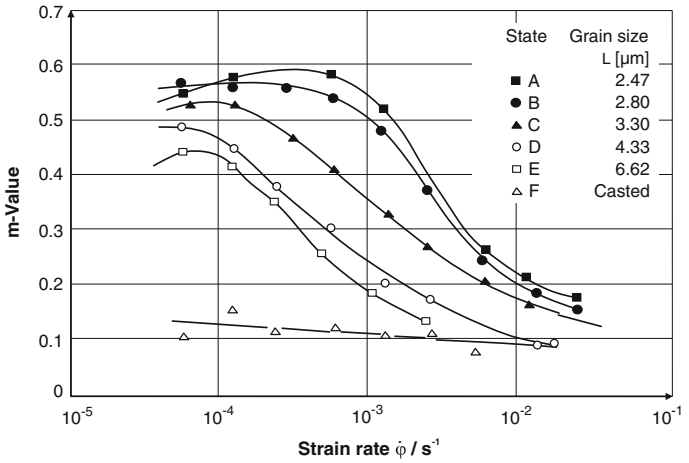


Fig. 3.75 Value of m as a function of forming speed for different grain sizes [AVER65]

Table 3.18 Superplastic alloys [PADM80]

Alloy system	Composition (mass %)	Grain size (μm) L	Forming temp. (°C) T_F	Forming speed (s^{-1}) $\dot{\varphi}$	Max. speed-exponent m	Yield stress (MPa) k_f
Tin–lead	62 % Sn; 38 % Pb	2.5	20	3×10^{-4}	0.6	10.0
Zinc-aluminium	78 % Zn; 22 % Al	1.8	250	1×10^{-4}	0.5	8.5
Magnesium–aluminium	67 % Mg; 33 % Al	2.2	400	3×10^{-2}	0.9	28.0
Aluminium-copper	67 % Al; 33 % Cu	5	523	4×10^{-4}	0.9	4.0
Steel, low alloyed	0.42 % C; 1.87 % Mn; 0.24 % Si; 0.02 % P; 0.02 % S	1.4	727	3×10^{-5}	0.7	21.0
Titanium-aluminium-vanadium	Ti; 6 % Al; 4 % V	7	953	1.5×10^{-4}	0.8	3.5
Titanium-aluminium-tin	Ti; 5 % Al; 2.5 % Sn	20	1013	6×10^{-4}	0.7	4.0
Nickel-based alloy	Ni; 15 % Co; 9.5 % Cr	–	1023	–	0.5	–
IN-100	Al; 5 % Ti; 3 % Mo					

does not play a major role and can thus be seen as negligent. The most simple and most widely accepted description is thus the following:

$$k_f = C \cdot \dot{\varphi}^m. \tag{3.12}$$

Consequently, the speed exponent m becomes:

$$m = \frac{\delta(\log k_f)}{\delta(\log \dot{\varphi})} \ . \tag{3.13}$$

The magnitude of the speed exponent m represents a measure for the superplastic behaviour of the material. Figure 3.75 [AVER65] shows the major influence of grain size on the value of m on the example of a eutectic tin–lead alloy with different heat treatments.

3.4.3.3 Superplastic Materials

Due to the abovementioned requirements placed on the fine graininess of the material, which remains intact during the forming process, the number of metals which can potentially be used is considerably limited. At first, only eutectic or eutectoid alloys were used for superplasticity. Among the superplastic alloys are zinc, aluminium, magnesium, copper, nickel and titanium alloys. Today, some

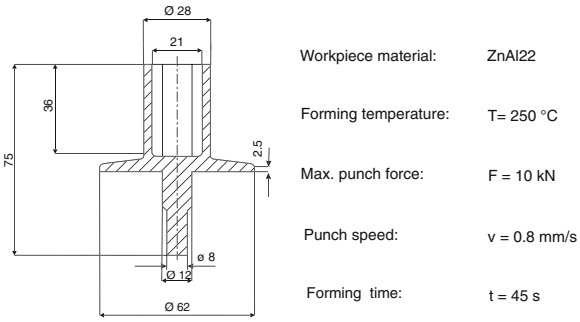


Fig. 3.76 Demonstration component—forming in a superplastic material state [SCHE76]

single-phase materials, such as nickel, can be subjected to a superplastic forming operation [FLOR67, HIRO90].

While aluminium alloys are very important for superplastic metal-sheet working, in massive forming mainly superplastic nickel and titanium alloys are used [SCHR93a].

Table 3.18 lists a large number of the materials with superplastic behaviour investigated until now along with recommended forming conditions [PADM80]. In order to keep the low grain size in the grain structure, some materials are prepared by powder metallurgy and then extruded, forged or rolled and also heat-treated.

3.4.3.4 Applications in Massive Forming

As a result of the low yield stress in the superplastic state, parts can be manufactured which cannot be manufactured in a normal plastic material state due to an excessively high required force and/or an excessively low forming capacity. The reduction of intermediate operations and the production of complex parts requiring large strains continue to be possible (Fig. 3.76).

Even though the principles of superplasticity have been known since the 1930s [PEAR34], the method has hardly been established until now as a massive forming process. Familiar examples are limited to a great extent to the isothermal forging of turbine components (see Sect. 3.4.1). Many but not all of the nickel-base or titanium alloys used in these cases are superplastically formable. Further applications are found in the area of sheet forming (see Sect. 4.6.2).

3.4.4 Thixoforging

The term thixoforging refers to a method of hot working at a temperature in which both solid and liquid phase content is present in the material. In this narrow temperature region, metallic materials can be formed with an extremely low

required force, in the process of which very high true strains can be achieved. This allows for the forming manufacture of complex structures which were once only producible using casting methods.

3.4.4.1 Process Principle and Prerequisites

The term "thixo" is derived from the Greek "thixis", meaning "touch". Thixotropy is the term for a flow behaviour in which the viscosity η of a liquid or partially solid material decreases with time t under a constant shear stress, approaching a constant low value (Fig. 3.77, left). The extent of the final decrease in viscosity after a specific stress duration T conforms to the magnitude of the applied shear rate or shear speed $\dot{\gamma}$. In a state of rest, the original state of the material is re-established, i.e. genuine thixotropy is always a reversible process.

The precondition for thixotropic material behaviour is that the material is composed of at least two phases possessing different solidus temperatures.

The most well-known example of thixotropic flow behaviour is ketchup. Different liquids and particles are present in this substance (water, fats, fibres, etc.) which in a state of rest are bound together by means of surface forces. The result is a pasty state. By applying shear, e.g. through shaking or mixing, the bonds are broken down and the viscosity drops with the time under shear stress. The ketchup becomes fluid, or better flowable. After the shear stress is suspended, the solid components agglomerate, i.e. they bond together again and form small accumulations.

The same applies to multiphase metallic materials. Even if a phase is already fluid in the region between the solid and liquid temperatures, material cohesion may still be provided through the solid phase. In this case, the cohesion of the solid grains can break down through an applied shear stress, so that individual solid material particles move relative to each other by means of rotation and translation within the liquid phase (Fig. 3.77, right) [HEUS96].

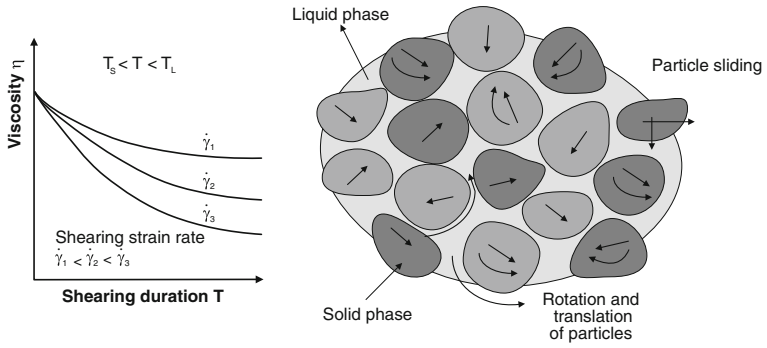


Fig. 3.77 Behaviour of materials in a thixotropic state; *left* viscosity as a function of shear rate and shear stress duration; *right* deformation mechanisms

This time- and shear-rate-dependent material softening is affected by two different, rapid processes. The first, rapid drop in viscosity is to be attributed to the disruption of the bonds between the solid grains (destruction of agglomerates); the second, later and clearly slower drop in viscosity is explainable by the rounding of the moving grains [KAPR98]. The material hardening which takes place in the subsequent state of rest (agglomeration of solid grains) takes considerably more time than the material softening.

3.4.4.2 Description of Thixotropic Material Behaviour

There are two fundamentally different approaches towards the mathematical description of material behaviour in a semi-solid state. On the one hand, the attempt is made to describe the material as a solid body despite exceeding the solidus temperature and to assign it a yield stress k_f. Other approaches define an apparent viscosity η_{Sch}, which changes depending on the fluid phase amount and thus describes the material as a fluid. This makes the application of fluid mechanics possible.

The main difference between the two approaches consists in k_f generally being determined through a time-independent deformation and η through a time-dependent deformation [HEUS96]. The latter approach thus accounts for both the influence of speed and the influence of the stress duration. The following will briefly describe both approaches.

Yield stress. The yield stress can be described using this equation:

$$k_f = C \cdot \dot{\varphi}^m. \tag{3.14}$$

As the yield stress is only affected by the preceding forming operation in the area of the solidus temperature and also only to a minor extent, the influence of the true strain can be left out. To ensure, however, that the equation is also capable of describing the material behaviour beyond the solidus temperature, m and C must be determined as functions of T. For this purpose, Heußen determined m and in tests for an aluminium alloy at different temperatures and described $m(T)$ and $C(T)$ as a third-degree polynomial [HEUS96].

The yield stress then shows a progression over which at first slopes down gently with increasing temperature and then drops dramatically when reaching the solidus temperature. When approaching the liquid temperature, it finally falls asymptotically to a value near zero. It should be noted that the duration of the shearing is not accounted for. However, the effectiveness of the approach can be improved by factoring in the influence of time.

Besides this, more complex models have already been developed which view the respective properties of the solid and liquid phases separately and combine them in a single formula, allowing for more exact calculation results [HEUS96, KIUS03].

Apparent Viscosity. In order to describe the time-dependent effects of thixotropy (dependency of yield stress on the duration of the shear stress), approaches have been developed which define an apparent viscosity η_{Sch} [HEUS96, KAPR98, MESS01]. This changes, depending on the liquid phase content, the shear speed and the stress duration:

$$\eta_{Sch} = f(f_l, \dot{\gamma}, t). \tag{3.15}$$

The time-dependent effects of thixotropy can then be determined by introducing a transport equation [MESS01]:

$$\frac{d\eta}{dt} = \frac{1}{\lambda} \cdot (\eta_\infty - \eta). \tag{3.16}$$

In this equation, t represents the time, λ the relaxation time and $\eta_\infty = f(f_l, \dot{\varphi})$ the equilibrium viscosity reached under constant shear stress after a sufficient amount of time. According to Joly [JOLY96, QUAA96], the equilibrium viscosity is calculated as

$$\eta_\infty = A \cdot e^{B \cdot f_l} \cdot \dot{\gamma}^m. \tag{3.17}$$

The liquid content f_l can be derived from the temperature using the Scheil equation [HEUS96, MESS01]:

$$f_l = 1 - \left(\frac{T_F - T}{T_F - T_L} \right)^{\frac{1}{k-1}}. \tag{3.18}$$

In this equation, T_F represents the melting temperature of the pure metal (e.g. $T_F = 659\,^\circ\text{C}$ for aluminium), T_L the liquidus temperature of the alloy (e.g. $T_L = 615\,^\circ\text{C}$ for AlSi7 Mg). k is the division ratio, also referred to as the distribution coefficient. This is a material-specific equilibrium constant which describes the material distribution between the phases.

3.4.4.3 Materials

Thixotropic materials are multicomponent systems which exhibit both liquid and solid phase content within the broadest-possible temperature range. These include multicomponent systems whose individual components have strongly varying melting temperatures. The materials should have a microstructure with fine, globular grains, so as to enable the forming mechanisms to act (Fig. 3.77, right). Dendritic (lamellar) microstructures are therefore unsuitable. For this reason, the treatment of the primary material is of critical importance [DOEG03].

Until now, the application of thixoforging has been limited largely to the processing of aluminium alloys. The reason for this lies primarily in the fact that the forming temperature of aluminium alloys, i.e. between 500 and 600 °C,

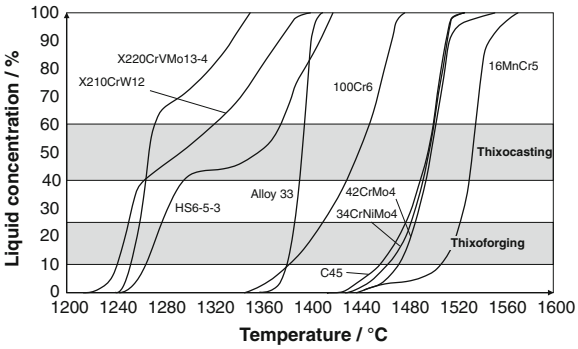


Fig. 3.78 Liquid phase progressions of different steels at a heating rate of 10 K/min [BLEC04]

is relatively low and more easily controllable compared to that of steel. The thermal tool stresses and required installation costs remain manageable within this range. Typical aluminium alloys for thixoforging are silicon, magnesium and copper-containing alloys, e.g. AlSi7Mg0.3 and AlSi6Cu3.

In contrast, the temperature range for steels within which thixoforging can be applied is between 1,250 and 1,500 °C, depending on the alloy (Fig. 3.78). This entails the use of special tool materials (e.g. ceramics) [DESE03, DOEG03], which considerable raise the production costs. Moreover, more effort must be invested in heating and temperature control. From an economical perspective, therefore, thixoforging is not yet a suitable forming process for steel [HIRT98, NN01c].

In principle, however, the thixoforging of steel is possible. It has already been realized several times under laboratory and near-industrial conditions [BLEC04, DOEG03, HIRT98]. Steels most suited in principle are, firstly, the subeutectoid steels, which also represent the majority of steels used in conventional forging. Due to their lower solidus temperatures and higher C contents, however, the supereutectoid steels are especially suited to thixoforging. The boundary of the C content lies among the eutectic steels which immediately and completely solidify upon cooling the melt. Above the eutectic (ca. 2 % C), the increased C contents lead in combination with the relatively rapid cooling in thixoforming to brittle materials. The goal of current studies is to develop specially adapted steel types which are characterized by good mechanical and metallurgical properties and simultaneously permit the lowering of process temperatures and an enlarging of the process window [DOEG03].

3.4.4.4 Processes and Application

Seen technologically, forming in the thixotropic material state is situated between foundry and forging technology (Fig. 3.79). Both technologies are possible for forming purposes, although a higher fluid phase content is aimed for as a rule in

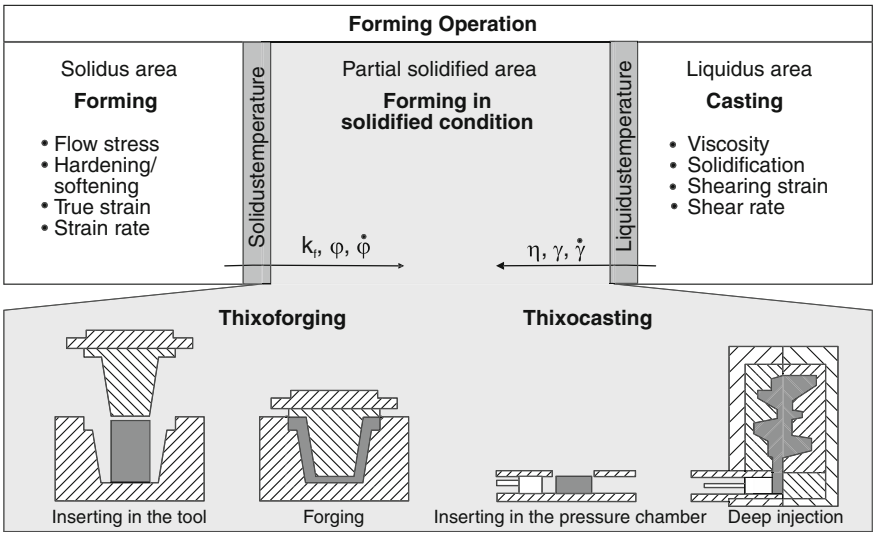


Fig. 3.79 Forming of steel in a partially solid state—distinction between thixoforging and thixocasting

so-called thixocasting (Fig. 3.78). The process is called thixoforging or thixocasting depending on whether forming processes are executed in a forging die or on a die-casting machine after heating [TIET93].

Some cases also allow for a process combination in which a forging process immediately follows casting. This is referred to as "cast-forging".

Today, thixoforging is predominately used in the manufacture of aluminium components [DOEG03, TIET93, WOLF03]. The main area of application is automotive construction. This area exploits the potential of the process for reducing weight through the use of aluminium alloys while simultaneously allowing for functional integration by producing complex, near-net-shape parts. The advantage over conventional casting lies in the creation of denser and, to the greatest extent possible, pore-free grain structures. More complex parts are producible in comparison to conventional forging, and there is even no need to subdivide the forming process into multiple stages [DOEG03].

A barrier which still exists in terms of the broad application this method for the purpose of processing steel is the high process temperatures involved, which must be controlled precisely. A tool technology is required for this which can balance out tool costs and tool service lives in an acceptable way [DOEG03, HIRT98].

3.5 Rolling as Remachining and Finish Machining Process

3.5.1 Profile Rolling of Prefabricated Components

Rolling methods used in the scope of remachining or finish machining are limited to the area of cold forming and are characterized in that only the rim zone of the component is plastically deformed.

The most common rolling methods used in remachining and finish machining are profile rolling, thread rolling and surface fine rolling, which will be described in detail in the following.

3.5.1.1 Principles and Overview of Rolling Methods

Different rolling methods and machines have been developed for the manufacture of rotationally symmetrical components with a profiled surface. These methods are subdivided in DIN 8583-2 [DIN03d] according to the following categories (see Fig. 3.80):

- kinematics (longitudinal, cross and skewed rolling),
- roll geometry (flat and profile rolling) and
- workpiece geometry (solid and hollow profile rolling).

The concepts of cross, skewed and longitudinal rolling describe the main forming and lay directions between the tool and workpiece axes (Fig. 3.81).

In longitudinal rolling, the tool moves along the workpiece axis, in cross rolling transversely to this axis. In skewed rolling, the tool axes are fixed at a certain angle oblique to the workpiece axis [SPUR83].

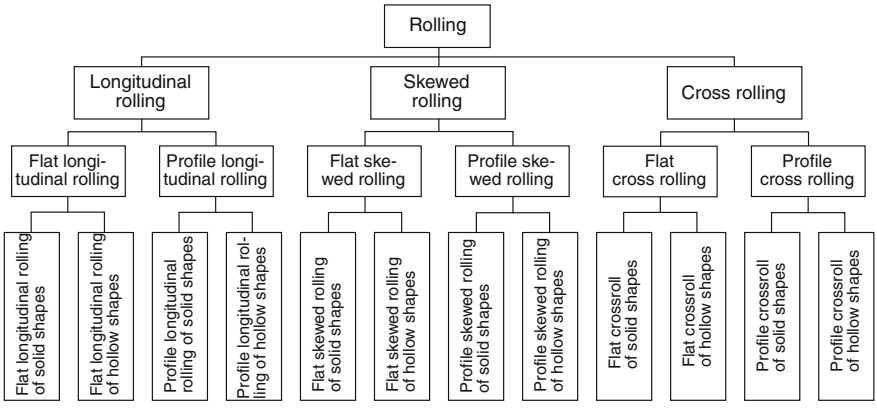


Fig. 3.80 Classification of rolling methods according to DIN8583-2 [DIN03d]

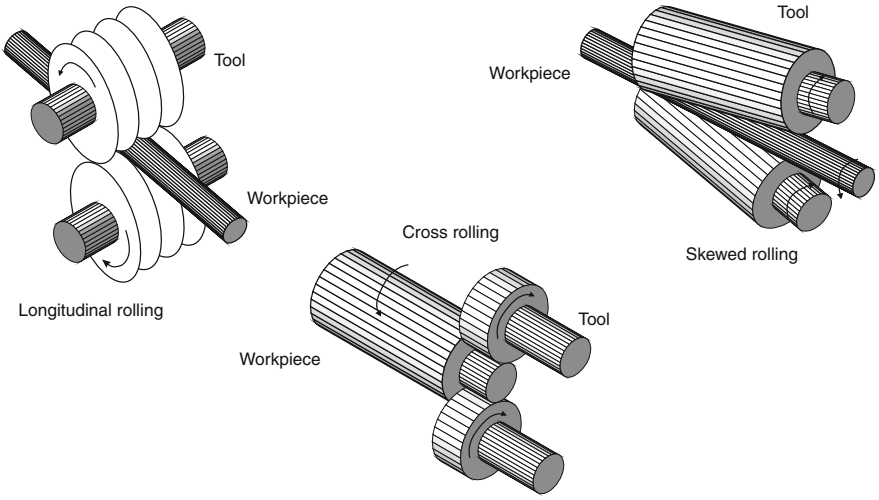


Fig. 3.81 Schematic diagram of the kinematics of the rolling process [SPUR83]

Rolling itself is counted among the compressive forming processes, i.e. the plastic forming action is induced largely by a compressive stress. Among the known methods of forming manufacturing of profiles, the rolling methods have come to have the widest application [LANG90b, SCHM81]. Their advantage lies in the relatively low forming forces involved, which is a result of the locally limited action zone of the tool and workpiece. Irrespective of the individual processes and process variants, the actual forming process can be represented as the penetration of a wedge-shaped tool into the raw part material. Figure 3.82 illustrates this process [EICH81, SHAH57].

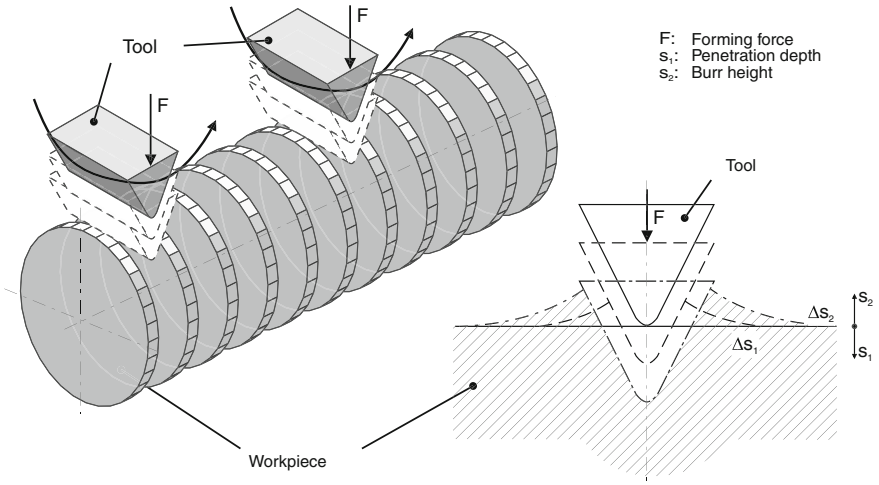


Fig. 3.82 General outline of the forming process in profile rolling

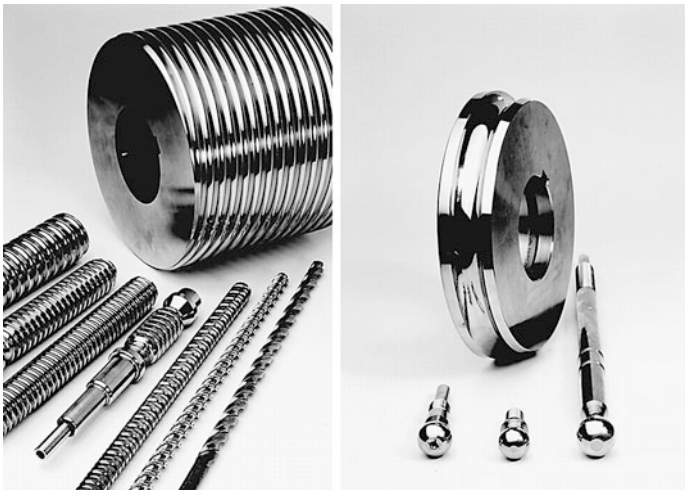


Fig. 3.83 Examples of profile rolling (*Source* Profiroll Technologies GmbH)

The tool displaces the material, which flows into the empty spaces in the tool contour. The rolling process is complete when the intended flow height of the material has been reached or the tool contour is filled with the workpiece material [VDI89]. The determination of the required raw part diameter is especially important for two reasons. Firstly, every deviation in manufacturing from the required premachining diameter has an adverse effect on the component geometry following the rolling process. Secondly, in case of an excessively large raw part diameter, deviations lead to a reduction of the tool life as a result of increasing forming forces. Assuming a constant surface, the premachining diameter can be determined approximately by means of the planimetry of the profile cross-sectional area (displaced material is equal in volume to the built-up material) and empirically optimized with diametrically stepped workpieces in subsequent rolling trials. In addition, analytical calculation methods offer the possibility of determining the premachining diameter in good approximation [KÖNI83].

Figure 3.83 shows typical tools and workpieces used in profile rolling.

3.5.1.2 Rolling of Tooth Profiles

Both rolling-off and moulding processes are used for manufacturing tooth profiles through cold rolling.

In the rolling-off process, the tooth profile is produced by means of the relative rolling motion between a tool set derived from a reference profile and the workpiece [DIN86c].

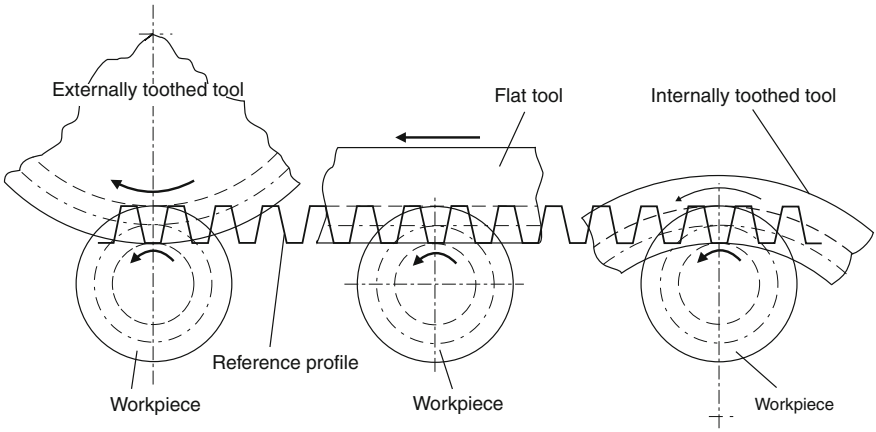


Fig. 3.84 Basic tool shapes for realizing the rolling-off principle in the cold rolling of tooth profiles

Figure 3.84 provides a schematic diagram of the basic principles which are technically realized for this purpose and the accompanying tool-workpiece arrangement [BART87].

In cold rolling processes working with round tools, the tool profile generating the tooth profile takes the form of a cylindrical external gearing which is represented by a rolling movement in the workpiece blank.

Today, for rolling tooth profiles from solid material with round tools, predominately double roller machines are used which usually represent further developments of thread-rolling machines [GLAU58, MÜLL60, SCHM81]. The photo on the left side of Fig. 3.85 provides a view of the working area of such a machine. The roller tools visible in the photo are set by a controllable drive into a synchronized, unidirectional rotary motion which is transferred during the rolling process to the workpiece guided between them. Figure 3.85, right provides a schematic diagram of the most important process variants.

In the throughfeed method, the workpiece is fed axially through the working area of the roller tools, which in this case are set at a constant centre distance. Their toothed outside surfaces are provided in the longitudinal direction with an inlet cone, a calibration area and an outlet cone. The toothing is thus profiled in such a way as to grow gradually in a widthwise direction, corresponding to the axial feed.

In the plunge-throughfeed rolling process, the workpiece is fixed in the machining plane in the axial direction. The toothing is rolled radially into the workpiece through the reduction of the centre distance of the cylindrical roller tools. In most machines, the feed motion required for this is executed by only one of the two tools. The other tool is rigidly attached. Here, the workpiece axis must be movable in the direction of feed so that it can be centred between the tools. Less common is the symmetrical feed with rigid workpiece axis [TURN71, NN81a].

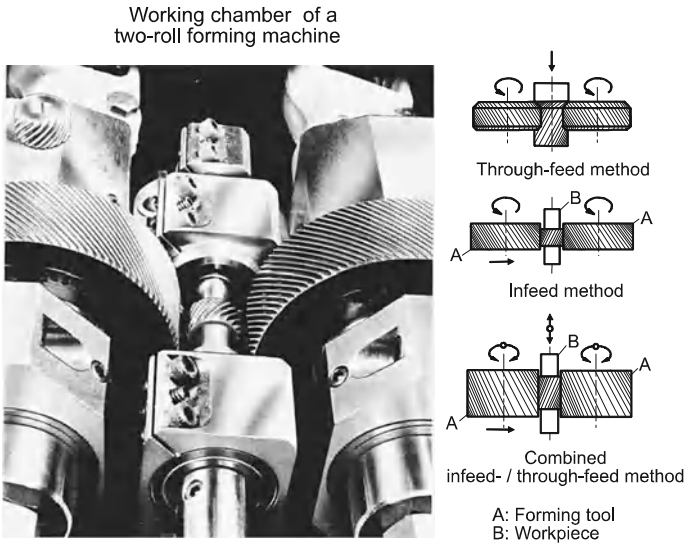


Fig. 3.85 Cold rolling of tooth profiles according to the double roll profile rolling method (*Source* Profiroll Technologies GmbH)

Combined plunge-throughfeed and throughfeed rolling is to be regarded as a special case of plunge-throughfeed rolling. In this process, the workpiece receives an axial feed motion, with the repeated reversal of the tool rotation movement ensuring that it remains within the machining area. Until the full profile depth is reached, the gear blank executes a reversing movement between the tool end faces which has a positive impact on the formation of the tooth curve.

The application limits of these double roller process variants depend on the type of toothing to be rolled and the size of the rolling machine [MÜLL60]. Both helical and straight tooth profiles can be rolled with diameters of up to $d = 100$ mm. Depending on the pressure and helix angles, cited modules have reached $m = 3.5$ [GLAU58, TURN71]. In plunge-throughfeed rolling processes, the toothing width is limited by the tool width, which can reach up to $b = 250$ mm. In throughfeed processes, workpieces of up to $b = 2{,}000$ mm can be processed on the relevant machines.

The Roto-Flo method developed in the USA (Fig. 3.86) is a realization of the model for creating involute tooth profiles in its original form through the use of tools which practically take on the form of the reference gear rack. A tool set consists of two straight rolling dies which, as shown in the schematic sketch in Fig. 3.86, are guided horizontally above and below the workpiece and are moved in synchronized opposition to each other. Their toothed functional surface consists of a chamfered inlet area, the work zone, a calibration zone with constant tooth height and a chamfered outlet area, the discharge zone.

At the beginning of the rolling process, the workpiece is taken up between the centres of the tools, which are moved apart. The working dies move in the

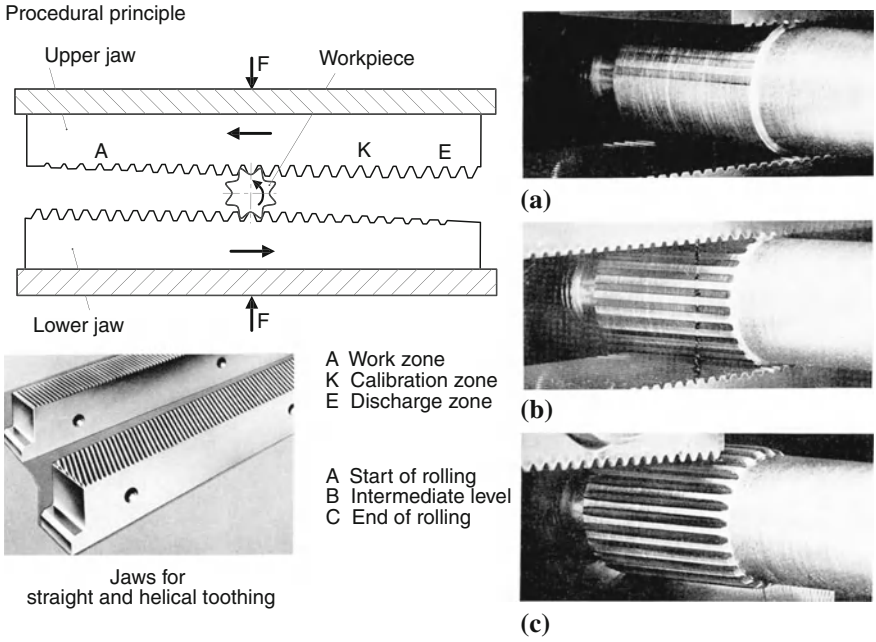


Fig. 3.86 Cold rolling of toothings according to the Roto-Flo method

respective tangential workpiece plane translationally towards the workpiece, capture it simultaneously and set it in rotation through friction. The profile is formed gradually with increasing tool tooth height in the work zone, which makes up about two thirds of the tool length, until reaching its full depth. It is post-formed in the adjacent calibration zone, where concentricity, tooth thickness and flank form are especially shaped. Finally, the discharge zone with decreasing tooth height continuously reduces the elastic deformation of the processing system and the vertical forces caused by them [KREI82, KREI83]. The forming process is complete after one working stroke. The right side of Fig. 3.86 shows three stages of this type of profile generation. With the correct tools, this process can be used to create both straight and helical toothings.

The relatively simple motion sequence is clearly suggestive of the very high productivity of this method. Depending on the material, geometry and automation, 200–400 rolls per hour have been cited, corresponding to cycle times of 17.5 s to 9 s [KREI82].

The realizable tooth geometries are limited by both the workpiece material properties and above all by the tool dimensions. Standard machines can accept tool lengths of roughly 1,200 mm, allowing for the machining of workpiece diameters of up to 60 mm and modules in the region of $m = 0.3$–2.0 mm with effective angles between 30° and 45°. The tooth width is determined by the die width, which is normally limited to 120 mm [KREI82, KREI83].

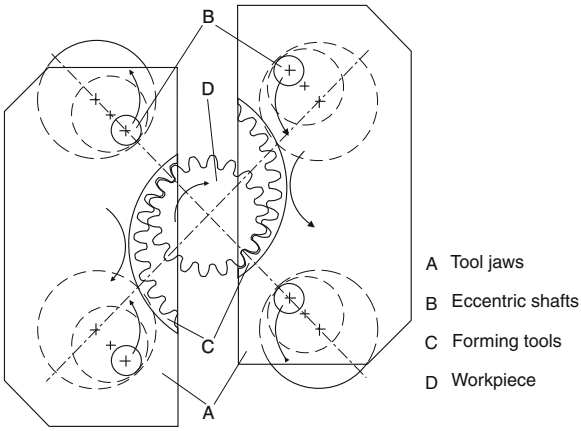


Fig. 3.87 Cold rolling of toothings according to the WPM method

The Roto-Flo method has established itself in mass production for the manufacture of oil grooves, involute spline shaft profiles (splines—sliding couplings and serrations—fixed couplings) and threads.

Tooth profiles are rolled in the WPM process according to the principle of rolling-off internal toothings [RYBK77, EICH86, MARC73]. The corresponding tool set comprises two internally toothed ring segments which are attached to the machine in moving dies (Fig. 3.87). Their toothed work surface is equipped in the longitudinal direction with a conical inlet area, a cylindrical calibration area and a conical outlet area.

The movement of the die jaws is controlled via two eccentric shafts, so that every point of the tool geometry describes a circular path. The midpoints of the tool arcs move with a phase shift of 180° around the workpiece axis and describe a circle whose diameter is to be set in accordance with the gear blank geometry. The tool positions shown in Fig. 3.88 demonstrate the motion sequence during a working cycle, composed of a movement of the mould and an empty movement.

During the mould movement, the tools roll on the rotating, but axially fixed workpiece, creating a toothed ring corresponding to the tool width. During the subsequent empty movement, the workpiece receives an axial jump feed. In the process, its rotation is maintained by means of a partial change gear drive in order to ensure the correct rotation angle position for the next forming cycle. The respective tooth profile is thus increasingly rolled gradually in the longitudinal direction.

The WPM method was mainly conceived for producing involute multi-spline profiles on shaftlike workpieces. Both helical and straight toothings can be manufactured with modules of up to $m = 3$ mm. For shaft lengths below $l = 50$ mm, maximum diameters of both $d = 120$ mm and $d = 75$ mm have been cited. The toothing width depends only on the axial path of motion of the feed unit and can amount to up to $b = 630$ mm [RYBK77, MARC79]. With respect to effective

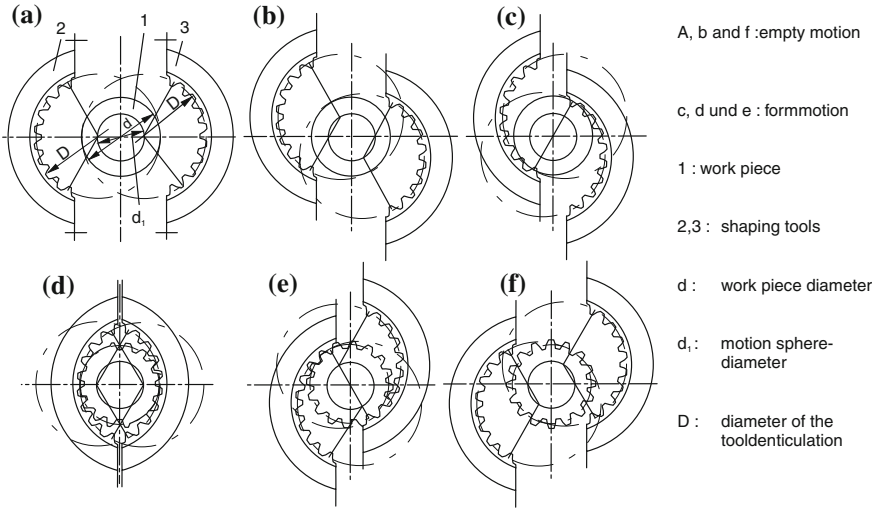


Fig. 3.88 Tool position in the cold rolling of toothings according to the WPM method

profile angles which can be rolled, no limitations apply, as the tool teeth designed as internal toothings are not very vulnerable to foot fracture.

The methods described thus far represent the most common cold rolling processes currently implemented for creating toothings which operate according to the rolling-off principle. They are also further characterized in that the workpiece axis is perpendicular to the working plane of the rolling tools. The machining direction thus runs transversely to the tooth spaces to be created [DIN03d].

The rolling off process is repeated according to the respective radial feed or to the inlet slants of the respective tool at different depths of immersion until the full profile depth has been reached. In the process, the material is formed in unequal cross-sections and with constantly changing direction and speed. The motion reversal of the rolling process in particular causes a hollowing-out of the material at the incoming flank and a bulging of the material at the outgoing flank. As a result, both the forming forces and consequently the forming process itself become asymmetrical. Gear wheels manufactured in this way are characterized by a deep asymmetrical depression of the tips and varying tooth tip heights.

When rolling using the mould method, the tooth spaces are formed using profiling tools which approximate the negative profile of the tooth spaces to be produced; the direction of the forming force remains constant during the overall forming process. The forming forces act symmetrically, and the material is predominately displaced in the radial direction. The tip depression which occurs here also, which is a typical feature for cold rolled toothings, forms symmetrically due to the even distribution of the material flow among the two flanks.

Among the mould methods which have been developed over the course of time for cold rolling tooth profiles, the only one which has achieved practical relevance is the method developed by Grob [GROB60, KRAP78a]. The basic principle of

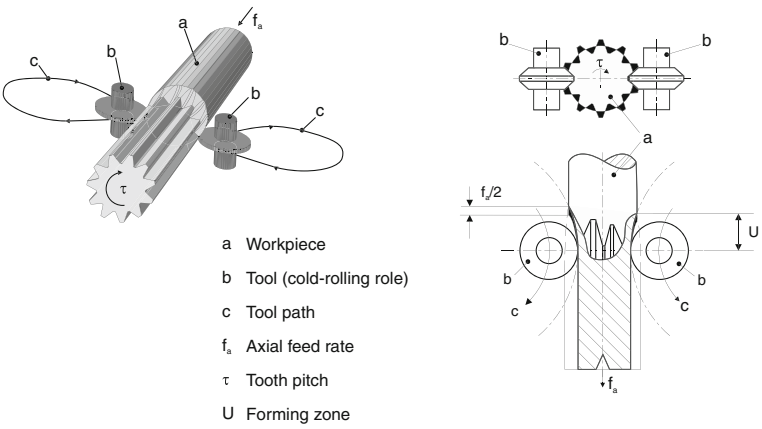


Fig. 3.89 Cold rolling of toothings according to the Grob method

this method, also known as planetary rolling, consists in the distribution of the total forming process into multiple partial forming processes. A profiled pair of rolls position in planetary fashion at the circumference of two opposing rolling heads has a forming effect.

As shown schematically in Fig. 3.89, the rolls process the workpiece guided between them simultaneously and symmetrically due to the opposed, synchronous rotation of the rolling heads, with the workpiece itself executing a rotational movement about its own axis. The rotations of the workpiece and the roller heads are kinematically connected to each other via a partial gear in accordance with the number of teeth on the gear blank. This motion sequence is superimposed by a continuous feed movement of the workpiece in the longitudinal direction, which causes the toothing profile to be formed in the axial direction.

Due to the use of a tool pair, the profile of the toothings runs along two helical lines which are shifted by half a work feed given an even number of teeth. The actual forming work is performed in the forming zone referred to in Fig. 3.89 as *U*, in which a sickle-shaped segment is rapidly formed with every tool passage. The tooth spaces are thus created in a large number of single short forming steps, with the material flow only being caused in a narrowly described outer rim zone.

The interrupted (discontinuous) workpiece rotational movement required purely for the forming process is created by ay special step gear which is synchronized with the rolling head rotation in such a way that the workpiece is motionless during the engagement of the rolls and further rotated by one tooth pitch during the subsequent empty movement.

Since the working direction of the tools in the longitudinal direction of the tooth spaces runs transversely to the profile with no relative movement, the Grob method allows for the production of any desired profile shape with uniform spacings and with either even or uneven tooth numbers. The toothing can also be cylindrical or conical in shape (Fig. 3.90) [KRAP78b].

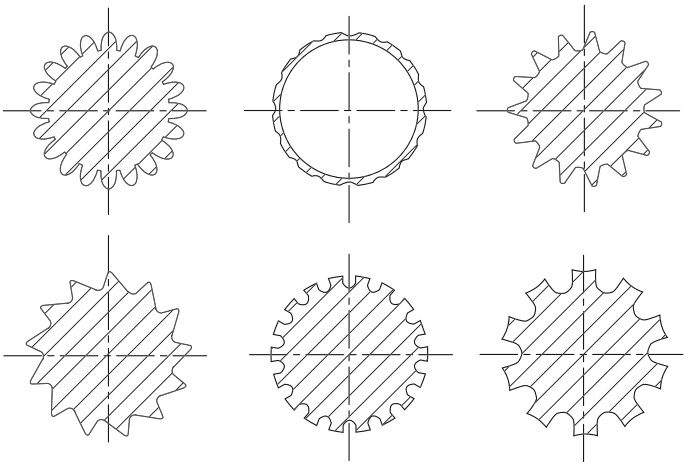


Fig. 3.90 Profile shapes which can be created using the Grob method of cold rolling [KRAP78a]

Due to the tool-workpiece kinematics, the discontinuous Grob method only allows for rolling straight toothings. The machines currently being manufactured allow for the production of toothings with modules of up to $m = 5$ and numbers of teeth in the region of $z = 10$–30 with outer diameters of up to $d_a = 120$. The settable rolling head rotational speeds which determine, together with the axial feed, the toothing rate are limited by the acceleration forces of the intermittently rotating workpiece to values in the region of n_R = 800–1,600 min^{-1} [GROB60].

Rolling with continuous workpiece rotation created with the aid of partial change gear drives is also possible using the Grob method. Due to the resultant relative motion arising transverse to the tooth space, this application requires that the axes of the rolling heads are swivelled at a certain angle corresponding to the workpiece rotation during tool engagement. The forming process is therefore superimposed with a minor amount of rolling. These kinematic conditions limit the producible profile shapes and accuracies. The continuous partial process is predominately used to produce toothings with low tooth depths and large tooth-space apertures angles, such as splines. This process variant allows for rolling head rotational rates of up to $n_R = 3.000\,\text{min}^{-1}$, with the transmission of the partial change gear drive being adjustable provided a number of gear blank teeth in the region of $z = 12$–96 [KRAP78a]. Typical parts produced using the Grob process include such automobile parts as rear axle shafts, clutch and brake camshafts, drive pinions, end-pieces for cardan shafts and steering shafts with conical gears [KRAP78b, KRAP84].

The method is also suitable for manufacturing toothed hollow parts. In this case, a toothed rolling mandrel is used hold the workpiece. The material is then moulded in the machining process by the rolling tools into the spaces of the rolling mandrel. Typical application examples for this process variant include toothed belt discs, gear rims for internal combustion engines and clutch disc carriers [KRAP79].

3.5.1.3 Thread Rolling

The trend which began in 1945 of manufacturing threads using largely chipless processes is mainly the result of the following advantages of thread rolling in contrast to thread cutting:

- high accuracy coupled with high output (hourly machine output with thread dimension M5 of max. 90,000) [NN79]
- unsanded smooth surfaces of the rolled threads
- increased material strength in the thread flanks
- increased fatigue strength
- reduced notch sensitivity
- savings on material due to the thread dimension in the premachining stage being smaller than the desired outer thread diameter
- materials with a strength of $R_m \leq 1,400$ MPa are also rollable in a heat-treated state

In thread rolling, the material rises to the flanks of the moulding tool as the tool penetrates the workpiece, tending to go more above than between the already rolled paths. Especially in sharp threads, this can lead to the formation of seams, which can reach up to 20 % of the thread depth. Hard material form deeper seams than soft materials. However, seams cause absolutely no reduction in the load capacity of the threads (Fig. 3.91, left).

This upward flow of the material causes a large strain in a narrowly limited area and an associated increase in strength (Fig. 3.91, right). This can easily reach twice

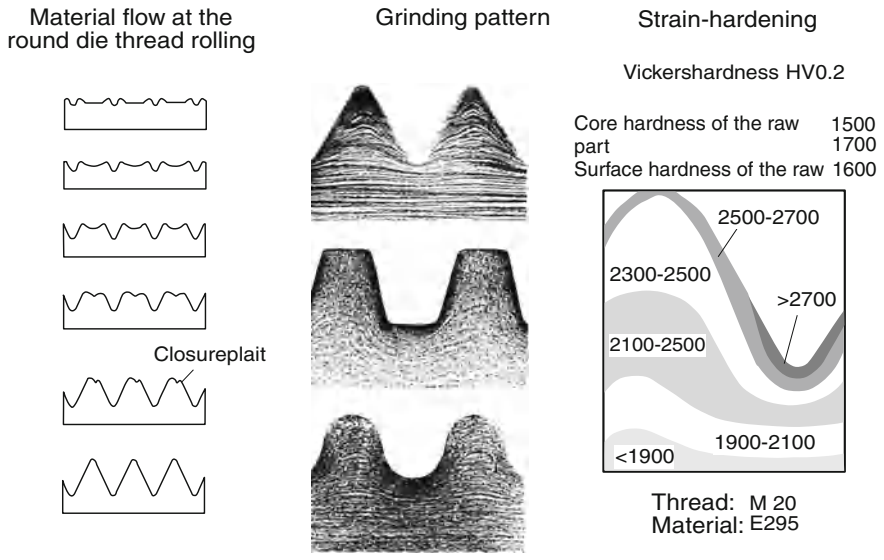


Fig. 3.91 Diagram of material flow and strain hardening in thread rolling [APEL53, SCHU89]



Fig. 3.92 Averaged roughness heights of thread profiles produced in different processes [APEL53]

Table 3.19 Compared reverse bending strength values of thread bolts manufactured in different processes [LANG90b]

Condition 1	Condition 2	$\sigma_{bw1}/\sigma_{bw2}$
Rolled-tempered	Tempered-rolled	~ 1 : 2
Tempered-cut	Tempered-rolled	~ 1 : 3
Cut-tempered	Rolled-tempered	~ 1 : 1

the value of the original material at some locations of the profile. As micrographs of rolled threads show (Fig. 3.91, centre), the individual material fibres are not cut, as in chipping thread production, but rather merely displaced. Figure 3.92 shows, moreover, that the roughness heights of the thread flanks are smaller than the cut thread flanks. The rolled surfaces thus have a characteristically high resistance to corrosion [SCHU89, BETH80, BETH82].

Strain hardening in conjunction with high surface quality (e.g. M10 for screws) causes an increase in the admissible loading capacity by about 12 %. Also, strain hardening has a considerably stronger effect on reverse bending strength (Table 3.19).

It must be taken into account, however, that heat treatment must be performed prior to rolling, as otherwise the strain hardening will break down when the material is heated.

It should be observed that, when pre-machining the workpiece, an elongation at the ends of the thread bold occurs in the forming zone exceeding the length of the core cross-section. This causes the formation of a concave end face. For this reason, it is necessary to chamfer the blanks as illustrated in Fig. 3.93. The angle α is determined as a function of the material strength. For materials with $R_m \leq 1,000$ MPa, this angle is ca. 15°, with higher tensile strengths up to 30°.

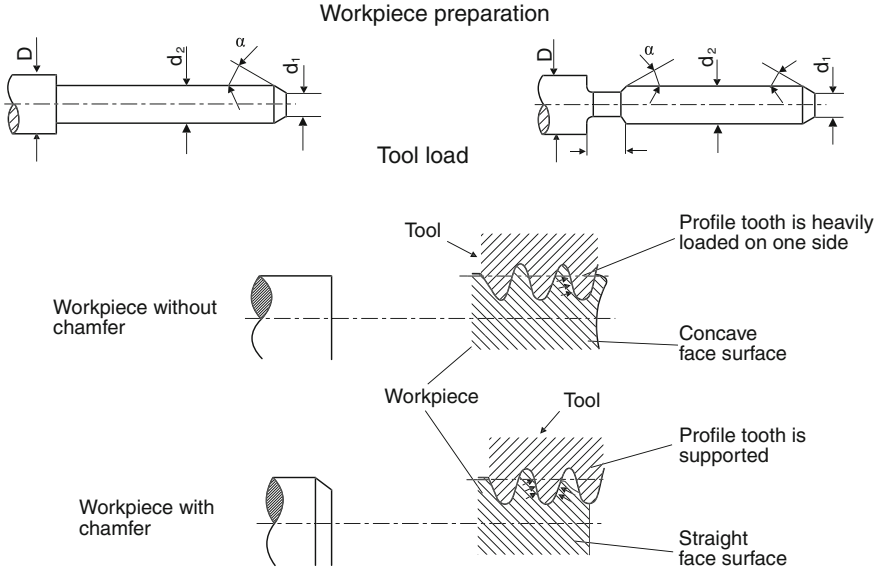


Fig. 3.93 Tool load and material flow as functions of workpiece pre-machining [APEL53]

The chamfer should be designed to in such a way that d_1 is smaller than the core diameter of the thread. In addition, the chamfer dominates the tool load and thus indirectly the tool life. An incorrect or even non-existent chamfer causes individual thread paths of the tool to be heavily loaded axially and, in extreme cases, to break. In contrast, a proper workpiece chamfer causes the axial stresses to break down slowly or almost compensate each other mutually [LANG90b, SCHU89].

Methods of non-cutting thread manufacture can be classified according to whether the thread is generated between driven or non-driven profiling tools. The use of single-purpose machines with driven rolls is referred to generally as thread rolling, whereas production with thread rolling heads or thread rolling irons on conventional machine tools are generally categorized as thread rolling. In the latter process, instead of being driven, the rolls are merely set in rotation by friction fit with the workpiece [SCHU89].

Both flat and round tools can be used in thread rolling machines. In process variants using flat tools, two rolling rods (threading dies) are used which engage with the rotating workpiece. The kinematics of the process corresponds to those of cold rolling toothings with flat die tools (Fig. 3.94).

Depending on the machine type, either the thread rolling rods run opposed to each other or one tool is held stationary in the machine body as the opposing tool moves relative to the fixed thread rolling rod. The stationary threading die in the inlet area is designed to be spherical. This area has a length 1.5 times that of the bolt circumference in which the actual thread forming process occurs. In the adjoining area (2–4 times the bolt circumference), the thread is merely smoothed

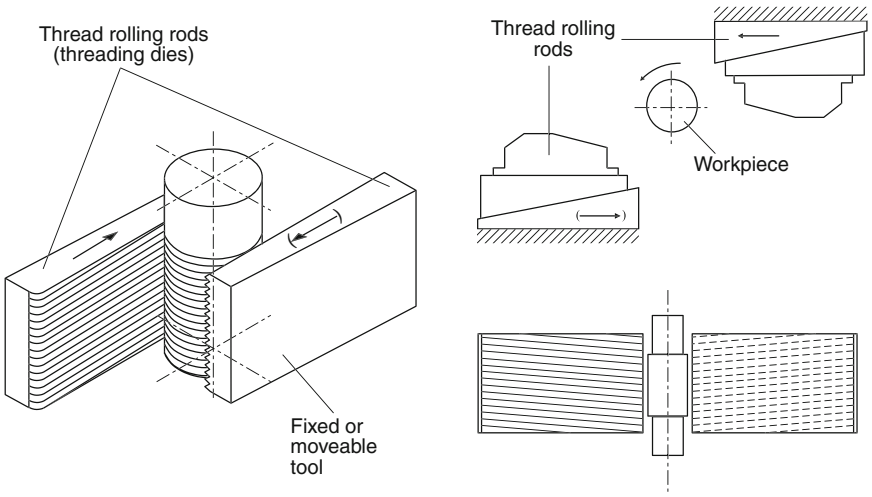


Fig. 3.94 Thread rolling with flat die tools [VDI89]

and calibrated. The outlet area of the fixed threading die is also spherical so as to prevent damage to the finished thread when it is expelled from the machine.

The respective thread pitch is already considered in the tool design, which means that no axial displacement of the workpiece takes place during rolling [VDI89].

The methods working with round tools can be subdivided into plunge-throughfeed and throughfeed processes. Common to the different methods is the use of two profiled tools rotating in the same direction, of which one can be stationary while the other is moved towards the workpiece. The workpiece is positioned as a rule either in the lower middle of the machine on a support ruler or in the middle between centres. Upon striking the workpiece, the driven tool sets the workpiece and the fixed tool in rotation by friction fit, in the process of which the tool profile reproduces itself in the workpiece. This basic sequence is altered or influenced in the different process variants in the following ways:

In the plunge-throughfeed process (Fig. 3.95), the profile of the rolling tools exhibits the same pitch angle as the workpiece, but the opposite pitch direction.

The workpiece only executes small compensatory movements in the axial direction. The width of the tools thus determines what thread lengths can be rolled. The method is used first and foremost for manufacturing high-precision threads, e.g. when high demands are placed on pitch accuracy.

Three different operating modes are possible for throughfeed thread rolling. These are illustrated in Fig. 3.96.

In the process variant represented in Fig. 3.96, left, the tools have pitchless grooves on the circumference with perpendicular orientation to the workpiece axis. For this reason, the tools must be inclined by an amount corresponding to the pitch angle of the intended workpiece about their horizontal transverse axis. Due to the

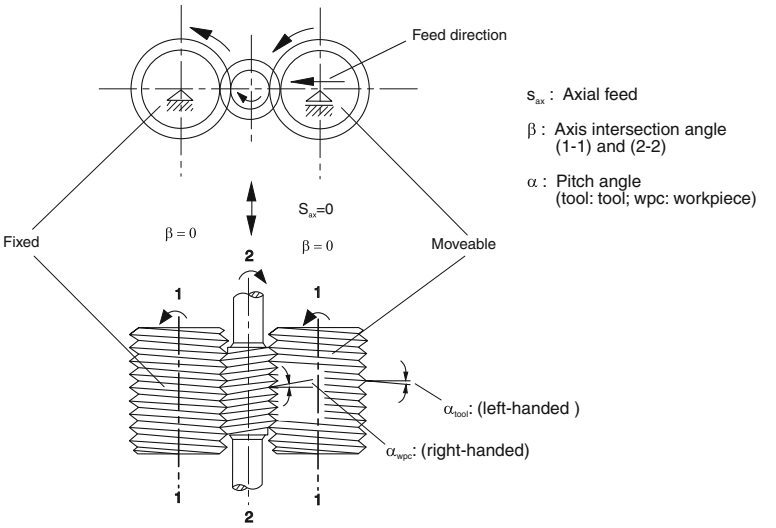
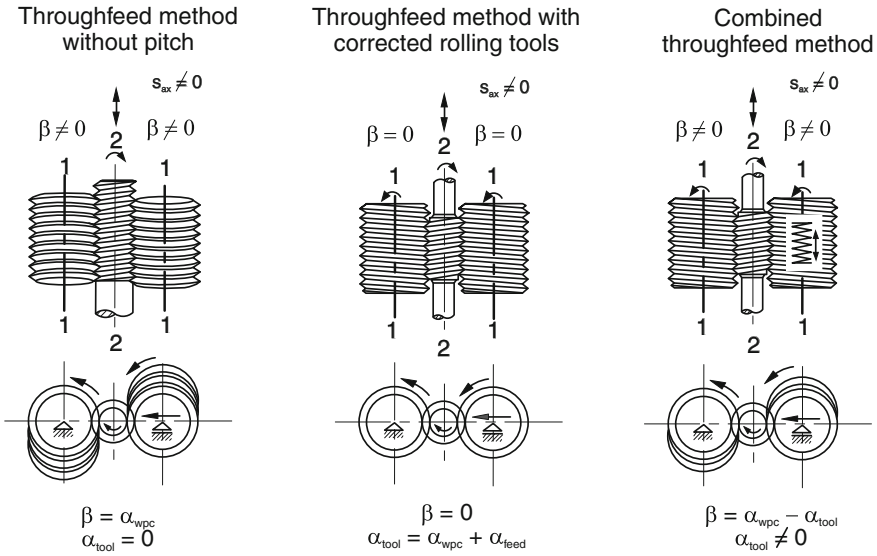


Fig. 3.95 Process principle of plunge-throughfeed rolling [VDI89]



B: Axis intersection angle (1 - 1) and (2 - 2)
α: Pitch angle; s_{ax}: Axial feed
tool: Rolling tool; wpc: Workpiece; feed: Resulting angle due to s_{ax}

Fig. 3.96 Process variants of throughfeed thread rolling

geometrical engagement conditions, there is a defined axial feed of the workpiece during the forming process. This operating mode is limited by the short contact length between the tool and workpiece coupled with large pitches. This variant is preferred in small-series production, as the same workpiece pitch can be rolled to a limited degree to different workpiece diameters with the same profile. A further advantage lies in that fact that the rolling tools can be resharpened repeatedly due to their workpiece-independent diameter.

In the process using corrected rolling tools (Fig. 3.96), the pitch angle of the tools is slightly larger or smaller than that of the workpiece. This causes a feed movement in the axial direction. However, the deviation of the angle α_{tool} from α_{wpc} may not be too large, since the thread flanks will otherwise be damaged. This method allows for the axially parallel arrangement ($\beta = 0$) of the tools, provided that the geometrical workpiece errors resulting from this are still tolerable. A correction of the pitch by inclining the rolling spindles ($\beta \neq 0$) is not possible. This process variant is used in serial manufacture, as the roller dimensions are only designed for one specific workpiece geometry.

The so-called combined throughfeed process represents a combination of both previously described process variants. The rolling tools have a pitch angle which is non-identical to that of the workpiece. As opposed to the process with corrected tools, however, the angular difference can be compensated by inclining the rolling spindles. As in the throughfeed process with grooved tools, there is a resultant axial movement of the workpiece during the forming process. This process is applied when major forming processes must be executed with large pitch angles and high accuracy is required [VDI89].

A further variation of thread rolling with round tool is thread rolling with three driven tools arranged at a 120° angle to each other. By means of a simultaneous linear feed movement, the workpiece is collected centrically and set in rotation. A support ruler and other holding devices are therefore unnecessary.

The three-roller method is used mainly for thread rolling on tube and hollow parts.

The last machine-fixed rolling method which should be mentioned in this context is the method using segment thread rolls (Fig. 3.97). In this process, up to three adjustable thread segments fixed in the machine body and furnished with inlet and outlet zones or with adjusted radii of curvature press the rotating, simultaneously fed workpieces against a driven thread roll. Due to the considerable output, this process is mainly used for mass-produced parts.

In addition to processes with driven tools on single-purpose machines, thread rolling heads and thread rolling irons have been developed for manufacturing difficult workpieces which have no drive and are used on machine tools such as automatic lathes, turret lathes and machining centres. This allows for the execution of both cutting operations and non-cutting thread rolling operations on a single machine in one clamping [BETH83]. This can lead in part to considerable savings in cost [BETH81].

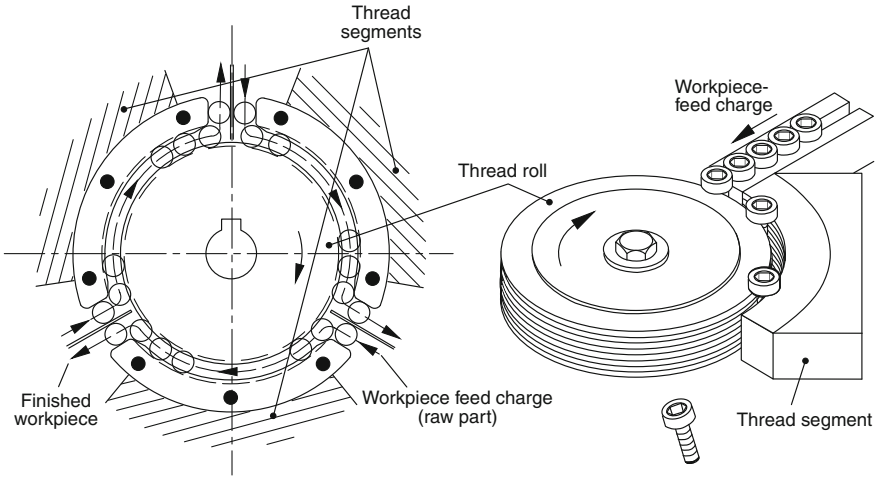
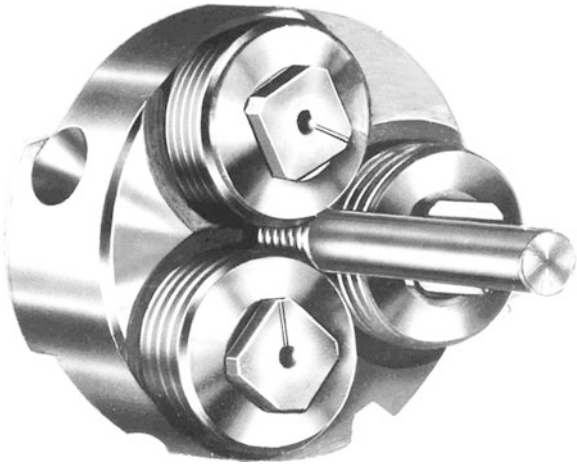


Fig. 3.97 Process principle of rolling with thread roll and thread segment

Fig. 3.98 Thread rolling iron



Another possible process for chipless thread manufacture on conventional machine tools is that of thread rolling with rolling irons. The thread rolling iron illustrated in Fig. 3.98 is a tool whose compact design allows for the chipless production of thread bolts, even given very small available space in the processing area of the machine. Producible thread lengths are limited exclusively by the machine tool used. Three thread rolls are supported by bolts on the front side of the main body. The support bolts are inserted at the pitch angle of the thread to be rolled in a 120° split in the main body. The rolls are not driven, but freely rotating. The rotational movement can be performed by the workpiece or the tool or both. The thread profile has a groove-shaped etching pattern without pitch on the outer diameter of the thread rolls. The thread pitch on the workpieces is created by

means of the support bolts, which are tilted to the pitch angle. The rolling process is initiated by advancing the thread rolling iron or the workpiece over one feed unit to the respective counter piece. The feed is to be set in correspondence with the thread pitch to be rolled. After the rolling process, the thread rolling iron must be rotated back in the pitch. This simple construction does not allow for an opening of the thread rolls, e.g. for reversing in a fast stroke. A delayed reversal is possible by using die stocks which disengage torquelessly after reaching the set thread length.

3.5.2 Surface Fine Rolling

Surface rolling is a process with which machined workpieces made of deformable materials are finished with the aid usually of multiple hardened, high-precision machined rolling elements, such as rollers or balls, under a material-dependent rolling force, and is used to improve surface quality, dimensional accuracy and strength properties.

The individual methods are also distinguished according to these workpiece improvement parameters (Fig. 3.99).

Smooth and deep rolling can be performed using a plunge-throughfeed process for short workpieces and a longitudinal feed process for longer workpieces. In the longitudinal feed process, either the workpiece or the tool executes the axial movement.

The plunge-throughfeed process does not include an axial feed. The surface lines of the contact surfaces of the workpiece and the roll are parallel to each other. The roll width corresponds to the length of the workpiece to be rolled. The procedure can be executed alternatively without centres or between centres.

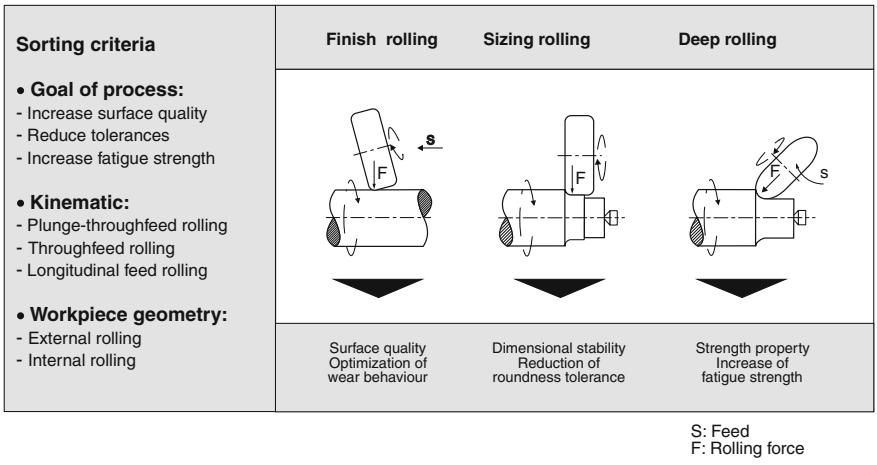


Fig. 3.99 Schematic diagram of the surface fine rolling process

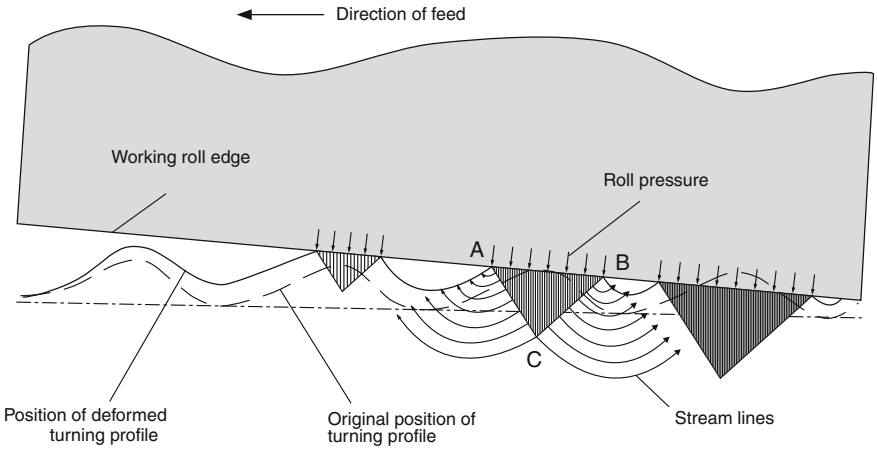


Fig. 3.100 Flow lines of the plastic motion of the material in surface rolling with feed [KÖNI54]

In the centreless longitudinal feed process, which is a throughfeed process, the longitudinal feed is effected by tilting the rolls. Three rolls with force-fit action are predominately used, of which at least one roll is driven.

In the positively controlled longitudinal feed process, on the other hand, the magnitude of the feed depends directly on the machine and indirectly on the number of rolls engaged with the workpiece. Generally, one to four rolls are used.

In the process, the surface lines are inclined to the rolling direction. The angle of inclination lies in the region of $\alpha = 20$–$40°$.

3.5.2.1 Smooth Rolling

The pressure of the smoothing rolls induces a forming of the workpiece which smoothes out the roughness profile. Figure 3.100 shows the material flow which occurs during surface fine rolling with feeding on a turned surface. The diagram demonstrates that almost rigid pressure wedges A-B–C form below the contact line A-B, on whose sides A-C and B–C the bordering material is displaced in the direction of the rotation grooves. This causes an elevation of the rotation groove base which continues until reaching the same level as the groove ridge [KÖNI54].

Figure 3.191 (above) shows the material flow in the circumferential direction on the example of a soldering joint running radially prior to rolling. In order to explain the tangential deformations, it is assumed that the no-slip point is found at position F (Fig. 3.101). Since the workpiece speed at point E is greater than the roll speed, there is a resultant backup of the material (upper deflection of the soldering joint) recognizable at the inlet side in the form of a bead. The material movements occurring in the longitudinal direction of the workpiece prevent an increase in the size of the bead from seam to seam. The lower curvature of the S-shaped material displacement is due to the shear stress arising in the workpiece.

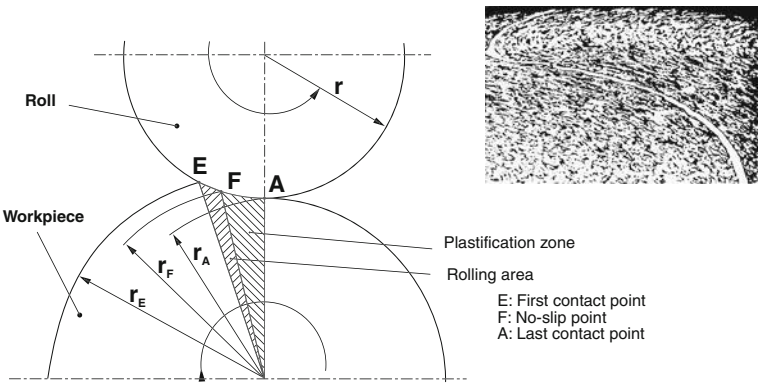


Fig. 3.101 Material flow in the circumferential direction and diameter change in the forming zone in surface fine rolling (acc. to Lange)

In the zone between the no-slip point F and the outlet point A, the shear stress at the workpiece surface assumes the value zero. However, as a shear stress maximum is already reached at a low depth under the workpiece surface, this stress slowly breaking down in the direction of the workpiece core, plastic flow can only occur in a zone below the workpiece surface [PAHL66, KROH65]. Thus an elastic, narrowly limited material zone "swims" on a plastic layer lying below the workpiece surface. Since the circumferential speed in zone F-A is lower than at the inlet area E due to the decreasing workpiece diameter, the elastic material zone moves at the same rate as the roll. This results in a displacement of the upper material zone in relation to the deeper zones. This displacement corresponds to the lower curvature of the soldering joint. The material displacements in the tangential direction increase with an increasing number of seams, with the depth of the maximum displacement and the formed zone remaining almost constant.

In surface fine rolling, the workpieces become defective as a result of the flaking off of the surface layer cause by an excessive tangential material displacement. This type of failure is attributable to excessively high relative rolling forces and the number of seams. With respect to the flaking-off of the surface layer, large numbers of seams are more unfavourable than large relative rolling forces.

Smooth rolling is used to create surfaces with low roughness heights and a high profile bearing length ratio, with the macrogeometric shape of the workpiece remaining ideally unchanged. The method is used to improve sliding, wear and corrosion properties of sliding components, such as bearing journals, valve stems, piston rods and sliding guides. It is applied as a pre-machining process for cylindrical workpieces intended for hard-chrome plating [HERM69]. Both inner and outer surfaces can be smooth rolled.

Since smooth rolling takes place in the region of the surface roughness, workpiece pre-machining is very important. Changes to the surface roughness due to pre-machining have a direct effect on deviations of diameter after rolling. As a

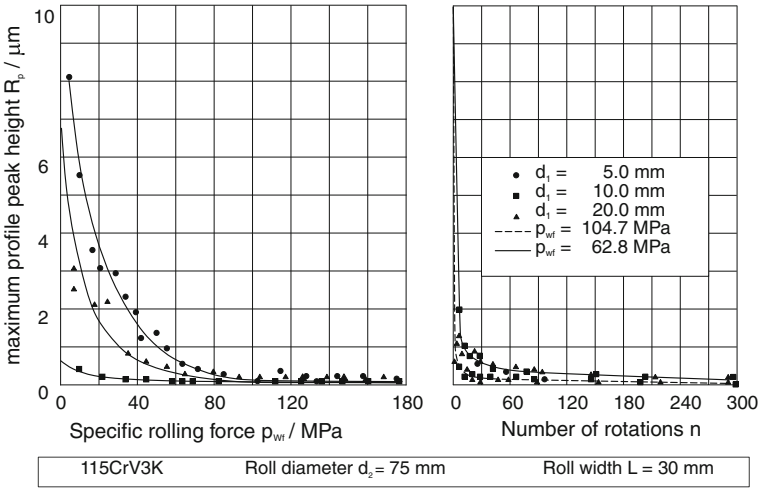


Fig. 3.102 The maximum profile peak height R_p as a function of the surface-related rolling force and the number of seams for different rotation roughness heights [PAHL66]

rule, a diameter change equal to the value of the starting roughness height R_t occurs in smooth rolling. Therefore, the allowance prior to rolling should amount to 1–1.5 times the pre-machining roughness height. Depending on the starting material, pre-machining roughness heights indicated as suited to smooth rolling are $R_{t0} = 30$ µm for steel and for grey cast iron workpieces $R_{t0} = 20$ µm [TELG80]. These values can be achieved by means of rotation.

The minimum workpiece roughness height achievable after this process amounts to 0.1–0.2 µm. Figure 3.102 shows the dependence of the maximum profile peak height R_p on the rolling force and the number of seams [PAHL66].

The rolling speed, however, has no effect on the target surface quality.

Figure 3.103 shows a hydrostatically mounted smooth rolling tool. A special design feature of this tool is that the rolling force is not generated via a spring assembly, but rather via a hydraulically activated piston. The advantage of this is that the same rolling force acts on the workpiece regardless of the workpiece diameter, thus guaranteeing consistent rolling results. By using a hydrostatically mounted ball as the rolling element, high contact stresses can be realized even with low rolling forces as a result of the small contact zone between the rolling ball and the workpiece. As a result, even small rolling forces lead to significant improvements of the surface.

The rolling tool can be equipped with steel or ceramic rolling balls. Steel balls are used for smooth rolling soft materials, ceramic balls for hardened and hard-machined workpieces. Smooth rolling hardened surfaces, i.e. hard smooth rolling, can be used to reduce the surface roughness by half and to considerably increase the bearing contact area ratio.

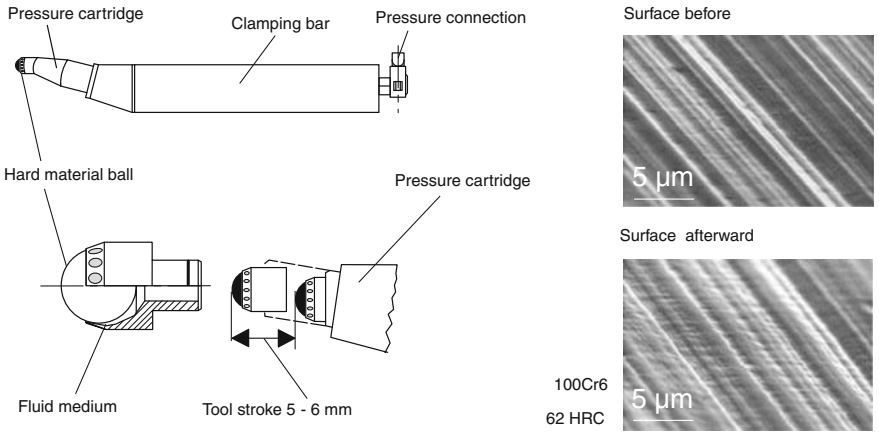


Fig. 3.103 Hydrostatically mounted smooth rolling tool, hard-turned and hard smooth rolled surface

3.5.2.2 Sizing Rolling

Whereas with large material diameters the application of rolling as a finishing method is limited to smooth rolling, as the diameter changes lie in the range of the starting roughness height, soft workpieces with small diameters ($d < 20$ mm) allow for a diameter change which goes way beyond this measure ($d \approx 0.1$ mm). This is then referred to as sizing rolling. With this process, workpieces with a diameter of 3 mm can be taken from tolerance quality IT 9–IT 5. Roundness errors of the pre-machined workpieces are similarly reduced (to ca. 1–1.5 µm).

3.5.2.3 Deep Rolling

In deep rolling, the goal of increasing the fatigue limit is essentially achieved by means of three factors:

- the removal of micro-notches on the workpiece surfaces,
- the strain hardening of the surface zone and
- the introduction of residual compressive stress into the workpiece surface zone which superimpose the load stresses, thus reducing the material stress in the tensile area.

The last factor dominates the effect on the fatigue limit of dynamically stressed components. Figure 3.104 shows the fatigue limit increases which can be realized using deep rolling with smooth and notched samples. The increase in the fatigue limit is plotted over the elastic limit $R_{p0.2}$.

Figure 3.104 (left) contains the achievable rotating bending fatigue limits of smooth, unfixed deep-rolled samples. It is clear that an increase in the fatigue limit

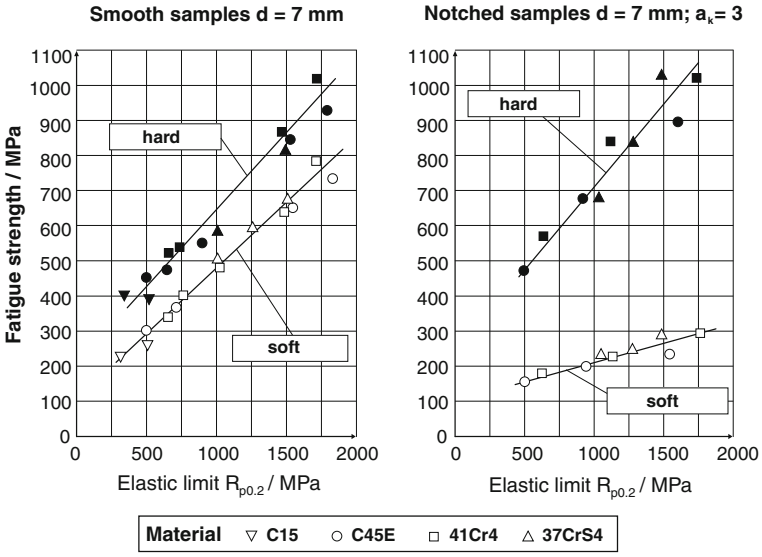


Fig. 3.104 Reverse bending strength of smooth and notched samples before and after deep rolling as a function of the 0.2 % elastic limit [LANG90b]

can be achieved in the regions of both low and high material strength. The increase in the fatigue limit achieved by means of deep rolling with a low elastic limit of up to approximately $R_{p0.2} = 900$ MPa is essentially due to an increased surface hardness, as the residual compressive stresses induced by deep rolling are almost completely broken down again through the external load [FUCH83, STRI71]. From an elastic limit of 1,400 MPa onwards, however, an increase in hardness is no longer possible. Consequently, the increase in fatigue limit in this case is exclusively achieved by inducing residual compressive stresses.

Figure 3.104 (right) shows the effects of deep rolling on fatigue strength behaviour for notched samples. It can be clearly seen that there is a relatively low increase in fatigue limit with increasing material strength in comparison to smooth, unfixed samples. In contrast, the notched deep-rolled samples demonstrate a considerable increase in the fatigue limit with increasing material strength. It follows that the increase in fatigue strength in the notched samples is more or less solely caused by the induction of residual compressive stresses. As a result of the large notch effect, strain hardening attributable to deep rolling only plays a subordinate role.

The introduction of residual compressive stresses therefore causes a considerable increase in the fatigue limit especially with brittle materials and notched components. A comparison of deep-rolled samples in smooth and notched states shows that the fatigue limit of the deep-rolled, notched samples is even higher. This makes it clear that, even with a large notch effect, the loss of fatigue strength present in an untreated state can be eliminated by deep-rolling the notch [FUCH83].

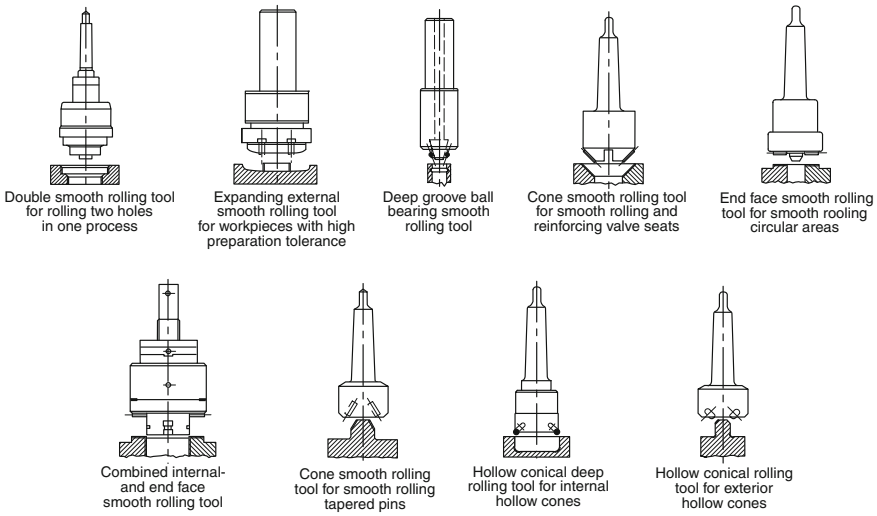


Fig. 3.105 Special tools for surface fine rolling (acc. to Ecoroll)

Typical components suited to deep rolling are hubs, knuckles, stepped shafts and crankshafts. In the case of crankshafts, for example, increases in fatigue limit of over 100 % can be achieved by deep rolling the grooves at the bearings [FELD84, TELG84].

In addition to single-purpose and special-purpose machines needed, for example, for deep rolling crankshafts, which usually operate in a force-fit manner, there is a series of special tools available for smooth and deep rolling bores and conical and plane surfaces (Fig. 3.105).

They offer the advantage of their small size and can be used in all conventional machine tools when finishing in a single clamping [FELD84].

Depending on the infeed system, they are to be categorized as form-locking, force-locking and expanding tools.

Prior to use, form-locking tools are set to the machining diameter. The tool diameter does not change during the machining process. The work result can be corrected by adjusting the tool diameter between machining operations.

Force-locking tools without presetting, on the other hand, are pressed against the workpiece surface with a defined force. The positioning of the smoothing rolls is determined by the workpiece geometry. Spring assemblies compensate both workpiece manufacturing tolerances and machine positioning errors and simultaneously provide an almost constant rolling force, thus guaranteeing consistent work results.

Expanding tools can change their working diameter during machining. The specified rolling force is set through mechanical, pneumatic or hydraulic impact.

For machining hydraulic and pneumatic cylinders, combined peeling and smooth-rolling tools are used (Fig. 3.106) which allow for peeling and smooth rolling in a single operation [TELG83].

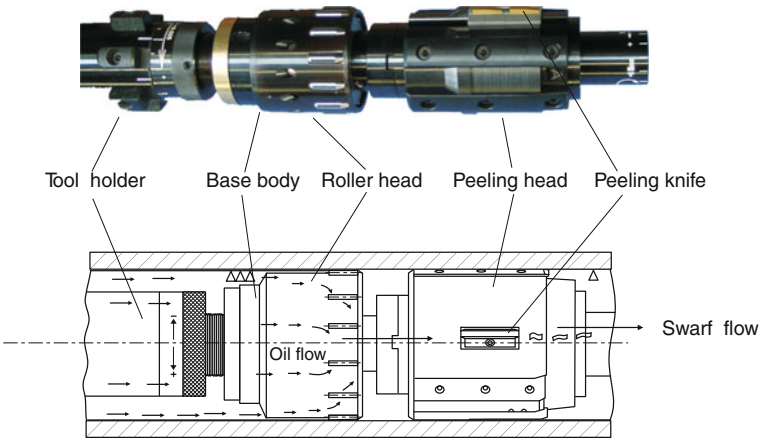


Fig. 3.106 Combined peeling and smooth-rolling tool (*Source* Ecoroll)

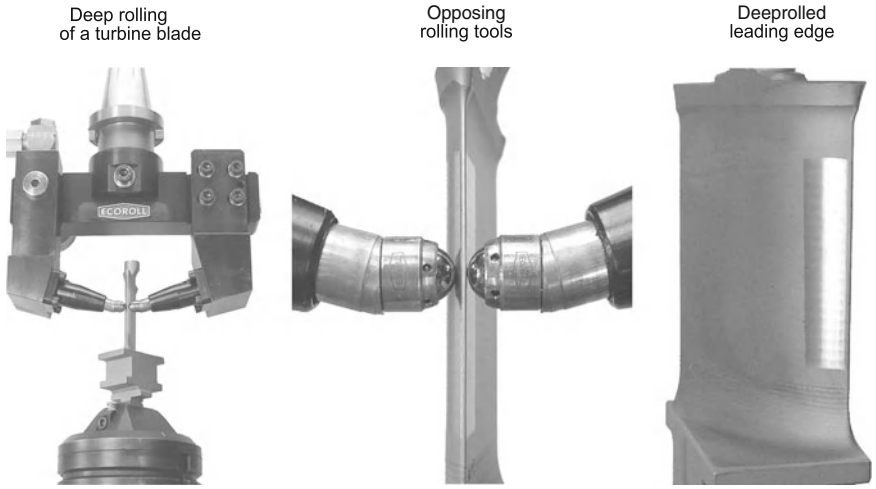


Fig. 3.107 Deep rolling of a turbine blade (WZL RWTH-Aachen)

Also, geometrically complex components are increasingly being subject to deep rolling processes. Figure 3.107 shows an example of this trend.

In the process illustrated, a turbine blade—i.e. a thin-walled workpiece with a free-formed surface—is subjected to a deep rolling operation in the area of the inlet edge. The deep rolling tool has two opposing hydraulically activated pistons with hydrostatically mounted balls which act on the blade from both sides. This construction both allows for the compensation of rolling forces and prevents the deflection of the thin-walled workpiece. As the rolling kinematics corresponds to a meander structure, the rolling tracks essentially run transversely to the blade and thus in the direction of potential crack propagation. Because high residual

compressive stresses are generated above all transverse to the rolling track, these are especially effective against crack formation and propagation. The process is of interest in particular for machining compressor blades for jet engines which are occasionally damaged by foreign objects drawn in the area of the blade inlet edges, from which cracks may propagate. The crack propagation rate can be significantly minimized by means of a deep rolling operation.

3.5.3 Materials Used in Rolling Processes

The question of rollable materials touches upon different issues, all of which, however, ultimately lead to the overarching question of acceptable production costs and tool lives. In principle, any plastically deformable material can be rolled.

The variety of rolling procedures for finishing purposes excludes any general statement regarding materials that can be used for these manufacturing processes. The local strains which take place in the individual processes represent the main criterion for the applicability of the materials.

For rolling tooth profiles according to the rolling-off principle, all alloyed and unalloyed carbon steels are basically suitable whose coefficient of expansion exceeds 7 %. The tensile strength R_m of these steels should lie between 600 and 800 MPa [KREI82]. For the Grob method of profile rolling, steels with less than 9 % elongation at fracture and tensile strengths $R_m > 1,200$ MPa provide limit values with respect to economical tool life [KRAP79].

Materials used in thread rolling should exhibit over 5 % elongation at fracture and tensile strengths $R_m < 1,200$ MPa. Structural and case-hardening steels, stainless steels and heat-treatable steels are thus appropriate. Other suitable materials are soft brass, copper, light metals and ferritic cast irons, such as GJS 400 and GJMB 350 [SCHU89, BETH82].

Materials unsuited to profile rolling are brittle materials with low elongation, such as grey cast iron, hard brass alloys and hardened materials.

The following materials can be surface fine-rolled, in part even in a hardened state [FELD84]:

- construction steels S185–E360,
- heat treatable steels C22–30 CrNiMo 8 in both a heat-treated and a non-heat-treated state,
- case-hardened steels C10–18 CrNi 8,
- spring steels 38 Si 6–58 CrV 4 with up to 1,500–1,600 MPa tensile strength,
- rust- and acid-resistant steels X 10 Cr 13 to X 10 CrNiMoNb 18,
- nonferrous metals, such as aluminium und Al alloys, duraluminium, anticorrodal, hydronalium, silumin, copper and Cu alloys, brass, bronze and red brass,
- cast irons from EN-GJS 140 to EN-GJS 300, malleable iron and especially spheroidal graphite cast iron (GGG).

In smooth rolling, the form of the graphite embedded in the cast iron should be fine-lamellar or spherolitic. The levels of quality achievable through smooth rolling cast iron do not correspond to the smoothing results possible for other materials [KROH65, GERL61].

The further development of micro-alloyed steels with the elements boron, niobium or vanadium, all of which exhibit the forming properties of unalloyed steels while still being able to reach the same strength values as chromium-alloyed steels when subjected to special heat treatments, also expands the range of applicable materials [DOMA80].

3.5.4 Tool Materials Used for Rolling Processes

Only general statements can be made regarding tool materials for rolling processes. For example, whereas in smooth rolling a uniform wear can be tolerated in part over the roll width and circumference, it necessarily leads to the replacement of the tool in thread rolling. The requirements placed on the tool materials in profile rolling are accordingly higher than for smooth rolling tools. In thread rolling, there is an additional increased notch sensitivity on the part of the tool, as the engraved profile is to be equated with a notch, which can lead to premature break-out of the rolls, especially given high forming activity. High chromium alloyed steels stand up to these wear criteria most effectively. The ledeburitic steel X 210 Cr 12 is recommendable in this case [APEL53]. Thread rolling tools are usually reground multiple times. When using the material mentioned above, this causes an up to 10 % reduction in the tool life of the reground tool, although the tools are heat-treated after grinding. The method of manufacturing of the thread rolls is also of special importance for tool life. In analogy to the increased loading capacity of rolled threads, the service life of thread rolling tools manufactured in a forming process is also about 90–100 % higher than that of ground tools [APEL53].

In recent times, high-speed steel (e.g. S-2-10-1-8) is increasingly used in the manufacture of profile rolling tools for rolling spline shafts. Newer developments have the aim of using high-speed steel prepared by powder metallurgy (e.g. ASP 60).

3.5.5 Friction and Lubrication

In thread and profile rolling, unlike chip-removing forming processes, lubricants are almost exclusively required for their lubricating effect. For this reason, typical drilling-oil emulsions are unsuited to these methods. They cause crooked thread flanks as a result of the direct contact between the workpiece and the tool and lead to a tool life reduction of up to 30 % [APEL53]. However, the abrasive wear of the

tools can be reduced by adding a high-pressure additive in the form of Molykote or colloidal graphite [APEL53, GERL61]. Tool life can also be significantly extended by phosphating the workpieces, as this measure essentially increases the absorption capacity and adhesiveness of the lubricant [SCHI62] (see Sect. 2.8.4.2).

For the purpose of surface formation in smooth rolling, lubricants can be dispensed with in part. *However, molybdenum disulfide compounds reduce the wear of the smoothing rolls* [APEL53]. The use of automatic smooth rolling units also requires workpiece cooling and the rinsing-off of very fine surface particles in addition to lubrication.

If the surface of the workpiece to be processed exhibits marked pores or high roughness heights, such as those found in cast iron, a lubricant may not be used, as the lubricant entering the pores can cause changes to the loading condition of the workpiece possibly leading to failure as a result of the hydrostatic pressure generated during rolling.

Chapter 4
Sheet Metal Forming

4.1 Deep Drawing

Deep drawing is the most important manufacturing process for producing sheet metal workpieces with a three-dimensional geometry. It is employed in large series production, such as in the automotive and packaging industries, and also in small series production, as typical of the aircraft industry. Deep drawing occupies a special place in sheet metal working. DIN 8584-3 [DIN03h] defines this process as follows: "Deep drawing is the forming of a flat sheet blank (or foil/plate, section/blank, depending on the material) into a hollow shape of a hollow shape to a hollow shape with smaller perimeter by pressing it through a die without intended change of the sheet thickness."

The essential prerequisites for achieving optimal work results in deep drawing are the correct control of the material flow, the determination of the blank dimensions, the knowledge of the limits to which the forming can be driven within a single operation and the estimation of the force required to shape the blank.

4.1.1 Principles of Deep Drawing

4.1.1.1 Process Principle

The process principle will be explained in the following on the example of a circular cylindrical drawn part. Figure 4.1 shows the corresponding tool used. The blank, in this case a circular sheet blank, is placed on the drawing die. When the punch is lowered, the sheet is drawn through the opening of the drawing die, with the sheet material flowing behind in such a way that the outer diameter of the circular sheet becomes smaller. After the drawing, during which the hollow shape is formed, the punch is raised again. Since the sheet expands, the upper edge of the drawn part strikes against the lower edge of the drawing die and the cup is stripped from the punch. The cup can also be stripped by means of other devices. This is especially required when the finished part is to have a flange neck, which would make a drawing of the sheet through the drawing die impossible. A blank holder is

F. Klocke, *Manufacturing Processes 4*, RWTHedition,
DOI: 10.1007/978-3-642-36772-4_4, © Springer-Verlag Berlin Heidelberg 2013

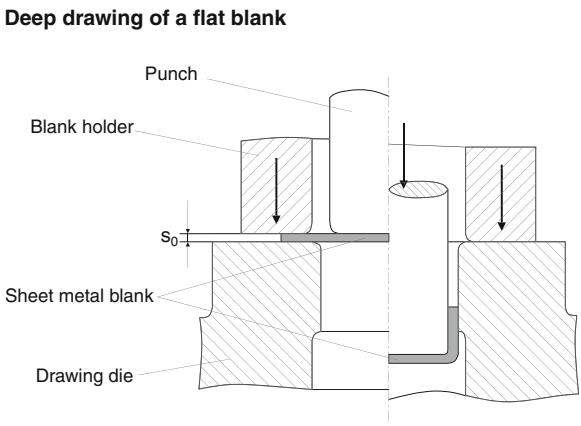


Fig. 4.1 Deep drawing of a cup from a *flat circular* sheet

indispensable as a rule. It fixes the circular sheet before the punch is applied, which prevents the formation of wrinkles in the area of the flange Fig. 4.2 shows sample applications of deep drawing.

During the forming of the flat sheet blank, the material is stretched and compressed (Fig. 4.3). The surface corresponding to the cup bottom is only minimally formed. The circular ring area between the initial circular sheet diameter d_0 and the inner cup diameter d_1 becomes the cylindrical skirt of the cup. The triangular parts b of the plate must be displaced during forming. By folding up the segments



Fig. 4.2 Sample applications: deep-drawn parts used in the automotive industry (*source* BMW AG)

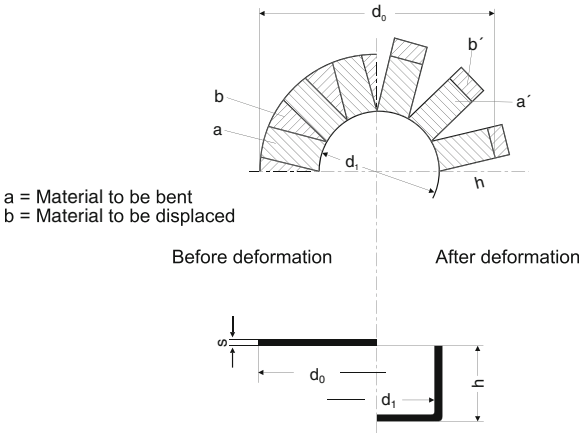


Fig. 4.3 Forming of a *circular* sheet

and adding up the surfaces b' (coextensive with b), one receives the final cup height h. This naturally only applies given a constant sheet thickness.

The dimensions and geometries of the initial blank sheet are thus chosen according to the shape and size of the workpiece to be manufactured. For circular drawn parts, the initial circular sheet form can be calculated relatively simply from the volume constancy. If one assumes that the sheet thickness remains constant during forming and is generally small in comparison to the external dimensions, one receives a circular sheet surface with the diameter d_0 from the finished part surface A_z:

$$d_0 = \sqrt{\frac{4}{\pi} \cdot A_z}. \tag{4.1}$$

For calculating round drawn parts, a subdivision into single surface elements is recommendable. The selection in Figure 4.4 is usually sufficient even for more complex shapes. Due to fluctuations in sheet thickness and other influence factors, the calculation is only approximate. A subsequent trimming of the workpiece or a correction of the blank is often necessary. This is executed using samples.

For more complex drawn parts, e.g. angular hollow bodies and car body parts with totally irregular geometries, the calculation of the dimensions of the blank is considerably more difficult. In these cases, the finished part must be unwound to give information about the form and dimensions of the initial blank sheet [TSCH77, HILB70, OEHL01, SIEB55].

4.1.1.2 Admissible Deformation

The force required for forming acts only indirectly on the plastic processes in the forming zone. This is because the forming zone lies in the flange and the area of the drawing die curvature, whereas the force from the punch is introduced via the

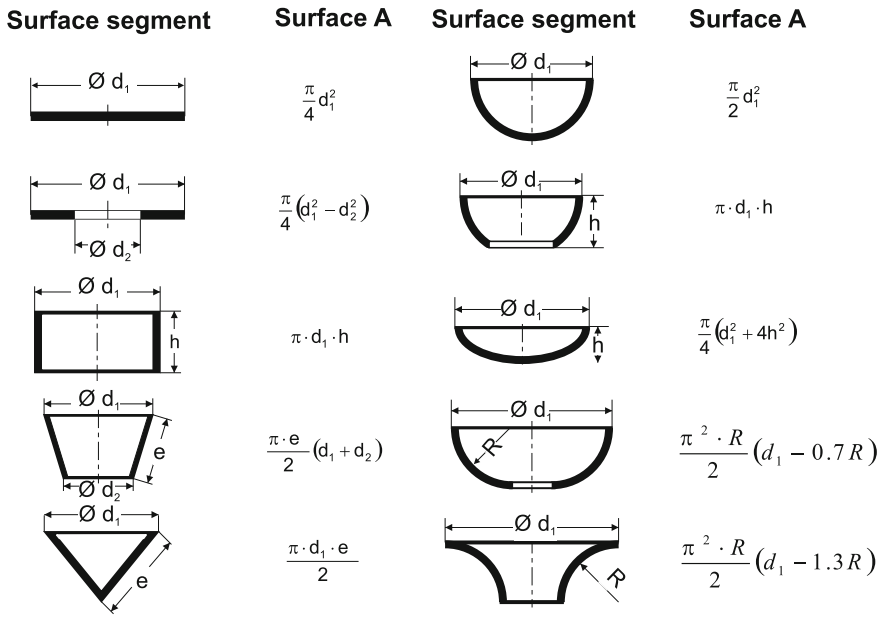


Fig. 4.4 Selected surface elements for calculating the blank dimensions (acc. to Oehler/Kaiser [OEHL01])

cup bottom, the transition of bottom to wall, and the wall itself. This causes high tensile stresses, above all in the cup wall and the area of the punch curvature, which can lead to wall losses and tends to cause crack formation in these locations.

Figure 4.5 shows the progression of a volume element during the different stages of the deep drawing process. As long as the element is still located in the

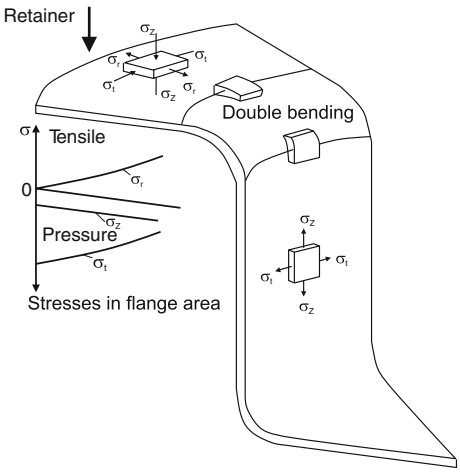


Fig. 4.5 Stress conditions during the deep drawing process

flange of the cup, tensile stresses arise in the radial (σ_r) direction and compressive stresses in the tangential (σ_t) direction. The element is stretched in the radial direction and compressed in the tangential direction.

If there is no blank holder and the buckling stability of the sheet is exceeded by the tangential compressive stresses, wrinkles will form in the flange area. The blank holder creates a compressive stress in the axial direction (σ_z) which acts against the formation of wrinkles. However, this compressive stress leads to additional friction between the sheet and the blank holder and between the sheet and the drawing die. If the blank holder pressure $p_N (p_N = \sigma_z)$ caused by the blank holder force does not exceed the maximum value $p_{Nmax} = 10$ MPa common in practice at the beginning of the forming process, the stresses are hardly influenced by it [SCHL77]. A more exact calculation of the blank holder pressure is provided by Eq. 4.8.

When proceeding from the flange to the cylindrical skirt, the sheet is subjected to a double bending stress. The sheet is bent at its radius at the beginning of the drawing die curvature. A reverse bending occurs at the end of the blank holder curvature into the straight, cylindrical part of the cup wall (Fig. 4.6). Finally, in the cup wall, tensile stresses predominate in the axial direction which result from the radial stress in the sheet flange, the bending stresses at the drawing die curvature and the friction influences [WILH75] .

Depending on the predominant stress condition, strains of the drawn parts are distributed among the main radial and tangential stress directions as well as perpendicular to the sheet plane. If the right-angled material element shown in Fig. 4.6 is stretched in its longitudinal direction, the length l_0 increases to l_1. The true strain φ_1 is characteristic for this. Because of the constant volume, the width b_0 is reduced to b_1 and the thickness s_0 to s_1. The sum of the true strains yields

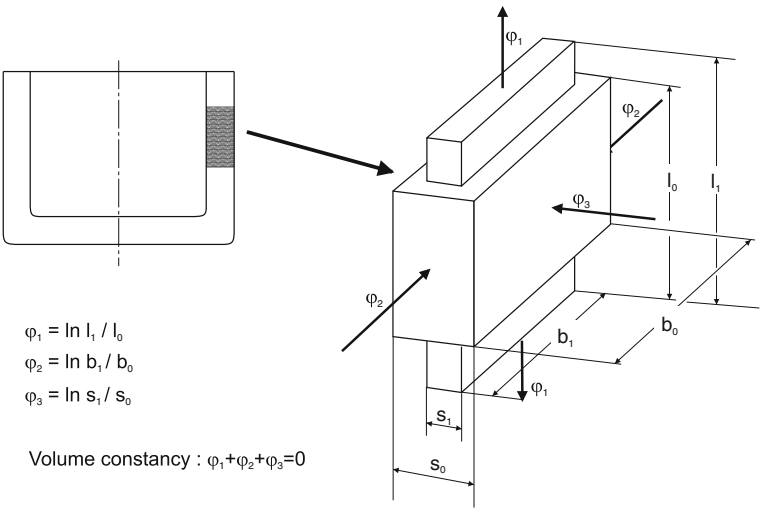


Fig. 4.6 Strains on a volume element

zero. In the case illustrated here, therefore, the strain φ_1 is positive and the strains φ_2 and φ_3 are negative.

Since the sheet is subjected during deep drawing to highly variant stress states, the true strains are distributed very unevenly in the finished cup. Directly after the punch is applied to the plate, the deformation is limited to the drawing die surface between the punch and the drawing die and to the final cup bottom. During this phase, a purely biaxial stress state prevails which is superimposed with an increasing punch path by a bending around the punch rounding and die radius [OEHL01]. For this reason, the original sheet thickness s_0 is only maintained at the cup bottom centre. It decreases considerable towards the bottom edge because of stretching. Its lowest value is reached in the area of the punch edge rounding. This is where cracks tend to appear.

If the sheet material attaches itself to the entire punch rounding, a tension–compression stress state is generated with an increasing punch path. Due to the tangential compression of the sheet, the sheet thickness increases again in the side wall of the finished cup as the cup height increases, reaching a maximum value at the upper cup edge which is greater than the initial sheet thickness s_0. In order to prevent a thinning of the material, however, the die clearance must be greater than the initial sheet thickness.

Since local strains cannot be calculated in advance and the sheet thicknesses can hardly be metrologically determined, especially given more complex shapes, line networks are usually used for experimentally determining the true strains. These are mounted on the circular sheet prior to the forming process (see Sect. 2.4.6). The true strains can be determined in the tangential and axial directions on the basis of the deformations of the measurement grid. The true strain in the direction of the sheet thickness is calculated with the continuity equation

$$\varphi_1 + \varphi_2 + \varphi_3 = 0. \tag{4.2}$$

Figure 4.7 shows the progressions of the true strains φ_1, φ_2 and φ_3 over the processing of a deep-drawn cup. The sheet thickness is either greater or smaller depending on the sign of true strain φ_3.

Especially in the case of complicated parts, it may be unavoidable to analyze the conditions at particularly critical locations with the aid of the line network method in order to take corrective measures with respect to the tool shape, the blank outline or even the sheet material, where applicable. In the case of rectangular drawn parts, for example, the material accumulates at the edges, while being drawn at the centres of the sides largely without hindrance, with the exception of a light bending stress. Due to arising stress differences, there is danger of tearing in the edge areas. Thus the material flow must either be relieved at the edges or hindered/stopped at the side centres. This can be achieved, for example by attaching so-called beads.

One can use the forming limit diagram (Sect. 2.7.3.5) to judge whether the respective stretch combinations lie in the critical area, causing a contraction of the sheet and thus possible cracks [MÜSC72].

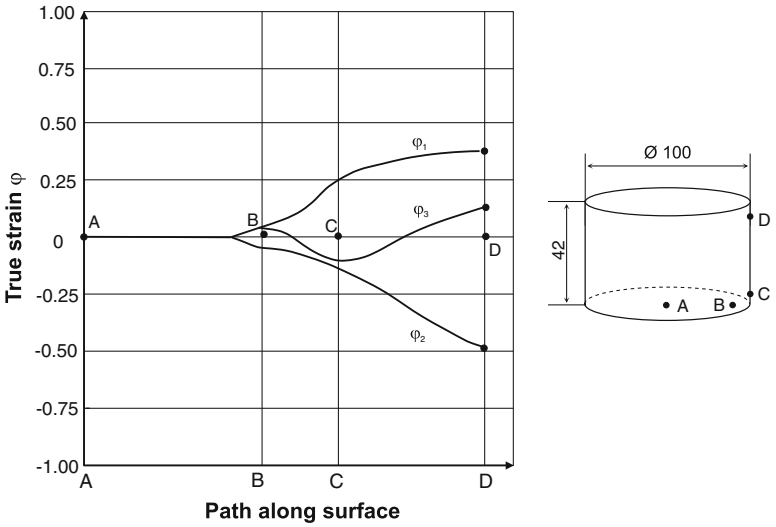


Fig. 4.7 Progression of the true strains over the processing of a deep-drawn sheet metal cup (acc. to Oehler/Kaiser [OEHL01])

With the effective strain

$$\varphi_V = \sqrt{\frac{2}{3}\left(\varphi_1^2 + \varphi_2^2 + \varphi_3^2\right)} \tag{4.3}$$

one can say something about the strength characteristics at the observed position of the workpiece by using the flow curve (see Sect. 2.4.2).

A variable describing the extent of the deformation of a drawing process is the drawing ratio β, defined as the quotient of the initial circular sheet diameter d_0 and the inner diameter d_1 of the cup (punch diameter) in the first draw.

$$\beta = \frac{d_0}{d_1} \tag{4.4}$$

For further draws, the drawing ratio is determined from the decrease of the inner cup diameter. To characterize the individual forming steps, the drawing ratio β is given an index. The index 0 refers to the first draw, the index 1 the first redraw, etc.

The drawing ratio has an upper limit. As the drawing ratio rises, the maximum draw force F_{Zmax} increases given equal conditions. Since this force must be transferred from the cylindrical skirt of the drawn part, when β is too high, the bottom rim tears as a result of an excessive tensile or elongation load. As characteristic value for the forming limit, the drawing limit ratio β_{max} may not be exceeded in the deep drawing process. High draw depths can only be achieved gradually by means of intermediary softening operations, where applicable.

The drawing limit ratio is a function of the dimensions of the blank and the tool geometry, but it is also influenced by further parameters, such as sheet material, blank holder force, and friction conditions. Thus the distinction must be made when choosing a drawing ratio between redraws with and those without prior intermediate annealing. In redraws, the drawing ratio during strain hardening is respectively smaller during the previous draws as in the last draw. For unalloyed soft steel sheets, for example, the drawing ratio in the first draw amounts to up to $\beta_0 = 2.0$, while in the first redraw without intermediate annealing a figure of is possible $\beta_1 = 1.3$, and with intermediate annealing $\beta_1 = 1.7$.

With increasing punch diameter relative to the sheet thickness, the drawing limit ratio decreases due to more unfavourable friction conditions. The friction behaviour is additionally influenced by the material combination of workpiece and tool, the surface condition of the friction partners, lubrication and the blank holder pressure, so changes to these parameters also affect the drawing limit ratio.

4.1.1.3 Forces

In order to design tools and select the appropriate machines, the forces must be determined in advance, among other things. Because of the many influence factors, the corresponding calculations are generally not made with the aid of the theory of plasticity, but rather by applying empirical formulae.

Drawing Force

When deep drawing a cylindrical cup (Fig. 4.1), the drawing force is primarily a function of the mean yield strength, the punch diameter, the circular sheet diameter and the sheet thickness.

As analogous to the stresses, the drawing force F_Z comprises the ideal drawing force F_{Zid} for lossless deformation and the increases in force arising from the friction on the drawing die rounding and the blank holder (F_R) and from the bending of the sheet on the drawing die rounding (F_b).

According to Siebel and Weiss [SIEB54], the increases in force are accounted for by an efficiency of deformation η_F:

$$F_{Zmax} = \pi \cdot d_m \cdot s_0 \cdot \left[1.1 \cdot \frac{k_{fm}}{\eta_F} \cdot \left(\ln \frac{d_0}{d_1} - 0.25\right)\right]. \tag{4.5}$$

In this equation, d_m is the mean cup wall diameter

$$d_m = d_1 + s_0, \tag{4.6}$$

k_{fm} the mean flow stress in the flange area and η_F the efficiency of deformation, defined as the quotient of the ideal deformation energy and total deformation energy actually used. The efficiency of deformation ranges in deep drawing

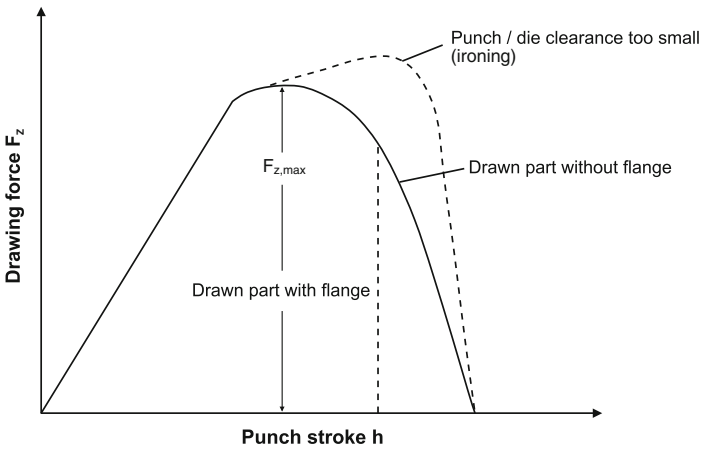


Fig. 4.8 Drawing force diagrams [OEHL01]

between 0.5 and 0.7, with the low values corresponding to thin-walled and the high values to thick-walled cups. For the average flow stress k_{fm} in the flange, the following connection to the initial tensile strength R_m can be roughly assumed:

$$k_{fm} \approx 1.3 \cdot R_m. \tag{4.7}$$

Equation 4.7 also takes account of the fact that the drawing force only achieves its maximum value after a certain punch path.

Figure 4.8 provides drawing force diagrams for the progression of the drawing force as a function of the punch path. At the start of the stroke, i.e. shortly after the punch is applied to the circular sheet, the drawing force rises sharply in proportion to the strain hardening of the material. According to Siebel and Beisswänger [SIEB55], the drawing force achieves its maximum value after approximately 25 % strain, i.e. when the current outer diameter of the circular sheet corresponds to ca. $0.75 \cdot d_0$ (see Eq. 4.5). If the die clearance is too narrow, there is a thinning of the material and thus a reduction in sheet thickness. The maximum value of the drawing force, however, is only reached after a larger punch path. If the drawn part is not completely drawn through because a flange is to remain, the drawing force sinks sharply to zero. Given a completely deep-drawn cup with no flange, the force curve falls more slowly, since the strain-hardened areas at the margin of the cup require additional force. The force required for deep drawing corresponds to the area beneath the respective drawing force curve.

Blank Holder Force

The blank holder has the task of preventing undesirable wrinkles formation caused by the buckling of the sheet flange by means of tangential compressive stresses. The fulfilment of the task requires a minimum pressure which the blank holder

applies to the circular sheet blank. However, the blank holder pressure may not be too great, as this would slow down the sheet too much, which can cause bottom tears (Sect. 4.1.5).

According to Siebel and Beisswänger [SIEB55], the blank holder pressure required to avoid wrinkles formation can be calculated using the following formula:

$$p_n = 0.002...0.003 \cdot \left[(\beta - 1)^3 + \frac{0.5 \cdot d_1}{100 \cdot s_0}\right] \cdot R_m. \tag{4.8}$$

The optimal blank holder pressure is therefore a function of the drawing ratio, the ratio of the punch diameter d_1 to the sheet thickness s_0 and the strength properties of the material to be formed. Figure 4.9 shows a nomogram for determining the blank holder pressure. The specifications relate as in Eq. 4.8 to round, cylindrical drawn parts. For irregular forms, the required blank holder pressures can hardly be determined without samples.

The force F_N exerted by the blank holder is calculated from the blank holder pressure and the surface A_N pressurized by the blank holder:

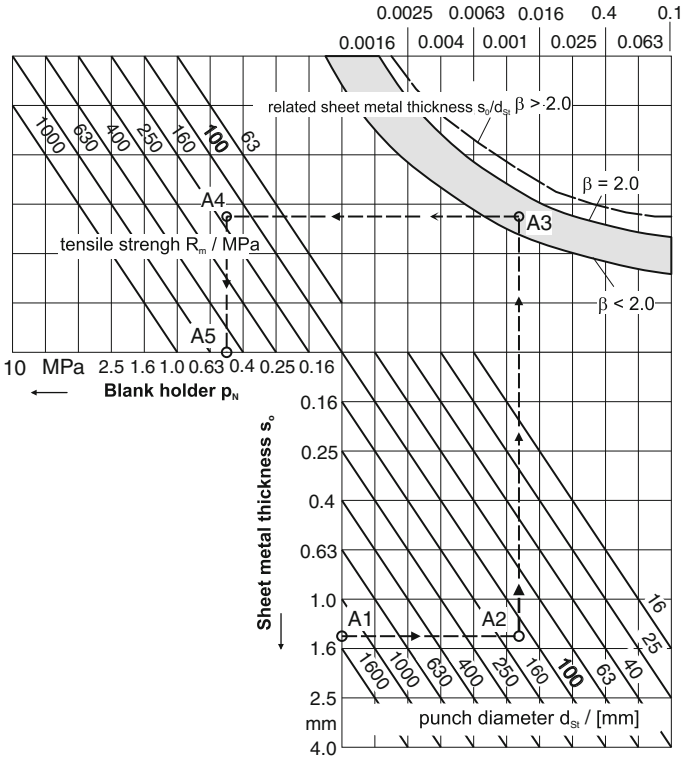


Fig. 4.9 Blank holder pressure for deep drawing *round*, *cylindrical* parts in the first draw [OEHL01]

$$F_N = p_N \cdot A_N. \tag{4.9}$$

To calculate the surface A_N, one must account for the initial circular sheet diameter d_0, the punch diameter d_1, the die clearance u_z, as well as the drawing die radius r_R.

$$A_N = \frac{\pi}{4} \cdot \left[{d_0}^2 - (d_1 + 2u_z + 2r_R)^2 \right]. \tag{4.10}$$

As a rule, the blank holder pressure is specified as initial pressure at the beginning of the deep drawing operation. The flange surface is reduced with increasing deformation, which causes an increase in the specific surface pressure given a constant blank holder force. The sheet thickness continues to increase on the outer edge during the necking. For this reason, there are several options for adjusting the blank holder force to the punch stroke. These will be treated in Sect. 4.1.3.

4.1.1.4 Friction, Lubrication

Friction conditions have a decisive influence on the deep-drawn product, especially when large parts, such as in automotive construction, or extremely thin sheets are drawn.

Friction between the tool and the circular blank is generated in three different zones:

1. on the sheet supporting surface on the drawing die or the blank holder,
2. on the die radius rounding,
3. on the punch edge rounding.

The friction in zones 1 and 2 significantly influences the extent of the required drawing force. A reduction in friction in these locations leads to a lower maximum drawing force, which means the true strains in the sheet flange are higher and greater drawing limit ratios β_{max} can be realized. The friction in these zones, which constitute the actual deformed zone, should thus be kept as low as possible. By means of a suitable lubricant [MANG83] and the use of plastic-coated steel sheets, the drawing limit ratio can be raised accordingly.

The percentage of friction forces in the total drawing force increases with increasing drawn part size or with decreasing sheet thickness s_0, i.e. with an increasing d_0/s_0 ratio (Fig. 4.10) [DOEG71].

As opposed to the friction in the flange area, the friction conditions in the area of the punch edge rounding positively influence the maximum punch force transferable from the drawn part bottom into the cup wall. The drawing limit β_{max} increases in proportion to the friction on the punch edge rounding, as a greater force is available for deformation.

Lubricants and protective coatings are used in practice in order to prevent drawing defects, especially the tearing of the material, even given relatively high true strains. At the same time, lubricants can reduce manifestations of tool wear and improve the surface quality of the workpiece.

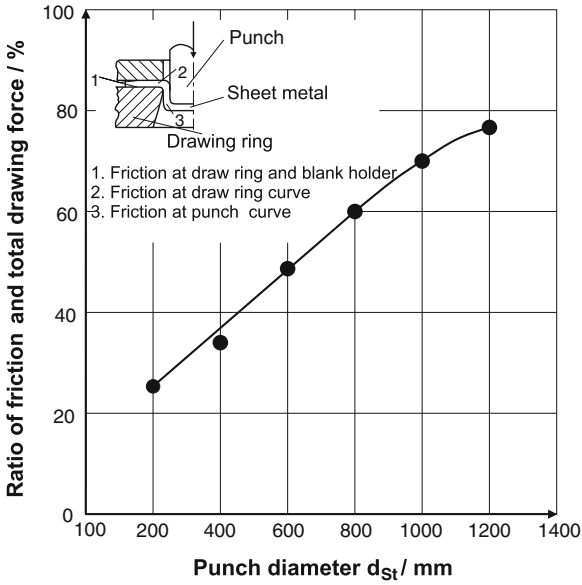


Fig. 4.10 Proportion of friction force in the total drawing force as a function of punch diameter [DOEG71]

Mang [MANG83] uses the sheet material and the level of difficulty as criteria for selecting lubricants and suggests suitable lubricants for the different classes. According to his model, primarily fluid lubricants (difficulty levels a to d), sometimes solid (difficulty levels c to e) or past-like lubricants with a fat or mineral-oil base are used for simple deep drawing steels (low-carbon thin sheets) [MANG83].

In addition to the pure oils, however, additives to fluid lubricants made from solid substances with a natural lubricant effect are also employed. If the sheet parts to be manufactured are to be subjected to a galvanic aftertreatment, it is recommendable to use sprayable or insertable plastic films which both protect the sheet surface and increase the tool life as a result of eliminating the metallic contact between the sheet and the drawing die [MANG83]. Such films are also used for austenitic, stainless high-grade steels. A measure rarely employed for reducing friction is, for example, to phosphate or copper-plated the sheets prior to forming, something only done under the most difficult forming conditions.

4.1.2 Process Variants and Examples of Use

4.1.2.1 Deep Drawing with Rigid Tools

Deep Drawing Without Blank Holder. The question of whether or not the use of a blank holder is necessary depends on the ratio of the sheet thickness to the diameter difference $d_0 - d_1$. The use of a blank holder is normally necessary if the following applies:

$$s_0 \leq 0.2 \cdot (d_0 - d_1). \tag{4.11}$$

For sheet thicknesses which do not fall into this range, i.e. for relatively thick sheets, a blank holder is no longer necessary, as the buckling stability of the sheet is then sufficiently great to bear the tangential compression occurring during the process without wrinkle formation in the flange area (Sect. 4.1.1.2). The advantage of deep drawing without a blank holder is that the tools are made up of more simple construction. Since any friction between the sheet and the blank holder does not apply here, the punch force required is reduced. Moreover, single-acting presses can be used.

However, deep drawing with no blank holder usually necessitates the use of a modified geometrical form for the drawing die. The simplest possibility consists in an enlargement of the rounding radius, which then allows a drawing limit ratio of up to $\beta_{max} = 2.8$ for steel sheets in the first draw. Another method is drawing the metal sheet through a conical infeed opening of the drawing ring. If possible, the starting diameter of this opening should be as large as the blank diameter of the circular sheet.

A so-called tractrix infeed (Fig. 4.11) allows a considerable reduction in punch force in comparison to the conventional drawing die shape. The use of a tractrix curve profile is based on the idea that the margin of the circular sheet is constantly supported by the drawing die. In this way, the lever length is constantly at a maximum, which minimizes the required bending force on the one hand while working against wrinkle formation by means of high surface pressure on the wall rim on the other [MAY61]. Other studies have demonstrated that varying the die radius geometry can help to reduce the normal contact stresses and thus the probability of tool failure. A proper adjustment of the infeed edge allows for an even distribution of the required surface pressure, thus reducing the maximum loading [KLOC04b].

When deep drawing without a blank holder, wrinkle formation and bottom tears set an upper limit for the achievable drawing ratio. But also falling below a certain drawing ratio can lead to a case of failure: so-called shell formation, in which a cup is formed without a cylindrical wall [KÜBE81, OEHL01].

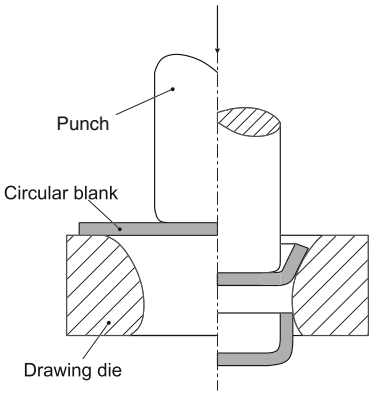


Fig. 4.11 Drawing die with tractrix infeed

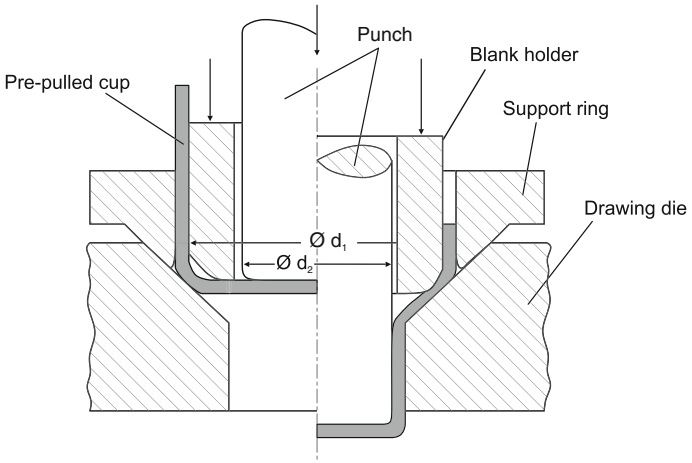


Fig. 4.12 Drawing tool for redraw

Multi-Stage Deep Drawing. Since the drawing ratio is limited by the maximum drawing force (Sect. 4.1.1.2), greater drawing heights can only be achieved in stages. Figure 4.12 shows a tool for a redraw of a predrawn cup.

Conical, spherical and parabolic shapes are often not producible in a single draw, even though the corresponding drawing limit ratio has not been exceeded. This is because a large section of the circular sheet (between the tip of the drawing punch and the shoulder of the drawing die) is not under the pressure of the blank holder. Until the sheet lies against the punch, therefore, this part of the surface would then have to be freely—i.e. without form-locking support—bent or deformed. A wrinkle formation would be inevitable in this case. For this reason, stepped cylindrical shapes are manufactured in multiple draws, being shaped in a calibration draw to the desired final contour.

Figure 4.13 shows the drawing steps for producing a lamp reflector. In order to prevent wrinkle formation reliably, the manufacture of the reflector in this example requires a subdivision into four predraws and one calibration draw. It is often inevitable that marks are made in the sheet by the individual drawing stages, which makes the subsequent polishing work more difficult. A remedy in this respect is provided in the form of deep drawing processes with active media (Sect. 4.1.2.2).

Deep Drawing With Beads. Draw beads are used in order to influence the material flow during the forming process. There are two kinds of draw beads: inflow beads and lock beads.

Inflow beads are fixed around the circumference of the die radius (Fig. 4.14). It functions to prevent wrinkle formation with conical, parabolic or spherical drawn parts on which there are relatively large material areas not directly subject to pressure. As a rule one wrinkle formed, it can no longer be removed. For this reason the condition in the deformed zone must be influenced in such a way that the tangential compressive stresses leading to wrinkle formation are kept as low as

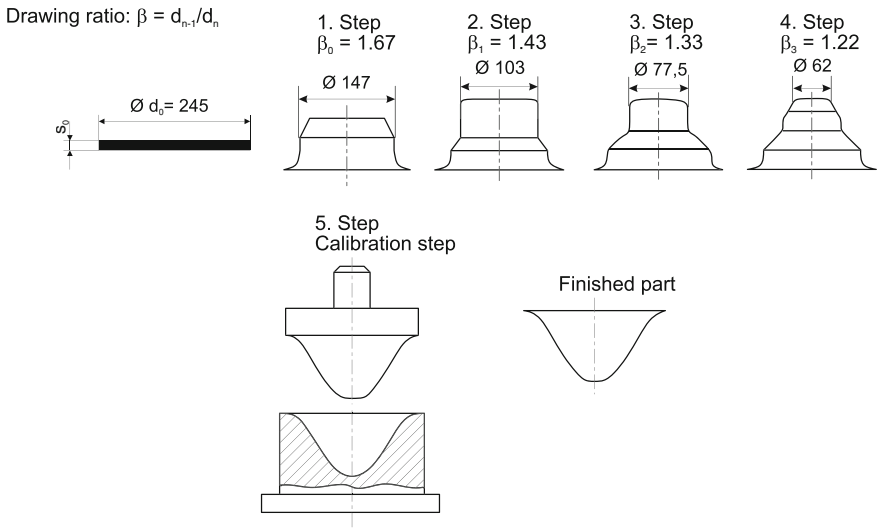


Fig. 4.13 Deep drawing of a *conical* workpiece with *cylindrical* intermediary draws

possible. The use of inflow beads achieves this insofar as the material is compressed slightly when slipping between the blank holder and the draw bead, since the die clearance is smaller than the sheet thickness and bent over the bead during the draw. This pre-deformation has the effect of increasing the radial stresses and lowering tangential stresses [VDI00].

Lock beads are important in the case of large-scale tools and especially of irregularly shaped, angular drawn parts, e.g. car body parts. They aid in controlling the material flow and are arranged on locations in which the material would slip

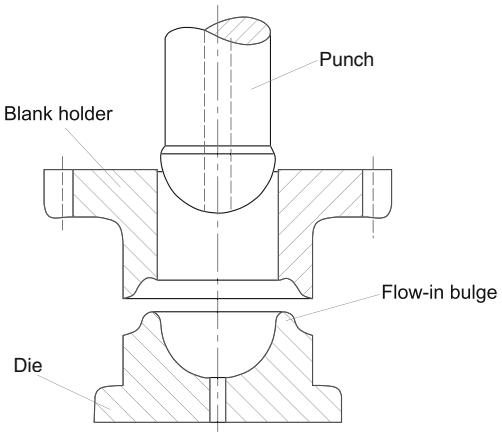


Fig. 4.14 Deep drawing using inflow beads

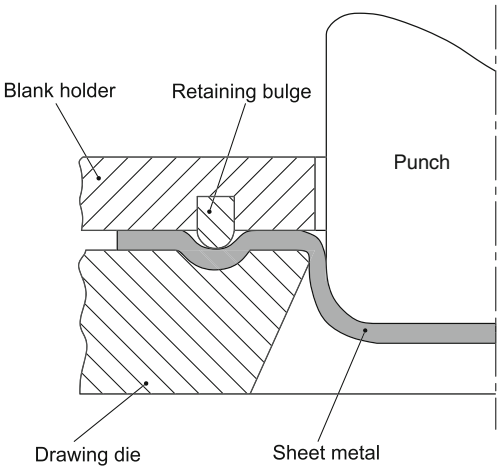


Fig. 4.15 Drawing tool with lock bead in the blank holder

too easily over the die radius. For this purpose, the drawing rods are placed in the blank holder of the deep drawing tool at a certain distance to the die radius (Fig. 4.15). Through the repeated redirection of the sheet in the flange, the sheet is subject to a local resistance at the relevant locations. In this way, the difference between the stresses in the side walls and the edges, one which could result in the failure of the operation, can be reduced, even given complicated parts. The material then flows almost evenly into the deformed zone, as in cylindrical drawing [HASE81]. In the case of rectangular parts, for example, the lock beads are only mounted on the side centres for this reason, although here there may be two, three or even more.

In addition to number and length, the height and rounding of the drawing rods are also decisive for the material flow. There are multiple ways to attach draw beads, provided that they aren't incorporated into the model for the casting mould [OEHL01, VDI00]. Exchangeability must be taken into consideration here. It may for example only become apparent over the course of production whether parts of the bead should be left out, other beads should be mounted or different geometrical shapes should be used. Recent studies [HASE80a] have concentrated more closely on the influence of drawing rods on the forming conditions.

Reverse Drawing. As opposed to deep drawing in steps, in which forming is executed in the same direction as the previous draw (Fig. 4.12), the punch in a reverse drawing operation moves in the opposite direction of the previous draw [DIN03h].

In the simplest case, the predrawn cup is placed on a reverse drawing ring and drawn by the punch through the die radius of the reverse drawing ring (Fig. 4.16 left). By reversing the direction of motion, the outer side of the cup now faces inwards and the inner side of the cup is turned inside out.

An important advantage of reverse redrawing lies in the fact that the first draw and the reverse draw are executed in a single operative step, i.e. with one tool during one press stroke (Fig. 4.16 right). This apparently increases the drawing ratio in one

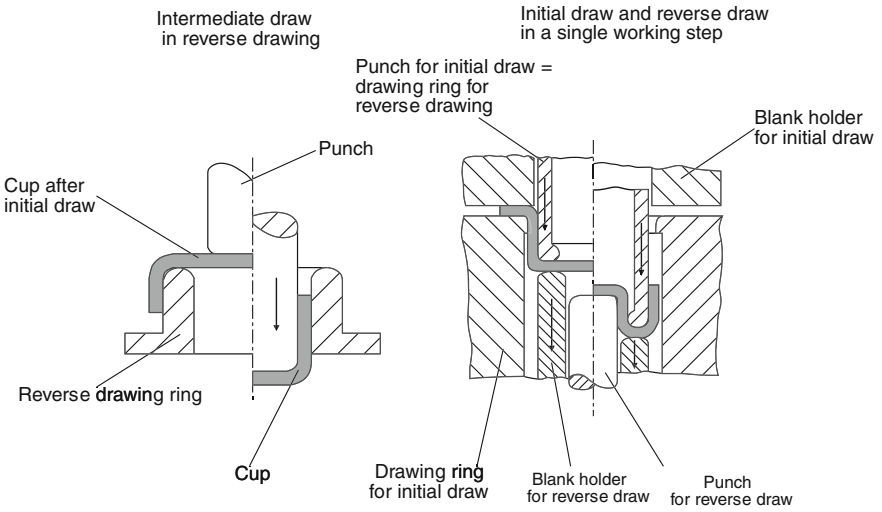


Fig. 4.16 Reverse redrawing

draw, though it is in fact a double draw in which the reverse drawing ring first serves as a hollow punch for the predraw and then as a drawing die for the reverse draw.

The tool arrangement is similar in operation to that of a lock bead and thus well suited to prevent wrinkle formation. One must not overlook the fact, however, that the tensile stresses superimposed in the process represent a strong load on the workpiece material and often lead to crack formation. Because of the high machine output required, therefore, the reverse drawing process is limited in practice with respect to maximum sheet thickness, the deep drawing properties of the material and the geometrical dimensions of the sheet-metal part to be formed. In addition, the process requires relatively long-stroke, sometimes triple acting presses. With respect to achieving the most even punch force progression possible via the press stroke, one must bear in mind that the cup bottom already steps onto the reverse drawing punch as long as a sheet flange is still present, and thus the predraw is not yet complete [OEHL64a, RADT65].

Ironing. As opposed to pure deep drawing, in which changes to wall thickness are unintended, ironing is used for workpieces for which the wall must have a lesser wall thickness than the bottom (e.g. beverage cans). The drawn parts are often preformed using another drawing tool in preceding work steps and then drawn to the required dimensions in an ironing draw. The drawing process is the same as for normal deep drawing. Differences in wall thickness arise by virtue of the fact that the gap between the punch and the drawing die corresponds to the desired lower sheet thickness (Fig. 4.17).

The forces which arise depend on the yield strength of the material, the ironing angle α, the friction conditions and the diameter change of the drawing die or the reduction of the wall thickness of the drawn part. The force transmission responsible for material forming between the ironing die and the punch is transferred via

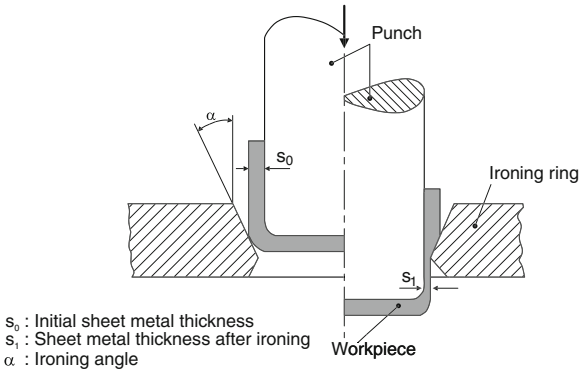


Fig. 4.17 Schematic diagram of ironing

the bottom of the drawn part and directly via the frictional engagement of the drawn part and the punch. Therefore, depending on the angle of the ironing die and the roughness of the punch, higher forces than the material strength in the bottom and wall areas can be transferred [PANK77]. Given a smaller ironing angle, higher reductions in wall thickness can be achieved in one work step.

Because of the wall thinning and the strain hardening of the material in the compressed zone, cracks form easily. For this reason, the change of wall thickness is executed in multiple stages. Also, the cup can be drawn out of a mechanical stop from an even circular sheet (Fig. 4.18). The sheet is pushed through several

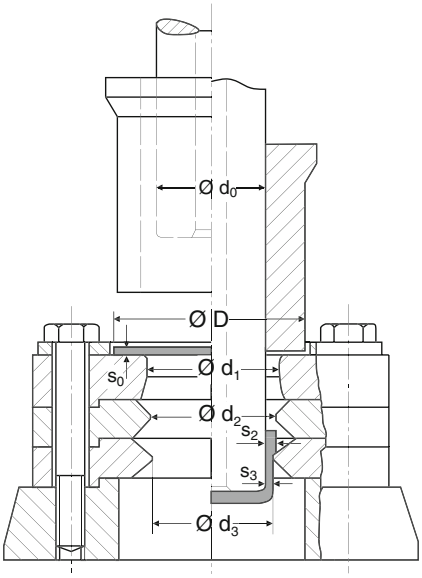


Fig. 4.18 Multi-stage ironing tool (acc. to Oehler/Kaiser [OEHL01])

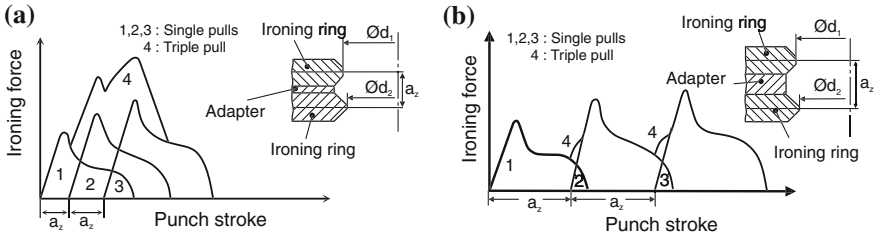


Fig. 4.19 Force progression for different ironing die distances (schematic), (**a**) smaller distance of ironing rings. (**b**) bigger distance of ironing rings

superimposed drawing rings, so that only a relatively small amount of material must be compressed for every drawing ring.

It is not recommendable to activate more than one ironing die during ironing [BUSC69, SACH74]. This is because the individual forces for each ironing draw add up, with the resultant force achieving potentially considerable values [BAND49, KUHN58]. By inserting adapters, the distances of the drawing dies can be increased to the extent that the forces at least do not add up at force peaks which occur, but rather in the lower areas (Fig. 4.19). This also entails higher punch strokes, however.

4.1.2.2 Deep Drawing with Elastic Tools and Active Media

The characteristic feature of these deep drawing methods lies in the fact that instead of two rigid tool halves being used, one of the tool parts—i.e. either the punch or the die—has a flexible design (Figs. 4.20 and 4.21). DIN 8584-3 [DIN03h] distinguishes between deep drawing processes with elastic tools (rubber

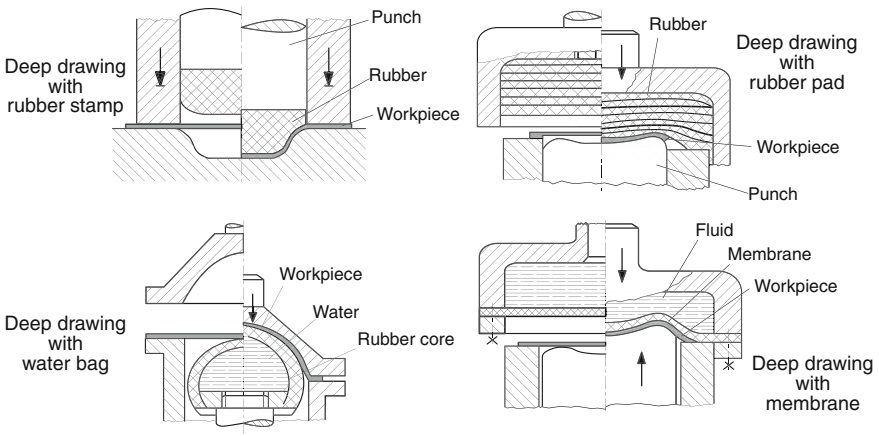


Fig. 4.20 Deep drawing with elastic tools and active media (part 1)

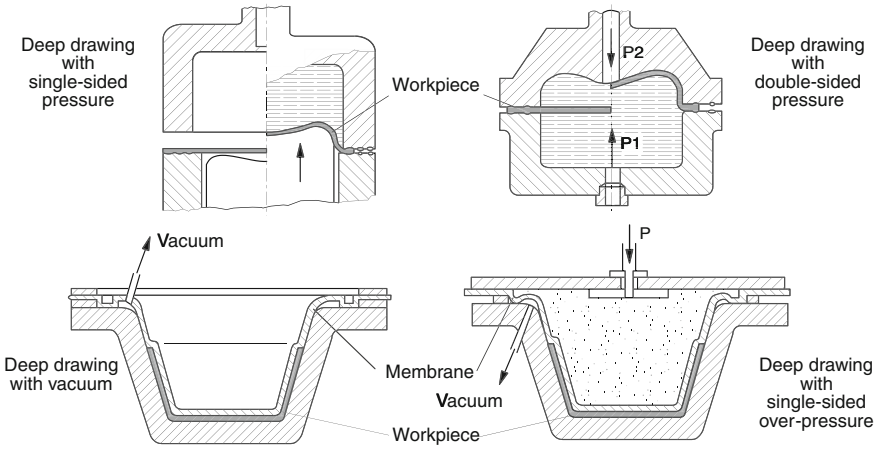


Fig. 4.21 Deep drawing with elastic tools and active media (part 2)

punch, rubber cushion) and those with active media, in which fluids are used together with a flexible membrane.

In deep drawing with a rubber cushion, the die consists of a cuboid made of soft to middle-hard rubber embedded in a case. For forming, the punch plunges into the rubber cushion. The medium nestles around the tool more or less flushly depending on the forming pressure, pressing the sheet against the punch contour. Since any blank holder which may be implemented is displaceable, workpieces with a vertical wall can also be produced without wall losses in the bottom area.

The required punch force is much higher than that required in conventional deep drawing processing, as a greater amount of the added energy is absorbed through the compression of the cushion. In comparison, the amount of force responsible for forming the sheet is negligible. Further disadvantages of this process must be ascribed to the relatively low service life of the tools. Furthermore, the output is lower than in conventional deep drawing.

The process is frequently employed in aircraft construction. A single aircraft requires up to 20,000 different individual components made of formed sheet-metal parts (Fig. 4.22). As a rule, however, a series of 1,000 units is not exceeded over a period of several years, and this favours both short tool changing times and low tool costs. These requirements are fulfilled by the use of both the rubber cushion and active media [KÖNI81b]. Both the rubber cushion and fluid-filled membrane are universally implementable. Since only one defined mould half is needed, the usually costly manufacture of the die shape and the time-consuming adjustment work of the tool halves are entirely dispensed with. Often the shape of the punch can be manufactured from hardwood.

Deep drawing with elastic tools or with active media can go beyond the process limitations of deep drawing with rigid tools. Figure 4.23 illustrates the production of a reflector. The drawing punch is not rigid, but rather bears a rubber bag filled with water at its upper end. The rigid die is responsible for shaping. During the

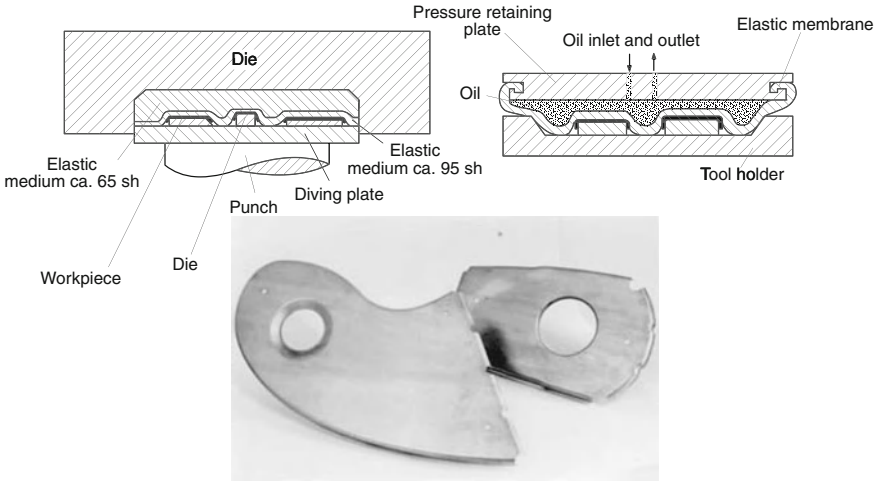


Fig. 4.22 Overview of processes and moulds used in aircraft construction

forming process, the plastic bag at first lies almost evenly on the workpiece, causing a reduction of the free, unguided surface area of the circular sheet to fit the dimensions allowable for deep drawing with a rigid tool. The individual forming phases show how the progression of the forming starts from the drawing die and goes further and further inwards. This prevents free, unguided surfaces and thus fold formation. The comparison in Fig. 4.23 shows that the five draws normally required for conventional deep drawing with a rigid tool can be reduced to one single work

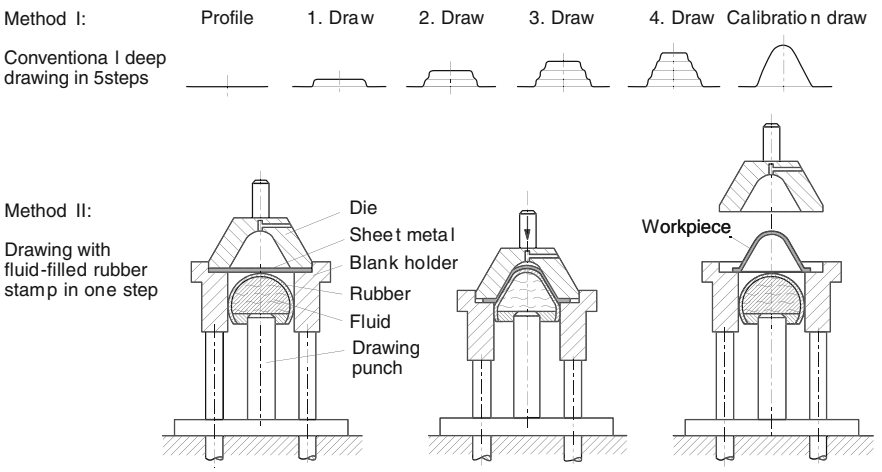


Fig. 4.23 Deep drawing of a reflector [OEHL01]

step. Moreover, because of the even pressure distribution on the sheet, a greater draw ratio can be achieved. The remaining processes in Figs. 4.20 and 4.21 operate in a similar way [BENS81, EBER67, OEHL01]. Section 4.6.4, p. 441 describes deep drawing processes with the use of explosive substances or magnetic fields.

4.1.3 Tools

4.1.3.1 Tool Design

The essential elements of a deep drawing tool are the punch, the die or drawing die, the blank holder and guiding elements. The tool parts are designed according to the special features resulting from workpiece quantity, the material to be formed, as well as the size and shape of the drawn part. Not every construction detail can be determined in advance. Frequently, samples must first be available to ascertain whether, how many and in which configuration drawing rods must be provided (Sect. 4.1.2.1). The situation is similar for tool ventilation. These generally refer to holes which prevent the adherence of the drawn part to the punch during stripping or the formation of an air cushion in the bottom part of the tool.

Die Radius Curvature. The radius of curvature of the die radius which the sheet must slip around during the forming process has a very important status. It is dependent on the dimension of the workpiece and the sheet thickness. If a die radius diameter is selected which is too small, then the resultant increasing cutting effect of the tool will cause bottom tears. In order to achieve a maximum drawing limit ratio with the lowest possible drawing force, the drawing die curvature should be large. Otherwise large drawing die radii cause a reduction in the flange surface pressurized by the blank holder (see Eq. 4.10).

According to Oehler and Kaiser [OEHL01], the curvature diameter r_R on the die radius can be calculated using the following empirical equation:

$$r_R = \frac{0.04 \cdot d_0}{d_1 \cdot \beta_{100}} \cdot [50 + (d_0 - d_1)] \cdot \sqrt{s_0}. \tag{4.12}$$

Here s_0 refers to the sheet thickness, d_0 to the blank diameter, d_1 to the punch diameter and β_{100} to the drawing limit ratio for a sheet thickness ratio $d_0/s_0 = 100$.

In this case too, reference values are provided to the designer in the form of table values. According to Sellin [SELL55], for example, the radius at the drawing ring should be determined according to the following relation:

$$r_R = (5 \ldots 10) \cdot s_0. \tag{4.13}$$

Punch Edge Curvature. Under no circumstances may the punch edge curvature r_{St} be smaller than the corresponding die radius curvature, since otherwise the danger arises that the punch may cut into the sheet. Sharp-edged draws can only be achieved by means of multiple draw stages or other deep drawing processes (Sect. 4.1.2).

The punch curvature should be roughly three to five times greater than the die radius curvature. For small drawn parts with large sheet thicknesses, a gradual transition is recommended, e.g. in the form of a tractrix curve, as for the drawing ring infeed.

Die Clearance. As long as the sheet is in a flow condition, the material is backed up at the draw opening during forming. Since a wall thickening also occurs over the wall height of the sheet part, a larger die clearance is needed as the extent of forming becomes greater.

When deep drawing round circular workpieces, the die clearance is measured according to this relation [OEHL01]:

$$u_z = s_0 + K \cdot \sqrt{10 \cdot s_0}. \tag{4.14}$$

$K = 0.07$ for steel sheets, $K = 0.02$ for aluminium alloys, $K = 0.04$ for other non-iron metals and $K = 0.02$ for high temperature alloys.

If the die clearance is too great, the cup is no longer a perfect cylinder, but rather remains widened at the upper edge. Also, wrinkle formation is possible. However, a widening of the cup is inevitable, even if to a very minor extent, as a result of elastic springback (Sect. 4.5.1.2). If the die clearance is too small, ironing occurs, which is linked to an increase of force. The risk of bottom tears becomes present in this case. Moreover, there may be an occurrence of cold welds between the drawing die and the workpiece.

A large problem to design the die clearance is presented in the form of inevitable fluctuations in sheet thickness owing to relatively large sheet thickness tolerances (± 0.05 mm). It may happen that a die clearance which is correctly measured for a normal sheet thickness leads with thin and medium-sized sheets both bottom tears and wrinkles.

One must also consider that a change in the gap width over the entire contour of the drawn part may make perfect sense for achieving optimal draw results, even with complicated shapes.

Blank Holder. The blank holder is driven on double-acting presses via a blank holder ram, which is separate from the drawing ram. The blank holder is controlled on mechanical presses via knee levers or cam discs in such a way that during the forming process it lies in its bottom dead centre on the drawing die or the sheet. The blank holder pressure can be set using springing elements in the blank holder ram.

On single-acting presses, the blank holder pressure is generated via springs between the top plate and the blank holder or via hydraulic or pneumatic die cushions present either additionally in the tool or already integrated in the machine (Fig. 4.24).

The pressure springs used should be as long as possible to avoid an all too great increase in the blank holder force during the drawing process. The disadvantage here is that any change to the blank holder pressure which may become necessary can only be made with great effort according to relevant sample draws. In contrast, hydraulic or pneumatic die cushions generally allow for an easy adjustment of the blank holder pressure. In addition, in these constructions, a pressure is usually given which is constant over the punch path.

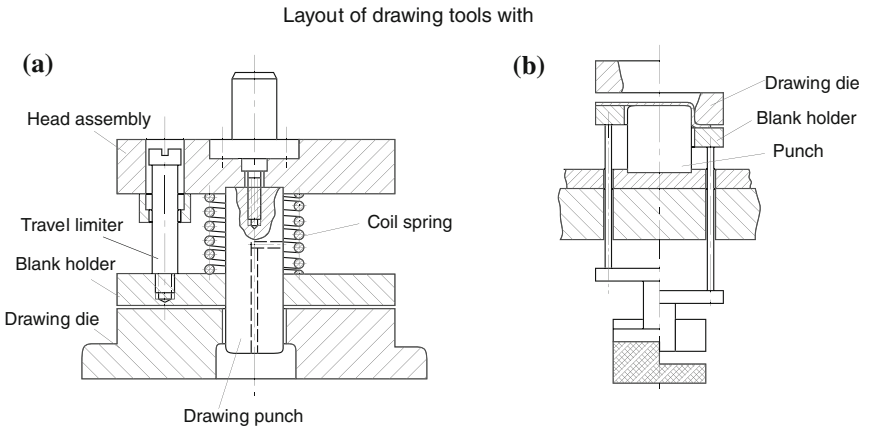


Fig. 4.24 Blank holder design on drawing tools (acc. to Hilbert/Wilhelm [HILB70], [WILH75]), (**a**) spring operated blank holder (**b**) blank holder drive unit over draw-cushion

Guides. Machine guidance, i.e. the ram guide in the machine bed, cannot replace the separate tool guidance. Only in smaller tools for small series production can one dispense separate guidance if a self-centring takes place within the tool. In order to achieve the most precise guidance possible, the press centre should coincide with the force application point.

4.1.3.2 Surface Treatment

A careful surface treatment of areas affected by friction is important. After hardening and tempering, they must be ground, lapped and as well polished as possible. This effort results in trouble-free operation, good workpiece quality, higher service life and longer tool life. This does not apply, however, to the end face and curvature of the punch. A greater force can be transferred from the sheet through repeated friction at these locations (Sect. 4.1.1.4).

Undesirable pick-ups or material deposits may also occur at the die radius of deep drawing tools and at the punches of cutting tools. In addition, a continuous abrasive wear is more or less pronounced depending on the sheet material. The results are a shorter tool life and a higher surface damage on the drawn workpieces. Different surface treatment processes are available to prevent these effects [EVER04, HAEF87, HORT01, OEHL01, VDI92, WEBE04].

A distinction is made between processes for influencing the surface zone, e.g. nitriding, case hardening, carbonitriding and boration as well as coating processes in which thin layers of hard materials (CVD/PVD: TiC, TiN, DLC etc.; galvanic: hard chrome) are deposited on the tool surfaces (Sect. 2.8.5.3). The relevant guidelines for executing these processes must be taken into consideration in order to prevent rejects and shortened tool life.

By coating especially stressed tool parts with titanium carbide, titanium nitride or other metal carbides and nitrides, tool life can be increased considerably. The layer thickness is up to 5 μm for PVD layers (15 μm through special measures) and up to 10 μm for CVD layers. Layers typical for industrial use have hardness values ranging between 1,700 HV (for CrN) and 3,500 HV (for TiAlN or TiCN multilayers). Coating temperatures lie between 180 °C for plasma-assisted CVD processes (PACVD), about 500 °C for cathode sputtering using arcs (ARC-PVD) and up to 1,000 °C for classic CVD processes.

Amorphous carbon layers (a-C:H, a-C:Me, DLC, among others) have in recent times started to complement coatings used until now [VDI04]. They can in many cases reduce friction forces and adhesive wear, although they have lower adhesive strengths, which makes them usable for higher stresses only in combination with other hard material layers.

A disadvantage of electro-galvanic hard chrome plating is that the chrome layer can flake off on sharp edges and sometimes even on smooth surfaces if there is no good bonding with the basic material. Hardness values of about 1,000 HV are achieved. Temperatures for hard chrome plating lie at approximately 50 °C, thus no dimensional or microstructural changes are to be expected in conjunction with a decrease in hardness [IBIN80].

Further extension of tool life can be realized by means of different nitriding processes. Good results can be achieved in particular with the combination of a plasa-nitriding treatment and a subsequent PVD or CVD coating.

4.1.4 Workpiece Materials

Demands for more complex geometries, higher shape accuracies, strength values and reduced workpiece mass have led to a series of new materials developments and to new "material layouts". Section 2.7.1.1 already introduced a series of these new materials developments.

4.1.4.1 Sheet Metal Qualities

Not every sheet is suitable for deep drawing. Important factors for deep-drawability are the mechanical parameters of the material which give information about formability (limit of elasticity, tensile strength, uniform elongation, elongation at fracture and the strain hardening coefficient) on the one hand and, on the other, parameters derived from test processes developed especially for deep drawing (Sect. 2.7.3.5).

In addition to platinum, gold and silver, good deep drawing properties can also be found in iron and zinc and, in particular, nickel, copper and their different alloys.

Quantitatively, deep drawing steel sheets have major importance. The further development of metallurgical and metal forming processes for deep drawing sheets made of steel have made it possible that today not only so-called soft-qualities can be deep drawn, but also steels with carbon content of up to 1 %, heat-treatable steels alloyed with manganese, chromium and molybdenum, stainless steels as well as structural steels alloyed with manganese and silicon [LANG81b].

For years, there have been made attempts in the automotive industry to save on fuel through weight reduction. Since components with greater strength can have a thinner design, easily formable micro-alloyed fine-grained steels have gained in significance. These are largely processed as cold-rolled thin sheets [MÜSC74].

Another approach in this context is tailored blanks. This approach exploits the specific advantages of different sheet metals. Sheets of varying quality (e.g. strength, hardness, surface etc.) and/or thickness are joined prior to the forming operation [MICH93]. The joining operation is executed by means of either mash seam welding or laser beam welding. The sheet formed in this way can be subsequently deep drawn. Figure 4.25 provides a schematic diagram of the process flow. Advantages of tailored blanks are the weight optimization of deep-drawn components, the reduction of the parts and the savings on assembly work [SCHN92]. The deep-drawn tailored parts are used above all in the automotive industry. The combination of joining and deep drawing is used in this sector to produce, for example, suspension strut supports, tread plates, door panels, side members and wheel housings.

In order to increase productivity and the accuracy of large parts which had once been welded together from individually formed parts, such components are produced in a single forming step. Materials with high formability have been developed for this purpose. Sheet metals with very high drawing quality were developed on the basis of steels with low carbon content. Micro-alloyed steels

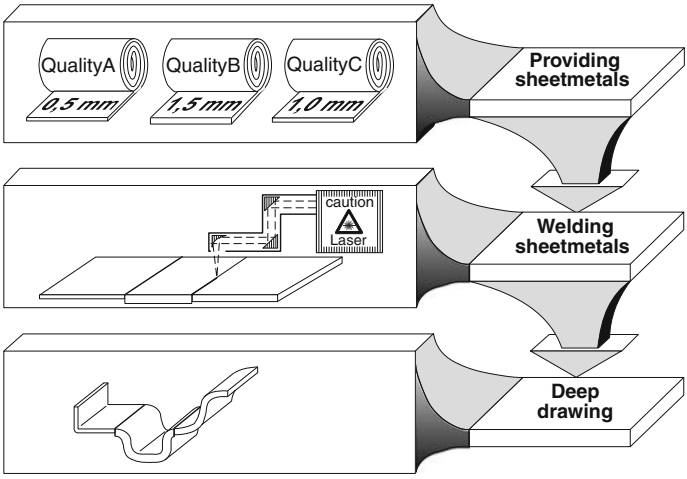


Fig. 4.25 Process steps for deep drawing tailored blanks

containing Ti and Ni achieve elongations of 50–60 % and a high strain hardening [NAKA93].

An additional alternative to frequently used steel materials can be found in the use of the specifically lighter material aluminium.

While pure aluminium sheets are distinguished by good formability with low hardness and strength [LANG81b], high-strength aluminium alloys exhibit a lower formability than deep drawing steel sheets and thus an inferior suitability for deep drawing. The primary reasons for this are their lower values for uniform elongation and their perpendicular anisotropy [BLAI81]. In contrast, sheets made from special aluminium alloys, also referred to as superplastic materials, can be elongated at temperatures of about 470 °C to an extent ten times its original length. Because of their lower strength values, they are most often used for covers, housings and casings [EICH80]. Given suitable temperature control, other sheet materials can also be deformed in this state [OEHL01]. Technically pure titanium, used in the form of thin sheets both in the chemical industry and in aircraft manufacture, can also be deep drawn [RÜDI81].

A classification of thin sheets according to sheet qualities is made by DIN EN 10139 [EN97] and DIN EN 10268 [EN03].

Composite materials are also partially suited to deep drawing and are used primarily in car body construction. An example of these is sandwich sheets, in which a 40–100 μm-thick plastic layer lies between 0.15 and 1.6 mm-thick steel sheets. They are used, for example, for vibration damping in oil sumps [NAKA93].

4.1.4.2 Heat Treatment

During the deep drawing process, the material is strain hardened, with the formability decreasing with increasing true strain. Because of the varying geometries of the drawn parts, the strains on the workpiece are of varying magnitude, leading to varying strength properties. By means of suitable heat treatments, irregular strain hardening can be eliminated and the desired strength properties can be set. The required annealing temperature and time depend on the alloy components of the materials on the one hand and the extent of previous deformation on the other. For steel materials, there is a basic distinction between the following three annealing processes:

- stress relieve annealing,
- spheroidizing,
- subcritical annealing.

Stress Relieve Annealing. The residual stresses caused by strain hardening in the workpiece can lead to warpage or even crack formation. These stresses can be broken down by means of stress relieve annealing (400–600 °C). Other properties of the workpiece remain unaffected by the process.

Subcritical Annealing. By means of subcritical annealing, a completely new, unstressed microstructure is created, allowing for the adjustment of special material properties given the proper combination of parameters (degree of deformation, annealing temperature, annealing time, cooling conditions). Below a critical true strain, an annealing of the material no longer causes the formation of new grains, but rather leads as a rule to grain growth, causing a degradation of the workpiece properties. The recrystallization temperature and the annealing time both decrease with increasing true strain.

4.1.5 Manufacturing Accuracy

In deep drawing, the draw result is mainly dependent on four superordinate influence factors [DOEG76]:

- tool geometry,
- material behaviour,
- friction conditions,
- the machine used.

Although with respect to its guiding accuracy and rigidity the forming machine has no little importance for the deep drawing result [DOEG80], its influence will not be discussed here. In addition to actual deep drawing defects with their different failure modes, other factors influencing manufacturing accuracy are shape deviations, surface texture and component properties.

4.1.5.1 Deep Drawing Defects

On the basis of Figure 4.26, the following will discuss the most important deep drawing defects, their outer appearance and measures for preventing them [OEHL01, WILH75].

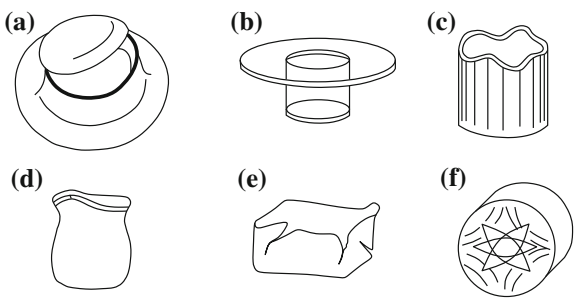


Fig. 4.26 Deep drawing defects [WILH75], (**a**) bottom tear, (**b**) shearing, (**c**) earing, (**d**) lip formation, (**e**) body rupture, (**f**) flow figures

Bottom tears belong to the frequent defects in deep drawing. In this case, the bottom tears off after a short cup wall begins to form, so that it is only attached to the wall via a narrow web (Fig. 4.26a). One of the main causes of this defect is that the drawing ratio for the material to be formed and for the selected tool geometry is too great. It may also be that wrinkles in the flange area can be pulled into the die clearance and ironed there. The increase in drawing force associated with this causes bottom tears.

In the case of excessively sharp-edged die radius curvature, far too little die clearance, too great drawing speed and too great blank holder pressure, the drawing tool acts as a cutting tool, with the result that the bottom is torn off at all sides before the wall is formed (Fig. 4.26b). This can be resolved by changing the parameters mentioned.

An inevitable phenomenon occurring with all sheets with plane anisotropy is earing on the wall rim or the sheet flange with not completely deep drawn parts (Fig. 4.26c). All that can be done here is to use sheets with low plane anisotropy.

If the wall is bulged in the middle or lips form on the upper wall rim (Fig. 4.26c), this is to be attributed to an excessively large die clearance.

Especially with parabolic, spherical and conical drawn parts, wrinkles tend to appear in the areas between the bottom of the drawn part and the sheet flange due to the unguided sheet surface between the drawing die and the drawing punch. For this reason, drawn parts with such shapes are frequently produced using special drawing processes (Sect. 4.1.2).

When deep drawing rectangular (Fig. 4.26e) but also other irregularly shaped hollow bodies, defect pieces with cracks are usually attributable to the construction of the blank. Further causes may be an uneven sheet thickness, unsuitable lubrication, worn punch and drawing die radii, as well as excessively small die clearances in the edges.

Figure 4.26f provides a schematic diagram of stretcher strain marks which usually appear after minor deformations with high stresses, i.e. frequently on the bottoms of drawn parts, rarely on the walls. When producing flat, not cylindrical drawn parts, such as car body parts which are lacquered or sprayed over a large area, such stretcher strain marks are particularly undesirable for optical reasons. They occur mainly after small plastic strains of materials susceptible to ageing which have a pronounced elastic limit. If the strains are greater in an additional drawing process, the marks become effaced and can no longer be seen. When deep drawing, therefore, sheets which are susceptible to ageing should be further processed as quickly as possible after rolling. Although steels with these properties are hardly used any longer, the tendency to form stretcher strain marks can also be observed when deep drawing AlMg alloys [BLAI81].

4.1.5.2 Dimensional and Shape Deviations, Surface Texture

Because of a locally and temporally changing stress state, deep drawn cups usually exhibit different wall thicknesses over the cup height (Sect. 4.1.1.2). The

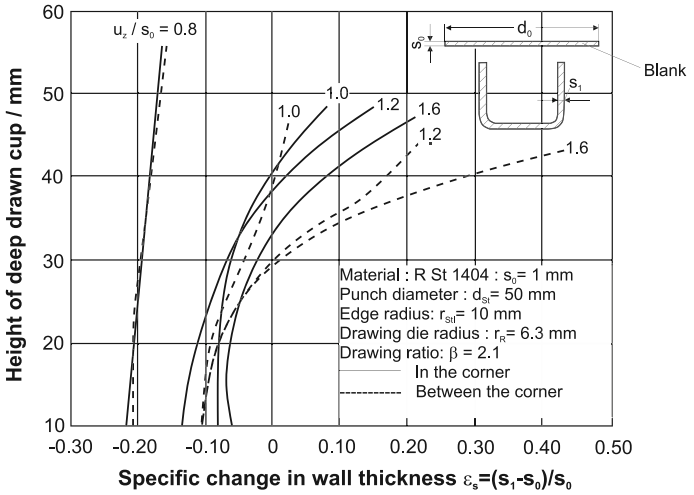


Fig. 4.27 Progression of the relative change to wall thickness over the cup height for different relative die clearances (acc. to Wilhelm [WILH75])

anisotropy of the sheet material causes both a change to the wall thickness over the length of the wall and earing, entailing extensive reworking of the drawn parts in some cases.

The die clearance relative to the sheet thickness u_z/s_0 represents an essential influence on the progression of the wall thickness (Fig. 4.27) [WILH75]. Only if the workpiece is ironed in addition to deep drawing ($u_z/s_0 < 1$) can improved accuracy of the diameter over the cup height and a regular wall thickness be achieved in this work step. The smaller the selected die clearance, however, the smaller the deviations are from the cylindrical shape, from the nominal inner diameter, as well as from roundness. In the case of materials with pronounced plane anisotropy, roundness deviations cannot be entirely eliminated [SIEB55]. After ironing, the tolerances possible for the cup diameter lie in the IT 6-9 tolerance range and IT 11-12 with respect to wall thickness [OEHL01].

Earing and the relative die clearance also have an influence on the usable cup height. With a smaller die clearance, the cup height becomes larger. Any ears which form must be removed in a subsequent cutting process.

Little has been documented with respect to the alteration of the surface condition through forming processes. Studies by Dannenmann [DANN69] have shown that there are basic differences between the inside and outside of a deep drawn cup in this respect. No change in the surface condition can be initially observed in the bottom area of the cup because of the minimal strains in this area. The roughness on the inner side of the wall increases with increasing cup height and with greater strains. The roughness of the outer side of the cup is almost unchanged relative to the original circular sheet. It is assumed that here too a roughening takes place during the forming process, though it is eliminated by compressive normal stresses

when the die clearance is passed through. The same applies to the surface condition on the inner side in the transitional zone between the bottom and the wall, which exhibits lower roughness in comparison to the outer side and to the starting circular sheet.

4.2 Flange Forming

Flange forming is generally understood as a process in which rims or flanges are formed usually on cut out internal contours which may be found on both flat and arched surfaces. The flanges can function in terms of mounting, fixing or distancing. The main area of application is apparatus construction, where it is used in thin-walled sheet parts to produce a geometrical element for thread cutting, pressing in bolts, soldering on pipes, and producing neck flanges from sheet metal waste.

4.2.1 Principles of Flange Forming

4.2.1.1 Process Principle

Before the actual flange forming process, the sheet is pierced. A rounded punch presses into the cut out hole, having a diameter greater than that of the hole, so that the sheet, which is lying on a die, fold around the die radius. The hole diameter is expanded, in the process of which a basically cylindrical rim forms (Fig. 4.28).

The stress conditions which prevail during forming are different for flange forming than for deep drawing a cup. Whereas in the case of cup drawing the sheet is compressed due to the reduction of the outer diameter in the flange area, in

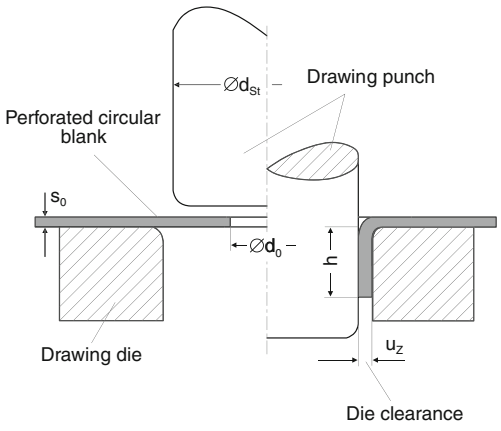


Fig. 4.28 Principle of flange forming

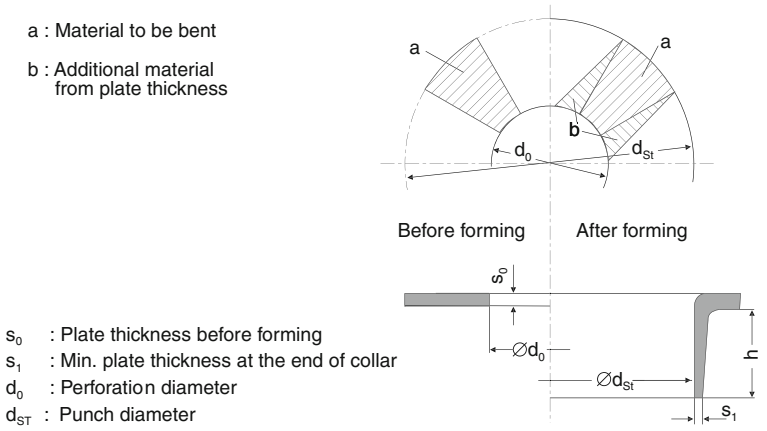


Fig. 4.29 Flange forming

flange forming the expansion of the diameter mainly causes an elongation (Fig. 4.29). As a result, the wall strength in the flange decreases with increasing flange height. The flange is thus formed at the partial expense of the sheet thickness.

The flange height h is roughly calculated as follows:

$$h = \frac{1}{2} \cdot (d_{St} + 2s_0 - d_0). \tag{4.15}$$

In the equation, d_{St} is the punch diameter, s_0 the initial sheet thickness and d_0 the pre-pierced hole diameter. However, this relation only applies for gap widths lying in the region of the starting sheet thickness s_0 and for sharp-edged die curvatures. Also, complex formulae must be applied for so called narrow flanges ($d_{St} < 4s_0$) if the flange height is to be known in advance [LANG90c, OEHL72, OEHL01].

The flange height is almost entirely unaffected by the shape of the punch on the face side. A punch with tractrix form or an approximated tractrix form is often used for flange forming. The advantage of the tractrix profile is that, similar to the drawing die shape for deep drawing without a blank holder (Sect. 4.1.2.1), the punch remains in line contact with the cut out hole margin during the entire forming process [REIS76], which maximizes the lever arm length, thus minimizing the required punch force.

4.2.1.2 Admissible Strains

As in deep drawing, the material elements are subjected to varying stress conditions. A bending takes place around the drawing die and a second bending around the punch edge curvature. Compressive stresses in the radial direction and tensile stresses in the tangential direction cause the strains, which result in a sheet

thickness reduction with an expansion of the diameter. Strains in the axial direction are barely observable [LANG90c, REIS76].

In analogy with the drawing limit ratio in deep drawing, the maximum possible strain for defect-free flange production is determined in flange forming by means of the expansion limit ratio. This value is defined as the quotient from the punch diameter d_{St} and the prepierced hole diameter d_0, in which there is no crack formation as of yet. Additionally, the parameter d_0/d_{St} [HILB70, KÜPP71, OEHL01] and the logarithm $\ln d_{St}/d_0$ [HILB70, KÜPP71, OEHL01] have been used to measure strain. The expansion limit ratio is dependent on the following [RAUT75, SCHM88]:

- the workpiece material,
- the prepierced hole diameter relative to the sheet thickness,
- the geometry/surface condition of the tools,
- the ratio of sheet thickness to punch diameter,
- the production type or the quality of the sheared edge of the prepierced hole.

The punch shape has no influence on the expansion ratio. However, the condition of the prepierced hole is especially important. Any possible burrs and greater roughness margin [KIEN68]. This is why the expansion ratio is smaller for cut prepierced holes than for pre-drilled holes.

According to Brambauer [BRAM71], improvements to the expansion limit ratio by means of increased hole quality can reach a figure of 100 %. For economic reasons, however, subsequent machining prepierced holes should only be executed when extremely large flange heights are required. Larger expansion ratios can be achieved for larger sheet thicknesses (prepierced hole diameter to sheet thickness $d_0/s_0 < 50$). Section 4.2.4 treats the expansion ratios achievable for different materials.

Also, the expansion limit ratio can be increased by changing the stress state on the edge of the prepierced hole, this is being achieved by creating an additional compressive stress in the axial or radial direction with the aid of a counterholder (Fig. 4.30).

4.2.1.3 Forces

Calculating the punch forces in advance is especially difficult due to the complex relationships involved. Few studies have been conducted in this area until now. By using a calculation model for a cylindrical punch form with a flat end face and rounded edges, Rauter and Reissner [RAUT75] have put forward relationships based on geometrical and plastic-theoretical connections which enable the determination of the punch force at all times during the process. A comparison of the measured and calculated values demonstrated good conformity (Fig. 4.31).

According to Wilken [WILK58], the punch force can be subdivided into a bending component and an expanding component. The bending component is

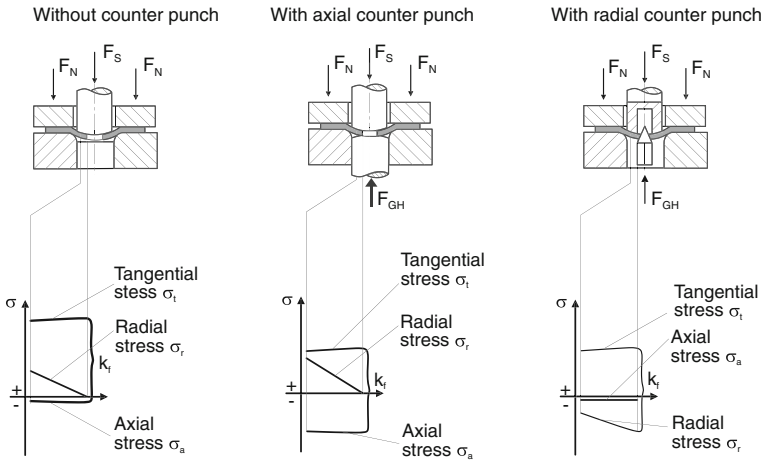


Fig. 4.30 Stress states in flange forming [SCHM88]

almost entirely independent from the expansion ratio, whereas the expanding component increases with a rising expansion ratio d_{St}/d_0.

In contrast to the maximum possible expansion ratio, the punch shape has a major influence on both the maximum punch force and the progression of the punch force over the punch path (Fig. 4.32).

By distinguishing the different punch forms, the tractrix geometry proves to have the lowest forces. The disadvantages of this geometry are in the difficult and costly manufacture and the greater machine stroke required. While they are easier to manufacture, hemispherical or conical punch forms also require greater punch forces. Cylindrical punches with edge curvature require the greatest force while simultaneously having the shortest punch path.

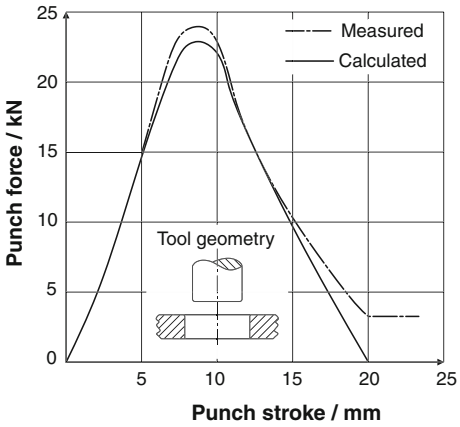


Fig. 4.31 Force-path diagram for flange forming [RAUT75]

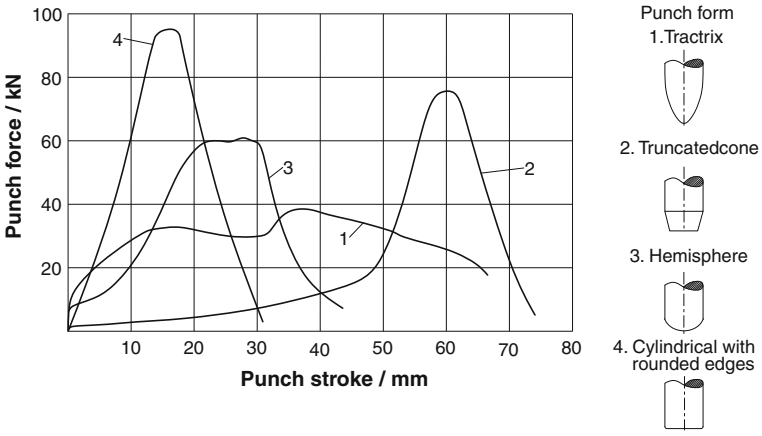


Fig. 4.32 Force-path diagrams for different *punch shapes* [WILK58]

An approximate calculation of the punch force can be made using the following relation [HILB70]:

$$F_{St} = U \cdot s_0 \cdot R_m. \tag{4.16}$$

In this equation, U represents the flange circumference, s_0 the starting sheet thickness and R_m the tensile strength of the sheet material.

4.2.1.4 Friction, Lubrication

The friction conditions between the sheet and the tool influence the work result in flange forming, as well. Increased friction of the sheet on the punch and the draw-through hole reduces the flange height because of a slowed material deformation. For this reason, the punch and die should be high-gloss polished to minimize friction. An additional friction reduction can be achieved with a conical die opening [STRA80].

The punch of a flange forming tool is subject to great friction stresses, especially when the prepierced holes cannot be produced without burrs. Therefore, after they are polished, the punches are generally hard chrome-plated or coated to protect against wear (see Sects. 2.8.5.3 and 4.1.3.2).

4.2.2 Process Variants and Manufacturing Examples

One generally distinguishes between narrow and wide ($d_{St} > 4s_0$) flanges. Narrow flanges are used to fasten screws or bolts to sheets or as hollow grooves. Wide flanges are used, for example, in the construction of pressure vessels.

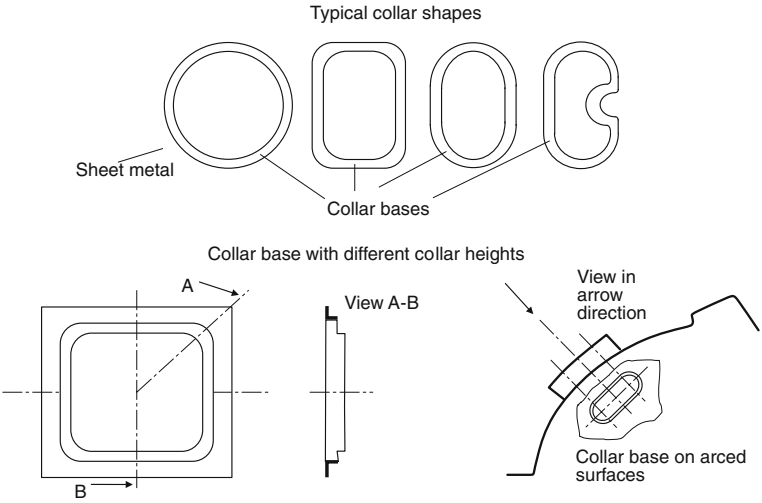


Fig. 4.33 Different *flange shapes* [HILB70]

As in deep drawing a cup, the possibility of ironing exists in the flange forming process, as well. If the gap u_z between the punch and the material is smaller than the starting sheet thickness, larger flanges with a simultaneous improvement of accuracy are the result. However, the ratio between the initial sheet thickness and the ironed sheet thickness may not be too small, as the entire flange could tear off in consequence.

In addition to round flanges, other types of flange geometries can also be drawn through, such as rectangles, long holes or more complex forms for which the flange height exhibits a specified progression over their contour (Fig. 4.33). However, different stress conditions arise, e.g. in the edge areas, which must be taken into account accordingly when designing the sheet outline for prepiercing [FISC72].

A very old method is pressing flanges into pre-pierced pipes (Fig. 4.34). The sphere as the pressure piece determines the outer shape of the flange. The process is used in the bicycle industry to manufacture bottom bracket shells and pipe connecting sleeves [OEHL01].

Tears on the outer edge of the flange are often unavoidable when approaching the limit of the expansion ratio. If the flange is nevertheless to have a certain height and a sheet thickness reduction is undesired, i.e. ironing is not possible; a cup-shaped shape is predrawn in a preceding operation. After prepiercing, the flange is then drawn to the desired height in a second operational step.

Oehler [OEHL72, OEHL01] recommends similar preparatory forming steps in a progressive compound tool for manufacturing with large flange heights for threads. In addition to prepiercing, the thread is also cut during the piercing process in the progressive tool.

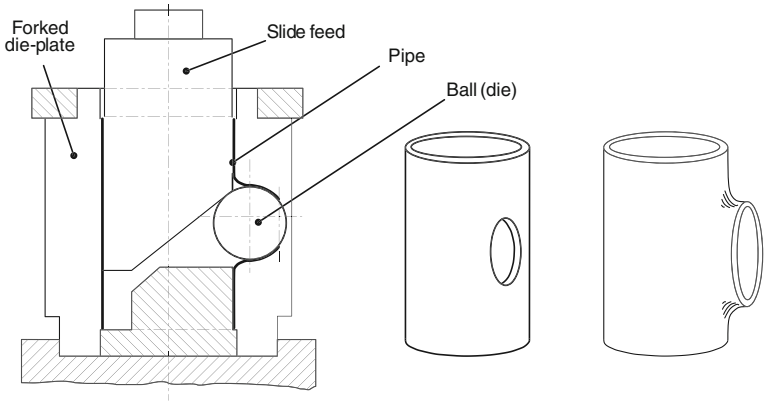


Fig. 4.34 Flange formation in pipe interiors [OEHL01]

The compound operation mode, i.e. prepiercing and flange forming in a progressive tool, can in some circumstances be executed with one double-acting punch in one stroke [STRA80] (Fig. 4.35 left). The face-side geometry is for piercing, the curvature for the subsequent flange forming. The punch shape is determined according to sheet thickness and sheet material, hole diameter and flange height. If the sheet metal blank is to flexible due to an unfavourable ratio of flange diameter to sheet thickness, a spring-loaded die must be provided accordingly.

Even without a previous hole, the sheet can still be torn and pulled with the aid of a plunging punch (Fig. 4.5 right). While this is the simplest and most cost-effective tool design, the flanges produced exhibit lower quality and an unsatisfactory appearance. The use of this method is thus limited to applications in which

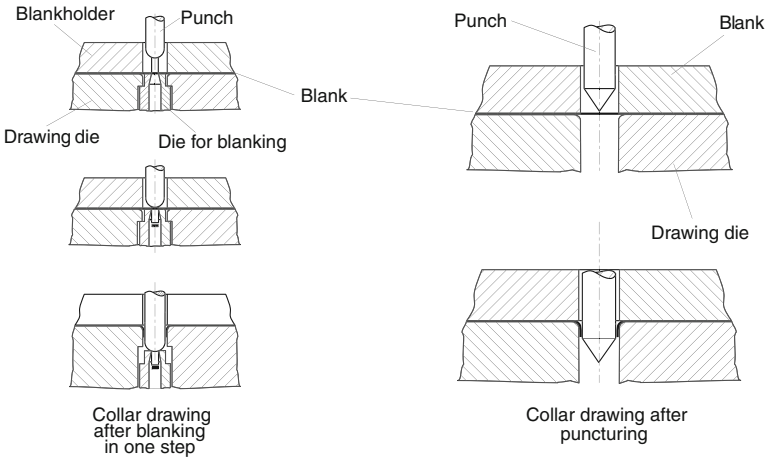


Fig. 4.35 Punch shapes in flange forming for simultaneous prepiercing and plunging

low costs or a rough margin are functionally required (e.g. solder clips, graters) [STRA80]. If necessary, excess material is sheared off during [DIN83].

Flange forming is often used for flanging container bases to allow for the fastening of pipes. In addition to a smooth transition, which can be important for fluid-mechanical reasons, the increased stiffness of the bottom in the transition area resulting from the flange is also advantageous [EHRE75]. Simple, mobile devices allow for an additional application in large container construction. The work result can be improved by supplying heat during the forming process. An even distribution of heat is important here.

4.2.3 Tools

In addition to the expansion ratio, the shape and design of the individual tool parts have an essential influence on the formation of the flange. The most important tool elements are the punch and the die. As in deep drawing, a blank holder may in some situations become necessary in order to prevent a wrinkle formation of the sheet and an increased continued flow of the material.

The drawing clearance should be as close as possible or smaller than the sheet thickness. The greater the drawing clearance, the stronger the resultant indentation and conicity of the wall. An ironing with $u_z < s_0$ increases the height of the flange. Also, a reduction of the punch edge radius increases the flange height, although this causes a decrease in the expansion limit ratio leading to crack formation. An opposite effect is observable in the drawing die curvature; the flange height increases with increasing drawing die radius [KÜPP71]. According to Kienzle [KIEN68], the most favourable radius of curvature for the die opening amounts to 10–20 % of the hole diameter of the die.

When using compound tools also including other metal sheet forming processes, one must note that the bulging punch should not be designed too long and should not act with other forming steps. A tensile loading of the punch strips, e.g. caused by a deep drawing operation, can otherwise cause the relatively thin tips of the plunging tool to break off or varying wall thicknesses to occur [OEHL01]. Also, multiple flanges should not be located to closely to each other, so as to avoid creating unwanted influence factors.

4.2.4 Materials

The central parameter for practitioners, i.e. the maximum achievable flange height, is in addition to the factors already mentioned also dependent on the material properties of the sheet used. Since flange forming involves mainly an elongation process, deep drawing sheets with high ductility and high tensile strength allow for

Table 4.1 Expansion ratios achievable in flange forming with different sheet materials [KIEN54]

Material	Expansion ratio d_1/d_0
Ms 63 w	2.3
Cu Zn 37 F 30	2.3
Al 99.5 h	2.3
St 13	2.4
St VIII	2.5
Al 99.5 w	3.4

higher flanges than normal steel sheets. Also, soft materials offer more favourable conditions than materials with stronger qualities [STRA80].

Table 4.1 provides an overview of the expansion ratios achievable for different materials [KIEN68, KIEN54].

Because of the stresses arising during flange forming, it could be assumed that sheet materials with higher uniform elongation provide better results with respect to the achievable flange height. However, studies on the behaviour of stainless thin sheets during flange forming could not confirm this assumption [KÜPP71]. In the case of the sheets examined, an inverse ratio can be observed between uniform elongation and the expansion limit ratio.

4.2.5 Manufacturing Accuracy

Flange forming defects include both crack formation and geometrical irregularities. The tool geometry has a considerable influence on the formation of these irregularities. The larger the radius of the punch edge curvature and the more sharp-edged the drawing die, the more cylindrical in form the flange wall becomes [KÜPP71].

A change to the face-side punch profile also affects the shape of the flange bottom. The tractrix geometry mentioned above provides the best results in this regard (Sect. 4.2.1.1). Following the forming, the bottom surface of the flange runs roughly parallel to the unformed sheet plane. By means of a hemispherical punch, the annular surface of the flange is transformed into a conical surface sloping outwards and, with smaller curvatures of a pointed-cone-shaped punch, into an inner cone [OEHL01]. A vertically running flange outer wall is obtained when the following relation between sheet thickness s_0, die diameter d_M and punch diameter d_{St} is fulfilled [OEHL72]:

$$\frac{2 \cdot s_0}{d_M - d_{St}} \geq 2.0. \tag{4.17}$$

For producing flange draws for threads, there are special prerequisites regarding the required core diameter, punch diameter and pre-pierced hole diameter. In the case of non-cylindrical flange shapes, the full height is not usable. Corresponding

numerical values for the manufacture of certain thread diameters are given in DIN 7952 [DIN86b]. Regarding the estimation of transmittable forces, it should be noted that a load opposite to the drawing direction allows for a roughly 15 % higher stress level. For this reason, screws should preferably be screwed in in the drawing direction [OEHL72, OEHL01].

4.3 Stretch Drawing

Stretch drawing is a process implemented in the aerospace industry, in automotive construction and shipbuilding for the manufacture of sheet metal formed parts. The large-surface workpieces, which can have dimensions exceeding 50 m^2 and in some cases up to 100 m^2, are generally bent over their entire expanse in one or more planes [SANS67].

While conventional forming processes like deep drawing or bending become unusable due to large workpiece size, production on stretch drawing devices can be performed both in one work step and in multiple stages.

The largest known stretch drawing device was built in 1957 and was employed in aircraft construction. It was designed to form up to 35 m long, 3 m wide and 6 mm thick sheets for aircraft wings [OEHL64b].

The shaping process takes place incrementally. After one area has been formed, the workpiece is transported further by means of feeding units, allowing the sheet section which is respectively connected to be formed. A staged forming of the planking-path reduces the joining work, thus eliminating fatigue phenomena which could otherwise have appeared on the joints [KURS60].

4.3.1 Process Principle

Stretch drawing uses rectangular, oval, trapezoidal or kidney-shaped sheet blanks which are firmly clamped on two opposite edges. Clamping is realized either by using rigid, rotary mounted clamping elements or with the aid of collets able to move in rotation or in translation, with these collets potentially providing an additional tensile load. The forming process consists in the sheet blank being loaded by the tensile load above the flow limit and fitted in a plastic state to the contour of a forming tool. In the process, the sheet thickness is reduced as the blank surface is simultaneously enlarged. In terms of procedure, one distinguishes between simple and tangential stretch drawing (Fig. 4.36).

In simple stretch drawing, the actual forming process is initiated solely by the movement of the punch. In tangential stretch drawing, blanks are shaped both by the movement of the forming block and by means of processes involving collets. The individual movements are adjusted to the respective forming process.

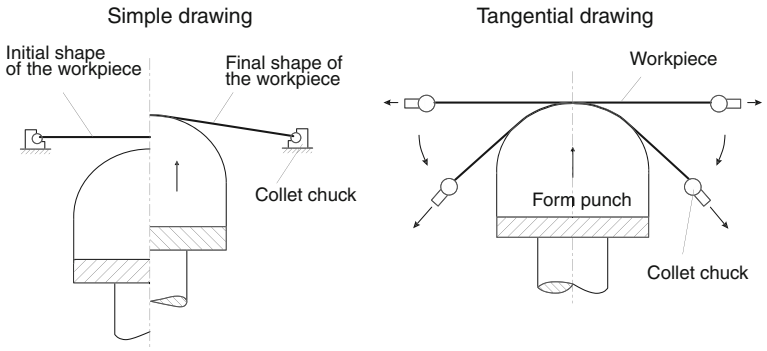


Fig. 4.36 Process principles of stretch drawing [DIN03j]

4.3.2 Process Variants

4.3.2.1 Simple Stretch Drawing

The simplest form of stretch drawing consists in the production of bent sheet parts with shaping in one plane, i.e. with no spatial bends. The stretch drawing devices required for this essential consist of a machine bed, sliding guidance for the clamping elements, a sheet holding device, a hydraulically driven press table and a drive unit with control system (Fig. 4.37).

The basic stretch drawing process proceeds as follows: The sheet blank is clamped at two opposing sides with collets or with other rotary mounted clamping devices. The clamping elements, which are arranged to be displaceable on five guide blocks, retain their position during the forming process. The stresses needed for forming are generated by the punch (Fig. 4.38). The shaping tool moves upwards by means of a generally hydraulically functioning table. The tool has the inner contour of the part to be manufactured as its outer contour. The sheet first touches the tip of the tool, initially beginning to stretch elastically with the further

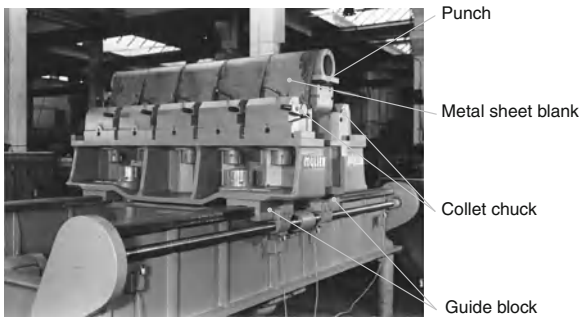


Fig. 4.37 Device for simple stretch drawing, press force: 1,500 kN, table width: 2,000 mm

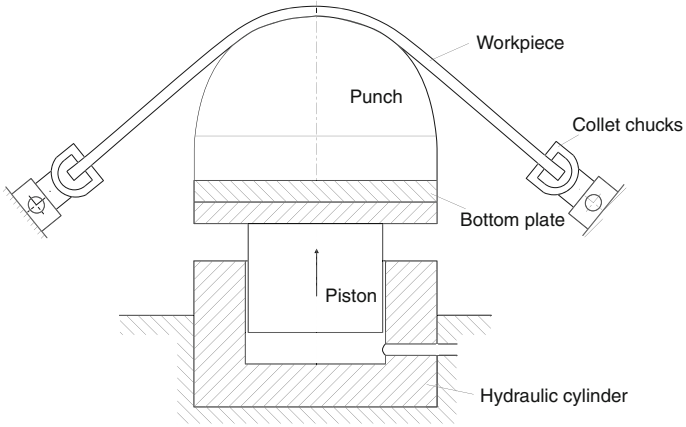


Fig. 4.38 Diagram of a stretch drawing press

upward movement of the punch. After the elastic limit is reached, the material is plastically deformed. As the material flows from the sheet thickness, the contact surface between the punch and the sheet blank increases in size. The friction forces acting between the forming tool and the sheet surface already touching prevent an even stretching and act against a further surface enlargement of the already formed parts of the sheet [SCHU64]. The material at these locations is not loaded to the limit of its stretchability. In contrast, it is primarily the areas of the sheet not lying on the forming tool which are stretched with increasing punch path.

The stretch drawing process is over when the sheet blank shows the contour of the shaping block. The punch is then lowered, and then the workpiece can be removed when the clamping elements are released.

Due to the friction conditions, only minor stretches can be achieved with simple stretch drawing. As a result, this process is only used with low true strains for lightly bent parts [PANK66b]. While the influence of friction can be reduced by lubrication or by covering the wooden mould with a metal sheet, it cannot be fully eliminated. If stretching on the upper and lower sides of the sheet is impeded through friction, bending effects may result which cause an undesirable elastic springback [KALC60].

4.3.2.2 Tangential Stretch Drawing

Whereas in simple stretch drawing the process is executed in a single operational stage and the tensile stresses required for shaping are generated only via the punch, tangential stretch forming is distinguished by the fact that the forming process is defined by two separate operations (Fig. 4.36).

First, the sheet to be formed is inserted into the clamping device of the stretch drawing machine and firmly clamped, as in simple stretch drawing. The clamping

elements run away from each other horizontally, which gives the sheet a tensile load which, according to the workpiece material, induces a plastic stretching of 2–5 % [BATH65, KURS69, SANS67]. As long as the workpiece is fully even, a uniform elongation of the entire sheet blank is achieved in this way.

If the sheet to be formed, however, exhibits uneven points, such as buckles and warps, a uniform elongation is initially hampered. The tensile load generated by the clamping elements causes stress peaks at the uneven points and leads to local plastic deformations of varying size. These deformations betray an orientation of the uneven points in the draw direction [KURS60, KURS65, KURS69]. If the tensile load is increased, the parts of the sheet which until then had not been stretched are also plastically deformed, so that an elongation of the entire blank is initiated at this point [KURS69, KURS71, MÖHR62].

The actual shaping process is executed in a second subsequent operation with the aid of a moulding tool. While the tensile load generated by the clamping elements is maintained, the pre-stretched sheet is attached tangentially to the forming tool in a continuous, speed-regulated operation. In the process, no relative motion may occur between the sheet blank and the forming tool. The movements needed for this are executed either by the clamping tools mounted on guide blocks alone or simultaneously by the collets and the tool punch [DIN03j].

In both cases, the position and the speed of the clamping elements are regulated in such a way that the generated tensile load constantly acts tangentially to the tool contour. In the process, the sheet areas not yet contacting the forming tool are uniformly stretched. In this way, the stretchability of the material can be exploited in every area of the sheet. Since a relative motion between the punch and the contacting sheet is largely avoided, no disturbing friction influences arise as in simple stretch drawing.

In many cases, the actual stretch drawing operation is followed by a re-stretching of the almost finished shape with an increased stretch drawing force in order to compensate for springback and minimize the deviation from the target contour of the workpiece caused thereby. Machines used for tangential stretch drawing often have numerical control systems for the exact and reproducible coordination of the movement sequence between the clamping jaws and the forming punch [SPAL81].

Tangential stretch drawing can produce workpieces with relatively large bends in two planes. Inherent to the process flow is that the workpiece material is under tensile load during the entire forming process. No bending occurs which can lead to compressive stresses and thus to a buckling of the finished sheet part [BATH65, KURS69, SCHU64]. For this reason, workpieces can be manufactured with much more narrow tolerances by tangential stretch drawing than by simple stretch drawing.

Other advantages of tangential stretch drawing lie in the smaller sheet blanks with less material waste [HOFM63, NN72] and in the possibility to undercut the moulding tool (Fig. 4.39). Given a suitable tool design, not only smooth sheets can be stretch drawn, but also corrugated sheets, asymmetrically milled sheets and deep-etched metal sheets [KURS60, KURS65].

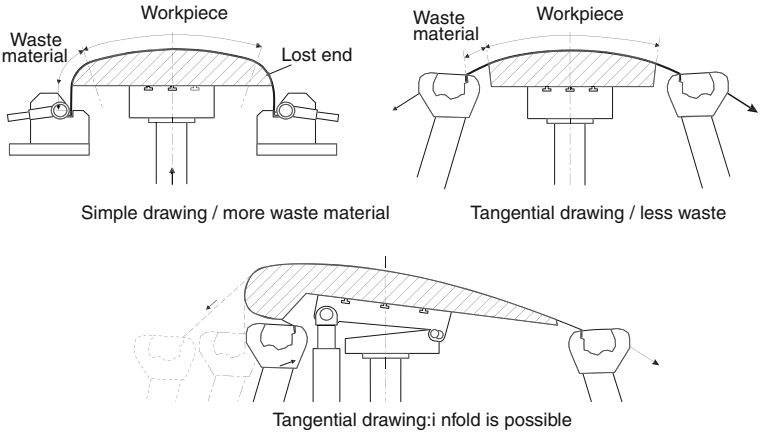


Fig. 4.39 Advantages of tangential stretch drawing

4.3.2.3 Stretch Drawing with a Counter Tool

Multiply bent shaped sheet parts and parts with flanged collars, recesses and breakthroughs etc. can be manufactured using stretch drawing with a counter tool. The manufacturing procedure comprises a tangential stretch drawing operation followed by a forming operation performed by a counter tool.

The stretch drawing device with counter tool shown in Figs. 4.40 and 4.41 are used in the aircraft industry and for shaping aluminium sheets. The maximum dimensions of the workable sheets are 11 m × 2.5 m × 8 mm. Figure 4.40a shows the opened tool, in which both the upper and the lower part of a deep drawing tool are clearly recognizable. In the foreground, one can recognize one of the two clamping elements of the stretch drawing device. In Fig. 4.40b, the sheet is already clamped and is then formed in the closed tool (Fig. 4.41c). In Fig. 4.40b, both clamping devices are recognizable. These comprise several clamping jaws which can be tilted against each other. The hydraulic cylinders next to the shaping block serve to clamp the counter tool (Fig. 4.41c).

In the following example, the use of a counter tool is required because the workpiece to be processed (Fig. 4.41d) is oriented in an unfavourable way to the stretch drawing direction due to its size and shape [NN82b]. Forming is executed in the following steps:

1. The sheet which is corrugated due to a previous heat treatment is locked in the clamping elements of the stretch drawing device and pre-stretched according to the contour of the forming tool. The clamping elements move apart in the process and are lowered vis-à-vis the forming tool. Not all parts of the sheet lie on the forming tool in this pre-stretched state.
2. The final shape of the workpiece is created by means of the counter tool. Forming takes place while the counter tool rests on the sheet, drawn by clamping cylinders against the forming tool, with all areas of the workpiece to

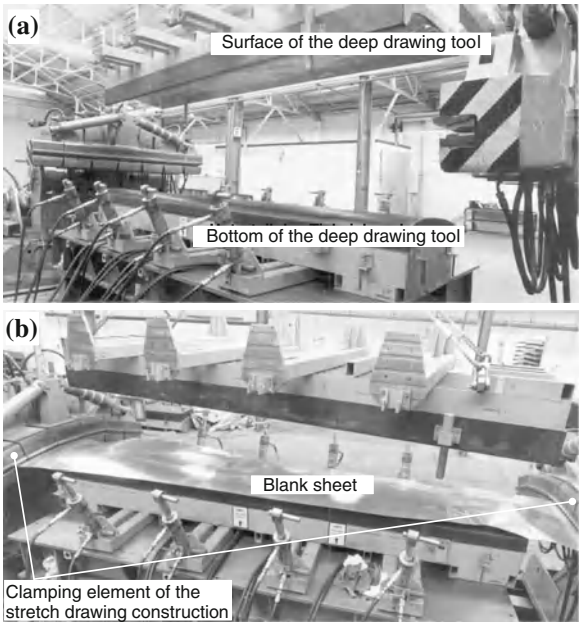


Fig. 4.40 Stretch drawing with counter tool I

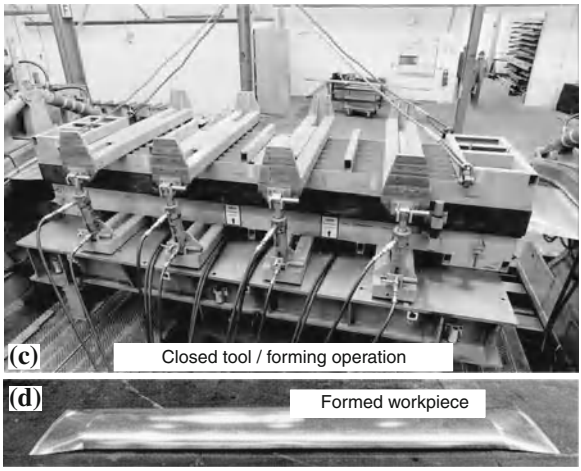


Fig. 4.41 Stretch drawing with counter tool II

be produced restrained by the mould. The clamping elements move in line with the movement of the counter tool. They move towards each other so as to avoid local overstretching.

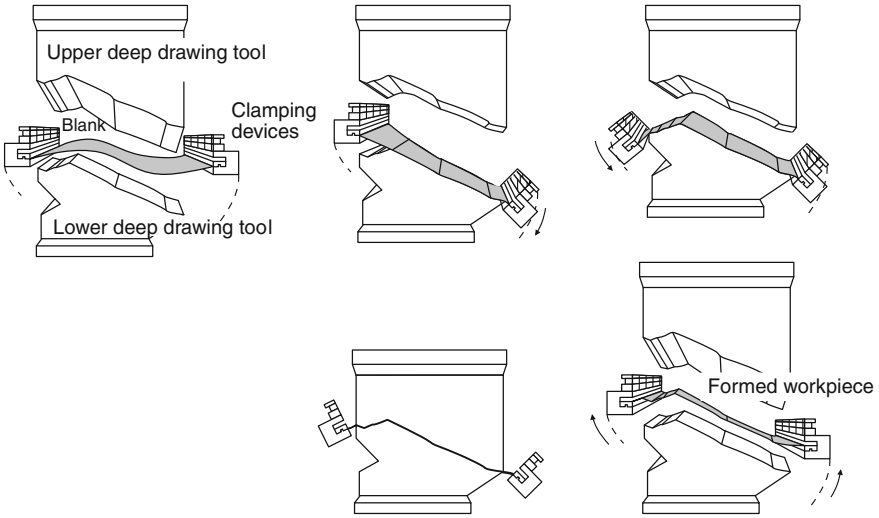


Fig. 4.42 Combined stretch and deep drawing

3. At the end of the forming operation, the forming tool and the counter tool are opened. The clamping elements move back to their starting position, allowing to workpiece to be removed.

The workpiece is first formed through a stretch drawing process and then through a deep drawing process (Fig. 4.42). At the start of the operation, the sheet blank is inserted into the stretch drawing device and firmly clamped when the hydraulic clamping jaws are closed. When the clamping units move away from each other, the sheet is stretched by 2–4 % of its length. The right clamping unit is then lowered, so that the metal sheet already receives a local deformation through the contour of the lower tool. After the left clamping unit is also lowered, the forming process is completed with the placing of the upper tool. The advantages of a combined stretch and deep drawing process lies above all in the savings on material in comparison to pure deep drawing, reaching values of 10–15 %. This is a result both of the lower starting size of the sheet blank, which is not located on all sides under a counter holder as in pure deep drawing, but is rather only clamped on two sides, and of the enlarged blank surface caused by the stretch drawing process [BATH65]. Because of the more uniform strain distribution in the shaped part achievable with the combined stretch and deep drawing, these workpieces are more stable.

4.3.2.4 Stretch Drawing Profiles

In addition to flat materials, profiled sheets can also be manufactured in a stretch drawing process to formed parts such as bent covering profiles [KURS71]. The

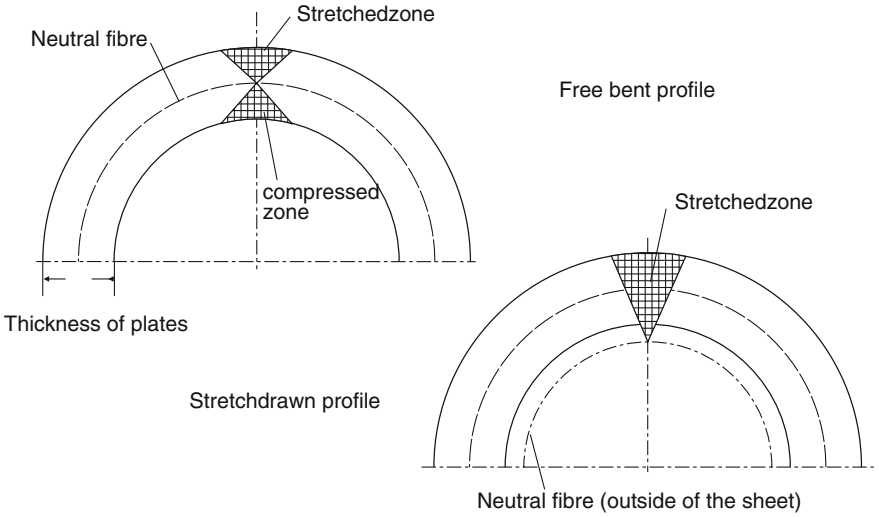


Fig. 4.43 Neutral axis in stretch drawing and bending

forming tools and the clamping elements must be adjusted to the respective profile shape. The clamping jaws comprise individual segments corresponding to the profile contour. These segments are mounted in a conical clamp chuck in such a way that they close tighter with increasing tensile load.

The special advantages of profile stretch drawing become apparent through a process comparison with free bending (Fig. 4.43).

Bending processes are characterized by the material beeing stretched on the outer radius and compressed on the inner radius, which can lead to local bulging, especially with thin-walled profiles [KURS71, LANE55b, LANE55a]. In profile stretch drawing, on the other hand, the workpiece is stretched in a straight condition through pulling, and this so strongly that the neutral axis lies outside of the workpiece upon subsequent bending. As opposed to bending, the radial springback of the workpiece is minimal, since no residual stresses of opposite sign are active in it. This effect is also exploited for straightening shapes.

4.3.2.5 Hot Stretch Drawing

Though stretch drawing is generally executed in room temperature, titanium alloys with sheet thicknesses over 1 mm, such as used predominately in airframe construction, cannot be formed without heating [HAUB67]. The forming temperatures in such processes depend on the titanium alloys to be formed and range between 480 and 590 °C. In order to avoid an undesirable transmission of heat from the workpiece to the tool which negatively impacts the forming process, heated tools made of heat-resistant tool steels or ceramic materials are used in hot stretch drawing.

4.3.3 Strains, Workpiece Materials and Forces

The stretch drawing process is characterized by a primarily generated tensile load causing a material flow from the sheet thickness. In order to avoid local necking, the sheet is normally stretched so strongly that the mean strain over the entire clamping length of the sheet does not exceed the value of the uniform elongation A_g.

At first, the only materials suited to stretch drawing were aluminium and copper alloys with uniform elongation values in the order of $A_g = 40$ %. Today, the range of materials used includes both soft and high-strength materials. These include low-carbon deep-drawing steels and high-alloy ferritic and austenitic steels, acid-resistant steels and magnesium and titanium alloys [KRAU66, LANG90c].

At room temperature, uniform elongation values lie in the order of 5–8 % for titanium alloys, 10–30 % for aluminium alloys, 20–35 % for deep-drawing steels, 45–50 % for brass and 50–60 % for austenitic sheet steels [LANG90c].

The equation

$$\varphi_g = n = \ln(1 + A_g) \tag{4.18}$$

can be used to derive information from the flow curve of a steel material about its stretch drawing capacity. This is because the strain hardening exponent, i.e. the slope of the flow curve in a double logarithmic coordinate system, is equal to the true strain given uniform elongation. Strong strain hardening and thus a high uniform elongation leads to a regular strain distribution [SPUR85]. The resultantly high numerical values for the strain hardening exponent n suggest favourable stretch drawing properties [GRUN76, PANK70, WEND71, ZIKA72]. This correlation applies without restrictions only to steel materials.

Stretching the workpiece material beyond the degree of uniform elongation causes local necking and cracks as a possible result [ADLE66]. Generally, three types of failure due to crack formation are distinguished (Fig. 4.44).

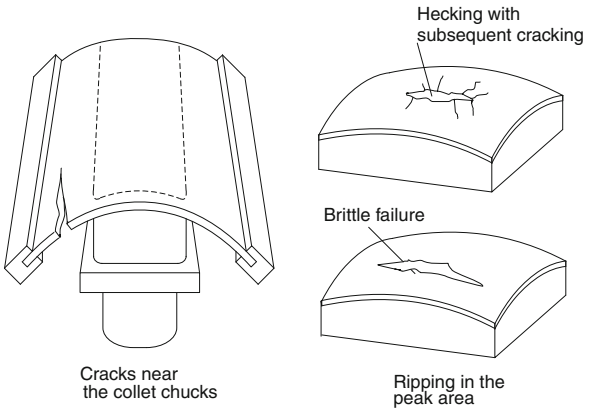


Fig. 4.44 Potential failure modes in stretch drawing

In easily formable materials, cracks result from overstraining, tending to form in the area of the clamping jaws and on parts of the sheet not yet lying on the moulding tool. The failure modes necking and brittle fracture tend rather to appear in the central area of the shaped sheet part, but especially at the top of the forming punch.

Whereas brittle materials which cannot be adjusted to the tool shape because of their relatively difficult formability exhibit failures early on, ductile materials show necking in the top area only at a later point in the forming process. Causes for these failures are an insufficient forming capacity of the workpiece material or an excessively large friction forces arising during stretch forming [PANK66a]. In the case that local necking is allowed in the stretch drawing operation, the critical parameter for failure is not uniform elongation, but rather elongation at fracture.

The punch force F_{St} required for a stretch drawing operation on a ca. 1 mm thick sheet is calculated according to [LANG90c] as

$$F_{St} = \frac{A_1}{\eta_F} \cdot k_{fm} \cdot \ln \frac{A_0}{A_1}. \tag{4.19}$$

In the equation, A_1 represents the surface between the clamping positions of shaped sheet part enlarged by stretch drawing, A_0 for the starting surface of the sheet and k_{fm} for the average yield stress. Friction losses arising during the forming process are summarized by the strain efficiency factor η_F. Typical values for the strain efficiency factor η_F lie at approximately $\eta_F = 0.7$ for stresses distributed evenly over the entire sheet and $\eta_F = 0.5$ for an uneven stress distribution. If the sheet thickness deviates significantly from 1 mm, the cross section of the clamping width and the sheet thickness subject to tensile load must be included in the calculation.

The highest admissible stretch drawing force F_{St} which can just be raised without tearing the sheet to be formed can be calculated based on equilibrium considerations (Fig. 4.45) as:

$$F_{St,max} = c \cdot 2 \cdot F_{Sp,max} \cdot \cos\gamma \text{ and} \tag{4.20}$$

$$F_{St,max} = 2.4 \cdot R_m \cdot s \cdot b \cdot \cos\gamma. \tag{4.21}$$

The friction forces arising during forming are summarized by the correction factor $c = 1.2$; the maximum tractive force F_{Sp} transmittable through the shaped sheet part, which is transmitted to the collets, results from the tensile strength R_m of the clamping width b and the sheet thickness s [LANG90c].

4.3.4 Tools

Material and production costs are generally low for manufacturing tools for stretch drawing process. The shaping tools, which are processed according to the shape of

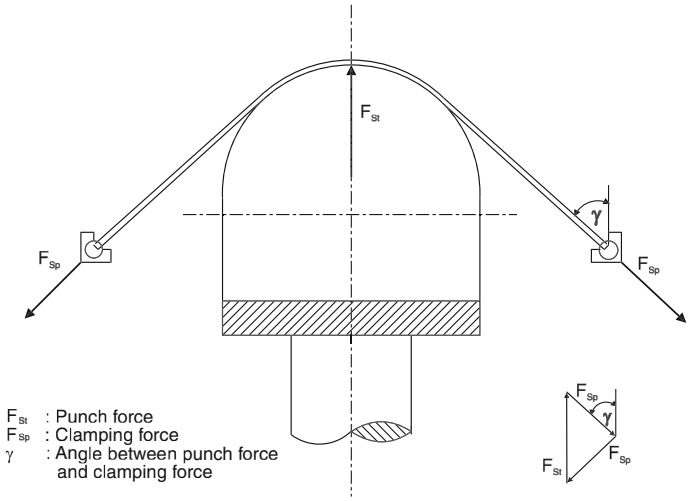


Fig. 4.45 Forces in stretch drawing

the shaped sheet part to be produced, are usually mad of relatively cost-effective, easily mouldable or castable and easily processed materials. The tool materials used for stretch drawing are not distinct from those used in other sheet forming processes. Because of the proportionally low relative movement between the workpiece and the tool, this process can dispense with complex and thus costly tools.

4.4 Metal Spinning

The metal spinning manufacturing process is used to produce rotationally symmetrical hollow bodies. The starting shape of the workpiece is a circular sheet or a pre-shaped hollow body.

The wall strengths of the initial and final shape are almost the same in conventional metal spinning. In the process variants projection straightening and shear spinning, the wall strength of the starting shape is reduced.

4.4.1 Process Principle

This section will discuss the process principles of the following variants:

- conventional metal spinning,
- projection lengthening and
- shear spinning.

4.4.1.1 Conventional Metal Spinning

According to DIN 8584-4 [DIN03i], conventional metal spinning is the tensile compressive forming of a sheet blank to a hollow body or the alteration of the circumference of a hollow body. In the process, a circular sheet is firmly clamped between the spinning chuck, which matches the inner shape of the workpiece to be produced, and the counterholder (Fig. 4.46). After the main spindle is set in rotation, the circular sheet is formed with the spinning tool (spinning roller) in one overrun or usually in stages until the final shape is reached. The forming is purely local.

Whereas in the past the tool was manually guided, which demanded great skill, today mainly NC machines are used.

Starting from prefabricated hollow bodies, metal spinning can also be used to manufacture hollow vessels with a bulged or drawn-in shape. According to DIN 8584-4 [DIN03i], conventional metal spinning has the following shaping functions:

- necking and expanding,
- creating inner and outer ribs,
- neck forming,
- thread spinning (Fig. 4.47).

Dividable spinning chucks are usually used, e.g. for expanding (Fig. 4.47). Flexibility is increased by means of metal spinning against a rotating profile roller, e.g. for necking (Fig. 4.47).

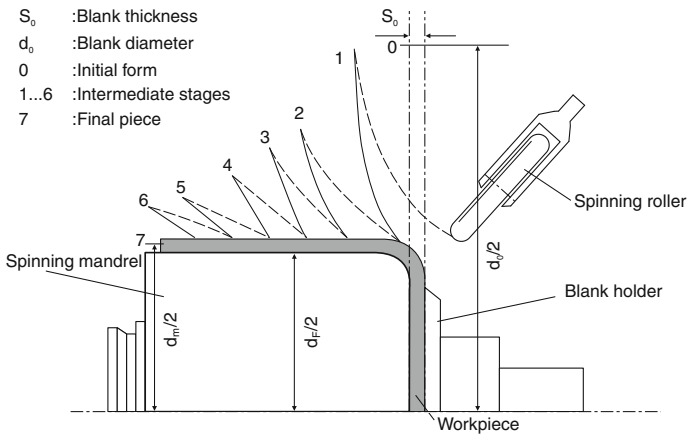


Fig. 4.46 Principle of the metal spinning process with intermediate stages according to DIN 8584-4 [DIN03i]

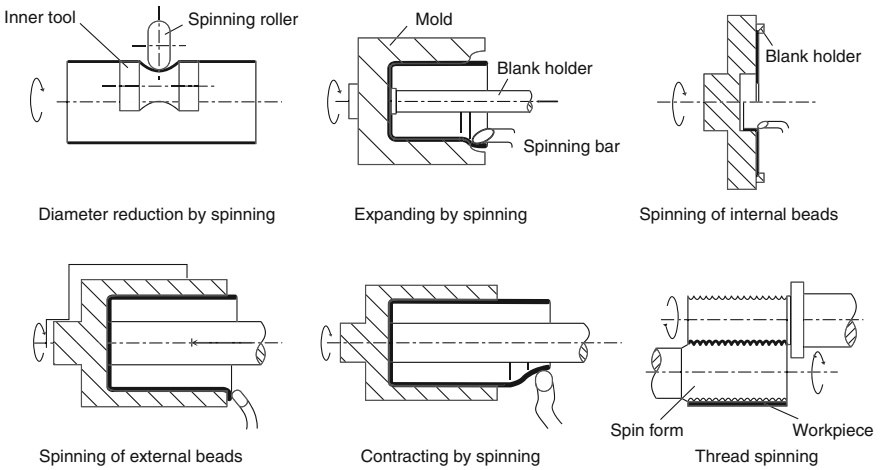


Fig. 4.47 Metal spinning process variants

4.4.1.2 Projection Lengthening

Projection lengthening is used to produce rotationally symmetrical hollow bodies with conical, concave or convex walls. In the forming process, the wall strength of the starting shape is reduced in such a way that every volume element of the workpiece is displaced parallel to the axis of rotation. The outer diameters of the starting and final shape thus remain identical [LUDW69]. The spinning roller moves at a corresponding distance parallel to the contour of the spinning chuck (Fig. 4.48). The final form is usually created in one overrun, with the wall strength s_1 being calculated from the wall strength of the starting shape s_0 and the half aperture-angle α:

$$s_1 = s_0 \cdot \sin(\alpha). \tag{4.22}$$

Conical workpieces can be made with aperture angles between $12^\circ < \alpha < 85^\circ$ [BRAC80, LUDW69].

When projection lengthening workpiece shapes with convex or concave surface lines, the wall strength of the final shape also changes as a result of the altered tangential angle (Fig. 4.49). Here too, the progression of the wall strength can also be ascertained with a variable α according to Eq. 4.22.

DIN 8583-2 [DIN03d] categorizes projection lengthening and shear spinning, treated below, under the compressive forming manufacturing processes (subcategory: rolling) and designates both processes as flow turning.

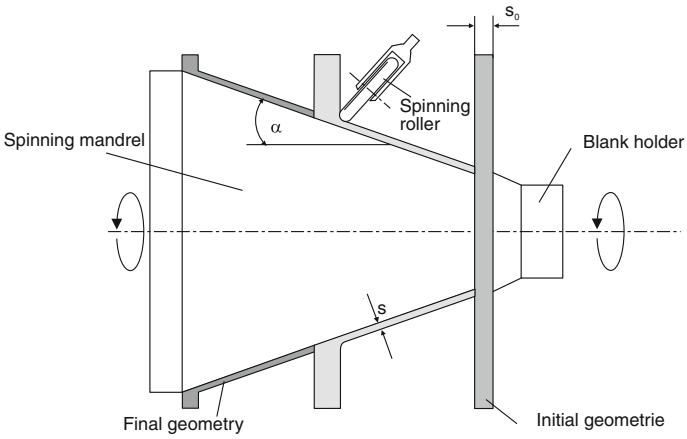


Fig. 4.48 Projection lengthening of a *conical* hollow body [LUDW69]

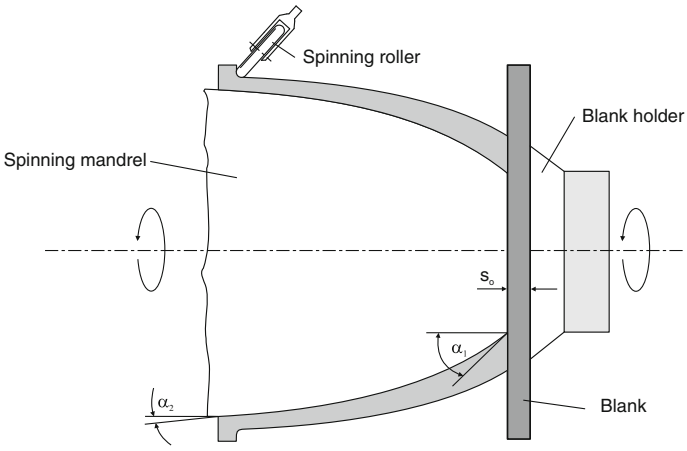


Fig. 4.49 Projection lengthening of a workpiece with a *convex* surface *line*

4.4.1.3 Shear Spinning

Shear spinning is used to manufacture cylindrical hollow bodies. In one or multiple overruns of the spinning roller parallel to the axis of rotation of the spinning chuck, the wall strength of the workpiece is reduced, with the inner diameter usually maintained. However, a circular sheet can also be selected as the starting shape. Because of the constant volume, the workpiece height stands in direct proportion to the wall strength reduction [BRAC80].

With respect to the kinematics of the spinning process, one distinguishes between co-rotating and counter-rotating processes. Whereas in co-rotating processes, feed and material movement run in the same direction, the material flow in

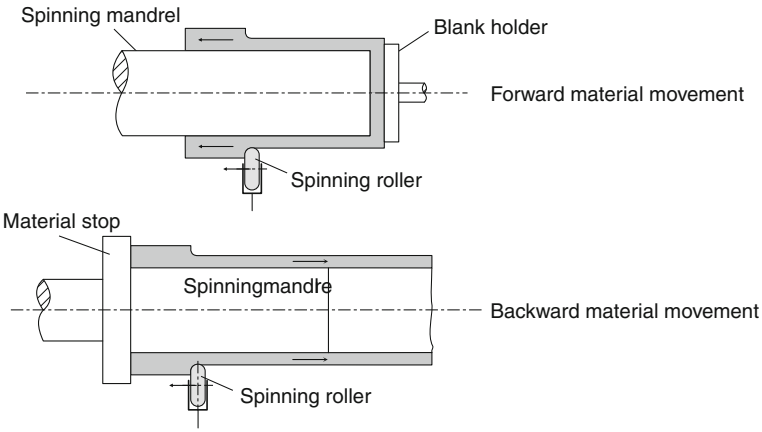


Fig. 4.50 Co-rotating and counter-rotating shear spinning processes

counter-rotating processes runs in the opposite direction of the tool movement (Fig. 4.50).

The application area of shear spinning can also be expanded to the manufacture of conical, convex and concave shaped parts. In contrast to projection lengthening, workpieces can be produced with defined wall strengths by controlling the motion of the rollers [LUDW69, SCHW87].

4.4.2 Admissible Strains

Axial and radial tensile stresses and tangential tensile and compressive stresses arise in the workpiece during the spinning process. These stresses increase with increasing strain as a result of strain hardening. If the deformation capacity of the material is exceeded or if process instability ensues, the following manufacturing defects can appear (Fig. 4.51) [GÖBE04, KLEI02]:

- Wrinkle formation—During forming, the circular sheet is not supported over its entire circumference, but rather only in the area of the spinning rollers. Through tangential compressive stresses, folds may form which can no longer be smoothed upon further rolling without a counter holder for the circular sheet.
- Radial cracks—After the formation of smaller folds, the continued spinning operation can lead to radial cracks due to tangential compressive and bending stresses or tangential tensile stresses.
- Tangential cracks—Tangential cracks appear as the result of excessively high radial or axial tensile stresses. To avoid such defects, on must know the process limitations of metal spinning [KÜHN82].

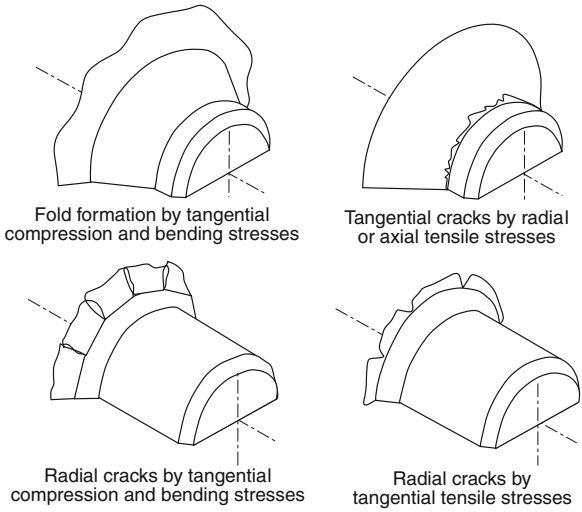


Fig. 4.51 Manufacturing defects in pressing a cup [KÜHN82]

In analogy to deep drawing, the spinning ratio

$$\beta = \frac{d_0}{d_1} \tag{4.23}$$

is defined as measure for strain. In order to prevent the abovementioned manufacturing defects, the maximum admissible spinning ratio β_{max} may not be exceeded. Figure 4.52 shows the effect of different geometrical values on β_{max}. With rising sheet thickness, the tendency towards fold formation decreases, allowing for greater spinning ratios. Tangential cracks caused by high axial stresses can be avoided by enlarging the roller radius.

With projection lengthening and shear spinning, the greatest strain is in the radial direction [KÜHN82]. From the wall thickness reduction, one acquires the logarithmic strain

$$\varphi_r = \ln \frac{s_1}{s_0}, \tag{4.24}$$

which with projection lengthening given the relation

$$s_1 = s_0 \cdot \sin \alpha \tag{4.25}$$

is simplified to (Fig. 4.48)

$$\varphi_r = \ln(\sin \alpha) \tag{4.26}$$

The maximum admissible wall thickness reduction is primarily dependent on the material, the feed and the roller shape. During shear spinning, bulge formation

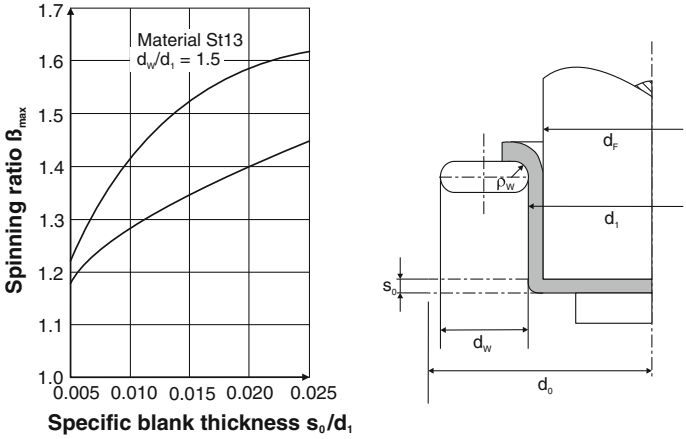


Fig. 4.52 Maximum admissible spinning ratio [DRÖG54]

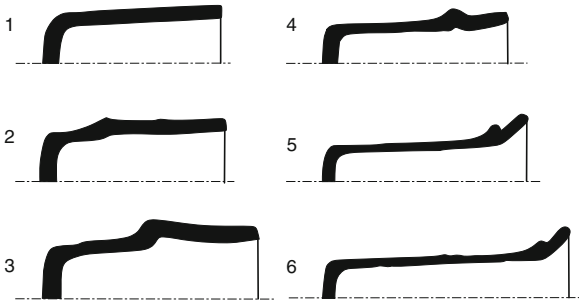


Fig. 4.53 Bulge formation and expansion at different stages of the shear spinning process [THAM61]

is observable in conjunction with an expansion of the workpiece, especially given a large reduction in wall thickness (Fig. 4.53).

Smoothing the bulge leads to an additional strain on the material. If the formability of the material is exhausted, the result may be a scale-like material detachments from the workpiece surface or crack formation [THAM61].

4.4.3 Forces

In addition to the mechanical properties of the material, the forming forces necessary for the different spinning processes also depend on geometrical, kinematic and process-specific factors. The forming force can be analyzed into the following three components (Fig. 4.54):

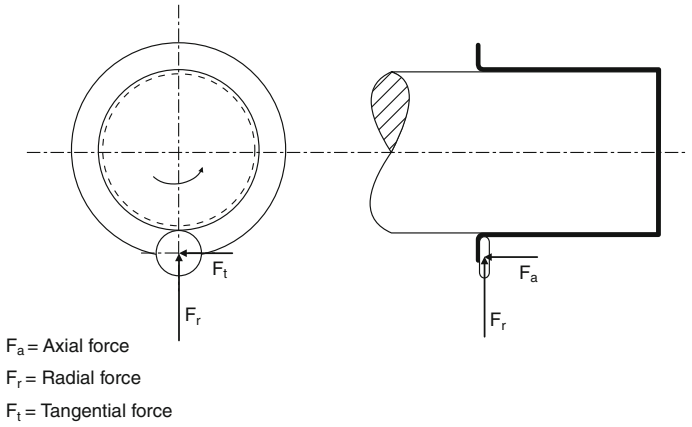


Fig. 4.54 Force components in metal spinning

- radial force F_r,
- axial force F_a,
- tangential force F_t.

Given the same material, both an increase in feed per rotation and a greater starting sheet thickness cause an increase in the forming forces. The radial and axial forces continue to be influenced when spinning without reducing the sheet thickness by the spinning ratio β and the radius of curvature ρ_w of the spinning roller (Fig. 4.55). The tangential component can generally be ignored [DRÖG54].

With projection lengthening, a decreasing inclination angle α leads to a greater reduction in sheet thickness. Due to the greater strain, the force components F_r and

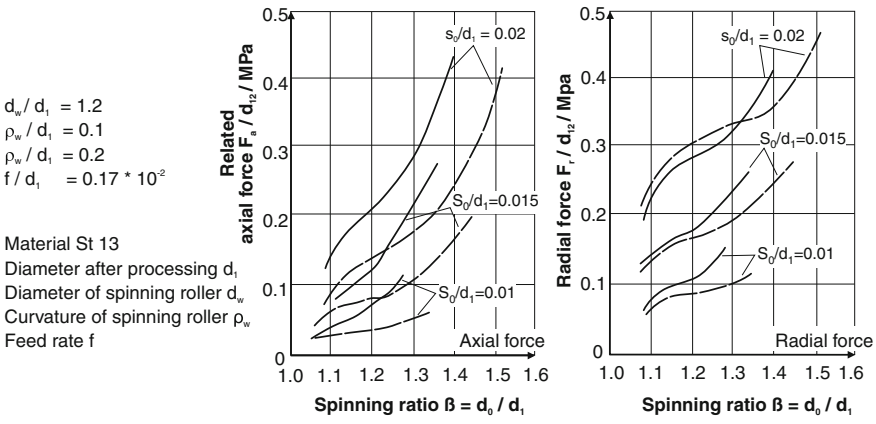


Fig. 4.55 Axial and radial forces in metal spinning [DRÖG54]

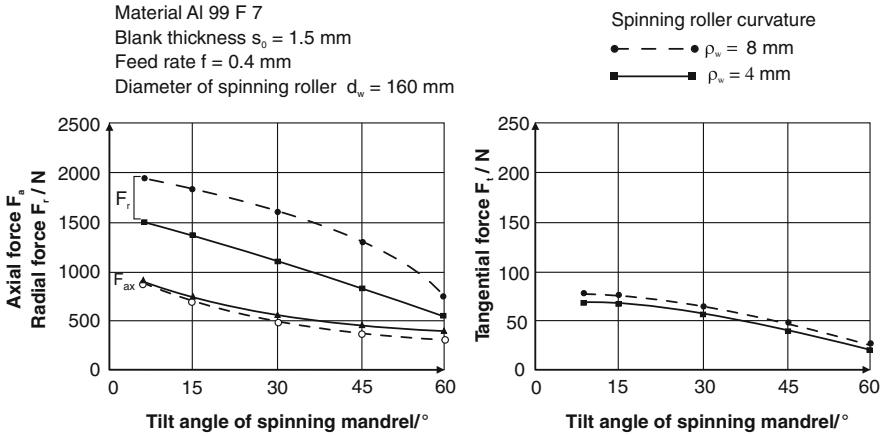


Fig. 4.56 Forces in projection lengthening

F_a increase (Fig. 4.56). The radius of curvature ρ_w of the spinning roller primarily influences the radial force [LUDW69].

With shear spinning, a greater strain also leads to higher forces. The shape and dimensions of the spinning roller influence the ratio and the magnitude of the axial and radial forces. Usually, the deformation occurs in the radial direction, thus making the radial force greater [LUDW69].

4.4.4 Manufacturing Examples

The area of application of metal spinning processes is extremely large. It includes the manufacture of:

- barrels and drums,
- cooking pots and pans,
- hubcaps and silencers for motor vehicles,
- lamp and radar reflectors,
- V-belt pulleys,
- tank bottoms,
- rims for passenger cars, trucks and tractors,
- brake and hydraulic cylinders,
- precision tubes,
- jet engine, rocket and projectile parts.

Figure 4.57 shows a number of metal spinning parts made of rust- and acid-resistant steels, titanium, aluminium, copper and brass; Fig. 4.58 shows a part family of aluminium reflectors.



Fig. 4.57 Metal spinning parts from different materials (*source* Thate gedrückte Präzision GmbH)



Fig. 4.58 Aluminium reflectors for different application areas (*source* Leifeld Metal Spinning GmbH)

Metal spinning is economically advantageous for bicycle wheel manufacture and especially for truck rims, since inexpensive flat material can be used (Fig. 4.59). Conventional manufacture using profile-rolled material, on the other hand, requires a specific profiled semi-finished product for each rim type and size.

Figure 4.60 provides a schematic diagram of the sequence of operations in the manufacture of taper base rim rings. The production of the associated wheel discs begins with a circular sheet. Through a combination of metal spinning, projection lengthening and shear spinning, the wall thickness can be varied arbitrarily. The rim ring and the wheel disc are manufactured separately and then welded together.

The demand for a reduced weight for passenger car wheels makes metal spinning manufacturing processes an attractive option. Figure 4.61 shows the



Fig. 4.59 One- and two-piece aluminium rims (*source* Leifeld Metal Spinning GmbH)

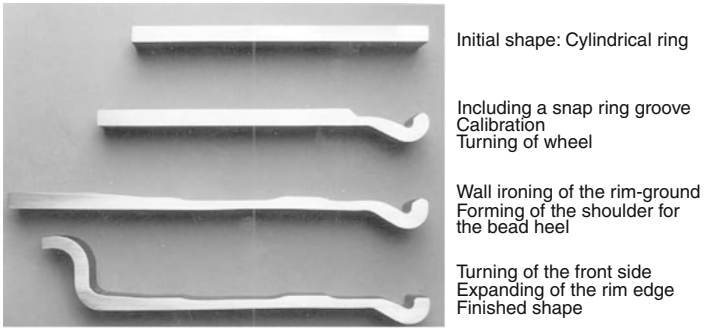


Fig. 4.60 Sequence of operations in the manufacture of taper base rim rings (*source* Leifeld Metal Spinning GmbH)

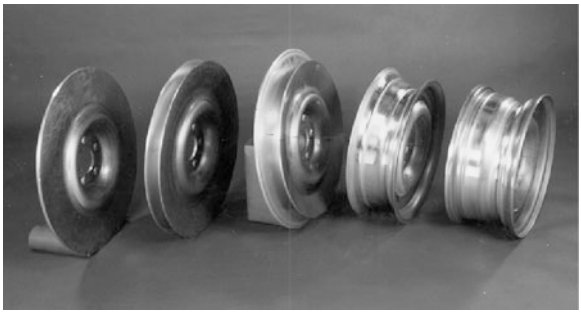


Fig. 4.61 One-piece aluminium split-rim wheel (*source* Leifeld Metal Spinning GmbH)



Fig. 4.62 Precision tube made of 14 CrMoV 5 9 (*source* Leifeld Metal Spinning GmbH)

sequence of operation in the manufacture of a one-piece aluminium split-rim wheel. This wheel is approximately 50 % lighter than a steel plate wheel of the same size and carrying capacity.

The process generally used for manufacturing precision tubes is shear spinning. This is usually executed in overruns. Collar steps and conical transitions can be created given a corresponding control of the spinning rollers. Figure 4.62 shows a precision tube made of the material 14 CrMoV 5 9, which was produced in two overruns. The wall thickness tolerance is 0.01 mm, the concentricity accuracy 0.05 mm. Given large tube lengths, a reverse spinning process is used. This allows for the shear spinning manufacturing of tubes, for example, made of X 5 CrNi 18 9 with a length of 6 m and a wall thickness of 0.5 mm.

4.4.5 Tools

In addition to the spinning chuck, whose shape is based on that of the workpiece to be manufactured, the metal spinning process makes almost exclusive use of spinning rollers. Spinning rods are rarely utilized by industry nowadays.

The spinning rollers are mounted in a fork. The axial and radial forces generated during the forming process are absorbed by the bearings. Depending on the machining operation, one distinguishes between the following roller types, among others [LUDW69]:

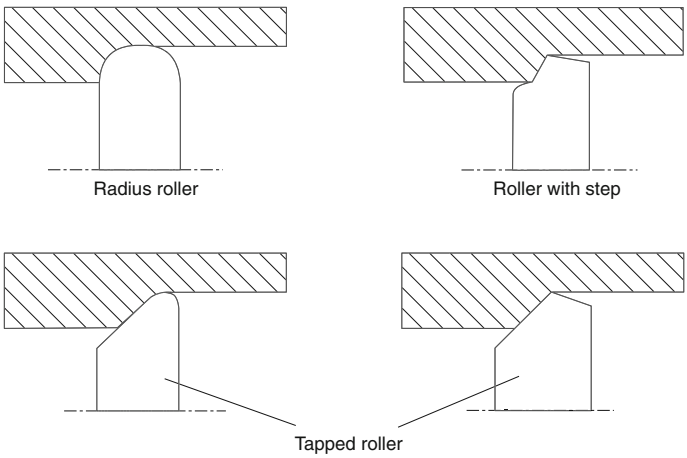


Fig. 4.63 Spinning roller shapes for shear spinning

- pressing rollers,
- smoothing rollers,
- calibrating rollers,
- drawing rollers,
- projection lengthening rollers, etc. [LUDW69].

The rollers are made of alloyed, wear-resistant tool steel and are hardened. Plastic rollers are also used to process soft metals, bronze rollers for stainless steel [LUDW69]. The shape and size of the rollers (roller curvature ρ_W, roller diameter d_W) are adjusted to the dimensions and shape of the workpiece. Shear spinning generally calls for higher forming forces than conventional metal spinning. One distinguishes between the following spinning roller shapes (Fig. 4.63) [GORB78, LUDW69]:

- radius roller,
- offset roller,
- tapered roller (double tapered roller).

Compared to radius and tapered rollers, offset rollers can be used to achieve greater wall thickness reductions per overrun, since a hindrance caused by bulging is largely avoided with the inlet cone [LUDW69].

The material used for the rollers is tool steel with a hardness of 62–65 HRC [GORB78]. The high strains are often accommodated by the use of three spinning rollers offset by 120°.

This allows for a regular distribution of force on the workpiece and prevents the stretch-chuck from deflecting [NN80].

Today, the different metal spinning processes make increasing use of machines with NC-controlled spinning rollers which guarantee greater flexibility and shorter

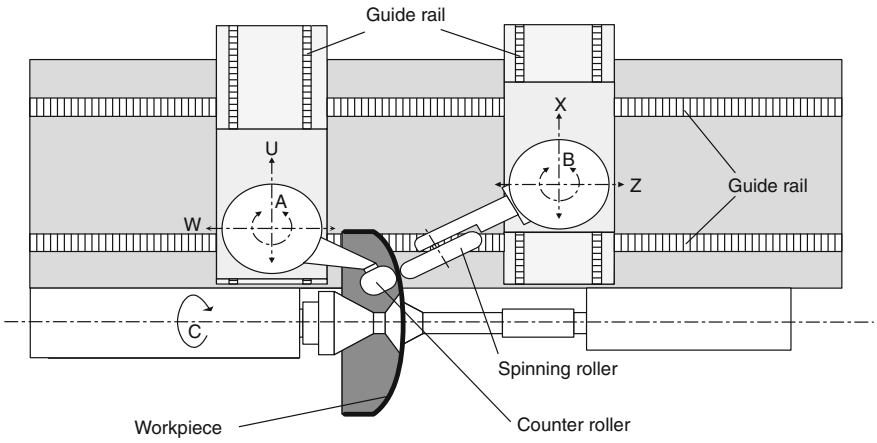


Fig. 4.64 NC-controlled spinning roller and counter-roller

changeover times [BRAC80]. Moreover, the spinning chuck can also be replaced by an NC-controlled counter-roller (Fig. 4.64).

4.4.6 Materials

Almost any malleable sheet material can be processed through metal spinning [LUDW69]. Typical materials are the following [NN82a]:

- unalloyed and low-alloy carbon steels,
- rust- and acid-resistant steels,
- light metals (aluminium, aluminium alloys with manganese, magnesium, silicon, as well as titanium),
- nonferrous heavy metals (lead, copper, brass, nickel, tin and zinc),
- precious metals.

The metal spinning process is particularly favoured by a great formability and a low strain-hardening tendency. Materials with a low strain capacity, such as some of the Al–Mg alloys, wolfram and titanium, as well as steel sheets with a thickness over 50 mm or precious metals over 20 mm [NN82a] must be hot formed [LUDW69]. In this case, the material is warmed locally during the metal spinning process with a gas burner [LUDW69].

In some cases, a gradual forming with intermediate annealing is also necessary to remove any strain hardening. New perspectives can be gained here through the selective heating of the deformed zone by means of a laser beam [KLOC04f]. Developments in construction and process technology with respect to laser-assisted metal spinning and application examples for laser-assisted forming processes are described in Volume 5 of this book series.

Table 4.2 Achievable working accuracy in metal spinning

Without contour control		With contour control	
Workpiece diameter (mm)	Tolerance (mm)	Workpiece diameter (mm)	Tolerance (mm)
<600	0.8–1.6	≤500	±0.2
600–1200	1.6–3.2		
1200–3000	3.2–6.4	>500	±0.4

4.4.7 Manufacturing Quality

4.4.7.1 Dimensional and Shape Accuracy

Springback following the spinning process influences the dimensional and shape accuracy of the workpieces. Defects in this respect can be reduced via a correction of the spinning roller movement. Table 4.2 shows the achievable dimensional accuracies. When spinning with an automatic contour control (copy spinning, NC spinning), considerably more narrow tolerances can be observed than with manual spinning roller control.

In comparison to metal spinning without wall thickness reduction, projection lengthening allows for improved shape accuracy, since in this case hardly any springback occurs [NN82a].

Wall thickness deviations are mainly dependent on the accuracy of the starting shape (circular sheet, preform) and lie, depending on the workpiece shape and size, between 0.01 and 0.2 mm [LUDW69]. In shear spinning, achievable diameter tolerances are in the order of 0.02 mm (for a 100 mm diameter), wall thickness deviations up to 0.01 mm.

4.4.7.2 Surface Quality

The surface quality in metal spinning and projection lengthening can be improved by selecting a smaller feed or through the use of a spinning roller with a larger radius of curvature [GROC04]. The more the shape of the tool surface line deviates from a straight line (concave or convex), the worse the surface is [LUDW69].

When shear spinning, the shape of the spinning roller causes a finish rolling of the workpiece surface [LUDW69]. The quality of the inner surface of the spinning part depends on the surface of the spinning chuck, which is frequently polished for this reason. The achievable mean roughness values range between $R_a = 0.02$ µm and $R_a = 0.2$ µm [LUDW69].

4.4.8 Metal Spinning: Advantages and Disadvantages, Criteria for Use

Manufacturing processes that compete with metal spinning for the production of rotationally symmetric hollow bodies are deep drawing, turning and wiper bending with subsequent welding.

Deep drawing requires a decisively higher amount of force, since forming is executed in a circumferential segment and not, as in metal spinning, in a local, narrowly limited area. Deep drawing is thus limited in terms of the construction size of workpieces [NN81b]. The choice is between the higher tool costs for deep drawing on the one hand, which requires a punch and a die and often, for complex shapes, more than one tool, and the longer machining times and associated higher labour costs for metal spinning on the other hand.

Figure 4.65 shows a fuel tank bottom for a civil carrier rocket made from a circular aluminium sheet with an outer diameter of three meters. In 2004, a metal spinning machine was first constructed with which fuel tank bottoms with an outer diameter of six meters were made for the "Ariane 5" rocket. Because of the size of the component, the resultant machining forces and costs, as well as the required precision, metal spinning is the only process alternative in the field of forming technology.

Due to the lower tool costs, the metal spinning processes can also be used in small-series production. Depending on the material and the workpiece shape, metal spinning cylindrical hollow bodies can be economically viable starting with series of 700–1,500 parts [HAYA81].

The production of hollow bodies by means turning can to high material waste levels. For this reason, metal spinning represents a cost-effective alternative as the



Fig. 4.65 Metal spun fuel tank bottom for a civil carrier rocket (*source* Leifeld Metal Spinning GmbH)

case arises. In addition to saving on material, another advantage is that the walls of the hollow bodies are strain hardened and thus exhibit higher strength.

As opposed to metal spinning, the manufacture of hollow bodies by means of wiper bending and welding can be highly time-intensive, requiring several work steps. Also, no variants are possible, such as wall thickness alterations and geometrical deformations (cones, spheres, cups etc.) [NN81b].

4.5 Bending

According to [DIN03k], bending or bend forming is the forming of solid bodies in which the plastic state is created essentially by means of a bending stress. In addition to metallic materials described in this chapter, others suited to bending are any other "malleable" materials.

Areas of application of bend forming are, on the one hand, individual production in boiler, container and ship construction and the mass production of smaller workpieces in motor vehicle construction as well as the manufacture of varying types of profiles and corrugated sheets on the other. With respect to sheet metal working, bending stands at the top alongside deep drawing. Besides sheet metal, ribbons, pipes, wires and rods are formed using very different bending processes. Typical forming machines are used in the process, such as presses, folding machines, profile rolling machines and bending machines with rolls. Figure 4.66 provides an overview of the different process variants of bend forming.

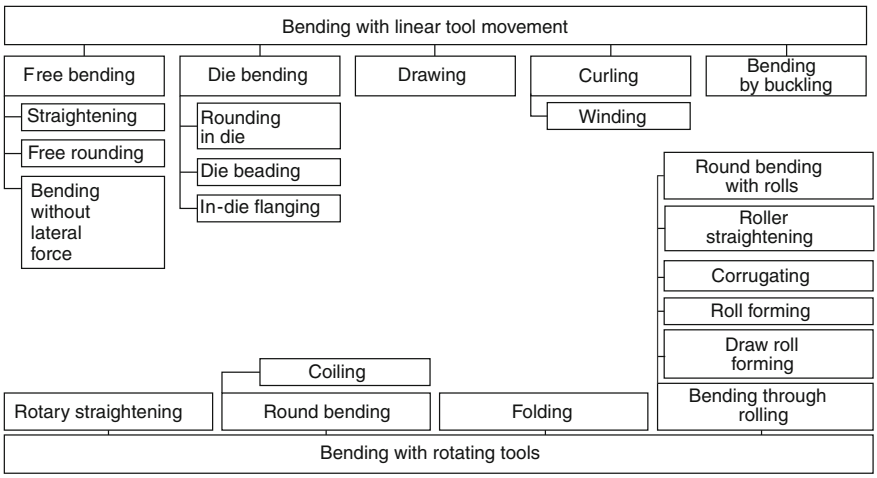


Fig. 4.66 Classification of bending processes [DIN03k]

4.5.1 Principles of Bending

4.5.1.1 Process Principle

The following will explain the mechanical principles of bend forming on the example of bending without lateral force. Although this bending process is lacking in practical relevance, it affords insights into the elastic springback after bending, the type of strain (bending radius) and the bending forces. For bending without lateral force, it is assumed that only a constant bending torque is active along the bending arc.

The classic theory of bending is based on the idea of a neutral fibre or an unstretched layer supposedly located in the centre of the sheet cross-section in which no longitudinal stresses are present. However, this hypothesis only applies for $r_i/s \geq 50$, whereas for most bending processes the ratios lie in the range of $r_i/s < 50$ ($r_i =$ inner bending radius, $s =$ sheet thickness). In this case, the unstretched fibre no longer lies in the centre of the cross-section. Instead, it is shifted to the inside with increasing bending angle (Fig. 4.67). As a result of stretching, flattening occurs in the outer fibre (outer radius), so that the outer radius of curvature is larger at the centre of the curvature than in the lateral areas of curvature. The internal fibre is generally subjected to compression.

4.5.1.2 Springback

Compression and stretching caused in the bending zone of the workpiece must be compensated by material displacement. This causes stresses released in part after the bending process which in turn cause the springback of the bent legs.

It has been found that an only weakly bent sheet with a bending radius r which is much greater than its thickness s has a stronger tendency to spring back to its original position in comparison to a workpiece bent to a sharp-edged contour. Thus the springback depends on the ratio of the bending radius to the sheet thickness.

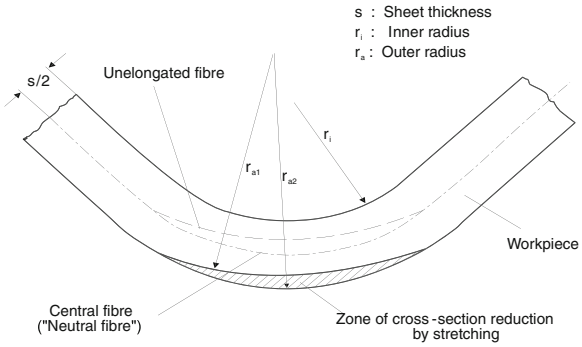


Fig. 4.67 Bending zones in workpieces with a bending angle of 90°

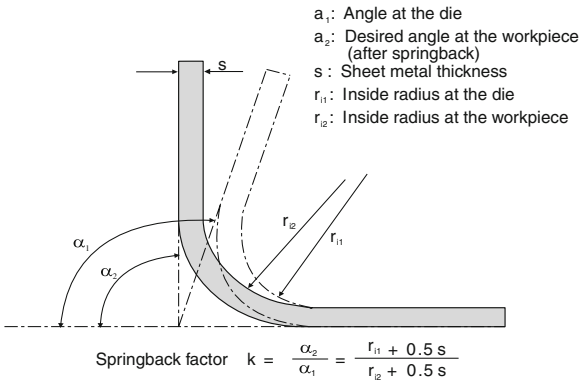


Fig. 4.68 Definition of the springback factor

This springback behaviour should be noted in all bending processes. This includes bending using a press, a folding machine, a profile rolling machine or a bending machine with rolls. Whereas in the latter case the springback can be affected by the setting angle of the rolls, with free bending it is enough to lower the punch more deeply and, with folding, to set a larger swivel angle for the bending apron. If an accurate, form-locking bending is required, however, the springback must be determined in advance for the sake of the constructive design of the workpieces. The ratio k of the target bending angle α_2 to the required angle of the bending tool α_1, which compensates the springback

$$k = \frac{\alpha_2}{\alpha_1} \tag{4.27}$$

depends on the material properties and the abovementioned ratio r/s (Fig. 4.68). Figure 4.69 provides the progressions of the values for k as a function of the bending radius/sheet thickness ratio $(k = f(r/s))$ for different materials.

The comparison of different materials in Fig. 4.69 shows that the k value increases with material strength given the same modulus of elasticity. This connection is also made apparent by the equation

$$r_{i1} = \frac{r_{i2}}{1 + \frac{r_{i2} \cdot R_m}{s \cdot E}}, \tag{4.28}$$

which links the required radius r_{i2} of the workpiece, the sheet thickness s and the ratio of the tensile strength R_m and the modulus of elasticity E with the radius to be defined. According to 4.28, no springback would occur given a rigid-plastic material with an infinitely high modulus of elasticity. Conversely, a large springback occurs given a high-strength material with a finite modulus of elasticity.

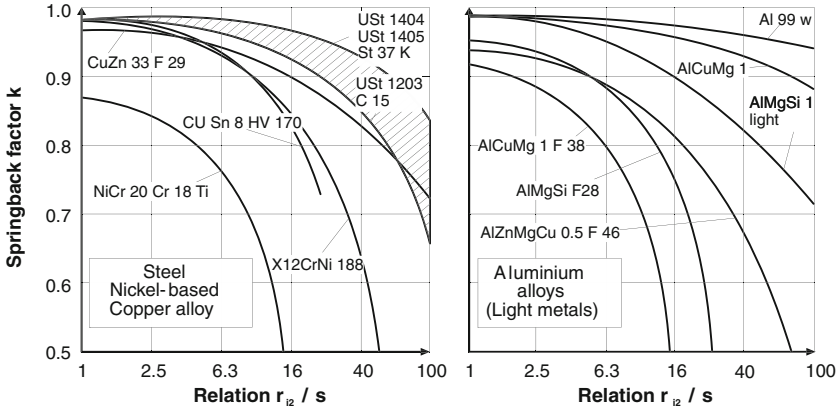


Fig. 4.69 Springback diagram for different materials [OEHL63]

In recent times, the bending process is increasingly simulated by numerical calculations with the aid of FEM analyses. This also allows predictions with respect to springback and residual stresses [KAHL82, FINC88].

4.5.1.3 Smallest Possible Bending Radii

Because of the compressions and stretchings which increase during bend forming in the direction of the sheet edges, strain hardening occurs in these areas. However, the increasing edge elongation on the outer side associated with the higher strength can lead to crack formation. One must therefore not fall below the smallest possible bending radius $r_{i,min}$. This value is determined by the degree of deformation in the extreme fibres. The deformation must thus be large enough on the one hand to allow for the desired bend, but on the other hand may not cause cracks in the area of the bending arc.

The minimum radius $r_{i,min}$ can be calculated via the maximum admissible elongation in the outer fibre ε_{aB}, with the flow properties of the material representing major influence factors. The following connection applies between $r_{i,min}$ and the edge elongation ε_{aB} [OEHL63, LANG90c]:

$$r_{i,min} = \frac{1}{2} \cdot s \cdot \left(\frac{1}{\varepsilon_{aB}} - 1 \right) = c \cdot s. \tag{4.29}$$

In the equation, c represents the minimum rounding factor, which is listed in Table 4.3 for different materials.

A factor which affects the variable ε_{aB} is the direction of the bending axis in comparison to the direction of rolling of the sheet. If they are parallel, crack formation can be assumed even with smaller edge elongations. This is because, due to the specified preferential direction of the grains, the material cannot easily

Table 4.3 Minimum rounding factors for different materials [OEHL63]

Material	C-factor	Material	Condition	C-factor	Material	Condition	C-factor
Sheet steel	0.6	Aluminium	Semi-hard	0.9	AlMn	Soft	1.0
Deep drawing sheet	0.5		Hard	2.0		Hard-pressed	1.2
Stainless steel (ferritic martensitic)	0.8	AlMg 3	Soft	1.0		Hard	1.2
Stainless steel (austenitic)	0.5		Semi-hard	1.3	AlCu	Soft	1.0
Copper	0.25	AlMg 7	Soft	2.0		Cured	3.0
Tin bronze	0.6		Semi-hard	3.0	AlCuMg	Soft	1.2
Aluminium bronze	0.5	AlMg 9	Soft	2.2		Hard-pressed	1.5
CuZn 28	0.3		Semi-hard	5.0		Cured	3.0
CuZn 40	0.35	AlMgSi	Soft	1.2	AlCuNi	Annealed	1.4
Zinc	0.4		Cured	2.5		Unannealed	3.5
Aluminium, soft	0.6	AlSi	Soft	0.8	MgMn		5.0
			Hard	6.0	MgAl 6		3.0

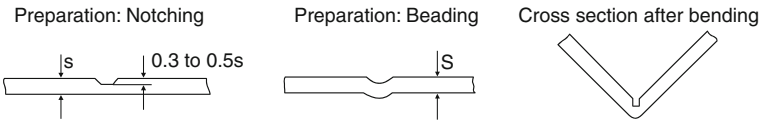


Fig. 4.70 Possibilities for achieving sharp bending edges

bear a load transverse to it. According to [DIN75], the values for $r_{i,min}$ are about 0.5 s higher than for bending perpendicular to the direction of rolling.

If the design calls for a sharp-edged contour of the bending edge, the workpiece must either be heated prior to forming or a previous notching (cross-section reduction) or, in the case of thin sheets, beading must be performed (Fig. 4.70). This can compensate the thickening of the sheet on the inner bending radius.

4.5.1.4 Edge Deformation

Deformations can appear at the outer edge of the bending arc which are undesirable for certain processing cases. This applies, for example, to hinges or bent components which are laterally guided after construction and must thus also exhibit a clean, rectangular edge in the area of the bending arc.

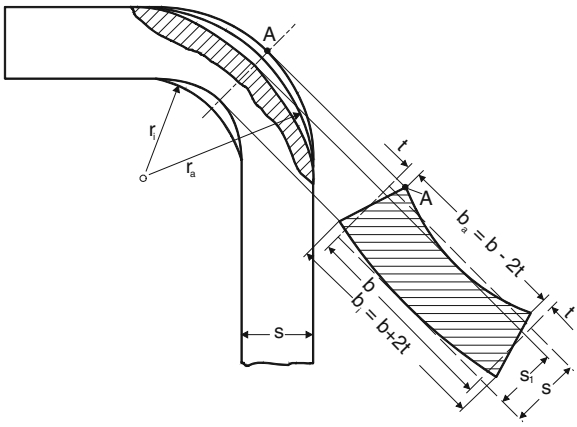


Fig. 4.71 Edge deformation in bending [OEHL63]

Disturbing edge deformations occur mainly when forming thick sheets with a small bending radius [LIPP59]. Since the material lying on the inner bending edge is compressed, it tries to deviate laterally at the edge. The starting width b thereby increases by a measure of $2t$ (Fig. 4.71). The material fibres running towards the outside exhibit the opposite behaviour. When they are elongated, the starting sheet thickness s is reduced on the one hand, often by more than 10 %, to s_1. On the other hand, the width b also shrinks to b_a by a measure of $2t$, as the material tends to flow inwards.

The cross-section in the bending area thus no longer corresponds to the shape of a rectangle, but rather more to that of a trapezoid (Fig. 4.71). In fact, however, as a result of the outwardly directed compressive forces on the inner edges, a lateral arching-up of the edge occurs together with the inwardly directed "shrinking forces" on the outer side of the bend. Past studies [OEHL44, LEHM58] have determined an approximate value for soft construction steel for the width difference (measure $4t$) between the inner and outer bending surface of approximately

$$4 \cdot t = 1.6 \cdot \frac{s}{r_i}. \tag{4.30}$$

If the lateral protrusion of the bulge over the starting workpiece width is disturbing for either constructive or functional reasons, a prior free machining operation can be used to prevent it. With easily formed materials, springback and thus the manufacturing tolerances for die bending processes (V-block) can be narrowly limited by means of a coining operation or a calibration pass. For this, the tools must be designed as in Fig. 4.72. The bending angle is to be set in these cases at 90°.

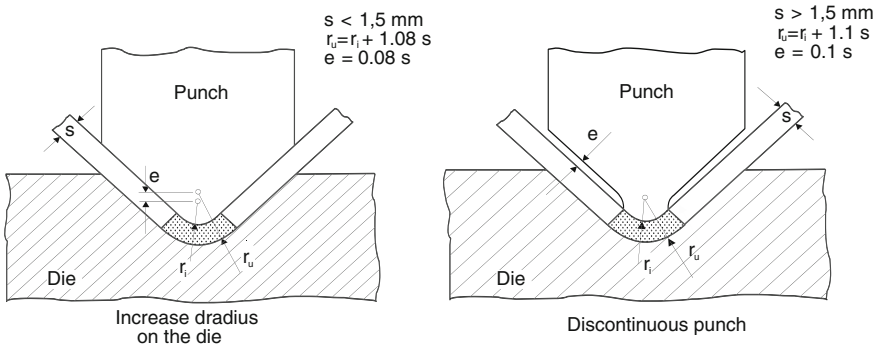


Fig. 4.72 Tool design for bending with coining

4.5.2 Process Variants

4.5.2.1 Free Bending

Free bending is described in [DIN03k] as bending with the free forming of the workpiece shape. The desired shape is this not specified by the geometry of the individual tools used in the bending process (punch, support plate), but rather by their position and direction of force.

Figure 4.73 shows two methods of free bending: the free bending of a sheet mounted on two sides with a punch attacking between the support plates (Fig. 4.73

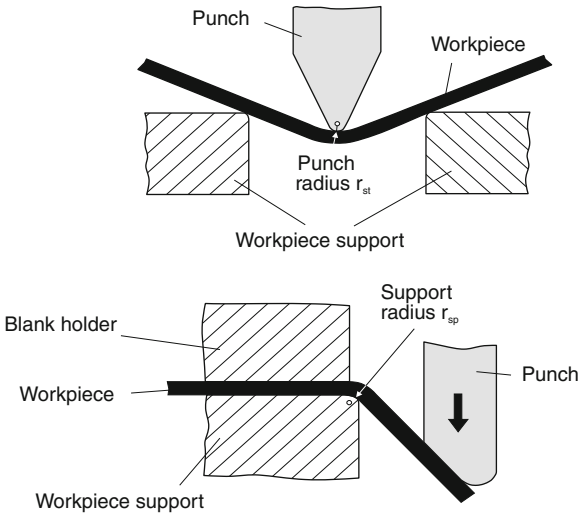


Fig. 4.73 Free bending with lateral force

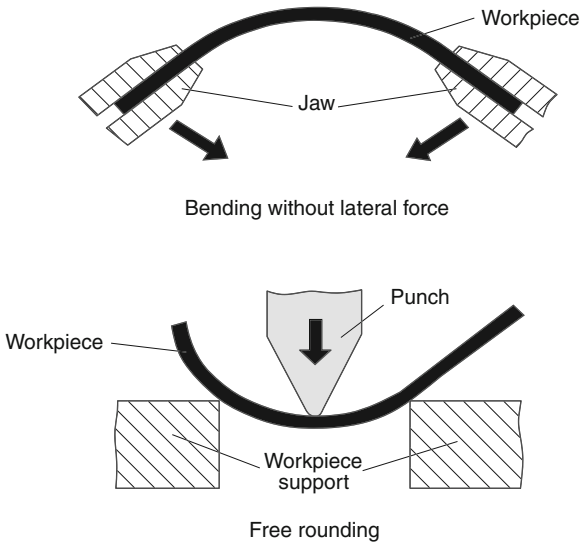


Fig. 4.74 Process variants of free bending

above) and the free bending of a sheet clamped on one side with a punch attacking at the end (Fig. 4.73 below).

These cases, however, are only free bending processes in the strict sense if the smallest inner bending radius of the workpiece is larger than the punch radius or the radius of the workpiece support plate. Other types of free bending are:

- bending without lateral force,
- free round bending,
- bend straightening.

Figure 4.74 provides examples for the first two process variants. Bending without lateral force is a forming process under pure moment loads, with the bending radius remaining constant over the length of the arc.

Free round bending refers to a gradually progressing bending of the workpiece. Because the punch moves in a straight line, the bent component must be pushed further after every stroke. In this way, a freely self-adjusting, round workpiece shape is created (Fig. 4.74 below).

Whereas the processes introduced until now serve to create curvatures on even or straight workpieces, bend straightening has the task of removing already existing, undesired curvatures, e.g. arising through irregular cooling after forming or residual stresses released during machining. Typical parts which must be straightened before finishing, e.g. grinding, include short rods, stepped shafts or crank shafts.

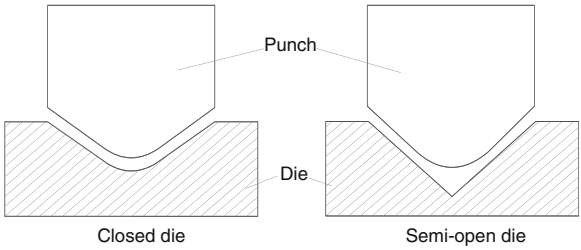


Fig. 4.75 Different tools for bending with V-block

4.5.2.2 Die Bending

In die bending, the workpiece is bent between the bending punch and the bending die until it assumes the required shape. The process can be combined with that of coining in an impression die, which refers to resqueezing of the workpieces to achieve the required accuracy. resqueezing is also referred to as forming to size or as sizing (Sect. 4.5.1.4). The most important die bending process which is also used most frequently in practice is bending with a V-block. This process utilizes open and half-open tools (Fig. 4.75).

Irrespective of the tool shape, die bending comprises two sequential processes:

The first process is free bending. This begins with the setting of the punch on the workpiece. The process is complete when the legs of the bent part are in contact with the die walls or when an inner bending radius develops on the workpiece which is smaller than the punch radius.

A resqueezing process follows. This adjusts the workpiece to the tool shape. A decisive role is played in the process by the ratio r_i/r_{St}.

If $r_i/r_{St} > 1$, the bent component is initially supported at two points against the die and at one against the punch (Fig. 4.76 left). Upon the further lowering of the punch, the support points on the die are displaced in the direction of the die centre and the free legs of the bent part are set laterally on the punch (Fig. 4.76 centre). A further approach causes the free legs to bend back until the workpiece assumes the shape of the tool in the final position (Fig. 4.76 right).

However, given a ratio of $r_i/r_{St} < 1$, the tool shape for the sizing process must be taken into account. If a closed tool is used, the contact points sketched in Fig. 4.77 above exist between the tool parts and the workpiece. The final shape then results as the bending arc is pressed in more and more. If a half-open tool is used, however, the tip of the bending arc cannot be supported on the die (Fig. 4.77 below). Thus bending processes can occur in which the workpiece centre is not set on the punch.

Another frequently implemented die bending process is U-die bending. This refers to the simultaneous bend forming of two legs connected by a web by 90° to a U-shaped workpiece. There are two process variants:

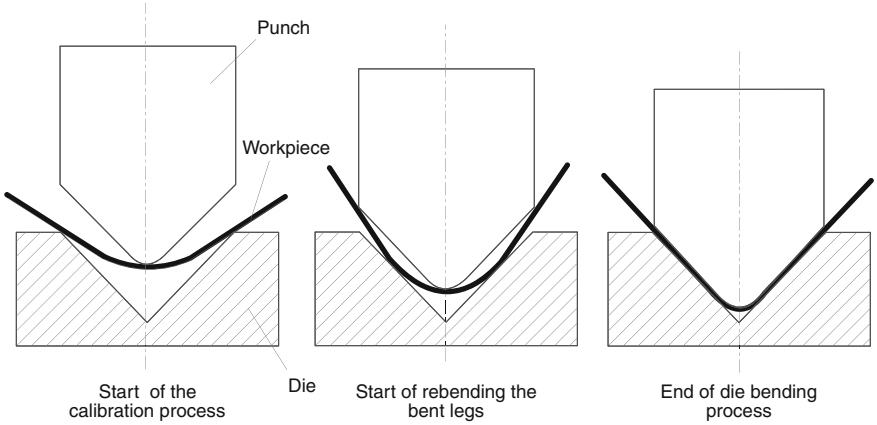


Fig. 4.76 Bending with a 90° die with small punch radius (half-open tool)

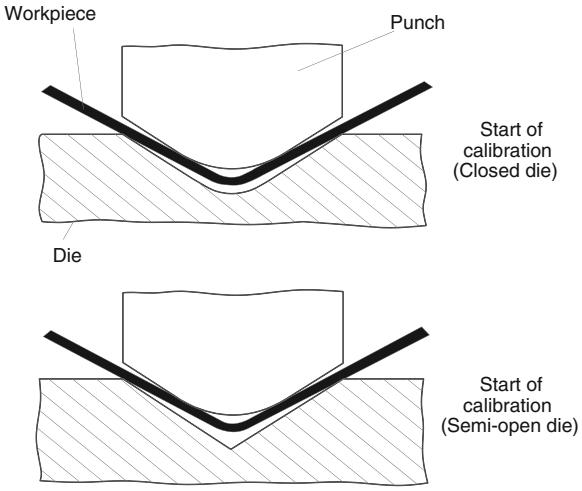


Fig. 4.77 Bending with a 90° die with a large punch radius

1. U-bending without a counter holder (Fig. 4.78 left)

First, there is an elastic deflection running in an arc shape in the area of the web. When the punch is lowered, the legs fold upwards. This causes an increase in the curvature of the web. As soon as the rounding of the web touches the die bottom, the process of resqueezing begins, in which the web first arches upwards and is then press upwards. The legs of the bent component are in contact with the punch during the process.

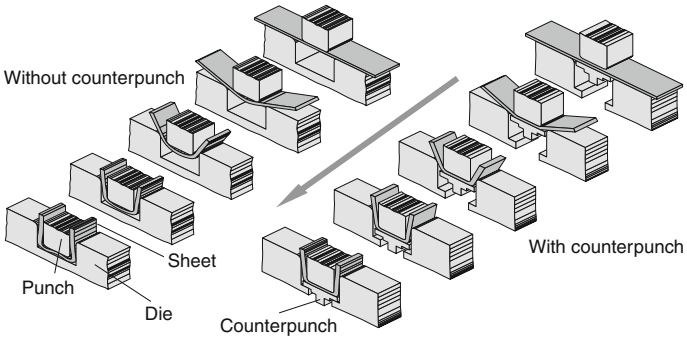


Fig. 4.78 Bending with a U-shaped die, with (*left*) and without (*right*) counterholder [OEHL63]

2. U-bending with a counter holder (Fig. 4.78 right)

The counter holder has the task of pressing the web firmly to the punch bottom during the entire bend forming process. The process is largely the same as that without a counter holder, except that no resqueezing process is involved. As studies have shown, the required force of the counter holder is roughly 0.3 times the force needed to raise the legs [VATE70]. Resqueezing requires three times this amount if no counter holder is used.

4.5.2.3 Folding

As opposed to die bending, the active tool in folding machines executes a swing movement instead of a linear movement. The sheet to be bent is clamped between the upper and lower wings and its protruding free end is formed by swinging the bending wing, thus folding the workpiece (Fig. 4.79). The swing angle corresponds to the bending angle of the sheet plus the springback value. FEM simulations can be executed in order to define the required swing angle and the residual stresses remaining in the sheet after bending [SCHI93].

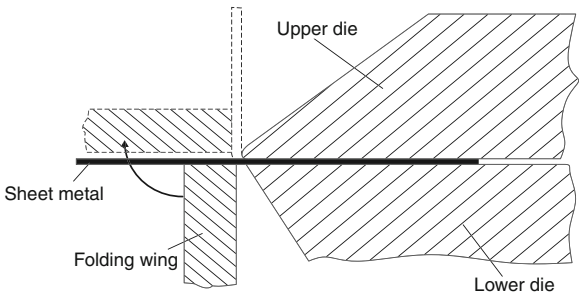


Fig. 4.79 Principle of folding

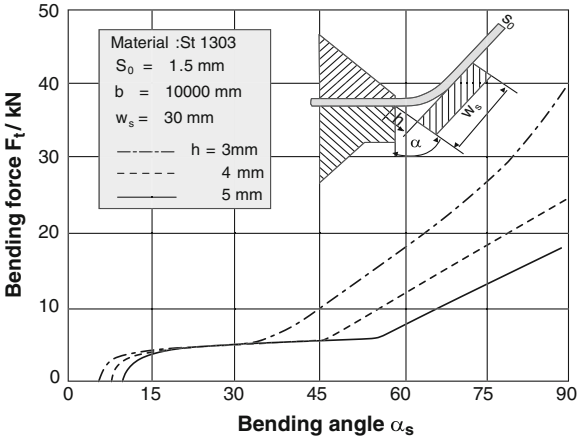


Fig. 4.80 Bending force as a function of bending angle and wing distance [FAIT87b, FAIT87a]

The bending line and the forces arising during folding show a strong dependency on the kinematics of the folding wing. If one selects a large bending lever arm and a large distance between the folding wing and the clamping tool elements, a large inward bending curvature is the result. This setting requires a relatively low amount of force (Fig. 4.80). For the sharpest possible bending radii, the wing distance must be reduced correspondingly [FAIT87b, FAIT87a].

4.5.2.4 Roll Bending

Roll bending, which is also a bend-forming process with rotating tool movement, is subdivided into the following process variants:

- round bending with rolls
- roller straightening
- corrugating
- roll forming
- draw roll forming

Round Bending With Rolls. The forming process referred to as round bending with rolls serves primarily to round fine, medium and coarse sheet metals for the manufacture of tubes and tube-shaped workpieces, e.g. for container and apparatus construction. Conical sections are also bent with this process. Also, round bending machines with rolls can be used to manufacture shapes deviating from rotational symmetry, such as ovals, rounded rectangles or coils to be used as parts for containers, housings and luminaires. In line with this area of application, different construction types of round bending machines with rolls have been established which can be categorized essentially according to the number, arrangement and adjustability of the bending rolls.

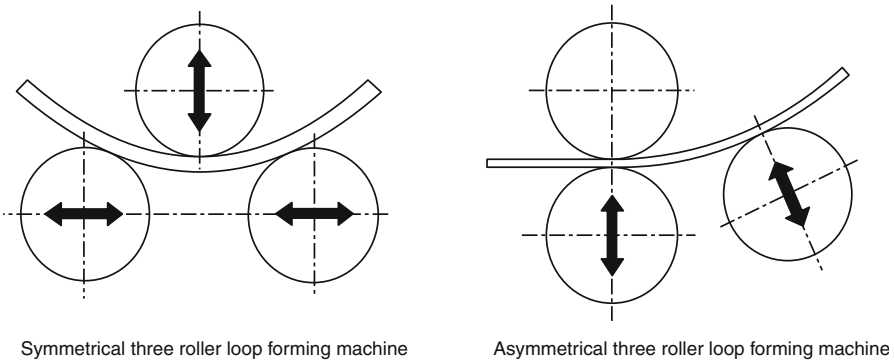


Fig. 4.81 Roll arrangement for a three-roll round bending machine [ZICK79]

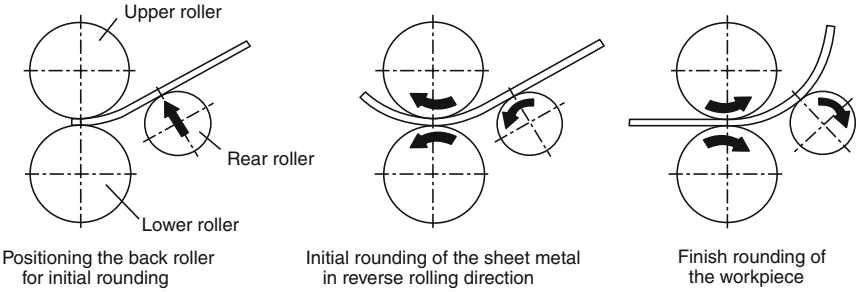


Fig. 4.82 Bending and finish round bending on an asymmetric three-roll round bending machine [ZICK79]

Frequent designs are three-roll and, especially for large units, four-roll machines. Two-roll machines are exclusively light machines made for low sheet thicknesses in which an unwound folded sheet is inserted into a corresponding slot of the upper or lower roll.

Symmetrical three-roll round bending machines are constructed for rounding coarse sheets. These are generally equipped with horizontally movable lower rolls and vertically movable upper rolls (Fig. 4.81 left). These are distinct from asymmetrical three-roll machines used for fine and medium sheets (Fig. 4.81 right). A characteristic feature of these is that the sheet part is moved while being constantly clamped by the two front rolls, whereas the back rolls initiate the bending process. For process engineering reasons, there is a wide variety of variants between these two basic designs. For example, cylinder-shaped workpieces cannot be manufactured on asymmetrical three-roll round bending machines in a single run or clamping. The sheet part must be bent at one end, which can be achieved under a press or by means of an initial reverse insertion and bending in the round bending machine (Fig. 4.82) [MASS93].

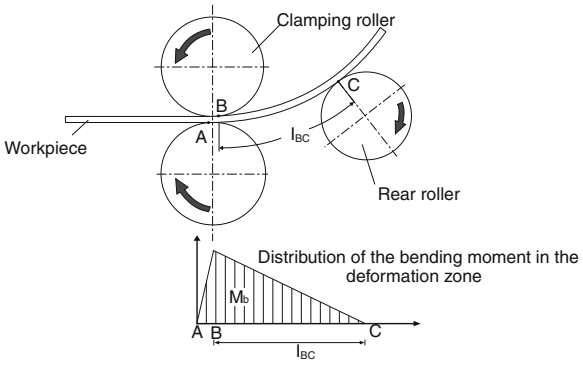


Fig. 4.83 The loading and the progression of the bending moment for round bending with rolls on an asymmetrical three-roll round bending machine [ZICK79]

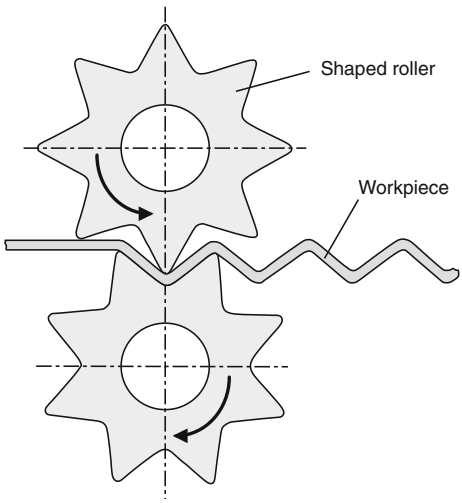
Figure 4.83 shows the loading and the corresponding progression of the bending moment for round bending with rolls on an asymmetric three-roll round bending machine [ZICK79]. The current state is comparable to a cantilever: The clamping point is the contact zone of the sheet between the drive rolls, with the load being generated by the back roll at point C. The displaced position of points A and B for connecting the midpoints of the clamping rolls results from the elastic deformation of the rolls and from the elastic–plastic deformation of the sheet. The traversed distance in part causes the "unbent end" in bending, which is specified as 1.5–4 times the sheet thickness.

To manufacture conical sections, the sheet must be cut in the form of an annular section. The different diameters are then created by tilting the lower rollers. Round bending with rolls also offers the possibility of manufacturing rotationally asymmetrical containers and housings [ZICK79, LUDO81]. In such processes, the feeding of the sheet and the adjustment of the rollers must be controlled continuously.

Corrugating. Corrugating refers to the roll bending of metal sheets, wires or tubes with rollers profiled in the circumferential direction, with the roller axes usually standing perpendicularly to the plane of bending (Fig. 4.84).

Roll Forming. Roll forming offers a cost-effective way to create profiles from metal sheet strips. In this process, metal strips are formed to profiles by means of roller pairs located one behind the other. Figure 4.85 shows the manufacture of a U-profile, a basic example of roll forming. The gaps between the upper and lower rollers of the two stages changes in the process from a strip shape to the final profile shape. The strip thickness and thus the size of the cross-section remain constant, as in all other bending processes. The process can also be used to manufacture complex or composite profiles. The rolling speed can run up to 100 m/min, which makes the process competitive not only with die bending, but also with bar extrusion and hot rolling of profiles [WEIM68].

Fig. 4.84 Corrugating



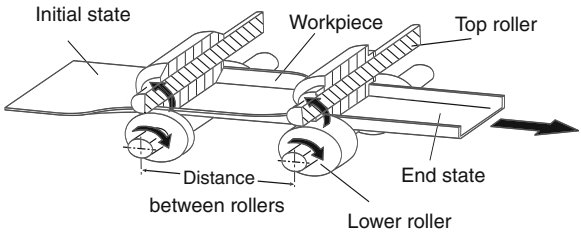


Fig. 4.85 Production of a U-profile by roll forming

Difficulties arise in roll forming in the form of edge warps which can form as a result of local elongations [MILC78, TÖLK70, WEIM66, WEIM68]. The reason for the warps is that bending does not occur over the entire width of the sheet. The following measures can be taken to reduce edge stretching:

- avoiding bending long legs,
- further bending by only a few degrees per step,
- inclining the roller pairs toward each other in order to superimpose a compression load on the otherwise stretched profiles,
- profiling by means of stretching (overfeed) using a gradually increasing roller diameter with a constant rotational speed—although entailing the danger of heavy roller wear and scratching the profile,
- continuous straightening of the curved profiles by means of straightening rolling in the opposite direction of the direction of curvature otherwise present [WEIM68].

Draw Roll Forming. Draw roll forming is a bend forming process in which the tools causing the shaping process are not driven. Instead, workpieces (bands, sheet strips) are drawn through the roller gap. The design of the rollers is similar to that for roll forming.

Table 4.4 Basic profile shapes [OEHL63]

Description	Profile Shapes			Cranks and lugs	
	Sharp-edged	Rounded off	Totally rounded	Simple	Reversed
V-profile					
L-profile					
U-profile					
C-profile					
O-profile					
Z-profile					

4.5.3 Tools and Workpiece Shapes

The large number of different bending processes entails a correspondingly large number of bending tools. These can be categorized as follows:

- Tools used for forming small workpieces. These generally involve processes with straight tool movement, i.e. die bending, curling or bending by buckling.
- Tools for large workpieces requiring the use of a special bending machine. The processes already mentioned are also used here.
- Tools for processes with rotating tool movement (draw roll forming, round bending or folding) which are all applied without exception using special bending machines.

In order to shorten set-up times and to increase flexibility in production, the tools increasingly have a modular design and are equipped with an automatic changing device [ISIN93, STAH93, NN94b].

To distinguish and classify the different workpiece profile shapes, upper-case letters are used corresponding to the cross-sectional shapes of the profiles, resulting in V, L, U, C, O and Z basic profiles (Table 4.4).

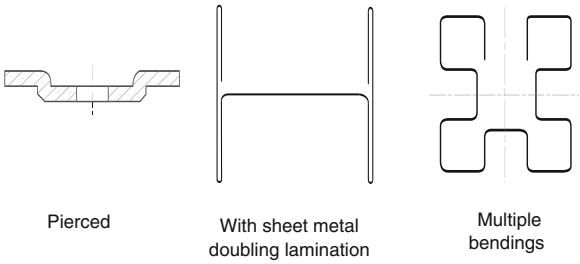


Fig. 4.86 Special shapes in draw roll forming

In addition to these basic profile shapes, more complex profiles are also draw roll formed for special applications (Fig. 4.86).

The attainable accuracies depend on the respective process. Die bending without a counterholder can only be used to manufacture sheet parts with lower accuracy (IT 11). Bending with counter pressure is used to produce workpieces with medium accuracy (IT 10). Higher accuracies (ca. IT 8–IT 9) are only attainable in a bending process if the sheet is centred in the tool beforehand. The same accuracy, however, is also attainable by employing an additional calibration pass. A number of additional requirements must be fulfilled in order to achieve the desired accuracy of the bent part [ROMA71]:

- The minimum bending radius should only be preset in exceptional cases. In general, the most favourable radii for thin sheets are $2s \geq r_i \geq s$ and, for thick sheets, $r_i \geq 2s$.
- If less ductile materials with the smallest radii $r_i \leq 0.5s$ are bent, the bending line should lie at a right angle to the direction of rolling. If $0.5s < r_i < s$, however, the position of the direction of rolling is not significant.
- In the case of brittle materials (e.g. bronze, brass or spring band steel) forming must occur at a right angle to the direction of rolling, as otherwise a crack may start to form due to the preferential direction of the grains.

4.5.3.1 Bending With Straight Tool Movement

Tool construction for bend forming is similar to that for deep drawing or cutting. The bending die replaces the drawing or blanking die, the bending punch the drawing or cutting punch (Fig. 4.87).

For very simple tools, punch and die are fixed directly on the table or on the press rams, for complex tools in supporting frames. Since the workpieces sometimes adhere to the punch following bending, they must be loosened from the punch by means of strippers or a spring-loaded pressure piece. Stops in the form of pins or bars simplify the insertion of the workpieces.

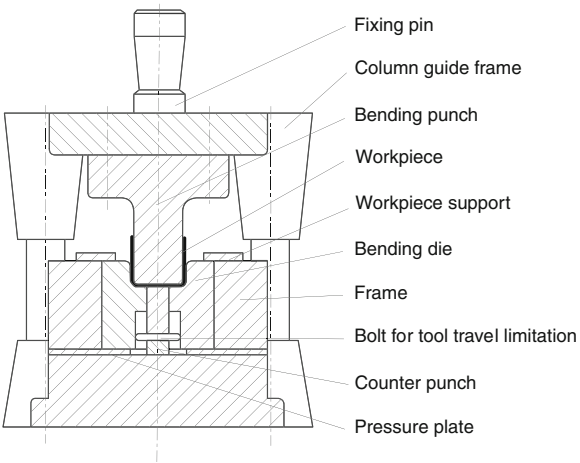


Fig. 4.87 Folding tool with pillar guidance

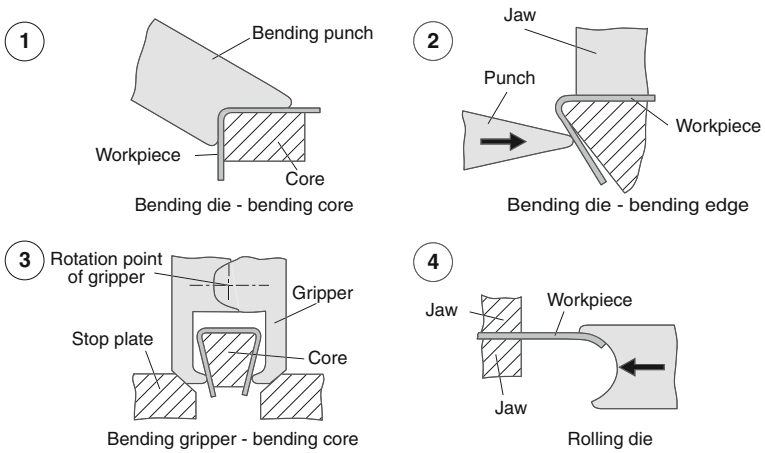


Fig. 4.88 Bending tool types [BRÜL78a]

Irrespective of the processing machine used, different types of bending tools can be implemented [BRÜL78a] (Fig. 4.88):

Bending Punch and Bending Core (1). Both tool parts are similar in contour except around the workpiece thickness. This contour corresponds to the shape of the bending section. The springback of the part should be taken into account.

Bending Punch and Bending Edges (2). The workpiece is bent freely vis-à-vis a fixed clamping location or between two support points. The final position of the bending punch determines the bending form according to springback. The bending can be corrected by regulating the final position of the punch. Because of the uncertainty involved in precorrecting springback, bending angle measurement

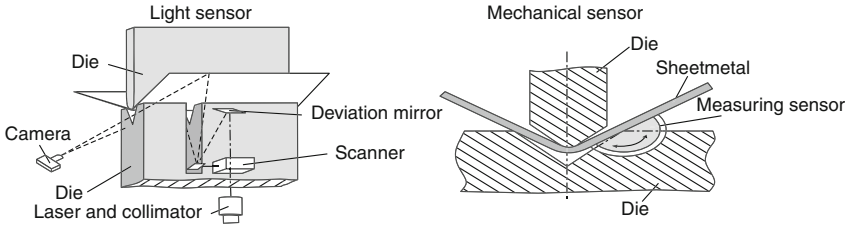


Fig. 4.89 Optical and mechanical measurement of the bending angle [GEIG93a]

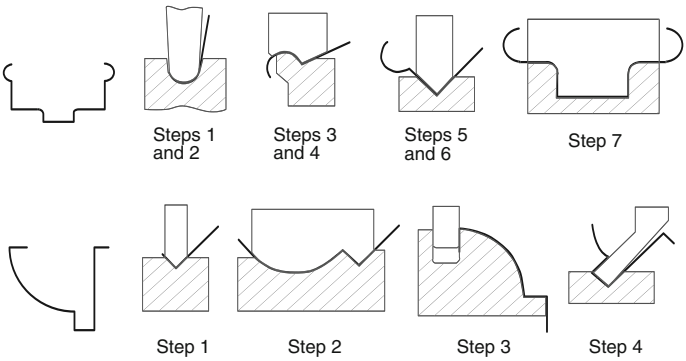


Fig. 4.90 Example of operations for the production of different profiles using die bending [OEHL63]

systems have been developed which determine the springback following punch retraction.

These values aid the press control in the online calculation of the required final position of the punch. There are two different measuring methods, one of which makes use of an optical light section sensor [GEIG93a] to determine the angle of the sheet, the other of which uses a mechanical sensor [HUXH93] (Fig. 4.89).

Bending Wrenches and Bending Core (3). The bending punch or punches are mounted in a tong-like manner. During the lowering process, the material can be formed around the bending core by opening and closing the tongs via the stops.

Rolling tool (4). A cup-shaped tool is moved against the specified end of the material. Starting materials used for the punch and die are high-speed steels, carbide-tipped tool parts and, in special cases, ceramics. Figure 4.90 illustrates the forming steps for manufacturing two profiles as an example for complicated bent parts.

Special dies are required in the second and third work step for the undercut groove profile (Fig. 4.90). The second work step can also be executed in three individual stages with normal dies. The upending in work step 4 is only possible with a highly offset upper beam rail. The manufacture of such an undercut profile can also conceivably be executed in a single work step, albeit with the use of a

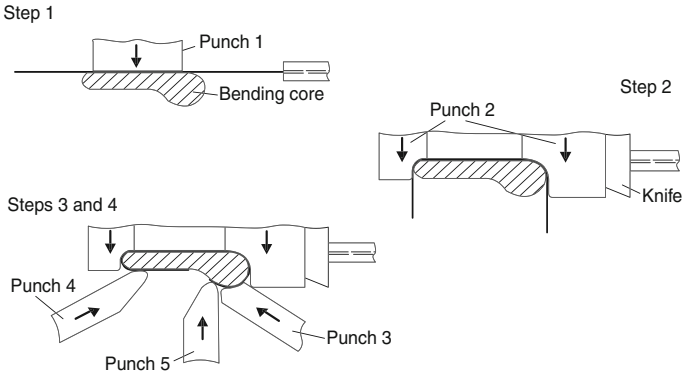


Fig. 4.91 Bending on bending machines

special die and an additional swivel-mounted auxiliary rail for creating the inward overlap of the profile edge.

Figure 4.91 shows the manufacture of an almost entirely closed workpiece. Using conventional working methods, this piece can only be produced on different workplaces and also entails inserting work.

In this particular case, all bending is executed at a right angle to the direction of rolling, which allows for small bending radii. Modern die bending machines are NC controlled and can change tool elements automatically. For highly accurate bending operations on large sheets, the machines have a hydraulic deflection compensation of the die which is adjusted to the respective press force. Further manufacturing examples can be found in [BRÜL78a, BRÜL78b, HILB70, KLIN56a, KLIN56b, KLIN56c, OEHL63, OEHL01, RADT79, ROMA71].

4.5.3.2 Bending With Rotating Tool Movement

Among the different bend forming operations which work with a rotating tool, the following will only treat

- folding and
- roll forming,

including the tools involved in each process and some manufacturing examples.

Folding. The construction of folding machines is shown in the cross-section on the left side of Fig. 4.92. It is important that the bending wing have as light a design as possible so as to achieve short cycle times. By adjusting the bending wing, one can change the bending lever arm and the inward bending curvature. Folding has found increased employment in recent years, especially for small and medium quantities, as it is considerably more flexible in application than die bending. With folding, many different workpiece shapes can be bent with a single

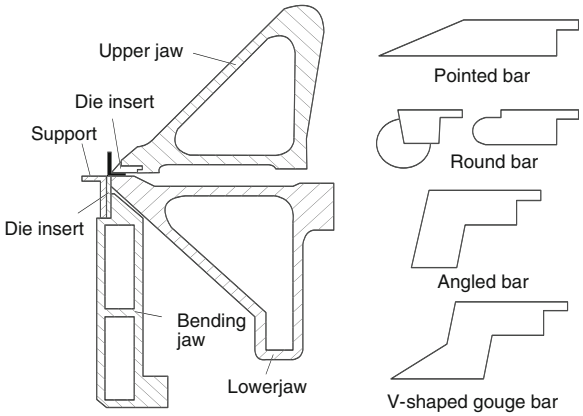


Fig. 4.92 Cross-section of a folding machine and the main bending rail profiles used

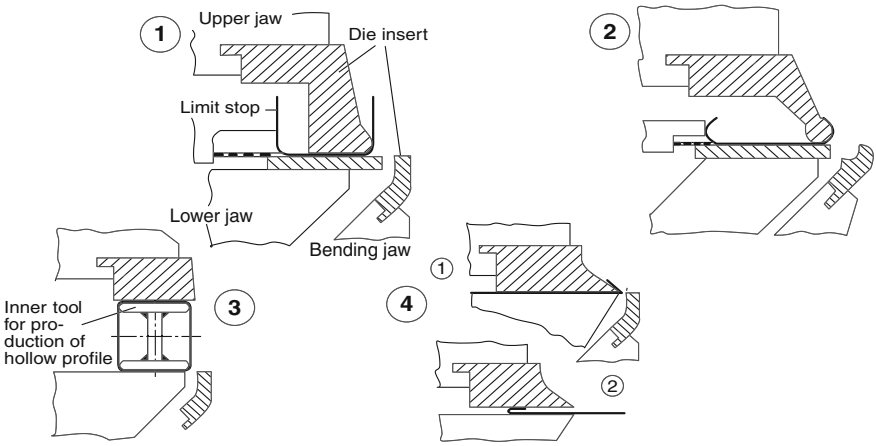


Fig. 4.93 Examples of the folding of different profiles [OEHL63]

tool set by controlling the bending wing and the stops. This reduces both set-up time and tool costs, although the basic machine costs are higher.

The performance of folding machines has proved to be increased significantly through the use of multiple NC-controlled axes, such as stops, swing angle and wing arrangement. As tools, different bending rails can be used. There are four main categories of such tools (Fig. 4.92 right).

Figure 4.93 provides examples for the manufacture of simple basic profile shapes:

To manufacture a rounded U profile, a suitable machine should be selected so that the sheet can initially be set against the lower (back) stop prior to raising and the first leg against the upper (front) stop following the folding operation (Fig. 4.93 (1)).

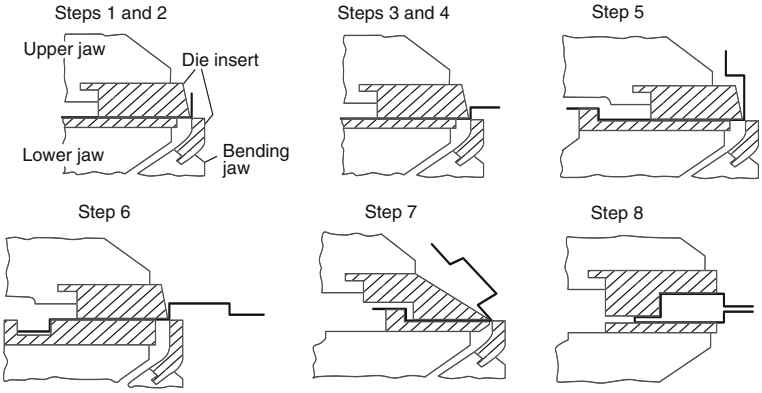


Fig. 4.94 Manufacture of a door frame profile (folding) [OEHL63]

When bending a rounded C profile, the bending wing is swivelled, if possible, around the midpoint of the curve profile. In any case, a well-defined and secure positioning against the stop locations should be provided for. The inner side of the bending rails should correspond to the curvature to be created (Fig. 4.93 (2)).

For the hollow profile "rounded O profile", installations should be provided for folding. These must be extracted from the sides when the manufacturing process is complete (Fig. 4.93 (3)).

Two work steps are required for sharp-edged fillister-bending (Fig. 4.93 (4)).

Another manufacturing example containing multiple work steps is the production of a door frame profile (Fig. 4.94)

The reason why folding has a larger number of stages is that the process is unable to produce direct Z-shaped profile forms in a single work step, as in die bending. On the other hand, folding requires no change of the upper beam bending rails in the first six work steps. Today, bending machines are largely constructed with segmented tools which allow for a reduction of changeover time by up to 50 %, thereby increasing productivity [STAH93].

A special process variant of folding is curling, in which the swivelling movement of the bending wings is superimposed with a linear movement (Fig. 4.95). This NC-controlled, superimposed kinematics prevents the relative movement between the tool and the sheet which is otherwise typical of almost all bending processes. This helps to avoid scratches on the sheet surface [STAH92].

Roll Forming. The roll forming process is described in Sect. 4.5.2.4. Machines used for roll forming are usually constructed according to the modular design principle. This way, units with one or two roller pairs can easily be constructed together to form machines with fewer rolling stands for manufacturing simple profiles. For highly complex parts, however, installations with up to 30 roller pairs have been constructed. The process is economically viable when profiles are needed in very large quantities or lengths.

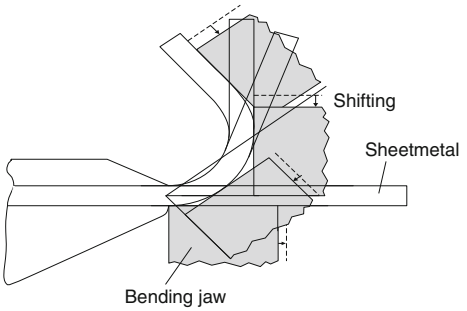


Fig. 4.95 Kinematics of curling (acc. to Reinhardt GmbH Sindelfingen)

The design of a roll forming pair is based on bending stage plan. To optimize the forming process, the profile should lie as flat as possible so as to eliminate or at least minimize vertical walls and to minimize overlapping and slip between the strip and the rollers. The workpiece should continue to be upwardly open for easy observability, its flat sections lying parallel to the roller axes.

The material properties and workpiece geometry indicate the number of stages in which a single profile leg should be bent. This number is large if the elastic limit, bending angle, leg length and modulus of elasticity increase or if the deformation length decreases.

The number of stages and the partial bending angle is individually determined for the bending of each edge. They are both also dependent on the sequence in which the individual edges must be profiled and on the position of the profile in the machine. The bends are further combined in such a way that several edges can always be formed, with an equal number of edges on both sides of the symmetry axis and never more than four simultaneously [SACH51].

It is recommendable to bend the edges in the centre of the profile first, since the rims of the strip are not yet clamped and thus the strip cannot be drawn back or stretched at the finished edges perpendicular to the direction of movement. If many edges are formed at the same time, the tools must follow the edges, which move together more and more closely to ensure that there is enough material between the bordering edges remaining for the forming process. Also, given initially large radii, there is the possibility of drawing the material from one leg to the other in the event of small inaccuracies. Tubes are purposefully formed with a constant radius from the outside inwards. The tube is closed by means of side rollers.

In conclusion, the following forming processes should be avoided as much as possible [JEME47, TRIS64]:

- drawing material over edges,
- compressing material into corners,
- walls standing perpendicular to the roller axes,
- excessively high profiles as a result of different circumferential speeds of rollers and resultant friction,

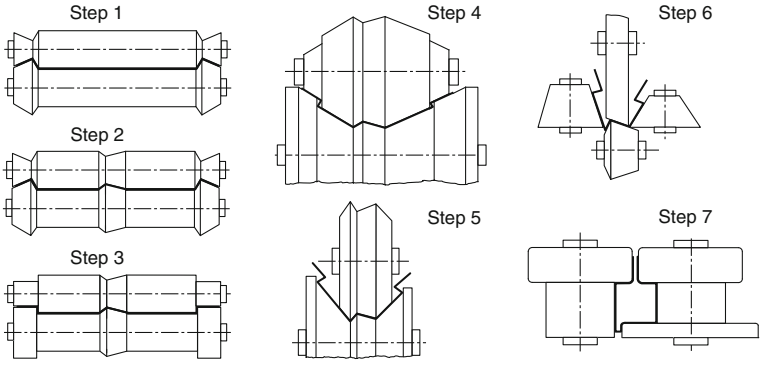


Fig. 4.96 Manufacture of a door frame profile (roll forming) [OEHL63]

- excessively small profile opening, as otherwise a high roller wear occurs,
- undercuts, as the profile is not surrounded by the tools on all sides,
- long legs if the strip edges have not been stiffened,
- strong or abrupt bendings,
- small bending radii,
- excessively large bending radii (springback),
- rolling out the strip due to high local tool pressure,
- pressing the sharp strip edges with rollers or guides.

Already mentioned in the context of die bending and curling, door frame profiles can also serve as the first manufacturing example for roll forming (Fig. 4.96). In the production process, the outer parts are first prerolled and then the inner areas formed. In final position 7, it is recommendable to mount one of the two rollers of every axis diagonally, since the circumferential speeds of the rollers vary and the profile to be produced would thus otherwise be bent by additional friction. It is also favourable to add an additional stage with a driving upper and lower roller which simultaneously takes over the function of closing of the profile.

Roll forming can also be employed to manufacture compound workpieces in a process in which, for example, a steel sheet profile is wrapped around a plastic strip, a strip of wood or another sheet profile. This can be applied to die bending machines, by means of curling, or on a roll bending machine. Because of springback, however, a very tight closure of compound profiles for these bend forming processes can only be achieved with great difficulty. For this reason, production under roll formers is more efficient, especially since in this case it is easier to encase the inner profile with the outer under prestress, so that the parts actually sit firmly in each other. Roll forming offers a lot of freedom with respect to forming profiles. Even perforated profiles can be made, with the perforation occurring during the forming process via a roller cutter. A highly sharp-edged bending between the rolls is also possible, achieving a sheet doubling.

4.6 Special Processes of Sheet Metal Forming

4.6.1 Internal High-Pressure Forming

Internal high-pressure forming refers to forming processes using active media in which the stress in the workpiece required for forming is introduced via an active medium. There are different active principles (force- or energy-bound) and active media (fluids, gases and formless solids) [VAHL04]. Internal high-pressure forming is an innovative manufacturing process of forming technology used increasingly for producing workpieces from sheet metal for lightweight automotive construction [DOHM93a, KLAA93].

The beginnings of internal high-pressure forming can be traced back to the second half of the 19th century. The first areas of application were in sanitary engineering and concerned bending and calibrating pipe bends [PISC95]. Because of the frame conditions of the time, the process was unable to see broader use. For the industrial use of internal high-pressure forming, presses with good accessibility, high holding forces, exact and fast-reacting control systems and high-pressure generators are necessary [MÜCK95]. Only at the beginning of the 20th century was systems engineering far enough for all requirements to be fulfilled. Large-series application of the process in the automobile industry has been taking place since the end of the 20th century [HEIZ03].

According to the classification made by the VDI Guideline 3146, internal high-pressure forming belongs to the internal high-pressure processes, along with internal high-pressure separation and internal high-pressure joining [VDI99b]. Internal high-pressure forming is divided in turn, depending on the blanks used, into the subcategories internal high-pressure forming of hollow profiles and internal high-pressure forming of sheets.

Advantages of internal high-pressure forming compared to conventionally produced components are the following:

- no joining operations, thus improved dimensional stability and reproducibility,
- improved flow properties of transitions, as well as wall thickness suited to both functionality and stresses,
- reduced mass though low wall thickness and thus improved material utilization,
- complex shaping and thus better use of critical installation spaces.

4.6.1.1 Internal High-Pressure Forming of Sheets

A process which has not yet secured a place in serial production is internal high-pressure forming of metal sheets or sheet metal pairs. Due to the highly varying process limitations and parametric constraints, this process remains largely in the research phase. For this reason, the following will only provide a short account of the process principle and process limitations.

Process Principle. As opposed to processes of hydromechanical deep drawing (cf. Sect. 4.1.2.2), the active tool element used in internal high-pressure forming of sheets is replaced by an active fluid medium introduced into the hollow space between the two sheets or between the sheet and the docking system [NOVO02]. The basic advantages of this process in comparison to other deep-drawing processes are the following [ROLL01]:

- The large proportion of stretch drawing contributes to achieving a uniformly high strain hardening of the material. Thus components with lower wall thicknesses can be used under the same loads.
- Since shaping is only partially dependent on rigid tool elements, there is a high flexibility with respect to process integration.
- Because the punch is not rigid, two-shell hollow bodies can be produced in a single forming step by means of internal high-pressure forming of welded or non-welded sheet metal pairs.
- The flexible tool offers greater freedom with respect to shaping potential. Drawing stages can be spared for parts with inclining frame. Undercuts can also be produced.
- In general, the tool costs for internal high-pressure forming tend to be lower, as only a negative shape has to be produced and the number of tool sets is reduced as a result of the lower amount of required drawing stages.
- Springback after the removal of the component is significantly reduced as a result of the uniform plasticizing of all workpieces areas, improving component accuracy [VOLL00].

If a sheet metal pair is used instead of a single sheet as the starting semifinished product in internal sheet-metal forming, two-shell hollow bodies can be produced in a single forming step. This method places additional demands on the sealing of the sheets. These demands can be met either though a preceding welding operation or through sealing by means of a sufficiently high blank holder force [NOVO02]

Figure 4.97 provides a sketch based on DIN 8584-3 showing different variants for forming sheet metal pairs with internal high pressure, i.e. deep drawing with internal high pressure [GROC03].

Before the actual forming process, the blank is supplied and, if necessary, preformed. After the tools are closed, the fluid is conveyed into the hollow space formed by the blank and the docking system and the internal pressure is increased by adding more of the pressure medium [BOBB00]. The actual forming process which now follows can be divided into two steps:

1. Free expansion:

   The material can flow from the blank holder area.

2. Calibration of the component:

   The pressure required for calibration entails that large areas of the sheet already touch the tool, with the resultant friction between the sheet and tool preventing

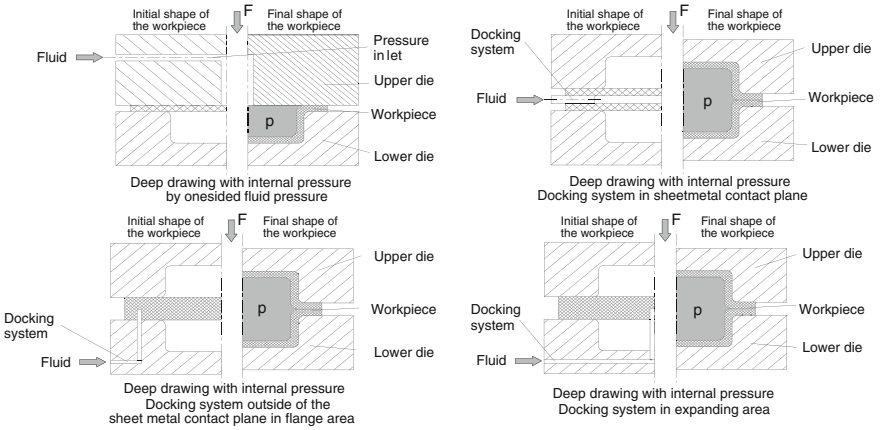


Fig. 4.97 Variants of deep drawing with internal high-pressure based on DIN 8584-3 [GROC03]

further flowing. The forming process which follows from this point results to the greatest possible extent from a single sheet thickness reduction.

Sealing the hollow space formed between the sheets and the docking system is very important in internal high-pressure forming of sheet metal pairs. In order for the internal pressure needed for the forming process to be achieved, this hollow space must be sealed off from the active medium, i.e. leakages must be smaller than the added fluid flow [BOBB00].

Egress of the fluid between the sheets is usually prevented by a weldseam along the outer contour or, in the case of non-welded blanks, by a sufficiently high closing force of the blank holder. If the sheets are joined, the weldseam is subjected to different stresses. The joined sheet metal pair must withstand the surface pressure generated by the tools and also the friction forces arising during the process when the fluid flows into the flange area. If the surface pressure generated by the blank holder between the two sheets is too low, the internal pressure also acts on the weldseam and can lead to a failure, especially if parts of the flange do not lie under the blank holder [BOBB00].

If the sheets remain unwelded during the entire forming process, the sealing must be provided by a sufficiently high surface pressure in the flange area of the sheets. Also, it is often desirable to feed the sheet for complete shaping in order to avoid stretching [DICK97]. An improved sealing effect can also be realized by introducing seals between the sheets in the flange area. Another possibility is using a sealing strip in the flange area, which can reduce the required sealing force [HEIN99].

4.6.1.2 Internal High-Pressure Forming of Hollow Profiles

Process Principle. To insert the blank and to remove the formed workpieces, the tools must be split. The production process follows the following steps [LANG93] (Fig. 4.98):

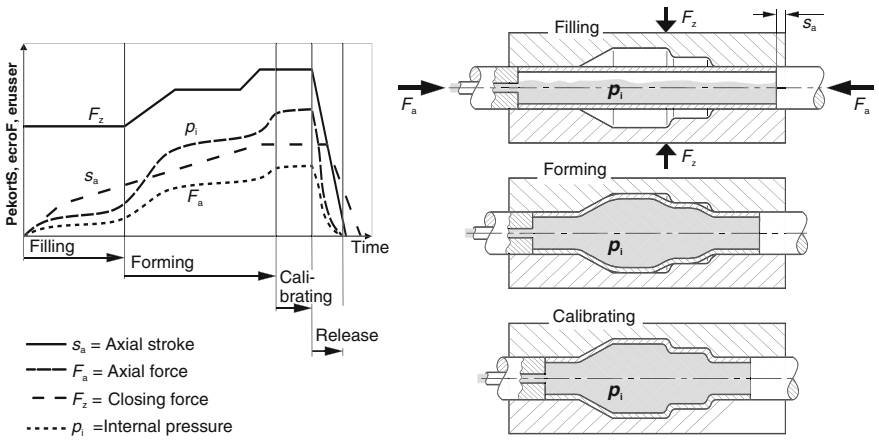


Fig. 4.98 Process sequence for internal high-pressure forming in a longitudinally split tool

1. The tubular blank is inserted into the open tool and flooded with the hydraulic fluid.
2. The tool is closed and the end faces of the tool are sealed.
3. The forming process: High pressure is applied to the workpiece from the inside, which causes it to deform outwards. After the first expansion, it lays more and more along the inner contour of the tool.
4. Material must be displaced axially by means of a tool movement, since the circumference and thus the surface of the workpiece has increased.

For transversely split tools, one can distinguish between two basic principles (Fig. 4.99):

- Expanding in a closed die, for which the moulding tool is closed prior to forming and the workpiece is pushed together axially with inner punches.
- Expansion compression, for which the moulding tool is first closed by the axial forming movement executed during the process itself.

In expanding in a closed die, the material exhibits a relative movement to the enclosing moulding tool during the process, which causes friction. The axial punches must therefore contribute certain force components to meet the following demands:

- overcoming wall friction,
- forming the workpiece and
- overcoming the hydraulic counterpressure.

For expansion compression, the first force component is not required because the relative movement is negligible. Due to the larger surface, however, the third force component is higher in expansion compression than for expanding in a closed die [DOHM93b]. Irrespective of the active principle, the axial direction of

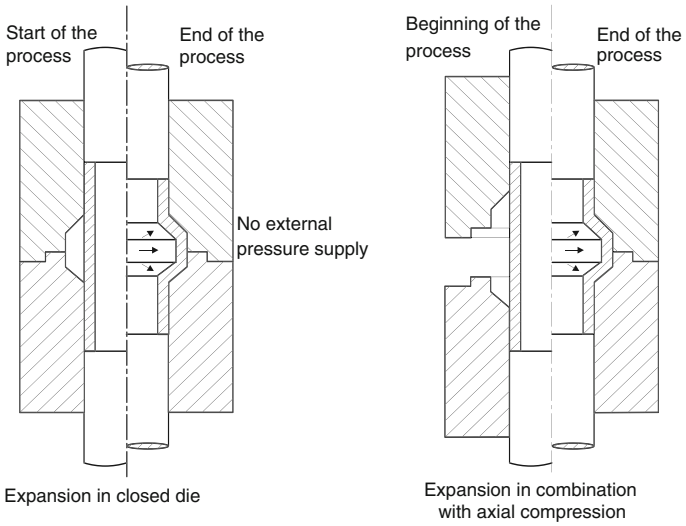


Fig. 4.99 Principles of internal high-pressure forming in a transversely split tool [DOHM93b]

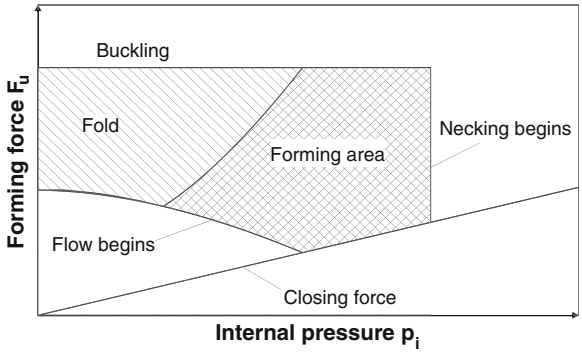


Fig. 4.100 Working diagram for expansion [DOHM93b]

pressure and both the corresponding forming force and the internal pressure must be adjusted exactly to the geometry, material and other process variables.

Figure 4.100 shows the resulting forming area as a function of pressure and force. It is obvious from this that the forming area is very small and that satisfactory results can only be obtained with proper process control. An unfavourable selection of process parameters can lead to the buckling of the workpiece or to fold formation. In extreme cases, the tube can even break on locations with abrupt transitions in cross-section (Fig. 4.101).

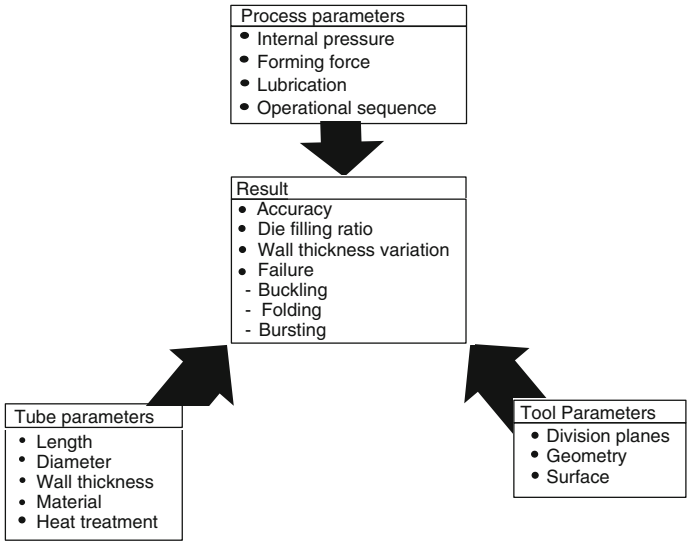


Fig. 4.101 Factors influencing the work result

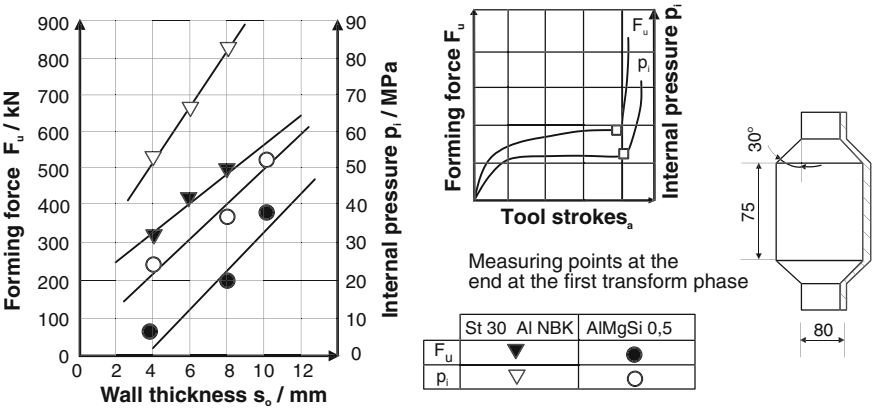
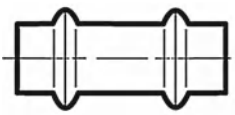
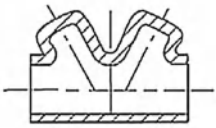
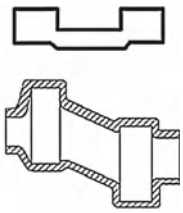
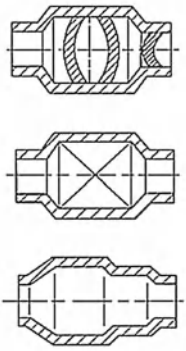
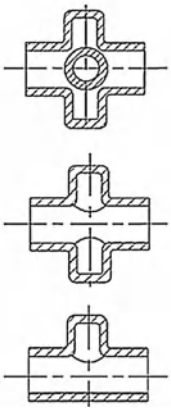


Fig. 4.102 Forming force and internal pressure as a function of the starting wall thickness [DOHM93b]

The admissible forming area shown is shifted according to the starting wall thickness and workpiece material to higher or lower values for forming force and internal pressure. The relationship shown in Fig. 4.102 applies to the phase of the process in which the workpiece first touches the tool contour but the corner areas are not yet narrowly shaped. After this first forming phase, the forces and pressures increase sharply and can reach values of 20,000 bar, depending on the material and the geometry.

Table 4.5 Shape classification for internal high-pressure forming

	rotationally or axially symmetrical parts	with a partial expansion	pushed through or displaced
With undercut			
Without undercut			

4.6.1.3 Producible Shapes and Process Limitations

Internal high-pressure forming can be used to produce many different shapes. There are three classes of these shapes (Table 4.5):

- rotationally or axially symmetrical parts (also oval, polygon-shaped or polygonal),
- with a partial expansion in one or more planes and directions and
- pushed through or displaced, e.g. excentric.

These shape classes can also be combined and realized with undercuts. The workpiece geometry is limited by the admissible tool strains and by the admissible process parameters. Suitable workpiece materials are all metallic materials with sufficient formability. These range from light metals through unalloyed and case-hardening steels to heat-treatable and stainless steels [VDI99b]. High-strength steels can also be used. The yield stress and strain hardening of the material affect the forces and internal pressures, as well as the formable radii [HESS91, HESS92].

4.6.1.4 Accuracy and Workpiece Qualities

The achievable dimensional accuracy of the workpieces is influenced by a number of process- and workpiece-side boundary conditions. According to DIN ISO 286-1 [ISO90], tool-based outer diameters can have an accuracy of about IT 14–IT 12 (in special cases even IT 10). The total length can have a tolerance of ±0.8 mm (Fig 4.102).

An extreme deviation of material and a corresponding strain hardening occurs in regions of sharp-edged cross-sectional transitions. Thus these geometries cannot be completely filled. The dimension of the smallest possible outer radius when shaping depends above all on the wall thickness, the material and the internal pressure (Fig. 4.103).

Since the inner contour is formed by the pressure medium and not by moulded tools, there is a practically free material flow in this area. There are therefore local fluctuations in wall thickness according to strain hardening, geometry and material flow over the component (Fig. 4.104). Given great changes in diameter without an axial advancement of the material through the punches, the wall thickness can be reduced considerably during the expansion process. Conversely, it is also possible to achieve a targeted local increase in wall thickness, within certain limits, by means of a great axial punch path.

The strength of the formed workpieces increases through strain hardening. Additionally, it is favourable that the material fibres lie tangentially to the contour, resulting in a good loading behaviour on the part of the components. The surface quality of the starting pipe remains largely intact during the forming process, and it can be improved at radial transitions given a suitable tool shape. In areas of free expansion, however, it is possible for the surface roughness to increase [KLAA93].

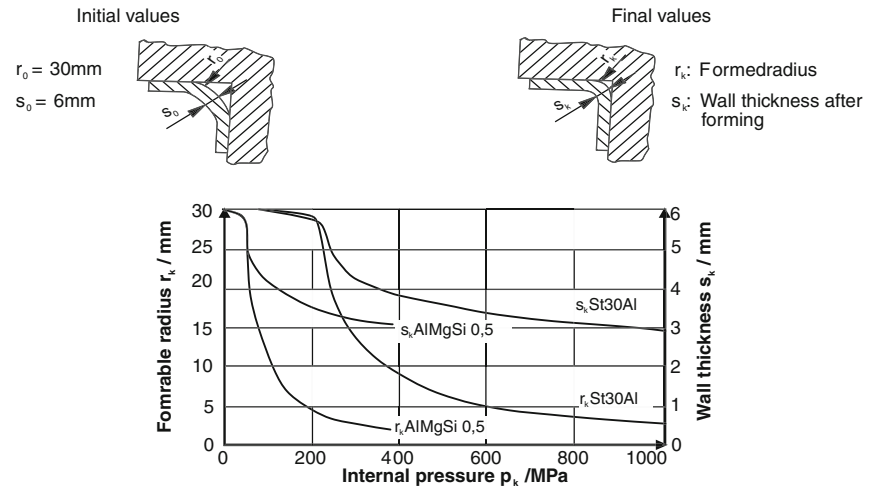


Fig. 4.103 Shapeable radii for steel and aluminium [DOHM93b, LANG93]

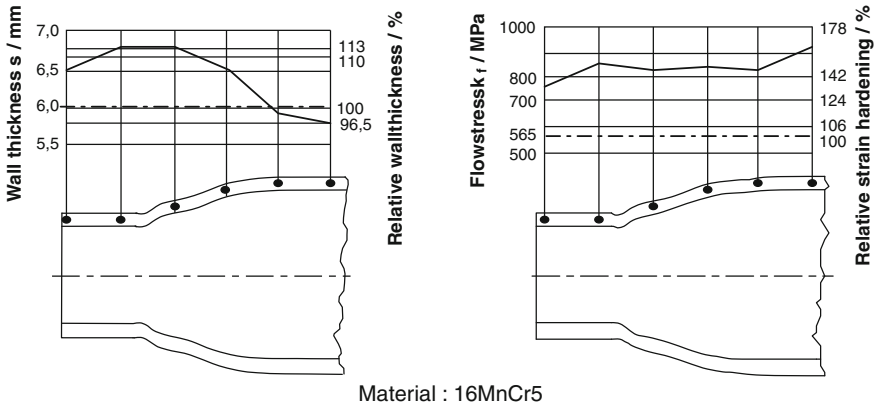


Fig. 4.104 Changes to wall thickness and strain hardening through internal high-pressure forming

4.6.1.5 Tools and Forming Media

The shapes of forming tools depend principally on the necessary dividing planes and travel paths. A good choice for rotationally symmetrical components without undercuts is a transverse division, since in this case the tool production is more cost-effective and more precise than for a longitudinal division (Fig. 4.105 left). Also, the forming machine only requires one working direction for the rams.

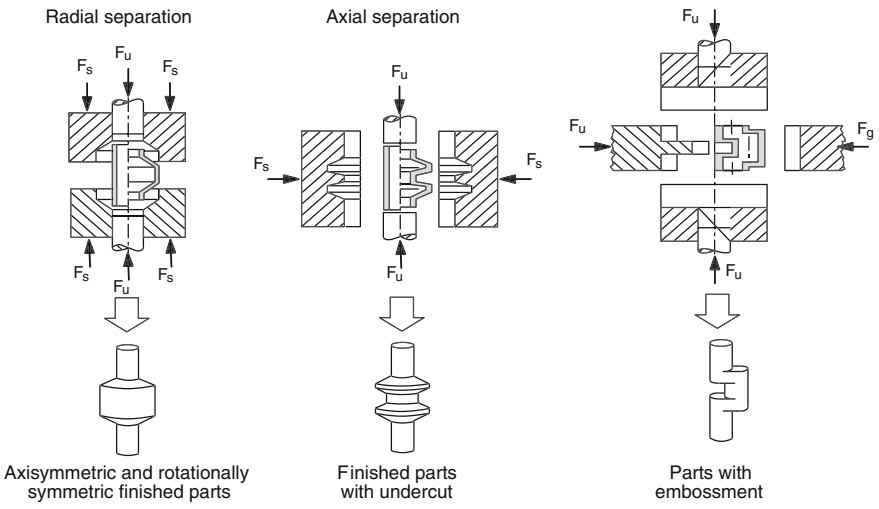


Fig. 4.105 Tool designs [DOHM93b]

The transverse division is not possible for components with undercuts. For demouldability reasons, the longitudinal division is the only possible choice. The only process adapted to this tool design is expanding in a closed die, as the closing direction of the mould halves stand perpendicular to the punch direction (Fig. 4.105 centre). In the case of embossed parts, tools with two or more divisions are even required allowing for three independent tool movements (Fig. 4.105 right). The machine expenditure is very great in this case. The rams used in machines for internal high-pressure forming are generally driven hydraulically.

The pressure medium used for forming is often an oil-in-water emulsion pumped via a hydraulic unit with a pressure intensifier into the component [PETE04]. Depending on the geometry and material, a lubrication of the workpiece may be necessary prior to forming.

4.6.1.6 Special Applications

Because of the radial expansion of the workpieces, internal high-pressure forming lends itself to a simultaneous joining process during the forming process. This joining and forming process combination has been applied in the manufacture of camshafts. The process starts with a long tube, onto which the individual, cams with holes are mounted. Internal pressure is then applied to the tube in the tool mould halves, so that the outer wall of the tube is in firm contact with the cam bores and a shrink fit develops (Fig. 4.106). The advantages of this construction are low mass and greater admissible tolerances for the cam bores. The material of the cams can be selected irrespectively of the material of the tube.

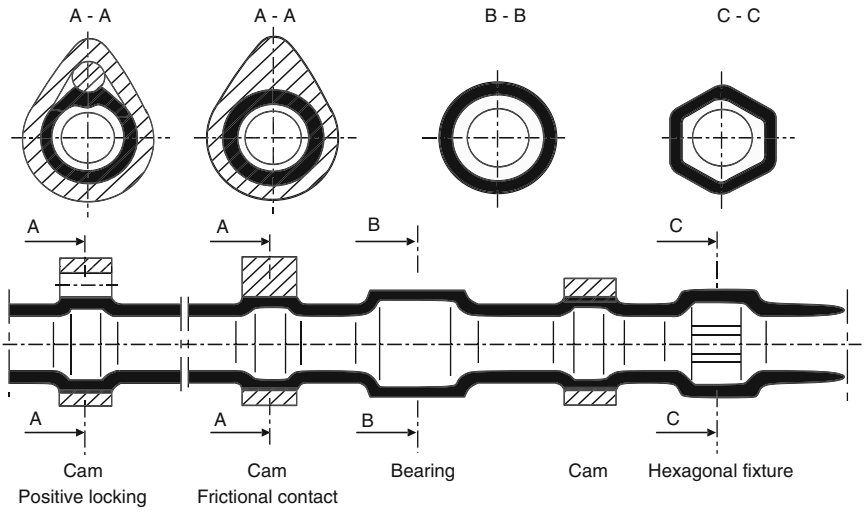


Fig. 4.106 Joined Camshaft

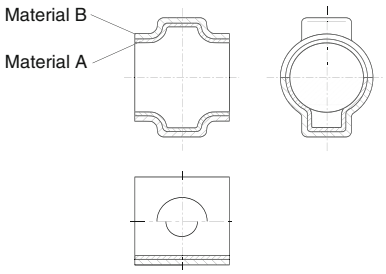


Fig. 4.107 Workpiece with composite construction

The production of composite components goes in a similar direction. Two tubes with different materials are pushed inside each other and internal high-pressure forming is executed on both simultaneously. After forming, both starting parts are positively connected to one another (Fig. 4.107). This composite construction can be used to advantage when aggressive or corrosive media are to be conveyed though the component. A thin, chemically resistant tube material can be selected for the inner tube, whereas for the outer tube an inexpensive and mechanically stable material is used.

4.6.2 Superplastic Sheet Metal Forming

4.6.2.1 Superplasticity

The state of a metallic material is referred to as superplastic if it exhibits a very high formability with an extremely low yield stress in comparison to a normal plastic state. The following conditions must be fulfilled in order for this material state to be reached and to be practical for forming purposes:

- a highly homogeneous and fine-grained structure (grain diameter $d < 10$ µm),
- a forming temperature which is higher than half the melting temperature and
- very low strain rates ($10^{-5}\mathrm{s}^{-1} < \dot{\varphi} < 10^{-1}\mathrm{s}^{-1}$).

Section 3.4.3 provides a more detailed description of the behaviour of superplastic material and of the process principle as well as an overview of the relevant materials.

Due to the low yield stress in the superplastic state, sheet parts can be made which cannot be realized in a normal plastic material state. Under conventional forming conditions, the formability of sheet material is limited to an elongation at fracture of circa 50 %, corresponding to a true strain of $\varphi \approx 0.4$. Usual elongations of superplastic sheet materials lie according to tensile test at 500 % ($\varphi \approx 1.6$). At

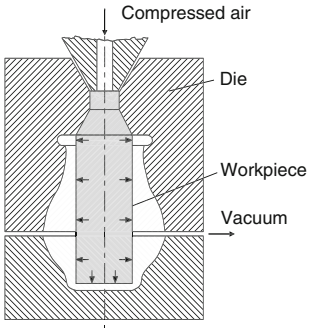


Fig. 4.108 Vacuum forming of a hollow body [THOM69]

present, the boundary for superplastic forming lies at 8,000 % ($\varphi \approx 4.4$), achieved using commercial bronze in a uniaxial tensile test [VULC04].

4.6.2.2 Process Principles

Superplasticity offers advantages above all when drawing ratios in deep drawing are particularly high [SIEG92] or if high true strains are required when forming with fluid or gaseous media [VULC04]. For deep drawn parts, two pneumatically functioning processes, so-called blow processes, have been established [WERL95].

- In pneumatic stretch forming with the die method, the sheet is clamped between two pressure chambers at the start of the process and then pressed by means of gas pressure into one of the two pressure chambers, which has the negative shape of the finished part. This method is suitable for large-surface, flat workpiece geometries with a primarily convex contour [VULC04].
- The male mould process also uses gas pressure. Here, the firmly clamped sheet is first pressed through gas pressure into one of the two chambers and thereby deformed into a bubble. When the desired bubble size is reached, a punch (the male mould) is guided from the inside into the spherical hollow shape of the bubble made in the previous step. At the same time, the pressure conditions are reversed, so that pressure is applied to the bubble from the outside, causing it to touch the contour of the punch. Compared to the die method, the male mould process is distinguished by higher achievable true strains, more constant component wall thicknesses and a more easily controllable strain rate [WERL95].

Hollow bodies can also be formed by means of compressed air and a vacuum, as in internal high-pressure forming (Fig. 4.108) [THOM69].

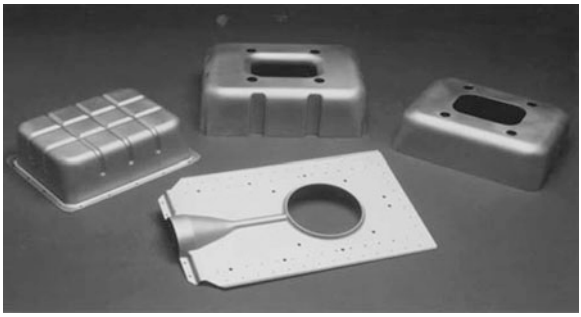


Fig. 4.109 Superplastically formed aluminium sheet components (*source* Alcan)

4.6.2.3 Materials and Areas of Application

Superplastic sheet materials made of aluminium and aluminium alloys are most widely used, as well as titanium and titanium alloys [FRIE88, HOJA91, THOM69, VULC04, SCHR93a].

Elongations achieved with the superplastic aluminium alloys available currently can reach up to 800 %, corresponding to logarithmic true strains of up to $\varphi \approx 2$. The main areas of application for superplastic aluminium components are, in descending order of their respective market shares, the aerospace industry (40 %), rail vehicle construction (39 %), the building industry (10 %), as well as small series production in automotive manufacture (7 %) [VULC04]. Figure 4.109 shows deep drawn parts made of aluminium used in aviation which have been superplastically formed.

Because of their heat resistance and high strength with respect to weight, titanium materials are used primarily in aviation [ADAM98, FRIE88, FURL88]. They are generally too costly for other applications. Titanium alloys are used, for example, in thrust reversers in jet engines, as here sheet parts are required which withstand high temperatures [ADAM98].

Overall, however, the industrial use of superplastic forming is not very advanced. This is due to the special systems engineering required and to the high production costs of the components. One problem is that the fine-grain materials required for superplastic forming are relatively expensive; another is that very long cycle times are entailed to guarantee low strain rates. This limits superplastic forming to applications in small series production.

4.6.3 Forming With Laser Radiation

As opposed to large series manufacture of sheet parts, in which forming is often executed with the aid of costly moulding tools, the high costs and time expenditure

associated with this tool manufacture represents a serious disadvantage for prototype and small series production. For example, the individual body components made during the development of a new vehicle type are subjected to numerous modifications until the final form is reached. The costs for the modifications cause an additional increase in the overall costs for tool manufacture. The need for flexible sheet metal forming processes is correspondingly great in this area of application, processes which produce the desired component geometry in a fast and cost-effective way, i.e. with no or few moulded tools.

As a process still in development, forming by means of laser radiation expands the range of flexible forming techniques used currently in industry. The essential hallmark of this forming technique is that it dispenses with moulding tools. Sheet forming is executed in this case exclusively by means of a contact-free induction of thermal stresses with the aid of a laser beam. In addition to prototype and very small series manufacture, a further area of application is the straightening of sheet parts.

4.6.3.1 Process Principle

Figure 4.110 shows a schematic diagram of the process principle of laser beam forming of metallic semi-finished part. The sheet moves with a constant feed rate below the fixed laser beam along a defined bending line. The energy of the laser beam absorbed on the workpiece surface is converted to thermal energy, causing a rapid heating of the edge layer due to the high intensity of the laser beam.

The temperature is equalized in the workpiece by means through heat conduction, which causes a temperature field to generate below the irradiated surface.

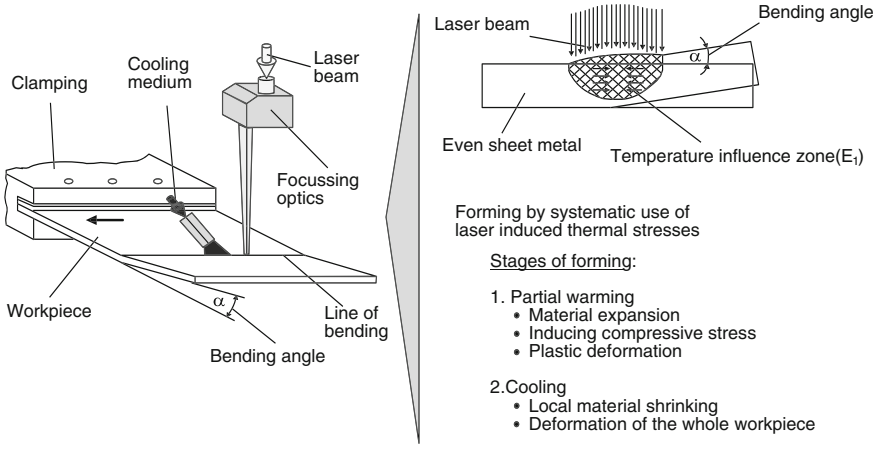


Fig. 4.110 Laser beam forming; process principle (schematic)

Seen two-dimensionally, this temperature field can be described as heat-influence zone E1. Depending on the temperature, a varyingly strong thermal expansion and reduction of the elastic limit of the material occurs in this zone. However, since this heat-related material expansion is retarded by the colder material of the directly neighbouring environment, compressive stresses arise in the heated zone. These are limited in intensity by the high-temperature limit of elasticity of the material corresponding to the relative temperature. If the high-temperature compressive stress reaches this value, plastic compressive deformations develop. The heating does not damage the material, as the formability of the material increases with increasing temperature [HENN01, VOLL96].

When the heating phase is complete, the plastified area contracts as a result of the temperature drop in the direction of the sheet thickness and width. The degree of the contraction effective in the form of a bending angle is influenced by the size of the heat-influence zone, the extent of the temperature gradient from the heat-influence zone to the neighbouring material, the elastic limit and thermal expansion coefficient of the material as well as its modulus of elasticity, but also in a decisive way by the stiffness of the component [FRAC90, GEIG91, KITT93, KÖNI93b].

The use of a laser beam offers advantages over other sources of heat with respect to its good focussing ability and precise controllability of beam intensity. Lasers can be used to heat areas which are in part clearly delimited, so as to introduce the forming mechanism described. Both gas (CO_2) and solid-state lasers (Nd:YAG) can be used as radiation sources. Both source types provide the beam power in the kilowatt range required for forming sheets with thickness exceeding 1 mm. Differences consist primarily in the wavelength of the laser beam and the resultant absorption properties. Whereas in the case of a CO_2 laser absorption-promoting coating layers e.g. of graphite must be applied to the workpiece surface, this is not required for processing using the Nd:YAG laser, as it has a wavelength of 1.06 μm, 10 times shorter than that of the CO_2 laser. Also, the beam of a solid-state laser is guided by means of optical fibres, which increases the flexibility of the process. However, the maximum output power of current Nd:YAG lasers is lower than that of CO_2 lasers.

4.6.3.2 Basic Technology

The essential factors and parameters underlying the laser beam forming process include component-related variables, such as material type and sheet thickness, as well as process-specific variables, such as laser type, power, beam dimension in the focal spot and feed rate. Figure 4.111 shows basic connections between the true strain and the process parameters for a simple forming task. With a sheet thickness of 0.75 mm and constant feed rate, only minimal changes to the bending angle can be observed with increasing laser power. On average, the bending angle

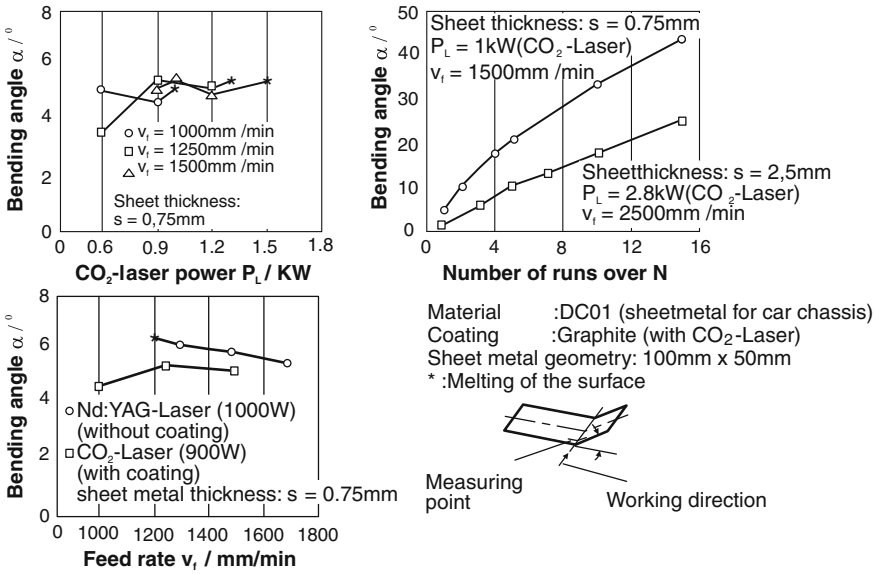


Fig. 4.111 Dependence of the bending angle on essential process parameters and cause variables

is 5° per overrun. Larger bending angles can be achieved by running over the same bending line multiple times, although there is a degressive connection between the number of overruns and the bending angle. The reason for this is a decrease of the amount of heat absorbed due to the fact that the irradiation conditions of the laser beam become less favourable with increasing bending angle and to the damaging of the graphite layer caused with the repeated application of the beam. Other process advantages can be achieved by processing with a Nd:YAG laser. In contrast to the CO_2 laser, the Nd:YAG laser can be used to increase the bending angle by ca. 20 %. A comparison of different materials shows that the bending angle which can be achieved with a single overrun increases linearly with an increasing ratio of the thermal expansion coefficient to the volume-related heat capacity. Accordingly, increasing bending angles are yielded in order by steel, titanium, high-grade steel, copper, brass and aluminium alloys [GEIG93b, KÖNI93b, VOLL96].

As a result of local heat effects, changes to grain structure occur during laser beam forming in the heat-influenced areas. These changes must be taken into account with respect to the case of application concerned and the required performance characteristics of the component. The type and extent of the effect on the grain structure depend on the material, the maximum process temperature and the respective cooling conditions. Investigations of body sheet metal made of DC 01, for example, yielded a clear grain refinement associated with a low increase in

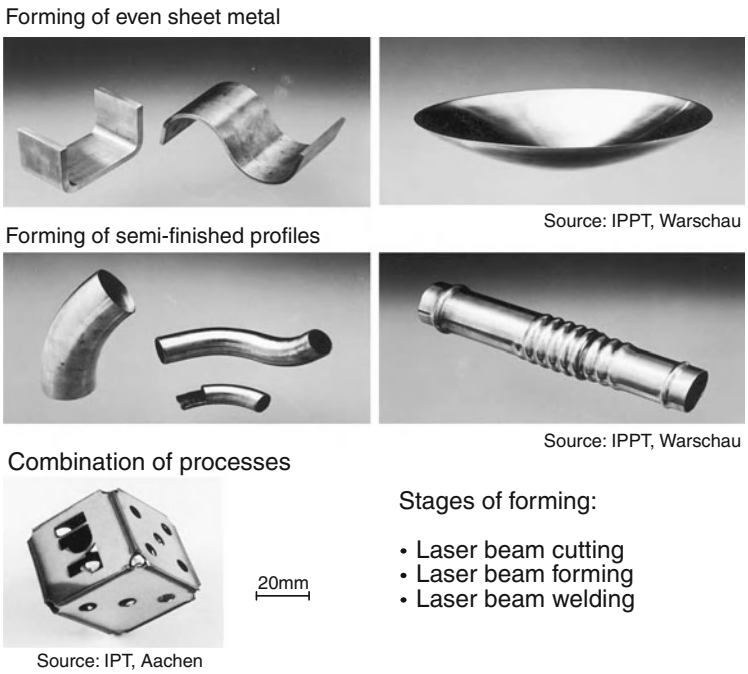


Fig. 4.112 Laser beam forming; sample components

hardness in the deformation zone by approximately 10 %. Considerably higher increases in hardness occur in steels with carbon content >0.2 % when the austenitizing temperature required for martensite formation is exceeded during the forming process. Also, precipitations may form at the grain boundaries through the repeated introduction of heat during forming. These lower the corrosion resistance of the materials, as in the case of Al–Mg alloys [KITT93, VOLL96].

4.6.3.3 Fields of Application

The high flexibility of lasers gives laser beam forming a broad application potential. Future application stresses are expected in the sectors of automotive manufacture, plant construction, aerospace engineering, as well as general mechanical engineering and microelectronics. In addition to the prototype and small series production, other possible areas of application include thermal straightening and forming high-strength and brittle materials (titanium, cast iron). Advantages can also be derived in combination with other laser processes, such as cutting and welding, potentially allowing for the complete processing of sheet parts. However, further development work is required before a wide industrial

Table 4.6 Characteristic values of high performance processes

Principle or machine	Tool* or rather workpiece** velocity (m/s)	Process time for small forming strokes (s)	Power (kW)	Achievable pressure (MPa)
Forging hammer	* 5	10^{-1} to 10^{-2}	10^4	10,000
Pneumatic–mechanical forming	* 20	10^{-2} to 10^{-3}	10^5	10,000
Electromagnetic forming	** to 300	10^{-4}	10^4 to 10^5	3,000–5,000
Electrohydraulic forming	** to 300	10^{-3}	10^4	10,000
Explosive forming with fluids	** to 300	10^{-3}	10^6	60,000

application of the process can be realized, especially with respect to the manufacture of complex components.

Figure 4.112 demonstrates the current state of development of laser beam forming on the basis of a series of sample components producible by the process.

The spectrum ranges from simple geometries, e.g. angles and arches with wall thickness of up to 8 mm, to more complex formal elements, such as spherical caps with a convex contour formed from flat sheet metal semi-finished products. Also, both open and close semi-finished profiles, such as tube, square, rectangular and U profiles can be bent by laser beam. With tubes, additional partial expansions and reductions of the nominal diameter can be realized.

4.6.4 High Rate Forming

The concept of high rate forming refers to processes which clearly differ from conventional forming processes with respect to process time and speed. Table 4.6 shows a comparison between forging as a "conventional" process and the most common high rate forming processes. All the processes listed in the table are considered as high performance processes, as they all, as the table shows, realize a similarly high performance level. However, high rate forming processes only include pneumatic-mechanical processes, magnetic forming, electrohydraulic forming and explosive forming. Pneumatic-mechanical processes use a strongly compressed gas (e.g. oil-free air or nitrogen) to accelerate a mass which then performs the work. In magnetic forming, magnetic fields are used to accelerate the workpiece and to press it with the aid of its particular kinetic energy into a tool mould. Electrohydraulic processes, also referred to as hydrospark processes, cause water or a wire spanning the spark gap to vaporize

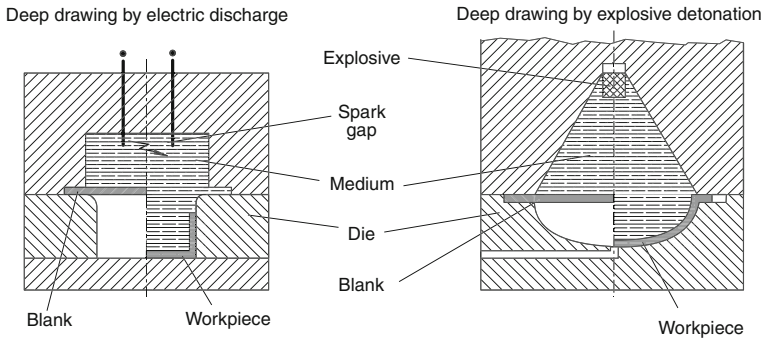


Fig. 4.113 Deep drawing with electrical discharge and explosive detonation [DIN03h]

by means of a sudden discharge of electric energy stored in capacitors. The shock wave thus generated is used for the forming operation. In explosive forming, a similar shock wave is created by igniting explosive materials [LANG93]. The following discussion will be limited to explosive forming and electromagnetic forming.

4.6.4.1 Explosive Forming

Processes which derive the energy required for forming from explosive materials have been already known since the turn of the century. However, they have only become relevant in recent years in the processing of materials difficult to form. Processes have been developed above all in the construction of aircraft, rockets and reactors as well as in medical technology which exploit electrical discharges under water or explosive materials as sources of energy (Fig. 4.113).

In forming with explosive detonation, for example, a shock wave is generated upon ignition which moves radially outwards from the midpoint of the explosion. When the shock wave strikes the sheet to be formed, it exerts a normal stress on its surface. Shock-wave propagation rates between 1,000 and 8,000 m/s lead to pressures of up to 10,000 MPa [OEHL01], thus also allowing high-strength sheet materials to be formed.

Common areas of application of explosive forming are the production of large-surface parts for which the nominal force of conventional presses is insufficient, the production of workpieces with complicated geometries and made of materials difficult to form, as well as small series and prototype manufacture [LANG90c, VOVK04]. Along with forming through underwater spark discharge, which is usually referred to as hydrospark processes, explosive forming processes have the following advantages:

- variety with respect of the geometries to be produced,
- considerably lower tool costs,

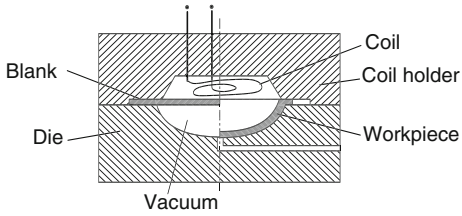


Fig. 4.114 Deep drawing under the action of a magnetic field

- reduced number of work steps because of the higher drawing ratios possible due to the greater strain rate,
- in comparison to conventional processes, an adherence to close tolerances is usually possible.

Mentionable disadvantages are the long set-up times and strict safety regulations.

4.6.4.2 Electromagnetic Forming

The processes described up to now require a medium to transfer the necessary forming forces. In contrast, forming using processes based on active energy occurs via pressure generated within the workpiece itself. Until now, the only process variant made known is electromagnetic forming (Fig. 4.114). Electromagnetic forming is an electrodynamic high rate manufacturing process in which the workpiece is formed by means of the action of forces produced by pulsed magnetic fields of very high intensity. There is usually no mechanical contact with the tool [MÜLL69, DIET75]. Stored in capacitors, the energy is discharged impulsively via a coil. A temporally varying magnetic field is generated between the workpiece and the coil by means of the discharge current with damped oscillation. This magnetic field induces eddy currents in the conductive workpiece. The interaction of the magnetic field and the eddy currents creates the force necessary for forming [LANG90c].

Only relatively flat parts can be produced when deep drawing with the aid of this process. This is because material flow over the die radius is prevented as a result of the inertia forces arising with high accelerations. A greater reduction in sheet thickness can be expected in the formed area in comparison to conventional deep drawing processes [OEHL01]. The process is therefore not so much applied to deep drawing as to bulging, expanding and necking thin tubes or hollow profiles [BÜHL66] and to joining by forming, as in crimping cable shoes on cables or tubular samples or tubes on solid profiles, and also to the creation of permanent connections [LANG90c, OEHL01].

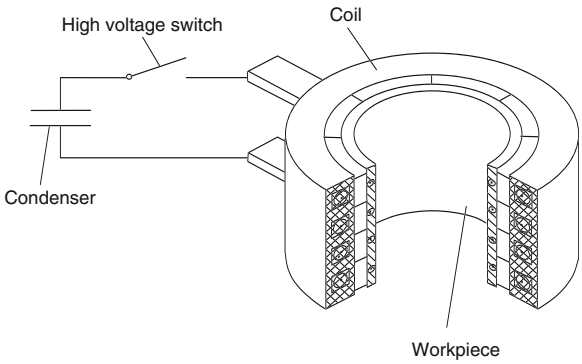


Fig. 4.115 Principle construction of a device for magnetic forming (acc. to Puls Plasmatechnik)

An essential advantage of this process is that, because of the lack of moving parts on the machine, maintenance costs are low. In addition, no transfer medium is required, which means that this process can be used in series manufacture. A particular disadvantage, however, is the limited selection of easily processable materials. The most suitable material is aluminium, as it is a good conductor of electricity with low yield stress. The installation (tool/coil, capacitor bank, etc.) must be adjusted to the forming task [RISC04]. Moreover, the size of the machine is limited for economic reasons [LANG09c].

Magnetic Forming: Process Principle and Requirements. Electromagnetic forming is based on the physical principle of induction. A primary, temporally varying magnetic field is created by the primary current of the tool coil. This induces a secondary current in the workpiece which in turn leads to the generation of a secondary magnetic field. Since the magnetic fields of the primary and secondary currents are opposing, they repel each other, causing an acceleration of the workpiece. The amount of acceleration depends primarily on the magnetic flux density B of the primary magnetic field and on the inductivity of the sheet material, which determines the magnitude of the induced currents and thus the magnetic flux density of the secondary magnetic field [LANG93].

To generate magnetic fields suited to magnetic forming, shock capacitors are charged to store energy and then discharged within several 10 µs via a coil adjusted to the workpiece geometry (Fig. 4.115).

The amount of the induced currents and of the inductivity of the sheet depends especially on the electrical conductivity of the workpiece material. In the case of materials with good conductivity, such as copper and aluminium, magnetic pressures of a few thousand MPa act on the workpiece surface. These pressures must be high enough that the yield stress in the workpiece is exceeded. If the currents and thus the forming pressures are too low due to poor conductivity, it is possibly to increase inductivity and thus current strength by enclosing the workpiece with a

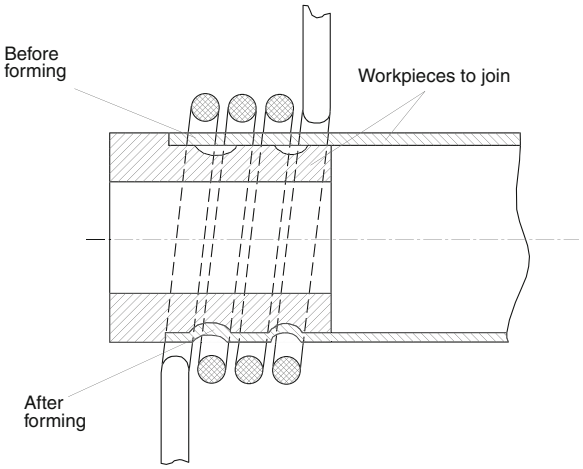


Fig. 4.116 Compression of tube-shaped components (acc. to Puls Plasmatechnik)

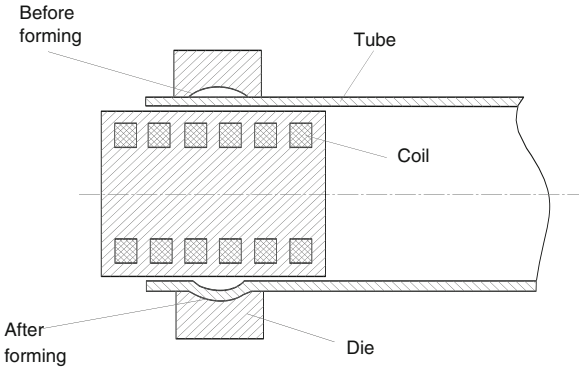


Fig. 4.117 Expansion of tube-shaped components (acc. to Puls Plasmatechnik)

so-called driver made of aluminium or copper. The magnetic forces then act on the driver, not on the actual workpiece [DENG91].

Application of Magnetic Forming. Frequently, magnetic forming is used for form-locking joining two components. In such a process, the one component usually encloses the other. Three process variants are distinguished on the basis of shape and direction of movement:

- compression
- expansion
- flat forming

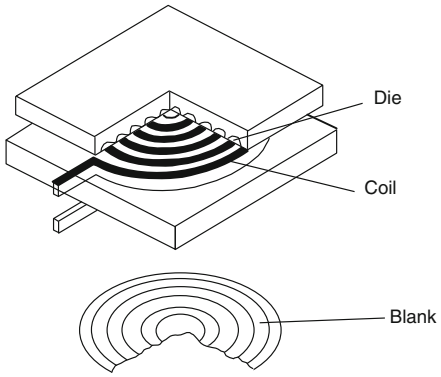


Fig. 4.118 Flat forming (acc. to Puls Plasmatechnik)

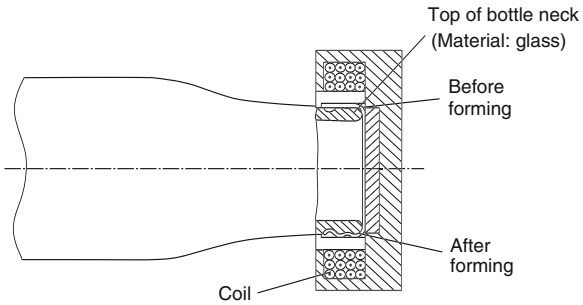


Fig. 4.119 Sealing of milk bottles by electromagnetic forming (acc. to Steingröver)

The most frequently applied variant is compression. In this process, a cylindrical coil is used as the working coil. The forces acting on the outer workpiece are directed inwards, with the pressure being applied on the shaping inner workpiece.

Regular, planar forces arise on the circumference of the workpiece in the process of magnetic forming. For this reason, magnetic forming is especially predestined for shrinking tubes or rings onto brittle materials, such as ceramics (Fig. 4.116).

In expansion, tubes or rings are expanded or pressed into a surrounding mould. The forces acting radially outward are created by a cylindrical coil located inside the workpiece (Fig. 4.117).

Figure 4.118 illustrates flat forming of flat sheets. The magnetic field is created in the vicinity of the sheet, pressing it into a depression of a die. The flat coil, arranged parallel to the workpiece, often has the shape of an Archimedes spiral. Besides aluminium and steel materials, studies also have investigated the

processing of magnesium materials at processing temperatures of ca. 300 °C [UHLM04].

Electromagnetic forming is applied in large series production for sealing aluminium caps for milk bottles (Fig. 4.119). Because of the low sheet thickness, perfectly tight join connections are possible using small amounts of energy with an output of several thousand units per hour.

Chapter 5
Sheet Metal Separation

Besides pure forming processes, separation methods are also especially important in sheet metal working. The manufacture of a sheet metal part is almost always associated with separation processes. The necessity of separation presents itself both in the production of blanks and in the manufacture of the final workpiece contour. The separation process is carried out either mechanically by cutting processes or thermically by flame or laser cutting.

5.1 Cutting

According to DIN 8588 [DIN03l], cutting processes belong to the group "Splitting" and are subdivided into shearing, knife edge cutting, cutting with two approaching blades, cleaving, separating by drawing and breaking (Fig. 5.1).

While the processes of knife edge cutting, cutting with two approaching blades, cleaving, separating by drawing and breaking play a minor role in the metalworking industry, shearing enjoys a broad application. Typical implementation areas are in the automotive industry (metal sheets for body, levers, fittings), the electrical industry (stator and rotor laminations, transformer cores), precision mechanics (parts for film and photo cameras, sewing machines, clockworks) and in the household appliance industry (cutlery, dishes, sinks).

5.1.1 Cutting Principles

For cutting, a tool is needed which comprises a punch and a cutting die as its main components (Fig. 5.2).

The aperture of the cutting die is greater than the cross section of the punch, so as to yield a shearing gap between the edges of the punch and the die.

F. Klocke, *Manufacturing Processes 4*, RWTHedition,
DOI: 10.1007/978-3-642-36772-4_5, © Springer-Verlag Berlin Heidelberg 2013

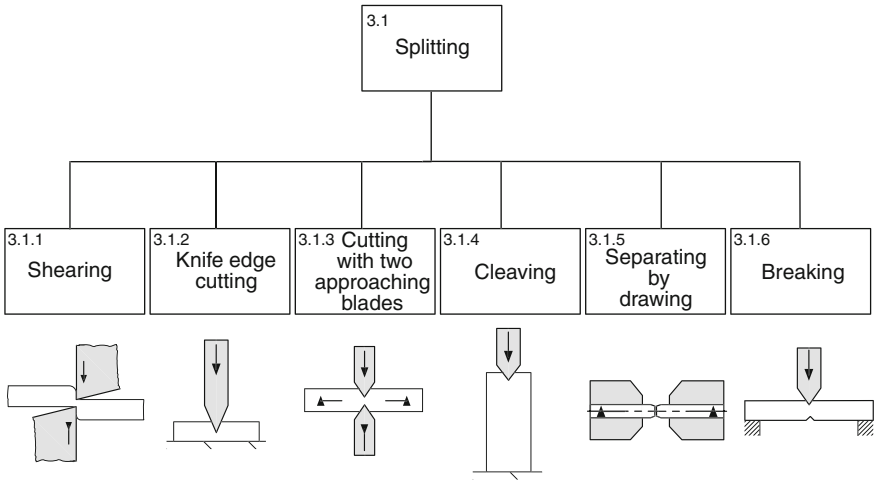


Fig. 5.1 Splitting processes [DIN03l]

5.1.1.1 Process Principle

The most important steps in the cutting process should be explained on the example of blanking a disc from a sheet metal strip. The assumption here is that the diameter of the disc to be cut out is great in comparison with the sheet thickness ($d \gg s$).

The cutting forces are transferred to the workpiece from the end face of the punch and from the cutting die. Due to the elastic resilience of the sheet, it flexes between the punch and the die (Fig. 5.2a).

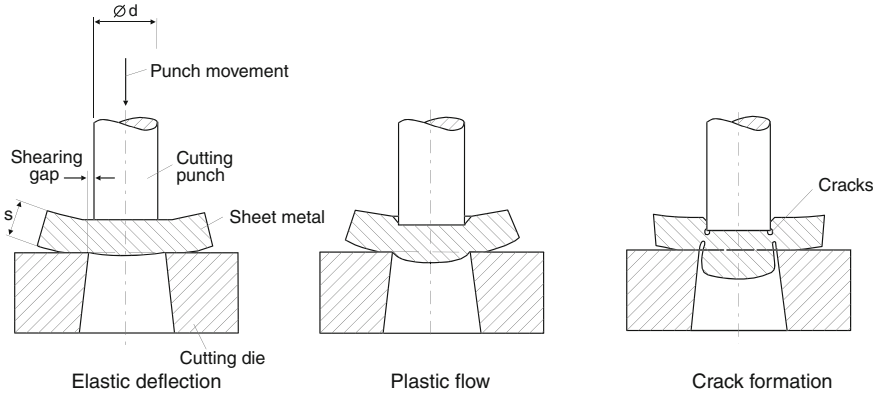


Fig. 5.2 Phases in the shearing process. **a** Elastic deflection. **b** Plastic flow. **c** Crack formation

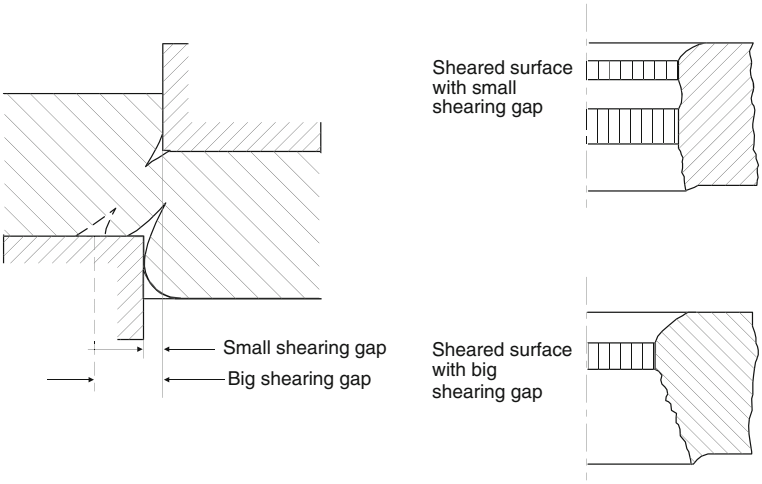


Fig. 5.3 Influence of the shearing gap on crack formation and the formation of the sheared edge [JAHN81]

An increase in the force acting on the punch causes a plastic deformation of the material, which then begins to flow. The punch then penetrates into the sheet (Fig. 5.2b).

As a result of the flowing of the material in and vertical to the cutting direction, die-roll occurs on the punch-penetrating side of the lead frame and on the blank to be cut out on the die-side (Fig. 5.2b). With an increasing cutting stroke, the edge deformation is transformed into a smooth shearing surface (smooth shearing zone) whose size is basically determined by the forming capacity of the workpiece material. As a rule, cracks form from the direction of the cutting die if the flow capacity of the workpiece material in the shearing zone is exhausted (Fig. 5.2c). These lead to material separation caused by fracturing and to the fracture surface typically associated with it.

Depending on the properties of the material and the size of the shearing gap, these cracks may run from the cutting edge of the cutting die to that of the punch, thereby causing a sudden separation and leaving a fracture surface in the shearing zone (Fig. 5.3). However, they may also run past each other originating from the die and the punch, leaving a narrow web behind which is squeezed and sheared. Multiple fracture surfaces form as a result, with intermittently distributed, narrow smooth shearing zones. This phenomenon, also called earing, most often occurs when the shearing gap is small and with soft materials.

Figure 5.4 shows the typical appearance of the cut surfaces of the blank and the lead frame.

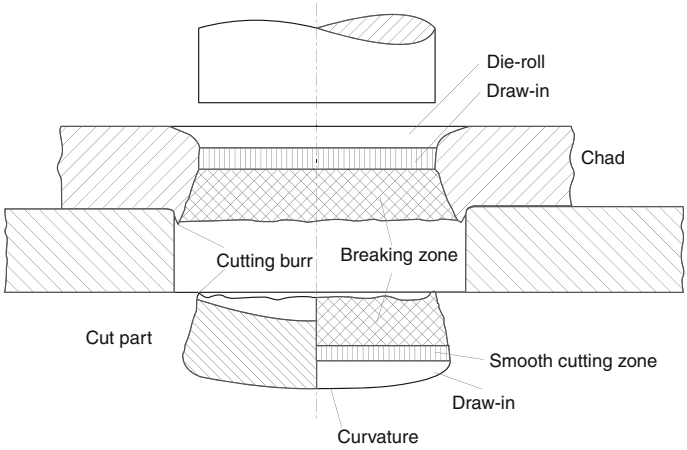


Fig. 5.4 Sheared edge formation in the shearing process

5.1.1.2 The Shearing Gap

While manufacturing accuracy is improved with smaller shearing gaps, also known as die clearance, [NN96], the deformation of the workpiece material increases in the shearing zone. This is associated with an increased strain hardening and with greater cutting forces. The design of the shearing gap represents an optimization problem, as its enlargement can reduce the power demand by up to 15 % and the work demand by approximately 40 % [LANG90c]. The ideal therefore is to have a minimal cutting force while maintaining a sufficient level of manufacturing accuracy. Reference values and rough estimates exist for the shearing gap u_s, generally related to the sheet thickness s.

Given an open cutting line (cf. Sect. 5.1.2.1), a shearing gap of u_s = 3–4 % of the sheet thickness s is selected. Given a closed cutting line, according to [OEHL01], a shearing gap of

$$u_s = c \cdot s\sqrt{\tau_B} \tag{5.1}$$

is selected for thin sheets of up to 3 mm sheet thickness.The factor c is taken as c = 0.005 for achieving a good sheared edge quality and as c = 0.035 for low cutting force. For carbide tools, c assumes a value between 0.015 and 0.018. For the shearing strengthτ_B, the approximation $\tau_B \approx 0.8 \cdot R_m$ is applied.

The empirically determined correction coefficient c accounts for the cutting line shape, the workpiece material quality and the sheet thickness. As a rule, shearing gaps of u_s = 5–10 % of the sheet thickness are selected.

Figure 5.5 provides an overview of the conventional shearing gap sizes with varying materials, as well as the expectable sheared edge qualities. However, because of the multiple factors influencing the cutting result, the optimum value will tend to deviate from these guideline values in any particular application.

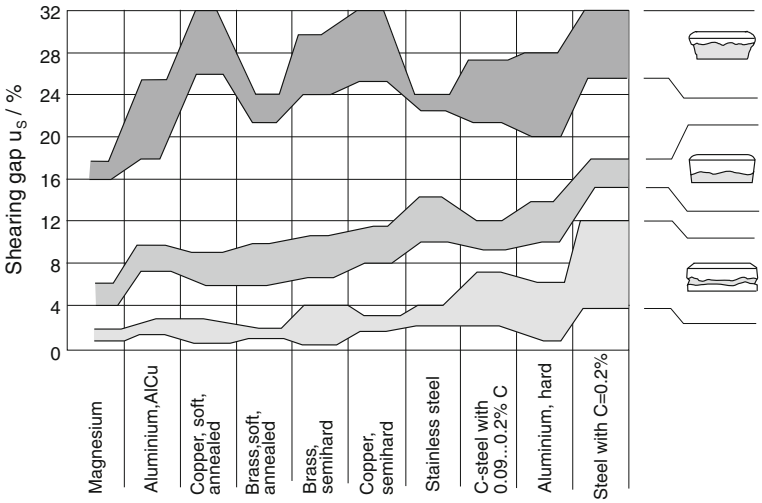


Fig. 5.5 Sheared edge quality as a function of shearing gap [JAHN81]

5.1.1.3 Cutting Force and Cutting Work

Forces arising during the separation process represent an essential parameter for machine and tool design.

The following factors exert an influence on the cutting force:

- the shear strength τ_B of the sheet material,
- sheet thickness s,
- length of the cutting line l_s,
- shearing gap u_s,
- cutting line geometry,
- tool wear,
- tool surface quality,
- lubrication.

In order to account for all factors when determining the cutting force, comprehensive calculations are necessary [KRÄM68] which have proved to be too laborious in practice [LANG90c]. Instead, the maximum cutting force $F_{S\max}$ required for cutting can be determined with sufficient accuracy by applying Eq. 5.2:

$$F_{S\max} = s \cdot l_s \cdot k_s. \tag{5.2}$$

In Eq. 5.2, s refers to the sheet thickness, l_s to the length of the cutting line and k_s to the shear resistance. The latter is defined as the quotient of the maximum cutting force and the sheared surface A_s:

$$k_s = \frac{F_{S\max}}{A_s}. \tag{5.3}$$

For given ratios of punch diameter to sheet thickness larger than 2, the shear resistance k_s can be calculated roughly from the tensile strength R_m [JAHN81, LANG90c, ROMA71, SEML73, STRO70]:

$$k_s \approx 0.6 \ldots 0.9 \cdot R_m. \tag{5.4}$$

For a soft, easily formable grain structure with low tensile strength (from $R_m = 350$ MPa), the relative shear resistance k_s/R_m is 0.8–0.9, for harder ferrite-pearlite structures (up to $R_m = 700$ MPa) 0.6–0.65 [HELL94, SPUR85]. Jahnke indicates a relative shear resistance for aluminium alloys of 0.6 [JAHN81]. In addition to tensile strength, the shear resistance k_s is also dependent on other material parameters, such as carbon content and elongation at fracture, as well as from the process values shearing gap, cutting line form, sheet thickness, tool wear and lubrication [SPUR85]. Figure 5.6 shows the effect of different influence factors on shear resistance.

Radial compression stresses are active between the punch and the sheet strip and between the cut-out and the cutting die. They cause friction forces which must be overcome when the punch is retracted. Depending on the friction conditions (lubrication, surface quality of the outer punch surface) and the radial stresses (dimensions, materials, tool shape), the retracting forces can assume values from 1 to 40 % of the cutting force [JAHN81, LANG90c, SEML73].

Figure 5.7 shows how the cutting force (F_S) on the punch is broken down to a horizontal component (F_H) and a vertical component (F_V). The cutting force causes a reaction force (F'_S) in the cutting die which can also be resolved into a

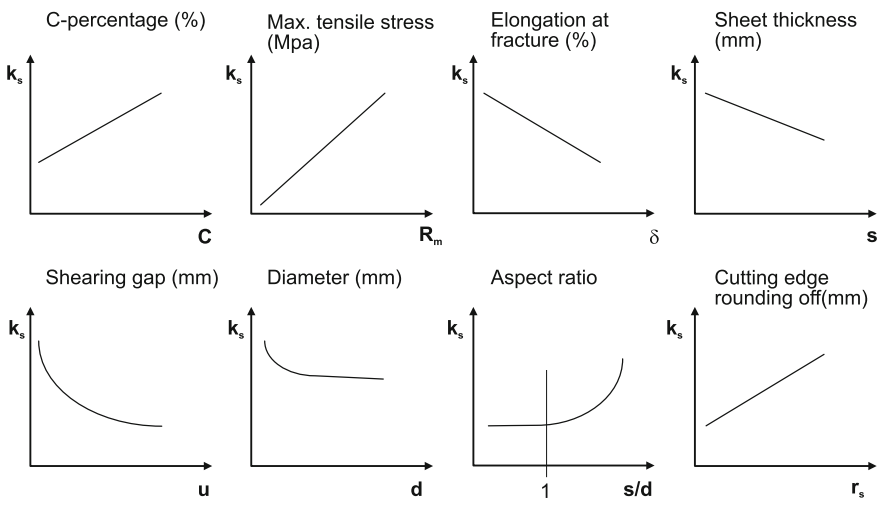


Fig. 5.6 Effect of different influence factors on the shear resistance k_s [JAHN81]

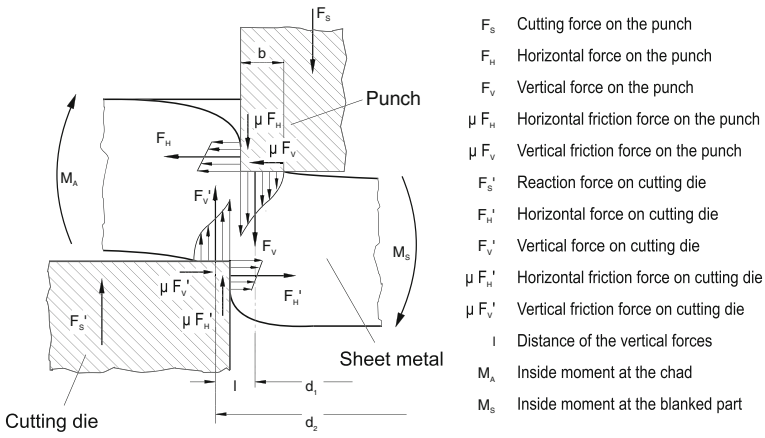


Fig. 5.7 Cutting force components in the shearing process

horizontal (F'_H) and a vertical (F'_V) component. The vertical forces (F_V and F'_V) starting from the punch and the die cause compression stresses which arise during the cutting process in a narrow area of the punch end face or the pressure surface of the cutting die. Since there is material glide at these positions [BÜHL70, LANG90c, SEML73, TIMM56], friction forces result which defend on the friction coefficients and the vertical forces F_V and F'_V. These friction forces are responsible for the wear of the cutting die and the punch [BIRZ97]. Due to the distance l of the vertical forces, a moment M arises in the sheet which stands in equilibrium to the bending stresses in the sheet and the horizontal forces F_H. The bending stresses in the sheet lead to a deflection of the sheet strip.

Figure 5.8 shows the cutting force-path progression. At the start of the cutting process, the sheet is elastically deformed. When the yield stress is exceeded, the cutting force increases degressively, reaching its maximum at roughly 30–50 % of the cutting path. It then decreases until the end of cutting. Crack propagation causes a rapid reduction of the cutting force. In the case of earing (cf. also Sect. 5.1.1.1), one or more inflection points appear in the cutting force-path progression after the cutting force maximum is reached [LANG90c]. If crack formation yields a crack which does not spread into the shearing plane, an ear forms between this crack and the shearing plane. This effect is observable when the shearing gap is too large and may occur repeatedly on the cut height [OEHL01].

The demand for lower cutting force can be met through a suitable geometry of the cutting elements. Given an open cutting line (Fig. 5.9), if the cutting edge of a shearing knife tilts at the aperture angle α_s, the cutting force is reduced because not the entire sheared edge is separated simultaneously. A disadvantage is that the cutting path becomes larger and the cut strips (blanks) are deformed.

When piercing, the cutting force can be lowered if the end face of the punch is bevelled. In this way, while the piercing chads are deformed, this prevents their being torn along with the punch when the latter is retracted. Such measures can

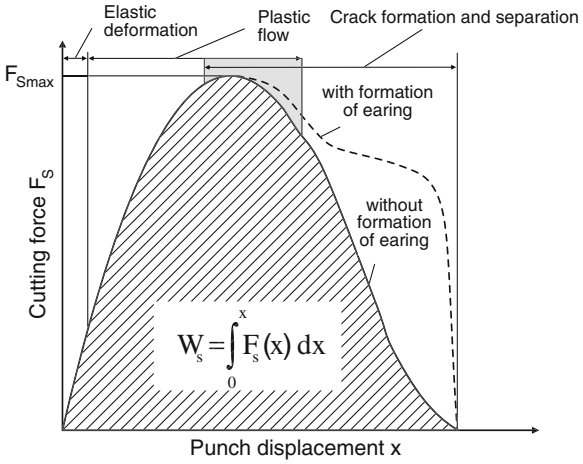


Fig. 5.8 Qualitative progression of the cutting force over the cutting path

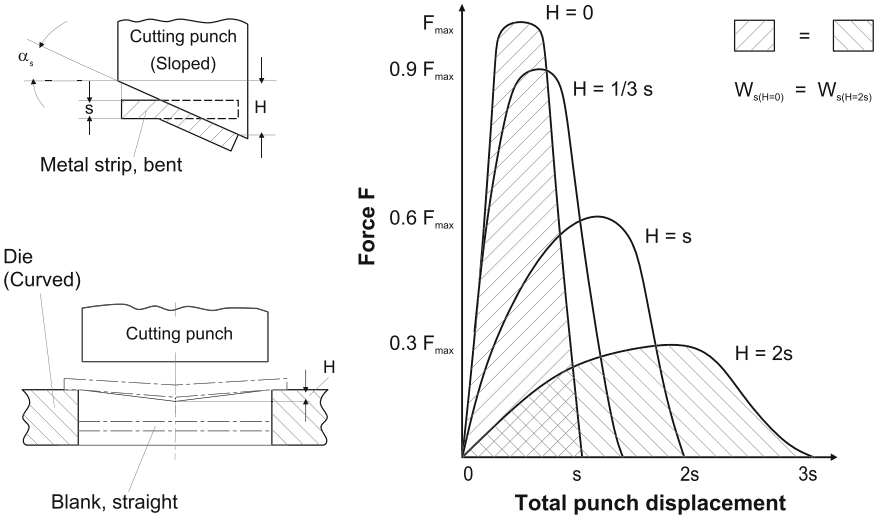


Fig. 5.9 Cutting force reduction through tool modification

reduce the cutting force significantly. A bevelling at the height of twice the sheet thickness can lower the maximum cutting force to 30 % of the value yielded if the entire cutting line is engaged from the start of cutting. The cutting force reduction caused by the bevelled cutting elements is associated with a greater cutting path. The required cutting work W_s, however, is not influenced significantly. This value corresponds to the integral

$$W_s = \int_0^{x_g} F_s(x)dx, \tag{5.5}$$

with x as the cutting path and F_s the current cutting force. Given straight cutting elements, the cutting path corresponds approximately to the sheet thickness s. If influence factors like material properties, the actual cutting path, the shearing gap size and friction force are comprised in a correction value c, Equation 5.5 can be reformulated as

$$W_s = c \cdot x_g \cdot F_{S\max}. \tag{5.6}$$

The cutting work, shown in the cutting force-path diagram (Fig. 5.8) as the area under the curve, results in a correction value $c \approx 0.3$–0.5.

5.1.1.4 Permissible Blanked Part Geometry

An economically viable tool life for cutting tools can only be realized if certain rules are observed when determining the geometry of the blanked parts.

If the ratio of the workpiece cross section to the cutting line length is reduced, the load on the cutting elements is greatly increased, particularly that on the punch. In this case, blanked parts with long, narrow slits or webs are to be avoided, as are acute-angled cuts. Tips and edges must be rounded, whereby the radius of curvature may not fall below a minimum value corresponding to half the sheet thickness ($r = 0.5s$). When piercing steel, a hole diameter of 1.2 times the value of the sheet thickness functions as the lower boundary to be observed in order to guarantee a sufficient strain resistance for the punch. Despite the demand for low chad quantities and thus for low web width between individual cutting operations and, as a result, for the narrowest possible lead-frame edge webs, certain minimum values must nevertheless be observed. The webs are generally to be selected at a size great enough that the material to be cut remains uninfluenced by the previous cutting operation. If the cut part is subjected to a further forming process, no piercing may be carried out in the area of the later forming, as this would lead to impermissible stress concentrations and thus to the formation of cracks. Thus [ROMA71] calculates the minimum distance a between the bending point and the cutting line on the basis of the bend radius r and the sheet thickness s:

$$a \geq r + 2s. \tag{5.7}$$

If multiple holes are punched into a sheet, the hole distances b must amount to at least

$$b \geq 2 \ldots 3s \tag{5.8}$$

of the sheet thickness *s*. The hole rim should have a minimum distance equal to the sheet thickness *s* to an outer edge. If multiple holes are to be punched parallel to the outer edge, the distance should amount to at least 1.5*s*.

5.1.1.5 Tool Wear and Lubrication

Since the dimensional and shape accuracy of the workpiece is determined by the quality of the tool used, the tool precision must generally exceed workpiece precision by 2 ISO qualities. As a result of the loads caused during the cutting process, the tools are subjected to wear. This has a negative effect on the quality of the blanked parts and the required cutting work [OEHL01, RENT97, TOUS00]. If the extent of wear occurring under the operating conditions is known, certain piece quantities can be prescribed until the tool has to be replaced or reworked in order to keep the required tolerance. At first, tool wear exhibits a progressive behaviour. This transitions into a linear increase in the rate of wear. This wear behaviour makes it possible to exchange/rework the production tools after a certain measure of wear provided that the dimensional change caused by the wear is known. Wear measuring quantities are the following [TOUS00]:

- outer wear surface length (in mm) or outer wear surface (in mm^2),
- front wear surface length (in mm) or front wear surface (in mm^2),

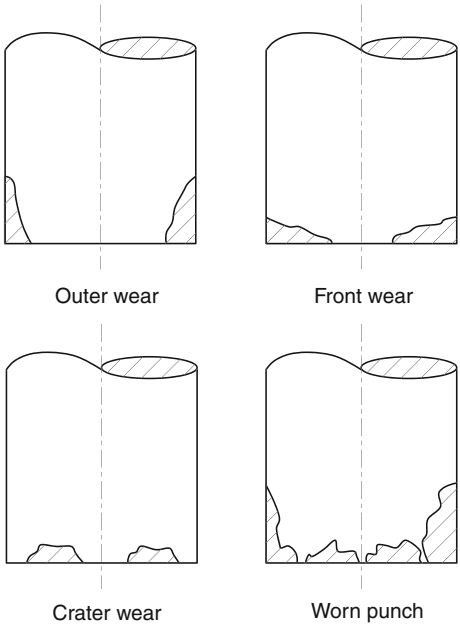


Fig. 5.10 Wear shapes on punches (schematic)

- crater wear (in mm^2),
- 45° wear (in mm), which describes the displacement of the cutting edge.

The causes of wear and thus of burr formation can be read from the behaviour of the cutting edges during the cutting process. As a result of the gliding motion occurring between the workpiece and the tool, for example, particles of the material are constantly deposited on the tool cutting edge. Figure 5.10 provides a schematic illustration of this edge wear.

Front wear surfaces, including crater wear, occur primarily on thin metal sheets ($s < 2$ mm), since they result from the horizontal movement of the material during cutting. Outer wear surfaces develop through friction parallel to the cutting direction occurring during punch penetration and retraction. This is found primarily among thicker steel sheets ($s \geq 2$ mm). With increasing wear, the burr height on the blanked parts generally rises as well. Wear and burr formation are not always easily predeterminable.

Practically all components which take part in the cutting process function as influence factors for tool wear. These include the tool (material, hardness, surface, guidance, shearing gap), the workpiece (alloy, strength, hardness, dimensions, shape) and the machine (design, stiffness).

Depending on the pairing of tool to workpiece material, certain characteristic wear profiles may develop. In order to keep the wear to a minimum, oils are used to lubricate the tools (Sect. 2.8.4). Their job is to form a separating layer between the workpiece material and the tool. The composition and properties of these oils are tuned to the sheet thicknesses and material quality of the material to be processed. [MANG83] recommends seven different groups of lubricant for four classes of sheet thickness and six classes of workpiece material which are distinguished on the basis of kinematic viscosity v (generally 10–100 mm^2/s) and degree of use of EP additives and polar parts.

5.1.2 Process Characteristics and Variants

5.1.2.1 Cutting Line Geometry

A principle distinction in shearing is between open and closed cut [DIN03l]. If the entire cutting line lies within the sheet strip, not cutting the edges, then it is a closed cut or otherwise an open cut (Fig. 5.11).

Closed Cut. Closed cuts serve either for blanking a desired blanked part from a metal sheet or for creating an internal form on the blanked part, i.e., piercing (Fig. 5.12). In the blanking process, the sheet strips remaining after the cut is chad. The cut out part (completed part) is led away through the cutting die opening or ejected from an ejector punch fixed at the cutting die opening. The piercing and blanking processes can be applied simultaneously or in sequence, e.g., in an intermediate stage.

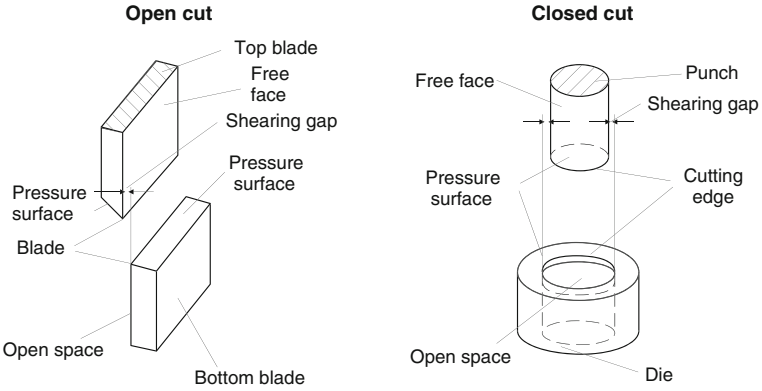


Fig. 5.11 Open and closed cuts in shearing

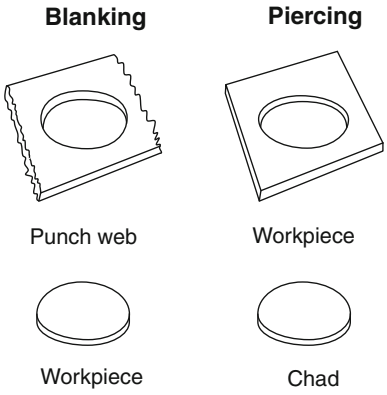


Fig. 5.12 Blanking versus piercing

Open Cut. Typical cutting processes with an open cutting line include all shearing-off processes as used for cutting flat and profiled material to length. They also include notching, partial cutting and nibbling, processes in which the cutting line is not closed in itself [DIN03l]. These processes may be applied to a workpiece both individually and in combination. In many cases, the cutting processes are complemented by forming processes. These are then referred to as compound processes.

Figure 5.13 provides an overview of the different types of open cutting. Cutting-off is a complete separation of the finished or half-finished part from the sheet. Notching is used when pieces are cut out at an external or internal boundary. Trimming is the separation of pieces or finish allowances by means of an open or closed cut. Finally, partial cutting is implemented for a partial separation of the material so as to subsequently form in by bending.

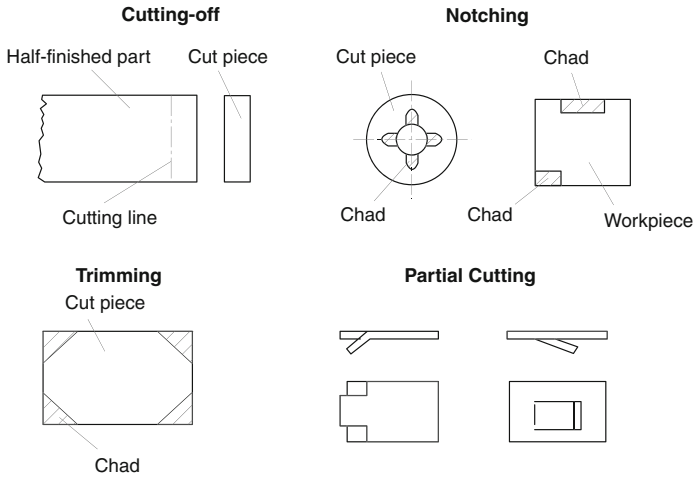


Fig. 5.13 Open cut variants [DIN031]

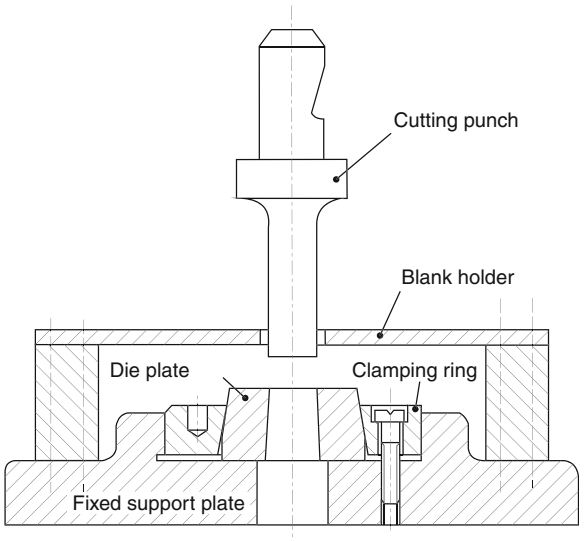


Fig. 5.14 Free punch tool

5.1.2.2 Tool Guidance

The constructive design and operation of a tool have a decisive influence on the work result. The construction of a tool and the selection its mode of operation should therefore be in line with the given conditions (machines present, processing task, quantity, tolerances).

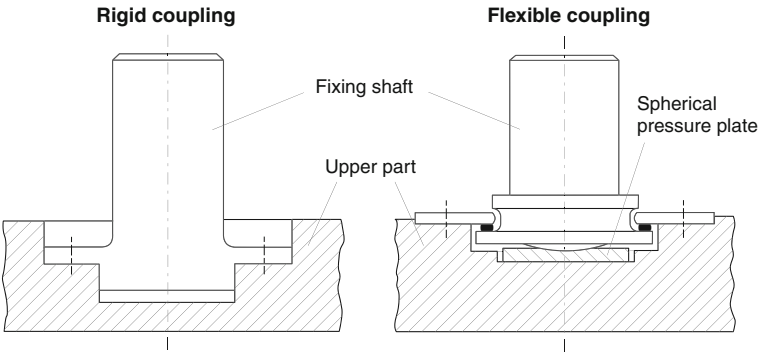


Fig. 5.15 Comparison of rigid and flexible clutches

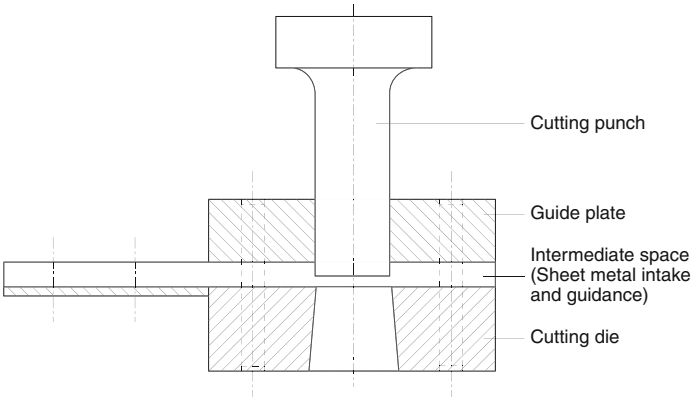


Fig. 5.16 Guided punch tool [MIKK70]

Free Punch Tool. The free punch represents the simplest and most economical option for producing simple cuts with a massive punch. The cutting tool elements are not guided against each other (Fig. 5.14). For this reason, the accuracy of the cut depends on the precision of the machine guidance.

Due to their simple design, free punch tools are the most inexpensive cutting tools. They are consequently used most frequently for small quantities. A disadvantage of these tools is that it is difficult when setting them in the press to adjust the gap between the cutting die and the punch equally on all sides. An unequal setting can lead to greater wear, especially when the shearing gap is only a few hundredths mm, as when cutting sheets below 1 mm. According to [MIKK70], the resilience of C-frame presses can be reduced by implementing a flexible clutch between the spigot and the punch. This reduces the negative influence of the punch displacement (Fig. 5.15).

Guided Punch Tool. In the case of a guided punch tool, the punch is guided via a plate arranged closely above the metal sheet strip (Fig. 5.16). The punch fits into

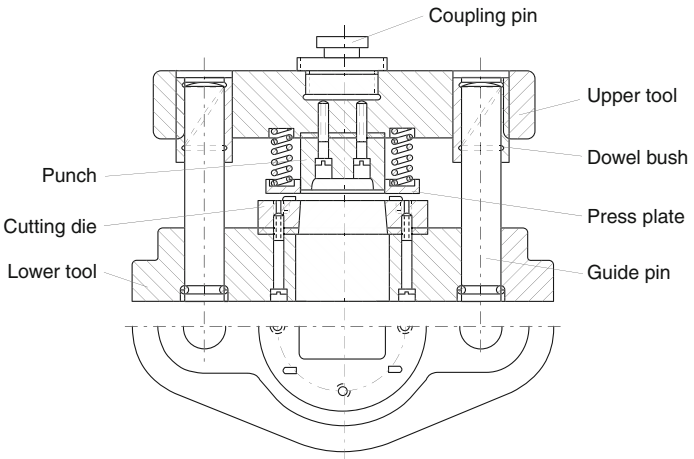


Fig. 5.17 Die set with tooling

the guide hole with almost zero clearance. The position of the guidance plate in relation to the cutting die is secured through alignment pins. The components for taking up and guiding the material strip are found between the guide plate and the cutting die.

The guidance plate reduces tool position errors arising when the tool is installed into the press and displacement position errors which can occur during the springing-back of the press or in case of imprecise or worn ram guides. Furthermore, the guidance plate, which simultaneously serves as stripper, lowers the danger of buckling in the case of narrow punches.

The effect of a guidance plate increases in proportion to how closely it can be brought to the sheet metal strips to be processed, since in this way the protruding length of the punch and the potential for errors associated with it can be minimized. It must be borne in mind, however, that if the material canal is to narrow, a sheet strip which is not completely flat may not be able to be pulled through the tool. Also, the guide bore hole may become damaged by material particles sticking onto the outer punch surface (material transfer through adhesion wear) if the distance of the guidance plate to the sheet strip is shorter than the stroke of the punch.

Highly accurate parts can be created by means of guided punch cutting. However, a guided plate can only be used for a single application. A change in the punch shape usually entails a change of the plate. The guided punch cut is consequently inflexible and thus costly. For this reason, it is only used for larger workpiece quantities or when manufacturing highly accurate parts.

Die Set with Tooling. A die set with tooling separates the functions of guiding and cutting (Fig. 5.17). The upper part of the tool with punch and stripper is connected to the tool lower part via 2, 4 or more pillars, depending on the load. The

pillars can be guided either in bushings (high stiffness) or in ball cages (low friction).

Since the relative positions of the cutting die and the punch to each other are already fixed when the tool is assembled, the installation of a die set with tooling into a press is simple and quick and therefore cost-effective. Tool position errors are reduced to a minimum. Displacement position errors caused through imprecise ram guides or the springing-back of the press frame can be reduced in a similar way as in guided punch tools. Because of the limited stiffness of the pillar guides and the usually high forces involved, however, they cannot be eliminated entirely.

When the demands on accuracy are high, additional guide plates are installed in the pillar frame which are fixed onto the cutting die by means of locking bolts when the press ram goes down.

Because of their elaborate construction, die sets with tooling are highly costly. However, they offer the following advantages:

- The tool can be entirely preset. Machine downtimes are kept short through rapid tool changes.
- The high cost can be compensated by the use of tool systems which consist for the most part of standardized single parts (upper and lower parts, pillars, ball bearing guide). Only the active elements, such as the punch and the cutting die must be designed according to the specific work.
- The precision of guided punch tools can be reached by employing additional guide plates.
- Because of these advantages, die sets with tooling have seen more and more use and now cover a large area of application.

5.1.2.3 Process Flow

Only in the rarest of cases is only one single cutting operation executed on a single part. If multiple cutting processes are required for one part, these can either be performed simultaneously with a blanking and piercing tool or sequentially with a progressive tool.

Blanking and Piercing Tool. The blanked part is finished in a single stroke. The more complex the part, the more difficult and thus more expensive is the tool (Fig. 5.18). This process is often unemployable in the case of more complicated shapes, as a suitable tool cannot be manufactured.

The special advantage of this mode of operation, however, lies in the high accuracy of the cut parts. This depends essentially on the precision of the tool and is free from influences on the part of the strip feed. The blanking and piercing tool is preferably used when not excessively complicated parts are to be manufactured with a demand for minimal position and dimensional errors.

Progressive Tool. In this case, the blanked part is created in a tool with several punches arranged in sequence (Fig. 5.19). After every ram stroke, the material

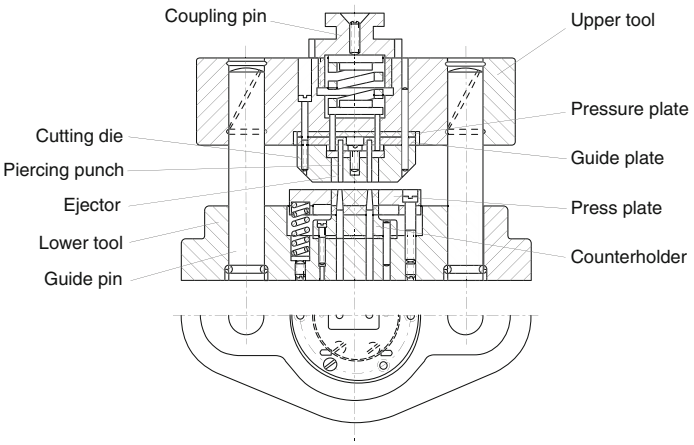


Fig. 5.18 Blanking and piercing tool with pillar guidance

strip is moved down one station, meaning that all punches are simultaneously at work and every press stroke yields a single part. This method can be used to manufacture complicated workpieces, allowing for an optimal exploitation of the material, since different parts can be produced from a single metal sheet strip (Fig. 5.20).

Even with complex parts, the individual punches can still have a simple construction. The progressive tool has seen increased use for that reason, especially because it allows for the integration of forming operations (progressive compound tools).

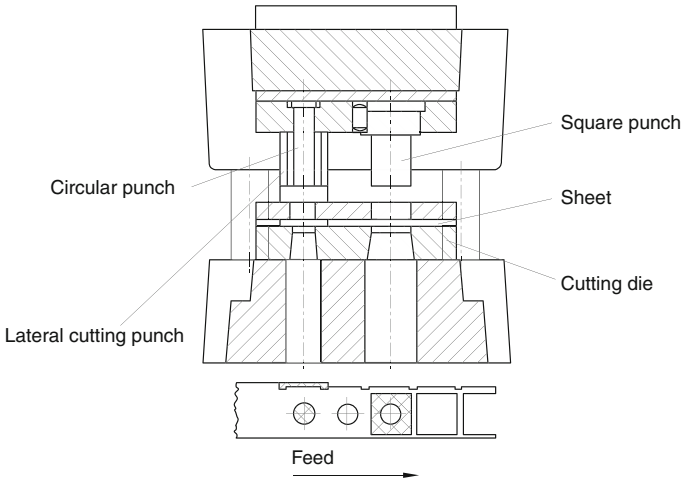


Fig. 5.19 Progressive tool [LANG90c]

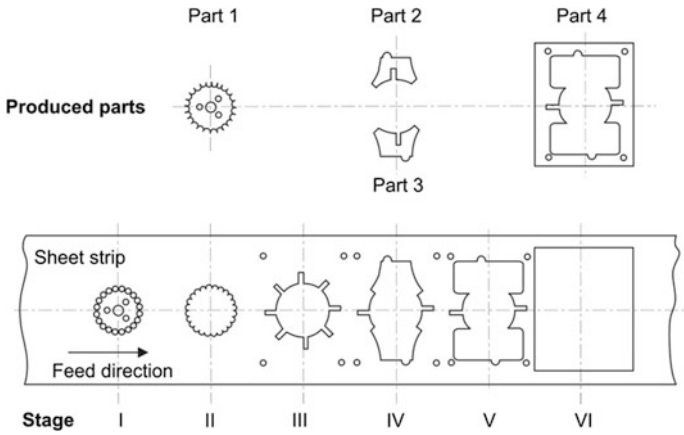


Fig. 5.20 Example of progressive blanking

A disadvantage of progressive tools lies in the fact that the accuracy of the finished parts depends not only on the tool, but also on the feed limit. Feed errors have the immediate effect of position errors and must therefore be kept to a minimum.

- In progressive blanking, the feed can be limited through:
- button stops or stop pins,
- pilots or capture pins,
- pilot punches,
- feed control/regulation by mean of roll feeds.

Button stops tend to be used with manual feed and with relatively small workpiece quantities and thin sheets because the strip can only be regulated when retracted. Stop pins are suitable for thicker sheets, provided they are sufficiently rigid (Fig. 5.21a).

Pilots and capture pins act to limit feed when this is automated (Fig 5.21b). It compensates for small feed errors and forces the sheet strip into the correct position. For this reason, it must have a conical design. Its cylindrical cross section must have reached the prepunch margins before the punch begins cutting. It is thus considerably longer than the punch.

If holes are already present in the blanked part, they can be used as pilot holes. Otherwise one must make special punch holes in the sheet strip.

The most precise feed limitation is provided by the pilot punch (Fig. 5.21c). This is an additional punch on the cutting tool which cuts off a section from the sheet strip with the length of the feed with every working stroke of the press ram. Then the strip is fed until the section created by the pilot punch lies firmly against the limit stop. If only one pilot punch is used, the feed limiting would stop when the end of the strip is reached, with a section of the strip remainder corresponding to the tool length going wasted. For this reason, two pilot punches are

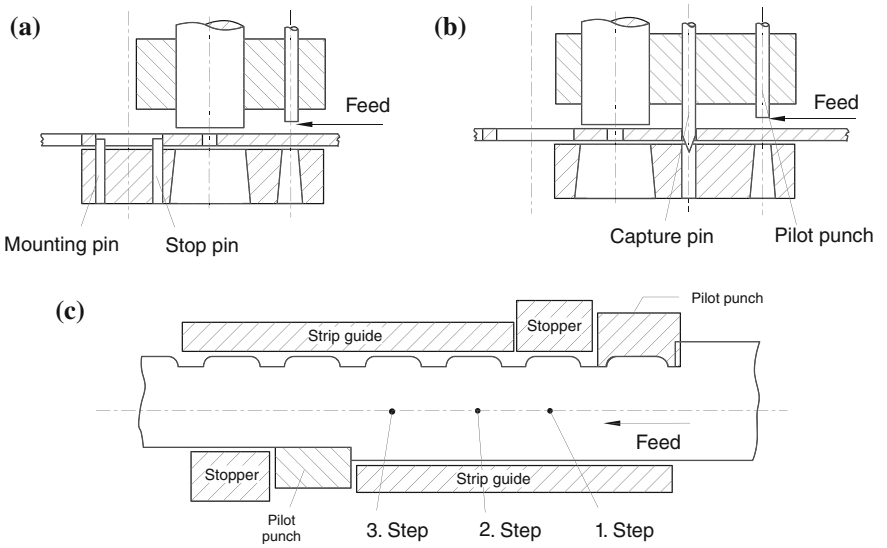


Fig. 5.21 Feed limits. **a** Stop pin. **b** Capture pin. **c** Pilot punch

arranged diagonally, one in front of the first, the second behind the last progressive station.

After prolonged use of the pilot punch, the increasing edge rounding leads to the formation of a burr. This burr reaches the limit stop sooner than the sheet edge lying perpendicular to the feed direction. The danger thus arises of the sheet strip jamming because of the burr left in the material channel.

This disadvantage can be avoided by the form pilot punch illustrated in Fig. 5.21c. Even given burr formation, an edge cut true to the dimensions always arrives at the limit stop. The burr can be bent within the material channel towards the remaining free spaces, thus preventing the jamming of the sheet strip.

Over the course of time, there has been a strong increase in the operating speed of modern presses, reaching stroke rates of 2.000 min^{-1} and higher. This in combination with feed rates of up to 60 m/min has made the implementation of pilot punches impossible. For such applications, roll feed systems with electric stepper motors and hydraulic torque amplifiers or with controlled-position drives have proven useful. These systems guarantee both the required dynamic properties and a positioning accuracy of a few hundredths of a millimetre [LANG90c]. The sheet strip is clamped between two or more rolls with a non-slip coating which give the strip its feed movement by rotating at a defined axis.

5.1.2.4 Special Process: Nibbling

Nibbling is a method for blanking arbitrary shapes from sheet metal plates [DIN031]. It is only used in individual or small batch production. Examples

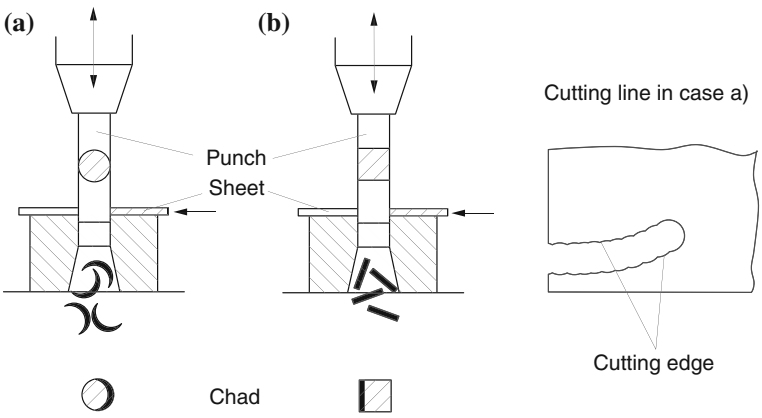


Fig. 5.22 The nibbling principle

include the manufacture of templates for copy lathes and milling machines or sheet metal parts for prototypes. Nibbling is a punching process with an open cutting line (Fig. 5.22).

Workpieces are cut out as follows: consecutive holes are made on the contour in such a way that only the front part of the punch is engaged. The feed from hole to hole is therefore smaller than the diameter of the punch. The shape of the sheared edge depends on the feed per hole and on the shape and size of the punch. Since crooked contours are generally made using nibbling, round punches are used which allow for changes in direction during the feed.

Modern nibbling machines are equipped with a tool change system which both has different punch geometries and can also execute machining production processes, such as thread cutting. An additional laser fitting also allows the nibbling machine to produce narrow slits in sheet parts manufactured by nibbling. Both the contour to be nibbled and that to be cut by the laser are created by the processing of the sheet stretched on a numerically controlled table.

5.1.3 Manufacturing Accuracy

The design of the cutting elements is of decisive importance for achievable accuracy. Already when setting tool tolerance margins, for example, one must take into consideration whether blanking or piercing is to be executed. The part located in the cutting die springs apart after being discharged from the cutting die aperture, which means that the plate size should lie at the lower limit of the tolerance range. Because of the low spring-back of the material and the punch wear, bore hole sizes are smaller than that of the punch. The punch dimensions correspond to the upper tolerance limit of the workpiece. Depending on sheet thickness, dimensions and

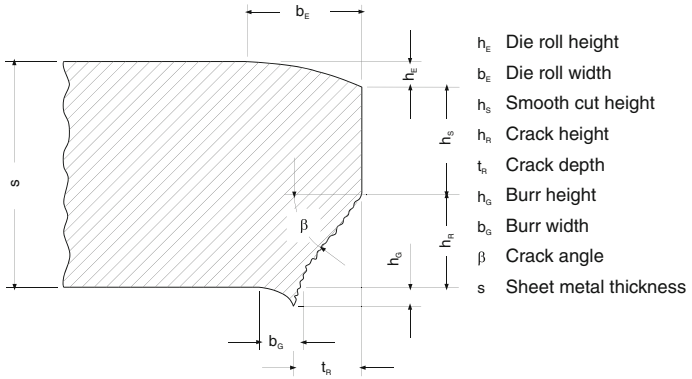


Fig. 5.23 Form errors on cut parts [BIRZ97]

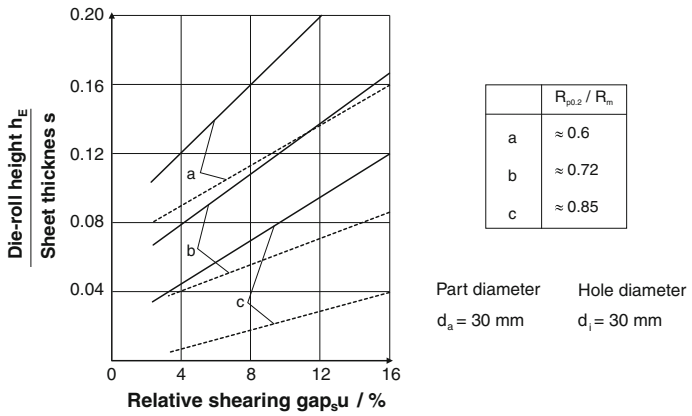


Fig. 5.24 Relative shearing gap over edge deformation height [GUID65]

the shape of the cutting line, the accuracies achievable are, according to [LANG81b, ECKS03], 0.02–1 mm for blanking and 0.01–0.25 mm for piercing.

Figure 5.23 shows form errors on the cut part. Other important factors besides dimensional errors and flatness deviations (camberings) are die roll height h_E, burr height h_G and the crack depth t_R. The die roll height is related to the deformation zone, the crack depth to the fracture zone.

Figure 5.24 clarifies the connection between the relative edge deformation height h_E/s and the relative shearing gap u_s. The die roll height increases in proportion to the size of the shearing gap and can very well amount to 20 % of the sheet thickness depending on the material's ratio of the limit of elasticity R_p/R_m. Materials with a small ratio of the limit of elasticity tend to have a greater die roll height that those with a large ratio of the limit of elasticity.

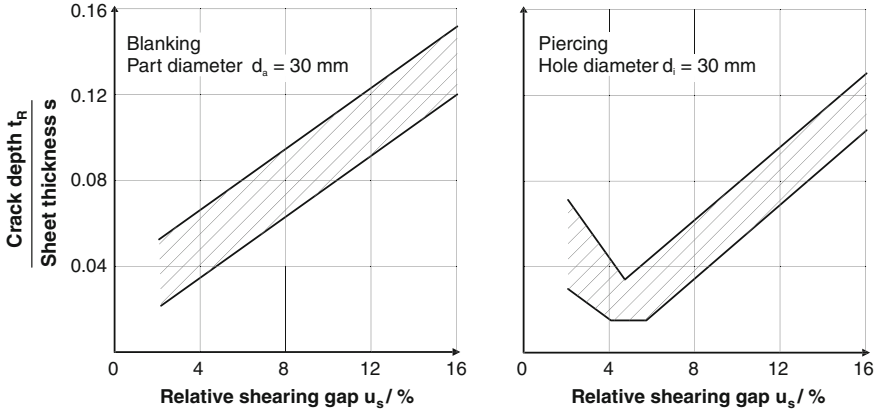


Fig. 5.25 Relative shearing gap over crack depth [GUID65]

When piercing, a larger shearing gap influences the crack depth as negatively as when blanking. While the crack depth remains minimal in its relation to the shearing gap, it increases linearly when blanking with an increasingly large shearing gap (Fig. 5.25).

Burrs are an undesirable accompanying effect found on blanked parts and must generally be removed in a reworking process, since they both constrict the upper plate of the part and represent a hazard with respect to handling. The height of the burr h_G is both a measure of the manufacturing quality of a blanked part and a parameter of the wear condition of the cutting tool. The burr height increases with

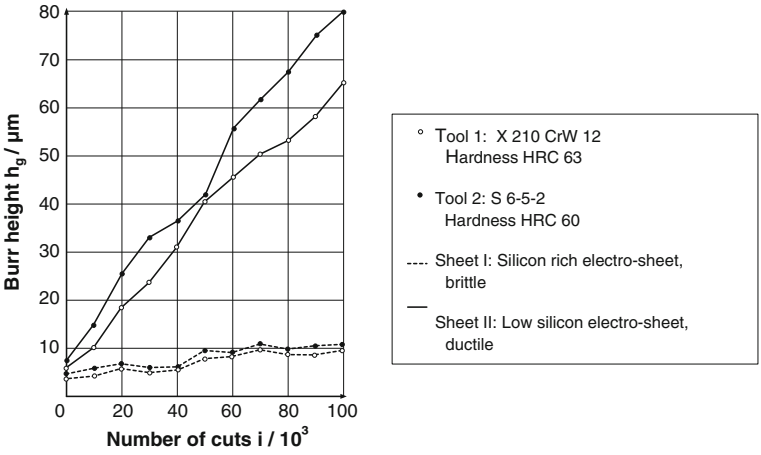


Fig. 5.26 Connection between burr height and number of cuts with different tool and workpiece materials

an increasing number of cuts and is determined not only by the tool wear or the shearing gap, but also by the workpiece material (Fig. 5.26).

Since the elongations which occur until a crack appears are greater on ductile materials than on brittle materials, blanked parts made of low-silicon magnetic steel sheets exhibit greater burr heights that those made of high-silicon, brittle steel materials. In comparison to high speed steel, the greater hardness of tools made of cold work steel proves to be a positive characteristic in view of the lower burr heights which can be attributed to lower tool wear.

5.2 Fine Blanking

Fine blanking is a separation process belonging, as a shearing method, to the group "Splitting" according to DIN 2003. In this process, which is associated with special tool and machine designs, parts can be created whose sheared edges are perfectly smooth throughout the thickness of the sheet. The parts cut in a single operation exhibit high dimensional and form accuracy and are ready for installation following deburring. Parts are mainly produced by means of fine blanking when there is a demand for high surface qualities with low dimensional tolerances, when surfaces with a good optical quality are desired, when the limits of normal stamping are exceeded [VDI94] and when the opportunity presents itself of combining fine blanking operations with forming operations.

Figure 5.27 shows a selection of typical fine-blanked parts. Originally, only small, fine blanked parts were produced, such as those made for the watchmaking, calculating machine, and camera industries (thus the designation "fine" blanking).

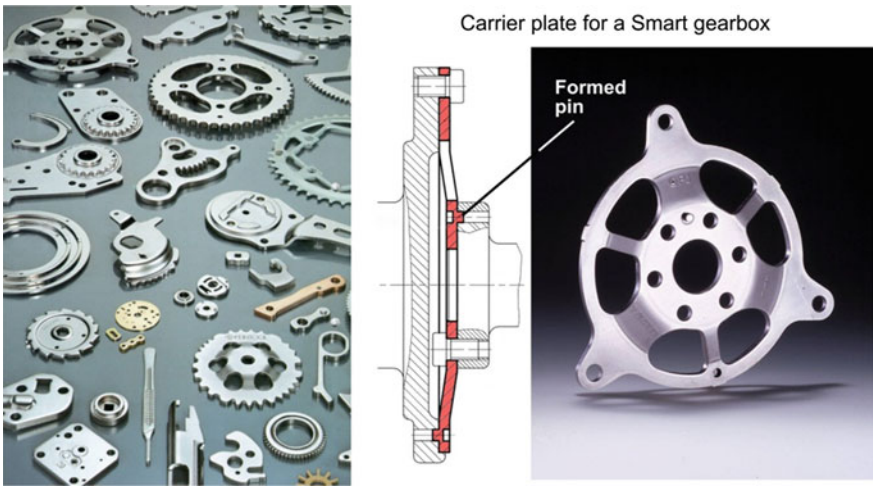


Fig. 5.27 Fine-blanked parts (*Source* Feintool AG)

Over the course of time, however, the range of products extended to functional and safety parts for the household appliances industry, as well as for the textile, automotive, medical and electrical industries [BIRZ93, BIRZ96, SCHÄ93]. A broad application of fine blanking is also found in combination with other forming operations, allowing for the production of workpiece with a higher functional integration [BIRZ96, BOET90].

The combination of fine blanking and forming operations makes it possible to save on additional production steps and components (e.g., positioning units). For example, the combined fine blanking and forming operation employed in the production of driving plates for Smart transmissions leads to a weight savings of circa 70 % (Fig. 5.27).

5.2.1 Principles of Fine Blanking

In normal cutting, about one third of the sheared edge is a smooth cutting zone and two thirds a fracture zone. In contrast, the smooth cutting zone may be extended over the entire sheet thickness if required (Fig. 5.28).

5.2.1.1 Process Principle

The fine blanking process includes the following characteristics absent in conventional blanking [DIN03l, VDI94, GUID65, BIRZ97, KRÄM69] (Fig. 5.29):

- press plate (guide plate) with knife-edged ring,
- counterholder,
- very small shearing gap,

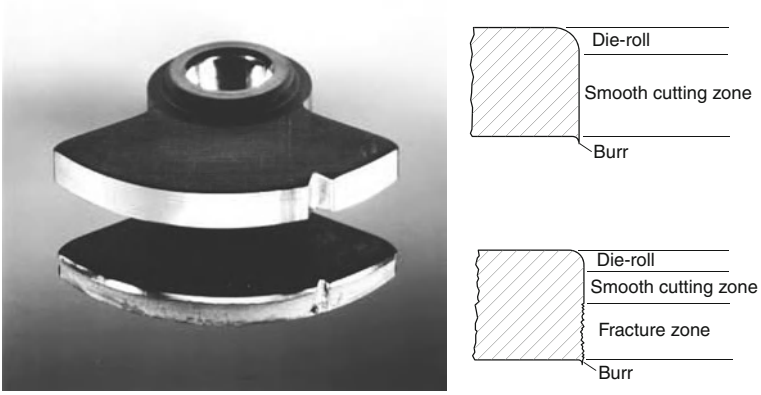


Fig. 5.28 Comparison of conventionally blanked and fine-blanked sheared edges (*Source* Feintool AG)

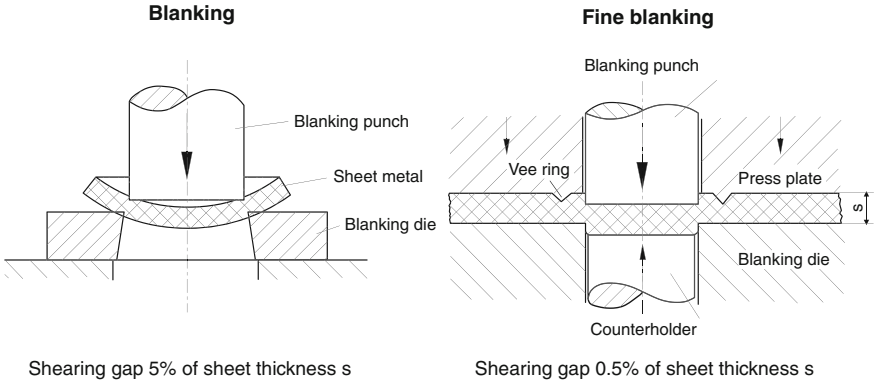


Fig. 5.29 Normal blanking versus fine blanking [BIRZ97]

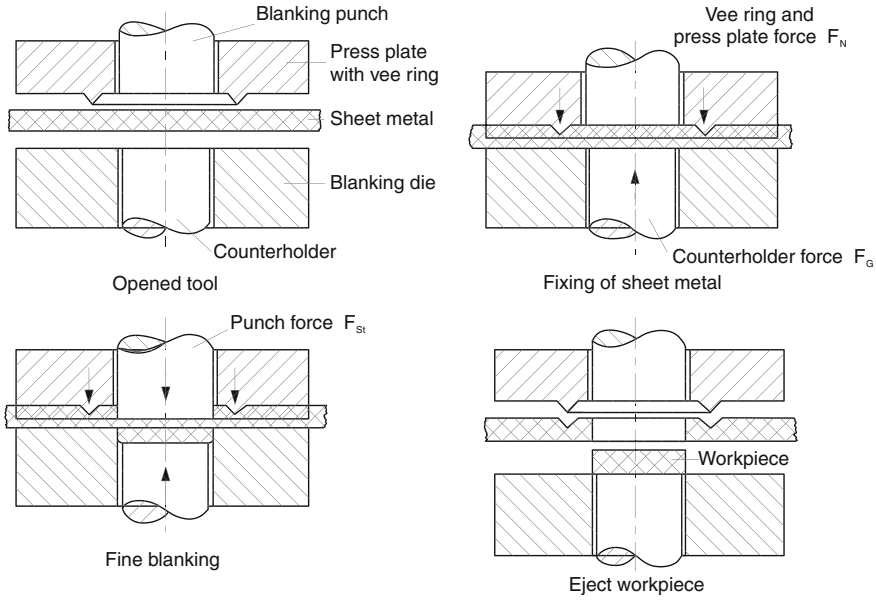


Fig. 5.30 Process steps in fine blanking

- three forces,
- cutting force-path progression.

After inserting the sheet strip, the tool closes, clamping the workpiece between the press plate equipped with a knife-edged ring and the cutting die (Fig. 5.30). The press plate has the additional task of guiding the punch.

The V-shaped knife-edged ring is pressed into the material outside of the cutting line. Within the cutting line, the material is stretched between the punch and the counterholder by means of a defined pressurization of the counterholder.

In order to initiate the actual blanking process, the punch force acting on the punch must be increased so that it penetrates the material when the yield stress is exceeded. The V-ring force applied to the press plate and the opposing force acting on the counterholder remain almost constant during the cutting process, so that the part to be cut out is clamped under pressure. After the punch has completely penetrated the sheet, the tool is opened. The press plate strips off the lead frame, inner forms are discharged and the workpiece is ejected from the counterholder.

The penetrating punch creates plastic material flow in the cutting zone. A smooth sheared edge is created as long as this flow can be maintained. However, a strain hardening of the material occurs in the cutting zone as a result of an increasing cutting path. Crack formation and an associated, undesirable fracture zone appear if the forming capacity of the material is exhausted. As opposed to shearing, this point should only be reached in fine blanking when the punch has penetrated the entire thickness of the sheet. The forming capacity is first and foremost dependent on the material, but also on the strain and stress conditions (Sect. 2.3.7.1). With progressive forming during the plastic flow, gliding dislocations dam up on obstacles in the crystal lattice. A stress field develops in the area of a barrier to dislocation movement, which leads to the rupturing of the crystal lattice in the form of a micro-crack when a critical value is exceeded. This crack formation is introduced by the prevalent shear stresses in the shearing zone. In shearing, the direction of crack propagation does not run parallel to the shearing zone, but rather into the material interior. Thus it can be concluded that the tensile stresses in the material are responsible for the propagation of shear-stress-induced cracks. In fine blanking, because of the large hydrostatic stress component, the tensile stresses are significantly lower, which means that crack propagation only happens as a result of the high shear stresses parallel to the shearing zone [HERR92]. It is thus possible to limit or even entirely to prevent crack propagation though sufficiently high compressive stresses. These are induced in fine blanking through the use of a counterpressure punch and a knife-edged ring. The small shearing gap u also guarantees the formation of a tension-free shearing zone (Fig. 5.31). At the start of the cutting process, the midpoint of Mohr's stress circle lies in the pressure range. As the cutting process progresses, σ_m is displaced further in the direction of the tensile area [ROTT84]. In fine blanking, given favourable process parameters, tensile stresses develop in the shearing zone only toward the end of the cutting process.

In order to determine the properties of a workpiece, it is important to know which stresses and strains may arise in the corresponding material. In all cold-forming processes, including fine blanking, deformations occur in the lattice in the deformed zones. In the process, the grains are stretched in the direction of the deformation, which is usually attended by a strain hardening of the material. This causes an increase in strength values, such as elastic limit, tensile strength and hardness with a decrease in material ductility in the form of elongation at fracture, contraction at

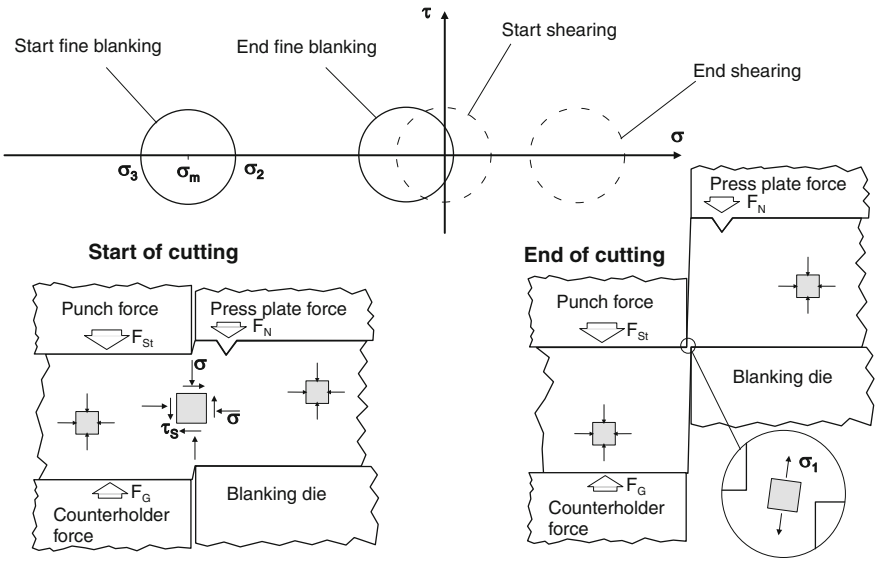


Fig. 5.31 Stresses in the cutting zone typical of fine blanking

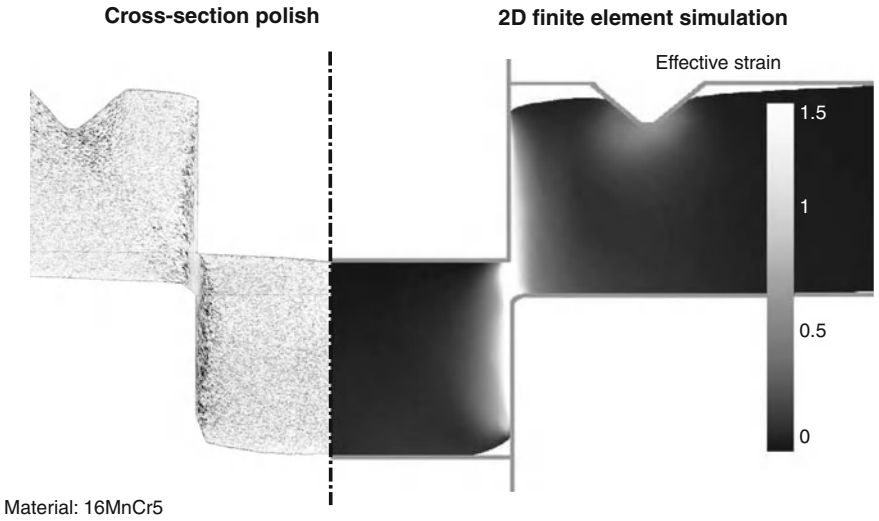


Fig. 5.32 Comparison of a cross-section and an FE-simulation derived from fine blanking of 16MnCr5

fracture and impact strength. In contrast to shearing, fine blanking places an equally high demand on the forming properties of materials as such processes as bending, coining and deep drawing. The left half of Fig. 5.32 illustrates the fibre pattern in the shearing zone and in the area of the knife-edged ring in the fine blanking

of 16MnCr5 steel. The lattice demonstrates a recognizably extreme cold forming of the grains which occurs strongly in the area of the sheared edge. Thus the cold forming increases from the edge deformation side to the burr side and decreases from the sheared edge to the material interior. A measurement of the hardness in the area of the shearing zone would yield a similar distribution (Fig. 5.47). The right half of Fig. 5.32 shows the comparative degree of forming in the shearing zone as calculated in a 2D FE-simulation. The comparative degree of forming also shows a similar distribution to that of strain hardening. The degree of forming along the sheared edge increases with the cutting path drops from the sheared edge to the material interior. The maximum degree of forming in the shearing zone depends greatly on the shape of the cutting edge and the edge rounding as well as from the size of the shearing gap and can reach very high values in small areas in front of the cutting edge.

5.2.1.2 Quality Characteristics and Influence Factors

The demand for a perfectly smooth sheared edge determines, among other things, the quality of a fine-blanked part. Since in practice the ideal of a 100 % straight cut is not always required, the sheared edge is judged on the basis of information about the existing clean-cut portion h_s/s and about the type of fracture surfaces, which can be found in the form of torn-off or ruptured surfaces. The minimum width of the clean-cut zone, which is related to the sheet thickness, is taken as the measure for the clean-cut portion [ROTT85, VDI94]. The quality of the clean-cut surface can be judged, for example, on the basis of the arithmetic mean roughness value

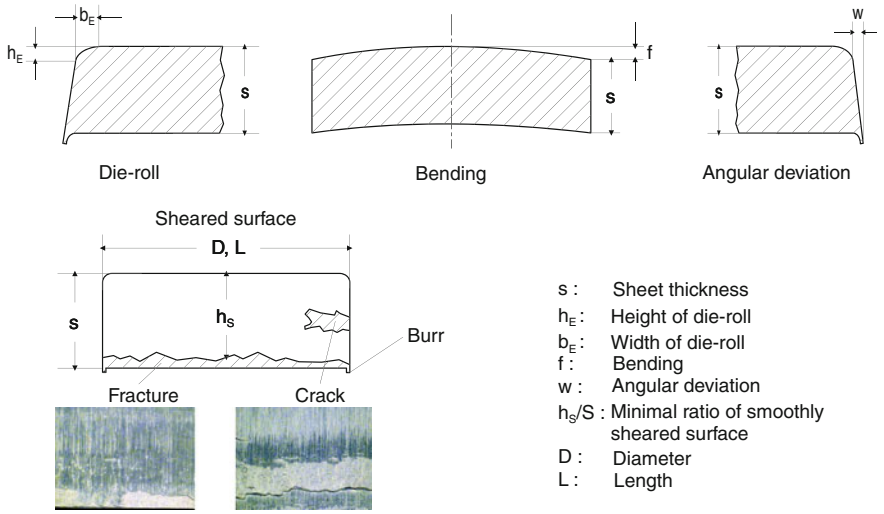


Fig. 5.33 Quality characteristics of a fine-blanked part

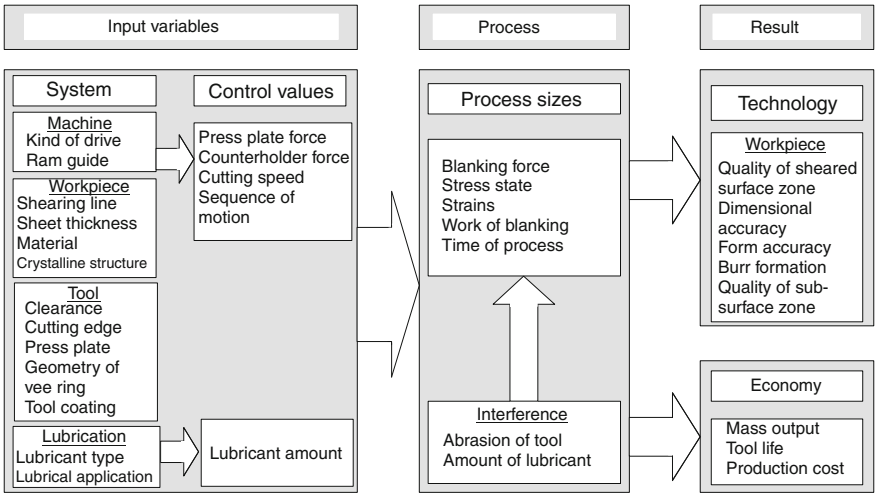


Fig. 5.34 Connections between input values, process values and the work result in fine blanking

R_a, which is to be measured in the middle of the sheared edge perpendicular to the cutting direction. In addition to dimensional accuracy (length, diameter), the following form deviations are used to determine the quality of a blanked piece [BIRZ96, HAAC79, BIRZ97] (Fig. 5.33):

- size of the edge deformation,
- angular deviation of the sheared edge,
- deflection of the blanked part.

The actual fine blanking process is set up by means of a combination of preset system parameters (machine, workpiece, tool, lubrication) with the correcting variables of the knife-edged ring force, the opposing force, the cutting speed and the lubricant quantity (Fig. 5.34). The process is characterized above all by the maximum required cutting force.

5.2.1.3 Permissible Sheared Edge Forms

Fine blanking thin, extended parts is easier than fine blanking narrow ridges or rings with high sheet thickness. Also, obtuse-angled edges with large radii are more suited to fine blanking than acute-angled edges with small radii.

As a result of experience, degrees of difficulty for fine blanking processes are specified on the basis of the three difficulty levels S1 (easy), S2 (medium) and S3 difficult (Fig. 5.35). The main criteria here are the geometry of the cutting line and the sheet thickness. The cutting line geometry is further analysed into simple geometric forms, such as corner radii, hole diameters, slit widths and ridge widths. The relationship of the geometrical dimension describing the cutting line to the

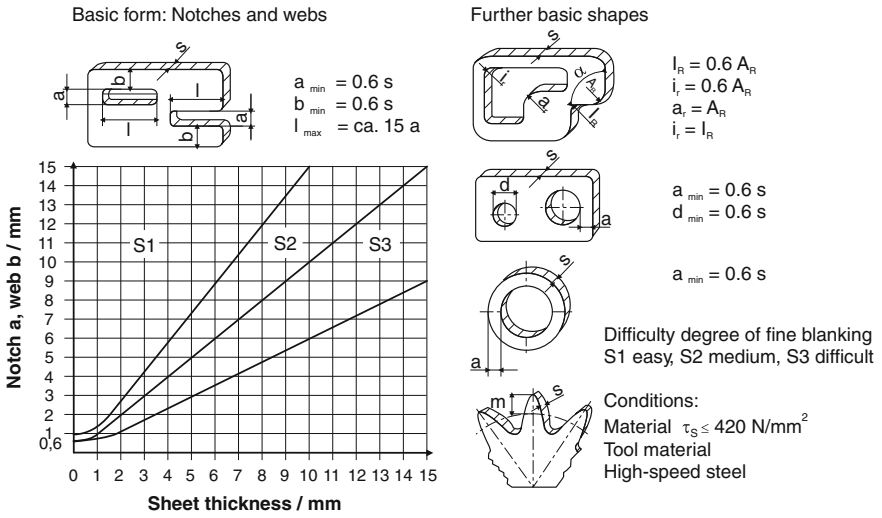


Fig. 5.35 Determination of the degree of difficulty for fine blanking (*Source* Feintool AG)

sheet thickness yields the degree of difficulty for fine blanking, which increases in proportion to sheet thickness. The highest single degree of difficulty results in the total degree of difficulty of the fine-blanked part.

The difficulty levels shown in Fig. 5.35 apply under the assumption that the cutting elements of the tool possess a 0.2 proof stress of $R_{p0.2} = 3.000$ MPa and the tensile strength of the material to be processed does not exceed $R_m = 500$ MPa.

In order to prevent the material from flowing away from the cutting edge, the ridge/edge widths of the lead frame and of the workpiece must have a certain minimum value. These must be large enough that the knife-edged ring can fully press into the material the sheet strip is not unduly deformed. Generally, the edge/ridge widths are to be kept low so as to minimize the consumption of material. One reference value is that the dimensions of edge/ridge width amount to roughly 60 % of the sheet thickness. This value can vary depending on the quality of the material and on the geometry of the cutting line.

5.2.1.4 Shearing Gap

Successful fine blanking depends on a small shearing gap. This is because it is favourable for pure shearing and prevents adverse bending tensile stresses in the cutting zone. The shearing gap becomes greater with increasing sheet thickness [GUID65, BIRZ97]. As in conventional blanking, the size of the shearing gap is also related to the sheet thickness in fine blanking, generally amounting to $u_s = 0.5$ % (cf. Sect. 5.1.1.2).

Studies have shown that this size can vary according to the geometry of the cutting line, the sheet thickness and the quality of the material [JOHN68, KÖNI82b, KÖNI84, MAED68]. A small ratio of workpiece width to sheet thickness, for example, leads to greater values for the shearing gap. Also, partial changes to the shearing gap can be made along the cutting line.

A general empirical formula, however, dictates that the clean-cut section of a sheared edge increases with smaller shearing gaps, with the result that, for fine blanking, the shearing gap should not be larger than 1 % of the sheet thickness.

5.2.1.5 Cutting Edge Geometry

For fine blanking a smooth outer contour, the cutting edge of the cutting die is rounded and the punch is sharp-edged. When fine blanking smooth hole walls, the punch is rounded and the cutting die is sharp-edged. A rounding of the cutting edges of both cutting die and punch is not executed, so as to avoid bends as much as possible and to favour pure shearing. Figure 5.36 shows the schematic structure, the active elements and the blanked components involved on the example of a disc to be fine blanked.

The size of the cutting edge radius is 5–10 % of the sheet thickness and is determined among other things by the quality of the material and the geometry of the cutting line. Higher material strengths require greater cutting edge radii [KÖNI84]. The cutting edge rounding should be just large enough so that the fine-blanked part exhibits smooth sheared edges. Too much of a rounding is to be avoided, since this can have a negative effect on the dimensional and form accuracy of the part.

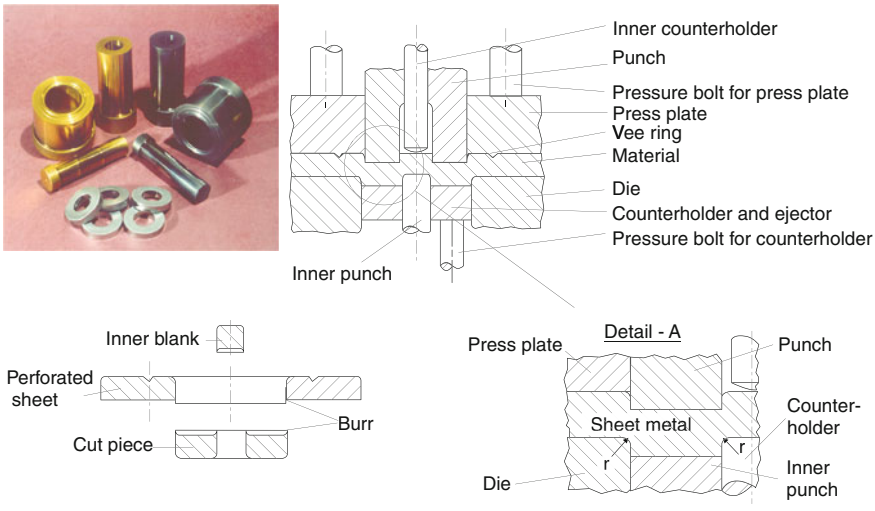


Fig. 5.36 Fine blanking a disc (schematic diagram)

In addition to rounding, the cutting edges are also given chamfers or a tractrix curve. The shape elements are specially adapted to the employed material, as well as to the required precision and geometry of the parts. Recent studies have shown that the shearing gap in association with the cutting edge geometry has a decisive influence on the quality of the cutting part.

5.2.1.6 Knife-Edged Rings

The knife-edged ring is usually also mounted on the press plate or on the press plate and the cutting die, running parallel to the cutting line a certain distance away from it.

Although studies have shown that perfectly smooth sheared edges can be made under certain conditions without the aid of a knife-edged ring [KIEN63, KÖNI82b, KÖNI84, ROTT84], industrial manufacturing has come to favour the use of a press plate with knife-edged ring as a result of the improved dimensional and form accuracies achieved. The V-shaped ring follows the cutting line at a certain distance, with both the distance and the height of the knife-edged ring increasing with increasing sheet thickness (Fig. 5.37).

With sheet thicknesses over $s = 5$ mm, a second knife-edged ring mounted on the cutting die must inevitably be employed [BIRZ97]. A knife-edged ring guidance running parallel to the cutting line would be optimal, but this is not always possible for manufacturing reasons. In the case of re-entrant sections with small ratios of slit width to sheet thickness, the knife-edged ring is guided past the slit.

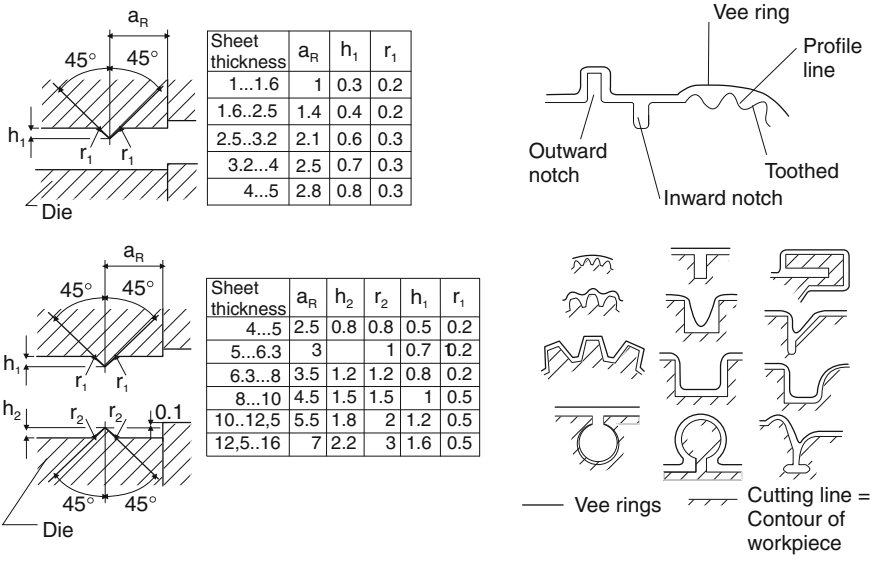


Fig. 5.37 Geometry and progression of the knife-edged ring (*Source* Feintool AG)

This same applies to gearings (Fig. 5.37, upper right). A knife-edged ring is not typically used outside of the cutting line when fine blanking a hole, because the notch of the knife-edged ring would remain in the workpiece. A knife-edged ring is only necessary within the outline of a hole when the dimensions of the inner form amount to a multiple of the sheet thickness in all directions of the sheet plane [KRÄM69].

5.2.1.7 Knife-Edged Ring Force

The knife-edged ring force is needed to impress the knife-edged ring(s) into the sheet strips and to clamp the material outside of the cutting line between the press plate and the cutting die. It must in any case be great enough that the knife-edged right can fully penetrate the sheet, since otherwise the sheet may deflect.

In general, the required knife-edged ring force should amount to between 30 and 100 % of the cutting force. Beyond this, one can apply the following formula [SIEB52]:

$$F_R \approx 4 \cdot l_R \cdot h_R \cdot R_m. \tag{5.9}$$

with the variables in the formula referring to:

- the knife-edged ring force (F_R),
- the total length of the knife-edged ring (l_R),
- the total height of the knife-edged ring (h_R),
- the tensile strength of the material (R_m).

However, the knife-edged ring force calculated in this way only represents an approximate value. In the construction design of fine blanking tools and presses, today's manufacturers resort to in-house developed nomograms in which the necessary knife-edged ring force is registered as a function of the knife-edged ring geometry, sheet thickness, material strength and grain structure. The final fine-tuning happens in the tool setting process, which influences the extent of the clean-cut section. With increasing knife-edged ring force, the clean-cut section can reach a maximum value of 100 %—in certain circumstances, a completely clean cut can prove impossible in spite of maximum knife-edged ring force. If this is required, however, constructive alterations must be made to the tool.

5.2.1.8 Opposing Force

Through the opposing force, a constant pressure is applied to the fine-blanked part being formed during the cutting process. The effect of the opposing force on sheared edge quality is different with blanked parts than with holes. Only a subordinate role is attributed to the opposing force in terms of the sheared edge quality

for blanked parts. For the fine blanking of holes, however, higher opposing forces lead to greater clean-cut sections [KÖNI81a, KÖNI82a, MAED68].

The main effect of opposing forces is to prevent the cambering of the blanked part. For this reason, its magnitude depends primarily on the sheet thickness and the size of the blanked part. Its value is usually specified as 10–20 % of the cutting force and can be calculated approximately according to the formula

$$F_G = A_q \cdot q_g \tag{5.10}$$

with A_q as the surface of the blanked part and q_g a specific opposing force whose value can range between $q_g = 20$ N/mm^2 for thin parts with a small area and $q_g = 70$ N/mm^2 for thick parts with a large area.

5.2.1.9 Required Cutting Force

The following factors are distinguished in cutting operations in the context of influences on required force:

- cutting force F_S,
- shear resistance k_S,
- shear strength factor c_1.

The load of the punch required for the fine blanking process, i.e., the punch force F_{St}, comprises the cutting force F_S necessary for the actual material separation and the opposing force F_G required for clamping the material (Fig. 5.38).

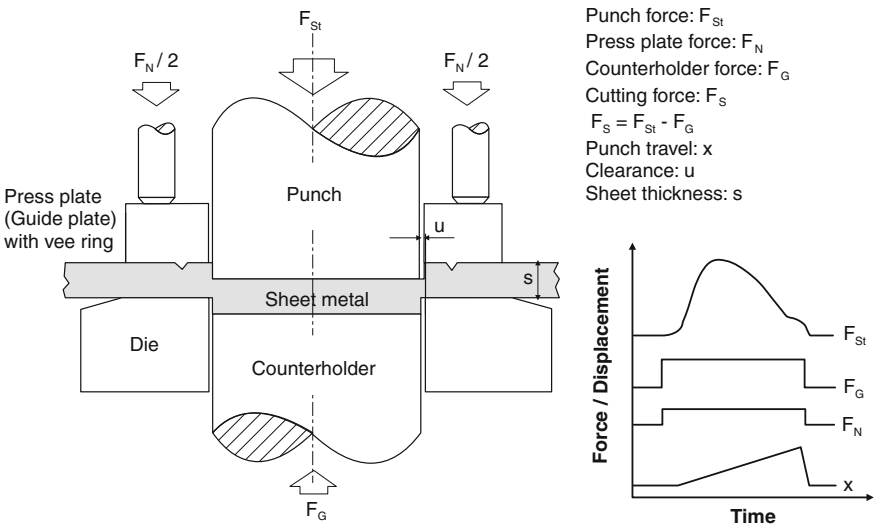


Fig. 5.38 Forces in fine blanking

The cutting force F_S is thus a result of the difference of the punch force F_{St} to be generated and the applied opposing force:

$$F_S = F_{St} - F_G. \tag{5.11}$$

The shear resistance represents the maximum cutting force related to the entire sheared edge. In addition to the force required for forming and material separation, the shear resistance also includes the friction forces between the tool and the workpiece. The shear strength depends on the sheet material.

The shear resistance k_S is calculated from the ratio of maximum cutting power to the shearing area:

$$k_S = \frac{F_{S\max}}{A_S} = \frac{F_{S\max}}{l_S \cdot s}. \tag{5.12}$$

The ultimate shear strength c_1 represents the ratio of shear resistance k_S to tensile strength R_m:

$$c_1 = \frac{k_S}{R_m}. \tag{5.13}$$

According to [BIRZ97], the cutting force is determined with the following formula:

$$F_S = l_g \cdot s \cdot \tau_S = c_1 \cdot l_g \cdot s \cdot R_m. \tag{5.14}$$

The variables in the formula refer to:

- the sum of the cutting line lengths (l_g),
- the material thickness (s),
- the ultimate shear strength (τ_S),
- a factor based on ratio of the limit of elasticity (c_1),
- the tensile strength of the material (R_m).

According to [HAAC79], the factor c_1 is specified as $0.6 < c_1 < 0.9$. The factor increases with a rising ratio of the limit of elasticity R_p/R_m.

In addition to the length of the cutting line, sheet thickness and material properties, other factors which can influence the cutting force are the geometrical form of the workpiece, the size of the shearing gap, the form of the cutting edges of the punch and the cutting die, the surface condition or coating of the cutting elements, as well as lubrication. Since no one has been able as yet to specify the extent of these influences exactly, it is recommendable for safety reasons to assume the factor $c_1 = 0.9$ to calculate the cutting force [HAAC79].

FE methods can also be used to determine the required cutting force. It also allows for the determination of stresses and strains both in the tool and in the workpiece [KLOC02a, KLOC03c] (cf. also Sect. 2.5.11.1).

5.2.1.10 Friction and Lubrication

The main source of tool wear is friction, which is found predominantly in the areas of interaction between the punch or the cutting die and the workpiece material. Since this tool wear results in bad workpiece quality and can also lead to tool breakage, one must guarantee through the use of suitable lubricants that the oxidation, abrasion and adhesion wear is reduced to a minimum. It should be borne in mind, however, that today tool materials and above all tool coatings have an equally high importance for wear protection (see Sect. 2.8.5.3).

Besides

- lubricity
- pressure and temperature resistance
- wettability
- viscosity or applicability (spraying, rolling)

one must also consider environmental and skin compatibility when selecting a lubricant. Equally as important is good corrosion protection, washability (or residue-free use) as well as the compatibility of the lubricant with possible downstream processes, such as welding, bonding or lacquering.

Due to the required lubricant properties, the extremely narrow shearing gap and the demand after fine blanking for a simplest-possible parts cleaning, oils are used almost exclusively.

Because of high pressure and temperature strains, the oils employed contain extreme pressure and passive extreme pressure additives (EP and PEP additives) (see Sect. 2.8.4.4). These additives form a physical or chemical protective film on the surfaces of the friction partners. In this way, they prevent partial weldings and reduce abrasive wear, friction and heat generation. This increases the precision of the parts and the tool life. In the past, chlorine compounds (chlorinated paraffins) were mainly used as EP additives. These have been largely replaced by formulas made from sulphur and phosphorus compounds (EP additives) and by esters (polar parts) and over-based sulphonates (PEP additives). As a rule, the formulations prepared today contain little ($\ll$50 %) or no mineral oils. However, since the chlorine additives are the most efficient EP additives, the search for alternatives remains a current topic [SCHU04a]. They have been indispensable up to now for the most difficult fine blanking operations, such as cutting thick high-grade metal sheets.

The viscosity of fine blanking oils ranges between 100 and 250 cSt and is selected at a value which is high in proportion to the estimated difficulty of the respective cutting operation. The viscosity is limited by applicability. The lubricant is applied to the sheet by spraying or rolling. In the case of a spraying application, the oil drops must run together to form a thick film so that it can act along the entire cutting line. This is often difficult when the smallest quantities of oil (lubricant film thicknesses) with high viscosities are to be applied [MANG83]. This endows importance to the wettability of the lubricant. It is determined through the polar surface energies of the lubricant fluid and the material surface [BOBZ00].

However, not only the properties of the lubricant influence the work result, but also the quantity. While there must be enough of the lubricant available so as to supply the surfaces in contact with the layer-forming additives, the lubricant oil layer may not be too thick, as this could lead to the formation of a pressure pad in the area enclosing the knife-edged ring. This pressure pad causes a deflection of the blanked part and prevents the complete penetration of the knife-edged ring. Also, a sparing use of fine blanking oils is advantageous in view of the considerable costs of high additive contents.

The quantity of lubricant required is thus applied when possible along the contours of the parts at the exact places on the blank or in the tool where it is really needed. This process is entirely free of oil mist. Since the lubricant is applied exclusively along the part contours, both the pressing waste and the lead frame remain largely free of lubricant. This greatly reduces the work required for parts degreasing and lowers disposal costs. Impairments with respect to operators or the environment are excluded [HIPT03].

5.2.1.11 Economic Efficiency

The result of the fine blanking process must be seen from both technological and economical points of view. The quality of the workpiece is the most important technological consideration. The economic efficiency of the result is influenced mainly by tool wear. In this regard, both the workpiece quantity manufactured between two sharpening operations applied to the active elements and the total die life is decisive. A further main criterion for an economically viable operation is the amount of material used. In order to minimize material usage, CAD-supported software is used which guarantees an optimal parts nesting in the sheet strip. Furthermore, process reliability is crucial when selecting a suitable manufacturing process. Fine blanking is a highly process-reliable operation which allows for the achievement of an overall process availability of over 95 % given optimized production.

5.2.2 Tools

The construction design, the machining type and the tool material type determine the workpiece quality and the tool costs, and these in turn have a decisive influence on the required costs when seen in connection with tool wear and batch size/quantity.

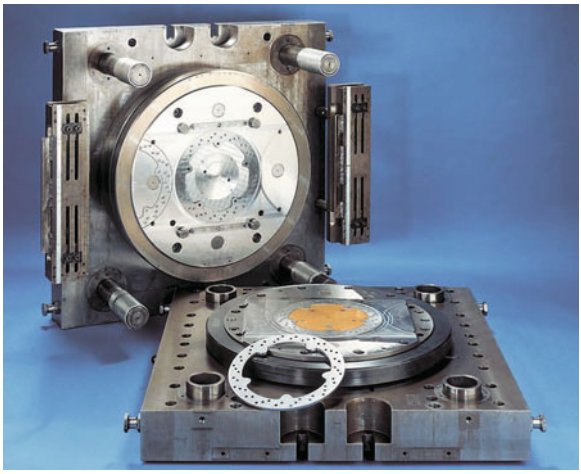


Fig. 5.39 Fine blanking with a blanking and piercing tool (*Source* Feintool AG)

5.2.2.1 Tool Types

In both fine blanking and conventional cutting, one distinguishes with respect to modes of operation between:

- blanking and piercing tools,
- progressive tools and,
- progressive compound tools.

In blanking and piercing tools, workpieces are fine-blanked in a single strike, with the outer and inner contours generated at the same time. The burrs of the inner and outer shapes lie on the same side (Fig. 5.36). Provided that the tool exhibits the appropriate level of precision, the workpieces which are manufactured in a blanking and piercing tool are characterized by high dimensional and form accuracies and by high flatness. Figure 5.39 shows a blanking and piercing tool for manufacturing a brake disc for a motorcycle.

In progressive tools, the manufacturing process is broken up into several sequential cutting steps. A prepunching of the sheet strip is always required at the beginning of the process to allow for the exact positioning of the sheet strip in the tool (see Sect. 5.1.2.3, p. 466). The burrs on the inner and outer shapes lie opposite each other (Fig. 5.40). Since prepunching and blanking are performed in sequence and certain feed tolerances occur in spite of positioning pins, fine-blanked parts produced in progressive blanking cannot have as close tolerances as in a blanking and piercing tool. The tool shown in Fig. 5.40 is a progressive tool for manufacturing a plate for an automatic transmission. In the first step, the plate is blanked and then, in a second step, positioned diagonally to the feed direction of the sheet.

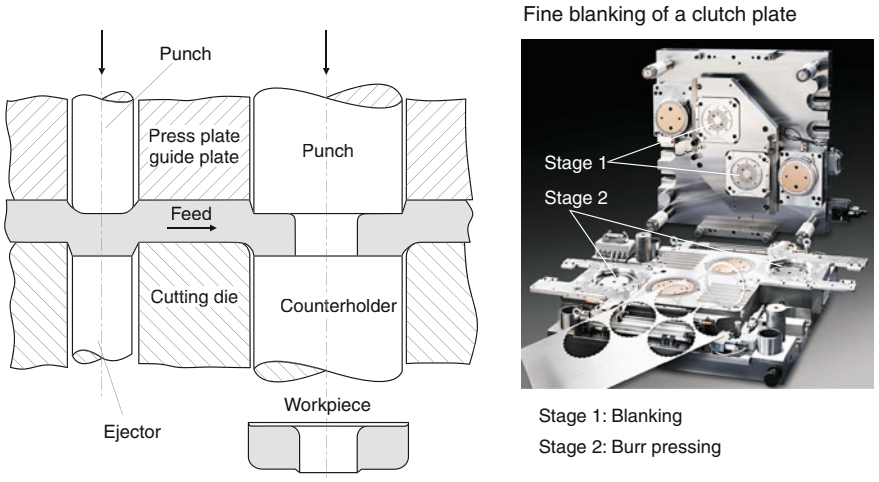


Fig. 5.40 Fine blanking with a progressive tool; *right*—progressive tool with integrated part transfer and burr pressing (*Source* Feintool AG)

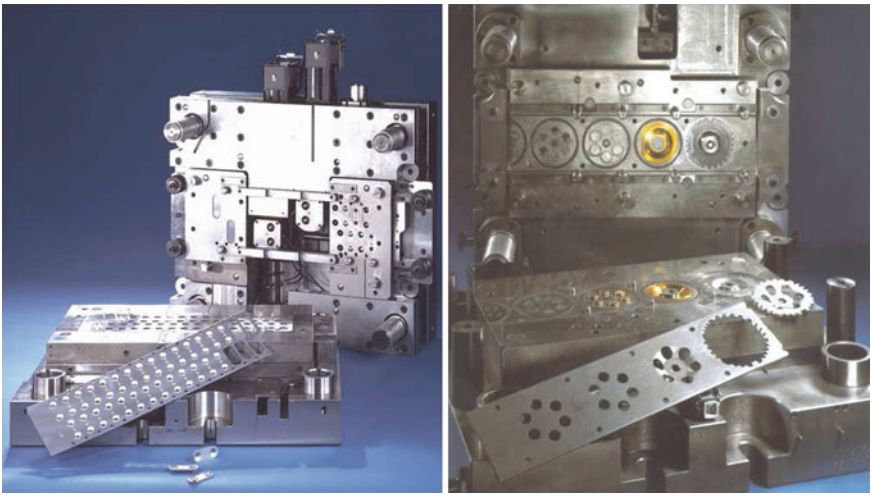


Fig. 5.41 Fine blanking with a progressive compound tool; *left*—progressive compound tool with integrated thread-forming unit; *right*—manufacture of a gear in four steps (*Source* Feintool AG)

The burr is then completely pressed in this step. The plates are ready for installing with no additional reworking.

The same applies to progressive compound tools. In these tools, not only are cutting operations performed according to the concept of progressive blanking, but also forming operations such as bending, coining and upsetting, which are executed in a second or third step. Figure 5.41 shows two progressive compound

tools. The left side shows a tool with an integrated thread-forming unit. In the second to last step, the thread is introduced in a rolling operation and then the component is blanked in the final step. The right side of Fig. 5.41 shows a progressive compound tool for manufacturing a gear in four steps.

Especially important with respect to progressive compound tools are both the exact manufacture of the tool elements and the tool guidance.

In order to guarantee an exact positioning of the punch even when the cutting or forming process is underway, so-called locking bolts and supporting strips are mounted in addition to the column guides. The locking bolts are submerged into the cutting die, absorbing transverse forces which arise when the cutting contour is irregular. Supporting strips prevent the tool from tipping, which can happen particularly at the beginning and end of the strip.

With large workpiece quantities, it is worthwhile to employ complicated at therefore highly costly multiple progressive compound tools. Their active elements must be manufactured with particular care in order to minimize wear and thus achieve a long tool life. In small batch production, one would tend to select a somewhat simpler tool, accepting the possible need for additional production steps [HASH84].

5.2.3 Materials

Materials suitable for fine blanking are all metallic materials which can also be easily cold-formed. Those of greatest interest to industry are the broad range of steels, comprising about 90 % of fine-blanked parts, as well as the NE metals aluminium and copper with their alloys.

5.2.3.1 Steels

Steels comprise the majority of the materials processed in fine blanking. They are processed as strip material or from coil in fine blanking machines. The use of strip material is advantageous because of the comparatively lower amount of defects in the fine-blanked parts, while working from coil allows for a higher production rate. The diverse steels are available today in the form of hot-rolled strip, cold-rolled strip and flat steel [BIRZ76, KÖNI82a, STRA82]. Raw materials are chosen on the basis of the required properties and ultimately economic considerations. The quality characteristics of the raw material is determined above all through

- mechanical and metallographic material properties,
- surface quality,
- dimensional and form tolerances.

Table 5.1 Fine-blankable steels [BIRZ99]

Group of materials	Numerical alloy designation (former designation)	Material number	DIN standard
Soft, unalloyed steels	DD13 (StW24)	1.0335	DIN EN 10111
	DC04 (St4/St14)	1.0338	DIN EN 10130
	S235J2G3 (St37-3)	1.0116	DIN EN 10025
	S275JO (St44-3)	1.0143	DIN EN 10025
Fine-grained structural steels	S420MC (QStE420 TM)	1.0980	DIN EN 10149-2
	S500MC (QStE500 TM)	1.0984	DIN EN 10149-2
	H240 (ZStE260)	1.0480	–
	H360 (ZStE380)	1.0550	–
	H400 (ZStE420)	1.0556	–
Case hardening steels	C10E (C10)	1.1121	DIN EN 10084
	C15E (C15)	1.1141	DIN EN 10084
	16MnCr5 (16MnCr5)	1.7131	DIN EN 10084
Quenched and tempered steels	C35E (Ck35)	1.1181	DIN EN 10083-1
	C45E (Ck45)	1.1191	DIN EN 10083-1
	42CrMo4 (42CrMo4)	1.7225	DIN EN 10083-1
Nitriding steels	34CrAl6 (34CrAl6)	1.8504	DIN EN 10085
	34CrAlMo5 (34CrAlMo5)	1.8507	DIN EN 10085
Flame and induction hardenable steels	C35G (Cf35)	1.1183	DIN 17212
	C53G (Cf53)	1.1213	DIN 17212
Cold-rolled strips for springs	C67E (Ck67)	1.1231	DIN 17222
	50CrV4 (50CrV4)	1.8159	DIN 17221
Cryogenic steels	11MnNi5-3 (11MnNi5-3)	1.6212	DIN EN 10216-4
	10Ni14 (10Ni14)	1.5637	DIN EN 10216-4
Tool steels	C80U (C80W1)	1.1525	DIN EN ISO 4957
	100Cr6 (100Cr6)	1.3505	DIN EN ISO 683-17
Stainless steels	X6Cr13 (X6Cr13)	1.4000	DIN EN 10088-3
	X5CrNi18-10 (X5CrNi18-10)	1.4301	DIN EN 10088-3
	X2CrNi19-11 (X2CrNi19-11)	1.4306	DIN EN 10088-3

One should find an optimal raw material with respect to quality, price and processing costs for every workpiece which is fine blanked or both fine blanked and formed.

Untreated hot-rolled strip plays a minor role in fine blanking. This is because the hard, adhering scale flakes off during blanking, clogging the shearing gap and causing major tool wear. Pickled hot-rolled strips have properties which allow them to compete with cold-rolled strips, which apply especially to soft-annealed and normalized hot-rolled strips. The advantage of cold-rolled strips, however, lies in the wider range of properties which can be adjusted to individual process steps.

Flat steels no longer play an appreciable role as raw material in Western Europe, the USA and Japan. In fine blanking processing, they have come to be replaced by hot-rolled strip. The variety of flat products with their special properties makes it possible for steels to be fine-blanked whose qualities range from soft deep-drawing steel to high-strength, micro-alloyed fine-grained steel.

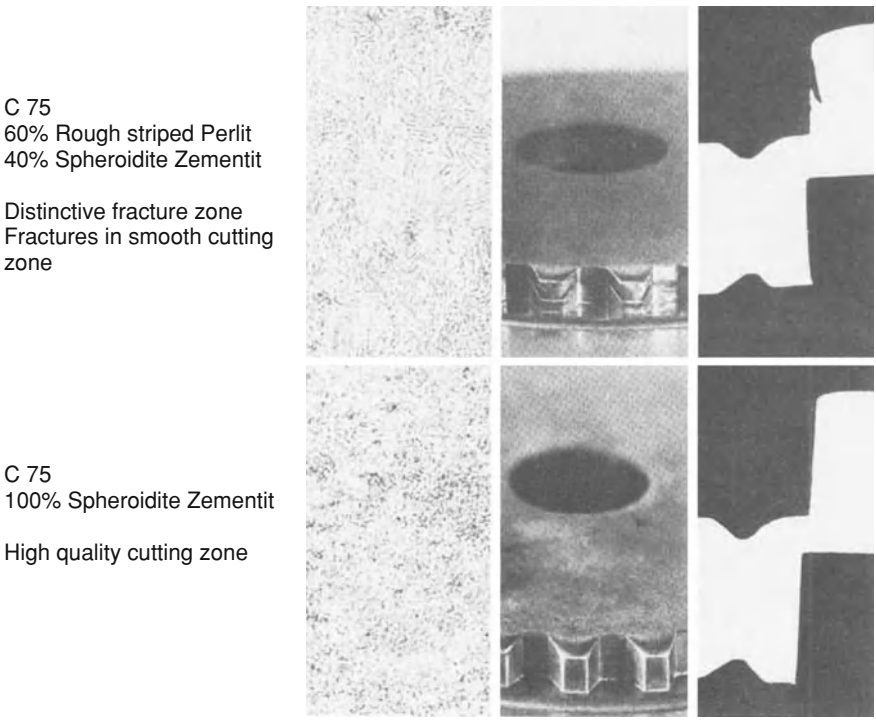


Fig. 5.42 Sheared edge quality with varying workpiece material grain structures (acc. to Kurzhöfer)

Table 5.1 provides a list of the most typical steels used in fine blanking technology.

For fine blanking, properties are required of the material which maximizes its forming potential. The material is assessed on the basis of the following parameters:

- tensile strength,
- limit of elasticity,
- elongation at fracture,
- contraction at fracture,
- hardness,
- degree of moulding, grain size and distribution of carbides,
- ferrite grain size.

As in all cold-forming processes, soft, low-carbon and low-alloy steels can be easily fine-blanked. The strength values of these materials are low, while elongation and contraction at fracture are relatively high. The main metallographic constituent of steels with up to ca. 0.1 % carbon content is ferrite, which is easily formable. The strength of the material rises in proportion to carbon and alloy

Table 5.2 Fine-blankable NE metals

Group of materials	Numerical alloy designation (former designation)	Material number	DIN standard
Non-age-hardenable aluminium-magnesium alloys	EN AW-3004 (AlMn1Mg1)	3.0526	DIN EN 584-2
	EN AW-5754 (AlMg3)	3.3535	DIN EN 584-2
	EN AW-5086 (AlMg4Mn)	3.3545	DIN EN 584-2
Cold- and warm-curable aluminium alloys	EN AW-6082 (AlMgSi1)	3.2315	DIN EN 584-2
	EN AW-6061 (AlMg1SiCu)	3.3211	DIN EN 584-2
	EN AW-2017A (AlCuMg1)	3.1325	DIN EN 584-2
Wrought copper alloys	Cu-DLP (SW-Cu)	2.0076	DIN EN 1652
	Cu-DHP (SF-Cu)	2.0090	DIN EN 1652
Copper-zinc alloys (brass types)	CuZn10 (CuZn10)	2.0230	DIN EN 1652
	(CuZn28)	2.0261	DIN EN 1652
	CuZn37 (CuZn37)	2.0321	DIN EN 1652
Copper–tin alloys (tin bronze types)	CuSn4 (CuSn4)	2.1016	DIN EN 1652
	CuSn6 (CuSn6)	2.1020	DIN EN 1652
Copper-nickel-zinc alloys (nickel silver types)	CuNi12Zn24 (CuNi12Zn24)	2.0730	DIN EN 1652
	CuNi25 (CuNi25)	2.0830	DIN EN 1652
Copper–aluminium alloys (aluminium bronze types)	(CuAl8)	2.0920	DIN EN 1652
Copper-beryllium alloys (hardenable)	(CuBe1,7)	2.1245	DIN EN 1652
	CuNi2Be (CuNi2Be)	2.0850	DIN EN 1652

content, while the pearlite content additionally present in the grain structure increases, debasing the fine blanking properties along with the carbides.

Materials with higher carbon and alloy content must therefore be soft-annealed prior to forming and fine blanking, as lamellar cementite and carbides are hard to fine blank. These metallographic constituents are too brittle and cause ruptures on the sheared edge [BECK73, BIRZ74, BIRZ76, HAAC79, SING76, VDI94]. Figure 5.42 shows examples of such ruptures.

As a rule, workpieces made from soft-annealed steel must be subjected to a heat treatment after fine blanking if the component is to satisfy certain strength requirements. The same applies to hard marginal zones, which are surface-hardened by means of nitriding, cementing or carbonitriding.

As opposed to higher-strength carbon and heat-treatable steels which are and difficult to fine-blank and whose strength increases with increasing carbon/alloy content, high-strength micro-alloyed fine-grained structural steels are well suited to fine blanking [BIRZ78, KÖNI82a, STRA82].

5.2.3.2 NE Metals

The fine blanking capacity of NE metals and their alloys depend largely on their chemical composition, the cold-rolling degree of the sheet material and the degree of age hardening. Pure aluminium and pure copper are good for fine blanking, and

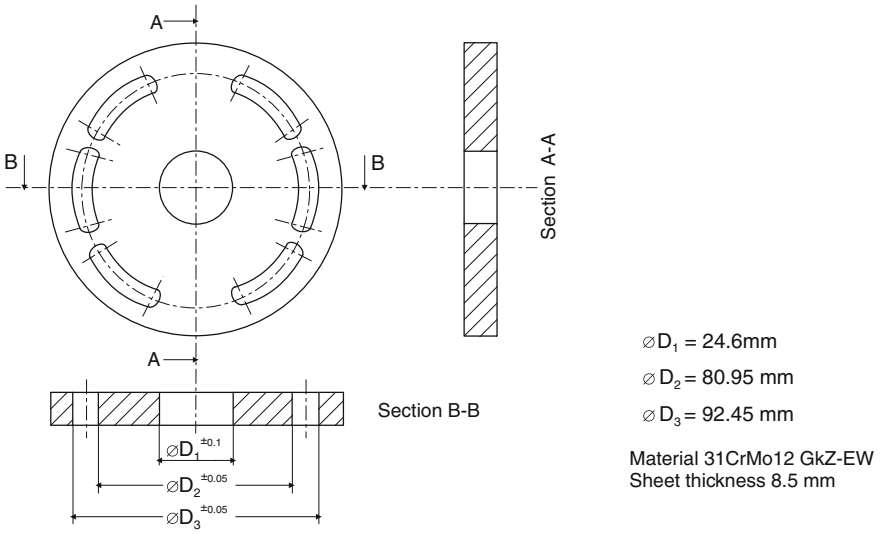


Fig. 5.43 Fine-blanked control plate manufactured in a blanking and piercing tool (*Source* Feintool AG)

the same applies to non-age-hardenable aluminium-magnesium alloys, such as AlMg1 and AlMg3, whose stretch values in the soft state amount to at least 17 % [HAAC79]. The same applies to copper-zinc alloys (brass types) with up to ca. 30 % zinc content, as they are still relatively soft. Table 5.2 provides an overview of typical fine blanking NE metals.

The fine blanking capacity decreases with increasing zinc content. The brass types CuZn37 and CuZn40 are typical in this regard. When the zinc content is even higher, the amount of brittle phases becomes so large that ruptures and torn-off parts are inevitable.

One can generally note that the fine blanking capacity is degraded in proportion to the material strength. In this respect, it is unimportant whether the increase in strength is due to mixed crystal hardening or cold-rolling (dislocation hardening). Highly age-hardenable aluminium alloys are also difficult to fine blank, or at any rate not without rupture formation.

5.2.4 Process Variants and Manufacturing Examples

The palette of products made by fine blanking range from very small, thin parts as used in the camera and electronic industries to large-area workpieces with a sheet thickness of 16 mm employed in the automotive industry and in agricultural machinery.

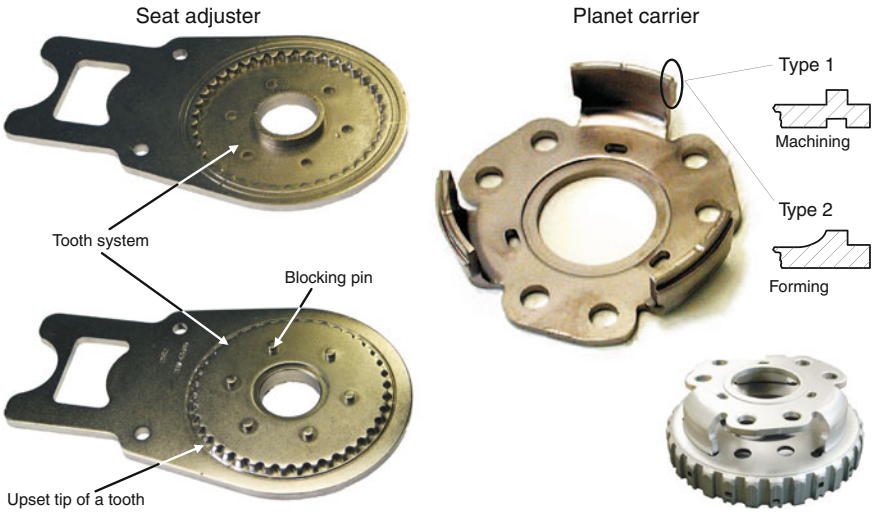


Fig. 5.44 Planet carrier and seat adjustment (*Source* Feintool AG)

Figures 5.43, 5.44 and 5.45 show examples of parts used in different industrial branches. Manufacturing can be performed in a blanking and piercing tool, in a progressive tool, or by means of a combination of fine blanking and forming processes like coining, bending and upsetting. The control plate shown in Fig. 5.43 is manufactured in a blanking and piercing tool.

Although the control plate for a hydraulic pump was originally manufactured purely by machining, fine blanking has proved to be more economically viable, since all the required tolerances and properties can be achieved through this process.

The degree of difficulty of a fine blanking operation is determined by a dimensional tolerance of ±0.05 mm, high material strength on the finished part and a very small ratio of slit width to sheet thickness (see also Fig. 5.35). The slits fixed in kidney-shaped fashion in the disc must have narrow tolerance in order to precisely control the oil flow regulated via turning the disc. Furthermore, the part must continue to be perfectly even on all surfaces, exhibit low surface roughness and resist abrasion.

The control plate is fine-blanked from an 8.5 mm thick strip, deburred and subsequently surface-hardened. All fine-blanked surfaces have 100 % straight cut, and the surface roughness generally amounts to $R_z < 1$ µm.

The combination of forming and fine blanking endows even greater importance to the material selection, since normally the material must first be formed and thus strain-hardened and subsequently fine-blanked. A further difficulty arises due to the different process steps, e.g., cutting, coining, bending or extrusion, which can be performed during the process at different points in time. The working speed must be adjusted to each individual process step so as to optimize the quality of the



Fig. 5.45 Shifting gate (*Source* Feintool AG)

finished parts and the tool life. Modern control systems allow for the working speed to be adjusted exactly to these requirements [HIPT03].

Figure 5.44 shows extreme material deformation on the example of a planet carrier and a seat adjustment manufactured by means of forming and fine blanking operations.

The geometric shape of the planet carrier and the strength properties it requires make it complicated to manufacture. Although not only its very low dimensional tolerances but also the required workpiece geometries speak for a combined forming and machining operation (variant 1), a pure forming and fine blanking operation was able to be developed in the form of a "reverse engineering" process (variant 2), so that the planet carrier is now manufactured ready-to-install in a progressive compound tool with no machining. This has led to a considerable savings for this component.

Seat adjustment mechanisms consist almost entirely of fine-blanked components. Rising requirements on adjusting comfort, safety and standardized, small construction volumes place new demands on tool and production technology. The manufacture of the seat adjustment shown in Fig. 5.44 involves embossing a gear and different locking pins. Since the gear is embossed through the entire sheet thickness, the tooth heads are additionally bulged on the non-functional side. By this means, the component receives increased torsion stiffness while maintaining minimal sheet thickness. The central bore is produced in a combined forming and fine blanking operation. This guarantees a higher perpendicularity between the seat adjustment and the shaft slid into the bore.

Due to narrow form and position tolerances and to the complicated, costly tool technology, combining the processes of fine blanking, forming and bending can entail some disadvantages (Fig. 5.45).

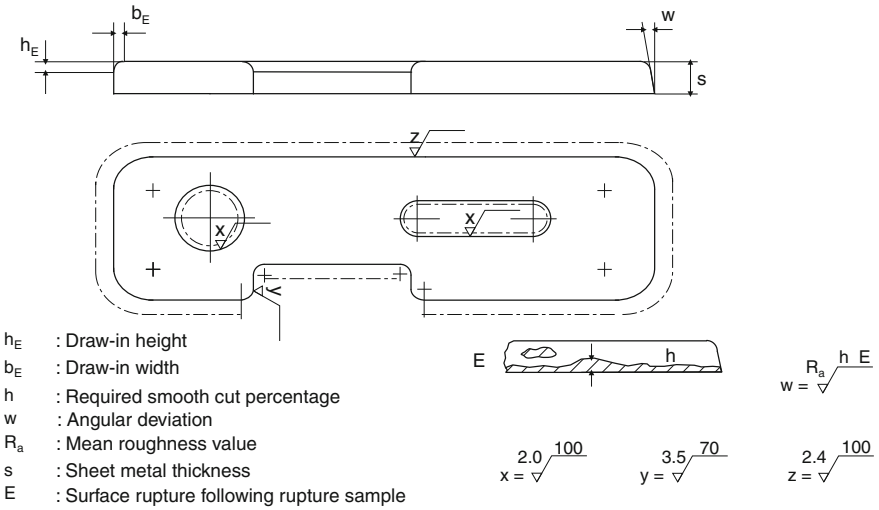


Fig. 5.46 Dimensioning of fine-blanked parts

The originally planned variant mad use of bent fins that failed to fulfil the form and position tolerances. For this reason the shifting gate is now manufactured from multiple individual parts which are joined by laser welding. The two side parts and the carrier are manufactured in a blanking and piercing tool, while the shifting gate is produced in a progressive tool due to its curvature. The substitution of a bending operation successfully reduced the number of operation steps, shortening the processing time by 40 %. It also allowed for a savings of ca. 50 %.

5.2.5 Manufacturing Accuracy and Component Properties

In addition to the commonly accepted construction dimensioning, the sheared edge is dimensioned according to VDI guideline 2906-5, as in the diagram shown in Fig. 5.46 [VDI94].

In addition to fully smooth blanked edges, one also makes the distinction between those with ruptures or torn-off parts, with the sheared edge quality being expressed by a symbol containing the maximum permissible mean roughness value R_a as well as the minimum proportion of clean-cut surface h_s/s expressed as a percent of the sheet thickness s in the case of torn-off parts. In order to determine the sheared edge quality more easily, one can take recourse to a surface reference standard. This contains examples of different clean-cut sections with ruptures and torn-off parts and also provides four qualitatively different rupture forms and six different surface profiles with surface roughness values ranging from $R_a = 0.2$ µm to $R_a = 3.8$ µm.

Table 5.3 Dimensional tolerances for fine-blanked parts

Material thickness (mm)	Tensile strength up to 500 MPa			Tensile strength above 500 MPa		
	Inner forms ISO-quality	Outer forms ISO-quality	Distance between holes (mm)	Inner forms ISO-quality	Outer forms ISO-quality	Distance between holes (mm)
0.5–1	6–7	7	±0.01	7	8	±0.01
1–2	7	7	±0.015	7–8	8	±0.015
2–3	7	7	±0.02	8	8	±0.02
3–4	7	8	±0.02	8	9	±0.02
4–5	7–8	8	±0.03	8	9	±0.03
5–6	8	9	±0.03	8–9	9	±0.03
6–	8–9	9	±0.03	9	9	±0.03

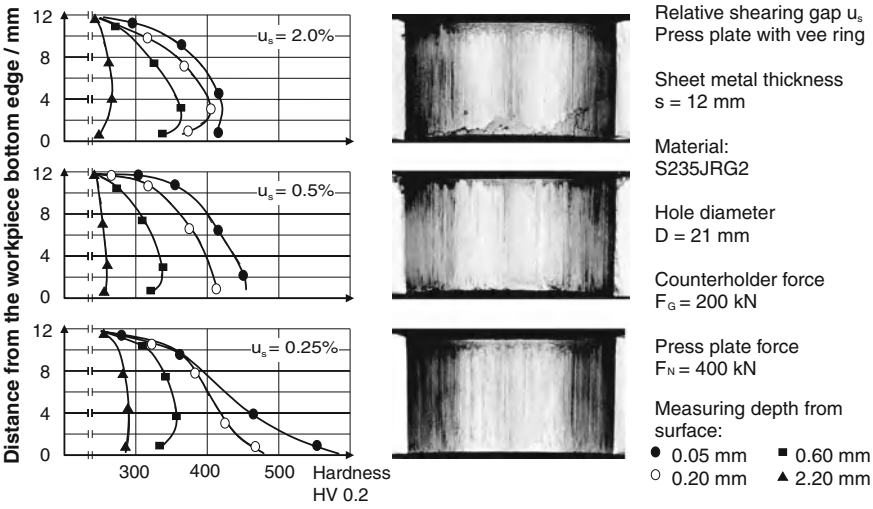


Fig. 5.47 Sheared edge quality and the condition of the marginal zones of fine-blanked holes as a function of the shearing gap

Typical characteristics of fine-blanked parts are edge deformation and burr formation. Edge deformation is a function of the geometrical form of the blanked part. While the edge deformation height increases with a decreasing edge radius and an increasing sheet thickness, it is reduced through higher material strength. The edge deformation height can reach an extent of ca. 20 % of the sheet thickness and the edge deformation width ca. 30 % of the sheet thickness.

Burr size, on the other hand, is entirely dependent on the material quality and the condition of the cutting edges. The softer the material is and the more worn the tool edges are, the greater the burr formations. These must be removed by a suitable process, e.g., belt grinding, barrel finishing or an electrochemical process. Since these procedures constitute an additional working step and as such entail no

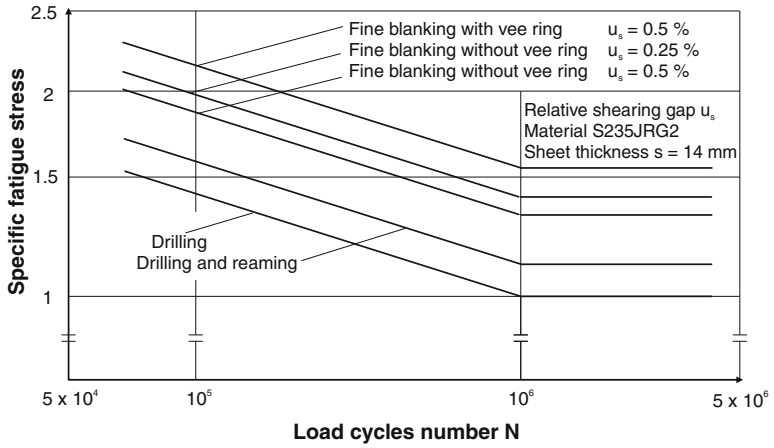


Fig. 5.48 Wöhler diagram for bored samples produced by fine blanking and machining [FRIT83]

small additional costs, the company Feintool has developed the method of "burr pressing". In this working step, the burr is completely pressed and thus removed without leaving residues. The operation is highly process-reliable, rendering any post-processing steps unnecessary, which means that the part is ready to install [HIPT03].

The dimensional tolerances of fine-blanked parts lie in the range of a hundredth millimetre. Table 5.3 lists tolerances for outer and inner forms [HAAC79, SCHW87].

Since fine-blanked surfaces are made by plastic material flow, a strain hardening of the marginal zone appears with an increasing cutting path. Principle differences in hardness are made apparent via hole walls cut with shearing gaps of varying size which are perfectly smooth on the one hand and have torn-off parts on the other. Figure 5.47 shows the appearance of the hole walls and the hardness progression in the marginal zones.

In addition to its function as wear-retarding layer, the strain hardening of the marginal zones also has a positive effect on the component behaviour of the workpieces. Studies of the fatigue limit of internally bored flat bars have shown that the fine blanking process is superior to conventional machining processes with respect to the fatigue limit [KÖNI82b]. The fatigue limit values of fine-blanked samples lie above the values of the machined samples (Fig. 5.48).

A friction operation performed after drilling causes an increase in the fatigue strength, though these values are also lower than those of fine-blanked samples. A small shearing gap of $u_s = 0.25$ % relative to the shearing gap causes an increase in the fatigue limit in comparison to a shearing gap of $u_s = 0.5$ %. What is striking is that, against expectations, the notch impressed by the knife-edged ring concentrically around the hole positively influences the fatigue limit.

Modern materials technology has made it possible today to produce steels, even high-strength steels, with strength values of up to 900 MPa with a very good fine blanking quality. Micro-alloyed fine-grained steels render a heat treatment for increasing hardness and strength, such as is unavoidable in the case of low-strength steels, superfluous. In combination with the strain-hardening caused by the fine blanking and forming process, the strength of these steels is sufficient for the achievement of the required component strength. This completely eliminates the considerable costs of heat treatment.

Chapter 6
Joining by Forming

6.1 Punch Riveting and Clinching

By means of punch riveting and clinching, local punctiform joints can be made between two and even multiple thin-walled components. The processes differ from traditional riveting inasmuch as neither require the premiering of the parts to be joined, which is advantageous in terms of both cost and time. Both processes are described in DIN 8593-5 [DIN03 m] as local forming methods by means of which sheets, pipe parts and profile parts are joined with and without auxiliary elements.

The methods differ insofar as punch riveting requires an additional joining element, referred to as a punch rivet. In clinching, no additional element is required. Joining takes place solely on the basis of the workpiece material. The higher cost of punch riveting is justified largely by the fact that it can generally absorb higher static and dynamic pressures than joints produced by clinching. The following will discuss both methods as well as the joint strength values that can be achieved with them.

6.1.1 Punch Riveting

Punch riveting essentially makes use of two different rivet types, by means of which two very different rivet joints can be created respectively. To produce the joint, either stationary or mobile hydraulic joining equipment is implemented which must exhibit high rigidity. The rivets are fed to the stamping tool by means of different conveyance concepts. Punch rivets are basically categorized as either belted or loose. This distinction is based on whether they are fed by means of the belt feed directly attached to the rivet system or by means of vibratory conveyors with subsequent singularization. The punch rivet materials used must be harder than the parts to be joined. Materials generally used are steel, high-grade steel, copper and aluminium with different surface coatings. The advantages and disadvantages of both punch rivet joints with solid and semi-hollow rivets will be discussed in the following.

F. Klocke, *Manufacturing Processes 4*, RWTHedition,
DOI: 10.1007/978-3-642-36772-4_6, © Springer-Verlag Berlin Heidelberg 2013

6.1.1.1 Punch Riveting with Solid Rivets

In punch riveting with solid rivets, the joining point of the components to be joined are positioned on the die (Fig. 6.1). The upper part of the riveting unit, which consists of a blank holder and a riveting die, moves onto the sheets to be joined. Simultaneously, the rivet is automatically fed and positioned below the riveting die. First, the spring-loaded blank holder comes into contact with the sheets, by means of which these are tightened and fixed between the die and the blank holder (Pos. 1)

Then the rivet is punched through the joining parts via the riveting die (Pos. 2). The punching operation is complete when the rivet head ends flush with the sheet surface (Pos. 3). The blank holder is subsequently lowered in a defined manner, which causes a compression of the sheets between the blank holder and a raised, annular step of the die. The material reacts to this compression with a transverse elongation, as a result of which especially the die-side sheet material is plastically deformed into the annular groove of the solid rivet (Pos. 4). The joining process is over when the joining tools are raised. The joint exhibits a form lock due to the undercut and a friction lock due to the remaining compressive stresses within the joint. The rivet itself is not subjected to a plastic deformation.

6.1.1.2 Punch Riveting with Semi-Hollow Rivets

Punch riveting with semi-hollow rivets differs from that with solid rivets particularly through the circumstances that a semi-hollow rivet is selectively plastically deformed and that the die-side sheet material is only formed, not blanked (Fig. 6.2) [HAHN96].

First, the joining point is positioned over the die. When the upper part of the riveting unit, also consisting of a blank holder and a riveting die, is set, the semi-hollow rivet is fed and the sheets are tightened and fixed between the blank holder and the riveting die (Pos. 1).

As the riveting die is progressively lifted, the material is locally displaced from the sheet plane and attaches itself on the die side to a raised expanding mandrel (Pos. 2), which causes the expansion and compression of the semi-hollow rivet. As a result, the punch-side sheet is punched through and the die-side sheet is

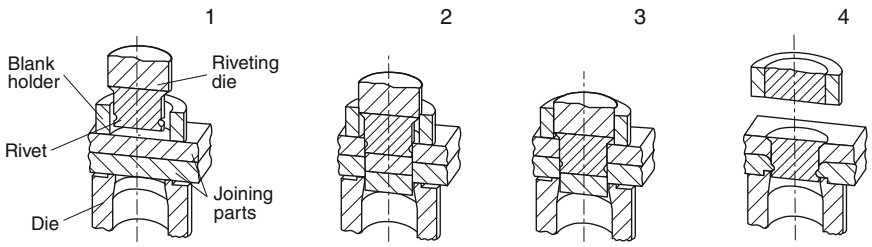


Fig. 6.1 Process steps for punch riveting with solid rivets [HAHN96]

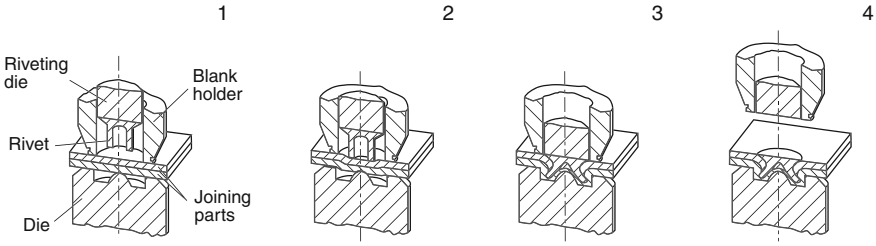


Fig. 6.2 Process steps for punch riveting with semi-hollow rivets [MATT03]

plastically deformed into a closing-head with a collar (Pos. 3) The punched sheet material of the upper sheet remains within the semi-hollow rivet. A gap-free form lock of the joining parts is achieved through the compression of the punch rivet (Pos. 4). Also, a friction lock is introduced into the joint as a result of the axial and radial tensioning of the punch rivet [MATT03].

6.1.2 Clinching

In clinching, joints are created through a common joining in the form of a mechanical clamping of two sheets caused by a local plastic deformation using a punch and a die. The joining force is generally conveyed orthogonally to the component surface via the punch. The material beneath the punch is displaced from the sheet plane and then compressed in such a way that a radial material flow arises from spreading, or a kind of lateral extrusion, and an undercut is formed. A local material separation can be purposively achieved or prevented during the clinching movement. Unlike riveting, the joint requires no auxiliary element, since it is obtained solely by means of component deformation. The joint exhibits an elastic friction lock which is distinguished by its combination of a form lock for transmitting great forces and a friction lock for avoiding backlash.

The method has seen increased employment since the mid-1990s, and a number of process variants have been developed. These may be categorized into one-step and multiple-step processes, respectively with or without cutting. The following will treat one-step cutting and non-cutting processes and will close with a discussion of a two-step clinching process.

6.1.2.1 Clinching with Cutting

In clinching with cutting, the joining element is created as a result of the local effect of a combined cutting and clinching process with subsequent cold-heading. As shown in Fig. 6.3, the punch cuts through the joining parts in the direction of the cutting edge of the punch die (Pos. 2).

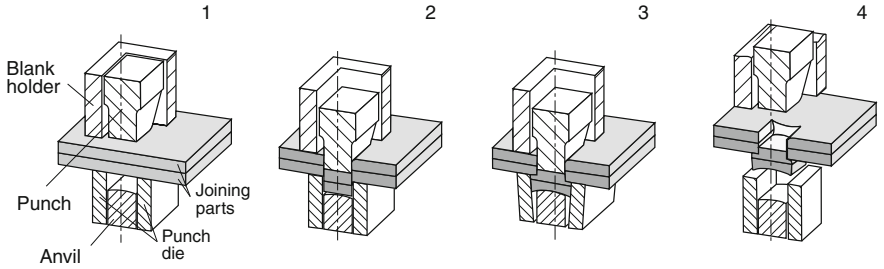


Fig. 6.3 Process steps for clinching with cutting [MATT03]

Outside the pressed-out, ridge-shaped volume range, however, the connection with the original piece remains intact. In the further course of the manufacturing process, the material is pressed against the anvil of the punch die, which is lower. This compression process causes a lateral extension by means of which the joining parts are compressed outwards radially (Pos. 3). This lateral elongation is rendered possible by the expansion of the spring-loaded cutting jaws of the punch die [MATT03].

6.1.2.2 Clinching Without Cutting

Clinching without cutting has been developed over the last 10–15 years on the basis of the cutting clinching method. It indicates the advantage of creating tight and high-strength joints. Similar to cutting clinching, a form- and force-fit joint is created though extrusion in a combined clinching and cold-heading process. No material is cut in this process, however. The process is further subdivided on the basis of the implementation of wither a closed or a split die. In the case of the closed die, the undercut relevant to the form fit is achieved through an annular channel in the die (Fig. 6.4).

The die-side material flows into the die by means of the lateral elongation of the punch-side material, forming an elevated margin. The thus created undercut can be considerably increased by using a split die. Its mobile die segments are displaced

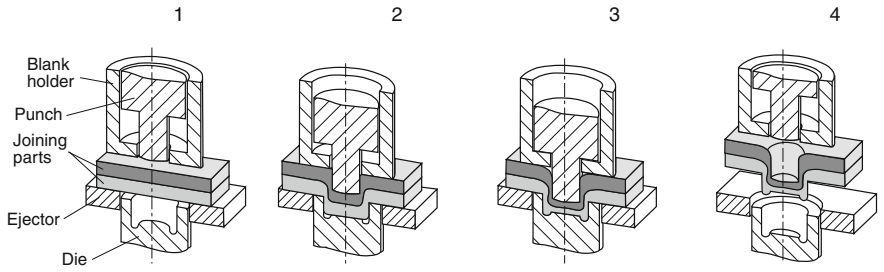


Fig. 6.4 Diagram of the non-cutting clinching process with closed die [MATT03]

radially outwards by means of the lateral elongation, which allows a lateral elongation not only of the punch-side material, but also of the die-side material (Fig. 6.5; Pos. 3).

According to the flow direction, not only an elevation, but also a widening of the margin is achieved, which means that the form fit is more pronounced than in the case of a closed die.

The goal of reducing process forces for clinching has led in recent years to the use of more complex tool kinematics, as a result of which the clinching process has become an incremental forming process. A rotation has been superimposed onto the axial lifting motion of the punch, by which the midpoint of the punch shaft is deflected from the translation axis (Fig. 6.6). The punch shaft midpoint can move in circular orbit around the translation path or on a hypotrochoid path. There is no rotation of the punch about its own central axis. This process is referred to as wobble or radial clinching and, through the reduction of the temporary local

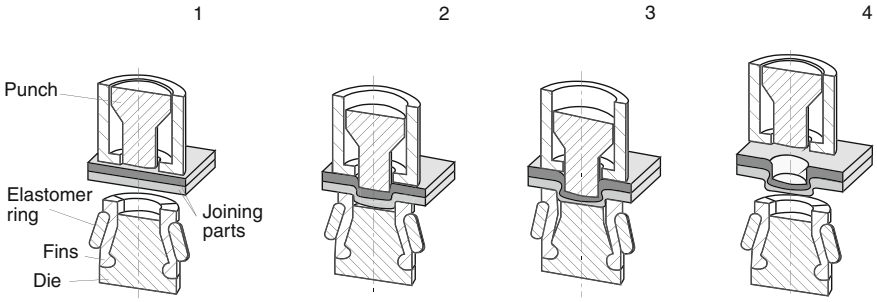


Fig. 6.5 Diagram of the non-cutting clinching process with split die, acc. to Böllhoff

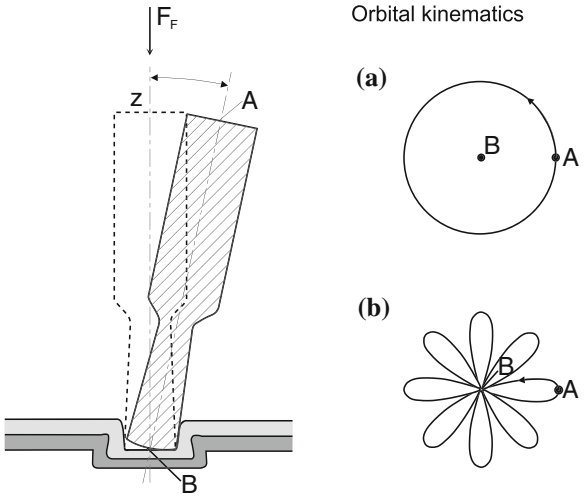


Fig. 6.6 Kinematics of wobble clinching, acc. to [WEST03]

forming zone, enables a reduction of the punch force by about half [WEST03]. In this way, the mass of the clinching system can be reduced or the outreach of the clinching system with C-Frame enlarged. The disadvantages of this process are the more intricate systems engineering and the somewhat longer process time.

6.1.2.3 Multi-Step Clinching

In addition to the one-step processes described above, in which the punch covers the full punch movement in a single operation and is then withdrawn from the joint, there are also multi-step processes. Depending on the technology used, one or more additional process steps may follow in which, for example, the base of the die is moved in the opposite direction of the punch, thus guaranteeing the development of the undercut within the joint. Figure 6.7 illustrates one such multi-step process.

Multi-step clinching is advantageous because it does not necessarily require a blank holder, allows for the use of a tool set for varying sheet thicknesses and requires lower forming forces. These advantages, however, are compensated for by a greater mechanical effort with respect to the joining device.

6.1.2.4 Materials

Different materials with different sheet thicknesses can be joined by means of clinching. What is absolutely required, however, is that they are plastically deformable. In practice, the materials most frequently joined by clinching are steel, aluminium and other non-iron metals with varying surface coatings. Since it is limited entirely to positioning and securing the components, the preparation needed for the joining process is low. For clinching, the joining point must be accessible on both sides. Surface coatings, such as foils or varnishes, must not be removed. However, depending on the process used, there may be a partial destruction or damaging of these surface coatings in the area of the joining connection [BEHR04b].

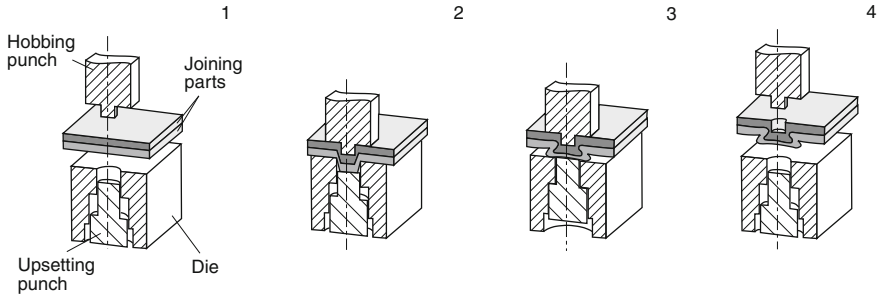


Fig. 6.7 Joining process for two-step clinching without cutting [BUDD95]

6.1.2.5 Joining Equipment

Joining equipment should have high rigidity. In clinching, the forming behaviour of the joining device has a decisive influence on the geometry of the joining element. A frame with insufficient rigidity cannot sufficiently guarantee the proper guidance of the tool set, with an unsymmetrical joining element as the result. For this reason, the devices all exhibit a minimal throat depth or a correspondingly massive frame structure. Devices used to produce the joints may either be mobile hand- or robot-guided, or even stationary devices (Fig. 6.8).

6.1.3 Static and Dynamic Strength

Most joints have the purpose of transmitting forces between their joined parts. For this reason, the following will discuss the static and dynamic strength of clinch and punch-riveted joints. When forming a joint between sheets, it is important to consider the design of the shear or peel loading of the joints. Also, one must distinguish between a static or dynamic strain on the joint. Figure 6.9 illustrates the elastically permissable force of a sheet joint made by punch riveting, clinching and resistance welding for a shear and peel load.

The welded joints can bear significantly higher shear loads. The welding point of the easily weldable sheet made of H320 exhibits the statically most fixed joint. In the case of materials which are difficult to weld, such as aluminium, alternatives are required which exploit the advantages of forming manufacturing processes.

In the case of dynamic stresses, such as those frequently occurring in automobile construction, joints exhibit even higher load capacities than those materially joined by means of welding (Fig. 6.10).

Punch riveting generally leads to higher strength values than clinching. This advantage is offset by additional costs for the joining element and its feeding.

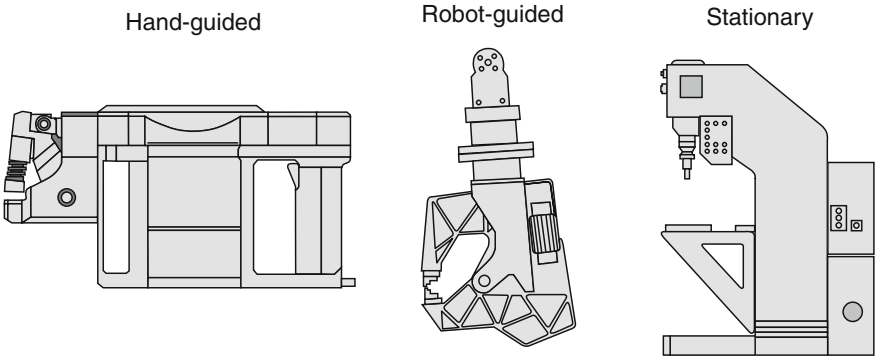


Fig. 6.8 Hand-guided, robot-guided and stationary joining devices

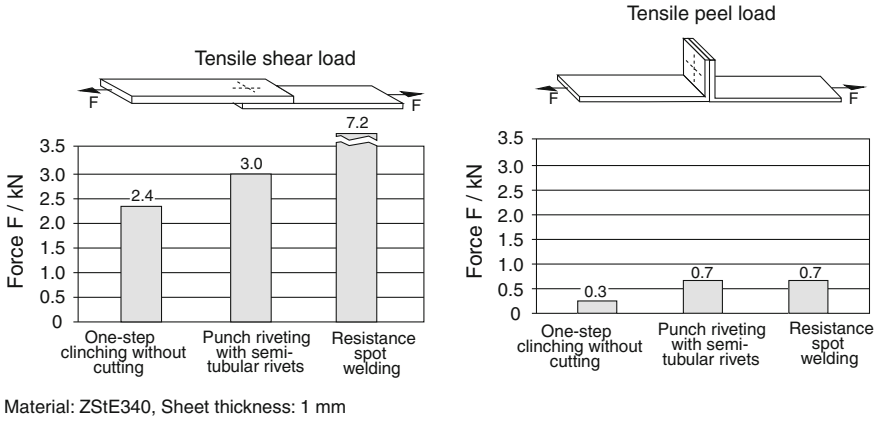


Fig. 6.9 Static rigidity of different joint types [HAHN96]

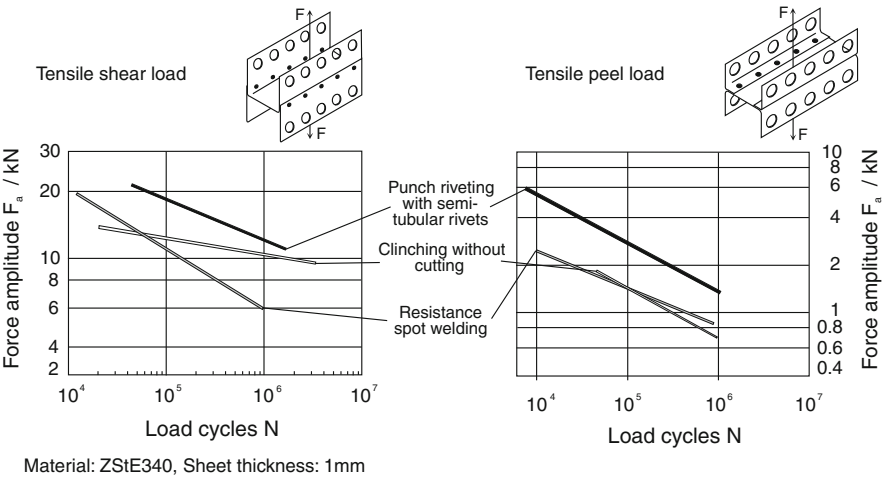


Fig. 6.10 Diagram of the dynamic strength of different binding types

6.2 Flanging and Seaming

According to [VDI79], both the flanging and seaming processes belong to the category of direct joints. Direct joints differ from indirect joints insomuch as the former require no additional joining means.

A direct joint generally desirable because indirect joints both require additional costs for the joining means and prolong the joining time.

In the case of direct joints, joining is achieved by forming one or both joining parts. In addition to the two processes discussed here, others using direct connection include notching, bending, expanding, necking-in, spread forming,

beading, rolling-in, enwinding, twisting, weaving and knotting. All these processes require costly tools which are only economical in serial production. Flanging is used to connect boards and pipes, seaming to connect two boards. In the flanging and seaming processes, the workpiece ends of the sheets to be joined are bent as to create a form-fit. The joints made are generally non-disconnectable. These manufacturing processes are categorized according to [DIN03 m] under the main group 4 "Joining" and further under the group 4.5 "Joining by Forming."

6.2.1 Flanging

The normal definition of joining by flanging (reference number 4.5.2.6) is as follows: "In joining by flanging, one end of a tubular workpiece is joined form-fittingly. Flanges can also be produced together on two joining parts pushed into each other." Flanging is generally understood as the placing of workpiece edges of sheet parts at an angle. If straight edges are flanged, it is purely a bending process. In the case of non-straight edges, an additional tangential compression (convex edges) or stretching (concave edges) occurs.

In joining by flanging, flanges are fixed to either one or both of the workpieces to be joined. Components with flanges and contact faces are formed in such a way that non-disconnectable, fixed connection is created after combining the parts, inserting them into each other and clenching them together. The flanged component must consist of an easily formable material. Such a requirement is not placed on the joining part, which means that it can also be brittle-hard. As a result, glass lenses and ceramic parts can also be joined with flange parts. Forming the joining parts yields a high joining strength. The forming process also leads to a compression of the surface [SPUR86]. The flanging manufacturing process is illustrated in Fig. 6.11.

As a joining process, flanging is predominately used in tank construction. The edge of the tank or that of a tube is partially deformed in such a way that a form-fitting joint is made with another workpiece (e.g. a stiffening edge of a tank). The higher the flange is, the greater the compression/stretching work. In order to prevent a rupture or the formation of folds, flanges should be kept as low as possible [DRAE65].

6.2.2 Seaming

Seaming (reference number 4.5.2.7) is described according to the DIN standard as follows: "Seaming is the process of joining by deformation in such a way that sheet metal parts with prepared ends are placed or pushed into each other and obtain a form fit by folding over the ends" [DIN03 m]. Sheets are thus joined at their margins by being bent, hooked and compressed together.

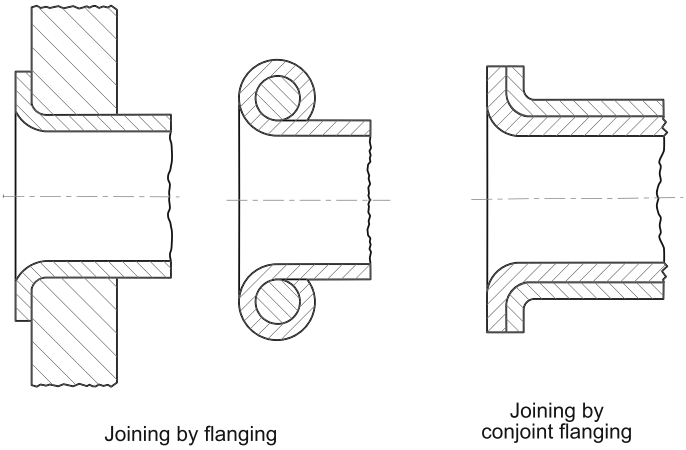


Fig. 6.11 Joining by flanging [DIN03 m]

Seaming is a joining process for sheet metal parts. At least one workpiece must firmly enclose the second by bending. To do this, the ends of the sheet metal parts to be joined are pre-bent, usually by machine (e.g. flanged). After pushing the ends into each other, the seam is compressed. When compressing, relative movements may occur at the joint. These are greater in proportion to how easily the parts hook together. In addition, these displacements lead to hollow spaces within the seam. In combination with a bonding process, a good corrosion protection may be achieved [SPUR86]. Different fold types can be manufactured manually or by machine in accordance with the intended use [BITZ96].

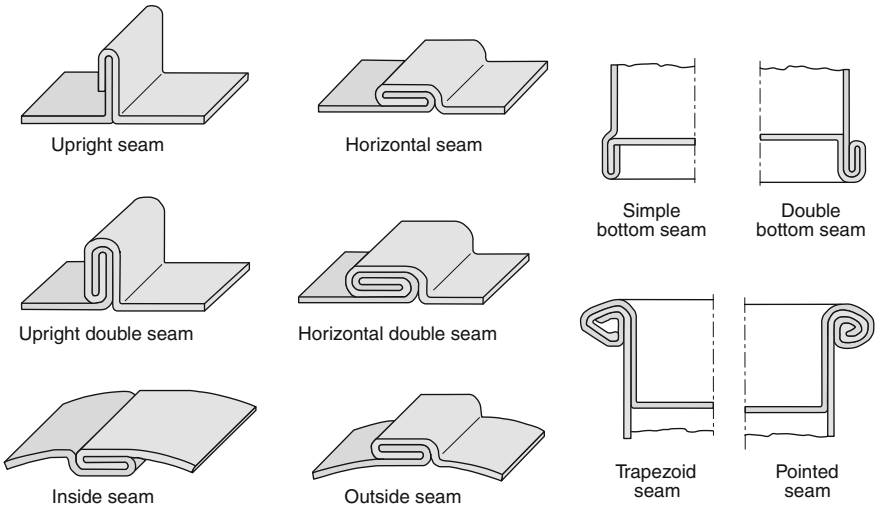


Fig. 6.12 Joining by seaming [RIED03]

The seaming manufacturing process is illustrated in Fig. 6.12.

It should be noted that there are a large number of different fold types used in seaming. Flat seams and bulge seams are employed very broadly. Bulge seams are usually used when seals are to be fixed onto workpiece edges [RIED03].

Seaming is only applicable to materials which retain a high ductility in cold conditions. A suitability test is performed in the form of a folding test [EN01b] and a to-and-fro bending test [ISO00]. In order to achieve a further corrosion protection, zinc-plated or plastic-coated sheet steels are used additionally.

A suitable alternative in the case of an unprotected cutting edge is double seaming, which guards agains the rusting and damage [SPUR86].

6.3 Examples of Use

New materials and construction concepts call for new connecting technologies. Special attention in this regard is being directed to innovative joining technologies. Whereas in the past only welded and blind rivet joints were employed, punch riveting and clinching now enjoy the broadest use (Fig. 6.13).

Given a European demand for beverage cans reaching 38 billion in the year 2003, the tear-open tab of a beverage can is certainly the most well-known component fixed with a clinching point. In this process, a small area of the lid is formed into the tear-open lid and a die by means of a punch in a deep drawing

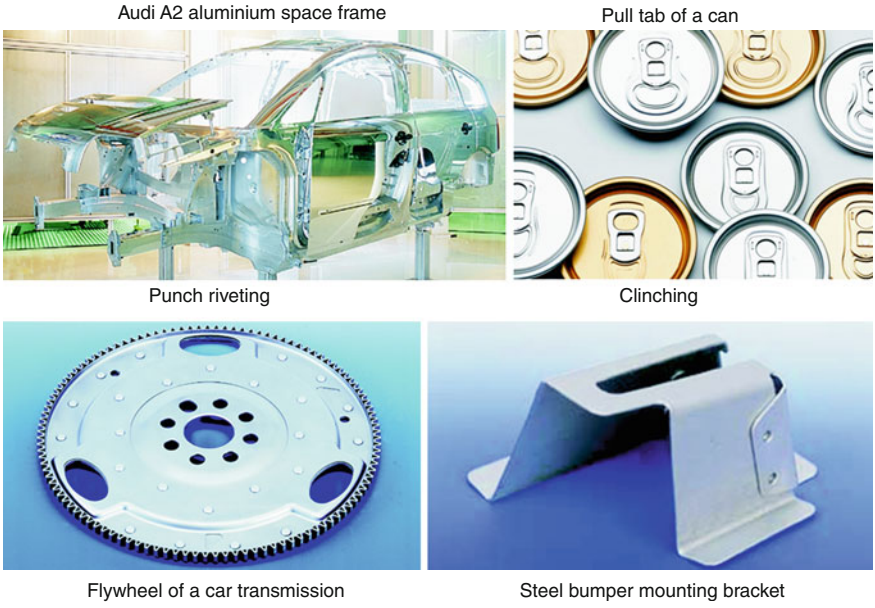


Fig. 6.13 Applications of punch riveting and clinching

process with no preliminary operations. The result is a gas-tight and liquid-tight joint in the form of a non-releasable pushbutton. The surface coatings remain largely intact. After the clinching process is complete, a cylindrical impression is formed on the inside of the lid and a elevation is formed on the tear-open tab. The lid and the beverage can are joined by means of a combined flanging and seaming process. Also, the deep-drawn and extended beverage can is loaded onto a sleeve and pressed axially into a flanging head. The open end of the can is bent outwards by means of the rotating flanging head and rolls distributed around its circumference and shaped into a flange corresponding to the geometry of the neck rolls. After being placed on the filled can, the lid is joined to it in a seaming process.

As it is dependent on lightweight construction, aeronautical technology is also dependent on mechanical joining. Mechanical joining methods and especially riveting technology thus occupy an important place in aeronautics. This is particularly apparent when considering the amount of joints used in the construction of the Airbus, an amount in the order of approximately two million per aircraft. The joints are visible in the shell structure. The sheer number of these joints highlights the importance of the optimization of the construction technology involved in their production. In addition the mechanical joints manufactured with rivets, seaming and flanging are also used in aeronautical engineering as connecting technologies. Typical seaming and flanging connections are used both in areas in which different sheet components are joined together and in which a superior component rigidity is required for construction reasons.

In addition to aeronautics, joining by forming is being used increasingly in the automotive industry. In 1994 Audi AG introduced the A8, ushering in a new trend in lightweight automotive construction. For the first time in serial car manufacture, aluminium found a greater employment as body material, placing special demands on connecting technology. Conventional resistance spot welding reached its limits, in particular with respect to the desired process reliability. Punch riveting would become the favoured process because it allowed for especially high dynamic strengths. 1,000 punch rivets per body were processed per body for the A8, a number which would rise to 1,800 in 1999, the year the entry-level model A2 was introduced. This is a reflection both of the continuous further development of this technology for use in serial manufacture and of the increasing trend to substitute undesirable welding spots. With the body shell of its Series 6, BMW has taken a further step towards lightweight construction [GORO04]. A large variety of materials are used in the process. If the passenger compartment is constructed primarily from steel plate, aluminium is chosen for the front structure. Add-on parts like doors and the front hood are manufactured from aluminium. Thermoplastic resin is still used for the front side walls and SMC for the rear hatch. In the aluminium front structure, deformed aluminium tubes, castings, extruded profiles and deep-drawing steel sheets are used alternately. This combination of materials places great demands on joining technology. BMW, for example, prevents contact corrosion caused by the contact of aluminium and steel by applying an epoxy resin glue. This acts as a sealed insulation layer with electrochemical separation and also provides a force-locked connection. The components are then furnished with

punch rivets. Besides adding more strength, these also fix the as yet fresh adhesive bond so that the dimensional accuracy is retained. In every riveting process, the force curve is compared to a reference curve, depending on the path. To prevent contact corrosion on the punch rivets, as well, they are especially coated.

A further application of punch rivets are on the flywheels of passenger car transmissions. These comprise two units, one several millimetres thick disc with inductively hardened peripheral teeth and an insert for stiffening and the noise reduction. This flywheel is flanged directly onto the crankshaft, which means that the start-up motor engages the gearing of the flywheel to start the engine. The resultant forces try to deform the flywheel, so the insert for stiffening was conventionally connected to the flywheel by means of projection or spot welding. The large quantity of welding spots required because of the dynamic forces involved could be replaced by a smaller quantity of punch rivets. Clinching also proved to be economically viable in the manufacture of bumper mounts. In this case, clinching was shown as an effective means of joining a multiple bevelled steel sheet.

References

[ADAM98] Adam, P.: Fertigungsverfahren von Turboflugwerken. Birkhäuser Verlag, Basel Boston Berlin, (1998)

[ADLE66] Adler, G.: Umformen von Blech bei Raumtemperatur. In: Industrie Anzeiger vol. 88, No. 88, pp. 1823–1833 (1966)

[ADLO89] Adlof, W.W.: Die Vielfalt von Schmiedeteilen. In: VDI-Berichte, No. 774, pp. 17–37 (1989)

[ADLO04] Adlof, W.W.: Simulation in der Massivumformung. In: Info-Reihe Massivumformung, Extraausgabe, Industrieverband Massivumformung, p. 7 (2004)

[AHLR04] Ahlroos, T., Parikka, R. et al.: Tribological properties of environmentally acceptable lubricants for metal working applications. In: Proceedings of the 2nd International Conference on Tribology in Manufacturing Processes. Nyborg, Denmark (2004)

[AMBA79] Ambaum, E.: Untersuchungen über das Verhalten innerer Hohlstellen beim Freiformschmieden. Dissertation, RWTH Aachen (1979)

[APEL53] Apel, H.: Gewindewalzen. Carl Hanser Verlag, München (1953)

[AVER65] Avery, S.H., Backofen, W.A.: A structural basis for superplasticity. Trans. Am. Soc. Metals (ASM) **58**, 551–562 (1965)

[AYAD84] Ayada, T., Higashino, K., Mori, K.: Central bursting in extrusion of inhomogenous materials. Adv. Technol. Plast. Band 1. (1984)

[BAND49] Bander, U.: Ableitung von Verformungsbestwerten für das Tiefziehen von Hohlkörpern aus dicken Stahlblechen. Dissertation, TU Stuttgart (1949)

[BARG83] Bargel, H.J., Schulze, G.: Werkstoffkunde. VDI Verlag (1983)

[BARN04] Barnert, L.: Grundlagen des Gesenkschmiedens unter tribologischen Gesichtspunkten. In: Bartz, W.J. (Hrsg.) Tribologie und Schmierung bei der Massivumformung. Expert Verlag, Renningen-Malmsheim (2004)

DOI: 10.1007/978-3-642-36772-4, © Springer-Verlag Berlin Heidelberg 2013

[BART87] Bartsch, G.: Kaltprofilgewalzte Zylinderräder für Leistungsgetriebe—Untersuchungen zur Technologie und zum Bauteilverhalten. Dissertation, RWTH Aachen (1987)

[BART94] Bartz, W.: Additive—Einführung in die Problematik. In: Bartz, W. et al. (Hrsg.) Additive für Schmierstoffe. Expert Verlag, Renningen-Malmsheim (1994)

[BART00] Bartz, W., Möller, U.: Expert Praxislexikon Tribologie PLUS: 2010 Begriffe für Studium und Beruf. Expert Verlag, Renningen-Malmsheim (2000)

[BATH65] Bath, C.: Streckziehen von Karosserieteilen. In: Werkstatt und Betrieb **98**(3), 143–144 (1965)

[BATH96] Bathe, K.J.: Finite Element Procedures. Prentice Hall, London (1996)

[BAY94] Bay, N.: State of the art in cold forging lubrication. J. Mat. Process. Technol. **46**(1–2), 19–40 (1994)

[BECK73] Beck, G.: Die Bedeutung des Werkstückwerkstoffes beim Feinschneiden. Bänder Bleche Rohre **14**(8), 339–344 (1973)

[BEHR04a] Behrens, B., Mathieu, H.: Rückwärtssimulation von Massivumformprozessen zur schnellen Auslegung der Stadienfolge. Schmiede-J. 19–20 (2004)

[BEHR04b] Behrens, B.A., Hübner, S., Poelemeyer, J.: Clinchen lackierter Stahlbleche—Werkzeuggeometrieoptimierung mittels FEM zur Minimierung der Lackschädigung. VDI-Z Integrierte Produktion (10), 62–64 (2004)

[BEIT01] Beitz, W., Grote, K.H. (Hrsg.): Dubbel—Taschenbuch für den Maschinenbau. Springer, Berlin p. 20 Auflage (2001)

[BENS81] Bensmann, G. et al.: Möglichkeiten und Weiterentwicklung des hydromechanischen Tiefziehens. Werkstatt und Betrieb **114**(9), 679–685 (1981)

[BETH80] Bethlehem, W.F.: Das Verhalten unterschiedlicher Werkstoffe beim Radialgewinderollen. Industrie Anzeiger **102**(70), 46–51 (1980)

[BETH81] Bethlehem, W.F.: Mit antriebslosen Rollköpfen Gewinde spanlos formen. Drahtwelt **67**(5), 106–109 (1981)

[BETH82] Bethlehem, W.F.: Die Flankenverschleißfestigkeit läßt sich erhöhen mit dem Einsteckgewindewalzen. Maschinenmarkt **80**(3), 18–20 (1982)

[BETH83] Bethlehem, W.F.: Spanlos Gewinde herstellen. Industrie Anzeiger **105**(37), 20–22 (1983)

[BETT03] Betten, J.: Finite Elemente für Ingenieure, Band 1. Springer, Berlin, 2. Auflage (2003)

[BILL73] Billigmann, J., Feldmann, H.D.: Stauchen und Pressen. Hanser Verlag, München, 1. Auflage (1973)

[BIRZ74] Birzer, F.: Gefügestruktur und Feinstanzfähigkeit eines Stahles. Technisches Zentralblatt für praktische Metallbearbeitung **68**(3), 85–88 (1974)

[BIRZ76] Birzer, F., Haack, J., Kurzhöfer, G.: Feinschneiden und Feinschneidwerkstoffe. Feintool AG, Lyss, Schweiz, (1976)

[BIRZ78] Birzer, F.: Feinschneiden hochwertiger Feinkornstähle. Techn. Rundschau vol. 44, Bern (1978)

[BIRZ93] Birzer, F.: Präzionsfeinschnitteile für High-Tech-Anwendungen. In: VDI-Z-Special Blechbearbeitung, pp. 38–39 (1993)

[BIRZ96] Birzer, F.: Feinschneiden und Umformen—Wirtschaftliche Fertigung von Präzisionsteilen aus Blech. In: Verlag Moderne Industrie (1996)

[BIRZ97] Birzer, F., Lange, K. et al.: Umformen und Feinschneiden—Handbuch für Verfahren, Werkstoffe und Teilegestaltung. Verlag Hallwag AG, Bern Schweiz (1997)

[BIRZ99] Birzer, F.: Feinschneiden und Umformen. Verlag Moderne Industrie, Landsberg/Lech (1999)

[BITZ96] Bitzel, H. et al.: Faszination Blech. Dr. Josef Raabe Verlags GmbH, Stuttgart Berlin Bonn (1996)

[BLAI81] Blaich, M.: Umformeigenschaften von Blechen aus Aluminiumlegierungen. Industrie Anzeiger **103**(95), 32–33 (1981)

[BLEC04] Bleck, W.: Bericht des Sonderforschungsbereichs SFB 289, Teilprojekt F2—Werkstoffverhalten und Bauteilprüfung, Antragszeitraum 2002 bis 2004. RWTH Aachen (2004)

[BOBB00] Bobbert, S.: Simulationsgestützte Prozessauslegung für das Innenhochdruck-Umformen von Blechpaaren. Dissertation, Friedrich-Alexander-Universität Erlangen-Nürnberg (2000)

[BOBZ00] Bobzin, K.: Benetzungs- und Korrosionsverhalten von PVD beschichteten Werkstoffen für den Einsatz in umweltverträglichen Tribosystemen. Dissertation, RWTH Aachen (2000)

[BOBZ04] Bobzin, K., Lugscheider, E., Pinero, C.: Neue PVD-Schichtkonzepte für hoch beanspruchte Werkzeuge für umweltverträgliche Fertigungsprozesse. Materialwissenschaft und Werkstofftechnik **35**(10/11) (2004)

[BOET90] Boetz, F.: Einbaufertig nach Entgraten—Stand der Technik beim Feinschneiden als Verfahren der Massenproduktion. Maschinenmarkt **96**(43), 50–56 (1990)

[BOET98] Boetz, V.: Leichtmetall-Räder im Automobilbau. Werkstatt und Betrieb **131**(7–8), 668–671 (1998)

[BOWD50] Bowden, F., Tabor, D.: The Friction and Lubrication of Solids. Oxford University Press, Oxford (1950)

[BRAC80] Brackhoff, H.F.: Numerisch gesteuertes (CNC) Umformbearbeitungszentrum zum Drücken von Blechen. Industrie Anzeiger **102**(37), 7–21 (1980)

[BRAM71] Brambauer, E.: Ermittlung der maximalen Aufweitverhältnisse beim Kragenziehen. In: VEB Kombinat Umformtechnik Erfurt **3**(45–48) (1971)

[BRID44] Bridgeman, P.: The stress distribution at the neck of tension specimen. Trans. Am. Soc. Metals (ASM) **32**, 553–574 (1944)

[BROZ72] Brozzo, P., Luca, B.D., Rendina, R.: A new method for the prediction of the formability limits of metal sheets. In: 7th Biennal Congress of the International Deep Drawing Research Group. (1972)

[BRÜL78a] Brüller, E.: Konstruktion und Funktion von Stanz- und Biegeautomaten. Blech Rohre Profile **25**(4), 154–159 (1978)

[BRÜL78b] Brüller, E.: Stanz-Biege-Automaten im Einsatz, Teil 2. Drahtwelt (5), 181–186 (1978)

[BUCK68] Buckley, D.: The influence of the atomic nature of crystalline materials on friction. Trans. Am. Soc. Lubr. Eng. (ASLE) **11**(89) (1968)

[BUDD95] Budde, L., Pilgrim, R.: Stanznieten und Durchsetzfügen. Verlag Moderne Industrie, Landsberg (1995)

[BÜHL66] Bühler, H., v. Finckenstein, E.: Hochgeschwindigkeitsumformung rohrförmiger Werkstücke durch magnetische Kräfte. Bänder Bleche Rohre **7**(3), 115–123 (1966)

[BÜHL70] Bühler, H., Pollmar, F., Rose, A.: Einfluß von Werkzeugstoff und seiner Wärmebehandlung auf das Schneiden von Feinblechen. Archiv für das Eisenhüttenwesen **41**(10), 989–996 (1970)

[BÜLT96] Bülter, M.: Untersuchung zum Einfluß des Herstellungsprozesses auf die Oberflächenausbildung und die Umformeigenschaften von elektrolytisch verzinktem Feinblech. Dissertation, Universität Stuttgart (1996)

[BURG67] Burgdorf, M.: Über die Ermittlung des Reibwertes für Verfahren der Massivumformung durch den Ringstauchversuch. Industrie Anzeiger **89**(39), 799–804 (1967)

[BUSC69] Busch, R.K.: Untersuchung über das Abstreckziehen von zylindrischen Hohlkörpern bei Raumtemperatur. Dissertation, Universität Stuttgart (1969)

[CHUN98] Chung, W.J., Cho, J.W., Belytschko, T.: On the dynamic effects of explicit FEM in sheet metal forming analysis. Eng. Comput. Int. J. Compu. Aided Eng. Softw. **15**(6) (1998)

[CLIN67] Cline, H.E., Alden, T.H.: Rate-sensitive deformation in tin-lead alloys. Trans. Metall. Soc. Am. Inst. Min. Metall. Pet. Eng. (AIME) **239**, 710–714 (1967)

[CLOU60] Clough, R.: The finite element method in plane stress analysis. In: Proceedings of the 2nd ASCE Conference on Electronic Computation. Pittsburgh, PA, USA, (1960)

[COCK66] Cockroft, M., Latham, O.: A simple criterion of fracture of ductile materials. In: NEL Report. Glasgow, Band 240 (1966)

[COEN88] Coenen, H.P., Wetter, E.: Das Pressenschmieden von Kurbelwellen. Thyssen Technische Berichte (2), 349–353 (1988)

[COUL85] Coulomb, C.: Theorie des machines simples, en ayant égard au frottement de leurs parties et a la roideur des cordages. In: Memoires de mathematique et de physique de L'Académie des Sciences. Band 10 (1785)

[CRAH82] Crahay, J., Bragard, A.: Production of surfaces of textured work rolls by means of laser pulses. In: 12th IDDRG Congress. p. Margherita Ligure, Italien (1982)

[CZIC68] Czichos, H.: Über den Zusammenhang zwischen Adhäsion und Elektronenstruktur von Metallen bei der Rollreibung im elastischen Bereich. Trans. Am. Soc. Lubr. Eng. (ASLE) **11**(89) (1968)

[CZIC73] Czichos, H., Habig, K.: Grundvorgänge des Verschleißes metallischer Werkstoffe—Neuere Ergebnisse der Forschung. In: VDI-Berichte (194) (1973)

[CZIC03] Czichos, H., Habig, K.: Tribologie-Handbuch—Reibung und Verschleiß. Vieweg, Wiesbaden (2003)

[DANN69] Dannenmann, E.: Die Veränderung der Oberflächenbeschaffenheit beim Tiefziehen von Näpfen. Industrie Anzeiger **91**(93), 2253–2254 (1969)

[DANN83] Dannenmann, E.: Einfluß der plastischen Eigenschaften und der Oberflächenmikrostruktur von Feinblechen auf Zieh- und Biegevorgängen. Dissertation, Universität Stuttgart (1983)

[DAWN79] Dawnson, D.: History of Tribology. Langman, London (1979)

[DEIL03] Deiler, G., Lobemeier, J.: Tiefziehwerkzeuge aus Kunststoff—ideal für mittlere Serien. Blech InForm (1) (2003)

[DENG91] Dengler, K., Glomski, G.: Die Hochleistungsimpulstechnik—eine zukunftsträchtige Hochgeschwindigkeits-Umformtechnologie. Blech Rohre Profile **38**(4), 285–286 (1991)

[DESE03] Desery, C., Haller, B. et al.: Thixoschmieden—Entwicklung der Thixoformingtechnologie für hochschmelzende Stahlwerkstoffe. wt Werkstattstechnik online **93**(10), 689–694 (2003)

[DICK97] Dick, P.: Technologie des Hochdruckumformens ebener Bleche. Dissertation, Technische Hochschule Darmstadt (1997)

[DIET72] Dieterle, K., Schröder, G.: Fließkurven. Lehrbuch der Umformtechnik, Band 1. Springer, Berlin (1972)

[DIET75] Dietz, H., Hamann, F.: Hochgeschwindigkeitsverfahren zur Umformung metallischer Werkstücke. Siemens Forschungs- und Entwicklungs Berichte **4**(3), 141–147 (1975)

[DIET86] Dieter, G.E.: Mechanical Metallurgy. McGraw-Hill, New York, 3rd Edn (1986)

[DIN75] DIN 6935: Kaltbiegen von Flacherzeugnissen aus Stahl. Normenausschuss Werkzeuge und Spannzeuge (FWS), Oktober 1975

[DIN77] DIN 51350: Prüfung von Schmierstoffen; Prüfung im Shell-Vierkugel-Apparat. Normenausschuss Materialprüfung (NMP), Januar 1977

[DIN83] DIN 7952-4: Blechdurchzüge mit Gewinde, Teil 4: Maße für die Werkzeuge und deren Gestaltung. Normenausschuss Werkzeuge und Spannzeuge (FWS), März 1983

[DIN86a] DIN 7523-2: Schmiedestücke aus Stahl; Gestaltung von Gesenkschmiedestücken; Bearbeitungszugaben, Seitenschrägen, Kantenrundungen, Hohlkehlen, Bodendicken, Wanddicken, Rippenbreiten und Rippenkopfradien. Normenausschuss Eisen-, Blech- und Metallwaren (NAEBM), September 1986

[DIN86b] DIN 7952-1: Blechdurchzüge mit Gewinde, Teil 1: Maße. Normenausschuss Werkzeuge und Spannzeuge (FWS), Juli 1986

[DIN86c] DIN 867: Bezugsprofile für Evolventenverzahnungen an Stirnrädern (Zylinderrädern) für den allgemeinen Maschinenbau und den Schwermaschinenbau. Normenausschuss Maschinenbau (NAM), Februar 1986

[DIN93] DIN 17864: Schmiedestücke aus Titan und Titan-Knetlegierungen (Freiform- und Gesenkschmiedeteile). Normenausschuss Nichteisenmetalle (FNNE), Februar 1993

[DIN94] DIN V ENV 1071-3: Hochleistungskeramik; Verfahren zur Prüfung keramischer Schichten. Teil 3: Bestimmung der Haftung mit dem Ritztest. Normenausschuss Materialprüfung (NMP), Juni 1994

[DIN00] DIN 51347: Prüfung von Schmierstoffen—Prüfung im Mischreibungsgebiet mit dem Schmierstoffprüfgerät nach Brugger. Normenausschuss Materialprüfung (NMP), Januar 2000

[DIN02] DIN V ENV 1071-6: Hochleistungskeramik—Verfahren zur Prüfung keramischer Schichten. Teil 6: Bestimmung des Abriebwiderstands von Schichten durch eine Mikroabriebprüfung. Normenausschuss Materialprüfung (NMP), September 2002

[DIN03a] DIN 8580: Fertigungsverfahren. Einteilung. Normenausschuss Technische Grundlagen (NATG), September 2003

[DIN03b] DIN 8582: Fertigungsverfahren Umformen, Einordnung, Unterteilung, Alphabetische Übersicht. Normenausschuss Technische Grundlagen (NATG), September 2003

[DIN03c] DIN 8583-1: Fertigungsverfahren Druckumformen—Teil 1: Allgemeines; Einordnung, Unterteilung, Begriffe. Normenausschuss Technische Grundlagen (NATG), September 2003

[DIN03d] DIN 8583-2: Fertigungsverfahren Druckumformen—Teil 2: Walzen; Einordnung, Unterteilung, Begriffe. Normenausschuss Technische Grundlagen (NATG), September 2003

[DIN03e] DIN 8583-3: Fertigungsverfahren Druckumformen—Teil 3: Freiformen; Einordnung, Unterteilung, Begriffe. Normenausschuss Technische Grundlagen (NATG), September 2003

[DIN03f] DIN 8583-4: Fertigungsverfahren Druckumformen—Teil 4: Gesenkformen; Einordnung, Unterteilung, Begriffe. Normenausschuss Technische Grundlagen (NATG), September 2003

[DIN03g] DIN 8583-6: Fertigungsverfahren Druckumformen—Teil 6: Durchdrücken; Einordnung, Unterteilung, Begriffe. Normenausschuss Technische Grundlagen (NATG), September 2003

[DIN03h] DIN 8584-3: Fertigungsverfahren Zugdruckumformen, Teil 3: Tiefziehen. Normenausschuss Technische Grundlagen (NATG), September 2003

[DIN03i] DIN 8584-4: Fertigungsverfahren Zugdruckumformen—Teil 4: Drücken. Normenausschuss Technische Grundlagen (NATG), September 2003

[DIN03j] DIN 8585-4: Fertigungsverfahren Zugumformen—Teil 4: Tiefen; Einordnung, Unterteilung, Begriffe. Normenausschusss Technische Grundlagen (NATG), September 2003

[DIN03k] DIN 8586: Fertigungsverfahren Biegeumformen—Einordnung, Unterteilung, Begriffe. Normenausschuss Technische Grundlagen (NATG), September 2003

[DIN03l] DIN 8588: Fertigungsverfahren Zerteilen. Normenausschuss Technische Grundlagen (NATG), September 2003

[DIN03m] DIN 8593-5: Fertigungsverfahren Fügen, Teil 5: Fügen durch Umformen. Normenausschuss Technische Grundlagen (NATG), September 2003

[DIN04a] DIN 50125: Prüfung metallischer Werkstoffe—Zugproben. Normenausschuss Materialprüfung, Juli 2004

[DIN04b] DIN 51834: Prüfung von Schmierstoffen—Tribologische Prüfungen im translatorischen Oszillations-Prüfgerät. Normenausschuss Materialprüfung (NMP), März 2004

[DINK97] Dinkel, F.: Umformbarkeit von Aluminium-Karosserieblechen mit neuartigen Oberflächen. Dissertation, TU München (1997)

[DOEG71] Doege, E. et al.: Tiefziehen auf einfach- und doppeltwirkenden Karosseriepressen unter Berücksichtigung des Gelenkantriebes. Werkstatt und Betrieb **104**, 737–747 (1971)

[DOEG76] Doege, E.: Wichtige Einflussgrößen beim Tiefziehen. Werkstattstechnik, Zeitschrift für industrielle Fertigung **66**(11), 615–619 (1976)

[DOEG80] Doege, E. et al.: Einfluss der Umformmaschine auf die Werkstückgenauigkeit. HFF-Bericht (6) (1980)

[DOEG86] Doege, E., Meyer-Nolkemper, H., Saeed, I.: Fließkurvenatlas metallischer Werkstoffe. Hanser-Verlag, München (1986)

[DOEG01] Doege, E., Huskic, A. et al.: Verschleißreduzierung an Schmiedegesenken durch Einsatz neuer Technologien. In: Siegert, K. (Hrsg.): Neuere Entwicklungen in der Massivumformung. MAT INFO Werkstoff-Informationsgesellschaft, Frankfurt (2001)

[DOEG03] Doege, E., Haller, B. et al.: Thixo-Schmieden von Stahl. In: Siegert, K. (Hrsg.): Neuere Entwicklungen in der Massivumformung. MAT INFO Werkstoff-Informationsgesellschaft, Frankfurt (2003)

[DOHM93a] Dohmann, F.: Innenhochdruckumformen. In: Lange, K. (Hrsg.): Umformtechnik—Handbuch für Industrie und Wissenschaft, Band 4: Sonderverfahren, Prozesssimulation, Werkzeugtechnik, Produktion. Springer, Berlin, Band 2. Auflage (1993)

[DOHM93b] Dohmann, F., Hartl, C.: Möglichkeiten der Innenhochdruckumformung unter besonderer Beachtung des Formens von Strangpressprofilen. In: Neuere Entwicklungen in der Massivumformung. DGM Verlag, Oberursel, pp. 255–280 (1993)

[DOLV91] Dolves, J.: Electron beam texturing of rolls. Iron Steel Eng. **68**(8), 33–38 (1991)

[DOMA80] Domalski, H.H.: Stähle mit Mikrolegierungszusätzen. In: Reprints der 6. Tagung Kaltumformung. Düsseldorf (1980)

[DOMK86] Domke, W.: Werkstoffkunde und Werkstoffprüfung. W. Girardet Buchverlag, Düsseldorf, 10. verbesserte Auflage (1986)

[DRAE65] Draeger, E.: Das Herstellen von Borden an Feinblechen. Industrie Anzeiger **87**(23), 393–397 (1965)

[DRÖG54] Dröge, K.H.: Kräfte und Materialfluss beim Drücken. Dissertation, TU Stuttgart (1954)

[EBER67] Ebertshäuser, H.: Technologie der Blechverarbeitung. Michael Triltsch Verlag, Düsseldorf (1967)

[ECKS03] Eckstein, R.: Scherschneiden und Biegen metallischer Kleinstteile—Materialeinfluss und Materialverhalten. Dissertation, Friedrich-Alexander-Universität Erlangen-Nürnberg (2003)

[EHRE75] Ehrenberg, H.: Vorrichtung zum Aushalsen von Behälterböden. Schweißtechnik **6**, 98–100 (1975)

[EICH80] Eichner, A.J.: Fertigen komplexer Formstücke in kleinen und mittleren Serien aus superplastischem Aluminium. Werkstatt und Betrieb **114**(10), 715–718 (1980)

[EICH81] Eichner, K.W.: Beschreibung des Umformvorgangs "Rillenwalzen". Dissertation, TH Darmstadt (1981)

[EICH86] Eichner, K.W.: Zahnradwalzen mit innenverzahnten Werkzeugen. Industrie Anzeiger **75**(108), 43–44 (1986)

[EISE66] Eisenkolb, F.: Einführung in die Werkstoffkunde, Band I-V. 9. VEB Verlag Technik, Berlin (1966)

[ELMA01] Elmagd, E.; Abouridouane, M.: Einfluss der Umformgeschwindigkeit und -temperatur auf das Umformvermögen metallischer Werkstoffe. In: Kolloquium "Erweiterung der Formgebungsgrenzen", pp. 26–30 (2001)

[EN97] DIN EN 10139: Kaltband ohne Überzug aus weichen Stählen zum Kaltumformen. Normenausschuss Eisen und Stahl (FES), Dezember 1997

[EN98] DIN EN 10267: Von Warmformgebungstemperatur ausscheidungshärtende ferritisch-perlitische Stähle. Normenausschuss Eisen und Stahl (FES), Februar 1998

[EN99] DIN EN 12420: Kupfer- und Kupferlegierungen—Schmiedestücke. Normenausschuss Nichteisenmetalle (FNNE), März 1999

[EN00] DIN EN 10243: Gesenkschmiedeteile aus Stahl—Maßtoleranzen. Normenausschuss Eisen-, Blech- und Metallwaren (NAEBM), Juni 2000

[EN01a] DIN EN 12476: Phosphatierüberzüge auf Metallen—Verfahren für die Festlegung von Anforderungen. Normenausschuss Materialprüfung (NMP), Oktober 2001

[EN01b] DIN EN 13523-7: Prüfverfahren, Teil 7: Widerstandsfähigkeit gegen Rissbildung beim Biegen (T-Biegeprüfung). Normenausschuss Beschichtungsstoffe und Beschichtungen (NAB), Dezember 2001

[EN02] DIN EN 586: Aluminium und Aluminiumlegierungen—Schmiedestücke. Normenausschuss Nichteisenmetalle (FNNE), Februar 2002

[EN03] DIN EN 10268: Kaltgewalzte Flacherzeugnisse aus Stählen mit hoher Streckgrenze zum Kaltumformen. Normenausschuss Eisen und Stahl (FES), Januar 2003

[EN04] DIN EN 10130: Kaltgewalzte Flacherzeugnisse aus weichen Stählen zum Kaltumformen. Normenausschuss Eisen und Stahl (FES), Oktober 2004

[ENGE02] Engelhorn, R.: Verschleißmerkmale und Schleifeinsatzverhalten zweiphasig verstärkter Sol-Gel-Korunde. Dissertation, RWTH Aachen (2002)

[ESCH04] Escher, C., Henke, T.: Werkzeugwerkstoffe für die Verarbeitung von hochfesten Stahlblechwerkstoffen. In: Siegert, K. (Hrsg.): Neuere Entwicklungen in der Blechumformung. MAT INFO Werkstoff-Informationsgesellschaft, Frankfurt (2004)

[EVER04] Eversberg, K.: Schwerlasttaugliche Werkzeugbeschichtungen und deren Bedeutung für die Kaltumformung schwer umformbarer Edelstähle. In: Bartz, W. (Hrsg.): Tribologie und Schmierung bei der Massivumformung. Expert Verlag, Renningen-Malmsheim (2004)

[EXNE86] Exner, H.E., Hougardy, H.P.: Einführung in die Quantitative Gefügeanalyse. DGM Informationsgesellschaft, Oberursel (1986)

[FAIT87a] Fait, J.: Grundlagenuntersuchung zur Ermittlung von Kenngrößen für das CNC-Schwenkbiegen. Industrie Anzeiger **109**(10), 36–37 (1987)

[FAIT87b] Fait, J., Rothstein, R.: Beitrag zur Prozesssimulation des Schwenkund U-Biegens. Industrie Anzeiger **109**(10), 45–46 (1987)

[FELD84] Feldmann, H.D.: Glatt- und Festwalzen. Technisches Zentralblatt für praktische Metallbearbeitung **78**(3), 62–69 (1984)

[FELD01] Feldhaus, U.: Simulieren geht über Probieren. Schmiede-Journal 30–31 (2001)

[FINC88] von Finckenstein, E. et al.: Die Prozesssimulation beim Biegeumformen als Voraussetzung für eine rechnerintegrierte Fertigung, Band 694. VDI Verlag (1988)

[FINK32] Fink, M., Hofmann, U.: Zur Theorie der Reiboxidation. Archiv für das Eisenhüttenwesen **6**(161) (1932)

[FINK74] Fink, C.: Theorie der Walzenarbeit. Zeitung Berg-, Hütten- und Salinenwesen **22**(5), 220 (1974)

[FINZ03] Finz, K.: Neue Werkzeugstähle hoher Belastbarkeit für die Kaltmassivumformung. In: Siegert, K. (Hrsg.): Neuere Entwicklungen in der Massivumformung. MAT INFO Werkstoff-Informationsgesellschaft, Frankfurt (2003)

[FISC72] Fischer, H., Hentschel, B.: Ergebnisse der Untersuchungen über Langloch- und Rechteckdurchzüge. VEB Kombinat Umformtechnik Erfurt **3**, 41–47 (1972)

[FLOR67] Floreen, S.: Superplasticity in pure nickel. Scripta Metallurgia **1**(19–23) (1967)

[FRAC90] Frackiewicz, H., Kalita, W. et al.: Laserformgebung der Bleche. VDI-Berichte (876), 317–328 (1990)

[FRAN99] Frank, C.: Kunststoff als Werkzeugwerkstoff für das Tiefziehen von Feinblech. Dissertation, Universität Hannover (1999)

[FREU50] Freudenthal, A.: The Inelastic Behavior of Engeneering Metals and Structures. Wiley, New York (1950)

[FRIE88] Friedrich, H.E. et al.: SPF/DB on the way to the production stage for Ti and Al. Superplasticity and Superplastic forming. The Minerals, Metals and Materials Society, pp. 649–664 (1988)

[FRIE97] Friedrich, C.: Tribologische Problemlösungen mit PVD Hartstoffschichten zum Verschleißschutz. Dissertation, TU Darmstadt (1997)

[FRIE02] Friedrich, D., Gottschalk, C. et al.: Simulation von Fertigungsprozessen—Möglichkeiten und Grenzen der Bauteilauslegung. In: Eversheim, W. et al. (Hrsg.): Wettbewerbsfaktor Produktionstechnik—Aachener Perspektiven. AWK AachenerWerkzeugmaschinen-Kolloquium, Shaker Verlag, Aachen, pp. 217–267 (2002)

[FRIT83] Fritsch, R.: Untersuchungen zum Einfluss unterschiedlicher Bearbeitungsverfahren auf die Dauerfestigkeit. Technologiearbeitskreis, WZL, RWTH Aachen (1983)

[FUCH83] Fuchsbauer, B.: Ermüdungseigenschaften festgewalzter Probestäbe. In: Festwalzen und Glattwalzen zur Festigkeitssteigerung von Bauteilen. Deutscher Verband für Materialprüfung, Berlin (1983)

[FÜLL04] Füller, K., Baumeister, J., Herold, R.: Keramische Umformwerkzeuge zum Umformen höchstfester Stähle. In: Siegert, K. (Hrsg.): *N*euere Entwicklungen in der Blechumformung. MAT INFO Werkstoff-Informationsgesellschaft, Frankfurt (2004)

[FURL88] Furlan, R. et al.: Production of Ti 6 Al 4 V components. In: Superplasticity and Superplastic forming. The Minerals, Metals and Materials Society, pp. 665–677 (1988)

[GAHR87] Zum Gahr, K.: Microstructure and Wear of Materials. Elsevier (1987)

[GEIG91] Geiger, M., Vollertsen, F., Amon, S.: Flexible Blechumformung mit Laserstrahlung—Laserstrahlbiegen. Bleche Rohre Profile **38**(11), 856–861 (1991)

[GEIG93a] Geiger, M., Heckel, W.: 3D-Lichtschnittsensor zur Biegewinkelerfassung. Blech Rohre Profile **40**(3), 235–240 (1993)

[GEIG93b] Geiger, M., Vollertsen, F.: Laserstrahlbiegen von Eisen- und NELegierungen. Blech Rohre Profile **40**(9), 666–670 (1993)

[GEIL04] Geile, M.: Neue Entwicklungen von Werkzeugwerkstoffen für die Blechumformung. In: Siegert, K. (Hrsg.): Neuere Entwicklungen in der Blechumformung. MAT INFO Werkstoff-Informationsgesellschaft, Frankfurt (2004)

[GERB02] Gerbig, Y., Ortmann, S., et al.: Verbesserung des tribologischen Verhaltens durch In-Prozess-Strukturierung von Schichtoberflächen. In: Reibung, Schmierung und Verschleiß—Forschung und praktische Anwendung, Tribologie-Fachtagung. Gesellschaft für Tribologie e.V., Göttingen (2002)

[GERB03] Gerbig, Y., Gerbig, F., et al.: Weizen contra Raps: Eine vergleichende Studie zu anwendungsrelevanten Eigenschaften von Pflanzenölen. Tribologie und Schmierungstechnik **50**(1) (2003)

[GERL61] Gerlach, H.H.: Das Glattwalzen von Gußeisen. Dissertation, TH Hannover (1961)

[GFT91] GfT-Arbeitsblatt 2: Schmierung beim Umformen. Gesellschaft für Tribologie e.V., Januar 1991

[GFT02] GfT-Arbeitsblatt 7: Tribologie—Definitionen, Begriffe, Prüfung. Gesellschaft für Tribologie e.V., September 2002

[GIAN99] Giannuzzi, L.A., Stevie, F.A.: A review of focused ion beam milling techniques for TEM specimen preparation. Micron **30**, 197–204 (1999)

[GLAU58] Glaubitz, H.: Kaltverformte Verzahnungen. Klepzig Fachberichte **66**(11), 425–427 (1958)

[GÖBE04] Göbel, R., Henkenjohann, N., Kleiner, M.: Process optimization in sheet metal spinning by adaptive sequential design of experiments. In: Proceedings of the Fourth Annual Meeting of ENBIS. Copenhagen, Denmark (2004)

[GÖCK94] Göcke, R.: Präparation—Überblick über Präparationsmethoden. In: Schmidt, P.F. (Hrsg.): Praxis der Rasterelektronenmikroskopie und Mikrobereichsanalyse. Expert Verlag, Renningen-Malmsheim, (1994)

[GOLD01] Gold, P., Schmidtand, A., et al.: Viskosität-Druck-Koeffizienten von mineralischen und synthetischen Schmierölen. Tribologie und Schmierungstechnik (47) (2001)

[GOLO77] Gologranc, F.: Theoretische Betrachtung zur Aufnahme von Fließkurven im kontinuierlichen hydraulischen Tiefungsversuch. Blech **4**, 116–121 (1977)

[GORB78] Gorbauch, S., Heidel, K.H., Kühmel, S.: Entwicklungsstand und Anwendungsmöglichkeiten des Abstreckdrückens. Fertigungstechnik und Betrieb **28**, 174–177 (1978)

[GORO04] Goroncy, J.: Intelligenter Leichtbau. Automobil Industrie OEM 84–85 (2004)

[GOSH76] Gosh, A.: A criterion for ductile fracture in sheets under biaxial loading. Met. Tran. **7**, 523–533 (1976)

[GOTT98] Gottstein, G.: Physikalische Grundlagen der Materialkunde. Springer, Berlin 1998

[GRÄB83] Gräbener, T.: Entwicklung und Anwendung neuer Schmierstoffprüfverfahren für die Kaltmassivumformung. Dissertation, Stuttgart (1983)

[GRÄF93] Gräfen, H.: VDI-Lexikon—Werkstofftechnik. VDI Verlag, Düsseldorf (1993)

[GREE51] Green, A.: A theoretical investigation of the compression of a ductile material between smooth flat dies. Philos. Mag. **42**, 900–918 (1951)

[GROB60] Grob, E.: Kaltwalzmaschinen für Keilwellen und Zahnräder. Werkstattstechnik **50**(7), 351–357 (1960)

[GROC03] Groche, P., Metz, C., Kaufmann, M.: DIN-Fachbericht 137: Einbindung der Innenhochdruck-Verfahren in die Normenreihe DIN 8580 et seqq. Unterausschuss Wirkmedienbasiertes Umformen des Arbeitsausschusses Begriffe der Fertigungsverfahren (C.4) im Normenausschuss Technische Grundlagen (NATG), September 2003

[GROC04] Groche, P., Schäfer, R.: Simulation der geometrischen Oberflächenwandlung beim Drücken optischer Bauteile. Materialwissenschaft und Werkstofftechnik **35**(7), 454–460 (2004)

[GRUN76] Grundig, W., Liebig, H.P.: Das Gesetz der Volumenkonstanz als allgemeine Voraussetzung bei der Ermittlung von Streck- und Tiefziehfähigkeit aus Ergebnissen des Zugversuches. Archiv für das Eisenhüttenwesen **41**(1), 27–32 (1976)

[GUÉR99] Guérin, J., Bartysand, H., et al.: Finite element implementation of a generalized friction model: application to an upsetting-sliding test. Finite Elem. Anal. Des. **31**, 193–207 (1999)

[GUID65] Guidi, A.: Nachschneiden und Feinschneiden. Hanser Verlag, München (1965)

[GURS77] Gurson, A.: Continuum theory of ductile rupture by void nucleation and growth, part 1—yield criteria and flow rules for porous ductile media. J. Eng. Mat. Technol. 2–15 (1977)

[HAAC79] Haack, J., Birzer, F.: Feinschneiden—Handbuch für die Praxis. Feintool AG, Lyss, Schweiz, (1979)

[HABI68] Habig, K.: Zur Struktur- und Orientierungsabhängigkeit der Adhäsion und der trockenen Gleitreibung von Metallen. Materialprüfung **10**(417) (1968)

[HAEF87] Haefer, R.: Oberflächen- und Dünnschichttechnologie, Teil 1: Beschichtungen von Oberflächen. Springer, Berlin (1987)

[HAHN96] Hahn, O.: Fügen durch Umformen - Nieten und Durchsetzfügen—Innovative Verbindungsverfahren für die Praxis. Studiengesellschaft Stahlanwendung e. V. (1996)

[HALL71] Haller, H.: Handbuch des Schmiedens. Hanser Verlag, München Wien (1971)

[HANT94] Hantschke, H.: Röntgenmikroanalyse mit dem Rasterelektronenmikroskop. In: Schmidt, P.F. (Hrsg.): Praxis der Rasterelektronenmikroskopie und Mikrobereichsanalyse. Expert Verlag, Renningen-Malmsheim (1994)

[HASE77] Hasek, V.V.: Anwendung von Grenzformänderungsschaubildern. Industrie Anzeiger **99**(20), 343–347 (1977)

[HASE78] Hasek, V.V.: Untersuchung und theoretische Beschreibung wichtiger Einflußgrößen auf das Grenzformänderungsschaubild. Blech Rohre Profile **25**, 213–220, 285–292, 493–499, 613–627 (1978)

[HASE80a] Hasek, V.V.: Steuerung des Stoffflusses beim Ziehen von großen unregelmäßigen Blechteilen und Untersuchung von Möglichkeiten zur Vermeidung von Faltenbildung. Dissertation, Universität Stuttgart (1980)

[HASE80b] Hasek, V.V., Lange, K.: Das Grenzformänderungsschaubild und seine Anwendung bei Tiefzieh- und Streckziehvorgängen. In: Siegert, K. (Hrsg.): Neuere Entwicklungen in der Blechbearbeitung. Forschungsgesellschaft Umformtechnik mbH, Stuttgart (1980)

[HASE81] Hasek, V.V.: Beeinflussung des Werkstoffflusses durch Ziehwulste und Ziehstäbe. Industrie Anzeiger **103**(59), 26–27 (1981)

[HASH84] Hashish, M.: A modeling study of metal cutting with abrasive water jets. Trans. Am. Soc. Mech. Eng. (ASME) **106**, 88–100 (1984)

[HAUB67] Hauber, O.: Titanverarbeitung im Flugzeugzellenbau. Blech (10), 44–54 (1967)

[HAYA81] Hayama, M., Kawai, K.: Das Drücken von Blechen in der Kleinserienfertigung. Blech Rohre Profile **28**(1), 514–517 (1981)

[HEBE87] Heberer, K.: Funkenerodiermaschine zur Oberflächenbearbeitung von Kaltwalzen. Stahl und Eisen **107**(3), 109–110 (1987)

[HEID75] Heidemeyer, J.: Einfluss der plastischen Verformung von Metallen bei Mischreibung auf die Geschwindigkeit ihrer chemischen Reaktionen. Schmiertechnik, Tribologie **22**(84) (1975)

[HEIN99] Hein, P.: Innenhochdruck-Umformen von Blechpaaren: Modellierung, Prozessauslegung und Prozessführung. Dissertation, Friedrich-Alexander-Universität Erlangen-Nürnberg (1999)

[HEIZ03] Heizmann, J.: Wirkmedienunterstützte Umformtechnologien—Status und Ausblicke. In: Siegert, K. (Hrsg.): Hydroforming von Rohren. Strangpressprofilen und Blechen, Tagungsband der internationalen Konferenz Hydroforming. MAT INFO, Frankfurt, 3 (2003)

[HELL94] Hellwig, W., Semlinger, E.: Spanlose Fertigung: Stanzen. Vieweg & Sohn Verlag, (1994)

[HENN01] Hennige, T.: Flexible Formgebung von Blechen durch Laserstrahlumformen. Meisenbach Verlag, Bamberg (2001)

[HERM69] Hermanns, M., Telgentren, G.: Glattwalzen als Vorbehandlung zylindrischer Werkstücke zum Hartverchromen. Werkstattstechnik **59**(8), 369–372 (1969)

[HERR92] Herres, W.U.: Prozessüberwachung beim Feinschneiden. Dissertation, Rheinisch-Westfälische Technische Hochschule Aachen (1992)

[HESS91] Hessleressler, C.: Beitrag zur Entwicklung des hydraulischen Rohr-Innendruck-Umformens. Dissertation, TH Darmstadt (1991)

[HESS92] Hessler, C., Engel, B.: Komplizierte Leichtbau-Werkstücke durch hydraulisches Innendruckumformen. Werkstatt und Betrieb **125**(6), 477–481 (1992)

[HEUS96] Heussen, J.: Untersuchungen zum Materialverhalten von Metallen im Bereich der Solidustemperatur. Dissertation, RWTH Aachen (1996)

[HILB70] Hilbert, H.: Stanzereitechnik, Band 2: Umformende Werkzeuge. Carl Hanser Verlag, München (1970)

[HILL50] Hill, R.: The mathematical theory of plasticity. Engineering Science Theories. Clarendon Press, Oxford (1950)

[HIPT03] Op de Hipt, M.: Anlagentechnische Genauigkeit. In: ICAFT 2003 International Conference on Accuracy in Forming Technology, 10th Saxon Conference on Forming Technology. SFU (2003)

[HIRO90] Hirohashi, M., Asanuma, H.: Superplasticity of hypoeutectoid Al-Zn alloy sheets. Aluminium **66**(11), 1074–1078 (1990)

[HIRT98] Hirt, G., Witulski, T., et al.: Thixoforming: Eine zukünftige Alternative zur Herstellung komplex geformter Stahlschmiedeteile? In: 13. Aachener Stahlkolloquium "Umformtechnik Stahl- und NEWerkstoffe—Impulse für Produktivitätssteigerung und Arbeitsplatzsicherung". (1998)

[HOFM63] Hofmann, R.: Neuzeitliche Streckziehpressen, Konstruktionen. Technik und Forschung **47**(195), 893–894 (1963)

[HOJA91] Hojas, M., et al.: Superplastische Aluminiumbleche. Metall **2**(45), 130–134 (1991)

[HORL89] Horlacher, U.: Prüfung des Einflusses von Schmierstoffadditiven auf das Tribosystem bei der Kaltmassivumformung. Dissertation, Stuttgart (1989)

[HORT01] Hortig, D.: Werkzeugbeschichtungen mit Trockenschmierstoffeigenschaften für das Tiefziehen. Dissertation, Darmstadt (2001)

[HUBM94] Hubmann, A.: Grundöle—deren Abstimmung mit Additiven und Bedeutung für Bedeutung für die Anwendungseigenschaften der Schmierstoffe. In: Bartz, W.J., et al. (Hrsg.): Additive für Schmierstoffe. Expert Verlag, Renningen-Malmsheim (1994)

[HUEB82] Hbnueer, K.H., Thornton, E.A.: The Finite Element Method for Engineers, 2nd edn. Wiley, New York, Chichester Brisbane, (1982)

[HUSK02] Huskic, A., Berg, M.E.S.: Verschleißminderung an Schmiedegesenken mittels Kombinationsbehandlungen bestehend aus einer Plasmanitrierung und PACVD-Viellagenbeschichtung. Galvanotechnik **1** (2002)

[HUXH93] Huxholl, L.: Biegemaschinen auf der EMO 93. Blech Rohre Profile **40**(11), 824–827 (1993)

[IBIN80] Ibinger, K., Spalke, H.: Oberflächenbehandlung von Umformwerkzeugen. Werkstatt und Betrieb **113**(3) (1980)

[ISIN93] Ising, G.: Verwaltung inklusive. Industrie Anzeiger **35**, 65–67 (1993)

[ISLA03] Islamgaliev, R.K., Yunusova, N.F., et al.: Characteristics of superplasticity in an ultrafine-grained aluminum alloy processed by ECA pressing. Scripta Materialia **49**(5), 467–472 (2003)

[ISO90] DIN ISO 286-1: ISO-System für Grenzmaße und Passungen, Teil 1: Grundlagen für Toleranzen, Abmaße und Passungen. Normenausschuss Länge und Gestalt (NLG), November 1990

[ISO00] DIN EN ISO 7799: Bleche und Bänder mit einer Dicke unter 3 mm, Hin- und Herbiegeversuch. Normenausschuss Materialprüfung (NMP), Juli 2000

[ISO03] DIN EN ISO 20482: Bleche und Bänder—Tiefungsversuch nach Erichsen. Normenausschuss Materialprüfung (NMP), Dezember 2003

[ISO04a] DIN EN ISO 6507-1: Metallische Werkstoffe–Härteprüfung nach Vickers. Teil 1: Prüfverfahren. Normenausschuss Materialprüfung (NMP), Juli 2004

[ISO04b] DIN EN ISO 7438: Biegeversuch. Normenausschuss Materialprüfung (NMP), Mai 2004

[JAHN81] Jahnke, H., Retzke, R., Weber, W.: Umformen und Schneiden. VEB Verlag Technik, Berlin, 5. Auflage (1981)

[JANS99] Janschek, P.: Entwicklung einer Schmiedetechnologie zur Herstellung von Verdichterschaufeln aus γ-Titanaluminid. Schmiede-J. (9), 22–23 (1999)

[JEME47] Jemeljaneko, D.T., Zukovsskij, B.D.: Das Kalibrieren von Walzen der kontinuierlichen Rohrwalzenstraßen. Stahl (7), 616–626 (1947)

[JOHN68] Johnston, R., Fogg, B., Chisholm, A.W.: An Investigation into the FineBlanking Process. In: Proceedings of the 96th Machine Tool Design and Research Conference, pp. 397–410. Birmingham (1968)

[JOLY96] Joly, P.A., Mehrabian, R.: The rheology of partial solid alloy. J. Mater. Sci. (11), 1393 et seqq. (1996)

[JOST66] Jost, H.P.: Lubrication (Tribology) education and research—a report of the present position and industry's needs. Department of Education and Science, Her Majesty's Stationary Office, London (1966)

[KAEH92] Kaehler, K.: Zu neuen Einsätzen. Industrie Anzeiger **46**, 21–23 (1992)

[KAHL82] Kahl, K.W.: Vorausbestimmung des Biegewinkels. Industrie Anzeiger **104**(85), 22–24 (1982)

[KAJD98] Kajdas, C.: Tribochemistry of ceramics. Tribologia **2**, 148–167 (1998)

[KALC60] Kalckhoff, M.: Profil-Streckziehen im Flugzeugbau. Metall **14**(3), 224–227 (1960)

[KAPR98] Kapranos, P., Kirkwood, D.H., Barkhudarov, M.R.: Modeling of structural breakdown during rapid compression of semi-solid alloy slugs. In: Bhasin, A.K., et al. (Hrsg.) Proceedings of the 5th International Conference on Semi-Solid Processing of Alloys and Composites. Golden, Colorado, USA (1998)

[KIEN54] Kienzle, O., Timmerbeil, H.: Herstellung und Gestaltung durchgezogener enger Kragen an Fein- und Mittelblechen. Mitteilungen der Forschungsgesellschaft Blechverarbeitung, pp. 2–9, 41–43, 66–70 (1954)

[KIEN63] Kienzle, O., Meyer, M.: Verfahren zur Erzielung glatter Schnittflächen bei vollkantigem Schneiden von Blechen. Westdeutscher Verlag, Köln Opladen (1963)

[KIEN68] Kienzle, O.: Mechanische Umformtechnik; Plastizitätstheorie, Werkstoffmechanik. Springer, Berlin (1968)

[KITT93] Kittel, S., Küpper, F., et al.: Laserstrahlumformen von Blechen. Bänder Bleche Rohre (3), 54–62 (1993)

[KIUS03] Kiushi, M.: Neuere Entwicklungen auf dem Gebiet des Thixo-Schmiedens. In: Siegert, K. (Hrsg.): Neuere Entwicklungen in der Massivumformung. MAT INFO Werkstoff-Informationsgesellschaft, Frankfurt (2003)

[KLAA93] Klaas, F., Kaehler, K.: Herstellung innovativer Hohlteilformen mit dem Innenhochdruckverfahren. Umformtechnisches Kolloquium Hannover **14**, 9/1–9/10 (1993)

[KLEI02] Kleiner, M., Göbel, R., et al.: Combinded methods for the prediction of dynamic instabilities in sheet metal spinning. Annals of the CIRP **51**(1), 209–214 (2002)

[KLIN56a] Klinger, R., Krucker, E.: Praxis des Abkant- und Profilpressens. Technische Rundschau **48**(20), 17–29 (1956)

[KLIN56b] Klinger, R., Krucker, E.: Praxis des Abkant- und Profilpressens. Technische Rundschau **48**(21), 17–29 (1956)

[KLIN56c] Klinger, R., Krucker, E.: Praxis des Abkant- und Profilpressens. Technische Rundschau **48**(26), 17–33 (1956)

[KLOC02a] Klocke, F., Raedt, H.: Innovationen in der Feinschneidtechnik. Werkstatttechnik online **92**(6), 268–272 (2002)

[KLOC02b] Klocke, F., Raedt, H.W., et al.: Friction and wear in cold forming. In: Proceedings of the International Conference Recent Developments in Metal Forming Technology. Columbus, Ohio, USA (2002)

[KLOC03a] Klocke, F., Breuer, D.: FEM und KNN als Werkzeuge zur Bruchvorhersage in der Umformtechnik. In: Tagungsband 18. Jahrestreffen der Kaltmassivumformer (2003)

[KLOC03b] Klocke, F., Kuwer, C., et al.: Einsatz keramischer Werkzeuge in der Blechumformung. Abschlussbericht des AiF-Projektes 12575N. Forschungsvereinigung Stahlverformung (FSV), Hagen (2003)

[KLOC03c] Klocke, F., Massmann, T., Kuwer, C.: Aktuelle Ansätze zur Verschleißminimierung in der Blechumformung. ZWF Zeitschrift für wirtschaftlichen Fabrikbetrieb **98**(10), 472–475 (2003)

[KLOC04a] Klocke, F., Breuer, D.: Using the finite element method and artificial neural networks to predict ductile fracture in cold forming processes. In: Proceedings of the 8th International Conference on Numerical Methods in Industrial Forming Processes. Columbus, Ohio, USA, pp. 1944–1950 (2004)

[KLOC04b] Klocke, F., Kuwer, C.: Optimierung der Ziehkantengeometrie eines Keramikwerkzeuges. In: EFB-Kolloquium "Lösungen für die Verarbeitung moderner Blechwerkstoffe". Europäische Forschungsgesellschaft für Blechverarbeitung e. V., Fellbach (2004)

[KLOC04c] Klocke, F., Massmann, T., Grams, J.: Grundlagenuntersuchungen zum Einsatz umweltverträglicher Tribosysteme beim Zerspanen und in der Kaltumformung. Materialwissenschaft und Werkstofftechnik **35**(10/11) (2004)

[KLOC04d] Klocke, F., Massmann, T., et al.: Carbon based tool coatings as an approach for environmentally friendly metal forming processes. In: Proceedings of the 2nd International Conference on Tribology in Manufacturing Processes. Nyborg, Denmark, Band 2 Forming Tribology (2004)

[KLOC04e] Klocke, F., Massmann, T., et al.: On the tribological performance of newly developed rape oil based biodegradable lubricants for cold forging processes. Annalen der Wissenschaftlichen Gesellschaft für Produktionstechnik (WGP): Production Engineering **11**(2) (2004)

[KLOC04f] Klocke, F., Wehrmeister, T.: Laser-assisted metal spinning of advanced materials. In: Proceedings of the Fourth LANE, pp. 1183–1192. Meisenbach Verlag, Bamberg, Erlangen, (2004)

[KNOT92] Knothe, K., Wessels, H.: Finite Elemente—Eine Einführung für Ingenieure. Springer, Berlin, 2. Auflage (1992)

[KOBA89] Kobayashi, S., Oh, S.I., Altan, T.: Metal Forming and the Finite Element Method. Oxford University Press, Oxford (1989)

[KÖNI54] König, H.: Glattwalzen. Schriftenreihe Feinbearbeitung. Deutscher Fachzeitschriften- und Fachbuchverlag Stuttgart (1954)

[KÖNI81a] König, W., Rotter, F., Muhr, R.: Glattwandige massgenaue Löcher im Stahlbau durch Feinschneiden. Industrie Anzeiger **103**, 27–29 (1981)

[KÖNI81b] König, W., et al.: Blechumformung mit elastischen Wirkmedien. Industrie Anzeiger **103**(35), 20–23 (1981)

[KÖNI82a] König, W., Rotter, F., et al.: Neue Möglichkeiten der Feinschneidtechnologie durch hochfeste perlitarme Stähle. Technisches Zentralblatt für praktische Metallbearbeitung **76**(3), 52–58 (1982)

[KÖNI82b] König, W., Rotter, F., et al.: Stanzen von Löchern hoher Formtreue und Oberflächengüte in dickwandige Bauteile aus Stahl durch Anwendung der Feinschneidtechnologie. KfK-PFT Kernforschungszentrum Karlsruhe (18) (1982)

[KÖNI83] König, W., Weck, M., Bartsch, G.: Kaltwalzen von Zahnrädern für Leistungsgetriebe—Bestimmung von Werkzeugprofil und Rohteilgeometrie—Tragfähigkeitsvergleich. In: Siegert, K. (Hrsg.) Neuere Entwicklungen in der Massivumformung. Forschungsgesellschaft Umformtechnik mbH (FGU), Stuttgart (1983)

[KÖNI84] König, W., Rotter, F., Krapoth, A.: Feinschneiden dicker Bleche—Experiment und Theorie. Industrie Anzeiger **106**(14), 24–28 (1984)

[KÖNI93a] König, W., Koll, W.: Kaltfließpressen ohne Schmierstoff, Dünne Schichten—große Leistung. Umformtechnik **27**(5) (1993)

[KÖNI93b] König, W., Weck, M., et al.: Formgebung mit Laserstrahlung. VDI-Z **135**(4), 14–17 (1993)

[KÖNI02] König, W., Klocke, F.: Fertigungsverfahren, Band 1: Drehen, Fräsen, Bohren. VDI Verlag, Düsseldorf, 7. Auflage (2002)

[KOPP87] Kopp, R., Welschof, K.: Partielles Schmieden—ein flexibles Umformverfahren zur Verbesserung der Energie- und Rohstoffausnutzung. Aluminium **63**(2), 168–172 (1987)

[KOPP99] Kopp, R., Wiegels, H.: Einführung in die Umformtechnik. Verlag Mainz, Aachen, 2. Auflage (1999)

[KORF94] Korff, J.: Additive für Kühlschmierstoffe. In: Bartz, W.J., et al. (Hrsg.) Additive für Schmierstoffe. Expert Verlag, Renningen-Malmsheim (1994)

[KOST51] Kostron, H.: Zur Mathematik des Zugversuchs. Archiv für das Eisenhüttenwesen **22**, 317–325 (1951)

[KRÄM68] Krämer, W.: Beitrag zur Kraft- und Arbeitsermittlung beim Schneiden von Blech. Industrie Anzeiger **90**, 361–365 (1968)

[KRÄM69] Krämer, W.: Untersuchungen über das Genauschneiden von Stahl und NE-Metallen. Verlag W. Giradet, Essen (1969)

[KRAP78a] Krapfenbauer, H.: Kaltwalzen eng tolerierter Verzahnungen. Werkstatt und Betrieb **111**(10), 657–661 (1978)

[KRAP78b] Krapfenbauer, H.: Präzisionszahnräder, aus vollem Material kaltgewalzt. Technische Rundschau (21) Sonderdruck (1978)

[KRAP79] Krapfenbauer, H.: Kaltgewalzte Präzisionsverzahnungen. VDI Berichte (332) (1979)

[KRAP84] Krapfenbauer, H.: Neue Gesichtspunkte für die Fertigung von Stirnzahnrädern durch Kaltwalzen. In: Präzisions-Fertigungstechnik aus der Schweiz. Carl Hanser Verlag, München (1984)

[KRAU62] Krause, U.: Vergleich verschiedener Verfahren zum Bestimmen der Formänderungsfestigkeit bei der Kaltumformung. Dissertation, TH Hannover (1962)

[KRAU66] Krauss, W.: Neue Verfahren der Umformung von Blechen und Profilen aus den USA. Bänder Bleche Rohre **7**(7), 403–408 (1966)

[KREI82] Kreissig, B., Schulz, W.: Kaltwalzen von Evolventenprofilen mit Flachbackenwerkzeugen (Roto-Flo-Verfahren), Band 4/82. Technische Akademie Esslingen, Eislingen/Fils, Lehrgang Zahnradfertigung (1982)

[KREI83] Kreissig, B.: Kaltwalzen von Verzahnungen mit dem Roto-Flo-Verfahren. die maschine (dima) **37**(9) (1983)

[KROH65] Krohn, P.: Das Glattwalzen zylindrischer Werkstücke im Einstechverfahren. Dissertation, TH Braunschweig (1965)

[KÜBE80] Kübert, M.: Aufbringen und Auswerten von Meßrastern beim Blechumformen. Werkstatt und Betrieb **113**(7), 483–487 (1980)

[KÜBE81] Kübert, M.: Verfahrensbeschreibung und Anwendungsbeispiele zum Tiefziehen dicker Bleche mit und ohne Faltenbildung. Blech Rohre Profile **28**(9), 404–408 (1981)

[KUBL95] Kubli, W., Reissner, J.: Optimisation of sheet-metal forming processes using the special purpose program "Autoform". J. Mater. Process. Technol. **50**, 292–305 (1995)

[KUHN58] Kuhn, W.: Untersuchungen über das Streckziehen von Stahlhülsen mit mehreren Ziehringen. Dissertation, TH Zürich (1958)

[KÜHN82] Kühne, R.: Ermittlung von Verfahrensgrenzen beim Drücken. Industrie Anzeiger **104**(102), 22–23 (1982)

[KÜPP71] Küppers, W.: Das Verhalten nichtrostender Feinbleche beim Kragenziehen. Blech Rohre Profile **10**, 403–409 (1971)

[KURS60] Kursetz, E.: Blechumformung im amerikanischen Flugzeugbau. Blech **7**(5), 260–268 (1960)

[KURS65] Kursetz, E.: Umformung von Blechen und Profilen auf Streckformmaschinen. Maschinenmarkt **71**(75), 21–24 (1965)

[KURS69] Kursetz, E.: Kombiniertes Streckformen und Tiefziehen. Maschinenmarkt **75**(60), 1368–1370 (1969)

[KURS71] Kursetz, E.: Das Streckformziehen als modernes Verfahren der Blechformteilherstellung. Technisches Zentralblatt für praktische Metallbearbeitung **65**(8), 357–362 (1971)

[LANE55a] Lane, F.B.: Streckformen, eine neue Art der Blechumformung im Flugzeugbau. Luftfahrttechnik 91–96 (1955)

[LANE55b] Lane, F.B.: Streckformmaschinen. Werkstatt und Betrieb **88**(5), 247–249 (1955)

[LANG74] Lange, E.: Untersuchung des Tiefziehverhaltens von Feinblechen unter besonderer Berücksichtigung des Gelenkantriebes. Dissertation, TU Clausthal (1974)

[LANG81a] Lange, K., Gräbener, T.: Untersuchung der Möglichkeiten für eine technologische Schmierstoffprüfung für Verfahren der Umformtechnik. In: BMFT bei der DFVLR Köln (Hrsg.): Tribologie: Reibung, Verschleiß, Schmierung. Springer Verlag, Berlin Heidelberg New York, Metallurgie, Werkstoffentwicklung, Rückgewinnung (1981)

[LANG81b] Lange, K., Kling, E.: Entwicklungen in der Blechbearbeitungstechnik am Beispiel jüngerer Forschungsergebnisse. Blech Rohre Profile **28**(3), 99–104 (1981)

[LANG83] [LANG83]Lange, K.: Radialumformen—wirtschaftliche Herstellung von Halbzeugen im Rahmen gemischter flexibler Fertigungssysteme. In: Tagungsband: Flexible Fertigungssysteme, Kolloquium zum SFB 155. Universität Stuttgart (1983)

[LANG90a] Lange, K.: Umformtechnik—Handbuch für Industrie und Wissenschaft, Band 1: Grundlagen. Springer, Berlin (1990)

[LANG90b] Lange, K.: Umformtechnik—Handbuch für Industrie und Wissenschaft, Band 2: Massivumformung. Springer, Berlin (1990)

[LANG90c] Lange, K.: Umformtechnik—Handbuch für Industrie und Wissenschaft, Band 3: Blechbearbeitung. Springer, Berlin (1990)

[LANG93] Lange, K.: Umformtechnik—Handbuch für Industrie und Wissenschaft, Band 4: Sonderverfahren, Prozesssimulation, Werkzeugtechnik, Produktion. Springer, Berlin (1993)

[LEE67] Lee, D., Backofen, W.A.: Superplasticity in some Ti- and Zr-alloys. Trans. Metall. Soc. Am. Inst. Min. Metall. Pet. Eng. (AIME) **239**, 1034–1040 (1967)

[LEHM58] Lehmann, T.: Probleme des Blechbiegens. VDI-Z **100**(27), 1295–1300 (1958)

[LEYK78] Leykamm, H.: Berechnung der Fließkurve von Fließpressstählen und der Festigkeit, Bruchdehnung und Brucheinschnürung kaltumgeformter Werkstücke aus der Werkstoffanalyse nach Wagenbach. Draht **29**, 648–651 (1978)

[LI95] Li, J.: Untersuchung der Wirkflächenreibung für die Finite-Elemente-Simulation der Massivumformung. Dissertation, RWTH Aachen (1995)

[LIND65] Lindner, H.: Massivumformung von Stahl zwischen 600–900°—Halbwarmschmieden. Dissertation, TU Hannover (1965)

[LIPP59] Lippmann, H.: Ebenes Hochkantbiegen eines schmalen Balkens unter Berücksichtigung der Verfestigung. Ingenieur-Archiv **27**, 153–168 (1959)

[LOWA01] Lowak, H., Vollrath, K.: Aluminium-Schmiedeteile mit hochinteressanten Leichtbauoptionen. Maschinenmarkt (32), 44–46 (2001)

[LUDO81] Ludowig, G., Zicke, G.: Programmiersystem für das CNC Walzrunden. Werkstattstechnik, Zeitschrift für industrielle Fertigung **71**, 287–291 (1981)

[LUDW09] Ludwik, P.: Elemente der technologischen Mechanik. Springer, Berlin (1909)

[LUDW69] Ludwig, H.I.: Grundlagen und Anwendungsgebiete der Drückverfahren. Bänder Bleche Rohre **10**(9), 540–548, 623–629 und 667–676 (1969)

[LUIG90] Luig, H., Bobke, T.: Beanspruchung und Schadensarten an Schmiedegesenken. Tribologie und Schmierungstechnik **37**(2), 76–81 (1990)

[LUIG93] Luig, H.: Einfluß von Verschleißschutzschichten und Rohteilverzunderung auf den Verschleiß beim Schmieden. Dissertation, Hannover (1993)

[MACH81] Macherauch, E.: Praktikum in Werkstoffkunde. Vieweg Verlag (1981)

[MAED68] Maeda, T., Nakagava, T.: Experimental Investigation on fine blanking. Sci. Pap. Inst. Phys. Chem. Res. **62**, 65–80 (1968)

[MANG83] Mang, T.: Die Schmierung in der Metallbearbeitung. Vogel, Würzburg (1983)

[MANG01] Mang, T., Dresel, W.: Lubricants and Lubrication. Wiley-VCH Verlag, Weinheim (2001)

[MARC73] Marciniak, Z., Chodakowski, A., Kopacz, Z.: Neue Verfahren zum plastischen Kaltumformen von Maschinenteilen. VDI-Z **115**(1), 9–12 (1973)

[MARC79] Marciniak, Z., Kopacz, Z.: WPM and WPMR transverse cold rolling process. In: Proceedings of the 1st International Conference on Rotary Metalworking Processes (RoMP 1), pp. 367–380. London (1979)

[MASS93] Massberg, W.; Bugdoll, P.M.: Anbiegen im automatischen Walzrundprozeß. Blech Rohre Profile **40**(6), 476–480 (1993)

[MATT03] Matthes, K.J., Riedel, F.: Fügetechnik—Überblick, Löten, Kleben, Fügen durch Umformen. Fachbuchverlag Leipzig im Carl Hanser Verlag, Leipzig (2003)

[MAY61] May, O.: Die Traktrix-Kurve, Ziehring mit schraubenförmiger Schulter und das Abstrecken durch mehrere Züge. Werkstattstechnik **51**(9), 476–479 (1961)

[MCCL68] Mcclintock, F.: A criterion for ductile fracture by the growth of holes. Trans. Am. Soc. Mech. Eng. (ASME) J. Appl. Mech. **90**, 363–371 (1968)

[MEIE01] Meier, H., Gänsicke, B.: Verbesserung des Umformvermögens beim Walzrundbiegen mittels partieller Drucküberlagerung. Kolloquium "Erweiterung der Formgebungsgrenzen". pp. 14–18 (2001)

[MERK03] Merkel, M., Thomas, K.H.: Taschenbuch der Werkstoffe. Fachbuchverlag Leipzig (2003)

[MESS01] Messmer, G.: Simulation des Thixo-Schmiedens von Aluminiumlegierungen mit Flow-3D. In: Siegert, K. (Hrsg.): Neuere Entwicklungen in der Massivumformung. MAT INFO Werkstoff-Informationsgesellschaft, Frankfurt (2001)

[MICH85] Michaelis, R.: Präzisionsschmieden mit integrierter Wärmebehandlung. Dissertation, Universität Hannover (1985)

[MICH93] Michel, B.: In einem Arbeitsgang. Industrie Anzeiger **35**, 26–28 (1993)

[MIKK70] Mikkers, J.: Bänder Bleche Rohre **11**(4), 223–228 (1970)

[MILC78] Milcke, F.: Ermittlung der Längseigenspannungen in walzproflierten Kaltprofilen. Dissertation, TU Dortmund (1978)

[MISE13] Von Mises, R.: Mechanik der festen Körper im plastisch deformablen Zustand. In: Nachrichten der Gesellschaft der Wissenschaften in Göttingen. Mathematisch Physikalische Klasse, pp. 582–592 (1913)

[MÖHR62] Möhrlin, W.: Die grundlegenden Tiefziehverfahren. Industrie Anzeiger **84**, 1901–1904 (1962)

[MÜCK95] Mücke, K.: Innen-Hochdruck-Umformen in der Serienfertigung. Blech Rohre Profile **42** (1995)

[MÜLL60] Müller, M.: Möglichkeiten und Beispiele für das Kaltrollen von Formteilen. Fertigungstechnik und Betrieb **10**(10), 582–588 (1960)

[MÜLL69] Müller, H.: Vorgänge beim elektrohydraulischen und elektromagnetischen Umformen von metallischen Werkstücken. Berichte aus dem institut für umformtechnik, nr. 11, Universität Stuttgart (1969)

[MÜSC69] Müschenborn, W.: Untersuchungen der Formänderungen an zwei Ziehteilen mit Hilfe eines photochemisch aufgebrachten Netzgitters. Thyssenforschung **1**(3), 109–115 (1969)

[MÜSC72] Müschenborn, W., et al.: Die erzeugungsbedingten Gütemerkmale von kaltgewalztem Feinblech unter dem Blickwinkel der Kaltumformbarkeit. Thyssenforschung **4**(1+2), 43–55 (1972)

[MÜSC74] Müschenborn, W.: Herstellung und Eigenschaften von hochfestem kaltgewalztem Feinblech aus mikrolegiertem Stahl. Thyssen Technische Berichte **6**(1), 22–27 (1974)

[NAKA93] Nakagawa, T.: Neue Entwicklungen bei der Fertigung von Karosserieteilen. Blech Rohre Profile **40**(12), 906–909 (1993)

[NEUD04] Neudecker, T.: Tribologische Eigenschaften keramischer Blechumformwerkzeuge—Einfluss einer Oberflächenendbearbeitung mittels Excimerlaserstrahlung. Dissertation, Erlangen-Nürnberg (2004)

[NITT04a] Nittel, K.: Chemische Beschichtungssysteme als Schmierstoffträger für die Massivumformung. In: Bartz, W. (Hrsg.) Tribologie und Schmierung bei der Massivumformung. Expert Verlag, Renningen-Malmsheim (2004)

[NITT04b] Nittel, K.: Seifen und Festschmierstoffe für die Kaltmassivumformung. In: Bartz, W. (Hrsg.) Tribologie und Schmierung bei der Massivumformung. Expert Verlag, Renningen-Malmsheim (2004)

[NN72] NN: Streckziehpressen. Fritz Müller Pressenfabrik, Esslingen (1972)

[NN75] NN: Fabricating Wiggin Nickel Alloys, Band 3590. Henry Wiggin & Comp. (Ltd.), Hereford, England (1975)

[NN79] NN: Firmenschrift. Fa. Hilgeland (1979)

[NN80] NN: Fertigung von Präzisionsrohren mit CNC-gesteuerten Streckdrückmaschinen. Industrie Anzeiger **102**(43), 22–23 (1980)

[NN81a] NN: Das Incremental-Verfahren. Fa. Escofier & Cie., Chalon-sur Saöne, Frankreich (1981)

[NN81b] NN: Herstellung von rotationssymmetrischen Hohlkörpern durch Drücken. Industrie Anzeiger **103**(93), 22–23 (1981)

[NN82a] NN: Entwicklungen und Trends beim Metalldrücken. Blech Rohre Profile **29**(6), 255 (1982)

[NN82b] NN: Mitteilungen. Fa. MBB/VFh, Bremen (1982)

[NN86] NN: Niedriglegierte Kupferwerkstoffe. Deutsches Kupfer Institut e. V., Düsseldorf (1986)

[NN87] NN: Fertigungsprozesse mit neuen Leistungs- und Anwendungsbereichen. Produktionstechnik: Auf dem Weg zu integrierten Systemen. In: AWK, Aachener Werkzeugmaschinenkolloquium. VDI Verlag, pp. 301–348. (1987)

[NN88] NN: Kupfer-Zink-Legierungen Messing und Sondermessing. Deutsches Kupferinstitut e. V., Düsseldorf (1988)

[NN94a] NN: Schmiedeteile—Gestaltung, Anwendung, Beispiele. Infostelle Industrieverband Massivumformung e. V., Hagen (1994)

[NN94b] NN: Werkzeugwechsler für Gesenkbiegepressen. Blech Rohre Profile **41**(2), 116 (1994)

[NN95] NN: PARCOM Decision 95/1 on the phasing out of short chained chlorinated paraffins. Convention for the prevention of marine pollution from land-based sources, Paris (1995)

[NN96] NN: Handbuch der Umformtechnik. Springer, Berlin (1996)

[NN01a] NN: Forschung und Entwicklung—Wir denken Stahl weiter. Thyssen-Krupp Stahl AG, Duisburg (2001)

[NN01b] NN: Kupfer. Deutsches Kupfer Institut e. V., Düsseldorf (2001)

[NN01c] NN: Massivumformtechniken für die Fahrzeugindustrie—Verfahren, Werkstoffe und Entwicklung, Band 213 von Die Bibliothek der Technik. Verlag Moderne Industrie, Landsberg/Lech (2001)

[NN03] NN: Bronze—unverzichtbarer Werkstoff der Moderne. Deutsches Kupfer Institut e. V., Düsseldorf (2003)

[NN04] NN: Kupfer-Zinn-Knetlegierungen (Zinnbronzen). Deutsches Kupfer Institut e. V., Düsseldorf (2004)

[NOVO02] Novotny, S.: Innenhochdruck-Umformen von Blechen aus Aluminium- und Magnesiumlegierungen bei erhöhter Temperatur. Dissertation, Friedrich-Alexander-Universität Erlangen Nürnberg (2002)

[OEHL44] Oehler, G.: Scharfkantiges Biegen dicker Bleche. Werkstattechnik **38**, 157–158 (1944)

[OEHL63] Oehler, G.: Biegen. Carl Hanser Verlag, München (1963)

[OEHL64a] Oehler, G.: Das zylindrische Stülpziehen unter ölhydraulischen Pressen. Werkstatt und Betrieb **97**(10), 133–134 (1964)

[OEHL64b] Oehler, G.: Streckziehmaschine für Teile großer Abmessungen. Mitteilungen der Forschungsgesellschaft Blechverarbeitung (1/2), 20–22 (1964)

[OEHL72] Oehler, G.: Blechdurchzüge für Gewinde. Werkstattstechnik, Zeitschrift für industrielle Fertigung **62**(7), 386–388 (1972)

[OEHL83] Oehler, G.: Einfluss der Rückfederung auf Maßtoleranzen an Blechen. Bänder Bleche Rohre **30**(3), 99 (1983)

[OEHL01] Oehler, G., Kaiser, F.: Schnitt-, Stanz- und Ziehwerkzeuge. Springer Verlag, 7. Auflage (2001)

[OPIT62] Opitz, H.: Stand und Bedeutung der Technologie der Fertigungsverfahren. Industrie Anzeiger **9**(72), 1709–1720 (1962)

[OROW43] Orowan, E.: In: Proceedings of the Institute of Mechanical Engineers, vol. 150, pp. 140–167. (1943)

[OYAN80] Oyane, M., Sato, T., Okimoto, K.: Criteria for ductile fracture and their applications. J. Mech. Working Technol. **4**, 65–81 (1980)

[PADM80] Padmanabhan, K., Davies, G.J.: Superplasticity. Springer, Berlin (1980)

[PAHL66] Pahlitzsch, G., Krohn, P.: Über das Glattwalzen zylindrischer Werkstücke im Einstechverfahren. Werkstattstechnik **56**, 2–12 (1966)

[PANK64] Panknin, W.: Die Bestimmung der Fließkurve und der Dehnungsfähigkeit von Blechen durch den hydraulischen Tiefungsversuch. Industrie Anzeiger **49**, 915–918 (1964)

[PANK66a] Panknin, W.: Bedeutung der Werkstoffeigenschaften für die Verarbeitung von Blech. In: Grundlagen der bildsamen Formgebung. Verlag Stahleisen GmbH, pp. 364–383 (1966)

[PANK66b] Panknin, W.: Sonderverfahren der Tiefziehtechnik. In: Grundlagen der bildsamen Formgebung. Verlag Stahleisen GmbH, pp. 489–503 (1966)

[PANK70] Panknin, W.: Gesetzmäßigkeiten des Ziehens und Drückens bei der Blechumformung. Zeitschrift für Metallkunde **61**(6), 407–414 (1970)

[PANK77] Panknin, W.: Herstellung zweiteiliger Dosen durch Tiefziehen und Abstreckziehen. Werkstatt und Betrieb **110**(6), 380–384 (1977)

[PANK90] Pankert, R.: Aufrauhen von Arbeitswalzen in Kaltwalzwerken. Stahl und Eisen **110**(3), 55–60 (1990)

[PAWE64] Pawelski, O.: Ein neues Gerät zum Messen des Reibungsbeiwertes bei plastischen Formänderungen. Stahl und Eisen **84**(20), 1233–1243 (1964)

[PAWE76] Pawelski, O.: Wege und Grenzen der Plastomechanik bei der Anwendung in der Umformtechnik, Band 256. Westdeutscher Verlag (1976)

[PEAR34] Pearson, C.E.: The viscous properties of extruded eutectic alloys of lead-tin and bismuth-tin. J. Inst. Metals **54**, 111–124 (1934)

[PERE92a] Perevezentsev, V.N., et al.: The theory of structural superplasticity I. Acta metallurgica et materialia **40**(5), 887–894 (1992)

[PERE92b] Perevezentsev, V.N., et al.: The theory of structural superplasticity II. Acta metallurgica et materialia **40**(5), 895–905 (1992)

[PETE02] Peters, M., Leyens, C.: Titan und Titanlegierungen. Wiley VCH, Weinheim (2002)

[PETE04] Peter, A.: Entwicklung eines Modells zur Abbildung der Reibverhältnisse beim Innenhochdruck-Umformen. Dissertation, Technische Universität Darmstadt (2004)

[PETZ94] Petzow, G., Carle, V.: Metallographisches, keramographisches, plastographisches Ätzen. Bornträger, Berlin Stuttgart, 6. Vollständig überarbeitete Auflage (1994)

[PFES97] Pfestorf, M.: Funktionale 3D-Oberflächenkenngrößen in der Umformtechnik. Dissertation, Erlangen-Nürnberg (1997)

[PHIL82] Philippe, J., Muth, H.W., Lubich, V.: Werkzeugwerkstoffe für das Schmieden. VDI-Berichte (432) (1982)

[PISC95] Pischel, H.: Bewährtes Innenhochdruck-Umformen. Werkstatt und Betrieb **128** (1995)

[PÖHL84] Pöhlandt, K.: Vergleichende Betrachtung der Verfahren zur Prüfung der plastischen Eigenschaften metallischer Werkstoffe. Dissertation, Universität Stuttgart (1984)

[PÖHL99] Pöhlandt, K.: Werkzeuge der Kaltmassivumformung, Band 581 von Kontakt & Studium. Expert Verlag (1999)

[POPP04] Popp, U., Engel, U.: Micro texturing of cold forging tools—influence on tool life. In: Proceedings of the 2nd International Conference on Tribology in Manufacturing Processes. Nyborg, Denmark (2004)

[PRAG54] Prager, W., Hodge, P.G.: Theorie idealplastischer Körper. Springer, Wien (1954)

[PUGH70] Pugh, H.L.D.: The mechanical behaviour of materials under pressure. Elsevier Publishing Co. FtD., Amsterdam (1970)

[QUAA96] Quaak, C.J.: Rheology of partial solidified aluminium composites. Dissertation, TU Delft (1996)

[QUIN62] Quinn, T.F.J.: The role of oxidation in the mild wear of steel. Brit. J. Appl. Phys. **13**(33) (1962)

[RADT65] Radtke, H.: Der Umformvorgang beim Stülpziehen. Mitteilungen der Forschungsgesellschaft Blechverarbeitung (11), 185–195 (1965)

[RADT79] Radtke, H.: Scharfkantiges Formbiegen hochfester Blechwerkstoffe. Maschinenmarkt **85**(10), 158–160 (1979)

[RAED02] Raedt, J.W.: Grundlagen für das schmiermittelreduzierte Tribosystem bei der Kaltumformung des Einsatzstahles 16MnCr5. Dissertation, RWTH Aachen (2002)

[RAPA04] Rapaport, D.C.: The Art of Molecular Dynamics Simulation. Cambridge University Press, 2nd edn. (2004)

[RAUT75] Rauter, A., Reissner, J.: Ein Beitrag zur Theorie des Kragenziehprozesses. Bänder Bleche Rohre **11**, 461–463 (1975)

[REDD93] Reddy, J.N.: An Introduction to the Finite Element Method, 2nd edn. McGraw-Hill, New York. (1993)

[REIC51] Reicherter, K.: Untersuchungen über das plastische Verhalten zylindrischer Proben im Druckversuch. Dissertation, TH Stuttgart (1951)

[REIH59] Reihle, M.: Verhalten des Gleitreibungskoeffizienten von Tiefziehblechen bei hohen Flächenpressungen. Dissertation, TH Stuttgart (1959)

[REIH61] Reihle, M.: Ein einfaches Verfahren zur Aufnahme von Fließkurven von Stahl bei Raumtemperatur. Archiv für das Eisenhüttenwesen **32**, 331–336 (1961)

[REIS76] Reissner, J., et al.: Das Grenzaufweitverhältnis beim Kragenziehen in Feinblechen. Maschinenmarkt **82**(99), 1919–1920 (1976)

[RENT97] Rentsch, C.: Feinschneiden mit beschichteten Werkzeugen. Dissertation, RWTH Aachen (1997)

[RICE69] Rice, J.R., Tracey, D.: On the ductile enlargement of voids in triaxial stress fields. J.Mech.Phys. Solids **17**, 201–217 (1969)

[RIED03] Riedel, F., Lang, H., et al.: Fügetechnik. Fachbuchverlag Leipzig im Carl Hanser Verlag, München Wien (2003)

[RISC04] Risch, C., Beerwald, C., et al.: On the significance of the die design for electromagnetic sheet metal forming. In: Kleiner, M. (Hrsg.) Proceedings of the 1st International Conference on High Speed Forming. Dortmund (2004)

[ROLL81] Roll, K.: Stand moderner numerischer Lösungsverfahren für die Berechnung der Verfahrensgrößen beim Kaltmassivumformen. In: Siegert, K. (Hrsg.) Neuere Entwicklungen in der Massivumformung. Forschungsgesellschaft Umformtechnik mbH, Stuttgart (1981)

[ROLL93] Roll, K., Tekkaya, A.E.: Numerische Verfahren der Prozesssimulation in der Umformtechnik. In: Lange, K. (Hrsg.) Umformtechnik, Handbuch für Industrie und Wissenschaft. Springer, Berlin, Band 4: Sonderverfahren, Prozesssimulation, Werkzeugtechnik, Produktion (1993)

[ROLL01] Roll, K., Bobbert, S.: Potentiale und Perspektiven der wirkmedienbasierten Blechumformung im Fahrzeugbau. In: Siegert, K. (Hrsg.) Kolloquium Wirkmedienumformung. LFU, Dortmund, pp. 95–100 (2001)

[ROMA71] Romanowski, W.P.: Handbuch der Stanzereitechnik. VEB Verlag Technik, Berlin (1971)

[ROTT84] Rotter, F.: Feinschneiden dicker Bleche. Dissertation, RWTH Aachen (1984)

[ROTT85] Rotter, F.: Genaue Werkstücke wirtschaftlich fertigen. Industrie Anzeiger **26**, 17–21 (1985)

[RÜDI81] Rüdinger, K.: Zum Umformverhalten von bandgefertigtem Titanblech. Blech Rohre Profile **28**(6), 234–237 (1981)

[RUPP97] Rupp, M.: Möglichkeiten und Grenzen der Kaltmassivumformung zinkphosphatschichtfreier Drähte. Dissertation, TU Darmstadt (1997)

[RYBK77] Rybke, Z.K.J.: Profile rolling of involute splines. Metallurgia and Metal Forming 201–204 (1977)

[SACH24] Sachs, G.: Einfluss der Probenhöhe auf den Stauchversuch. Metallkunde **16**, 55–58 (1924)

[SACH27] Sachs, G.: Z. Zeitschrift für Angewandte Mathematik und Mechanik **7**, 235 (1927)

[SACH51] Sachs, G.: Roll forming and drawbench forming straight sections. In: Corporation, R.P. (Hrsg.) Principles and Methods of Sheet Metal Fabricating. New York (1951)

[SACH74] Sachs, G., Expey, G.: Effect of spacing between die in the tandem drawing of tubular parts. Trans. Am. Soc. Mech. Eng. (ASME) 139–143 (1974)

[SALM82] Salmang, H., Scholze, H.: Keramik, Teil 1: Allgemeine Grundlagen und wichtige Eigenschaften. Springer, Berlin (1982)

[SALM83] Salmang, H., Scholze, H.: Keramik, Teil 2: Keramische Werkstoffe. Springer, Berlin (1983)

[SANS67] Sanson, M.: Blechformung durch Streckziehpressen. Technisches Zentralblatt für praktische Metallbearbeitung **61**(3), 147–149 (1967)

[SCHÄ93] Schäfer, R.: Feinschneiden und Umformen elektrotechnischer Bauteile. Schweizer Präzions-Fertigungstechnik 30–34 (1993)

[SCHE76] Schelosky, H.: Beitrag zum Verhalten superplastischer Werkstoffe beim Massivumformen. Dissertation, Universität Stuttgart (1976)

[SCHI62] Schimz, K.: Kaltformfibel II. Draht-Welt. Triltsch Verlag, Düsseldorf (1962)

[SCHI93] Schilling, R.: Umform-Eigenspannungen in Blechen berechnen mit der FE-Methode. Bänder Bleche Rohre **34**(7), 29–32, 37–38 (1993)

[SCHL77] Schlosser, D.: Geometrische Eigenschaften tiefgezogener kreiszylindrischer Näpfe. Dissertation, Universität Stuttgart (1977)

[SCHM81] Schmoeckel, D., Eichner, K.W., Neff, F.J.: Lagebericht: Verzahnungen durch Umformen. Werkstatt und Betrieb **113**(12), 33–34 (1981)

[SCHM88] Schmoeckel, D., Schlagau, S.: Verbesserung der Verfahrensgrenzen beim Kragenziehen durch Überlagerung von Druckspannungen. Ann. CIRP **37/1**, 271–274 (1988)

[SCHM94] Schmidt, P.F.: Aufbau eines Rasterelektronenmikroskops. In: Schmidt, P.F. (Hrsg.) Praxis der Rasterelektronenmikroskopie und Mikrobereichsanalyse. Expert Verlag, Renningen-Malmsheim (1994)

[SCHN92] Schneider, C., Prange, W.: "Tailored blanks"—ein Werkstoff für neue Formen der Konstruktion. Thyssen Technische Berichte (1), 97–106 (1992)

[SCHR84] Schröder, G.: Isothermschmieden—Ein neuer Weg für die Präzisionsumformtechnik. In: der ehemaligen Mitarbeiter des Instituts für Umformtechnik Stuttgart e. V., V. (Hrsg.): Umformtechnik '84—Festschrift zum 65. Geburtstag von Professor Dr.-Ing. K. Lange, Stuttgart (1984)

[SCHR93a] Schröder, G.: Umformen bei besonderen Werkstoffzuständen. In: Lange, K. (Hrsg.) Umformtechnik, Handbuch für Industrie und Wissenschaft. Band 4: Sonderverfahren, Prozesssimulation, Werkzeugtechnik, Produktion. Springer, Heidelberg (1993)

[SCHR93b] Schröder, G.: Umformen von Nickelbasislegierungen (Superlegierungen). In: Lange, K. (Hrsg.) Umformtechnik, Handbuch für Industrie und Wissenschaft. Band 4: Sonderverfahren, Prozesssimulation, Werkzeugtechnik, Produktion. Springer, Heidelberg (1993)

[SCHR04] Schruff, I.: Der Einfluss des Werkzeugstahles auf den Werkzeugverschleiß beim Gesenkschmieden. In: Bartz, W. (Hrsg.) Tribologie und Schmierung bei der Massivumformung. Expert Verlag, Renningen-Malmsheim (2004)

[SCHU64] Schuler, L.: Handbuch für die spanlose Formgebung. Ernst Klett Verlag (1964)

[SCHÜ73] Schürmann, E., et al.: Zur Verzunderung von unlegiertem Stahl. Archiv für das Eisenhüttenwesen **44**(12), 927–934 (1973)

[SCHU89] Schunk, U.: Gewindeherstellung mit Rollköpfen. VDI-Z **131**(8), 106–110 (1989)

[SCHU04a] Schulz, J.: Alternativen zu chlorhaltigen Produkten. In: Tribologie-Fachtagung: Reibung, Schmierung und Verschleiß. Gesellschaft für Tribologie e. V., Göttingen (2004)

[SCHU04b] Schumann, H.; Oettel, H.: Metallographie. Wesentlich überarbeitete und erweiterte Auflage. Wiley-VCH, Weinheim, 14 (2004)

[SCHW87] Schwager et al.: Neue Verfahrenskombinationen Umformen-Spanen. In: Blech Rohre Profile **34**(11), 739–742 (1987)

[SEID04] Seidel, H.: Schmierstoffe für Massivumformprozesse im Warm- und Halbwarmbereich. In: Bartz, W. (Hrsg.) Tribologie und Schmierung bei der Massivumformung. Expert Verlag, Renningen-Malmsheim (2004)

[SELL55] Sellin, W.: Tiefziehtechnik. Springer, Heidelberg (1955)

[SEML73] Semlinger, E.: Stanztechnik. Vieweg Verlag, Braunschweig, 2. Auflage (1973)

[SHAH57] Shah, P.: Der Umformvorgang bei der Erzeugung von Rillen. Dissertation, TH Hannover (1957)

[SHAW63] Shaw, M.: The role of friction in deformation processing. Wear **6**, 140–158 (1963)

[SIEB27] Siebel, E.; Pomp, A.: Die Ermittlung der Formänderungsfestigkeit von Metallen aus dem Stauchversuch. Mitteilungen des Kaiser-Wilhelm-Institut für Eisenforschung **9**, 157–171 (1927)

[SIEB32] Siebel, E.: Die Formgebung im bildsamen Zustand. Verlag Stahleisen, Düsseldorf (1932)

[SIEB48] Siebel, E.; Schwaigerer, S.: Zur Mechanik des Zugversuchs. Archiv für das Eisenhüttenwesen **19**, 145–152 (1948)

[SIEB52] Siebel, E.: Werkstoffmechanik. VDI-Z **14**, 465–471 (1952)

[SIEB54] Siebel, E., Weiss, H.: Untersuchungen über das Abstrecken. Mitteilungen der Forschungsgesellschaft Blechverarbeitung (11) (1954)

[SIEB55] Siebel, E., Beisswänger, H.: Tiefziehen. Carl Hanser Verlag, München (1955)

[SIEB62] Siebel, E.: Grundlagen und Begriffe der bildsamen Formgebung. VDI Verlag, Düsseldorf (1962)

[SIEG92] Siegert, K., Werle, T.: Verfahrenskombination verbessert Umformteile aus Blech. Wissenschaft und Technik (4), 66–68 (1992)

[SIKO63] Sikorski, M.: Correlation of the coefficient of adhesion with various physical and mechanical properties of metals. Trans. Am. Soc. Mech. Eng. (ASME) **85**(279) (1963)

[SING76] Singer, H.: Wirtschaftliches Feinschneiden mit optimalen Werkstoffen. Technische Rundschau (12), 13–14, 19–21 (1976)

[SPAL81] Spallarassa, G., Gropetti, R.: Numerisch gesteuertes Streckziehen. Werkstatt und Betrieb **114**(8), 565–567 (1981)

[SPUR83] Spur, G., Söferle, T.: Handbuch der Fertigungstechnik Band 2/1 Umformen (1983)

[SPUR84] Spur, G., Söferle, T.: Handbuch der Fertigungstechnik Band 2/2 Umformen (1984)

[SPUR85] Spur, G., Söferle, T.: Handbuch der Fertigungstechnik Band 2/3 Umformen und Zerteilen (1985)

[SPUR86] Spur, G., Söferle, T.: Handbuch der Fertigungstechnik, Band 5: Fügen, Handhaben, Montieren. Carl Hanser Verlag, München Wien (1986)

[STAE98] Staeves, J.: Beurteilung der Topographie von Blechen im Hinblick auf die Reibung bei der Umformung. Dissertation, Darmstadt (1998)

[STAH92] Stahl, W.: Schonende Behandlung der Oberfläche. SMM Schweizer Maschinenmarkt **37**, 24–29 (1992)

[STAH93] Stahl, W.: Schneller Wechsel. Maschinenmarkt **99**(35), 32–35 (1993)

[STEE99] Steenberg, T., Olsen, J., et al.: Estimation of temperature in the lubricant film during cold forging of stainless steel based on studies of phase transformations in the film. Wear **232**, 140–144 (1999)

[STEI99] Steinhoff, K., Kapoor, A., Guillon, N.: Controlled wear as mechanism for the design of geometrically defined nanometric surface structures on forming tools. In: Advanced Technology of Plasticity. Springer, Berlin, Band 1 (1999)

[STEN65] Stenger, H.: Über die Abhängigkeit des Formänderungsvermögens metallischer Werkstoffe vom Spannungszustand. Dissertation, RWTH Aachen (1965)

[STEN82] Stenzhorn, F.: Beitrag zur empirisch-theoretischen Vorausplanung des Freiformschmiedens großer Blöcke mit Hohlräumen. Dissertation, RWTH Aachen (1982)

[STRA80] Strasser, F.: Blechdurchzüge. Werkstatt und Betrieb **113**(1), 50–52 (1980)

[STRA82] Straßburger, C., Maid, O., Müschenborn, W., König, W., Rotter, F.: Feinschneidbarkeit von Warmbändern aus höherfesten, mikrolegierten und sulfidkontrollierten Feinkornbaustählen. Thyssen Technische Berichte **2**, 146–153 (1982)

[STRI71] Strigens, P.: Zum Einfluss der Oberflächenverfestigung auf die Dauerfestigkeit von Stählen. Dissertation, TH Darmstadt (1971)

[STRO70] Stromberger, C., Pfaff, K.O.: Lochen von austenitischen Feinblechen mit Stempeln kleinen Durchmessers. Werkstatt und Betrieb **103**(2), 135–140 (1970)

[SU94] Su, J.: Auslegung von Fließpressmatrizen mit der Boundary-Element-Methode im Verbund mit CAD-Systemen. Dissertation, TU Stuttgart (1994)

[SUH73] Suh, N.: The delamination theory of wear. Wear **25**(111) (1973)

[SUY77] Suy, J.: Ziehen unregelmäßiger Blechteile. Industrie Anzeiger **99**, p. 1704–1706 (1977)

[TELG80] Telgentren, G.: Oberflächenfeinwalzen. Werkstatt und Betrieb **113**, 408–413 (1980)

[TELG83] Telgentren, G.: Aufbohren, Schälen und Glattwalzen von Rohren. Werkstattstechnik **73**, 695–696 (1983)

[TELG84] Telgentren, G.: Eingeebnet—Glätten von Oberflächen mit Walzverfahren. Maschinenmarkt **92**(24), 29–32 (1984)

[TERL01] Terlinde, G., Witulski, T., Fischer, G.: Schmieden von Titan. In: Siegert, K. (Hrsg.) Neuere Entwicklungen in der Massivumformung. MAT INFOWerkstoff-Informationsgesellschaft, Frankfurt (2001)

[THAM61] Thamasett, E.: Kräfte und Grenzformänderungen beim Abstreckdrücken zylindrischer, rotationssymmetrischer Hohlkörper aus Aluminium. Dissertation, TU Stuttgart (1961)

[THIE67] Thiessen, P., Meyer, K., Heinicke, G.: Grundlagen der Tribochemie. Akademie Verlag, Berlin (1967)

[THOM69] Thomsen, T.H., et al.: The forming of superplastic sheet-metal in bulging dies, Final Report "Deformation processing of anisotropic materials". Massachusetts Institute of Technology (1969)

[TIES02] Tiesler, N.: Grundlegende Untersuchungen zum Fließpressen metallischer Kleinstteile. Dissertation, Uni Erlangen (2002)

[TIET93] Tietmann, A.L.: Gießschmieden und Thixoschmieden von Aluminiumknetlegierungen. Dissertation, RWTH Aachen (1993)

[TIET94] Tietz, H.D. (Hrsg.): Technische Keramik. VDI Verlag, Düsseldorf (1994)

[TIMM56] Timmerbeil, F.W.: Der Einfluß der Schneidkantenabnutzung auf den Schneidvorgang am Blech. Werkstattechnik und Maschinen **46**, 58–66 (1956)

[TÖLK70] Tölke, K.D.: Unerwünschte Verformungen und Profilverkrümmungen beim Walzprofilieren. Dissertation, TU Hannover (1970)

[TOUS00] Toussant, A.: Einfluss des Werkzeugverschleißes auf die Teilequalität beim Scherschneiden von Elektroblechen. Dissertation, TU München (2000)

[TRES64] Tresca, H.: Sur l'écoulement des corps solides soumis á de fortes pressions. Comptes Rendus de l'Académie des Sciences (Paris) **59**, 754–764 (1864)

[TRIS64] Trisevskij, I.S., Klepanda, V.V., Skokov, F.I.: Kaltgeformte Stahlleichtprofile. Büro Neue Technik WB Stahl- und Walzwerke, Berlin (1964)

[TSCH77] Tschätsch, H.: Taschenbuch Umformtechnik: Verfahren, Maschinen, Werkzeuge. Hanser Verlag, München, 1. Auflage (1977)

[TURN71] Turno, A., Romanowski, M., et al.: Spanlose Herstellung von Zahnrädern und verzahnten Werkstücken. VDI Verlag, Düsseldorf (1971)

[UHLM04] Uhlmann, E., Jurgasch, D.: New impulses in the forming of magnesium sheet metals. In: Kleiner, M. (Hrsg.) Proceedings of the 1st International Conference on High Speed Forming, Dortmund (2004)

[ULLM04] Ullmann, R.: Tribologie und Schmierung in der Massivumformung—Fließpressöle für die Kaltmassivumformung. In: Bartz, W. (Hrsg.) Tribologie und Schmierung bei der Massivumformung. Expert Verlag, Renningen-Malmsheim (2004)

[VAHL04] Vahl, M.: Beitrag zur gezielten Beeinflussung des Werkstoffflusses beim Innenhochdruck-Umformen von Blechen. Dissertation, Friedrich-Alexander-Universität Erlangen-Nürnberg (2004)

[VATE70] Vater, M., Stapper, H.: Biegen von Grobblechen zu U-Profilen mit Gegenhalter. In: Mitteilungen der Deutschen Forschungsgesellschaft für Blechverarbeitung und Oberflächenbehandlung (DFBO) **21**, 153–155 (1970)

[VDI76] VDI 3137: Begriffe, Benennungen, Kenngrößen des Umformens. Verein Deutscher Ingenieure, Januar (1976)

[VDI77] VDI 3166: Halbwarmfließpressen von Stahl. Verein Deutscher Ingenieure, April (1977)

[VDI79] VDI/VDE 2251: Feinwerkelemente. Blatt 2: Stauch- und Biegeverbindungen. Verein Deutscher Ingenieure / Verband der Elektrotechnik Elektronik Informationstechnik, Januar (1979)

[VDI86] VDI 3176: Vorgespannte Presswerkzeuge für das Kaltmassivumformen. Verein Deutscher Ingenieure, Oktober (1986)

[VDI89] VDI 3174-1: Walzen von Außengewinden. Verein Deutscher Ingenieure, Juli (1989)

[VDI92] VDI 3198: Beschichten von Werkzeugen der Kaltmassivumformung—CVD- und PVD-Verfahren. Verein Deutscher Ingenieure, August (1992)

[VDI94] VDI 2906: Schnittflächenqualität beim Schneiden, Beschneiden und Lochen von Werkstücken aus Metall, Blatt 5 Feinschneiden. Verein Deutscher Ingenieure, Mai (1994)

[VDI97] VDI 3186-2: Werkstoffe für Kaltfließpresswerkzeuge—Anleitung zur Gestaltung, Bearbeitung und Eigenschaftenverbesserung. Verein Deutscher Ingenieure, April (1997)

[VDI98] VDI 3138-1: Kaltmassivumformen von Stählen und NE-Metallen. Verein Deutscher Ingenieure, März (1998)

[VDI99a] VDI 3138-2: Kaltmassivumformen von Stählen—Anwendung, Arbeitsbeispiele, Wirtschaftlichkeitsbetrachtung für das Kaltfließpressen. Verein Deutscher Ingenieure, August (1999)

[VDI99b] VDI 3146: Innenhochdruck-Umformen—Grundlagen und Bauteilgestaltung. Verein Deutscher Ingenieure (1999)

[VDI00] VDI 3141: Einfließwulste und Ziehstäbe in Stanzerei-Großwerkzeugen. Verein Deutscher Ingenieure, Januar (2000)

[VDI01] VDI 3824-4: Qualitätssicherung bei der PVD- und CVD Hartstoffbeschichtung. Blatt 4: Prüfplanung für Hartstoffbeschichtungen. Verein Deutscher Ingenieure, August (2001)

[VDI02] VDI 3824-1: Qualitätssicherung bei der PVD- und CVD Hartstoffbeschichtung. Blatt 1: Eigenschaftsprofile und Anwendungsgebiete von Hartstoffbeschichtungen. Verein Deutscher Ingenieure, März (2002)

[VDI04] VDI 3840: Kohlenstoffschichten—Grundlagen, Schichttypen und Eigenschaften. Verein Deutscher Ingenieure, Mai (2004)

[VOIG88] Voigtländer, O.: Perspektiven der Massivumformung in den 90er Jahren. Werkstatt und Betrieb **121(**7), 561–567 (1988)

[VOLL96] Vollertsen, F.: Lasergestützte Formgebung: Verfahren, Mechanismen, Modellierung. Meisenbach Verlag, Bamberg (1996)

[VOLL00] Vollertsen, F.: Accuracy in process chains using hydroforming. J. Mater. Process. Technol. **103**(3), 424–433 (2000)

[VOVK04] Vovk, V., Sabelkin, V.: New achievements in the field of impulse processing technologies. In: Kleiner, M. (Hrsg.) Proceedings of the 1st International Conference on High Speed Forming, Dortmund (2004)

[VULC04] Vulcan, M.: Superplastische Aluminium-Blechumformung. In: wt Werkstattstechnik online **94(**10), 500–501 (2004)

[WAGE99] Wagemann, A.: Umformwerkzeuge aus Hochleistungskeramik. Blech Rohre Profile (1/2), 28–29 (1999)

[WAGE00] Wagemann, A.: Umformwerkzeuge aus Hochleistungskeramik. Umformtechnik **4**, 20–21 (2000)

[WAGN96] Wagner, S.: 3D-Beschreibung der Oberflächenstrukturen von Feinblechen. Dissertation, Stuttgart (1996)

[WANH87] Wanheim, T., Bay, N.: Friction stress and normal stress in bulk metal forming processes. J. Mech. Working Technol. **14**, 203–223 (1987)

[WANH99] Wanheim, T., Bay, N.: Modelling and testing of friction and lubrication in bulk metal forming. Trans. Am. Soc. Mech. Eng. (ASME), J. Tribol. (1999)

[WEBE04] Weber, M., Bewilogua, K., et al.: Anwendung und Potenzial neuartiger hochbelastbarer Kohlenstoffschichten für die Umformtechnik. In: Dünne Schichten: Tagungsband zum EFDS-Workshop "Kohlenstoffschichten—tribologische Eigenschaften und Verfahren zu ihrer Herstellung". EFDS Europäische Forschgesellschaft, Dortmund (2004)

[WEIM66] Weimar, G.: Längsdehnungen und Verwerfungen beim Bandprofilwalzen. Dissertation, TH Hannover (1966)

[WEIM68] Weimar, G.: Messung und Beeinflussung von Kantendehnungen beim Walzprofilieren. Industrie Anzeiger **90**, 2012–2013 (1968)

[WEND71] Wend, E.F.: Aussagekraft der Werkstoffkenngrößen für das Umformverhalten rost- und säurebeständiger Bleche und Bänder. VDI-Z **113**(8), 582–588 (1971)

[WERL95] Werle, T.: Superplastische Aluminiumblechumformung unter besonderer Beachtung der Formänderungsgeschwindigkeit. Dissertation, Universität Stuttgart (1995)

[WEST03] Westkemper, E., Scharft, D.: Taumelclinchen, ein Verfahren zum kraftreduzierten Durchsetzfügen. Fraunhofer Institut Produktionstechnik und Automatisierung (2003)

[WILH75] Wilhelm, H.: Zugdruckumformen. In: LANGE, K. (Hrsg.): Umformtechnik, Handbuch für Industrie und Wissenschaft. Springer, Heidelberg, Band 3: Blechumformung (1975)

[WILK58] Wilken, R.: Das Biegen von Innenborden mit Stempeln. In: Mitteilungen der Forschungsgesellschaft Blechverarbeitung, pp. 56–63 (1958)

[WILL88] Willmann, G., Wielage, B.: Technische Keramik. Vulkan Verlag, Essen (1988)

[WITT80] Witthüser, K.P.: Untersuchung von Prüfverfahren zur Beurteilung der Reibungsverhältnisse beim Tiefziehen. Dissertation, Universität Hannover (1980)

[WITT89] Witt, S.: Präzisionsgeschmiedete Getriebeteile. Industrie Anzeiger **111**(28), 31–34 (1989)

[WOLF03] Wolf, A.: Thixo-Schmieden von Al-Mg-Si Legierungen. Dissertation, Universität Stuttgart (2003)

[WU00] Wu, W.T., Tang, J.P., Li, G.: Recent developments of process simulation and its applications to manufacturing processes. In: 1st International Conference on Thermal Process Modelling and Computer Simulation, Shanghai, P. R. China (2000)

[WU03] Wu, W.T., Jinn, J.T., Fischer, C.E.: Modeling techniques in forming processes. In: Dieter, G.E., Kuhn, H.A., Semiatin, S.L. (Hrsg.): Handbook of Workability and Process Design. ASM International, Materials Park (2003)

[WÜNS02] Wünsch, M., Pyka, P.: Chlorfreie Tiefziehöle für Edelstahl. In: Reibung, Schmierung und Verschleiß—Forschung und praktische Anwendungen. Tribologie-Fachtagung. Gesellschaft für Tribologie e.V., Göttingen (2002)

[ZIBU04] Zibulla, G.: Trocken schmieren—Moderne Entwicklung bei Schmierstoffen für die Blechumformung. In: Bänder Bleche Rohre (2004)

[ZICK79] Zicke, G.: Automatisierung in der Umformtechnik am Beispiel des Walzrundens. Industrie Anzeiger **101**(79), 72–76 (1979)

[ZIEN00] Zienkiewicz, O., Taylor, L.R.: The Finite Element Method: Volume 1—The Basis, 5th edn. Butterworth-Heinemann, Oxford Auckland Boston (2000)

[ZIKA72] Zika, J., Reißner, J.: Beanspruchungs- und fertigungsgerechte Werkstoffauswahl in der Blechumformtechnik. In: Fertigung (1), 9–15 (1972)

[ZIMN98] Zimnik, W., Ritterbach, B., Müll, K.: Pretex—Ein neues Verfahren zur Erzeugung texturierter Feinbleche für höchste Ansprüche. In: Stahl und Eisen **118**(3), 75–80 (1998)

[ZITZ95] Zitz, U.: Abschätzung der Rissentstehung bei der Kaltumformung. Dissertation, RWTH Aachen (1995)

[ZWIC74] Zwicker, U.: Titan und Titan-Legierungen. Reihe Reine und angewandte Metallkunde in Einzeldarstellungen Bd. 2. Springer, Heidelberg (1974)

Index

A
Abrasion, 129
Active plane, 16
Actual forming process, 39
Adhesion, 130
AFP steels, 89
Alkali soap, 138
Aluminium, 80
Analysis methods, 62
Anisotropy, 5, 76
Annular surface of the flange, 331
Atom shifting, 5

B
Bake-hardening steel, 74
Basic profile shape, 373
Bauschinger effect, 49, 170
Beading, 465
Beam intensity, 396
Bendability, 114
Bending
- bending angle, 360
- bending radius, 361
- die bending, 368
- edge deformation, 363
- edge elongation, 361
- folding, 370
- free, 366
- neutral fibre, 359
- roll bending, 371
  - - corrugating, 371
  - - draw roll forming, 373
  - - roll forming, 374
  - - round bending with rolls, 371
- springback, 361
- V-block, 366

Bending arc, 367
Bending punch, 376
Bending stage plan, 380
Bending test, 111, 113
Bending work, 192
Bending wrenches, 376
Bend straightening, 365
Bite ratio, 208
Blank holder, 315
Blanking, 422
Blanking and piercing tool, 422
Blasting treatment, 155
Blue brittleness, 201
Bond, 130
- covalent, 131
- force, 7
- ionic, 131
- metallic, 3, 131
- non-metallic, 100
- van der Waals, 131

Boundary friction, 120
Button stop pin, 424

C
Capture pin, 424
Carbide, 87
Carrying capacity, 139
Cementite, 87
Ceramic, 99
Chemisorption, 141
Chevrons, 179
Chlorinated paraffin, 142
Clamping element, 332
Clamping roll, 371
Clinching, 459
- multi-step, 462
- with cutting, 459
- without cutting, 460

Coarse grain, 13
Coating, 316

DOI: 10.1007/978-3-642-36772-4, © Springer-Verlag Berlin Heidelberg 2013

Coating material, 150
Coating methods, 149
Coating testing devices, 160
Cold forming, 169
Cold shut, 128
Collect chuck, 354
Complex phase steels, 75
Compound tool, 328
Compression yielding point, 147
Compressive forming, 169, 172
Condition of adhesion, 122
Constitutive law, 33, 48
Contact condition, 51
Contact normal stress, 161
Contact surface, 120
Continuity equation, 38
Continuous flow process, 229
Continuum element, 47
Continuum kinematics, 21
Continuum mechanics, 15
Continuum representation, 45
Contrasting, 71
Coolant, 242
Copper, 81
Coulomb friction coefficient, 160
Counterholder, 430
Crack, 62
Crack depth, 427
Crack propagation rate, 289
Cross-section simulation, 61
Crystal lattice, 4
Crystal orientation, 68
Crystal physics, 15
Crystal regeneration, 10
Crystal structure, 3
Cupping test, 111
Cutting, 407
- blanked part geometry, 415
- burr, 425
- burr height, 427
- clean-cut portion, 434
- crack formation, 413
- cutting force, 411
- cutting force reduction, 414
- cutting line, 410
- cutting line geometry, 417
- earing, 409
- manufacturing accuracy, 426
- retracting force, 412
- sheared edge, 429
- sheared edge forms, 435
- sheared edge quality, 410
- sheared edge comparison, 430
- shearing, 407
- shearing correction coefficient, 410
- shearing gap, 410
- shearing plane, 413
- shear resistance, 411
- shear strength, 411
- tool wear, 416
- - crater wear, 416
- - front wear, 416
- - outer wear, 416
Cylinder crush test, 107

D
Damage criteria, 31
Damage value, critical, 32
Decarburization, 235
Deep drawing
- blank holder, 294
- blank holder force, 293
- bottom tear, 302, 321
- buckling stability, 297
- circular sheet blank, 293
- defects, 322
- die clearance, 316
- die radius, 314
- die radius curvature, 315
- draw bead, 306
- drawing force, 300
- drawing limit ratio, 299
- elastic tools, 312
- forming limit, 298
- inflow bead, 307
- lock bead, 308
- manufacturing accuracy, 321
- punch edge curvature, 315
- reverse drawing, 309
- sheet blank, 293
- strain, 297
- stretcher strain mark, 322
- tool design, 314
- tools, 317
- without blank holder, 301
- workpiece materials, 318
Deep drawing grade, 73–74
Deep drawing test, 112
Deflashing, 221
Deformation analysis, 116
Deformation rates, 40
Degree of material difficulty, 248
Degrees of difficulty for fine blanking process, 435
Determining the flow curve, 101
Die, 170
Die method, 393

Die set with tooling, 421
Die stress, 252
Dimensional accuracy, 195
Disc model, 37
Discretizing, 43
Dislocation, 6
Dislocation migration, 7
Dispersion hardening, 89
Displacement, 6
Draw force, 299
Drawing force formula, 38
Drawing ratio, 299
Drive roll, 371
Dual phase steel, 74

E
Earing, 77
Economic feasibility, 197
Edge deformation, 454
Edge dislocation, 7
Edge web, 415
Effective forming speed, 28
Effective strain, 28, 40, 103
Effects of topography, 153
Efficiency of deformation, 36
Elastic limit, 7
Elasticity limit, 102
Electron beam, 65
Electron microscopy, 65
Element equation, 44
Element type, 44, 47
Elongation at fracture, 105
Elongation, logarithmic, 23
Elongation rate, 24
Elongation tensor, 24
Elongation, true, 23
Embedding, 70
Embedding medium, 71
Embossing, 211
Energy dispersive X-ray (EDX), 70
Energy method, 35
Energy requirement, 125, 188
Enwinding, 465
Erichsen cupping value, 113
Error Compensation Method (ECM), 42
Etching method, 73
Expanding in a closed die, 385
Expansion, 324
Expansion ratio, 326
Explosive forming, 400
Extrusion, 172
- backward, 173
- ejector, 177
- forward, 173
- lateral, 173
- manufacturing examples, 186
- processes, 172
- tools, 175
- with active media, 172

F
Falex testing machine, 158
Fatigue strength, 245
Fatigue wear, 132
Feasibility studies, 59
Feed flow process, 229
Feed limit, 424
FEM, 43
- crash, 59
- massive, 52
- sheet metal, 60
Ferrite, 86
FIB method, 71
Fibre structure, 73
Fillister-bending, 379
Fine blanking, 429
- cutting edge geometry, 437, 438
- forces
  - - cutting force, 440
  - - knife-edged ring force, 439
  - - opposing force, 439
- knife-edged ring, 438
- shearing gap, 436
Fine blanking oil, 442
Finished forging, 212
Finite element analysis, 50
Finite element method, 43
Flange, 328
Flange forming, 324–331
- manufacturing accuracy, 331
- manufacturing examples, 350
- Principles, 323
  - - tools, 331
Flanging, 465
Flash gap, 220
Flat crush test, 108
Flat path test, 164
Flow behaviour, 10
Flow curve, 27, 40
Flow line, 282
Flow rule, 25
Folding test, 114
Force requirement, 8
Foreign atom, 4
Forgeability, 92
Forging saddle, 236

Formability, 29
Forming limit, 32
Forming limit diagram, 116
Forming performance, 42
Forming rate, 13, 23, 29
Forming temperature, 13
Forming work, 36
Forming work, ideal, 36
Form saddle, 217
Four ball tester, 159
Fracture criteria, 31
Fracture strain, 29
Free bending, 364
Free punch, 419
Friction, 120
Frictional force, 120
Frictional shear stress, 121
Functional ceramics, 99
Friction law, 121
Friction parameter determination, 157
Friction work, 192
Further draw, 299

G
GKZ, 87
Grain boundaries, 5
Grain boundary sliding, 14
Grain size, 11
Grain size distribution, 58
Grain structure, 62
Groove profile, 376
Guided punch tool, 420

H
Hardness, 7
Hardness testing, 63
Hard smooth rolling, 284
Hard surfacing, 236
Heating, 232
Heat treatment, 13
Hexahedral element, 48
Higher-strength steel, 74
High rate forming, 399
High-temperature compressive stress, 396
Hollow mandrels, 211
Hooke's law, 20
Hot forming, 13, 201
- closed-die, 217
- - application examples, 222
- - closed-die forging, 217
- - isothermal, 251
- - lubrication, 241
- - precision, 248
- - preforming, 218
- - tools, 237, 238, 241
- forgings, 243
- open die, 219
- - application examples, 212
- - cavity creation, 211
- - drawing out, 207
- - separation, 211
- - spread forging, 210
- - tools, 212
- - upsetting, 209
Hot stretch drawing, 339

I
Ideal crystal, 4
IF steel, 75
Impact value, 244
Impression die, 366
Increasing the fatigue limit, 285
Indentation process, 211
Integration points, 45
Interfacial bond, 128
Internal high-pressure forming, 384–386, 388, 390, 391
Interpolation function, 44
Interstitial atom, 4
Interstitial impurity atom, 4
Ironing, 310
Ironing test, 167
Iron oxalates, 195
Isoparametric elements, 47

K
Knife-edge cutting, 212
Knotting, 465

L
Laser beam forming, 395
Laser remelting, 156
Lattice distortion, 40
Lattice fault, 4
Lattice structure, 4
Layer properties, 149
Limiting strain, 33
Line network method, 298
Lip formation, 320
L-IP steel, 75
Load spectrum, 118
Longitudinal feed process, 282
Lower roller, 371

Lubricant, 134, 194
- additives, 139
- base, 133
- carrier coating, 135
- dry, 144
- emulsion, 139
- grease, 139
- liquid, 139
- mineral oil, 140
- properties, 133
- requirement, 135
- solid, 143
- viscosity, 139
Lubricant film, 140
Lubricant pocket, 153
Lubricant testing equipment, 158
Lubrication, 134–146
Ludwik equation, 104

M
Machinability, 248
Male mould process, 393
Mandrel, 211
Manufacturing accuracy, 195
Material flow, 35
Material flow simulation, 57
Material model, 49
Materials, 74
- massive, cold, 79
- massive, hot, 89
- sheet metal, 74
Materials testing, 101
Maximum drawing ratio, 113
Measurement grid, 298
- method, 39
Membrane element, 47
Mesher, 51
Metal spinning
- admissible strains, 346
- conventional, 343
- criteria for use, 357
- dimensional and shape accuracy, 356
- forces, 350
- manufacturing examples, 350
- manufacturing quality, 356
- materials, 357
- projection lengthening, 347
- shear spinning, 342
- surface quality, 356
- tools, 354
Metallography, 62
Microgeometry, 117
Microhardness testing, 64
Microscopy, 63
Mixed friction, 153
Mohr's stress circle, 17
Molybdenum disulfide, 137
Molykote, 290
Moulding tool, 335
Multi-stage die, 223

N
Networking, 51
Nibbling, 425
Nickel, 85
Nitriding, 148
Non-linearity, 48
Non-stationary processes, 191
Normal stress, 15
Notching, 418, 464

O
Oberhofer etching, 73
Offsetting with drawing out, 211
One-step simulation, 62
Open-die, 206
Optical microscopy, 63
Oxalate coating, 136

P
Paraffin oil, 139
Partial upsetting in a die, 219
Path lines, 191
Penalty term, 45
Perlite, 86
Phase boundaries, 62
Phase transformation, 89
Phosphate coating, 136
Physisorption, 141
Pilot, 424
Pilot punch, 424
Pipe model, 36
Plasticity theory, 35
Plastics, 100
Plastomechanics, 37
Plunge process, 229
Plunge-throughfeed rolling, 267
Pore, 32, 62
Precipitation, 62
Preforming, 218
Preparation method, 70
Prepiercing, 328
Pre-processor, 51
Pressure absorption capacity, 159

Pressure, hydrostatic, 16
Principal line method, 38
Principal normal stresses, 16
Process kinematic, 52
Process simulation, 48
Profile bearing length ratio, 283
Profile stretch drawing, 339
Progressive compound tool, 444
Progressive tool, 422
Proportionality factor, 33
Punch riveting, 457
- hollow rivet, 458
- solid rivet, 458
Pushing-through, 172

Q
Quadratic element, 48

R
Radial forming method, 217
Radius of curvature, 350
Raffinate, 139
Real crystal, 5
Recrystallization, 10, 62
Recrystallization rate, 13
Reducer rolling, 219
Reduction in area, 7
Redundant work, 192
Reflected-light microscope, 63
Reichert's test, 159
Reinforcement rings, 176
Residual austenite steel, 75
Resqueezing, 366
Ring upsetting test, 161
Riveting die, 458
Roll feed, 425
Rolling, 264
- cold, 267
- cross, 265
- deep rolling, 286
- flow height, 266
- kinematics, 265
- longitudinal, 265
- materials, 285
- plunge-throughfeed rolling process, 268
- profile rolling, 264
- rolling irons, 276
- rolling-off process, 266
- sizing rolling, 285
- skewed, 264
- surface fine rolling, 281
- thread, 264
- thread rolling, 274
- throughfeed method, 268
- tool materials, 290
- tooth profile, 266
Rolling-in, 465
Roto-Flo method, 268
Runge-Kutta method, 38

S
Salts, 145
Scaling, 234
Scanning electron microscopy, 65
Scoring, 128
Seaming, 464
SF tester, 160
Shaping block, 334
Shear flow stress, 122
Shear forming process, 211
Shear friction law, 123
Shear strength factor, 440
Shear stress, 6, 16, 19
Shear stress theory, 19
Sheet doubling, 381
Sheet metal qualities, 317
Sheet metal forming testing procedures, 165
Sheet metal testing, 112
Sheet thickness reduction, 328
Shell element, 47
Simulation, 50
Single die, 223
Skin pass roll, 154
Slenderness ratio, 108
Slide plane, 7
Sliding, 6
Slip line method, 38
Smooth rolling, 282
Soaps, 142
Soft-annealing, 87
Solid forging, 212
Solid mandrels, 211
Solidus temperature, 89
Solution domain, 44
Solution method, 46
Specimen picture, 5
Speed of the heating process, 232
Spinning chucks, 347
Spinning ratio, 348
Splitting, 407
Spread forging, 210
Spread forming, 464
Springback, 61

Springback factor, 361
Stainless steel, 76, 87
Start of flow, 18
State of lubrication, 120
State of stress, 15, 16, 31
Stationary process, 191
Steel, stainless, 76
Stop pin, 424
Strain, 5, 189
Strain efficiency factor, 341
Strain hardening, 7
Strain hardening exponent, 105, 341
Strain strength, 21
Strength value, 7
Stress relieve annealing, 319
Stress tensor, 15, 26
Stretch drawing, 333
Stretch drawing force, 341
Stretch drawing test, 113
Stribeck curve, 135
Strict solution, 38
Strip drawing test, 165
Strip model, 37
Structural ceramics, 99
Subcritical annealing, 320
Subdomains, 44
Substitute atom, 4
Superplasticity, 394
Surface disruption, 132, 146
Surface energy, 149
Surface finish, 120
Surface microtopography, 154
Surface quality, 195, 198
Surface roughness, 284
Surface technology, 147
Surface treatment, 316
Swaging, 229
Symmetry, 50
System equations, 44

T
Tailored blanks, 318
Tangential stretch drawing, 336
Taper crush test, 109
Tensile compressive forming, 343
Tensile strength, 7
Tension test, 20
Tetrahedral element, 48
Texturing, 154
Thermal coupling, 46
Thixoforging, 258
Three-roller method, 279
Three-roll round bending machine, 370
Throughfeed method, 268
Time increment, 46
Titanium, 85, 394
To-and-fro bending test, 115
Tool coatings, 148
Tool impression, 217
Torsion Test, 111
Tractrix infeed, 305
Translation, 6
Transmission electron microscope, 63
Transmission electron microscopy, 68
Triangular element, 48
Tribochemical wear, 133, 147
Tribological system, 118
Tribology, 117
Tribometer, 160
TRIP steel, 75
True elongation, 22
True strain, 13, 23, 31
True upset strain, 212
Twinning, 6
Twisting, 226, 465
Types of damage, 240

U
U-die, 367
Uniform elongation, 7, 102, 340
Unit cell, 3
Upper bound method, 42
Upsetting, 169, 209
- manufacturing examples, 170
- significance, 169
Upward flow, 220

V
Vacancy, 5
Variational calculus problem, 42
Variation principal, 44
Velocity field, 39
Viscosity index, 139
Viscosity-pressure behaviour, 139
Viscosity-temperature behaviour, 139
Visioplasticity, 39
Volume constancy, 24
Volume element, 47

W
Wall thickness, 231
Warm forming, 201
Wavelength dispersive X-ray spectroscopy (WDX), 70

Wear, 127
Wear mechanisms, 128
Wear natures, 128
Weaving, 465
Wedge draw test, 168
Workpiece rotational movement, 272
Wrinkle formation, 305, 346
Wrought structure, 244

Y
Yield criterion after Tresca, 19, 36
Yield criterion after v. Mises, 19, 38
Yield locus curve, 78
Yield point, 25
Yield stress, 13, 21, 40
Young′s modulus, 101

Z
Zinc, 81
Zinc phosphate, 195